UNIVERSITAT AUTÒNOMA DE BARCELONA

Faculty of Science

Department of Chemistry

Part I. Hypervalent iodine species: reagents and intermediates in oxidative processes
Part II. Water-soluble metal nanoparticles (Rh, Au) in catalysis

Wusheng Guo

Supervisors:

Prof. Roser Pleixats

Dr. Alexandr Shafir

PhD in Chemistry

Doctoral Thesis, 2014

UNIVERSITAT AUTÒNOMA DE BARCELONA

Faculty of Science

Department of Chemistry

Part I: Hypervalent iodine species: reagents and intermediates in oxidative processes
Part II: Water-soluble metal nanoparticles (Rh, Au) in catalysis

Dissertation submitted for the degree of

Doctor

Wusheng Guo

Supervisors:

Prof. Roser Pleixats

Full professor of Organic Chemistry
Universitat Autònoma de Barcelona

Dr. Alexandr Shafir

Group leader in *Institut Català d'Investigació Química* (ICIQ)

Cerdanyola del Vallès, 20th April 2014

to my family, supervisors and my good friends

ACKNOWLEDGEMENTS

The present work has been performed at the Chemistry Department of Universitat Autònoma de Barcelona under the supervision of Prof. Roser Pleixats and Dr. Alexandr Shafir.

First of all, I would like to acknowledge my supervisor Professor Roser Pleixats for her expert guidance and financial support. I'll never forget her patience with me. I also give great thanks to my supervisor Dr. Alexandr Shafir. He really taught me a lot about reaction skills and always gave me insightful ideas whenever I lost somewhere in my project. Professor Jordi Hernando also helped me a lot in understanding some perplexing scientific questions.

The former group members, Amàlia Monge Marcet, Chao Liu and Dongmei Shen offered me very important and timely help with my research. They taught me how to work with efficiency, how to use the new equipments and how to perform the water-sensitive organic reactions. I also thank all the other colleagues of our organic group for their friendship and timely help.

Thanks to Emma Rossinyol and Anna Crespí, I could always get the XRD and TEM analysis results in the first time. Thanks also are given to the collaborators Enrico Faggi, Oriol Vallcorba and Teodor Parella.

I thank my parents, brothers and sisters. Special thanks are given to my wife, Yu Zhou. For more than three years she has patiently provided solid support from the other side of the earth, China. With her love I was full of strength everyday to perform the experimental work.

Thanks to China Scholarship Council (CSC scholarship) and the financial support from Spain (Projects CTQ2009-07881, CTQ2011-22649 and Consolider Ingenio 2010 (CSD2007-00006)), I have the chance to perform the research in Spain. I appreciated the help and facilities from the following services or organizations: *Servei d'Anàlisi Química de la UAB*, *Servei de Ressonància Magnètica Nuclear de la UAB*, *Servei de Microanàlisis del CSIC de Barcelona*, *Servei de Microscòpia Electrònica de la UAB.*

To all, again, thank you very much.

Wusheng
20th Mar 2014

List of publications based on this thesis

- M. Planellas, **W. Guo**, F. Alonso, M. Yus, A. Shafir,* R. Pleixats*, T. Parella,
  Hydrosilylation of internal alkynes catalyzed by tris-imidazolium salt stabilized palladium nanoparticles,
  Adv. Synth. Catal., **2014**, *356*, 179-188.

- **W. Guo**, O. Vallcorba, A. Vallribera, A. Shafir*, R. Pleixats*, J. Rius,
  Oxidative breakdown of iodoalkanes to catalytically active iodine species. A case study in the α-tosyloxylation of ketones,
  ChemCatChem, **2014**, *6*, 468-472.

- **W. Guo**, E. Faggi, R. M. Sebastián, A. Vallribera*, R. Pleixats*, A. Shafir*,
  Direct Arylation of Oligonaphthalenes Using PIFA/BF_3·Et_2O: From Double Arylation to Larger Oligoarene Products,
  J. Org. Chem., **2013**, *78*, 8169-8175.
  Highlighted in *Synfacts,* **2013***, 9,* 1177

- **W. Guo**, A. Monge-Marcet, X. Cattoën, A. Shafir*, R. Pleixats*,
  Sol-gel immobilized aryl iodides for the catalytic oxidative α-tosyloxylation of ketones, *React. Funct. Polym.*, **2013**, *73*, 192-199.

Manuscripts in preparation

- **W. Guo**, R. Pleixats*, A. Shafir*,
  Water soluble gold nanoparticles stabilized by a PEG-tagged nitrogen-rich compound as highly active, selective and recyclable catalysts for the reduction of nitroarenes in water at room temperature.
  Manuscript in preparation.

- **W. Guo**, R. Pleixats *, A. Shafir *, T. Parella,
  Rhodium nanoflowers stabilized by a PEG-tagged nitrogen-rich stabilizer as recyclable catalyst for the hydrosilylation of alkynes under solvent-free conditions.
  Manuscript in preparation.

Congresses and scientific meetings attended and work presented

- *8 Oct* **2013**, Barcelona, Spain
  W. Guo
  Assistance to workshop on Nanomedicine UAB-CEI: a challenging opportunity

- *25 - 28 Jun* **2013**, Vienna, Austria
  W. Guo, E. Faggi, R. M. Sebastián, A. Vallribera, R. Pleixats, A. Shafir
  14th Tetrahedron Symposium *(Poster: Direct arylation of oligonaphthalenes using PIFA/BF_3·Et_2O: from double arylation to four-component assembly)*

- *3 - 5 Jun* **2013**, Alicante, Spain
  W. Guo, A. Shafir, R. Pleixats
  VI International School on Organometallic Chemistry *Marcial Moreno Mañas (Poster and oral flash presentation: Synthesis and catalytic activity of water-soluble Au and Rh nanoparticles)*

- *15-17 May* **2013**, Barcelona, Spain
  W. Guo, A. Shafir, R. Pleixats
  Jornades Doctorals-2013 *(Poster and oral flash presentation: A) Studies on hypervalent organoiodanes in oxidative processes;B) Organic catalysis by water-soluble metal nanoparticles (Au, Rh))*

- *11 - 13 Mar* **2013**, Berlin, Germany
  W. Guo
  Assistance to Chemiedozententagung 2013 / Festsymposium 125 Jahre Angewandte Chemie.

- *2 - 4 Jul* **2012**, Jaca, Spain
  W. Guo, E. Faggi, R. M. Sebastián, A. Vallribera, R. Pleixats, A. Shafir
  V School on Organometallic Chemistry *Marcial Moreno-Mañas* (*Poster and oral flash presentation: PIFA/BF_3 Et_2O: A reagent for direct formation of extended polynaphthalenes*)

- *27 - 29 Jun* **2011**, Santiago, Spain
  W. Guo, R. Pleixats, A. Shafir
  IV School on Organometallic Chemistry *Marcial Moreno-Mañas (Poster: Heterogeneous and homogeneous organoiodine reagents as catalysts in oxidative processes)*

TABLE OF CONTENTS

ABBREVIATIONS

anh.:	anhydrous
Ar:	aryl
atm:	atmosphere
ATR (for IR):	Attenuated Total Reflectance
b.p.:	boiling point
BET:	Brunauer-Emmett-Teller
BJH:	Barrett-Joyner-Halenda
cat.:	catalyst
^{13}C-NMR:	13-Carbon Nuclear Magnetic Ressonance
CP-MAS:	Cross-Polarization Magic Angle Spinning
Cy:	cyclohexyl
Δ:	heating
d (NMR):	doublet
DBU:	1,8-Diazabicyclo[5.4.0]undec-7-ene
dd (NMR):	double doublet
δ (NMR):	chemical shift
DMF:	dimethylformamide
DMSO:	dimethylsulfoxide
DSC:	Differential Scanning Calorimetry
dt (NMR):	double triplet
EA:	elemental analysis
ee	enantiomeric excess
eq.:	equivalent
EtO:	ethoxy
Et_2O:	diethyl ether
Exp.:	experiment
GC:	Gas Chromatography

GC-MS	Gas Chromatography with Mass Spectrometry detector
^{1}H-NMR:	Proton Nuclear Magnetic Ressonance
HR-MS:	High Resolution Mass Spectrometry
ICP:	Inductively Coupled Plasma
^{i}Pr:	isopropyl
^{i}PrOH:	isopropanol
J (NMR):	coupling constant
λ:	wavelength
HTIB:	[hydroxy(tosyloxy)iodo]benzene
HMPA:	hexamethylphosphoramide
IR:	Infrared spectroscopy
lit.:	literature
M:	concentration in mol/L
mM:	concentration in mmol/L
m (for NMR):	multiplet
m:	*meta*
min:	minutes
Me:	methyl
MeO:	methoxy
Mes:	mesityl
mol%:	molar percentage
m.p.:	melting point
MS:	Mass Spectrometry
MW:	molecular weight
m-CPBA:	*m*-chloroperbenzoic acid
m-CBA:	*m*-chlorobenzoic acid
NMP	1-methyl-2-pyrrolidinone
NPs:	nanoparticles
v (IR):	frequency

o:	*orto*
Ox:	*oxidant*
p:	*para*
PIFA:	phenyliodine bis(trifluoroacetate)
p-TsOH:	*p*-toluenesulfonic acid
p-XRD:	Powder X-Ray Diffraction
q (NMR):	quartet
r.t.:	room temperature
s (NMR):	singlet
S_{BET}:	surface area measured by BET
SET	single electron transfer
SSNMR:	Solid State Nuclear Magnetic Ressonance
t (NMR):	triplet
TBAF:	tetrabutylammonium fluoride
^{t}Bu:	*tert*-butyl
TEOS:	tetraethoxysilane
TFA:	trifluoroacetic acid
TGA:	Thermogravimetry
TLC:	Thin Layer Chromatography
TMS:	trimethylsilyl
THF:	tetrahydrofuran
Ts:	tosyl
MW:	microwave
w/w:	weight percentatge
XPS	X-ray Photoelectron Spectroscopy

ABSTRACT

Hypervalent iodine reagents are known to act as efficient oxidants in a range of oxidative transformations. Kita and coworkers previously used the PIFA/BF_3·Et_2O system to achieve the dehydrogenative arene-arene coupling. Our group extended this methodology to a direct oxidative coupling of four molecules involving binaphthalene and arenes. Following the group's work in this field, we have prepared in this doctoral work new arylated tris-, tetra- and hexa-naphthalene oligomers, which constitute compounds of potential interest in the field of dyes and organic optical devices. As a separate topic on hypervalent organoiodanes, Koser *et al.* used stoichiometric amounts of PhI(OH)(OTs) in the oxidative formation of C-O bonds. Given that the hypervalent reagent reverts to the parent iodoarene, the process was made catalytic by Ochiai using sub-stoichiometric quantities of the aryl iodides in the presence of a terminal oxidant, with the hypervalent species being generated *in situ*. In this thesis we have developed recyclable sol-gel immobilized aryl iodides for the catalytic α-tosyloxylation of ketones. Unexpectedly, a hybrid silica derived from (3-iodopropyl)triethoxysilane was also catalytically active. Further investigations revealed that, unexpectedly, even iodoalkanes can act as pre-catalysts for this oxidative process. We found that in the presence of *m*-CPBA, the iodoalkanes undergo an oxidative breakdown to inorganic catalytic species (likely $IO^{\cdot-}$ or $IO_2^{\cdot-}$). Overoxidation of the *in situ* formed inorganic species resulted in catalyst deactivation *via* the formation of a hitherto unreported phase of the iodic acid (HIO_3), whose structure has been solved *ab initio* from the powder x-ray diffraction data.

As a second topic, metal nanoparticles are very useful in catalysis due to the particular properties imparted by their size and morphology. A stabilizing agent (**S**) is usually required to prevent the agglomeration of the NPs, as well as to control the reactivity at the surface. In this thesis, a new PEG-tagged nitrogen-rich stabilizer has been designed and synthesized to prepare water-soluble Au and Rh NPs. We found that by varying the molar ratio **S**/Rh, we can achieve size and morphology controllable Rh NPs from small atom clusters to nanoflowers. A similar phenomenon was also found for the gold NPs, with morphologies varying from small spheres to nanotadpoles, the sizes of particles depending on the amount of stabilizer. The nanomaterials have been fully characterized. The flower-like Rh NPs proved to be very effective to catalyze the stereoselective hydrosilylation of internal alkynes and they could be easily recycled. The Au NPs were efficient and recyclable catalysts for the selective reduction of various nitroarenes to the corresponding anilines in water at room temperature.

RESUM

Els reactius de iode hipervalent són oxidants eficients en diverses transformacions oxidatives. Kita havia utilitzat el sistema PIFA/$BF_3{\cdot}Et_2O$ per assolir acoblaments oxidatius arè-arè. El nostre grup va extendre aquesta metodologia a l'acoblament oxidatiu directe de quatre components (*four-component direct oxidative coupling*) en el que estaven implicats binaftalè i arens. Seguint amb el nostre interés en aquest tema, en aquesta tesi hem preparat diversos tris-, tetra- i hexanaftalens arilats, compostos que tenen potencial interès en les àrees dels colorants i dels dispositius òptics orgànics. Dins també del tema dels organoiodans hipervalents, Koser havia emprat una quantitat estequiomètrica de PhI(OH)(OTs) en la formació oxidativa d'enllaços C-O. Atès que el reactiu hipervalent reverteix al correspondent iodoarè, el procés fóu millorat posteriorment per Ochiai mitjançant l'ús de quantitats catalítiques de iodurs d'aril en presència d'un oxidant terminal, de manera que les espècies hipervalents es generaven *in situ*. En aquesta tesi hem desenvolupat iodurs d'aril immobilitzats pel mètode sol-gel com a catalitzadors reciclables en l'α-tosiloxilació de cetones. Inesperadament, una sílica híbrida derivada de (3-iodopropil)trietoxisilà també va mostrar activitat catalítica. A partir d'aquí, posteriors investigacions van revelar que els iodoalcans poden actuar també com a pre-catalitzadors en aquest procés oxidatiu. En presència d'un oxidant (*m*-CPBA), els iodoalcans experimenten una degradació oxidativa per donar espècies catalítiques inorgàniques (probablement IO^- o IO_2^-). La sobreoxidació de l'espècie inorgànica formada *in situ* produeix la desactivació del catalitzador i la formació d'una nova fase de l'àcid iódic (HIO_3), no descrita fins ara, estructura que s'ha resolt *ab initio* a partir de dades de difracció de raigs-X de pols.

Per altra banda, les nanopartícules (NPs) metàl.liques són molt útils en catàlisi degut a les particulars propietats derivades de la seva mida i morfología. Es requereix un agent estabilizant (**S**) per evitar l'aglomeració de les NPs i controlar la reactivitat en la superfície. En aquesta tesi s'ha dissenyat i sintetitzat un nou estabilitzant amb elevat contingut de nitrogen i cadenes de PEG, per preparar NPs d'or(0) i de rodi(0) solubles en aigua. Variant la relació molar **S**/Rh es controla la mida i la morfologia de les NPs de Rh(0), des de petits clústers a *nanoflowers*. Un fenòmen similar s'ha observat en les NPs d'Au(0), on la morfologia varia des de petites esferes fins a *nanotadpoles* i la mida depèn de la quantitat d'estabilitzant. Els nanomaterials s'han caracteritzat completament. Les NPs de Rh en forma de flor han mostrat bona activitat catalítica en la hidrosililació estereoselectiva d'alquins interns i s'han pogut reciclar fàcilment, mentre que les NPs d'Au són catalitzadors eficients i reciclables en la reducció selectiva de nitroarens a les corresponents anilines en aigua a temperatura ambient.

GENERAL INTRODUCTION

The discovery of the hypervalent iodine reagent in the late 19th century by Conrad Willgerodt[1] was the starting point for the future development of the chemistry of hypervalent organoiododanes. These compounds have, since then, attracted attention due to their peculiar reactivities and environmentally benign characteristics.[2] Thus, various organoiodane reagents have been prepared and found applications as oxidants and catalysts in different organic transformations. An overview of this subject is given in chapter 1 of part I.

Our group previously[3] performed a direct oxidative four-component coupling involving binaphthalene and arenes on the basis of the methodology proposed by Kita.[4] As an extension of this work, in this thesis we have achieved the direct dehydrogenative C-C coupling between linear ter- and quaternaphthalenes and substituted benzenes using the hypervalent PIFA/$BF_3{\cdot}Et_2O$ reagent (Part I, Chapter 2).[5]

In a separate but related study, Koser *et al.* used stoichiometric amounts of [hydroxy(tosyloxy)iodo]benzene in oxidative α-tosyloxylation of ketones.[6] Given that the hypervalent reagent reverts to the parent iodoarene, the process was improved by Ochiai[7] through the use of catalytic quantities of the aryl iodides and a stoichiometric amount of a cheaper oxidant, with the hypervalent species being generated *in situ*. In this thesis (Part I, Chapter 3), new hybrid silica materials derived from silylated aryl iodides have been prepared and used as recyclable catalysts in oxidative α-tosyloxylation of ketones.[8]

In further investigations (Part I, Chapter 4) we have found that catalytic amounts of iodoalkanes are also active pre-catalysts in this α-tosyloxylation reaction *via* their oxidative breakdown to the true inorganic catalytic species (likely IO^- or IO_2^-). The

---

[1] C. Willgerodt, *J. Prakt. Chem.* **1886**, *33*, 154-160.

[2] Zhdankin, V. V.; Stang, P. J. *Chem. Rev.* **2008**, *108*, 5299.

[3] Faggi, E.; Sebastian, R. M.; Pleixats, R.; Vallribera, A.; Shafir, A.; Rodriguez-Gimeno, A.; Ramírez de Arellano, C. *J. Am. Chem. Soc.* **2010**, *132*, 17980.

[4] Dohi, T., Ito, M.; Morimoto, K.; Iwata, M.; Kita, Y. *Angew. Chem. Int. Ed.* **2008**, *47*, 1301.

[5] **Guo, W.**; Faggi, E.; Sebastián, R. M.; Vallribera, A.; Pleixats, R.; Shafir, A. *J. Org. Chem.* **2013**, *78*, 8169

[6] Koser, G. F.; Relenyi, A. G.; Kalos, A. N.; Rebrovic, L.; Wettach, R. H. *J. Org. Chem.* **1982**, *47*, 2487.

[7] Ochiai, M.; Takeuchi, Y.; Katayama, T.; Sueda, T.; Miyamoto, K. *J. Am. Chem. Soc.* **2005**, *127*, 12244.

[8] **Guo**, **W.**; Monge-Marcet, A.; Cattoën, X.; Shafir, A.; Pleixats, R. *React. Funct. Polym.* **2013**, *73*, 192.

overoxidation of the *in situ* formed catalyst leads to its deactivation through the formation of a hitherto unreported phase of the iodic acid.[9]

Metal catalysis lies at the heart of chemical reactions, both in the academic research area and in the chemical industry. As a special case, metal NPs stand out due to their good catalytic properties imparted by their size and morphology, as reviewed in Chapter 1 of Part II. In chapter 2 we present the objectives of Part II of the thesis.

Continuing with the interests on NPs as catalysts in our group,[10] we have described the hydrosilylation of internal alkynes under catalysis by Pd NPs stabilized by tris-imidazolium salts.[11] Inspired from the previous fruitful results, we have designed and prepared, in the present thesis, a nitrogen-rich polyoxyethylenated stabilizer using a threefold [2+3] click reaction (CuACC). The stabilizer was used for the formation of water soluble Rh NPs and Au NPs (Part II, Chapter 3). The catalytic activity and recyclability of these metal NPs in different organic transformations have also been investigated (Part II, Chapter 4).[12]

---

[9] **Guo, W.**; Vallcorba, O.; Vallribera, A.; Shafir, A.; Pleixats, R.; Rius, J. *ChemCatChem*, **2014**, *6*, 468.

[10] (a) Villarroya, S. *Doctorial thesis*, Universitat Autònoma de Barcelona, **2002** (b) Tristany, M. *Doctorial thesis*, Universitat Autònoma de Barcelona, **2005**. (c) Serra-Muns, A. *Doctorial thesis*, Universitat Autònoma de Barcelona, **2008**. (d) Mejías, N. *Doctorial thesis*, Universitat Autònoma de Barcelona, **2011**. (e) Planellas, M. *Doctorial thesis*, Universitat Autònoma de Barcelona, **2012**.

[11] Planellas, M.; **Guo, W.**; Alonso, F.; Yus, M.; Shafir, A.; Pleixats, R.; Parella, T. *Adv. Synth. Catal.* **2014**, *356*, 179.

[12] The corresponding manuscripts are in preparation for publication.

Part I. Hypervalent iodine species: reagents and intermediates in oxidative processes

CHAPTER 1

Overview of structure and reactivity of hypervalent iodine reagents

Chapter 1. Overview of structure and reactivity of hypervalent iodine reagents

Since the first report of a polyvalent organoiodine compound by Conrad Willgerodt (1886),[1] the chemistry of hypervalent organoiodines has attracted a great deal of attention. Initially, this interest was due in large part to certain similarities in the reactivity of a hypervalent iodine reagent and that of Hg^{II}, Ti^{III} and Pb^{IV} species, thus leading to processes that are more environmentally benign. Recently, however, this analogy has been extended to the chemistry of common transition metal species; the subject of hypervalent iodine chemistry has been treated in several books and reviews.[2] Up until recently, this burgeoning area has been based on the stoichiometric uses of the hypervalent organoiodines as oxidizing reagents in various organic transformations.[2a-r] Recently, however, there has been a surge of interest in using catalytic amount of common organoiodines, such as iodobenzene, in the presence of a cheap oxidant for various organic transformations, made possible by the *in situ* regeneration of the hypervalent species.[2s-v] More recently, as a separate but related field of study, it was found that the inorganic iodine(+1) and iodine(+3) reagents (*e.g*. hypoiodites and iodites, respectively), commonly generated *in situ,* could also act as catalytic intermediates for various oxidative transformations.[3]

1.1 Structure and bonding of hypervalent iodine reagents

A hypervalent state is defined as a situation in which an atom expands its valence shell beyond the limits of the Lewis octet rule.[2a] All known stable hypervalent organoiodines can be divided into two categories, namely the iodine(III) and iodine(V)

---

[1] Willgerodt, C. *J. Prakt. Chem.* **1886**, *33*, 154-160.

[2] (a) Wirth, T., Ed. *Hypervalent Iodine Chemistry: Modern Developments in Organic Synthesis*; Topics in Current Chemistry Series 224; Springer: Berlin-Tokyo, 2003. (b) Varvoglis, A. *The Organic Chemistry of Polycoordinated Iodine*; VCH Publishers, Inc.: New York, 1992. (c) Varvoglis, A. *Hypervalent Iodine in Organic Synthesis*; Academic Press: London, 1997. (d) Zhdankin, V. V.; Stang, P. J. *Chem. Rev.* **2002**, *102*, 2523. (e) Moriarty, R. M.; Prakash, O. *Hypervalent Iodine in Organic Chemistry: Chemical Transformations*; Wiley-Interscience: 2008. (f) Wirth, T.; Hirt, U. H. *Synthesis* **1999**, 1271. (g) Stang, P. J. *J. Org. Chem.* **2003**, *68*, 2997. (h) Moriarty, R. M. *J. Org. Chem.* **2005**, *70*, 2893. (i) Stang, P. J.; Zhdankin, V. V. *Chem. Rev.* **1996**, *96*, 1123. (j) Wirth, T. *Angew. Chem. Int. Ed.* **2005**, *44*, 3656. (k) Varvoglis, A. *Tetrahedron* **1997**, *53*, 1179. (l) Zhdankin, V. V.; Stang, P. J. In *Chemistry of Hypervalent Compounds*; Akiba, K. y., Ed.; VCH Publishers: New York, 1999. (m) Koser, G. F. In *Chemistry of Halides, Pseudo-Halides and Azides, Suppl. D2*; Patai, S., Rappoport, Z., Eds.; Wiley-Interscience: Chichester, 1995. (n) Zhdankin, V. V.; Stang, P. J. *Chem. Rev.* **2008**, *108*, 5299. (o) V. V. Zhdankin, *Arkivoc* **2009**, 1. (p) E. A. Merritt, B. Olofsson, *Angew. Chem. Int. Ed.* **2009**, *48*, 9052. (q) V. V. Zhdankin, *J. Org. Chem.* **2011**, *76*, 1185. (r) R. D. Richardson, T. Wirth, *Angew. Chem. Int. Ed.* **2006**, *45*, 4402. (s) M. Ochiai, K. Miyamoto, *Eur. J. Org. Chem.* **2008**, 4229. (t) T. Dohi, Y. Kita, *Chem. Commun.* **2009**, 2073. (u) M. Uyanik, K. Ishihara, *Chem. Commun.* **2009**, 2086.

[3] Uyanik, M.; Ishihara, K. *ChemCatChem*, **2012**, *4*, 177.

species. Based on the IUPAC nomenclature guidelines, iodine(III) and iodine(V) compounds are denoted as λ^3- and λ^5-iodanes respectively. These are further classified by the type of ligands attached to the iodine center.[2a,2i,2o] The iodine atom in λ^3-iodane (species **a**, Scheme 1) has a total of 10 valence electrons and a geometry of a distorted trigonal bipyramid, with two ligands (B and C) occupying the apical positions and with the remaining ligand (A) and two stereoactive electron lone pairs in the equatorial positions. Ignoring these lone pairs, the three ligands form a T-shaped structure ubiquitous in λ^3-iodanes. Bonding in such species uses the nonhybridized 5p orbital of iodine for the formation of a linear three-center, four-electron (3c-4e) bond.

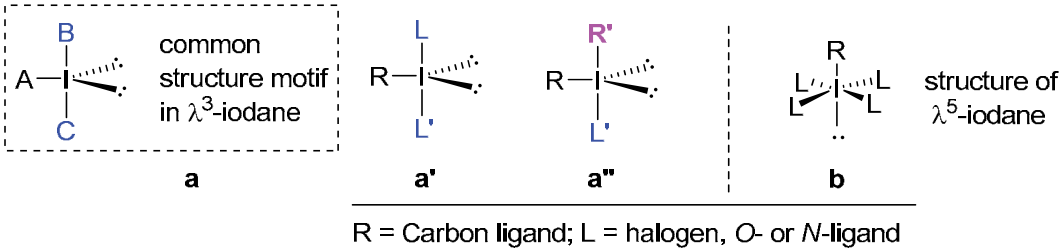

Scheme 1. Hypervalent organoiodanes: λ^3-iodanes (a) and λ^5-iodanes (b).

Organic iodine(III) derivatives can be further subdivided into two categories according to the nature of the remaining two ligands. In compounds with one carbon ligand **R** (species a', Scheme 1), the two electronegative (heteroatom) ligands **L** and **L'** are found in the apical positions, and the least electronegative carbon ligand **R** (along with the two lone pairs) in equatorial positions. Once again, such molecules are almost always T-shaped with the organic (usually aromatic) ligand occupying the "stem" of the T geometry. The second category (species a'', Scheme 1) includes compounds with central iodine bearing two organic ligands, almost always *aromatic* (or heteroaromatic), or in some cases *vinyl* substituents. For the hypervalent species a'', the nomenclature of "diaryl λ^3-iodane" has been widely accepted. The third (heteroatomic) ligand in such species is only loosely bound, often in the form of a cation-anion pair, leading to the second frequent denomination as diaryliodonium salts. The overall geometry is, once again, T-shaped, but for species with a non-coordinating anion (as in the BF_4^- salts), the geometry can be considered as 2-coordinate with the C_{Ar}-I-$C_{Ar'}$ angle close to 90°.

Organic λ^5-iodanes (species b, Scheme 1) have a distorted octahedral structure with the organic group **R** and the electron pair in the apical positions and four heteroatom ligands **L** in basal positions. Two orthogonal hypervalent 3c-4e bonds accommodate all ligands **L**, while the apical group **R** is connected to iodine by a "conventional" covalent bond using a hybridized orbital (5sp).[2b, 2o]

The structural studies of the hypervalent iodine compounds have been addressed by a large number of groups.[4,5] A practical and useful nomenclature to describe the hypervalent iodine species was introduced by Arduengo and Martin in a seminal 1980 publication.[5] The nomenclature, applicable in principle to any bonding pattern, is based on the descriptor N-E-L, where E is the chemical element, the N is the number of valence electrons and the L is the number of ligands bound to the center in question (Scheme 2).Thus, a radical sulfur species shown in Scheme 2 is classified as 9-S-3, while the parent carbene CH_2 is described as a 6-C-2 species (6 valence electrons and 2 hydrogen substituents). For the hypervalent iodine species, the nomenclature readily distinguishes between λ^3-iodanes with the three ligands firmly bound (the 10-I-3 family) and those that have undergone the dissociative loss of one of the X ligands (e.g. as cationic 8-I-2 salt).

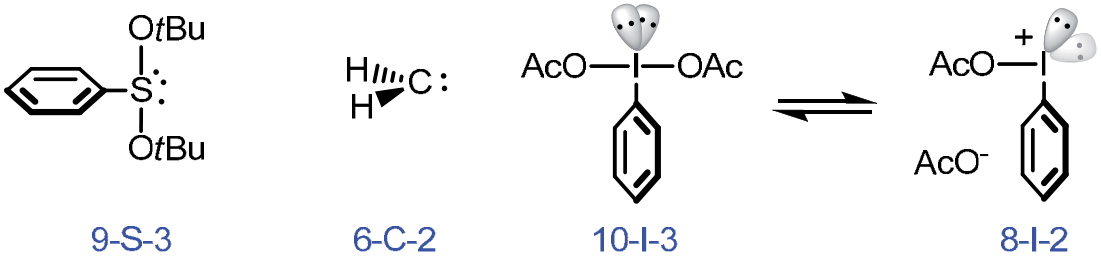

Scheme 2. The Martin-Arduengo classification of the λ^3-iodanes and other compounds.

1.2 Preparation and general reactivity of hypervalent organoiodine reagents

1.2.1 λ^3-Iodanes

The commonly used hypervalent iodine(III) reagents are summarized in Scheme 3. The (dichloroiodo)arenes (type **a**) and (difluoroiodo)arenes (type **b**) have been employed as halogenation reagents as well as oxidants in various organic transformations.[6]

---

[4] (a) Katritzky, A. R.; Savage, G. P.; Gallos, J. K.; Durst, H. D. *J. Chem. Soc., Perkin Trans.2* **1990**, 1515. (b) Katritzky, A. R. Savage, G. P.; Palenik, G. J.; Qian, K.; Zhang, Z.; Durst, H. D. *J. Chem. Soc., Perkin Trans. 2* **1990**, 1657. (c) Katritzky, A. R.; Duell, B. L.; Gallos, J. K.; Durst, H. D. Magn, *Res. Chem.* **1989**, *27*, 1007. (d) Katritzky, A. R.; Gallos, J. K.; Durst, H. D. Magn, *Res. Chem*. **1989**, *27*, 8154.

[5] Perkins, C. W.; Martin, J. C.; Arduengo, A. J.; Lau, W.; Alegria, A.; Kochi, J. K. *J. Am. Chem. Soc*. **1980**, *102*, 1153.

[6] (a) Yusubov, M. S.; Drygunova, L. A.; Zhdankin, V. V. *Synthesis* **2004**, 2289. (b) Yusubov, M. S.; Yusubova, R. J.; Filimonov, V. D.; Chi, K.-W. *Synth. Commun.* **2004**, *34*, 443. (c) Yusubov, M. S.; Drygunova, L. A.; Tkachev, A. V.; Zhdankin, V. V. *ARKIVOC* **2005**, 179. (d) Ibrahim, H.; Kleinbeck, F.; Togni, A. *Helv. Chim. Acta* **2004**, *87*, 605. (e) Jin, L.-M.; Yin, J.-J.; Chen, L.; Guo, C.-C.; Chen, Q.-Y. *Synlett* **2005**, 2893. (f) Benjahad, A.; Guillemont, J.; Andries, K.; Nguyen, C. H.; Grierson, D. S. *Bioorg. Med. Chem. Lett.* **2003**, *13*,

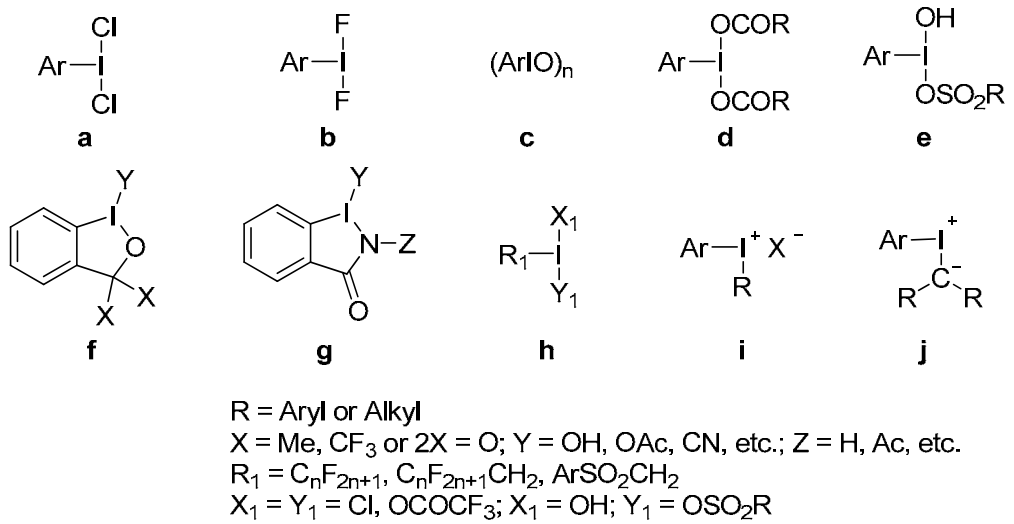

Scheme 3. Representatives of λ^3-iodanes used in synthetic applications.

The preparation of (dichloroiodo)arenes was first described by Willgerodt in the 19th century with the reaction of an iodoarene with Cl_2, and this process continues to be the method of choice for the large-scale applications, where the inconvenience of working with chlorine gas is compensated by the low cost of the process.[1,6a,7] Thus, $PhICl_2$ has been prepared on a multi-kilogram scale with the reaction between iodobenzene and chlorine at low temperature in a CH_2Cl_2 solution.[7] Other reagents prepared by this method include the corresponding hypervalent dichloride derivatives of the 4,4'-diiodo-biphenyl and the 3-iodobenzoic acid, with the latter serving as a recyclable (through acid-base extractions) iodoarene platform.[6a]

Small laboratory scale synthesis can be performed using a combination of an aqueous chloride solution (including HCl) with an oxidant (potassium permanganate, perchlorate, periodate and perborates, as well as various forms of hydrogen peroxide).[8] In all cases, the reaction may proceed either via the initial oxidation of the iodoarene, followed by the ligand exchange of the intermediate λ^3-iodane with the Cl^-,

---

4309. (g) Benjahad, A.; Oumouch, S.; Guillemont, J.; Pasquier, E.; Mabire, D.; Andries, K.; Nguyen, C. H.; Grierson, D. S. *Bioorg. Med. Chem. Lett.* **2007**, *17*, 712. (h) Prakash, O.; Kaur, H.; Batra, H.; Rani, N.; Singh, S. P.; Moriarty, R. M. *J. Org. Chem.* **2001**, *66*, 2019. (i) Prakash, O.; Sharma, V.; Batra, H.; Moriarty, R. M. *Tetrahedron Lett.* **2001**, *42*, 553. (j) Prakash, O.; Kaur, H.; Pundeer, R.; Dhillon, R. S.; Singh, S. P. *Synth. Commun.* **2003**, *33*, 4037. (k) Li, X.-Q.; Zhao, X.-F.; Zhang, C. *Synthesis* **2008**, 2589. (l) Cook, T. R.; Esswein, A. J.; Nocera, D. G. *J. Am. Chem. Soc.* **2007**, *129*, 10094. (m) Cotton, F. A.; Koshevoy, I. O.; Lahuerta, P.; Murillo, C. A.; Sanau, M.; Ubeda, M. A.; Zhao, Q. *J. Am. Chem. Soc.* **2006**, *128*, 3674. (n) Whitfield, S. R.; Sanford, M. S. *J. Am. Chem. Soc.* **2007**, *129*, 15142. (o) Khusniyarov, M. M.; Harms, K.; Sundermeyer, J. *J. Fluorine Chem.* **2006**, *127*, 200. (p) Hayton, T. W.; Legzdins, P.; Patrick, B. O. *Inorg. Chem.* **2002**, *41*, 5388. (q) Bastian, M.; Morales, D.; Poli, R.; Richard, P.; Sitzmann, H. *J. Organomet. Chem.* **2002**, *654*, 109.

[7] Zanka, A.; Takeuchi, H.; Kubota, A. *Org. Process Res. Dev.* **1998**, *2*, 270.

[8] Zielinska, A.; Skulski, L. *Tetrahedron Lett.* **2004**, *45*, 1087.

or, more likely, via the reaction of the *in situ* generated chlorine molecule with the iodoarene. A "textbook" example of the latter mode is exemplified by the recently reported generation of $PhICl_2$ using a combination of HCl with sodium hypochlorite (NaClO, *i. e.*, bleach). Indeed, the comproportionation between Cl^- and ClO^- to Cl_2 is rapid, and allows for the efficient chlorination processes, as observed in this case with iodoarenes (Scheme 4).[9]

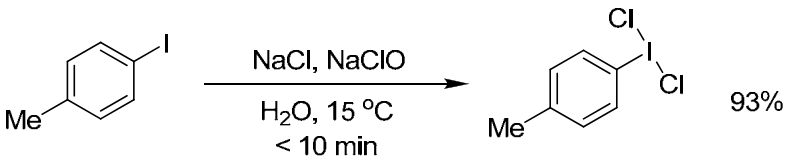

Scheme 4. Chlorination of iodoarenes using non-gaseous Cl_2 equivalents.

(Difluoroiodo)arenes are hygroscopic compounds making their preparation and crystallization extremely difficult. A clean and selective, but relatively expensive, procedure for their preparation consists of the treatment of iodoarenes with xenon difluoride in dichloromethane (Scheme 5) in the presence of anhydrous hydrogen fluoride.[10] Alternative methods involve the treatment of iodosylarenes with HF in dichloromethane at room temperature (Scheme 5).[11] A variety of other powerful fluorinating reagents were also tried to prepare this compound.[12]

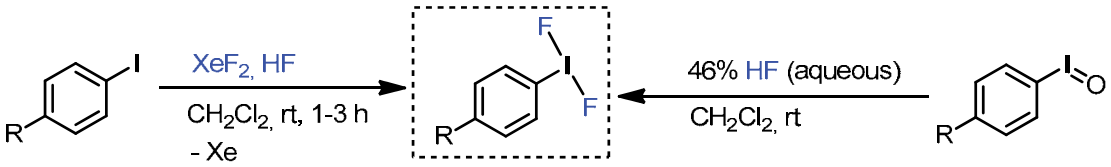

Scheme 5. Two approaches to the preparation of the (difluoroiodo)arenes.

The most common method for the synthesis of iodosylarenes (Scheme 3, type **c**) and derivatives is alkaline hydrolysis of (diacetoxy)iodobenzene or (dichloroiodo)arenes (Scheme 6). The structure of iodosobenzene is often represented with a double bond between the iodine and the oxygen atoms, namely PhI=O. This representation is operationally useful, as it allows for envisioning the use of this species

---

[9] Zhao, X.-F.; Zhang, C. *Synthesis* **2007**, 551.

[10] (a) Zupan, M.; Pollak, A. *J. Fluorine Chem.* **1976**, *7*, 445. (b) Gregorcic, A.; Zupan, M. *Bull. Chem. Soc. Jpn.* **1977**, *50*, 517.

[11] (a) Sawaguchi, M.; Ayuba, S.; Hara, S. *Synthesis* **2002**, 1802. (b) Arrica, M. A.; Wirth, T. *Eur. J. Org. Chem.* **2005**, 395.

[12] (a) Bailly, E.; Barthen, P.; Breuer, W.; Frohn, H. J.; Giesen, M.; Helber, J.; Henkel, G.; Priwitzer, A. *Z. Anorg. Allg. Chem.* **2000**, *626*, 1406. (b) Padelidakis, V.; Tyrra, W.; Naumann, D. *J. Fluorine Chem.* **1999**, *99*, 9. (c) Frohn, H. J.; Bardin, V. V. *J. Fluorine Chem.* **2005**, *126*, 1036.

as oxygen transfer agent. Nevertheless, iodosylarenes, in general, have a polymeric structure resulting in insolubility, which significantly restricts their practical usefulness. The majority of the known reactions[13] applying iodosylarenes require a hydroxylic solvent (water or alcohols) or a catalyst (bromine, Lewis acid, iodide anions or transition metal complex, etc.) which can depolymerize the $(PhIO)_n$, generating the reactive monomeric species.

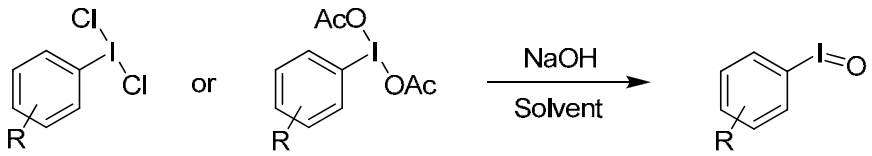

Scheme 6. Preparation of iodosylarenes.

It should be mentioned that for iodosylarenes, the structural studies in solution are often complicated by the reversible solvation (resulting in a new T-shaped species), as occurs in alcohols and with certain acids, and by the non-reversible solvent oxidation, as observed in some alcohols and DMSO (Scheme 7).

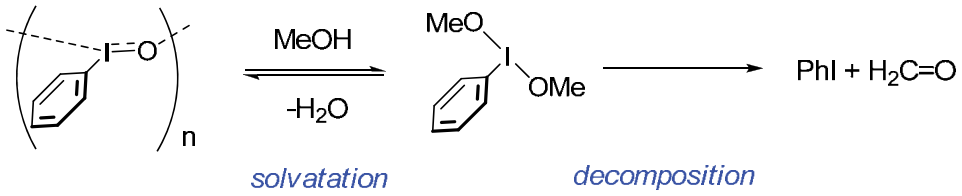

Scheme 7. Behavior of the iodosylbenzene PhI=O in methanol.

[Bis(acyloxy)iodo]arenes (Scheme 3, type **d**) are perhaps the most important and practically useful hypervalent organoiodine species. Of these, two are commercially available, namely (diacetoxyiodo)benzene (PIDA) and phenyliodinebis(trifuoroacetate), PIFA, and have enjoyed a widespread use as oxidizing reagents. The use of [bis(acyloxy)iodo]arenes as precursors to other iodine(III) compounds and as reagents

---

[13] (a) Tohma, H.; Takizawa, S.; Maegawa, T.; Kita, Y. *Angew. Chem. Int. Ed.* **2000**, *39*, 1306. (b) Miyamoto, K.; Hirobe, M.; Saito, M.; Shiro, M.; Ochiai, M. *Org. Lett.* **2007**, *9*, 1995. (c) Tohma, H.; Maegawa, T.; Takizawa, S.; Kita, Y. *Adv. Synth. Catal.* **2002**, *344*, 328. (d) Francisco, C. G.; Herrera, A. J.; Suarez, E. *J. Org. Chem.* **2002**, *67*, 7439. (e) Francisco, C. G.; Herrera, A. J.; Suarez, E. *J. Org. Chem.* **2003**, *68*, 1012. (f) Ueno, M.; Nabana, T.; Togo, H. *J. Org. Chem.* **2003**, *68*, 6424. (g) Lee, S.; MacMillan, D. W. C. *Tetrahedron* **2006**, *62*, 11413. (h) Fujita, M.; Lee, H. J.; Sugimura, T.; Okuyama, T. *Chem. Commun.* **2007**, 1139. (i) Miyamoto, K.; Tada, N.; Ochiai, M. *J. Am. Chem. Soc.* **2007**, *129*, 2772. (j) Ono, T.; Henderson, P. *Tetrahedron Lett.* **2002**, *43*, 7961. (k) Yusubov, M. S.; Gilmkhanova, M. P.; Zhdankin, V. V.; Kirschning, A. *Synlett* **2007**, 563.

for oxidation of alkenes, alkynes, alcohols, phosphorus, sulfur, etc., has been previously reviewed in detail by Zhdankin and Stang.[2d,2o]

Generally speaking, two ways are used for the preparation of [bis(acyloxy)iodo]arenes. One is the oxidation of iodoarenes in the presence of a corresponding carboxylic acid and appropriate oxidants, such as periodates, sodium percarbonate, *m*-CPBA, H_2O_2-urea or peroxodisulfate.[14] A convenient modification of this approach is the use of the arenes in the presence of molecular iodine and potassium peroxodisulfate in acetic acid, as shown in Scheme 8.[15] This approach offers the advantage of delivering a hypervalent iodine reagent without the need to prepare the intermediate iodoarene. However, the method's applicability is curtailed by the obvious limitation of being governed by the inherent chemoselectivity of the electrophilic aromatic iodination, with molecular iodine in this case (the intermediacy of the iodane $I(OAc)_3$ was discarded by the authors).

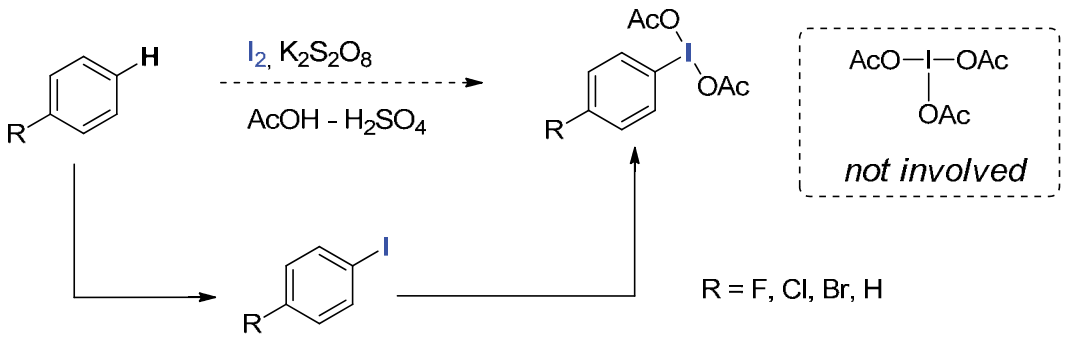

Scheme 8. Direct conversion of an arene into a [bis(acyloxy)iodo]arene.

The second common method is based on ligand exchange reaction of the readily available (diacetoxyiodo)arenes (*e.g.* PIDA) with an appropriate carboxylic acid, as illustrated in Scheme 9. In this example, PIDA is heated with carboxylic acid $R'CO_2H$ in a high boiling point solvent.[16]

---

[14] (a) Qian, W.; Jin, E.; Bao, W.; Zhang, Y. *Angew. Chem. Int. Ed.* **2005**, *44*, 952. (b) Handy, S. T.; Okello, M. *J. Org. Chem.* **2005**, *70*, 2874. (c) Chen, F.-E.; Xie, B.; Zhang, P.; Zhao, J.-F.; Wang, H.; Zhao, L. *Synlett* **2007**, 619. (d) Shang, Y.; But, T. Y. S.; Togo, H.; Toy, P. H. *Synlett* **2007**, 67. (e) Gallop, P. M.; Paz, M. A.; Fluckiger, R.; Stang, P. J.; Zhdankin, V. V.; Tykwinski, R. R. *J. Am. Chem. Soc.* **1993**, *115*, 11702. (f) Dohi, T.; Morimoto, K.; Takenaga, N.; Goto, A.; Maruyama, A.; Kiyono, Y.; Tohma, H.; Kita, Y. *J. Org. Chem.* **2007**, *72*, 109. (g) Moroda, A.; Togo, H. *Tetrahedron* **2006**, *62*, 12408. (h) Hossain, D.; Kitamura, T. *Synthesis* **2005**, 1932. (i) Page, T. K.; Wirth, T. *Synthesis* **2006**, 3153. (j) Lee, B. C.; Lee, K. C.; Lee, H.; Mach, R. H.; Katzenellenbogen, J. A. *Bioconjugate Chem.* **2007**, *18*, 514. (k) Ross, T. L.; Ermert, J.; Hocke, C.; Coenen, H. H. *J. Am. Chem. Soc.* **2007**, *129*, 8018. (l) Tohma, H.; Maruyama, A.; Maeda, A.; Maegawa, T.; Dohi, T.; Shiro, M.; Morita, T.; Kita, Y. *Angew. Chem. Int. Ed.* **2004**, *43*, 3595.

[15] Hossain, M. D.; Kitamura, T. *Tetrahedron Lett.* **2006**, *47*, 7889.

[16] (a) Das, J. P.; Roy, U. K.; Roy, S. *Organometallics* **2005**, *24*, 6136. (b) Koposov, A. Y.; Boyarskikh, V. V.; Zhdankin, V. V. *Org. Lett.* **2004**, *6*, 3613. (c) Stang, P. J.; Boehshar, M.; Wingert, H.; Kitamura, T. *J. Am.*

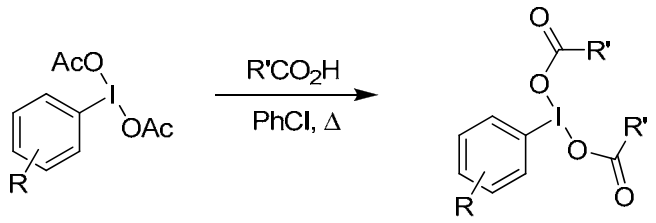

Scheme 9. Preparation of ArI(OCOR')$_2$ using ligand exchange.

Although aryliodine(III) compounds ArI(OX)$_2$ derived from strong inorganic acids HOX, such as H_2SO_4, HNO_3, $HClO_4$, CF_3SO_3H, $HSbF_6$ and HPF_6, have been found, they usually lack stability and can only be generated at low temperature under absolutely dry conditions.[2d, 2g] However, some aryliodine(III) compounds derived from organic sulfonic acids, *e. g.*, [hydroxy(organosulfonyloxy)iodo]arenes, ArI(OH)OSO$_2$R, (Scheme 3, type **e**), are relatively stable and they have been used in different organic transformations.

[Hydroxy(tosyloxy)iodo]arenes, as a special category of [hydroxy(organosulfonyloxy)iodo]arenes, are readily prepared by a ligand exchange reaction of (diacetoxyiodo)arenes with *p*-toluenesulfonic acid monohydrate in acetonitrile (Scheme 10, route **a**).[17] This method was later applied for the synthesis of [hydroxy(tosyloxy)iodo]heteroaromatic derivatives.[17a, 17d, 18] An other convenient procedure for the synthesis of various [hydroxy(sulfonyloxy)iodo]arenes consists of the one-pot reaction of iodoarenes and *m*-CPBA in the presence of sulfonic acids in a small amount of chloroform at room temperature, as exemplified in Scheme 10 (route **b**).[19] A similar modified method was developed to prepare organosulfonyloxy analogues using 4-nitrobenzenesulfonic acid, methanesulfonic acid or 10-camphorsulfonic acid.[20]

Chem. Soc. **1988**, *110*, 3272. (d) Sutherland, A.; Vederas, J. C. *Chem. Commun.* **2002**, 224. (e) Ray III, D. G.; Koser, G. F. *J. Org. Chem.* **1992**, *57*, 1607.

[17] (a) Koser, G. F.; Wettach, R. H. *J. Org. Chem.* **1977**, *42*, 1476. (b) Nabana, T.; Togo, H. *J. Org. Chem.* **2002**, *67*, 4362. (c) Dohi, T.; Maruyama, A.; Yoshimura, M.; Morimoto, K.; Tohma, H.; Shiro, M.; Kita, Y. *Chem. Commun.* **2005**, 2205. (d) Yusubov, M. S.; Funk, T. V.; Chi, K.-W.; Cha, E.-H.; Kim, G. H.; Kirschning, A.; Zhdankin, V. V. *J. Org. Chem.* **2008**, *73*, 295. (e) Hirt, U. H.; Schuster, M. F. H.; French, A. N.; Wiest, O. G.; Wirth, T. *Eur. J. Org. Chem.* **2001**, 1569.

[18] Lee, B. C.; Lee, K. C.; Lee, H.; Mach, R. H.; Katzenellenbogen, J. A. *Bioconjugate Chem.* **2007**, *18*, 514.

[19] Yamamoto, Y.; Togo, H. *Synlett* **2005**, 2486.

[20] (a) Koser, G. F.; Wettach, R. H. *J. Org. Chem.* **1977**, *42*, 1476. (b) Hatzigrigoriou, E.; Varvoglis, A.; Bakola-Christianopoulou, M. *J. Org. Chem.* **1990**, *55*, 315.

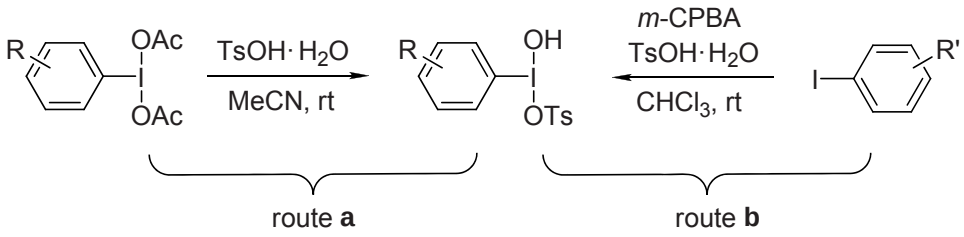

Scheme 10. Two routes for the preparation of [hydroxy(tosyloxy)iodo]arenes.

It is worth mentioning that, Koser and colleagues[21] in 1982, reported the use of stoichiometric PhI(OH)(OTs) (abbreviated as HTIB and also referred to as "Koser reagent"), as an especially effective oxidative reagent for introducing the -OTs group at the α position of ketones. Later on, the reaction scope was expanded to other [hydroxy(organosulfonyloxy)iodo]arenes (Scheme 11).[22]

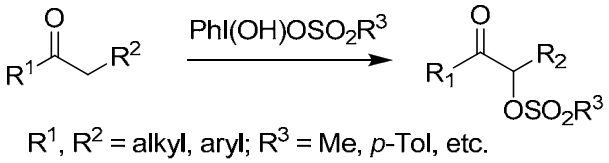

Scheme 11. α-Functionalization of carbonyl compounds by [hydroxy(organosulfonyloxy)iodo]arenes.

HTIB was found a great deal of applications in various oxidative rearrangements and fragmentations. Justik and Koser[23] found that the treatment of styrene derivatives with HTIB in methanol can achieve an oxidative rearrangement (Scheme 12a). A related oxidative rearrangement promoted by HTIB was recently utilized in the regioselective synthesis of Wighteone and in a diastereoselective total synthesis of (±)-Indatraline.[24] In particular, the key step in the synthesis of (±)-indatraline involved the HTIB-promoted diastereoselective ring contraction of a 1,2-dihydronaphthalene to construct the indane ring system (Scheme 12b).[24b]

The HTIB can also effectively achieve the oxidative rearrangement of alkenes.[25] Thus, Justik and Koser investigated the oxidative ring expansions of

---

[21] Koser, G. F.; Relenyi, A. G.; Kalos, A. N.; Rebrovic, L.; Wettach, R. H. *J. Org. Chem.* **1982**, *47*, 2487.

[22] Koser, G. F. *Aldrichim. Acta* **2001**, *34*, 89.

[23] Justik, M. W.; Koser, G. F. *Tetrahedron Lett.* **2004**, *45*, 6159.

[24] (a) Hossain, M. M.; Tokuoka, T.; Yamashita, K.; Kawamura, Y.; Tsukayama, M. *Synth. Commun.* **2006**, *36*, 1201. (b) Silva, L. F., Jr.; Siqueira, F. A.; Pedrozo, E. C.; Vieira, F. Y. M.; Doriguetto, A. C. *Org. Lett.* **2007**, *9*, 1433.

[25] (a) Justik, M. W.; Koser, G. F. *Molecules* **2005**, *10*, 217. (b) Silva, L. F., Jr.; Vasconcelos, R. S.; Nogueira, M. A. *Org. Lett.* **2008**, *10*, 1017.

alkylidenebenzocycloalkenes with the help of HTIB (Scheme 12c).[25a] A similar ring expansion of 1-vinylcycloalkanol derivatives to seven-membered rings using HTIB were also reported by other groups (Scheme 12d).[25b] HTIB is frequently used for the oxidative functionalization of arenes, alkenes and alkynes. For instance, the reaction of polycylic aromatic hydrocarbons (PAH) with HTIB in the presence of trimethylsilyl isothiocyanate results in the regioselective thiocyanation of the PAH, as exemplified by the reaction of anthracene shown in Scheme 12e.[26] Dihydropyridone derivatives can be iodinated by the treatment with *N*-iodosuccinimide (NIS) with the help of HTIB (Scheme 12f).[27]

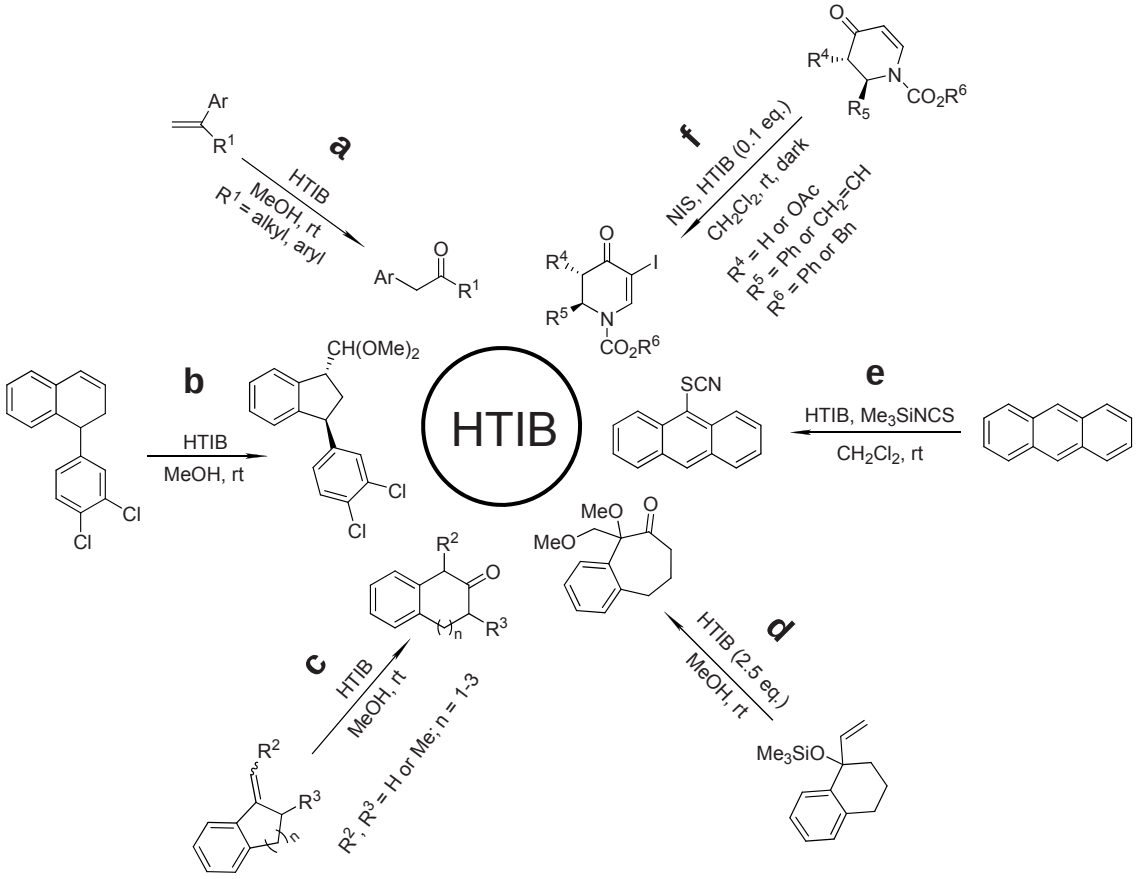

Scheme 12. Various oxidative rearrangements and fragmentations with HTIB.

In contrast, the iodine(III) heterocycles, corresponding to structure types f-g (Scheme 3), gained much less attention. Recent reports, however, demonstrate their applications as reagents in organic synthesis.[28] As an interesting example, Togni and

---

[26] Koser, G. F.; Telu, S.; Laali, K. K. *Tetrahedron Lett.* **2006**, *47*, 7011.

[27] Comins, D. L.; Kuethe, J. T.; Miller, T. M.; Fevrier, F. C.; Brooks, C. A. *J. Org. Chem.* **2005**, *70*, 5221.

[28] (a) Morales-Rojas, H.; Moss, R. A. *Chem. Rev.* **2002**, *102*, 2497. (b) Zhdankin, V. V. *Curr. Org. Synth.* **2005**, *2*, 121.

co-workers recently reported the use of a 1-trifuoromethylbenziodoxole derivative as a useful reagent for electrophilic trifluoromethylation of nucleophilic substrates. As shown in Scheme 13, this reagent reacts with β-ketoesters in the presence of potassium carbonate to afford an α-trifluoromethylated product.[29] The reagent has also been used to transfer a CF_3 group to other C-centered nucleophiles.[30]

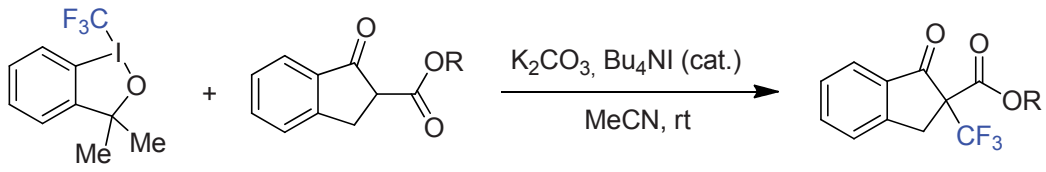

Scheme 13. Reaction of 1-trifuoromethylbenziodoxole derivative with β-ketoesters giving α-trifluoromethylated product.

Alkyl-substituted hypervalent iodine(III) reagents are unstable, in general, and can only exist as short-lived reactive intermediates in the oxidation of alkyliodides. The stability of the corresponding derivatives can be increased by steric or electronic modification of the alkyl moiety, preventing the decomposition of the molecule by either elimination or nucleophilic substitution pathways. It was found that the introduction of electron-withdrawing substituents in the alkyl chain, such as fluorine atoms or a sulfonyl group, is an effective method to achieve the stabilization of this type of λ^3-iodanes (Scheme 3, type **h**).[31] As a special case, the [bis(trifuoroacetoxy)iodo]-perfluoroalkanes, $C_nF_{2n+1}I(OCOCF_3)_2$, can serve as electrophilic perfluoroalkylating agents,[32] as precursors[32] for other (perfluoroalkyl)aryliodonium salts and they are applicable as effective and easily recyclable oxidative reagents.[21c-d]

Iodonium salts, $R_2I^+X^-$ (Scheme 3, type **i**), are defined as positively charged 8-I-2 species with two carbon ligands and a negatively charged counterion. Generally speaking, these salts do not show any significant oxidizing properties, but $Ar_2I^+X^-$ often react as aryl transfer agents, in part as a consequence of the excellent leaving group ability of the [ArI] fragment.[33] Stable iodonium salts have found numerous applications

---

[29] (a) Eisenberger, P.; Gischig, S.; Togni, A. *Chem. Eur. J.* **2006**, *12*, 2579. (b) Kieltsch, I.; Eisenberger, P.; Togni, A. *Angew. Chem., Int. Ed.* **2007**, *46*, 754.

[30] Eisenberger, P.; Kieltsch, I.; Armanino, N.; Togni, A. *Chem. Commun.* **2008**, 1575.

[31] (a) Umemoto, T.; Kuriu, Y.; Shuyama, H.; Miyano, O.; Nakayama, S. *J. Fluorine Chem.* **1986**, *31*, 37. (b) Umemoto, T.; Kuriu, Y.; Shuyama, H.; Miyano, O.; Nakayama, S. *J. Fluorine Chem.* **1982**, *20*, 695. (c) Tesevic, V.; Gladysz, J. A. *Green Chem.* **2005**, *7*, 833. (d) Tesevic, V.; Gladysz, J. A. *J. Org. Chem.* **2006**, *71*, 7433. (e) Yagupolskii, L. M.; Maletina, I. I.; Kondratenko, N. V.; Orda, V. V. *Synthesis* **1978**, 835.

[32] Umemoto, T. *Chem. Rev.* **1996**, *96*, 1757.

[33] Okuyama, T.; Takino, T.; Sueda, T.; Ochiai, M. *J. Am. Chem. Soc.* **1995**, *117*, 3360.

as cationic photoinitiators[34] and synthetic reagents.[35] Finally, iodonium ylides (Scheme 3, type **j**) usually serve as carbene precursors.[36]

1.2.2 λ^5-Iodanes

In general, the chemistry of organic λ^5-iodanes has been less developed, when compared with that of λ^3-iodanes. As summarized in Scheme 14a-f, the iodine(V) species of noncyclic iodylarenes (Scheme 14, type **a**), pseudocyclic iodylarenes (Scheme 14, types **b-e**) and Dess-Martin periodinane (Scheme 14, type **f**) have been developed in synthetic applications.

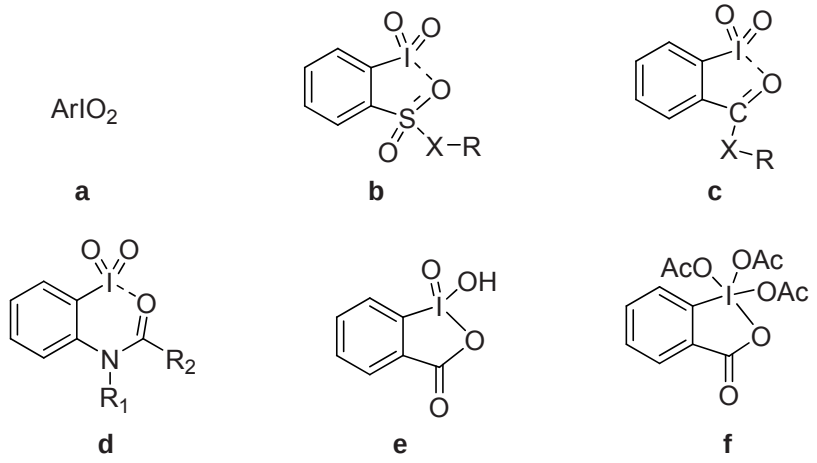

Scheme 14. Representatives of λ^5-iodanes used in synthetic applications.

Iodylarenes, $ArIO_2$, are commonly prepared by direct oxidation of iodoarenes with strong oxidants or by disproportionation of iodosylarenes.[37] The most common oxidants used for the preparation of iodylarenes include sodium hypochlorite, sodium

---

[34] (a) Shirai, A.; Kubo, H.; Takahashi, E. *J. Photopolym. Sci. Technol.* **2002**, *15*, 29. (b) VanderHart, D. L.; Prabhu, V. M.; Lin, E. K. *Chem. Mater.* **2004**, *16*, 3074. (c) Slegt, M.; Minne, F.; Zuilhof, H.; Overkleeft, H. S.; Lodder, G. *Eur. J. Org. Chem.* **2007**, 5353. (d) Tasdelen, M. A.; Kumbaraci, V.; Jockusch, S.; Turro, N. J.; Talinli, N.; Yagci, Y. *Macromolecules* **2008**, *41*, 295.

[35] (a) Chen, D.-W.; Ochiai, M. *J. Org. Chem.* **1999**, *64*, 6804. (b) Kalyani, D.; Deprez, N. R.; Desai, L. V.; Sanford, M. S. *J. Am. Chem. Soc.* **2005**, *127*, 7330. (c) Ochiai, M.; Ito, T.; Takaoka, Y.; Masaki, Y. *J. Am. Chem. Soc.* **1991**, *113*, 1319. (d) Carroll, M. A.; Wood, R. A. *Tetrahedron* **2007**, *63*, 11349. (e) Yan, J.; Hu, W.; Rao, G. *Synthesis* **2006**, 943. (f) Ozanne-Beaudenon, A.; Quideau, S. *Angew. Chem. Int. Ed.* **2005**, *44*, 7065. (g) Xue, Z.; Yang, D.; Wang, C. *J. Organomet. Chem.* **2006**, *691*, 247. (h) Fujita, M.; Mishima, E.; Okuyama, T. *J. Phys. Org. Chem.* **2007**, *20*, 241. (i) Oh, C. H.; Kim, J. S.; Jung, H. H. *J. Org. Chem.* **1999**, *64*, 1338. (j) Ochiai, M.; Kitagawa, Y.; Takayama, N.; Takaoka, Y.; Shiro, M. *J. Am. Chem. Soc.* **1999**, *121*, 9233.

[36] (a) Kirmse, W. *Eur. J. Org. Chem.* **2005**, 237. (b) Muller, P.; Allenbach, Y. F.; Chappellet, S.; Ghanem, A. *Synthesis* **2006**, 1689. (c) Muller, P. *Acc. Chem. Res.* **2004**, *37*, 243.

[37] (a) Kraszkiewicz, L.; Skulski, L. *ARKIVOC* **2003**, *6*, 120. (b) Kazmierczak, P.; Skulski, L.; Kraszkiewicz, L. *Molecules* **2001**, *6*, 881. (c) Meprathu, B. V.; Justik, M. W.; Protasiewicz, J. D. *Tetrahedron Lett.* **2005**, *46*, 5187.

periodate, dimethyloxirane and Oxone.[2o] Interestingly, a facile method has been developed by Zhdankin and coworkers (Scheme 15) using peracetic acid as an oxidant in the presence of the ruthenium trichloride catalyst.[38] With this methodology, several previously unknown iodylarenes bearing electron-withdrawing CF_3 group on the aromatic ring were successfully prepared. The Ru species in this process was shown to act as a highly efficient catalyst for the disproportionation of the initially formed iodine(III) species to iodoarene and the target $ArIO_2$, presumably through the intermediacy of the Ru=O unit.

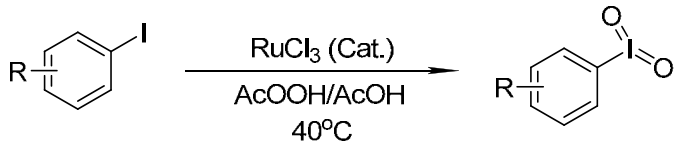

R = H, *p*-Me, *o*-Me, *o*-Cl, *m*-Cl, *p*-Br, *p*-F, *p*-CF_3, *p*-Cl, etc.

Scheme 15. Preparation of $ArIO_2$ under catalysis by $RuCl_3$.

Several aryliodyl derivatives (Scheme 14, types **b-d**) have been recognized in which a substituent appears *ortho to the* iodine.[39] These kinds of compounds are characterized by the presence of a pseudocyclic structure due to a strong intramolecular secondary bonding between the hypervalent iodine center and the oxygen atom of the *ortho*-substituents. Some practical applications of these reagents have been reported.[40]

2-Iodoxybenzoic acid (Scheme 14, type **e**) is the most important representative of pentavalent iodine heterocycles. A convenient procedure to prepare this reagent involves the oxidation of 2-iodobenzoic acid with Oxone (Scheme 16).[41] This reagent, often referred to as IBX, has attracted significant interest as a mild and selective oxidant in numerous total syntheses.[42]

---

[38] (a) Yusubov, M. S.; Chi, K.-W.; Park, J. Y.; Karimov, R.; Zhdankin, V. V. *Tetrahedron Lett.* **2006**, *47*, 6305. (b) Koposov, A. Y.; Karimov, R. R.; Pronin, A. A.; Skrupskaya, T.; Yusubov, M. S.; Zhdankin, V. V. *J. Org. Chem.* **2006**, *71*, 9912.

[39] (a) Zhdankin, V. V.; Koposov, A. Y.; Netzel, B. C.; Yashin, N. V.; Rempel, B. P.; Ferguson, M. J.; Tykwinski, R. R. *Angew. Chem. Int. Ed.* **2003**, *42*, 2194. (b) Zhdankin, V. V.; Litvinov, D. N.; Koposov, A. Y.; Luu, T.; Ferguson, M. J.; McDonald, R.; Tykwinski, R. R. *Chem. Commun.* **2004**, 106. (c) Zhdankin, V. V.; Koposov, A. Y.; Litvinov, D. N.; Ferguson, M. J.; McDonald, R.; Luu, T.; Tykwinski, R. R. *J. Org. Chem.* **2005**, *70*, 6484.

[40] (a) Karimov, R. R.; Kazhkenov, Z.-G. M.; Modjewski, M. J.; Peterson, E. M.; Zhdankin, V. V. *J. Org. Chem.* **2007**, *72*, 8149. (b) Koposov, A. Y.; Karimov, R. R.; Geraskin, I. M.; Nemykin, V. N.; Zhdankin, V. V. *J. Org. Chem.* **2006**, *71*, 8452.

[41] Frigerio, M.; Santagostino, M.; Sputore, S. *J. Org. Chem.* **1999**, *64*, 4537.

[42] (a) Frigerio, M.; Santagostino, M. *Tetrahedron Lett.* **1994**, *35*, 8019. (b) Paintner, F. F.; Allmendinger, L.; Bauschke, G. *Synthesis* **2001**, 2113. (c) Martin, C.; Macintosh, N.; Lamb, N.; Fallis, A. G. *Org. Lett.* **2001**, *3*,

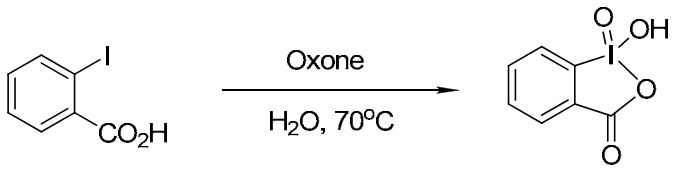

Scheme 16. Preparation of 2-iodoxybenzoic acid (IBX).

Closely related to IBX, the so-called Dess-Martin periodinane (Scheme 14, type **f**) was first introduced, as the reagent name implies, by Dess and Martin in 1984[43] and it is best prepared by the reaction of 2-iodoxybenzoic acid, IBX, with acetic anhydride in the presence of TsOH, as shown in Scheme 17.[44] This λ^5-iodane is especially useful for the oxidation of alcohols containing sensitive functional groups, such as amino groups, unsaturated moieties, silyl ethers, phosphine oxides, sulfides, selenides, etc., due to the high chemoselectivity and mild reaction conditions (room temperature, absence of acidic or basic additives). Moreover, this unique oxidizing property and convenience of use make it widely applicable in the synthesis of a great deal of biologically important natural products.[45]

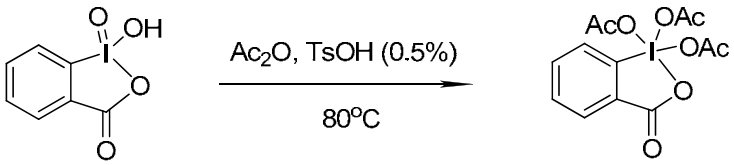

Scheme 17. Preparation of Dess - Martin periodinane.

1.2.3 Inorganic iodine reagents and their reactivity

It is well known that iodine can exist in the oxidation state of +1, +3, +5 or +7, although the most stable oxidation state in organic compounds is -1. In addition to the

---

1021. (d) Zhang, J.; Wang, X.; Wang, W.; Quan, W.; She, X.; Pan, X. *Tetrahedron* **2007**, *63*, 6990. (e) Vincent, A.; Prunet, J. *Synlett* **2006**, 2269. (f) Suzuki, K.; Takayama, H. *Org. Lett.* **2006**, *8*, 4605. (g) Kirkham, J. E. D.; Lee, V.; Baldwin, J. E. *Chem. Commun.* **2006**, 2863. (h) Kirsch, S.; Bach, T. *Angew. Chem. Int. Ed.* **2003**, *42*, 4685. (i) Iwamoto, O.; Koshino, H.; Hashizume, D.; Nagasawa, K. *Angew. Chem. Int. Ed.* **2007**, *46*, 8625. (j) Nicolaou, K. C.; Harrison, S. T. *Angew. Chem. Int. Ed.* **2006**, *45*, 3256. (k) Skouta, R.; Li, C.-J. *Tetrahedron Lett.* **2007**, *48*, 8343. (l) Kuboki, A.; Yamamoto, T.; Taira, M.; Arishige, T.; Ohira, S. *Tetrahedron Lett.* **2007**, *48*, 771. (m) Hosokawa, S.; Kuroda, S.; Imamura, K.; Tatsuta, K. *Tetrahedron Lett.* **2006**, *47*, 6183. (n) Ichikawa, Y.; Yamaoka, T.; Nakano, K.; Kotsuki, H. *Org. Lett.* **2007**, *9*, 2989. (o) Molander, G. A.; Petrillo, D. E. *J. Am. Chem. Soc.* **2006**, *128*, 9634.

[43] Dess, D. B.; Martin, J. C. *J. Org. Chem.* **1983**, *48*, 4155.

[44] Ireland, R. E.; Liu, L. *J. Org. Chem.* **1993**, *58*, 2899.

[45] (a) Nourry, A.; Legoupy, S.; Huet, F. *Tetrahedron* **2008**, *64*, 2241. (b) Li, P.; Majireck, M. M.; Korboukh, I.; Weinreb, S. M. *Tetrahedron Lett.* **2008**, *49*, 3162. (c) Trost, B. M.; O'Boyle, B. M. *Org. Lett.* **2008**, *10*, 1369. (d) Nicolaou, K. C.; Tang, Y.; Wang, J. *Chem. Commun.* **2007**, 1922. (e) Rein, C.; Demel, P.; Outten, R. A.; Netscher, T.; Breit, B. *Angew. Chem. Int. Ed.* **2007**, *46*, 8670. (f) Kozaka, T.; Miyakoshi, N.; Mukai, C. *J. Org. Chem.* **2007**, *72*, 10147. (g) Pouplin, T.; Tolon, B.; Nuhant, P.; Delpech, B.; Marazano, C. *Eur. J. Org. Chem.* **2007**, 5117. (h) England, D. B.; Padwa, A. *J. Org. Chem.* **2008**, *73*, 2792. (i) Zhang, W.; Wicks, M. N.; Burn, P. L. *Org. Biomol. Chem.* **2008**, *6*, 879. (j) Thongsornkleeb, C.; Danheiser, R. L. *J. Org. Chem.* **2005**, *70*, 2364. (k) Struble, J. R.; Kaeobamrung, J.; Bode, J. W. *Org. Lett.* **2008**, *10*, 957.

practical use of hypervalent organoiodine(III) and (V) reagents, as a separate but related research area, the inorganic iodine reagents, especially iodates (oxidation state +5) and periodates (oxidation state +7) have also been applied as powerful oxidants in a variety of processes.[46]

In contrast, the application of inorganic iodine compounds (I or III) in synthetic organic chemistry is less developed. Hypoiodite reagents, indeed, have been used for iodo-functionalization in organic transformations, such as iodoacetoxylation, azidoiodination, iodination of alkenes or arenes, etc..[47] However, the use of iodite reagents for synthetic purposes in organic chemistry is almost unknown due to their instability.

1.2.4 Iodine reagents or intermediates in catalysis

Interestingly, several recent publications describe that catalytic quantities of a common iodoarene, *e. g.*, PhI, can catalyze a great deal of reactions in the presence of a cheaper terminal oxidant via the *in situ* regeneration of organoiodine(III) species.[48] Thus, as pioneering works, Ochiai's group[49] and Kita's group[50] independently reported iodoarene as a catalyst in coupling reactions in the presence of a terminal oxidant, whereby the [bis(acyloxy)iodo]arene is regenerated *in situ*. For instance, Ochiai's group reported the α-acetoxylation of ketones with iodobenzene as a catalyst in the presence of *m*-CPBA as terminal oxidant, in which the hypervalent species (diacyloxyiodo)benzene was generated *in situ* (Scheme 18). Ligand exchange of a (diacyloxyiodo)benzene with an enol derived from the ketone produces an α-λ^3-iodanylketone, which undergoes a S_N2 displacement by acetic acid affording an α-acetoxy ketone with the regeneration of iodobenzene.

Since then, a rapid progress has been made in the development of iodoarenes as catalysts in various reactions with a cheap co-oxidant, such as *m*-CPBA, Oxone, H_2O_2,

---

[46] (a) Lang, J.-P. in Encyclopedia of Inorganic Chemistry, 2nd ed., Vol. II (Ed: King, R. B.), Wiley, New York, 2005, pp. 866-887. (b) Wee, A. G.; Slobodian, J.; Fernandez-Rodriguez, N. A.; Aguilar, E. in Encyclopedia of Reagents for Organic Synthesis, 2nd ed., Vol. 11 (Eds: L. A. Paquette, Crich, D.; Fuchs, P. L.; Molander, G. A.), Wiley, Chichester, 2009, pp. 8921-8930.

[47] (a) Kirschning, A.; Monenschein, H.; Wittenberg, W. *Angew. Chem. Int. Ed.* **2001**, *40*, 650. (b) French, A. N.; Bissmire, S.; Wirth, T. *Chem. Soc. Rev.* **2004**, *33*, 354. (c) Minakata, S. *Acc. Chem. Res.* **2009**, *42*, 1172.

[48] (a) Dohi, T.; Maruyama, A.; Yoshimura, M.; Morimoto, K.; Tohma, H.; Kita, Y. *Angew. Chem. Int. Ed.* **2005**, *44*, 6193. Two minireviews: (b) Richardson, R. D.; Wirth, T. *Angew. Chem. Int. Ed.* **2006**, *45*, 4402. (c) Dohi, T.; Kita, Y. *Chem. Commun.* **2009**, 2073.

[49] Ochiai, M.; Takeuchi, Y.; Katayama, T.; Sueda, T.; Miyamoto, K. *J. Am. Chem. Soc.* **2005**, *127*, 12244.

[50] Dohi, T.; Maruyama, A.; Yoshimura, M.; Morimoto, K.; Tohma, H.; Kita, Y. *Angew. Chem. Int. Ed.* **2005**, *44*, 6193.

TBHP, etc..[2s-v] A detailed discussion about this topic will be further introduced in Chapter 3 of Part I of this thesis.

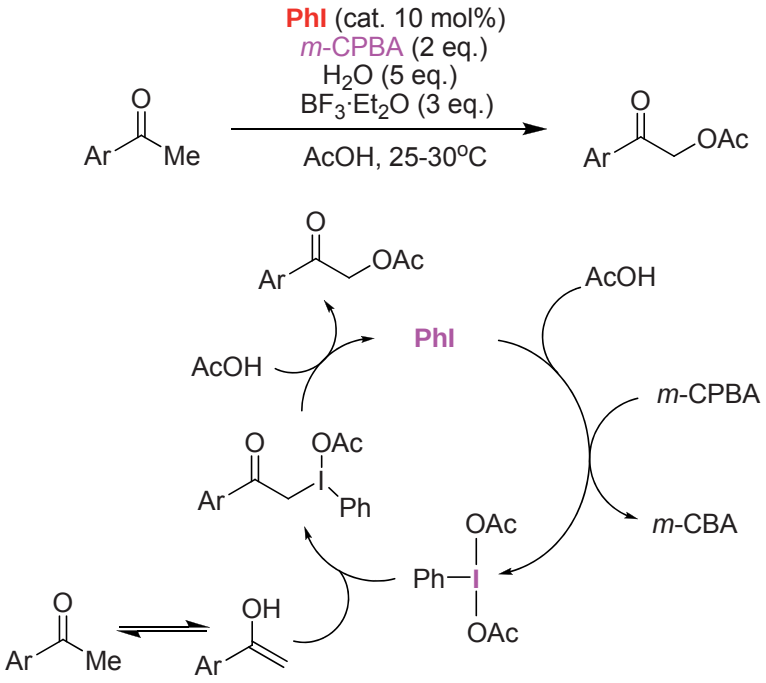

Scheme 18. Catalytic cycle for the α-acetoxylation of ketones with iodobenzene as a catalyst in the presence of *m*-CPBA as terminal oxidant.

What's more, some recent reports suggest that the hypoiodite or iodite species may arise as intermediates in processes catalyzed by inorganic iodine compounds (including molecular iodine), particularly in oxidative S-S,[51] C-O,[52] C-N[53] and C-C[54] coupling reactions, as exemplified in Scheme 19.[51]

[51] Kirihara, M.; Asai, Y.; Ogawa, S.; Noguchi, T.; Hatano, A.; Hirai, Y. *Synthesis* **2007**, 3286.

[52] (a) Chen, L.; Shi, E.; Liu, Z.; Chen, S.; Wei, W.; Li, H.; Xu, K.; Wan, X. *Chem. Eur. J.* **2011**, *17*, 4085. (b) Wei, W.; Zhang, C.; Xu, Y.; Wan, X. *Chem. Commun.* **2011**, *47*, 10827.

[53] (a) Froehr, T. C.; Sindlinger, P.; Kloeckner, U.; Finkbeiner, P. B.; Nachtsheim, J. *Org. Lett.* **2011**, *13*, 3754. (b) Ma, L.; Wang, X.; Yu, W.; Han, B. *Chem. Commun.* **2011**, *47*, 11333.

[54] Rodriguez, A.; Moran, W. J. *Org. Lett.* **2011**, *13*, 2220.

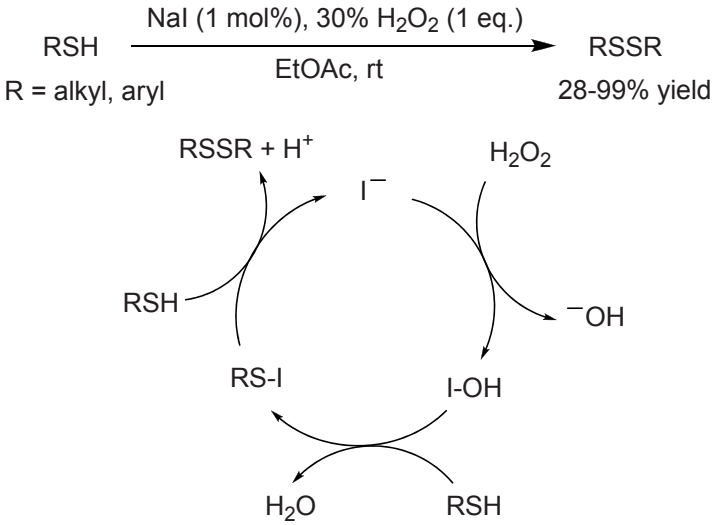

Scheme 19. *In situ*-generated hypoiodite-catalyzed oxidative homocouplings of thiols to disulfides.

Part I. Hypervalent iodine species: reagents and intermediates in oxidative processes

CHAPTER 2

Direct arylation of oligonaphthalenes using PIFA/BF_3·Et_2O: from double arylation to larger oligoarene products

Chapter 2. Direct arylation of oligonaphthalenes using PIFA/BF_3·Et_2O: from double arylation to larger oligoarene products

2.1 Introduction

The carbon-carbon (C-C) coupling between arenes is relevant to fields ranging from medicinal chemistry to materials science. In a canonical metal-catalyzed cross-coupling (Suzuki, Negishi, Stille, Hiyama, Kumada) the new C-C bond is formed by combining an aryl halide (or pseudohalide) with an appropriate organometallic reagent. Following the nomenclature adopted from aromatic nucleophilic substitution processes, the aryl halide component is considered an *electrophile*, and the organometallic component, a *nucleophile*. Although broadly applicable, these methods require independent synthesis and isolation of the two coupling partners. Moreover, these reactions generate stoichiometric inorganic salts as byproducts. In contrast, the C-C coupling between arenes *via* the transformation of the CH groups needs fewer steps and is more efficient, and therefore, is a particularly promising goal. In this field, the earlier stoichiometric methods, many in the form of the Scholl reaction,[55] have recently been complemented by the development of the metal-assisted catalytic dehydrogenative cross-coupling processes.[56] More recently, Kita and co-workers have developed a combination of BF_3·Et_2O with hypervalent iodine species (PIFA) that is highly effective and environmentally benign in promoting direct C-C coupling.[57]

2.1.1 Overview of C-C couplings from the reaction of aryl halides with organometallic reagents

The development of metal-catalyzed cross-coupling reactions began with some stoichiometric metal-promoted homocoupling processes,[58] as exemplified in Scheme 20a with the Ullmann reaction.[59] Advances of using organoalkali-metal reagents in C-C coupling reactions were made alongside the fledging progress in the metal-mediated

---

[55] (a) Scholl, R.; Seer, C. *Liebigs Ann. Chem.* **1912**, *394*, 111. (b) Kovacic, P.; Jones, M. B. *Chem. Rev.* **1987**, *87*, 357.

[56] (a) McGlacken, G. P.; Bateman, L. M. *Chem. Soc. Rev.* **2009**, *38*, 2447. (b) Yeung, C. S.; Dong, V. M. *Chem. Rev.* **2011**, *111*, 1215.

[57] Dohi, T.; Ito, M.; Morimoto, K.; Iwata, M.; Kita, Y. *Angew. Chem. Int. Ed.* **2008**, *47*, 1301.

[58] Please see the review and references therein: Johansson Seechurn, C. C. C.; Kitching, M. O.; Colacot, T. J.; Snieckus, V. *Angew. Chem. Int. Ed.* **2012**, *51*, 5062.

[59] Ullmann, F.; Bielecki, J. *Ber. Dtsch. Chem. Ges.* **1901**, *34*, 2174.

C-C homocoupling reactions at the beginning of 20th century.[58] For instance, in 1914, Bennett and Turner reported[60] the homodimerization of phenylmagnesium bromide through the use of stoichiometric quantities of chromium(III) chloride (Scheme 20b). Despite the remarkable achievements, the early metal-promoted reactions were limited in two key ways: 1) the application of poorly soluble, stoichiometric or superstoichiometric metal reagents and 2) issues of regioselectivities for the coupling processes. With time, catalytic amounts of metals had been shown to promote some C-C cross-coupling reactions (Scheme 20c).[61]

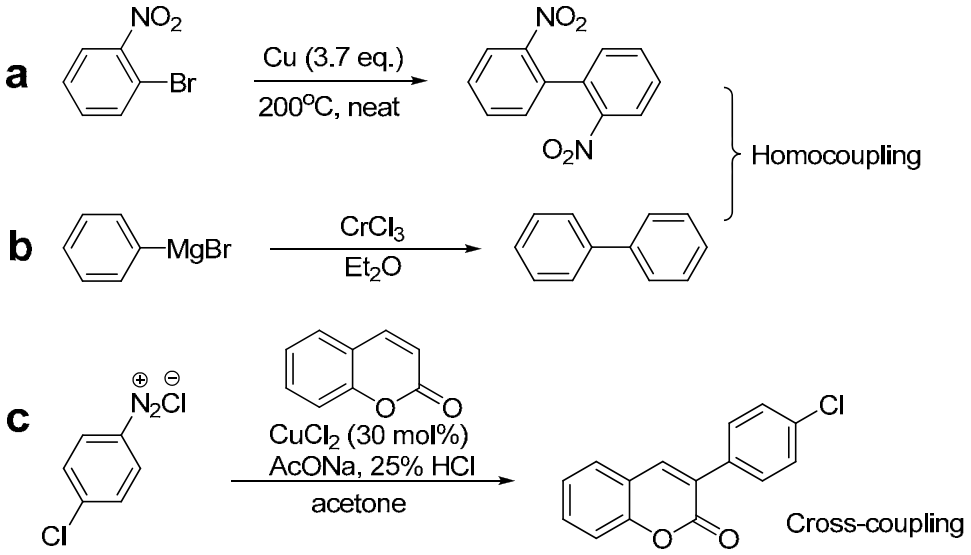

Scheme 20. Examples of homocoupling (a, b) and cross-coupling with metals (c).

On the basis of the achievements noted above, significant progress has been made in the last 40 years in the field of the transition metal-catalyzed cross-coupling, most famously the palladium-catalyzed processes using an arene substrate functionalized with a leaving group (*e. g.*, halogen, OTf) and an appropriate organometallic reagent as a partner.[62] In general, these methods require independent preparation of the two coupling partners before implementation of the cross-coupling. The main well-developed protocols of cross-coupling of two aryl moieties in recent years include those of the Kumada, Negishi, Stille, Suzuki and Hiyama coupling reactions (Scheme 21).

---

[60] Bennett, G. M.; Turner, E. E. *J. Chem. Soc. Trans.* **1914**, *105*, 1057.

[61] (a) Ullmann, F.; Sponagel, P. *Ber. Dtsch. Chem. Ges.* **1905**, *38*, 2211. (b) Corriu, R. J. P. *J. Organomet. Chem.* **2002**, *653*, 20. (c) Job, A.; Reich, R. *C. R. Hebd. Seances Acad. Sci.* **1923**, *177*, 1439.

[62] (a) JohanssonSeechurn, C. C. C.; Kitching, M. O.; Colacot, T. J.; Snieckus, V. *Angew. Chem. Int. Ed.* **2012**. *51*. 5062. (b) Molnar, A. *Chem. Rev.* **2011**, *111*, 2251. (c) Beletskaya, I. P.; Cheprakov, A. V. *Chem. Rev.* **2000**, *100*, 3009. (d) Yin, L.; Liebscher, J. *Chem. Rev.* **2007**, *107*, 133. (d) Li, H.; Johansson Seechurn, C. C. C.; Colacot, T. J. *ACS Catal*. **2012**, *2*, 1147.

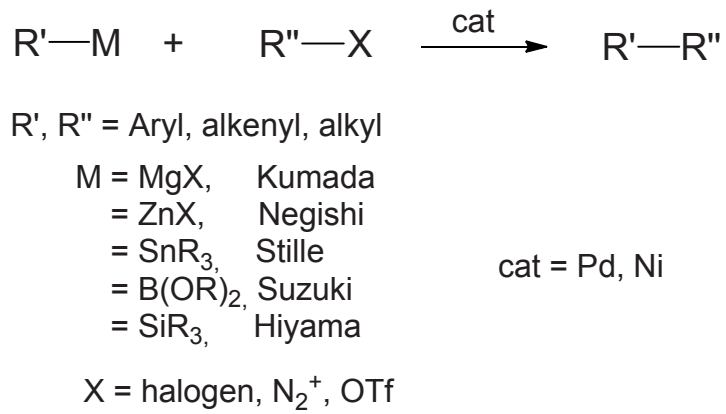

Scheme 21. Overview of cross-couplings by combining an aryl or alkenyl halide (or pseudohalide) with an appropriate organometallic reagent.

Corriu and Kumada in 1972 independently reported the nickel-catalyzed cross-coupling reaction of alkenyl halides with Grignard reagents,[63] and the reaction scope was later extended to achieve the coupling between arene derivatives,[64] as exemplified in Scheme 22.[64b] This reaction was recognized as a breakthrough, as it offered a solution to selectively achieve C-C cross-couplings with only traces (or none) of the homodimerization byproducts.

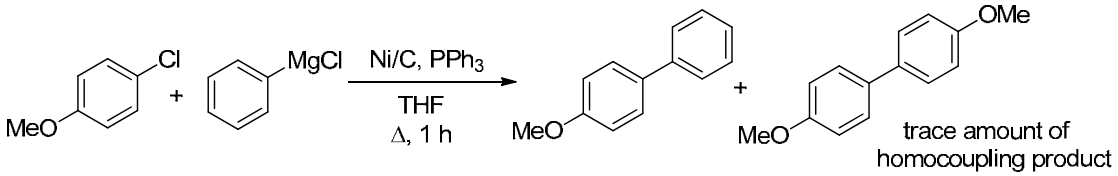

Scheme 22. The Kumada cross-coupling reaction between arene derivatives.

On the heels of the Kumada reaction, Negishi, in 1976, reported on the cross-coupling of organoaluminum reagents with nickel and palladium as catalysts (Scheme 23a).[65] Subsequently, the same group and others[66,67] disclosed the use of organozinc reagents as coupling partners (Scheme 23b). All of these findings indicated the organomagnesium coupling partner used in the Corriu-Kumada protocol could be

---

[63] (a) Corriu, R. J. P.; Masse, J. P. *J. Chem. Soc. Chem. Commun.* **1972**, 144. (b) Tamao, K.; Sumitani, K.; Kiso, Y.; Zembayashi, M.; Fujioka, A.; Kodama, S.; Nakajima, I.; Minato, A.; Kumada, M. *Bull. Chem. Soc. Jpn.* **1976**, 49, 1958; (c) Tamao, K.; Kiso, Y.; Sumitani, K.; Kumada, M. *J. Am. Chem. Soc.* **1972**, *94*, 9268; (d) K. Tamao, K. Sumitani,M. Kumada, *J. Am. Chem. Soc.* **1972**, *94*, 4374.

[64] (a) Ikoma, Y.; Ando, K.; Naoi, Y.; Akiyama, T.; Sugimori, A. *Synth. Commun.* **1991**, *21*, 481. (b) Tasler, S.; Lipshutz, B. H. *J. Org. Chem.* **2003**, *68*, 1190.

[65] Negishi, E.; Baba, S.; *J. Chem. Soc., Chem. Commun.* **1976**, 596.

[66] (a) Negishi, E.; King, A. O.; Okukado, N. *J. Org. Chem.* **1977**, *42*, 1821. (b) King, A.; Okukado, O. N.; Negishi, E. *J. Chem. Soc., Chem. Commun.* **1977**, 683.

[67] Fauvarque, J. F.; Jutand, A. *J. Organomet. Chem.* **1977**, *132*, C17.

extended to other organometallic species. Indeed, various organometallic derivatives such as aluminium, tin-based acetylenes, magnesium and zirconium involving C-C coupling reactions were subsequently studied in the same group.[68] Nevertheless, the term *Negishi cross-coupling* is taken today to denote the palladium or nickel catalyzed cross-couplings between organozinc compounds and organohalides. In general, the Negishi protocol offers advantages when compared with the Kumada coupling, due to the higher stability of the organozinc reagents, milder conditions and tolerance of the potentially electrophilic functional groups. Therefore, this reaction is widely used throughout the industrial, medical and academic research areas.[69] It should be noted, however, hat recently some very efficient Kumada reactions tolerating a wide range of functional groups have been published by Knochel as well as by other groups.[70]

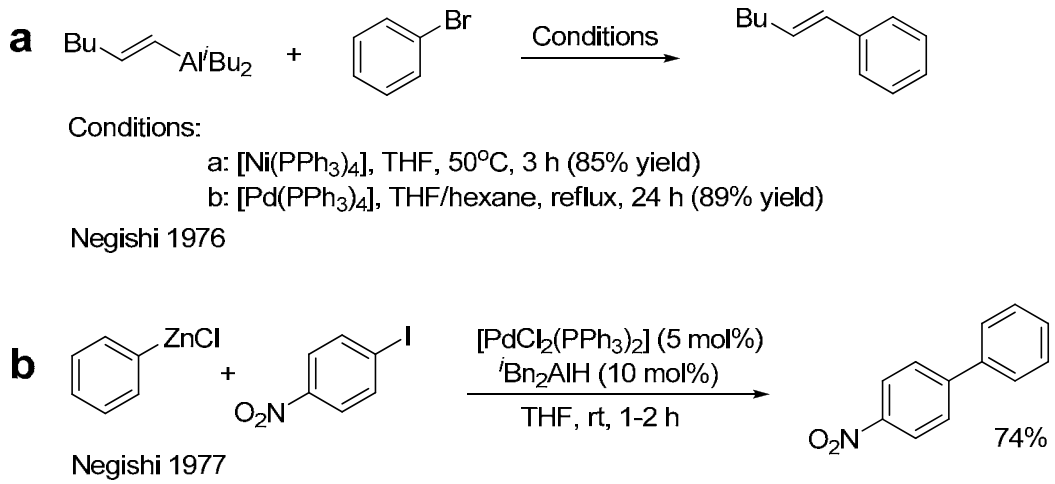

Scheme 23. The Negishi cross-coupling reaction.

As a seminal contribution, in 1976 the Eaborn group reported the use of palladium catalysis in the coupling of organodistannane reagents with aryl iodides to afford arylstannanes (Scheme 24a).[71] In this report, a byproduct of the homodimerization of the aryl halide was detected, and rationalized through the coupling between the target arylstannane, and the parent iodoarene substrate. Interestingly, shortly after, Migita's group[72] reported on the palladium-catalyzed cross-coupling of organotin reagents with aryl bromides (Scheme 24b). Following these precedents from the Eaborn and Migita

---

[68] Negishi, E.; Hu, Q.; Huang, Z.; Qian, M.; Wang, G. *Aldrichimica Acta* **2005**, *38*, 71.

[69] See the latest review and the references therein: Negishi, E. *Angew. Chem. Int. Ed.* **2011**, *50*, 6738.

[70] Knochel, P.; Thaler, T.; Diene, C. *Isr. J. Chem.* **2010**, *50*, 547.

[71] Azarian, D.; Dua, S. S.; Eaborn, C.; Walton, D. R. M.; *J. Organomet. Chem.* **1976**, *117*, C55.

[72] (a) Kosugi, M.; Sasazawa, K.; Shimizu, Y.; Migita, T. *Chem. Lett.* **1977**, 301. (b) Kosugi, M.; Shimizu, Y.; Migita, T. *J. Organomet. Chem.* **1977**, *129*, C36. For aryl halides, see; (c) Kosugi, M.; Shimizu, Y.; Migita, T. *Chem. Lett.* **1977**, 1423.

groups, Stille and Milstein[73] described the synthesis of ketones by combining aroyl chlorides with organostannanes in the presence of a palladium catalyst (Scheme 24c) under reaction conditions significantly milder than those reported by Migita *et al.*. In the early 1980s, the Stille reaction was further improved, and the method has since found a great number of applications in various total syntheses.[74]

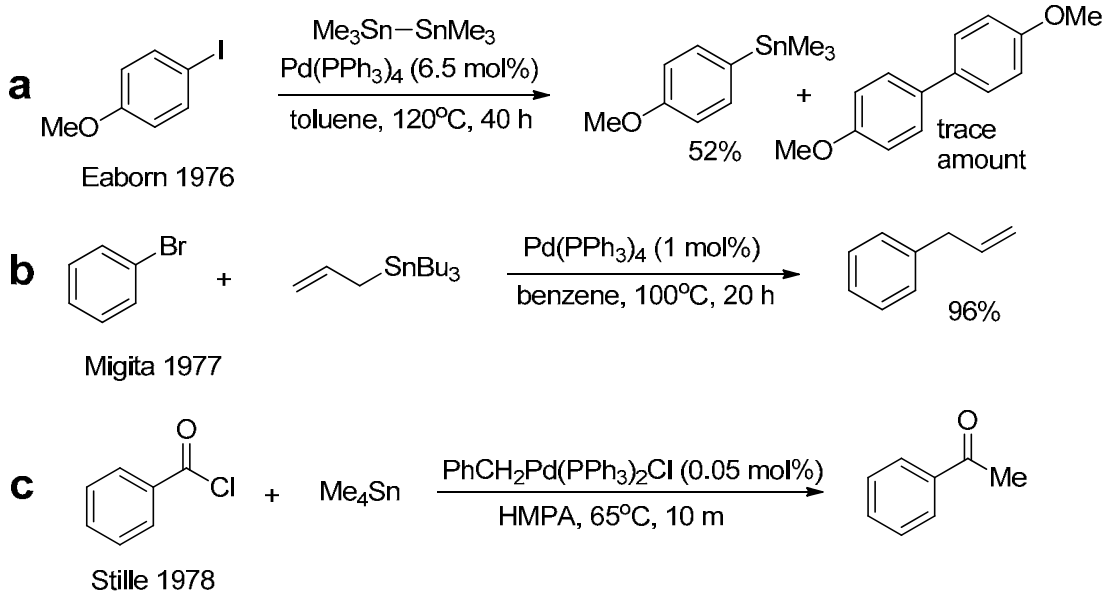

Scheme 24. The seminal stannane cross-coupling.

Today, the Stille reaction has been extended to the cross-coupling of various arene derivatives (Scheme 25).[75] Although the toxicity of the organostannanes in Stille reaction is recognized, this coupling reaction still attracts lots of attention worldwide, as evidenced by the number of publications and patents in which the method is used.[76]

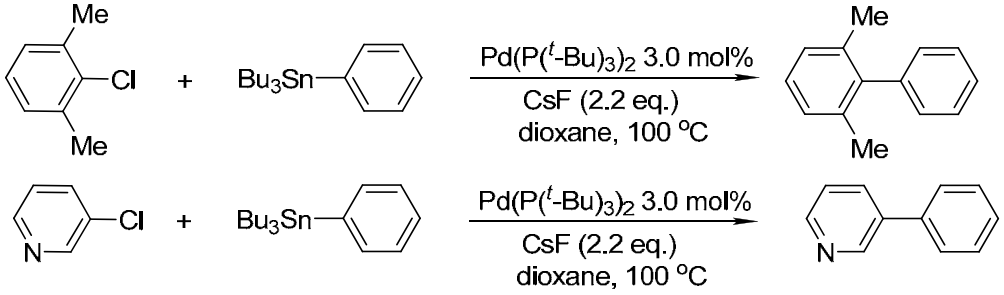

Scheme 25. Cross-coupling between aryl halides and organostannanes in the Stille reaction.

---

[73] Milstein, D.; Stille, J. K. *J. Am. Chem. Soc.* **1978**, *100*, 3636.

[74] (a) Kosugi, M.; Fugami K. in Handbook of Organopalladium Chemistry for Organic Synthesis (Ed.: E. Negishi), Wiley, New York, 2002, pp. 263 - 283. (b) Stille, J. K. *Angew. Chem. Int. Ed.* **1986**, *25*, 508.

[75] Littke, A. F.; Schwarz, L.; Fu, G. C. *J. Am. Chem. Soc.* **2002**, *124*, 6343.

[76] (a) Ragan, J. A.; Raggon, J. W.; Hill, P. D.; Jones, B. P.; McDermott, R. E.; Munchhof, M. J.; Marx, M. A.; Casavant, J. M.; Cooper, B. A.; Doty, J. L.; Lu, Y. *Org. Process Res. Dev.* **2003**, *7*, 676. (b) Farina, V.; Krishnamurthy, V.; Scott, W. *J. Org. React.* **1997**, *50*, 1.

Following the discoveries of the Negishi, Stille and Kumada cross-coupling reactions, the Suzuki group established[77] the C-C cross-coupling between aryl halides and organoboronic acids and boronates, as exemplified in Scheme 26,[78] in a manner similar to the organometallic Al, Mg, Zr, Zn or Sn reagents.

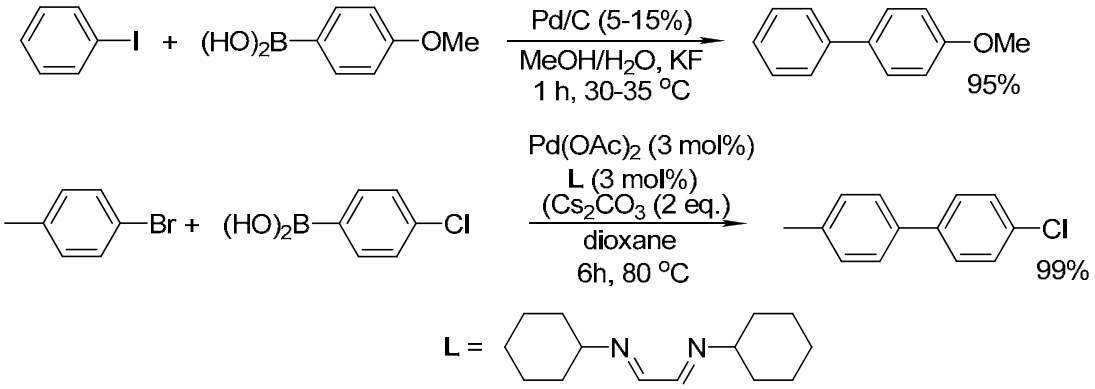

Scheme 26. Examples of Suzuki cross-coupling reactions.

This new protocol offers several advantages: mild reaction conditions and high product yields; water stability of the reagents; straightforward reaction setup both under aqueous and heterogeneous conditions; high regio- and stereoselectivity; tolerance of the substrate steric hindrance; need for a small amount of catalyst; nontoxic reagents and easy separation of the inorganic side product. What's more, comparing with the Kumada and Negishi coupling, the use of boronic acids as coupling partners instead of the strong basic and nucleophilic Grignard or organozinc reagents leads to a higher functional group tolerance in the Suzuki coupling. Notably, the Suzuki and the Negishi coupling reactions have developed into an extremely powerful and general tool for the formation of C-C bonds in the field of total synthesis,[79] reflecting the fertile evolution of the subject. In 2010, the Nobel Prize in Chemistry was awarded to profs. Akira Suzuki and Ei-ichi Negishi (along with prof. Richard Heck) because of their outstanding contributions in C-C coupling reactions.

The general mechanism for the palladium-catalyzed cross-coupling between organohalides and organometallic reagents is summarized in Scheme 27.[80] The

---

[77] See the latest review and the references therein: Suzuki, A. *Angew. Chem. Int. Ed.* **2011**, *50*, 6723.

[78] Polackova, V.; Hut'ka, M.; Toma, S. *Ultrason. Sonochem.* **2005**, *12*, 99.

[79] (a) Heravi, M. M.; Hashemi, E. *Tetrahedron* **2012**, *68*, 9145. (b) Suzuki, A. *Pure Appl. Chem*. **1994**, *66*, 213. (c) Miyaura, N.; Suzuki, A. *Chem. Rev*. **1995**, *95*, 2457. (d) Suzuki, A. *J. Organomet. Chem*. **1999**, *576*, 147. (e) Kotha, S.; Lahiri, K.; Kashinath, D. *Tetrahedro*n **2002**, *58*, 9633. (f) Suzuki, *J. Organomet. Chem.* **2002**, *653*, 83. (g) Kotha, S.; Lahiri, K. *Eur. J. Org. Chem.* **2007**, 1221. (h) Alonso, F.; Beletskaya, I. P.; Yus, M. *Tetrahedron* **2008**, 3047.

[80] (a) Metal-Catalyzed Cross-Coupling Reactions, (Eds.: de Meijere, A.; Diederich F.), Wiley-VCH, Weinheim, 2004. (b) Handbook of Organopalladium Chemistry for Organic Synthesis (Eds.: Negishi, E.; de Meijere,

process involves an oxidative addition between the aryl halide and the Pd^0 centre, followed by a transmetallation with the organometallic reagent and, subsequently, a reductive elimination step yielding the desired product and the regenerated catalyst.

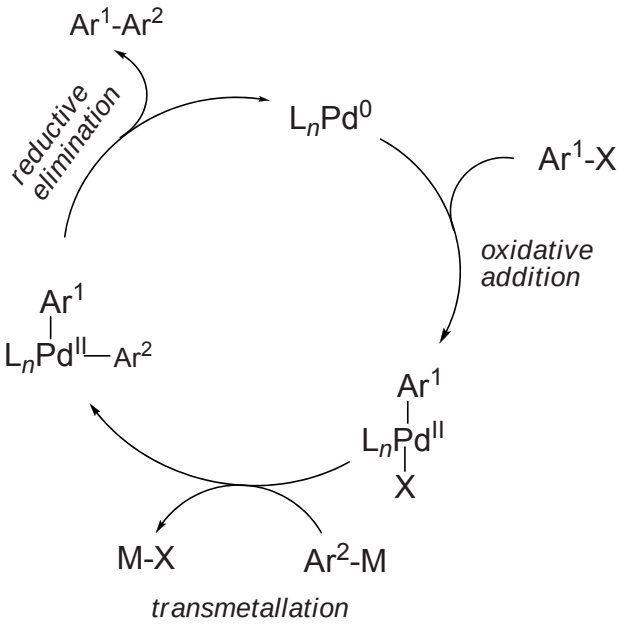

Scheme 27. General mechanism for the C-C cross-coupling under catalysis by palladium involving aryl halides and organometallic reagents.

Hiyama and co-workers, in 1988, described the palladium and nickel-catalyzed coupling of organosilanes with aryl halides or triflates in the presence of a fluoride source.[81] In this protocol, the fluoride species was shown to be crucial for the activation of the organosilane towards the transmellation by the formation of silicate intermediates. Nowadays, the Hiyama cross-coupling has been extended to reactions between various aromatic substrates, *i. e.*, aromatic organosilanes and aromatic halides,[82] as shown in Scheme 28.[82a,b] Moreover, this reaction has been applied to the synthesis of many natural products such as Papulacadin D, an anti-fungal agent.[83]

A.), Wiley, New York, 2002.

[81] Hatanaka, Y.; Hiyama, T. *J. Org. Chem.* **1988**, *53*, 918.

[82] (a) Molander, G. A.; Iannazzo, L. *J. Org. Chem.* **2011**, *76*, 9182. (b) Cheng, K.; Hu, S.; Zhao, B.; Zhang, X. -M.; Qi, C. *J. Org. Chem.* **2013**, *78*, 5022. (c) Raders, S. M.; Kingston, J. V.; Verkade, J. G. *J. Org. Chem.* **2010**, *75*, 1744.

[83] (a) Denmark, S. E.; Yang, S. -M. *J. Am. Chem. Soc.* **2004**, *126*, 12432. (b) Denmark, S. E.; Regens, C. S. *Acc. Chem. Res.* **2008**, *41***,** 1486.

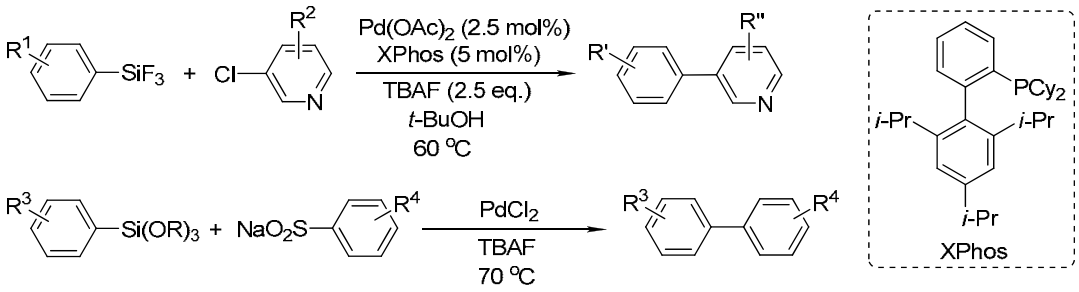

Scheme 28. Hiyama cross-coupling reactions.

2.1.2 Scholl reaction for C-C coupling *via* the transformation of the C-H groups

The first example of an oxidative dimerization of aromatic compounds was reported in 1871 (Scheme 29a).[84] What would later become known as the "Scholl reaction" was first introduced 39 years later, when Scholl found that a similar effect can be achieved by heating certain aromatic compounds with $AlCl_3$, as shown in Scheme 29b.[85] For many years, these two kinds of reactions were noticed. Nowadays, however, there is a mix-up in the scientific field, and the oxidative coupling of electron-rich aromatic substances is often called Scholl reaction.

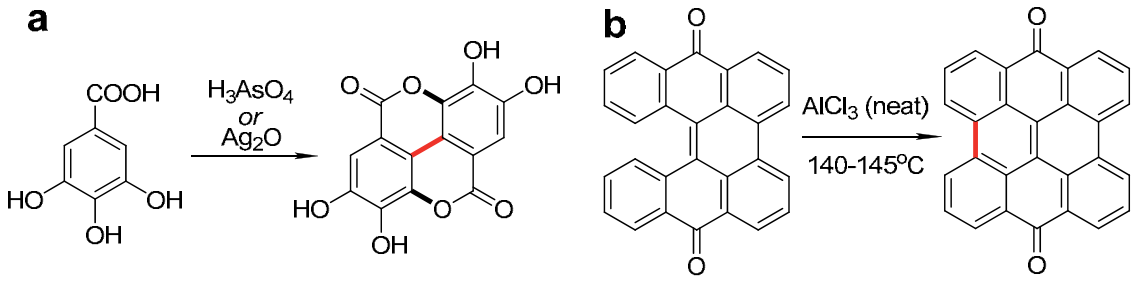

Scheme 29. C-C coupling reaction: a) oxidative dimerization; b) Scholl reaction.

Scholl reaction was further developed and numerous other examples, as listed in Scheme 30a-d, were published in the following years after 1910.[86] Since the early 1920s, this protocol was mainly utilized for the industrial synthesis of many antraquinone-derived dyes. After World War II, the focus on Scholl reaction shifted to

---

[84] (a) Lcwe, J.; *Chemie, Z.* **1868**, *4*, 603. (b) Grzybowski, M.; Skonieczny, K.; Butenschön, H.; Gryko, D. T. *Angew. Chem. Int. Ed.* **2013**, *52*, 9900.

[85] Scholl, R. Mansfeld, J. *Ber. Dtsch. Chem. Ges.* **1910**, *43*, 1734.

[86] (a) Homer, A. *J. Chem. Soc.* **1910**, *97*, 1141. (b) Scholl, R.; Seer, C.; Weitzenbock, R. *Ber. Dtsch. Chem. Ges.* **1910**, *43*, 2202. (c) Weitzenbcck, R.; Seer, C. *Ber. Dtsch. Chem. Ges.* **1913**, *46*, 1994. (d) Scholl, R.; Seer, C. *Monatsh. Chem.* **1912**, *33*, 1. (e) Scholl, R.; Seer, C. *Justus Liebigs Ann. Chem.* **1912**, *394*, 111. (f) Scholl, R.; Neumann, H. *Ber. Dtsch. Chem. Ges.* **1922**, *55*, 118. (g) Scholl, R.; Schwarzer, G. *Ber. Dtsch. Chem. Ges.* **1922**, *55*, 324. (h) Seer, C.; Dishendorfer, O. *Monatsh. Chem.* **1913**, *34*, 1493. (i) Scholl, R.; Dischendorfer, O. *Ber. Dtsch. Chem. Ges.* **1918**, *51*, 452.

the synthesis of extended aromatic hydrocarbons. During that period, various improved protocols appeared, including the use of $AlCl_3$/pyridine complex, $AlCl_3$ in high-boiling solvents such as dichlorobenzene and trichlorobenzene, low-melting complexes such as $AlCl_3/SO_2$, $AlCl_3/CS_2$, $AlCl_3/Cu(OTf)_2/CS_2$, etc..[87]

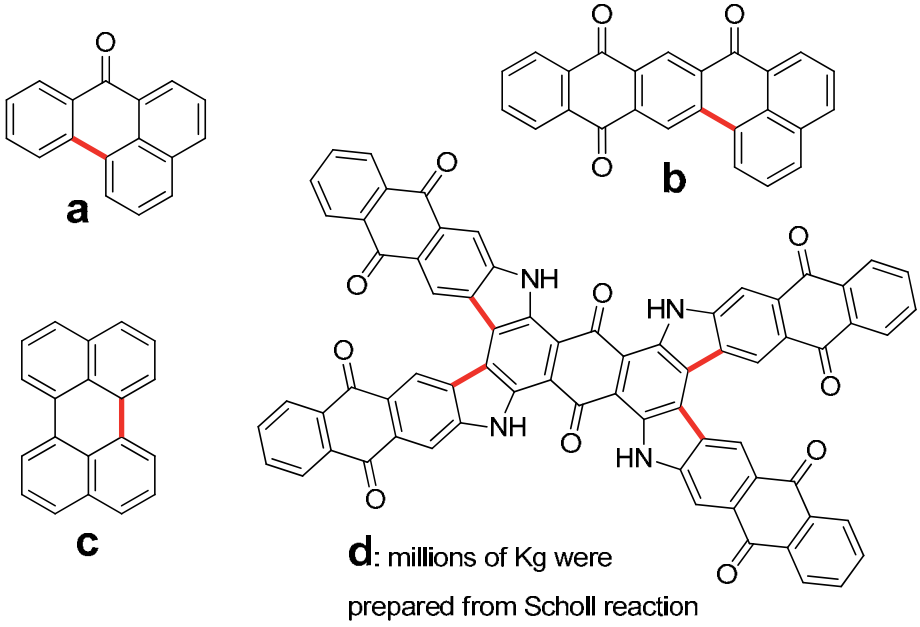

Scheme 30. Some products prepared from Scholl reaction.

However, there is still scientific controversy about the definition and mechanism of the Scholl reaction, which are the subjects of a recent review by Gryko, Butenschon and co-workers.[87] It seems that the main confusion arises from the difference between oxidative aromatic coupling and Scholl reaction. In that review, the authors proposed that, in a typical (non-Scholl) oxidative aromatic coupling, the electron-rich aromatic compounds, such as phenols, involve the formation of a radical cation from one molecule of the substrate, followed by substitution at the neutral second molecule and, finally, aromatizative convergence to the biaryl target product (Scheme 31). This mechanism generally requires a substrate that is reasonably electron rich, and the attack of the electrophilic radical cation occurs at the most electron-rich position of the second substrate molecule. Of course, other mechanistic pathways have also been discussed.[88]

---

[87] See the latest review and the references therein: Grzybowski, M.; Skonieczny, K.; Butenschön, H.; Gryko, D. T. *Angew. Chem. Int. Ed.* **2013**, *52*, 9900.

[88] (a) "Oxidative coupling of phenols and phenol ethers": D. A. Whiting in Comprehensive Organic Synthesis, Vol. 3. (Eds.: Trost, B. M.; Fleming, I.; Pattenden, G.), Pergamon, Oxford, 1991, pp. 659 - 703. (b) S. R. Waldvogel, D. Mirk, Handbook of CH-Transformations, Vol. 1 (Ed.: Dyker, G.), Wiley-VCH, Weinheim, 2005, pp. 251 - 261.

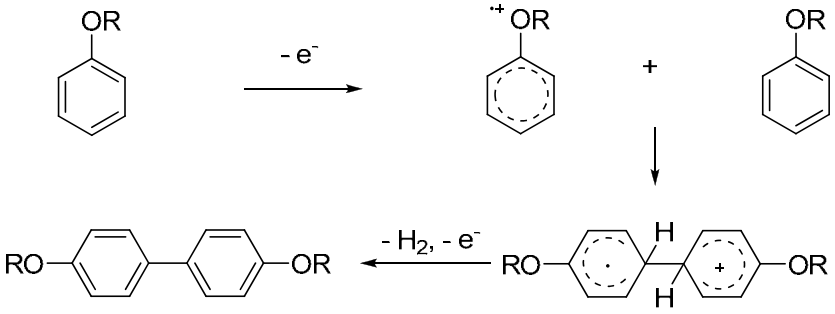

Scheme 31. The typical mechanism of oxidative aromatic C-C coupling.

The Scholl reaction, in the 1940s, was defined as the dehydrogenation of aromatic nuclei under the influence of aluminum chloride that results in the formation of a condensed ring system.[89] A definition that was later reformulated by Balaban and Nenitzescu,[90] as the elimination of two arylbonded hydrogens under the influence of Friedel-Crafts catalysts. Baddeley[91] was the first to propose the mechanism of the Scholl reaction, in which the formation of a σ complex between the Lewis or the Brönsted acid and the aromatic ring was followed by the formation of an arenium cation; this cation was attacked by a nucleophile (the other aromatic ring) and then the intermediate compound experienced a hydrogen elimination to yield the final product. This mechanism (Scheme 32) implies the protonation of the arene to form an electrophilic σ complex (H^+ is used for simplicity sake, but the manifold should be valid for a σ complex with a Lewis acid), which is subsequently attacked by the second aromatic ring to form a new C-C bond. Finally, the oxidative rearomatization affords the desired product. Numerous experimental data[92] and computational calculations[93] supported this mechanistic pathway, although a radical pathway was also proposed by others.[94] Scholl reactions are still widely applied nowadays, especially in the synthesis of extended aromatic derivatives.[95]

---

[89] (a) Kranzlein, G. Aluminium chlorid in der organischen Chemie, 3rd ed., Chemie, Berlin, 1939, p. 146; (b) C. A. Thomas, Anhydrous Aluminium Chloride in Organic Chemistry, Reinhold, New York, 1941, p. 648.

[90] "Dehydrogenation Condensation of Aromatics (Scholl and Related Reactions)": Balaban, A. T.; Nenitzescu, C. D. Friedel – Crafts and Related Reactions, Vol. 2 (Ed.: Olah, G.), Wiley, New York, 1964, pp. 979-1047.

[91] (a) Baddeley, G.; Kenner, J. *J. Chem. Soc.* **1935**, 303. (b) Baddeley, G. *J. Chem. Soc.* **1950**, 994.

[92] (a) Nenitzescu, C. D.; Balaban, A. T. *Chem. Ber.* **1958**, *91*, 2109. (b) Vollmann, H.; Becker, H.; Corell, M.; Streeck, H.; *Justus Liebigs Ann. Chem*. **1937**, *531*, 1. (c) Scholl, R.; Seer, C. *Ber. Dtsch. Chem. Ges.* **1922**, *55*, 330.

[93] (a) Rempala, P.; Kroulik, J.; King, B. T. *J. Am. Chem. Soc.* **2004**, *126*, 15002. (b) King, B. T.; Kroulik, J.; Robertson, C. R.; Rempala, P.; Hilton, C. L.; Korinek, J. D.; Gortari, L. M. *J. Org. Chem.* **2007**, *72*, 2279. (c) Rempala, P.; Kroulik, J.; King, B. T. *J. Org. Chem.* **2006**, *71*, 5067.

[94] Kenner, J. *J. Soc. Chem. Ind.* **1933**, *42*, 470. (b) Rooney, J. J.; Pink, R. C. *Proc. Chem. Soc.* **1961**, 142. (c) Clover, G. A. *J. Chem. Soc. C* **1968**, 2519.

[95] Wu, J.; Pisula, W.; Müllen, K. *Chem. Rev.* **2007**, *107*, 718.

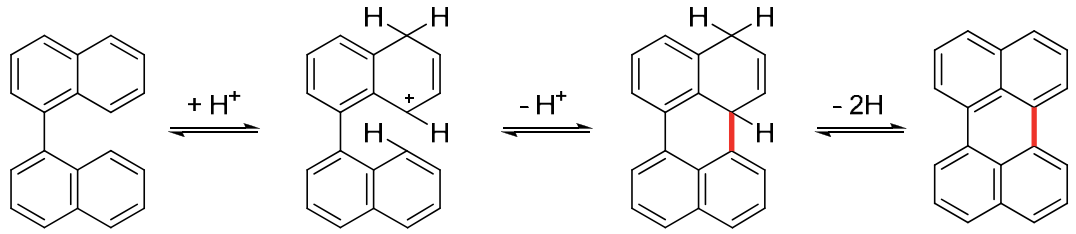

Scheme 32. An example of the Scholl reaction involving the formation of a σ complex and arenium cation.

2.1.3 Oxidative formation of C-C bond between arenes

In theory, the most direct approach for the construction of C-C bond between arenes can operate through either *Path a* or *Path b* (Scheme 33), with a net loss of hydrogen gas or two protons (and two electrons) in the presence of an oxidant, respectively. However, the thermodynamics of making a C-C bond with loss of H_2 is typically unfavourable. Indeed, examples of oxidative cross-coupling (Scheme 33, *Path b*) have been proven in the early 1960s, and a steady increase of research on this topic can be found in the last 15 years.[56]

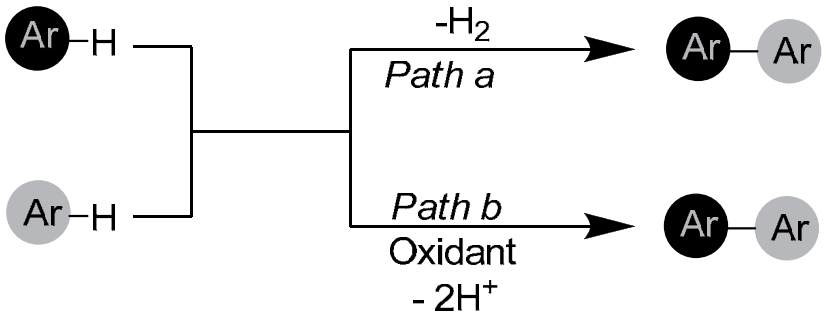

Scheme 33. Direct oxidative C-C cross-coupling.

An early example of this reaction in an intramolecular setting was demonstrated in the synthesis of (±)-glaucine from (±)-laudanosine in 43% yield by using vanadium oxyfluoride as oxidant (Scheme 34). Owing to the large number of natural products accessible through this strategy, considerable progress has been subsequently made in achieving intramolecular oxidative cross-coupling under mild reaction conditions.[96]

[96] (a) Kupchan, S. M.; Liepa, A. J.; Kameswaran V.; Bryan, R. F. *J. Am. Chem. Soc.* **1973**, *95*, 6861. (b) Churruca, F.; SanMartin, R.; Carril, M.; Urtiaga, M. K.; Solans, X.; Tellitu, I.; Dominguez, E. *J. Org. Chem.* **2005**, *70*, 3178, and references therein.

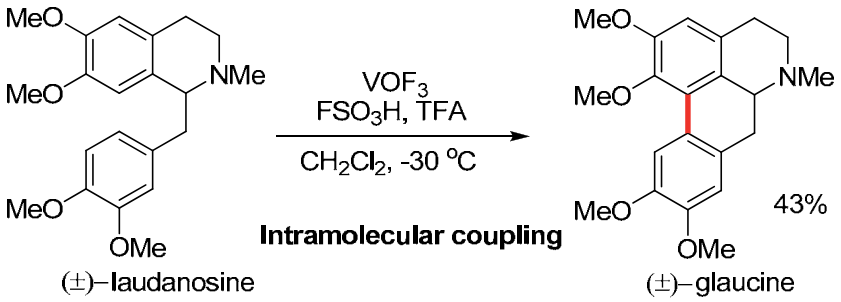

Scheme 34. Oxidative intramolecular coupling to prepare (±)-glaucine from (±)-laudanosine.

To extend this type of reaction to an intermolecular mode, however, two challenges have been encountered: 1) the reaction conditions must be carefully chosen to avoid the undesired homocoupling product and 2) the regioselectivity issue should be overcome. In the absence of activating/directing groups on the substrate, the position of the newly formed C-C bond is determined by the electronic and steric preferences of the two substrates.

2.1.3.1 Metal-catalyzed oxidative aromatic couplings

As one of the earliest description of regioselective arene-arene cross-coupling, Lu and co-workers, in 2006, achieved dehydrogenative C-C bond formation between naphthalene and simple arenes using $K_2S_2O_8$ as the terminal oxidant.[97] Selective cross-coupling was achieved by optimizing the relative concentration of the trifluoroacetic acid and of each of the arene substrates.

In 2007, as a ground breaking research, Fagnou and co-workers[98] reported the direct oxidative C2 or C3 cross-coupling of indoles with simple arenes, *e. g.*, benzene. With $Cu(OAc)_2$ as an oxidant, the palladium-catalyzed C3 arylation of *N*-acetylindoles was achieved using the arene coupling partner as solvent. Interestingly, choosing AgOAc as the terminal oxidant instead of $Cu(OAc)_2$, a reversal in regioselectivity and preference for C2 indole and pyrrole arylation is observed. The authors, as outlined in Scheme 35, proposed a catalytic cycle in this kind of transformations which begins with the electrophilic palladation of an arene to produce an arylpalladium intermediate Ar^1PdL. Later on this intermediate performs a selective C-H activation upon the second arene to produce a diarylpalladium(II) species which is, in principle, the same as that formed in the palladium-catalyzed cross-coupling reactions (see Scheme 27). This step

[97] Li, R.; Liang, L.; Lu, W. *Organometallics* **2006**, *25*, 5973.
[98] Stuart, D. R.; Fagnou, K. *Science*, **2007**, *316*, 1172.

is followed by a reductive elimination of the target biaryl and catalyst re-oxidation to complete the catalytic cycle.

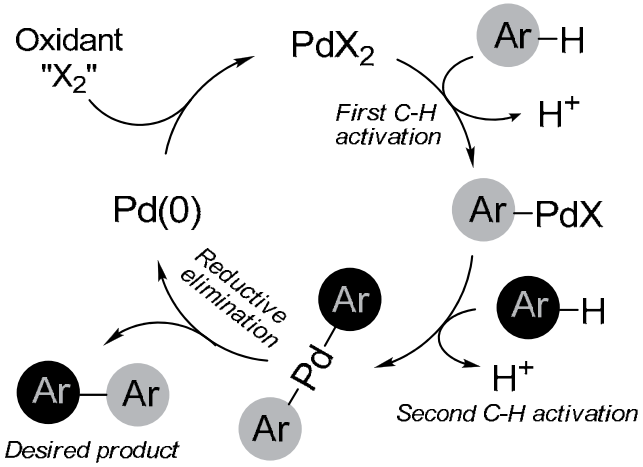

Scheme 35. Palladium-catalyzed oxidative arene-arene cross-coupling.

The same year, DeBoef and co-workers[99] also reported the oxidative arylation of indoles and benzofurans with O_2 as the terminal oxidant. In a later study, the same group confirmed that[100] the C2 and C3 regioselective arylation depends on the oxidant applied, with $Cu(OAc)_2$ favoring benzofuran arylation at C2 while AgOAc facilitating functionalization at C3 positions. Two years later, the group once again demonstrated[101] that electron-rich indoles are excellent cross-coupling partners in direct arylation. In this strategy, catalytic amount of palladium and stoichiometric quantities of pivalic acid and AgOAc can achieve a broad-scope oxidative C3 arylation of *N*-protected indoles.

Besides, a number of innovative methodologies have been published[102] providing cross-coupling products between two unactivated arenes in good yields. To date, various substrates can undergo oxidative biaryl C-C bond formation with palladium catalysts, including electron-rich arenes, arenes bearing pyridine, electron-deficient arenes and arenes bearing other directing groups, as exemplified in Scheme 36(a-d) where the newly formed C-C bonds are highlighted.[56]

---

[99] Dwight, T. A.; Rue, N. R.; Charyk, D.; Josselyn, R.; DeBoef, B. *Org. Lett.* **2007**, *9*, 3137.

[100] Potavathri, S.; Dumas, A. S.; Dwight, T. A.; Naumiec, G. R.; Hammann, J. M.; DeBoef, B. *Tetrahedron Lett.* **2008**, *49*, 4050.

[101] Potavathri, S.; Pereira, K. C.; Gorelsky, S. I.; Pike, A.; LeBris, A. P.; DeBoef, B. *J. Am. Chem. Soc.* **2010**, *132*, 14676.

[102] Please see the two following reviews and the references therein: (a) Yeung, C. S.; Dong, V. M. *Chem. Rev.* **2011**, *111*, 1215. (b) Ashenhurst, J. A. *Chem. Soc. Rev.* **2010**, *39*, 540.

Hu and You[103] found that other nitrogen-containing heterocycles can also undergo regioselective arylation with $Cu(OAc)_2$ as oxidant (Scheme 36a). This protocol exhibits excellent functional group compatibility and was found to tolerate aldehydes, nitriles and ketones.

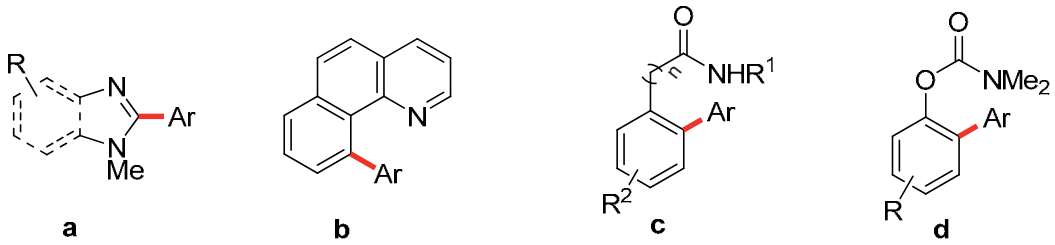

Scheme 36. Examples of palladium-catalyzed oxidative arene-arene cross-coupling.

In an approach differing from the above mentioned methodologies, the Sanford group[104,105] used directing groups (Scheme 36b) to achieve regioselective oxidative arylation. Benzo[*h*]quinolines and 2-phenylpyridines were found to react with simple arenes with the help of Ag_2CO_3 affording the cross-coupling products.[104] This strategy is suitable for a range of electron-rich, -neutral, and –deficient arene coupling partners.

Dong's group disclosed alternative catalytic conditions[106] amenable to a broad class of arenes, including phenylacetamides and benzamides (Scheme 36c), and *O*-carbamates (Scheme 36d). The methodology employs the relatively cheap combination of the TFA in combination with $Na_2S_2O_8$ as oxidant. *O*-phenylcarbamates bearing two reactive C-H bonds can undergo efficient diarylation in a 4-fold C-H (two pairs of CH per each new C-C bond) functionalization process due to the high reactivity of the catalyst.

Other metals, including nickel (Ni), copper (Cu), iron (Fe), have also found applications as catalysts to promote direct oxidative C-C coupling between arenes.[107] For instance, in 2012, Itami *et al.* implemented a C-H arylation of azoles with C-O electrophiles catalyzed by the combination $[Ni(cod)_2]$/dcype (cod = 1,5-cyclooctadiene, dcype = 1,2-bis(dicyclohexylphosphino)ethane) (Scheme 37).[108]

---

[103] Xi, P.; Yang, F.; Qin, S.; Zhao, D.; Lan, J.; Gao, G.; Hu, C.; You, J. *J. Am. Chem. Soc.* **2010**, *132*, 1822.

[104] Hull, K. L.; Sanford, M. S. *J. Am. Chem. Soc.* **2007**, *129*, 11904.

[105] Hull, K. L.; Sanford, M. S. *J. Am. Chem. Soc.* **2009**, *131*, 9651.

[106] (a) Zhao, X.; Yeung, C. S.; Dong, V. M. *J. Am. Chem. Soc.* **2010**, *132*, 5837. (b) Yeung, C. S.; Borduas, N.; Zhao, X.; Dong, V. M. *Chem. Sci*. **2010**, *1*, 331. For a recent mechanistic study on intramolecular oxidative coupling with $Na_2S_2O_8$, see: (c) Borduas, N.; Lough, A. J.; Dong, V. M. *Inorg. Chim. Acta* **2011**, *369*, 247.

[107] Mousseau, J. J.; Charette, A. B. *Acc. Chem. Res.* **2013**, *46*, 412.

[108] Muto, K.; Yamaguchi, J.; Itami, K. *J. Am. Chem. Soc.* **2012**, *134*, 169.

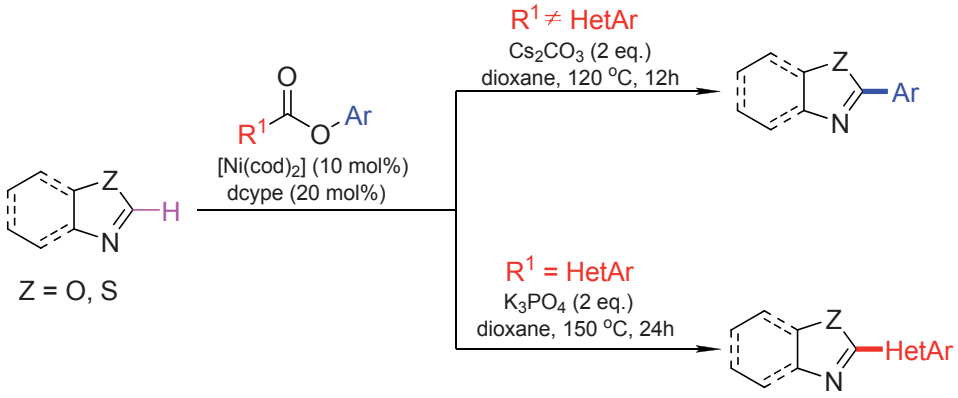

Scheme 37. Ni-catalyzed oxidative cross-coupling between arenes.

2.1.3.2 Oxidative C-C coupling between arenes with hypervalent iodanes

The oxidative C-C coupling between arenes promoted by hypervalent iodine reagents offers an alternative protocol, which may give products unobtainable by metal-catalyzed methods. In this area, initial efforts have been paid to achieve direct intramolecular C-C coupling.[109] For example, Kita group reported in 1996 the aryl-aryl intramolecular coupling with PIFA, as depicted in Scheme 38.

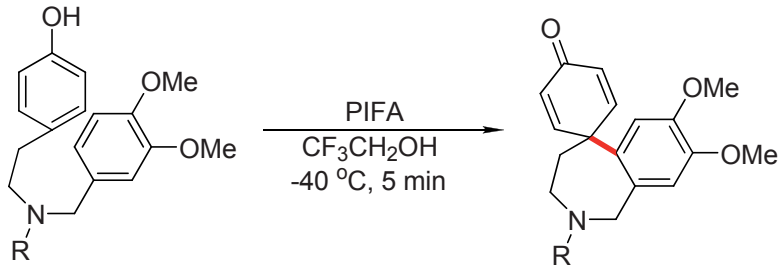

Scheme 38. PIFA promoted intramolecular C-C coupling.

Promisingly, the formidable challenge of C-C coupling in intermolecular systems with the use of hypervalent iodine, without the formation of homocoupling products, has been conquered by Kita and co-workers in the coupling of naphthalenes and electron-rich arenes.[110] In this work, as shown in Scheme 39, the authors propose that PIFA coordinates to the napthalene giving a π complex. Since the $BF_3{\cdot}Et_2O$ is essential, the

[109] (a) Tohma, H.; Morioka, H.; Takizawa, S.; Arisawa, M.; Kita, Y. *Tetrahedron* **2001**, *57*, 345. (b) Arisawa, M.; Utsumi, S.; Nakajima, M.; Ramesh, N. G.; Tohma, H.; Kita, Y. *Chem. Commun.* **1999**, 469. (c) Hamamoto, H.; Anilkumar, G.; Tohma, H.; Kita, Y. *Chem. Commun.* **2002**, 450. (d) Tohma, H.; Kita, Y. *Top. Curr. Chem.* **2003**, *224*, 209. (e) Moreno, I.; Tellitu, I.; Dominguez, E.; San Martin, R. *Eur. J. Org. Chem.* **2002**, 2126. (f) Kita, Y.; Takada, T.; Gyoten, M.; Tohma, H.; Zenk, M. H.; Eichhorn, J. *J. Org. Chem.* **1996**, *61*, 5857. (g) Kita, Y.; Arisawa, M.; Gyoten, M.; Nakajima, M.; Hamada, R.; Tohma, H.; Takada, T. *J. Org. Chem.* **1998**, *63*, 6625.

[110] Dohi, T., Ito, M.; Morimoto, K.; Iwata, M.; Kita, Y. *Angew. Chem. Int. Ed.* **2008**, *47*, 1301.

authors supposed that the BF_3 coordinates to a trifluoroacetoxy ligand of the formed π complex. Upon a SET process, a radical cation is formed, which subsequently undergoes nucleophilic attack by the electron-rich coupling partner to afford, upon further one-electron oxidation and deprotonation, the cross-coupling product. Several interesting relevant protocols were also developed based on this methodology.[111]

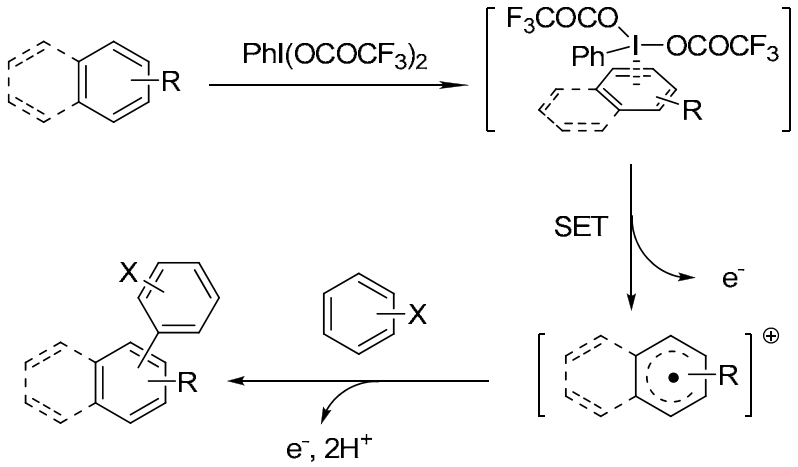

Scheme 39. Proposed mechanism of PIFA promoted oxidative C-C coupling by Kita.

Later on, the same group extended the reaction scope to the coupling of heteroarenes (Scheme 40).[112] In this method, the thiophene substrate was treated with Koser's reagents, PhI(OH)(OTs), in 1,1,1,3,3,3-hexafluoro-2-propanol (HFIP) at room temperature, affording an α-thienyl iodonium(III) intermediate, which was allowed to react with the sequentially added 1-methoxynaphthalene coupling partner in the presence of bromotrimethylsilane (TMSBr), to give the target cross-coupling product in 86% of yield.

[111] (a) Dohi, T.; Ito, M.; Yamaoka, N.; Morimoto, K.; Fujioka, H.; Kita, Y. *Tetrahedron* **2009**, *65*, 10797. (b) Ouyang, Q.; Zhu, Y.-Z.; Zhang, C.-H.; Yan, K.-Q.; Li, Y.-C.; Zheng, J.-Y. *Org. Lett.* **2009**, *11*, 5266. (c) Kar, A.; Mangu, N.; Kaiser, H. M.; Beller, M.; Tse, M. K. *Chem. Commun.* **2008**, 386. (d) Shen, D.-M.; Liu, C.; Chen, X.-G.; Chen, Q.-Y. *J. Org. Chem.* **2009**, *74*, 206. (e) Gu, Y.; Wang, D. *Tetrahedron Lett.* **2010**, *51*, 2004.

[112] Kita, Y.; Morimoto, K.; Ito, M.; Ogawa, C.; Goto, A.; Dohi, T. *J. Am. Chem. Soc.* **2009**, *131*, 1668.

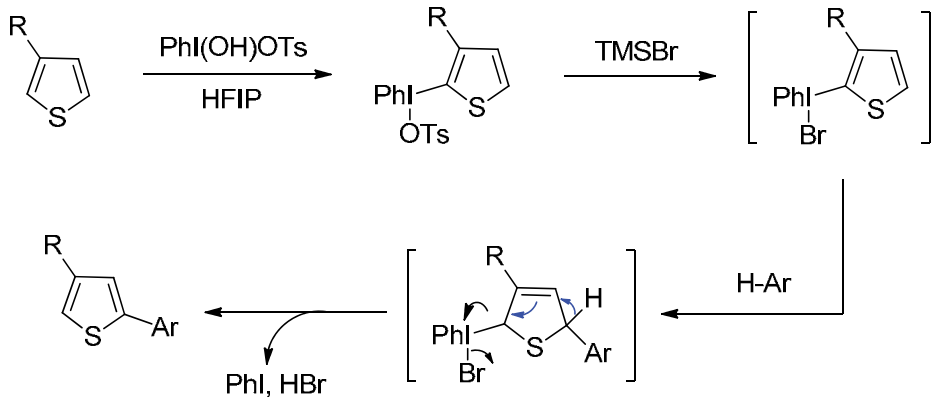

Scheme 40. PhI(OH)(OTs) promoted oxidative C-C coupling.

2.1.4 Precedents of oxidative C-C coupling in our group with hypervalent iodanes

During the course of a related research, Shafir and Faggi[113] in our group repeated the reaction between mesitylene and naphthalene (Nap_1) reported by Kita *et al*.[110] for the synthesis of 1-mesitylnaphthalene (Scheme 41). They found that, in addition to the target product, the thin-layer chromatography (TLC) of the reaction mixture also showed a ladder of spots that were fluorescent under 365 nm light irradiation. Further investigation suggested that the spots corresponded to oligonaphthalene derivatives **A**, **B** and **C**, respectively (Scheme 41). Considering that the formation of these interesting byproducts might be caused by an overoxidation process, the effect of the amount of PIFA employed on the reaction outcome was investigated. Indeed, the yields of 1-mesitylnaphthalene and compound **A** were found to be a function of the amount of PIFA used, with the yield of compound **A** peaking at 2 eq. of PIFA. Changing the amount of the mesitylene coupling partner did not improve the yield of product **A**.

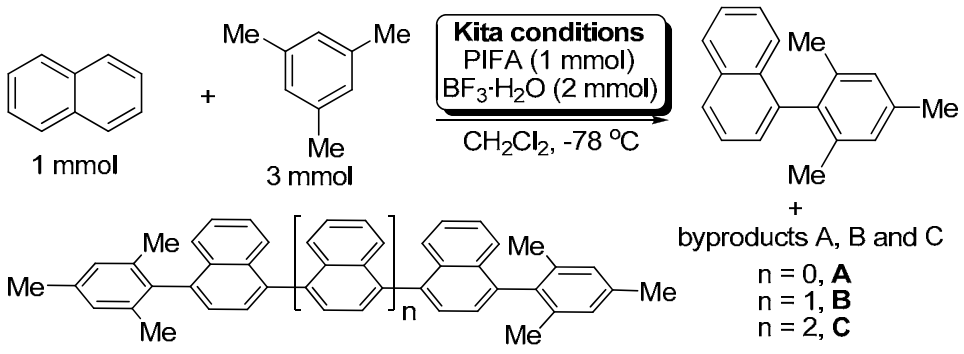

Scheme 41. Previous observations in the oxidative arylation of naphthalene with the system PIFA/BF_3 in our group.

[113] Faggi, E.; Sebastian, R. M.; Pleixats, R.; Vallribera, A.; Shafir, A.; Rodriguez-Gimeno, A.; Ramírez de Arellano, C. *J. Am. Chem. Soc.* **2010**, *132*, 17980.

Later on, the reactions of naphthalene with a series of electron-rich arenes (3 mol per mol of Nap_1) with the use of an excess of PIFA (1.5 mol per mol of Nap_1) were performed in the presence of BF_3·Et_2O (3 mol per mol of Nap_1) (Scheme 42a). The dimerization products were indeed isolated albeit with relatively lower yields (23-27%). Interestingly, when 1,1'-binaphthalene (Nap_2) was submitted to the reaction with mesitylene under the optimized conditions, a respectable 87% yield of the dimerization product was obtained (Scheme 42b). More reactions were performed and the yields of dimerization products varied with different electron-rich arenes.

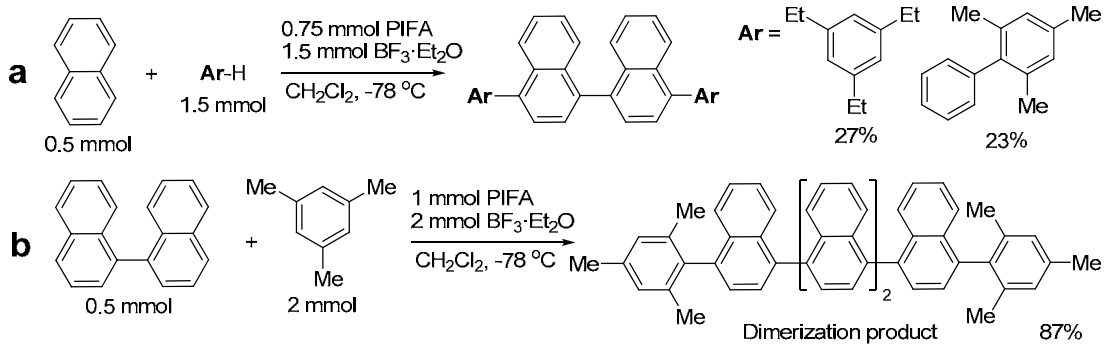

Scheme 42. Arylation of Nap_1 and Nap_2 under different reaction conditions.

Control experiments showed that in the case of the Nap_2, the formation of dimerization product follow either a dimerization/arylation sequence (Scheme 43, path a) or an arylation/dimerization sequence (Scheme 43, path b). Furthermore, the monoarylation product, an intermediate in path b, may undergo a second arylation to afford the final product (path c).[113] In fact, these experiments and the overall high efficiency for this formal dimerization arylation process suggested the use of longer chain oligonaphthalenes, such as the ter- and quaternaphthalenes (Nap_3 and Nap_4) might also be feasible.[114]

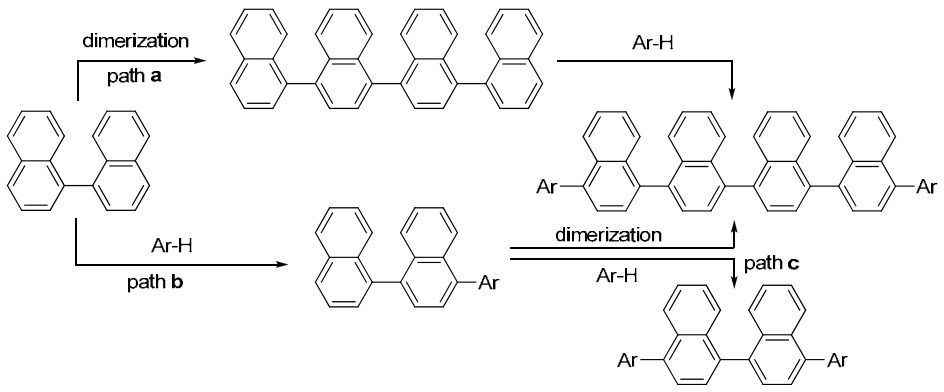

Scheme 43. Plausible reaction paths for oxidative arylation of Nap_2 by $PIFA/BF_3$.

[114] The 1:1',4':1'',4'':1'''-quaternaphthalene (Nap_4) has been previously accessed at Sony Corp. *via* Ni-catalyzed Kumada coupling: Takada, K.; Sakamoto, H.; Ichimura, M.; Tamura, S. Organic EL Light Emitting Element. JP 2005,019219 (A), Jan 20, 2005.

2.2 Objectives

Continuing the previous studies on oxidative C-C coupling with PIFA/BF_3·Et_2O system in our group, we planned the following aims for this chapter 2 of part I of the thesis:

a) The preparation of Nap_3 and Nap_4 via a bromination/Suzuki coupling sequence (Scheme 44).

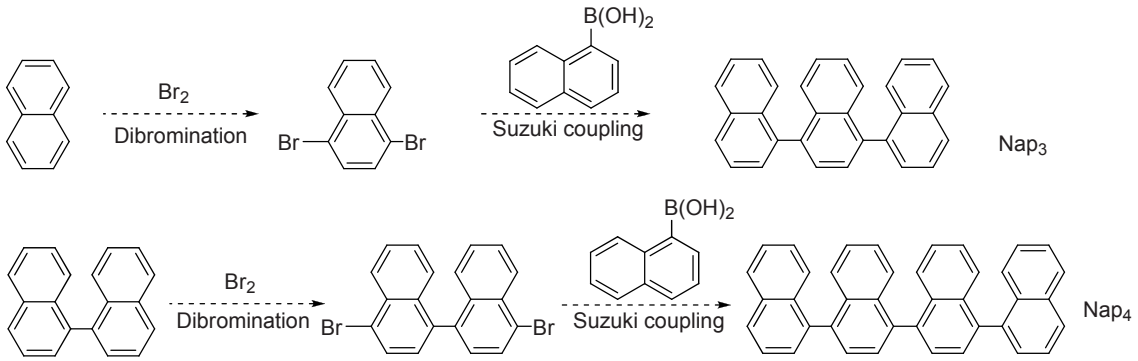

Scheme 44. Proposal for the preparation of Nap_3 and Nap_4 via bromination/Suzuki coupling sequence.

b) The arylation of Nap_3 with a range of electron-rich arenes using the PIFA/BF_3·Et_2O system, with the investigation of the effect of the reaction conditions (amounts of PIFA and arenes) on the reaction outcome (double arylation products *versus* octiarenes derived from diarylation/dimerization processes) (Scheme 45).

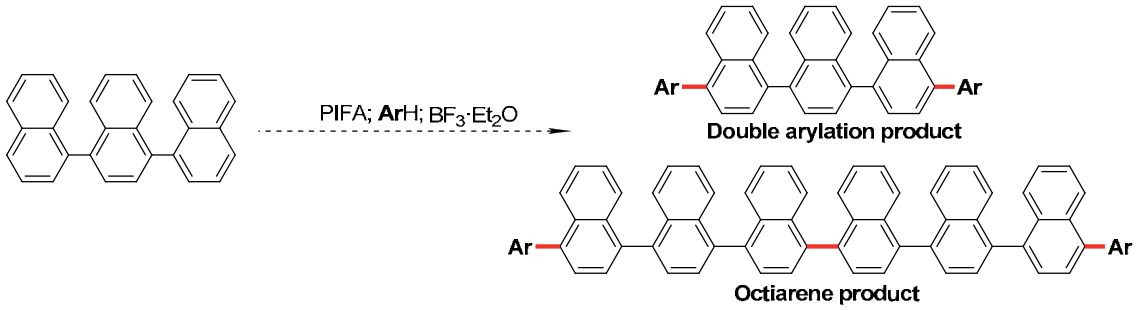

Scheme 45. Proposal for the arylation of Nap_3 with PIFA/BF_3 system.

c) The arylation of Nap_4 with various electron-rich arenes using the PIFA/BF_3·Et_2O system, in a similar study as described in objective b.

2.3 Results and Discussion

As described in the introduction section (2.1.4, Part I), Faggi and coworkers[113] in our group performed the arylation of naphthalene with PIFA/BF_3·Et_2O under Kita's conditions[110] and, in addition to the expected arylation product, they observed a ladder of spots on the TLC plate of the reaction mixture corresponding to a range of oligonaphthalene derivatives, *i. e.*, compounds **A**, **B**, **C** in Scheme 41. Based on these observations, we envisaged that a similar phenomenon could take place in the arylation of Nap_2 and Nap_3 under similar reaction conditions; in particular, we were interested in the obtention of the larger oligoarenes derived from diarylation/dimerization processes, compounds that could not be easily prepared by other methods in an efficient and selective manner.

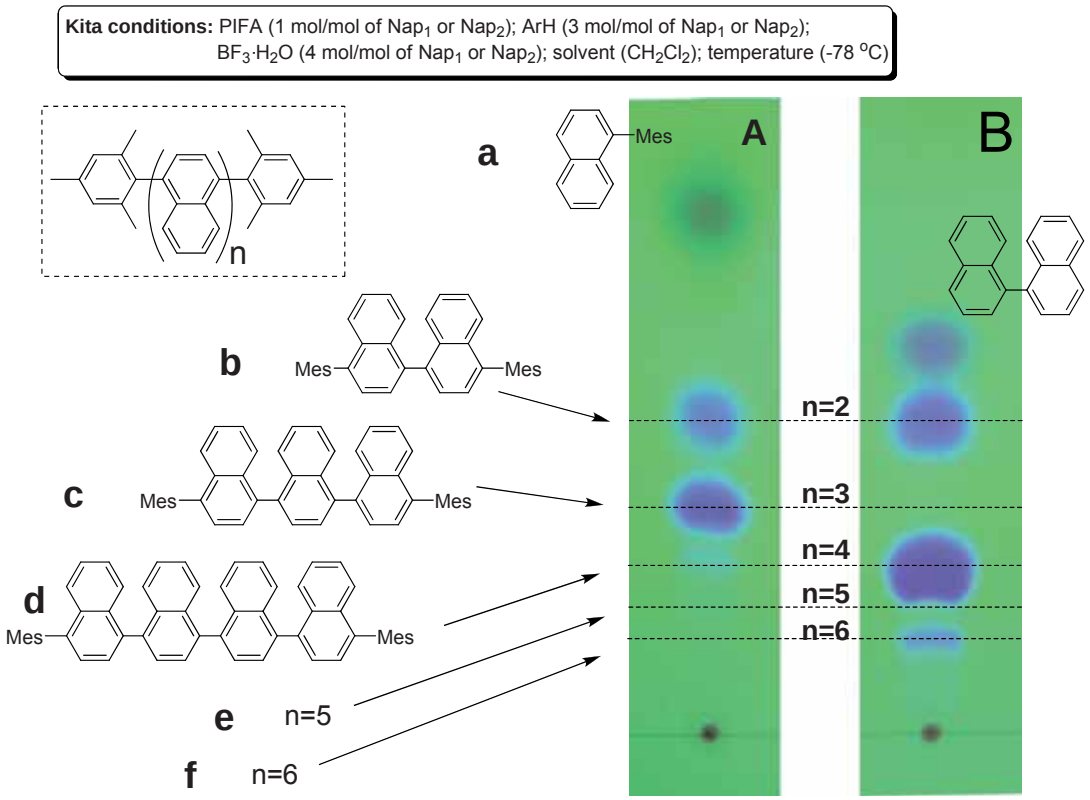

Figure 1. TLC traces for the coupling of mesitylene with: A) naphthalene, and B) 1,1´-binaphthalene.

Before undertaking the arylation of linear Nap_3 and Nap_4, the arylations of naphthalene and 1,1'-binaphthalene with mesitylene under Kita's conditions were performed. As shown in Figure 1, the TLC traces of the reaction mixtures give a nice visual comparison for the two outcomes. Trace A (Figure 1) shows that the arylation of naphthalene yields, in addition to compound **a**, oligonaphthalenes (**b**, **c**, **d**, etc.) capped

on both sides by a mesityl moiety. Indeed, while the *n*-even **b**, **d** are found on both traces (compound **f** can also be found in trace B), product **c** (n = 3) is absent in trace B which corresponds to the reaction mixture of the arylation of 1,1'-binaphthalene.

2.3.1 Preparation of ternaphthalene and quaternaphthalene

Following a reported procedure,[115] the parent linear Nap_3 was synthesized through a two-step procedure involving selective dibromination to offer 1,4-dibromonaphthalene, **1**, followed by the Suzuki-Miyaura coupling of product **1** with the 1-naphthaleneboronic acid (Scheme 46) to afford the desired compound **2** in good yield. It should be noted that in the dibromination step the reaction mixture should be well protected from the light to avoid the formation of the undesired 1,5-dibromonapthalene (Scheme 46b).[115]

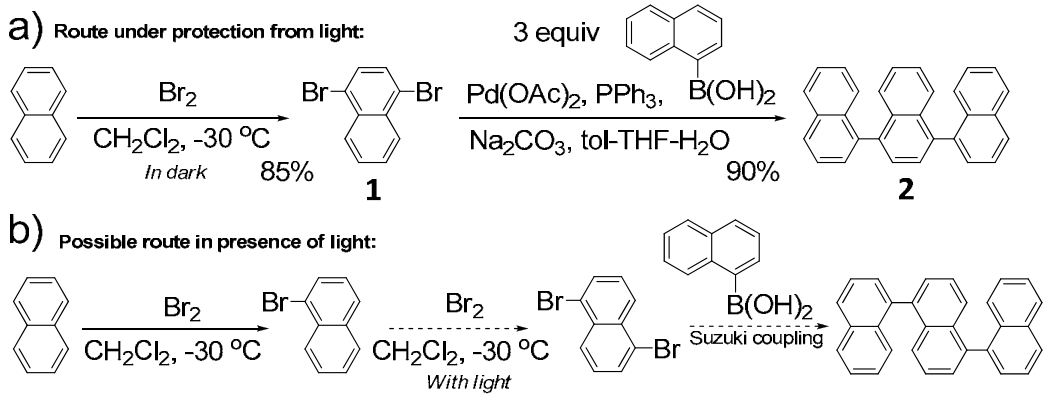

Scheme 46. a) Synthesis of Nap_3 (**2**) via a dibromination (under protection from the light)/Suzuki cross-coupling route and b) possible route in the presence of light.

The parent linear Nap_4 was prepared via a similar route, as reported previously from our research group (Scheme 47).[113] Thus, the treatment of Nap_2 with bromine in chloroform at 0 °C gave 4,4'-dibromo-1,1'-binaphthalene **3** in 94% yield. A Suzuki cross-coupling was performed between the compound **3** and 1-naphthaleneboronic acid affording the Nap_4 (**4**) in quantitative yield.

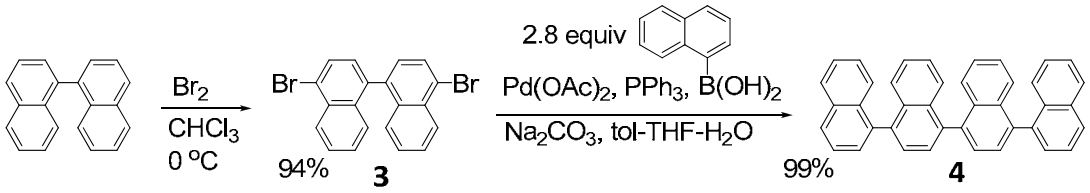

Scheme 47. Preparation of Nap_4 (**4**).

[115] Preparation of 1,4-dibromonaphthalene: Cakmak, O.; Demirtas, I.; Balaydin, H. T. *Tetrahedron*, **2002**, *58*, 5603.

Even for the simple Nap_3, the fairly complex ^{13}C NMR spectrum consists of a large number of the somewhat broadened peaks (Figure 2),[116] suggesting that the product exists as a mixture of the slowly interconverting atropisomeric *aRaR*/*aSaS* (*rac,* C_2) and *aRaS* (*meso* σ) forms. The procedure afforded multigram quantities of Nap_3 **2** and Nap_4 **4** in 77% and 93% yields, respectively, over the two steps.[117]

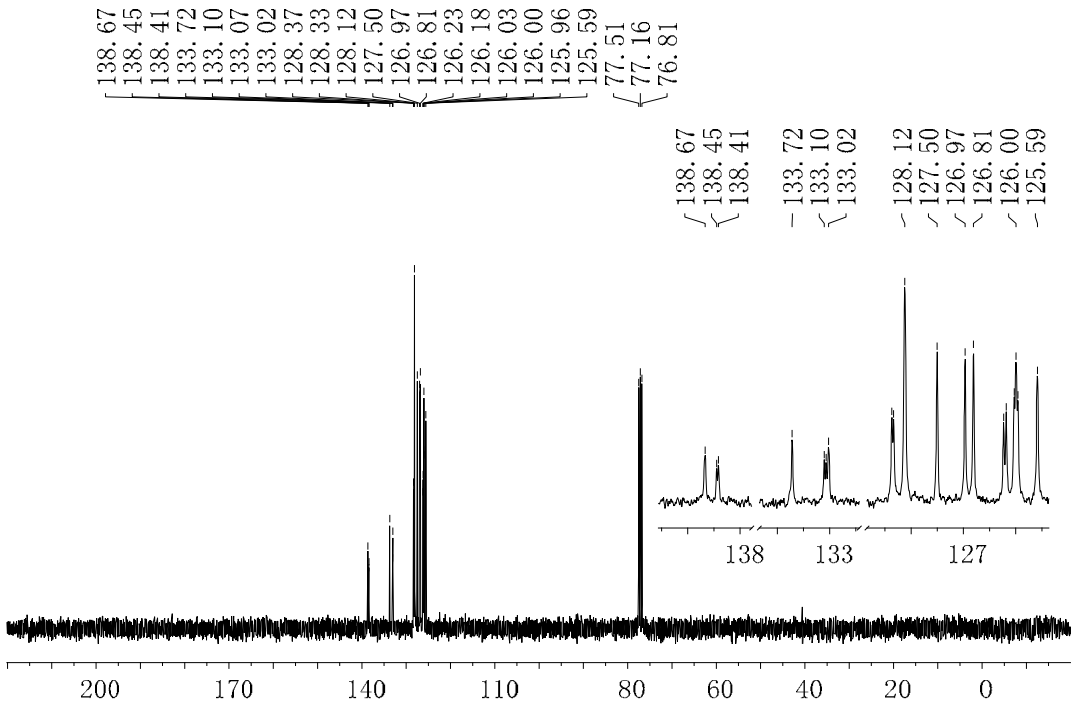

Figure 2. ^{13}C NMR spectrum of Nap_3 (90 MHz, $CDCl_3$).

2.3.2 Oxidative arylation of ternaphthalene (Nap_3) using PIFA/BF_3·Et_2O

As was the case for the parent 1,1'-binaphthalene, the Nap_3 (**2**) could be envisaged undergoing, in addition to the monoarylation, a double arylation to afford **5** (Table 1, *path I)*, or a formal dimerization/arylation to give the linear sexinaphthalene **6** (*path II*).

Thus, the reactivity of Nap_3 with mesitylene was examined under the conditions similar to those used for the binaphthalene.[113] The tests revealed that, unlike for Nap_2, the simple double arylation path I is somewhat preferred for Nap_3. Specifically, the addition of the PIFA/BF_3·Et_2O reagent (0.6 mmol/1.2 mmol) to a mixture of Nap_3 (0.3

---

[116] (a) A slow interconversion is consistent with a ~23 kcal/mol racemization/rotation barrier in 1,1´-binaphthalene: Cooke, A. S.; Harris, M. M. *J. Chem. Soc*. **1963**, 2365. (b) Pu, L. *Chem. Rev*. **1998**, *98*, 2405.

[117] An analogous procedure has been used previously to prepare substituted oligonaphthalenes, see: Bohnen, A.; Koch, K.-H; Lüttke, W.; Müllen, K. *Angew. Chem. Int. Ed.* **1990**, *29*, 525.

mmol) and mesitylene (1.2 mmols) led to a 90% yield of **5a**, a compound previously identified (see Figure 1) as a minor fraction in the arylation of naphthalene (Table 1, entry 1). The reactivity difference between Nap_2 and Nap_3 in the Kita-type arylation is noteworthy. Assuming the monoarylation as the first step, the preference for arylative dimerization in Nap_2 and for selective diarylation in Nap_3 indicates a significantly more favoured second arylation in the latter.

Table 1. Oxidative arylation of Nap_3 using PIFA/$BF_3{\cdot}Et_2O$.[a,b]

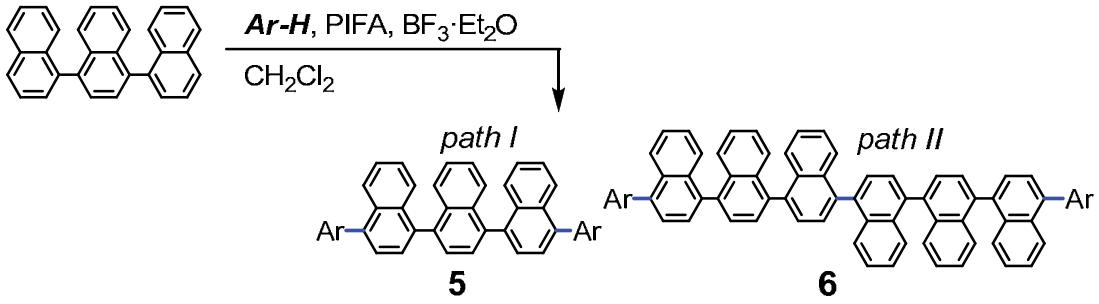

Entry	*Ar-H*				
1	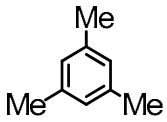	**5a**	90	**6a**	-
2	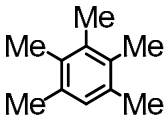	**5b**	89	**6b**	-
3	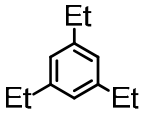	**5c**	71	**6c**	<5%
4	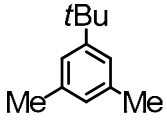	**5d**	33	**6d**	31
5	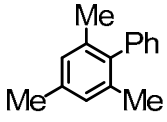	**5e**	32	**6e**	22
6	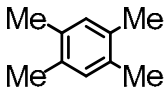	**5f**	31	**6f**	34

[a] Using 0.3 mmol Nap_3, 0.6 mmol of PIFA, 1.2 mmol of Ar-H and 1.2 mmol $BF_3{\cdot}Et_2O$ in CH_2Cl_2 at -78°C. [b] Yields of isolated products.

As previously documented for 4,4'-dimesityl-1,1'-binaphthyl,[113] two singlets are observed in the ^1H NMR spectrum of **5a** due to the diastereotopic *ortho* Me resonances within each mesityl; signal doubling is also observed for the aromatic *m*-H. A diastereotopic relationship between the two halves of the "hindered" mesityl group is a

consequence of their disposition over the two diastereotopic faces of the adjacent naphthalene (Figure 3). The two possible diastereomers of **5a** (*aRaR-rac* and *aRaS-meso*) should each give two *o*-Me signals, for a total of four peaks expected for a mixture. Observation of just two such signals may either mean the existence of a single isomer in solution, or a coincidence in chemical shift due to similar local chemical environments for the Me groups.

A good yield of the double arylation product was also obtained using pentamethylbenzene (Table 1, entry 2, 89%), and triethylbenzene (Table 1, entry 3, 71%). In contrast, the use of bulkier arenes drastically lowered the efficiency of the double arylation, and only a modest 33% of **5d** was isolated using 1-*tert*-butyl-3,5-dimethylbenzene (Table 1, entry 4). Similarly, the use of 2,4,6-trimethyl-1,1'-biphenyl gave **5e** in 32% yield (Table 1, entry 5). In the latter two cases, however, the decrease in the yield of **5** was compensated by the appearance of non-negligible quantities of the octi-arene products **6d** (31%; Table 1, entry 4) and **6e** (22%; Table 1, entry 5). An approx. 1:1 mixture of **5f**:**6f** was also obtained using 1,2,4,5-tetramethylbenzene (Table 1, entry 6).

The detailed experimental procedures can be found in the following experimental section. It should be noted that, to separate the double arylated products (**5c-f**) and the octiarene products (**6c-6f**) from the reaction crude by column is not easy and sometimes, three chromatographic purifications were required.

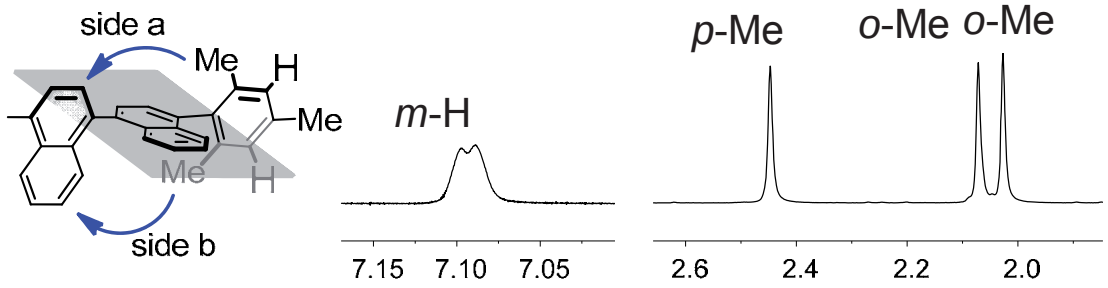

Figure 3. Different chemical environments for the two halves of the mesitylene and the resulting doubling of the ^{1}H pattern.

The formation, albeit in modest yields, of **6c**-**6f**, represents an assembly of a linear octiarene (counting the capping arenes) using simple aromatic building blocks, whereby three new C-C bonds have been formed in the process from six unactivated arene molecules. The new products appear at R_f lower than those of the corresponding

5d-**5f**. In addition to the ^{1}H and ^{13}C NMR spectra, the identity of the new species was also confirmed through high resolution MALDI TOF spectrometry (Figure 4).

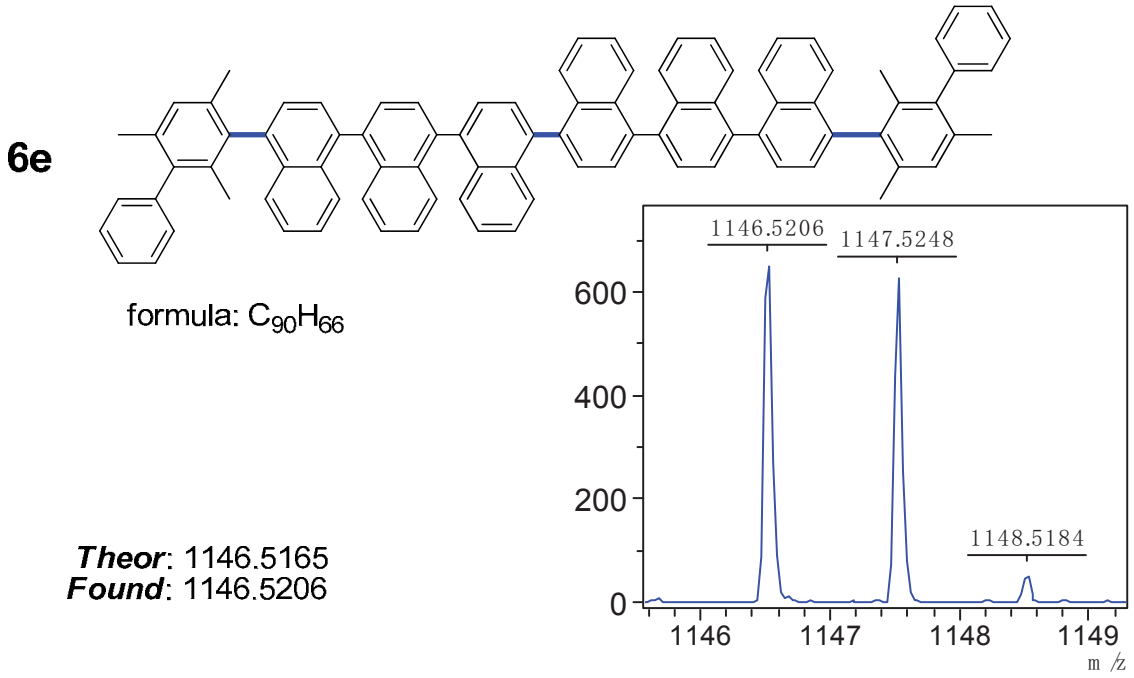

Figure 4. High resolution MALDI-TOF spectrum (experimental) of **6e**.

2.3.3 Effect of the amount of PIFA and arene on the reaction outcome in the oxidative arylation of ternaphthalene

Given that the product distribution in the arylation of Nap_2 was dependent on the amount of PIFA, we looked for a similar influence for Nap_3. Taking as a model the coupling between 1-*tert*-butyl-3,5-dimethylbenzene (entry 4, Table 1) and Nap_3 (ratio 4:1), the yields of the simple and formal dimerization/arylation products **5d** and **6d** were determined as a function of the equivalents of PIFA employed (Figure 5, A). It should be noted that the yields were measured by HPLC equipped with a Ph_2MeSi-functionalized column (reversed-phase, see experimental section for details), since the products were not volatile enough to be quantified by GC. Nap_2 was used as an internal standard. Thus, the yields of both **5d and 6d** grew steadily with increasing amounts of PIFA, with the **6d** reaching a maximum yield (32%) at 2 equiv. In turn, the yield of **5d** reached its maximum (40%) with 3 equiv. of PIFA (at the expense of **6d)**; a further increase in the PIFA loading was found to be detrimental to both. In a separate experiment, the yields of both **5d** and **6d** were found to peak at ~4-5 equiv of ArH added, with **5d** slightly favoured (as expected) at higher ratios of ArH (Figure 5, B).

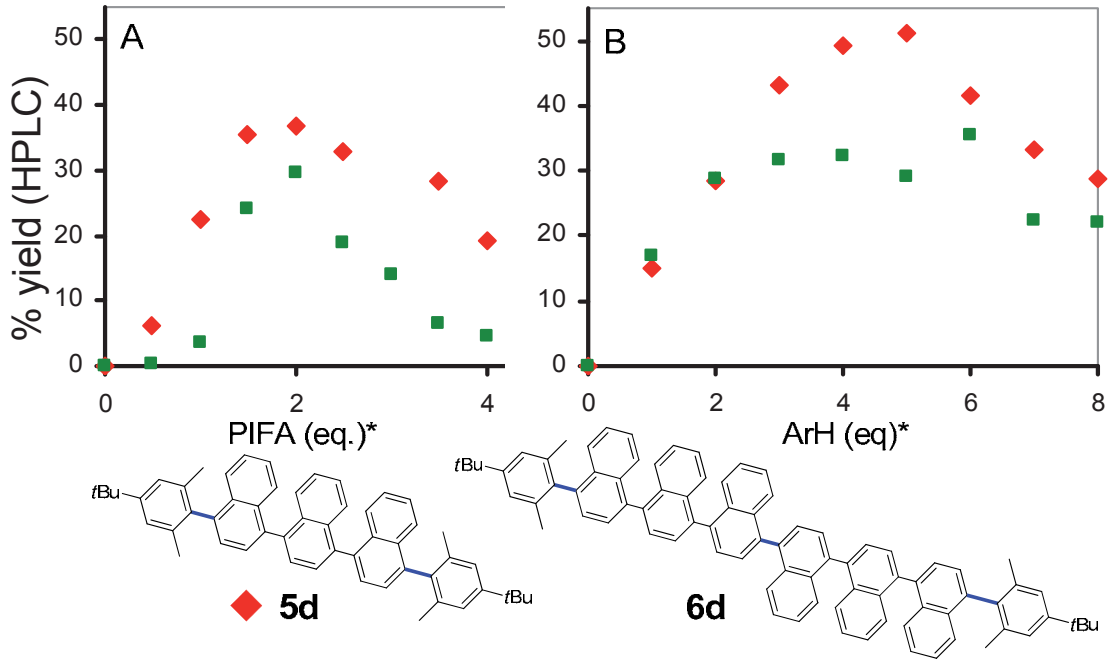

Figure 5. Yields of **5d** and **6d**, (% by HPLC, corrected) as a function of the amount of PIFA (**A**) and ArH (**B**) used. * eq. PIFA = mmol(PIFA)/mmol of Nap_3.

2.3.4 Oxidative arylation of quaternaphthalene using PIFA/BF_3·Et_2O

Finally, the oxidative arylation of the next higher homologue Nap_4 was explored (Scheme 48 and Figure 6). Previously,[113] the arylation of this substrate with mesitylene was found to give predominantly the arylated product **7a** (Figure 6), indicating the substrate's decreased ability to undergo the formation of the larger formally dimeric products, *e. g.*, the deciarene products **8**.

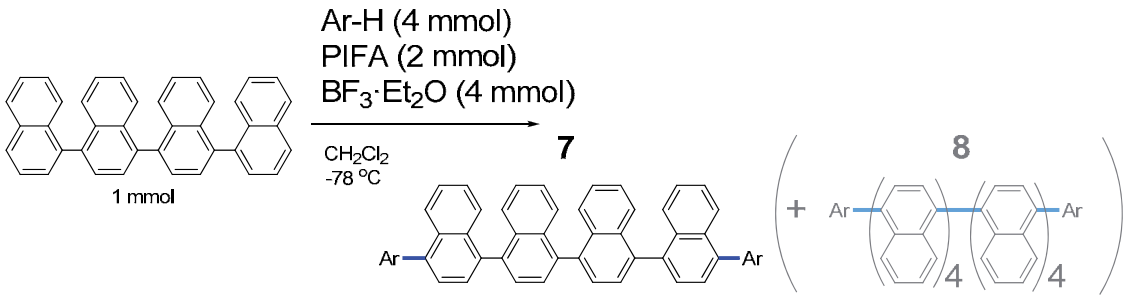

Scheme 48. Oxidative arylation of Nap_4 using PIFA/BF_3·Et_2O.

Building on that preliminary result, and after some optimization, we found that in addition to the 91% yield obtained for **7a**, good yields were reached for the pentamethylphenyl and triethylphenyl derivatives, **7b** (95%) and **7c** (77%), respectively.

Once again, arylation using the bulkier 1-*tert*-butyl-3,5-dimethylbenzene and 2,4,6-trimethyl-1,1'-biphenyl gave moderate yields of the corresponding products **7d** (52%) and **7e** (60%), respectively. In the case of 1,2,4,5-tetramethylbenzene, only a 37% yield of the double arylation product **7f** was obtained. This low yield was attributed to the further oxidative coupling at the *p*-H at the tetramethylphenyl unit of the newly formed **7f**, leading to an intractable oligomer.

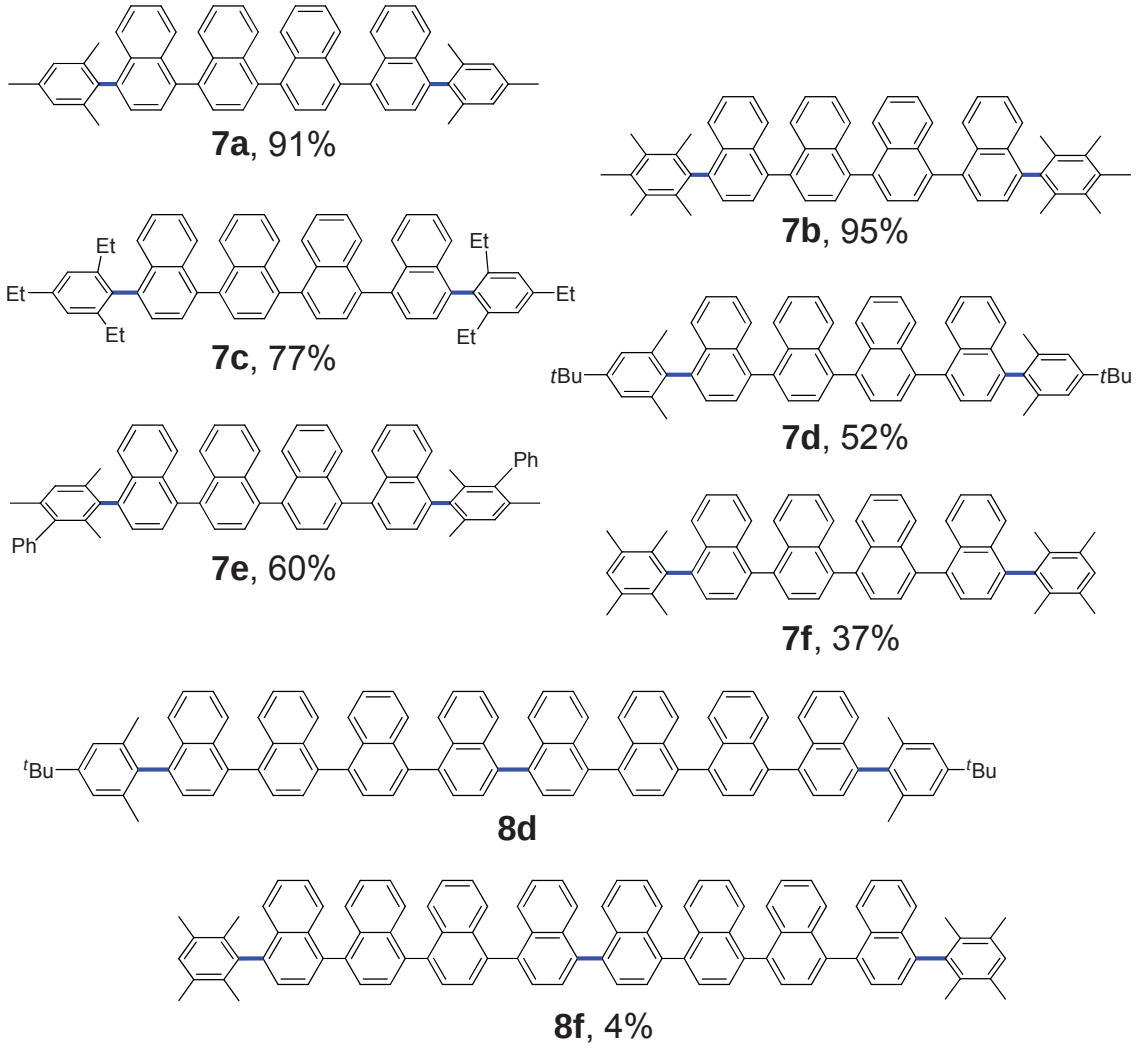

Figure 6. Products obtained via oxidative arylation of Nap_4 using PIFA/$BF_3{\cdot}Et_2O$.

Unlike in the case of Nap_3, however, the use of Nap_4 as substrate did not afford any significant quantities of the larger oligoarenes **8**. Nevertheless, small amounts of **8** were indeed detected in some cases. For example, the TLC analysis in the reaction mixture using 5-*tert*-butyl-*m*-xylene as substrate showed detectable traces of **8d**, which was further confirmed by MALDI-TOF analysis (Figure 7). However, attempts to separate product **8d** were unsuccessful. For 1,2,4,5-tetramethylbenzene as substrate, the TLC showed the principal leading fraction (product **7f**) trailed by a minor component,

consistent with the presence of a larger oligomer. Repeated purification of this fraction by preparative TLC afforded small quantities of the deciarene **8f**, whose identity was confirmed by the observation of a peak at 1274.5852 in the high resolution MALDI-TOF analysis (Figure 7).

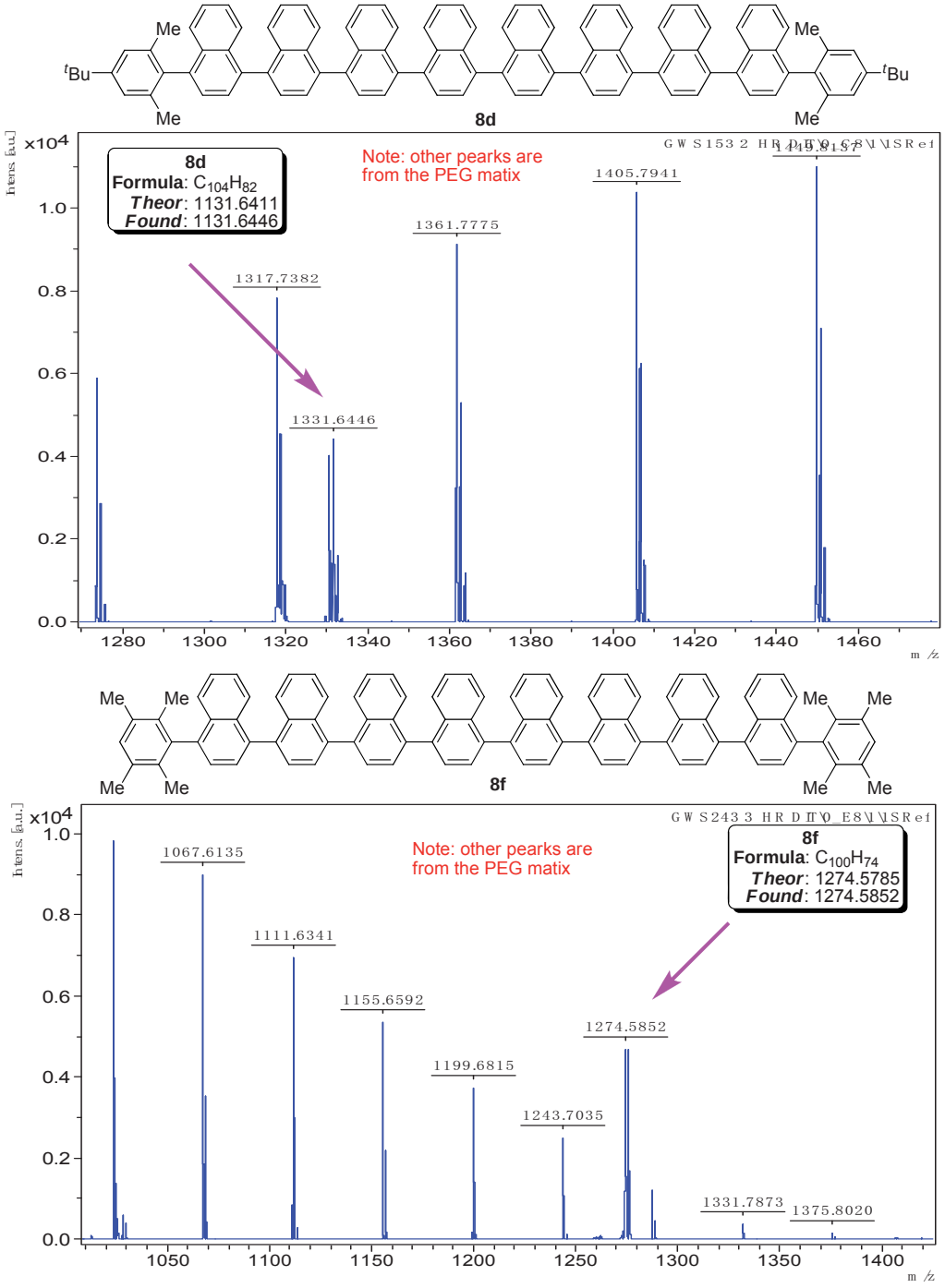

Figure 7. MALDI-TOF spectra (experimental) of **8d** and **8f**.

2.4 Conclusions[118]

In summary, the Kita-type direct dehydrogenative arylation protocol using the BF_3-activated PIFA has now been successfully applied to the arylation of the linear ter- and quaternaphthalenes. In contrast to the reactions using naphthalene and binaphthalene, the arylation of oligonaphthalenes has led predominantly to the double-arylation products **5** and **7**. Still, moderate yields of the larger multiarene **6** could be obtained in some cases for Nap_3. Such synthesis of an octiarene is remarkable, in that it constitutes a direct oxidative metal-free assembly of four unfunctionalized building block molecules. The interest in practical synthesis of such large oligonaphthalenes lies in their optoelectronic properties relevant in the design of solar cells or OLED devices.[119] Finally, small quantities of the formal dimerizative arylation products **8d** and **8f** have also been detected (4% isolated yield for **8f**), representing the one-pot assembly of a linear deciarene.

[118] **Guo, W.**; Faggi, E.; Sebastián, R. M.; Vallribera, A.; Pleixats, R.; Shafir, A. *J. Org. Chem.* **2013**, *78*, 8169

[119] Pschirer, N. G.; Kohl, C.; Nolde, F.; Qu, J.; Mullen. K. *Angew. Chem. Int. Ed.* **2006**, *45*, 1401.

2.5 Experimental section

2.5.1 General

All reagents were purchased from commercial sources and used as received. 1,4-Dibromonaphthalene was prepared following a reported procedure;[115] 2-phenylmesitylene was prepared following a Suzuki coupling protocol as previously described;[113] 4,4'-dibromo-1,1'-binaphthalene was prepared as already described.[113] Dichloromethane was dried by passing through a column of activated molecular sieves. Silica gel used corresponds to 230-440 mesh. Routine ^1H and ^{13}C NMR spectra were recorded on 250 and 360 MHz instruments. ^1H NMR chemical shifts are given relative to the residual proton signal of $CDCl_3$ (7.26 ppm). ^{13}C NMR spectra are given relative to the ^{13}C resonance of $CDCl_3$ (77.16 ppm). High resolution MALDI-TOF spectra were recorded using dithranol as the matrix and polyethylene glycol as internal reference. IR data were obtained using a spectrometer equipped with an ATR probe. The yields of compounds **5d** and **6d** related to conditions optimization (see Figure 5 for details) were determined by HPLC, using a column packed with diphenyl silica as stationary phase (Pursuit XRs Diphenyl from Agilent Technologies, particle size: 3 μm) and a mixture of hexane/acetonitrile/isopropanol (10/20/70) as a mobile phase with a flow rate of 0.6 mL/min. For all the analyses, 1,1'-binaphthalene was used as internal standard.

2.5.2 Syntheses of the parents ternaphthalene and quaternaphthalene

2.5.2.1 Synthesis of 1,4-dibromonaphthalene, **1**.[115]

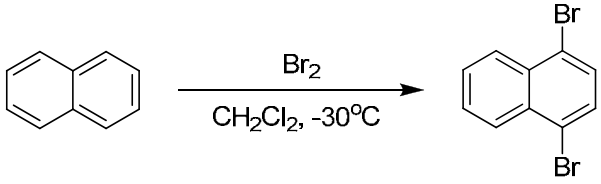

A stirred solution of naphthalene (8.970 g, 69.692 mmol) in dichloromethane (70 mL) was cooled to -30 °C and then bromine (33.600 g, 10.8 mL, 210 mmol) was added dropwise over 10 min under protection from the light while maintaining the temperature at -30 °C with constant magnetic stirring. The mixture was then stirred for 20 h under protection from the light at -25 °C. At this point, the excess of bromine was quenched with an aqueous solution of $NaHSO_3$. The organic layer was separated and further washed with aqueous solutions of $NaHSO_3$ and NaOH (2 M). The organic layer was then dried over anhydrous Na_2SO_4, and concentrated to dryness to afford the crude compound, which was further purified by silica gel chromatography using hexane as

eluent. White powder, yield: 17.000 g, 85%; mp 79-81 °C; lit[115]. 80-82 °C; ^{1}H NMR (360 MHz, $CDCl_3$): δ 8.25 (dd, *J* = 6.5, 3.3 Hz, 2H), 7.65 (dd, *J* = 6.4, 3.3 Hz, 2H), 7.63 (s, 2H) ppm. $^{13}C\{^{1}H\}$ NMR (90 MHz, $CDCl_3$): δ 133.1, 130.2, 128.3, 127.9, 122.7 ppm; IR (ATR) *v* (cm^{-1}): 3067, 1583, 1492, 1365, 1251, 959, 812, 749.

2.5.2.2 Synthesis of 1,1':4',1''–ternaphthalene (Nap_3), **2**.

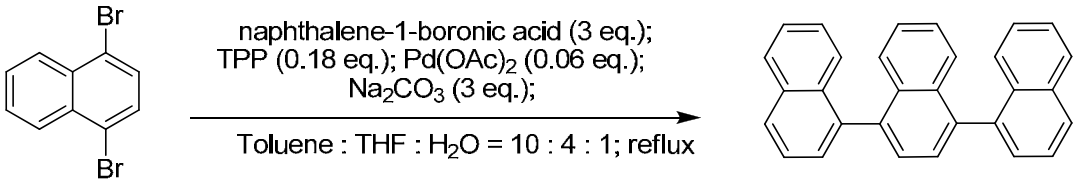

To a mixture of 1,4-dibromonaphthalene (2.000 g, 6.994 mmol), naphthalene-1-boronic acid (3.610 g, 20.990 mmol), $Pd(OAc)_2$ (94 mg, 0.42 mmol), PPh_3 (0.330 g, 1.258 mmol), and Na_2CO_3 (2.230 g, 21.038 mmol) were added H_2O (14 mL), THF (53 mL) and toluene (140 mL), and the resulting suspension was heated to reflux under N_2 for 22 hours. The reaction mixture was then cooled to room temperature and the solvent was evaporated. The crude product was purified by column chromatography (silica gel, hexane:AcOEt 20:1; R_f = 0.43) affording 1,1':4',1''-ternaphthalene. Cotton-like white solid, yield: 2.400 g, 90%; mp 188-190 °C; ^{1}H NMR (250 MHz, $CDCl_3$): δ 8.00-7.97 (m, 4H), 7.68-7.48 (m, 12H), 7.43-7.35 (m, 2H), 7.29-7.26 (m, 2H); $^{13}C\{^{1}H\}$ NMR (90 MHz, $CDCl_3$): δ 138.7, 138.5, 138.4, 133.7, 133.10, 133.07, 133.0, 128.37, 128.33, 128.1, 127.5, 127.0, 126.8, 126.23, 126.18, 126.03, 126.00, 126.96, 125.6. HRMS (MALDI-TOF) m/z calcd for $C_{30}H_{20}$ $[M]^+$:380.1554, found: 380.1569; IR (ATR) *v* (cm^{-1}): 3043, 1571, 1505, 1375, 1256, 776, 758.

2.5.2.3 Synthesis of 4,4'-dibromo-1,1'-binaphthalene, **3**.[113]

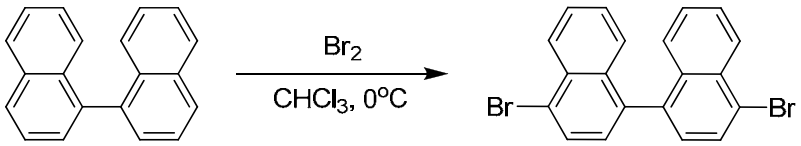

A stirred solution of 1,1'-binaphthalene (3.050 g, 11.993 mmol) in chloroform (96 mL) was cooled to 0 °C. Bromine (9.010 g, 2.9 mL, 56.383 mmol) was added dropwise over 10 min under protection from the light while maintaining the temperature at 0 °C and with a steady magnetic stirring. The mixture was stirred for 4 h protected from the light at 0 °C. At this point, aqueous $NaHSO_3$ solution was added to quench the excess of bromine. The organic layer was separated and washed successively with aqueous $NaHSO_3$ solution, aqueous NaOH solution (2 M) and water. The organic layer was

dried over anhydrous Na_2SO_4, and concentrated to dryness to afford the crude compound, which was recrystallized from boiling chloroform. White needle crystals, 4.600 g, yield: 94 %; mp 214-216 °C; lit.[115] 215-217 °C;. ^{1}H NMR (360 MHz, $CDCl_3$): δ 8.37 (d, *J* = 8.6 Hz, 2H), 7.90 (d, *J* = 8.6 Hz, 2H), 7.62-7.58 (m, 2H), 7.35-7.31 (m, 6H); $^{13}C\{^1H\}$ NMR (90 MHz, $CDCl_3$): δ 137.8, 134.0, 132.1, 129.6, 128.3, 127.6, 127.1, 123.1 ppm; IR (ATR) *v* (cm^{-1}): 3071, 1582, 1450, 1366, 1248, 954, 817, 754.

2.5.2.4 Synthesis of 1,1':4',1'':4'',1'''- quaternaphthalene (Nap_4), **4**.[113]

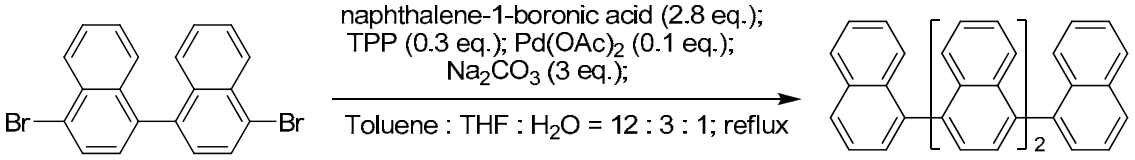

To a mixture of 1,4-dibromonaphthalene (2.470 g, 5.993 mmol), naphthalene-1-boronic acid (2.890 g, 16.803 mmol), $Pd(OAc)_2$ (135 mg, 0.601 mmol), PPh_3 (488 mg, 1.861 mmol), and Na_2CO_3 (1.910 g, 18.019 mmol), were added of H_2O (9 mL), THF (36 mL) and toluene (108 mL) and the resulting suspension was heated to reflux for 24 hours. Reaction was monitored by GC to ensure complete conversion of the dibromide as well as the intermediate monoarylation product. The reaction mixture was cooled to room temperature and the solvent was evaporated to dryness. The crude product was purified by column chromatography (silica gel, neat hexane; R_f = 0.1). Cotton-like white solid, yield: 3.000 g, 99%; mp 178-181 °C; ^{1}H NMR (250 MHz, $CDCl_3$): δ 8.01-7.99 (m, 4H), 7.77-7.49 (m, 16H), 7.45-7.32 (m, 6H); $^{13}C\{^1H\}$ NMR (90 MHz, $CDCl_3$): δ 138.7, 138.6, 138.5, 133.7, 133.13, 133.09, 128.40, 128.36, 128.2, 127.7, 127.6, 127.1, 126.8, 126.3, 126.2, 126.1, 125.6 ppm; HRMS (MALDI-TOF) *m/z* calcd for $C_{40}H_{26}$ $[M]^+$: 506.2029, found: 506.2019; IR (ATR) *v* (cm^{-1}): 3041, 1592, 1506, 1373, 1256, 800, 761.

2.5.3 Arylation procedure and relevant data of the products

2.5.3.1 General procedure for the oxidative arylation

To a solution of 1,1':4',1''-ternaphthalene, Nap_3, or 1,1':4',1'':4'',1'''- quaternaphthalene, Nap_4, (0.300 mmol) and the chosen arene (1.200 mmol) in dry dichloromethane (2 mL) at -78 ºC and under nitrogen atmosphere, were added BF_3•Et_2O (170 mg, 150 µL, 1.200 mmol) and a solution of PIFA (258 mg, 0.600 mmol) in dichloromethane (anhydrous, 2 mL). The resulting deep purple reaction mixture was kept below -50 ºC for 3 hours; the cold bath was removed and the mixture was allowed to stir for additional 20 hours. The mixture was quenched with saturated aqueous $NaHCO_3$ (5 mL)

and was transferred to a separatory funnel. The organic layer was separated and the aqueous phase was extracted with dichloromethane (2 x 20 mL). The combined organic fraction was dried over anhydrous Na_2SO_4 and concentrated to dryness. The crude product was purified by flash chromatography. Given the difficult separation due to similar R_f values for the major and the minor components, a second or even a third purification by flash chromatography were performed when needed. In some cases, preparatory paper TLC was used to obtain samples suitable for analysis.

2.5.3.2 4, 4''-Dimesityl-1,1':4',1''-ternaphthalene, **5a**.

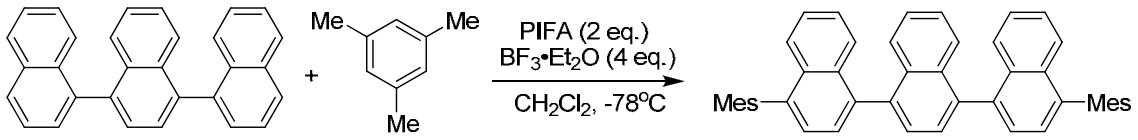

Following the general procedure, ternaphthalene, **Nap$_3$** (150 mg, 0.394 mmol) was allowed to react with 1,3,5-trimethylbenzene (230 µL, 0.846 g/mL, 1.610 mmol). Column chromatography: silica gel, hexane:AcOEt 70:1, R_f = 0.25. Light yellow powder, 223 mg, yield: 90%; mp 212-214 °C; ^{1}H NMR (360 MHz, $CDCl_3$): δ 7.72 - 7.59 (m, 8H), 7.52 - 7.44 (m, 2H), 7.41 - 7.33 (m, 8H), 7.10-7.09 (two overlapping s, 2H + 2H), 2.45 (s, 6H), 2.07 (s, 6H), 2.03 (s, 6H); ^{13}C{^{1}H} NMR (90 MHz, $CDCl_3$): δ 138.9, 138.6, 137.7, 137.2, 137.1, 137.0, 133.42, 133.36, 133.3, 133.2, 132.1, 128.3, 128.0, 127.7, 127.2, 127.0, 126.5, 126.0, 125.6, 21.3, 20.7 ppm. HRMS (MALDI-TOF) *m/z* calcd for $C_{48}H_{40}$ $[M]^+$: 616.3124, found: 616.3125; IR (ATR) *v* (cm^{-1}): 3038, 2919, 2854, 1374, 1260, 844, 762.

2.5.3.3 4, 4''-Bis(2,3,4,5,6-pentamethylphenyl)-1,1':4',1''-ternaphthalene, **5b**.

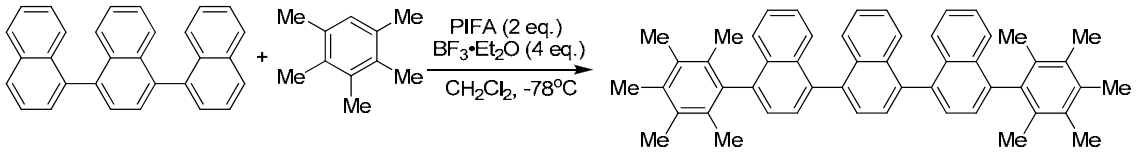

Following the general procedure, ternaphthalene (114 mg, 0.300 mmol) was allowed to react with 2,3,4,5,6-pentamethylbenzene (178 mg, 1.201 mmol). Column chromatography: silica gel, hexane:AcOEt 70:1, R_f = 0.16. Light yellow powder, 180 mg, yield: 89%; mp 198-201 °C; ^{1}H NMR (360 MHz, $CDCl_3$): δ 7.73 - 7.62 (m, 8H), 7.56 - 7.52 (m, 2H), 7.46 - 7.34 (m, 8H), 2.42 (s, 6H), 2.37 - 2.36 (two overlapping s, 6H + 6H), 2.01 (s, 6H), 1.96 (s, 6H); ^{13}C{^{1}H} NMR (90 MHz, $CDCl_3$): δ 140.9, 138.7, 138.6, 137.6, 137.55, 137.45, 134.4, 133.2, 132.73, 132.70, 132.65, 132.56, 128.0, 127.7, 127.1, 126.70, 126.67, 126.6, 126.0, 125.9, 18.6, 18.5, 17.1, 16.9 ppm. HRMS (MALDI-TOF)

m/z calcd for $C_{52}H_{48}$ $[M]^+$: 672.3751, found: 672.3752; IR (ATR) *v* (cm^{-1}): 3040, 2990, 2916, 1372, 906, 761, 731.

2.5.3.4 4, 4''-bis(2,4,6-triethylphenyl)-1,1':4',1''-ternaphthalene, **5c**.

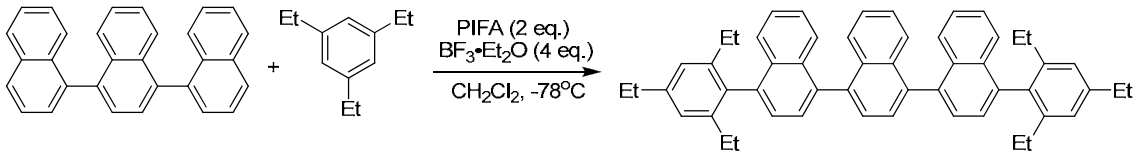

Following the general procedure, ternaphthalene (114 mg, 0.300 mmol) was allowed to react with 1,3,5-triethylbenzene (226 µL, 0.862 g/mL, 1.200 mmol). Column chromatography: silica gel, hexane : AcOEt gradient from 250:1 to 100:1 (R_f = 0.09). Light brown powder, 150 mg, yield: 71%; mp 135-138 °C; ^{1}H NMR (360 MHz, $CDCl_3$): δ 7.74 - 7.62 (m, 8H), 7.50 - 7.47 (m, 4H), 7.37 – 7.35 (m, 6H), 7.14 (two overlapping s, 2H + 2H), 2.82 – 2.76 (q, 4H, *J* = 7.4 Hz), 2.39 – 2.29 (m, 8H), 1.41 – 1.37 (t, 6H, *J* = 7.6 Hz), 1.11 – 1.03 (m, 12 H); ^{13}C{^{1}H} NMR (90 MHz, $CDCl_3$): δ 143.7, 143.2, 143.1, 138.3, 137.7, 136.0, 133.20, 133.18, 133.0, 127.8, 127.7, 127.12, 127.05, 126.0, 125.94, 125.91, 125.32, 125.29, 29.0, 27.02, 26.95, 15.9, 15.8, 15.7 ppm. HRMS (MALDI-TOF) *m/z* calcd for $C_{54}H_{52}$ $[M]^+$: 700.4064, found: 700.4078; IR (ATR) *v* (cm^{-1}): 3044, 2967, 2933, 2873, 1570, 1460, 1375, 840, 764.

2.5.3.5 4, 4''-bis(4-(tert-butyl)-2,6-dimethylphenyl)-1,1':4',1''-ternaphthalene, **5d**.

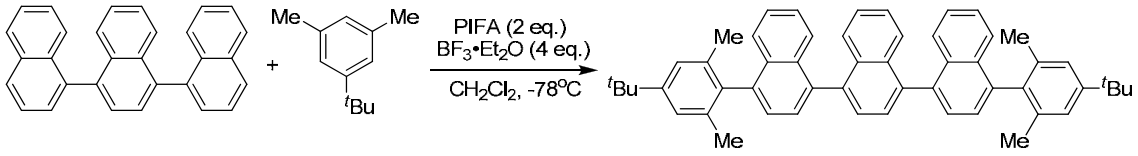

Following the general procedure, ternaphthalene (114 mg, 0.300 mmol) was allowed to react with 5-tert-butyl-*m*-xylene (195 mg, 225 µL, 1.200 mmol). Column chromatography: silica gel, hexane:AcOEt gradient from 250:1 to 100:1 (R_f = 0.21). Light yellow powder, 70 mg, yield: 33%; mp > 300 °C; ^{1}H NMR ($CDCl_3$): δ 7.72 – 7.58 (m, 8H), 7.52 - 7.44 (m, 4H), 7.40 - 7.33 (m, 6H), 7.25 (two overlapping s, 2H + 2H), 2.09 (s, 6H), 2.05 (s, 6H), 1.44 (s, 18H). ^{13}C{^{1}H} NMR (90 MHz, $CDCl_3$): δ 150.2, 139.1, 138.64, 138.58, 137.6, 136.9, 136.7, 133.3, 132.2, 128.0, 127.7, 127.2, 127.1, 126.4, 126.1, 126.0, 124.5, 34.6, 31.7, 21.1 ppm. HRMS (MALDI-TOF) *m/z* calcd for $C_{54}H_{52}$ $[M]^+$: 700.4064, found: 700.4068; IR (ATR) *v* (cm^{-1}): 3040, 2952, 2864, 1456, 1375, 841, 763.

2.5.3.6 4,4''''-Bis(4-*tert*-butyl-2,6-dimethylphenyl)-1,1':4',1'':4'',1''':4''',1'''':4'''',1'''''-sexinaphthalene, **6d**.

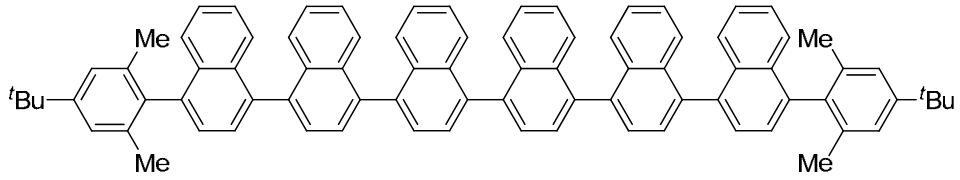

From the same experiment used to obtain **5d**, an additional product was isolated that corresponded to the hexanaphthalene **6d**. Light brown powder, 50 mg, yield: 31%. ^{1}H NMR (360 MHz, $CDCl_3$): δ 7.87 - 7.65 (m, 20H), 7.56 - 7.54 (m, 2H), 7.52 - 7.39 (m, 14H), 7.29 (two overlapping s, 2H + 2H), 2.14 – 2.09 (two s, 6H + 6H), 1.47 (s, 18H). ^{13}C{^{1}H} NMR (90 MHz, $CDCl_3$): δ 150.2, 139.1, 138.6, 137.6, 136.9, 136.7, 133.4, 133.2, 132.3, 128.0, 127.8, 127.2, 126.4, 126.1, 126.02, 125.97, 124.5, 34.6, 31.7, 21.1 ppm. HRMS (MALDI-TOF) *m/z* calcd for $C_{84}H_{70}$ $[M]^+$: 1078.5472, found: 1078.5488; IR (ATR) *v* (cm^{-1}): 3039, 2951, 1509, 1372, 837, 760.

2.5.3.7 4, 4''-Bis(2,4,6-trimethyl-[1,1'-biphenyl]-3-yl)-1,1':4',1''-ternaphthalene, **5e**.

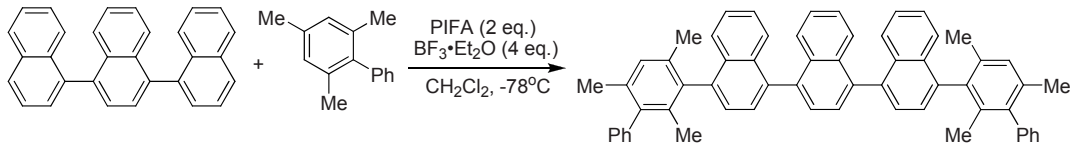

Following the general procedure, ternaphthalene (114 mg, 0.300 mmol) was allowed to react with 2-phenylmesitylene (235 mg, 1.200 mmol). Column chromatography: silica gel, hexane:AcOEt 70:1 (R_f = 0.15). Orange powder, 74 mg, yield: 32%; mp 209-212 °C; ^{1}H NMR (360 MHz, $CDCl_3$): δ 7.73 - 7.60 (m, 10H), 7.49 - 7.28 (m, 18H), 7.21 and 7.20 (two overlapping s, 1H + 1H), 2.16 (s, 6H), 2.11 (s, 3H), 2.06 (s, 3H), 1.78 (s, 3H), 1.73 (s, 3H) ppm; ^{13}C{^{1}H} NMR (90 MHz, $CDCl_3$): δ 141.7, 140.0, 139.3, 137.7, 137.6, 136.1, 135.4, 135.2, 133.4, 133.1, 132.2, 129.6, 129.5, 128.8, 128.6, 128.0, 127.7, 127.2, 127.0, 126.7, 126.5, 126.1, 126.0, 21.2, 20.8, 19.0, 18.9 ppm. HRMS (MALDI-TOF) *m/z* calcd for $C_{60}H_{48}$ $[M]^+$: 768.3756, found: 768.3774; IR (ATR) *v* (cm^{-1}): 3038, 2918, 1601, 1441, 1373, 763, 702.

2.5.3.8 4,4''''-Bis(2,4,6-trimethylbiphenyl-3-yl)-1,1':4',1'':4'',1''':4''',1'''':4'''',1'''''-sexinaphthalene, **6e**.

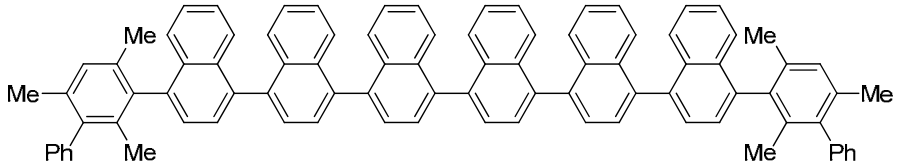

From the same experiment used to obtain **5e**, an additional product was isolated that corresponded to the hexanaphthalene **6e**. Light red powder, 38 mg, yield: 22%; mp 278-281 °C; ^{1}H NMR (360 MHz, $CDCl_3$): δ 7.85 - 7.62 (m, 22H), 7.53 - 7.29 (m, 24H), 7.23 and 7.21 (two overlapping s, 1H + 1H), 2.17 (two overlapping s, 3H + 3H), 2.12 (s, 3H), 2.08 (s, 3H), 1.79 (s, 3H), 1.75 (s, 3H); ^{13}C NMR (101 MHz, $CDCl_3$): δ 141.7, 140.0, 139.4, 138.7, 137.6, 136.1, 135.4, 135.2, 133.4, 133.2, 132.3, 129.7, 129.5, 128.8, 128.6, 127.8, 126.7, 126.6, 126.1, 21.2, 20.1, 19.0 ppm. HRMS (MALDI-TOF) *m/z* calcd for $C_{90}H_{66}$ $[M]^+$:1146.5159, found: 1146.5198; IR (ATR) *v* (cm^{-1}): 30378, 2918, 2856, 1371, 838, 760, 702.

2.5.3.9 4, 4''- Bis(2,3,5,6-tetramethylphenyl)-1,1':4',1''-ternaphthalene, **5f**.

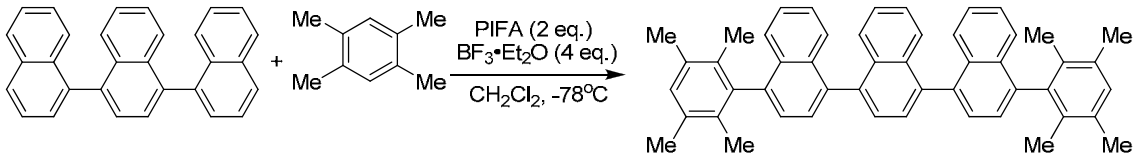

Following the general procedure, ternaphthalene (114 mg, 0.300 mmol) was allowed to react with 1,2,4,5-tetramethylbenzene (161 mg, 1.200 mmol). Column chromatography: silica gel, hexane : AcOEt 400 : 1 (hexane : AcOEt 50 : 1, R_f = 0.42). White powder, 60 mg, yield: 31%; mp 165-168 °C; ^{1}H NMR (360 MHz, $CDCl_3$): δ 7.74 - 7.63 (m, 8H), 7.49 - 7.37 (m, 10H), 7.15 (s, 2H), 2.37 (two overlapping s, 6H + 6H), 1.96 (s, 6H), 1.91 (s, 6H) ppm. ^{13}C{^{1}H} NMR (90 MHz, $CDCl_3$): δ 140.2, 139.9, 138.62, 128.56, 137.5, 133.7, 133.3, 133.2, 133.14, 133.11, 132.4, 130.8, 127.9, 127.7, 127.1, 127.0, 126.5, 126.4, 126.33, 126.31, 125.98, 125.95, 20.4, 17.34 and 17.25 (partial overlap of the latter two signals) ppm. HRMS (MALDI-TOF) *m/z* calcd for $C_{50}H_{44}$ $[M]^+$: 644.3438, found 644.3441; IR (ATR) *v* (cm^{-1}): 3039, 2918, 2863, 1466, 1369, 824, 761.

2.5.3.10 4,4''''-Bis(2,3,5,6-tetramethylphenyl)-1,1':4',1'':4'',1''':4''',1'''':4'''',1'''''-sexinaphthalene, **6f**.

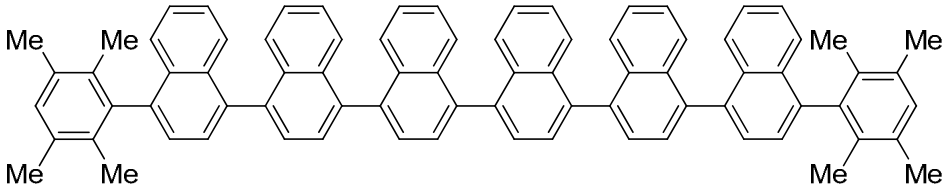

From the same experiment used to obtain **5f**, an additional product was isolated that corresponded to the hexanaphthalene **6f**. Peach powder, 52 mg, yield: 34%; mp 256-259 °C; ^{1}H NMR (360 MHz, $CDCl_3$): δ 7.86 - 7.65 (m, 20H), 7.49 - 7.39 (m, 16H), 7.15 (s, 2H), 2.39 – 2.37 (two overlapping s, 6H + 6H), 1.97 (s, 6H), 1.93 (s, 6H);

$^{13}C\{^{1}H\}$ NMR (62.5 MHz, $CDCl_3$): δ 140.29, 140.28, 139.9, 138.8, 138.7, 138.52, 138.48, 137.5, 133.8, 133.3, 133.14, 133.11, 132.5, 130.9, 128.0, 127.8, 127.1, 126.5, 126.4, 126.1, 126.0, 20.4, 17.4, 17.3. HRMS (MALDI-TOF) *m/z* calcd for $C_{80}H_{62}$ $[M]^+$: 1022.4852, found: 1022.4870; IR (ATR) *v* (cm^{-1}): 3038, 2917, 1370, 826, 759.

2.5.3.11 4, 4'''-Dimesityl-1,1':4',1'':4'',1''' – quaternaphthalene, **7a**.

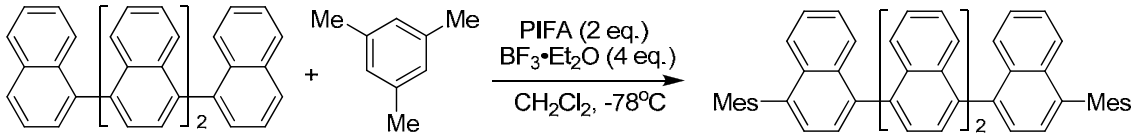

Following the general procedure, quaternaphthalene (203 mg, 0.400 mmol) was allowed to react with mesitylene (192 mg, 222 µL, 1.600 mmol). Column chromatography: silica gel, hexane : AcOEt 70 : 1 (R_f = 0.29). Off-white powder, 271 mg, yield: 91%; mp 203-205 °C; ^{1}H NMR (360 MHz, $CDCl_3$): δ 7.84-7.62 (m, 12H), 7.56 - 7.51 (m, 2H), 7.49 - 7.35 (m, 10H), 7.11 - 7.10 (two overlapping s, 2H + 2H), 2.46 (s, 6H), 2.08 (s, 6H), 2.04 (s, 6H); $^{13}C\{^{1}H\}$ NMR (101 MHz, $CDCl_3$): δ 139.0, 138.8, 138.7, 138.6, 138.5, 137.72, 137.71, 137.2, 133.4, 133.3, 133.2, 132.3, 128.3, 127.8, 127.2, 127.1, 126.5, 126.1, 126.0, 21.3, 20.7. HRMS (MALDI-TOF) *m/z* calcd for $C_{58}H_{46}$ $[M]^+$: 742.3594, found : 742.3605; IR (ATR) *v* (cm^{-1}): 3040, 2952, 2917, 2861, 1571, 1375, 839, 762.

2.5.3.12 4, 4'''-Bis(2,3,4,5,6-pentamethylphenyl)-1,1':4',1'':4'',1'''-quaternaphthalene, **7b**.

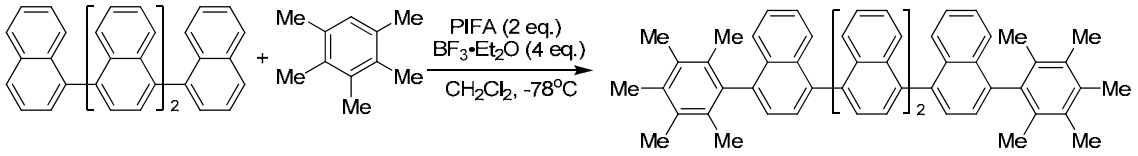

Following the general procedure, quaternaphthalene (152 mg, 0.300 mmol) was allowed to react with 1,2,3,4,5-pentamethyl benzene (178 mg, 1.201 mmol). Column chromatography: silica gel, hexane : AcOEt 100 : 1, (hexane : AcOEt 70 : 1, R_f = 0.13). Off-white powder, 227 mg, yield: 95%; mp 212-215 °C; ^{1}H NMR (360 MHz, $CDCl_3$): δ 7.83-7.37 (m, 24H), 2.44 (s, 6H), 2.38 (two overlapping s, 6H + 6H), 2.04 (s, 6H), 1.99 (s, 6H); ^{13}C NMR (62.5 MHz, $CDCl_3$): δ 141.0, 138.82, 138.76, 138.54, 138.49, 137.6, 137.4, 134.4, 133.3, 133.2, 132.73, 132.69, 132.6, 128.0, 127.8, 127.1, 126.71, 126.69, 126.1, 125.9, 18.6, 18.55, 18.46, 17.1, 16.9, 16.8 ppm. HRMS (MALDI-TOF) *m/z* calcd for $C_{62}H_{54}$ $[M]^+$: 798.4220, found: 798.4198; IR (ATR) *v* (cm^{-1}): 3038, 2915, 1508, 1372, 839, 760.

2.5.3.13 4, 4'''- Bis(2,4,6-triethylphenyl)-1,1':4',1'':4'',1'''-quaternaphthalene, **7c**.

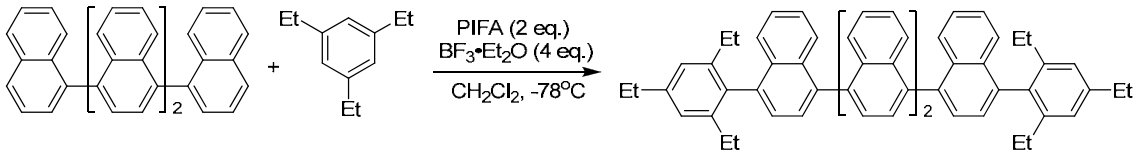

Following the general procedure, quaternaphthalene (152 mg, 0.300 mmol) was allowed to react with 1,3,5-triethylbenzene (195 mg, 226 µL, 1.200 mmol). Column chromatography: silica gel, hexane:AcOEt 60:1 (R_f = 0.26). Pale-yellow powder, 191 mg, yield: 77%; mp 165-168 °C; ^{1}H NMR (360 MHz, $CDCl_3$): δ 7.83 - 7.62 (m, 12H), 7.55 - 7.49 (m, 4H), 7.43 - 7.33 (m, 8H), 7.16 (s, 2H), 7.15 (s, 2H), 2.80 (q, *J* = 7.5 Hz, 4H), 2.43 - 2.28 (m, 8H), 1.42 (t, *J* = 7.5 Hz, 6H), 1.14 - 1.06 (m, 12H); ^{13}C{^{1}H} NMR (62.5 MHz, $CDCl_3$): δ 143.8, 143.2, 143.1, 138.8, 138.7, 138.6, 138.5, 138.4, 137.7, 136.0, 133.23, 133.19, 133.15, 133.06, 127.79, 127.76, 127.66, 127.14, 127.07, 126.6, 126.1, 126.0, 125.9, 125.33, 125.30, 29.0, 27.03, 26.96, 15.9, 15.8, 15.7 ppm. HRMS (MALDI-TOF) *m/z* calcd for $C_{64}H_{58}$ $[M]^+$: 826.4533, found 826.4538; IR (ATR) *v* (cm^{-1}): 3040, 2962, 2931, 2870, 1458, 1421, 1372, 838, 761.

2.5.3.14 4, 4'''- Bis(4-tert-butyl-2,6-dimethylphenyl)-1,1':4',1'':4'',1'''-quaternaphthalene, **7d**.

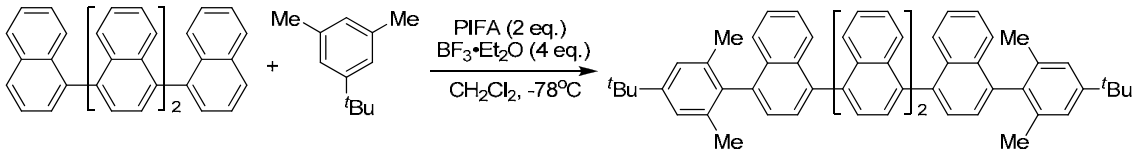

Following the general procedure, quaternaphthalene (152 mg, 0.300 mmol) was allowed to react with 5-tert-butyl-*m*-xylene (195 mg, 225 µL, 1.200 mmol). Column chromatography: silica gel, hexane:AcOEt 70 : 1 (R_f = 0.22). White powder, 130 mg, yield: 52%; mp 219-222 °C; ^{1}H NMR (360 MHz, $CDCl_3$): δ 7.81 - 7.62 (m, 12H), 7.52 - 7.48 (m, 4H), 7.40 - 7.37 (m, 8H), 7.27 (broad s, 4H), 2.11 (s, 6H), 2.07 (s, 6H), 1.45 (s, 18H); ^{13}C{^{1}H} NMR (90 MHz, $CDCl_3$): δ 150.3, 139.2, 139.1, 138.80, 138.75, 138.6, 138.51, 138.49, 137.6, 136.9, 136.66, 136.65, 133.4, 133.3, 133.2, 132.3, 128.0, 127.8, 127.1, 126.4, 126.04, 125.96, 124.5, 34.6, 31.7, 21.1 ppm. HRMS (MALDI-TOF) *m/z* calcd for $C_{64}H_{58}$ $[M]^+$: 826.4533, found: 826.4551; IR (ATR) *v* (cm^{-1}): 3040, 2953, 2865, 1481, 1373, 964, 837, 761.

2.5.3.15 4, 4''''''- Bis(4-tert-butyl-2,6-dimethylphenyl)-1,1':4',1'':4'',1''':4''',1'''':4'''',1''''': 4''''',1''''': 4''''',1''''''- octinaphthalene, **8d**.

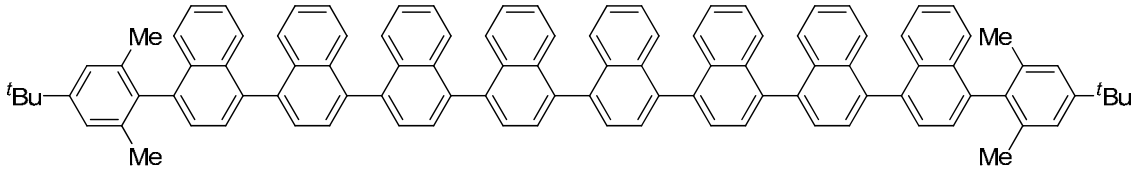

From the same experiment used to obtained **7d**, trace amount of an additional product was isolated that corresponded to the octinaphthalene **8d**. HRMS (MALDI-TOF) m/z calcd for $C_{104}H_{82}$ $[M]^+$: 1330.6411, found: 1330.6446.

2.5.3.16 4, 4'''- Bis(2,4,6-trimethylbiphenyl-3-yl)-1,1':4',1'':4'',1'''-quaternaphthalene, **7e**.

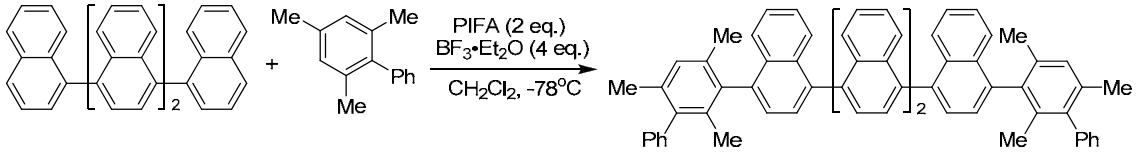

Following the general procedure, quaternaphthalene (152 mg, 0.300 mmol) was allowed to react with 2-phenylmesitylene (235 mg, 1.200 mmol). Column chromatography: silica gel, hexane:AcOEt 50:1 (R_f = 0.35). White powder, 160 mg, yield: 60%; mp 250-253 °C; ^{1}H NMR (360 MHz, $CDCl_3$): δ 7.80 - 7.61 (m, 14H), 7.53 - 7.28 (m, 20H), 7.22 (s, 1H), 7.21 (s, 1H), 2.16 (s, 6H), 2.12 (s, 3H), 2.07 (s, 3H), 1.79 (s, 3H), 1.75 (s, 3H); ^{13}C{^{1}H} NMR (90 MHz, $CDCl_3$): δ 141.8, 140.0, 139.4, 138.8, 138.5, 137.7, 137.6, 136.1, 135.4, 135.2, 133.4, 133.2, 132.3, 129.7, 129.6, 128.9, 128.6, 128.1, 127.7, 127.1, 126.6, 126.1, 21.2, 20.8, 19.0, 18.9 ppm. HRMS (MALDI-TOF) *m/z* calcd for $C_{70}H_{54}$ $[M]^+$: 894.4220, found: 894.4224; IR (ATR) *v* (cm^{-1}): 3038, 2949, 2918, 2860, 1441, 1372, 952, 838, 761.

2.5.3.17 4,4'''-Bis(2,3,5,6-tetramethylphenyl)-1,1':4',1'':4'',1'''–quaternaphthalene, **7f**.

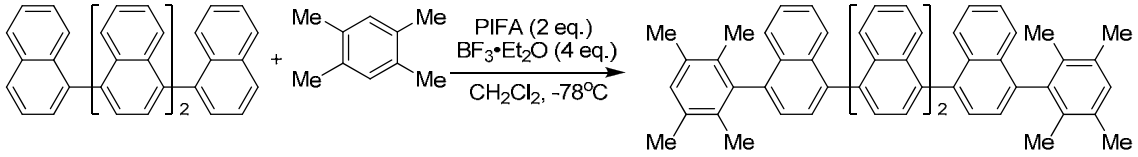

Following the general procedure, quaternaphthalene (152 mg, 0.300 mmol) was allowed to react with 1,2,4,5-tetramethylbenzene (161 mg, 1.200 mmol). Column chromatography: silica gel, hexane : AcOEt 50 : 1, R_f = 0.35. Pale yellow powder, 86 mg, yield: 37%; mp 212-215 °C; ^{1}H NMR (360 MHz, $CDCl_3$): δ 7.82 - 7.64 (m, 12H), 7.51 - 7.35 (m, 12H), 7.15 (s, 2H), 2.38 (s, 6H), 2.37 (s, 6H), 1.96 (s, 6H), 1.92 (s, 6H). ^{13}C{^{1}H} NMR (90 MHz, $CDCl_3$): δ 140.3, 140.0, 138.80, 138.76, 138.74, 138.56, 138.55,

137.55, 137.54, 133.8, 133.31, 133.27, 133.23, 133.20, 133.14, 133.11, 132.5, 130.9, 128.0, 127.78, 127.76, 127.1, 126.49, 126.46, 126.38, 126.35, 126.07, 126.02, 126.00, 125.98, 20.41, 20.39, 17.34, 17.32, 17.25 ppm. HRMS (MALDI-TOF) *m/z* calcd for $C_{60}H_{50}$ $[M]^+$: 770.3907, found: 770.3874; IR (ATR) *v* (cm^{-1}): 3038, 2918, 2864, 1450, 1378, 826, 764..

2.5.3.18 4,4’’’’’’-Bis(2,3,5,6-tetramethylphenyl)-1,1':4',1'':4’’,1’’’:4’’’,1’’’’:4’’’’,1’’’’’: 4’’’’’,1’’’’’’: 4’’’’’’,1’’’’’’’- octinaphthalene, **8f**.

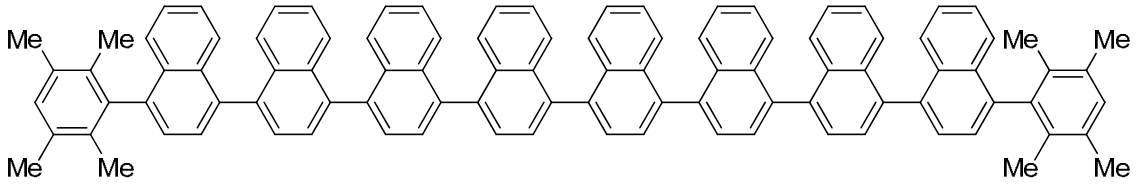

From the same experiment used to obtained **7f**, an additional product was isolated that corresponded to the octinaphthalene **8f**. Purple powder, 8 mg, yield: 4%; ^{1}H NMR (360 MHz, $CDCl_3$): δ 7.87 - 7.66 (m, 28H), 7.48 - 7.42 (m, 20H), 7.15 (s, 2H), 2.37 (s, 12H), 1.97 (s, 6H), 1.93 (s, 6H). HRMS (MALDI-TOF) *m/z* calcd for $C_{100}H_{74}$ $[M]^+$: 1274.5785, found: 1274.5852.

2.5.4 HPLC traces of the optimization process

The internal standard: 1,1’-binaphthalene, Nap_1

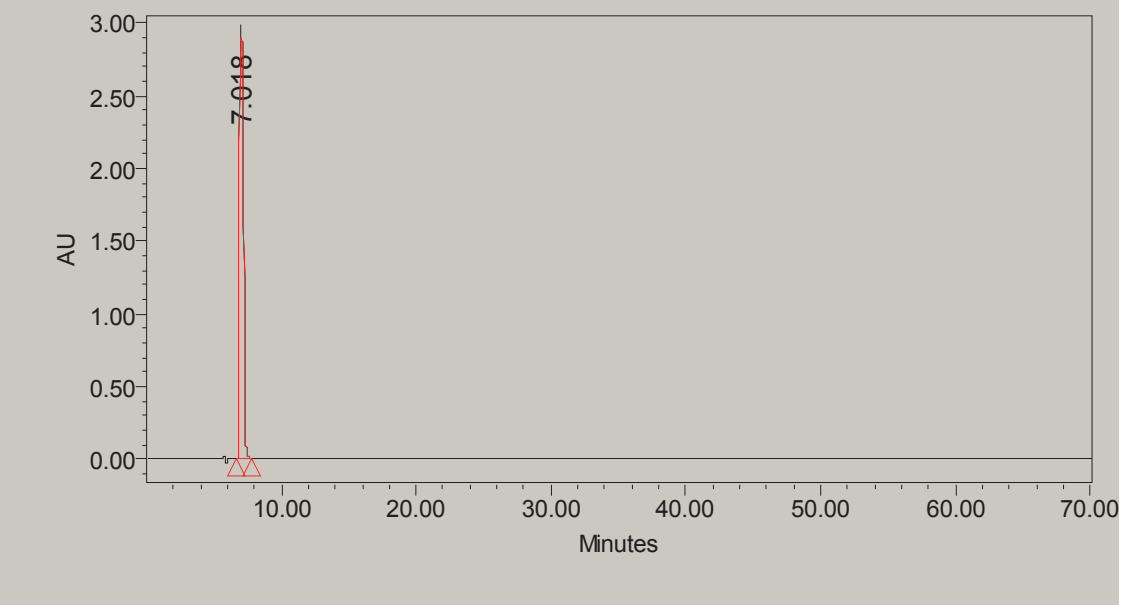

Peak	Retention Time	Area	% Area	Height
1	7.018	61448828	100.00	2902175

Starting material: ternaphthalene, Nap_3

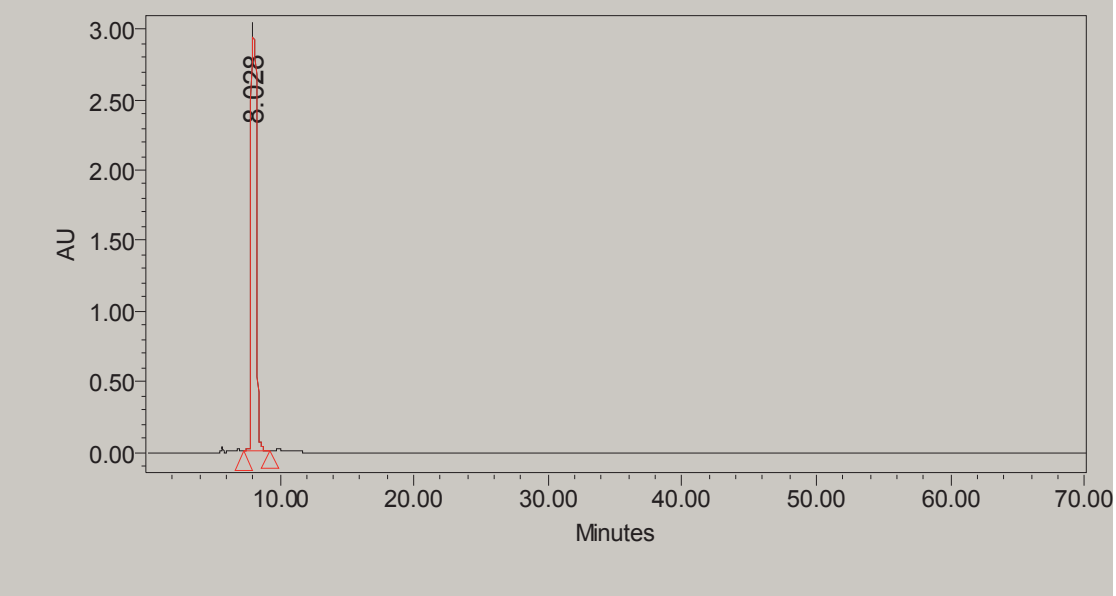

Peak	Retention Time	Area	% Area	Height
1	8.028	80931657	100.00	2945384

Product of 4, 4''-bis(4-(tert-butyl)-2,6-dimethylphenyl)-1,1':4',1''-ternaphthalene, **5d**

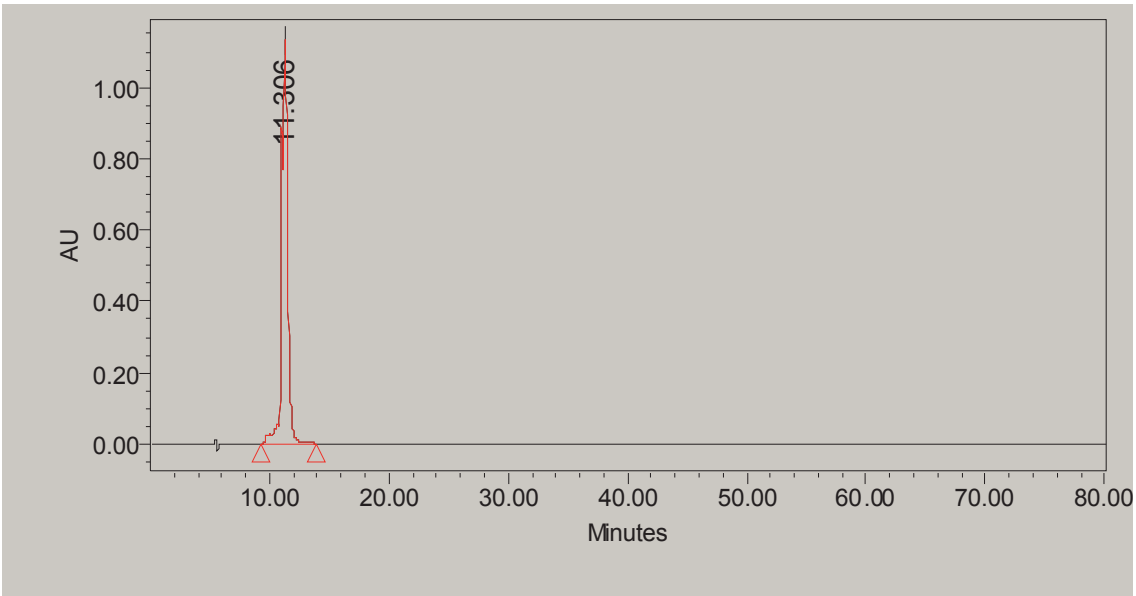

Peak	Retention Time	Area	% Area	Height
1	11.306	40186328	100.00	1129632

4,4’’’’’-Bis(4-*tert*-butyl-2,6-dimethylphenyl)-1,1':4',1":4’’,1’’’:4’’’,1’’’’:4’’’’,1’’’’’-sexinaphthalene, **6d**

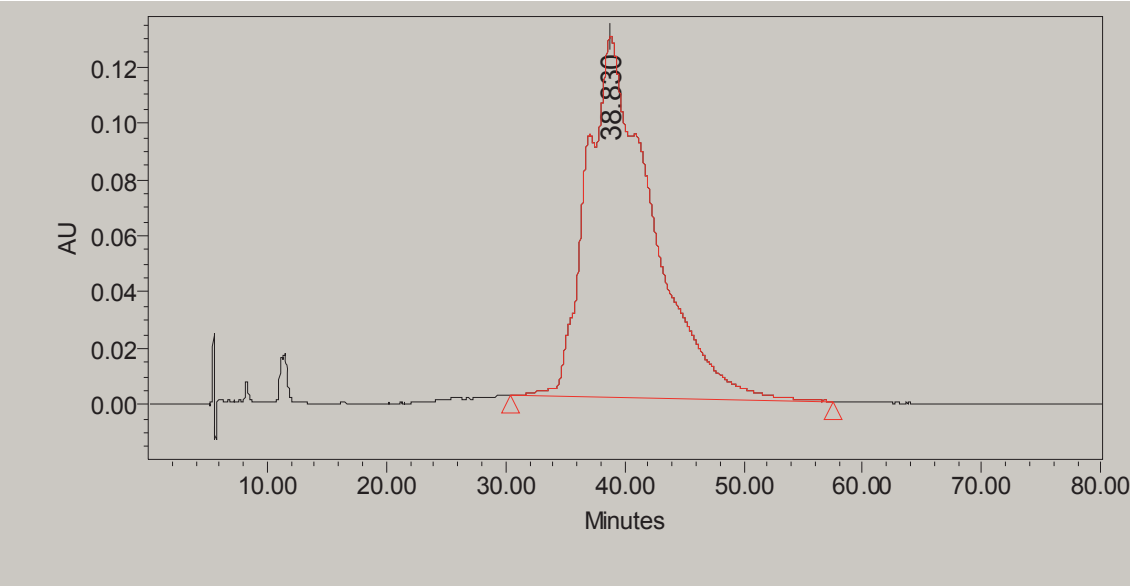

Peak	Retention Time	Area	% Area	Height
1	38.830	48736640	100.00	127803

A mixture of pure **5d** and **6d**

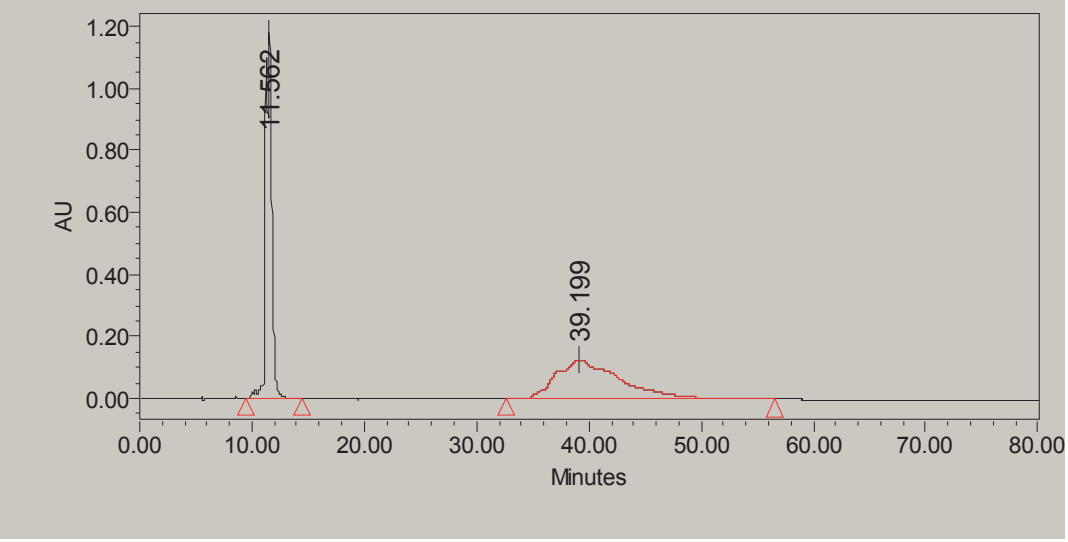

Peak	Retention Time	Area	% Area	Height
1	11.562	45402734	48.16	1182222
2	39.199	48878012	51.84	124908

An example of the reaction mixture including the **5d**, **6d** and the internal standard Nap_1

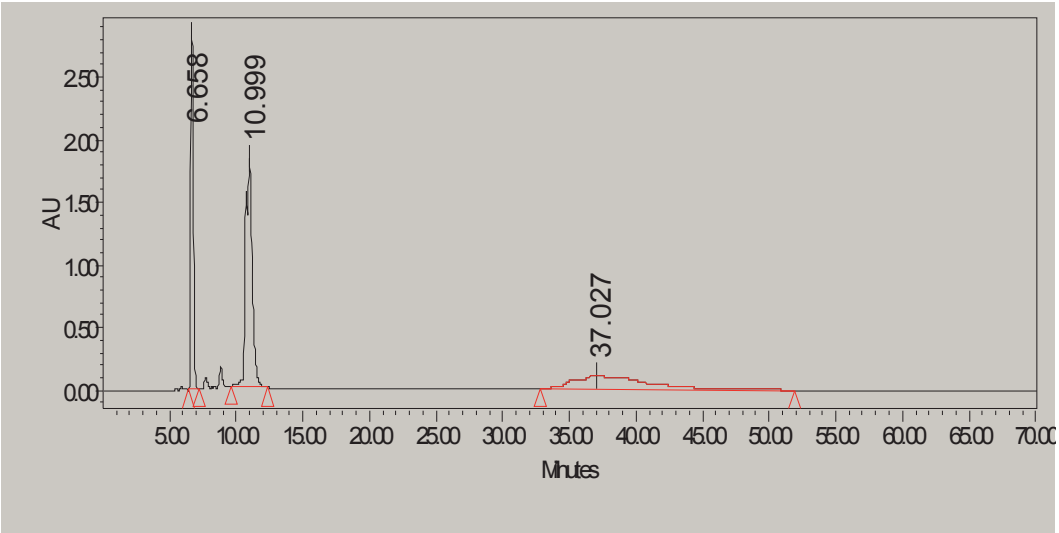

Peak	Retention Time	Area	% Area	Height
1	6.658	41414557	28.24	2827446
2	10.999	63520497	43.32	1823975
3	37.027	41707791	28.44	117923

Part I. Hypervalent iodine species: reagents and intermediates in oxidative processes

CHAPTER 3

Sol-gel immobilized aryl iodides for the catalytic oxidative α-tosyloxylation of ketones

Chapter 3. Sol-gel immobilized aryl iodides for the catalytic oxidative α-tosyloxylation of ketones

3.1 Introduction

Due to the good leaving ability of the -OTs group, α-tosyloxyketones are important building blocks for the construction of various heteroaromatic compounds, such as thiazoles, oxazoles, selenazoles, imidazoles, pyrazoles, and benzofurans.[120] α-Tosyloxyketones can be synthesized by the oxidative C-H functionalization at the α position of carbonyl compounds. The earlier methodologies for the preparation of α-tosyloxyketones required the toxic thalium[121] or a stoichiometric amount of hypervalent iodine oxidant.[120h] Later on, some improvements were achieved by only using a catalytic amount of iodine reagents with the help of a cheaper and easy accessible terminal oxidant.[122] More recently, efforts have been focused on the development of various recyclable iodine-based catalysts for this kind of transformations.

3.1.1 Oxidative α-tosyloxylation of ketones with iodine reagents

Koser, in 1982, described the stoichiometric use of hypervalent organoiodine(III) reagent, PhI(OH)(OTs), as an especially effective reagent for the oxidative introducing the -OTs group at the α position of ketones (Scheme 49).

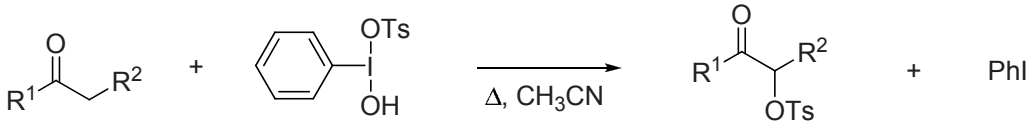

Scheme 49. α-Tosyloxylation of ketones by a stoichiometric amount of Koser's reagent with a full equivalent of iodobenzene as byproduct.

---

[120] See the following review articles and references therein: (a) Moriarty, R. M.; Vaid, R. K.; Koser, G. F. *Synlett* **1990**, 365. (b) Koser, G. F. *Aldrichimica Acta* **2001**, *34*, 89. (c) Prakash, O.; Saini, N.; Sharma, P. K. *Heterocycles* **1994**, *38*, 409. Papers: (d) Neilands, O.; Karele, B. *J. Org. Chem. USSR* **1970**, *6*, 885. (e) Koser, G. F.; Wettach, R. H.; Troup, J. M.; Bertram, A. F. *J. Org. Chem.* **1976**, *41*, 3609. (f) Koser, G. F.; Wettach, R. H. *J. Org. Chem.* **1977**, *42*, 1476. (g) Koser, G. F.; Wettach, R. H.; Smith, C. S. *J. Org. Chem.* **1980**, *45*, 1543. (h) Koser, G. F.; Relenyi, A. G.; Kalos, A. N.; Rebrovic, L.; Wettach, R. H. *J. Org. Chem.* **1982**, *47*, 2487. (i) Moriarty, R. M.; Penmasta, R.; Awasthi, A. K.; Epa, W. R.; Prakash, I. *J. Org. Chem.* **1989**, *54*, 1101. (j) Moriarty, R. M.; Vaid, R. K.; Hopkins, T. E.; Vaid, B. K.; Prakash, O. *Tetrahedron Lett.* **1990**, *31*, 201. (k) Tuncay, A.; Dustman, J. A.; Fisher, G.; Tuncay, C. I. *Tetrahedron Lett.* **1992**, *33*, 7647. (l) Moriarty, R. M.; Vaid, B. K.; Duncan, M. P.; Levy, S. G.; Prakash, O.; Goyal, S. *Synthesis* **1992**, 845. (m) Prakash, O.; Goyal, S. *Synthesis* **1992**, 629. (n) Prakash, O.; Rani, N.; Goyal, S. *J. Chem. Soc., Perkin Trans. 1* **1992**, 707. (o) Prakash, O.; Saini, N.; Sharma, P. K. *Synlett* **1994**, 221. (p) Vrama, R. S.; Kumar, D.; Liesen, P. J. *J. Chem. Soc., Perkin Trans. 1* **1998**, 4093. (q) Lee, J. C.; Choi, J.-H. *Synlett* **2001**, 234.

[121] Khanna, M.; Garg, C. P.; Kapoor, R. P. *Tetrahedron Lett.* **1992**, *33*, 1495.

[122] (a) Dohi, T.; Maruyama, A.; Yoshimura, M.; Morimoto, K.; Tohma, H.; Kita, Y. *Angew. Chem. Int. Ed.* **2005**, *44*, 6193. Two minireviews: (b) Richardson, R. D.; Wirth, T. *Angew. Chem. Int. Ed.* **2006**, *45*, 4402. (c) Dohi, T.; Kita, Y. *Chem. Commun.* **2009**, 2073.

In this process, as shown in Scheme 50, the reaction is initiated by the electrophilic addition of PhI(OH)OTs to the corresponding enol tautomers to yield intermediate α-phenyliodonio ketone. Nucleophilic displacement of iodobenzene from the α-carbon in the intermediate results in the final α-tosyloxyketone product accompanying with a full equivalent of iodobenzene as byproduct.[120h]

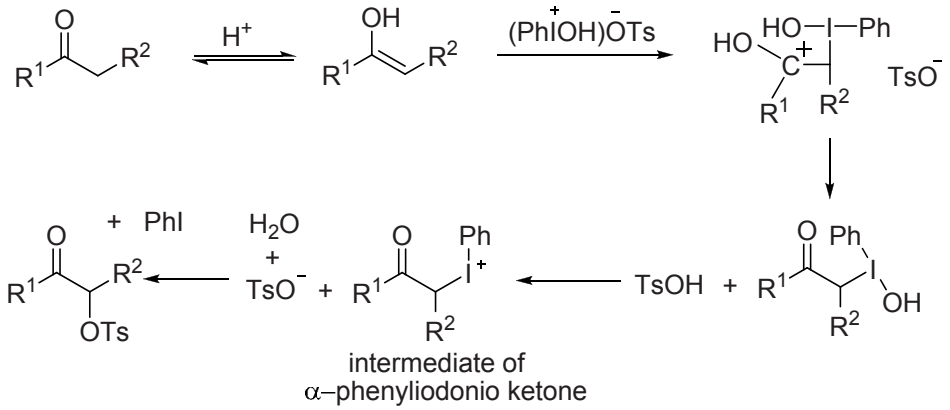

Scheme 50. Plausible mechanism of α-tosyloxylation of ketones by stoichiometric amount of PhI(OH)OTs.

Since this pioneer work on hypervalent iodine reagents, the synthetic use of hypervalent organoiodanes has become a hot topic due to the unique reactivity of these reagents beyond that of a simple oxidant.[2d,2i,2n] In addition, the use of a hypervalent iodine reagent may, in a number of cases, obviate the need for a metal additive, a particularly attractive feature in pharmaceutical chemistry. Moreover, hypervalent iodine reagent-based protocols may, in some extent, be more environmentally friendly, easily accessible and low cost than those of valuable metals such as Rh, Au, etc..[2,120]

Althought widely applicable, one can note that the stoichiometric use of hypervalent iodine reagents usually leads to the production of an equimolar amount of organic iodine waste, such as PhI. This iodoarene side-product may, in principle, be easily removed at the end of the reaction[2i,2n] and could, once again, be converted to a hypervalent iodane through a simple oxidation. Interestingly, several recent publications describe a modification of this process, whereby catalytic quantities of the aryl iodides are used in the presence of a cheaper terminal oxidant, which ensures the *in situ* regeneration of the organoiodine(III) reagent.[122] This budding area of research was recently the subject of two minireviews.[122b-c] In particular, following a 2005

publication by Ochiai and coworkers on the PhI-catalyzed α-acetoxylation of ketones,[123] Yamamoto and Togo[124] recently reported that iodobenzene also catalyzes the oxidative α-tosyloxylation of ketones (as illustrated in Scheme 51) under mild conditions using *m*-CPBA as an oxidant, with promising results achieved at 10 mol% of iodobenzene. In that process, on the basis of Koser's proposal, Togo proposed[124] the PhI(OH)(OTs) is first generated *in situ* through the oxidation of PhI by *m*-CPBA in the presence of *p*-toluenesulfonic acid. This species then reacts with the enol form of ketone to provide α-tosyloxyketone, thus regenerating PhI, and therefore, closing the catalytic cycle (Scheme 51).

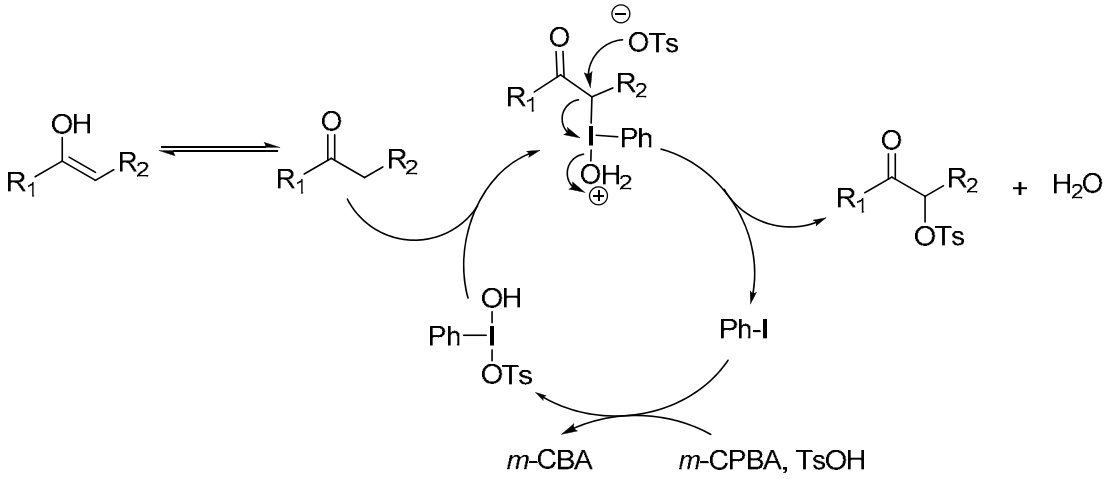

Scheme 51. Reaction pathway for PhI-catalyzed α-tosyloxylation of ketones in the presence of *m*-CPBA as stoichiometric oxidant.

The same group later reported[125] the same tosyloxylation transformation involving the use of the *m*-CPBA and *p*-toluenesulfonic acid combination in the presence of a catalytic amount of molecular iodine in a mixture of acetonitrile and 2,2,2-trifluoroethanol. It was found that the addition of *t*-butylbenzene improved the overall yield. The authors proposed that the α-tosyloxylation reaction was catalyzed, in this case, by the *in situ* generated iodoarenes, formed through the iodination (by I_2) of the *p*-toluenesulfonic acid or *t*-butylbenzene in the presence of *m*-CPBA (Scheme 52). Indeed, the treatment of *p*-toluenesulfonic acid monohydrate (2.1 mmol) and *m*-CPBA (2.2 mmol) in the presence of molecular iodine (2.4 mmol) in a mixture of acetonitrile (3 mL) and 2,2,2-trifluoroethanol (3 mL) at 60 °C for five hours provided 4-iodotoluene in

---

[123] Ochiai, M.; Takeuchi, Y.; Katayama, T.; Sueda, T.; Miyamoto, K. *J. Am. Chem. Soc.* **2005**, *127*, 12244.

[124] (a) Yamamoto, Y.; Kawano, Y.; Toy, P. H.; Togo, H. *Tetrahedron* **2007**, *63*, 4680. (b) Yamamoto, Y.; Togo, H. *Synlett* **2006**, 798.

[125] Tanaka, A.; Moriyama, K.; Togo, Hideo. *Synlett* **2011**, 1853.

54% yield. A similar methodology has been developed by others through the *in situ* formation of iodobenzene by the reaction of benzene and ammonium iodide in the presence of *m*-CPBA.[126]

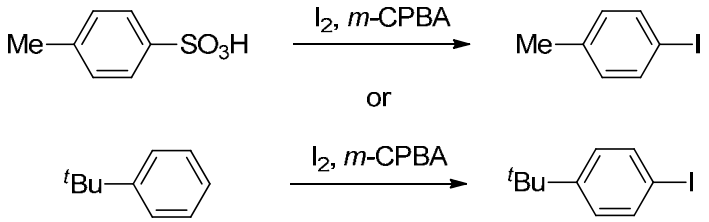

Scheme 52. Formation of iodoarenes from *p*-toluenesulfonic acid or *t*-butylbenzene by reaction with molecular iodine in the presence of *m*-CPBA.

Interestingly, the Togo group recently described that this kind of organic transformations can also proceed with Oxone as oxidant in the presence of a substoichiometric amount of iodine (0.7 eq.) (Scheme 53).

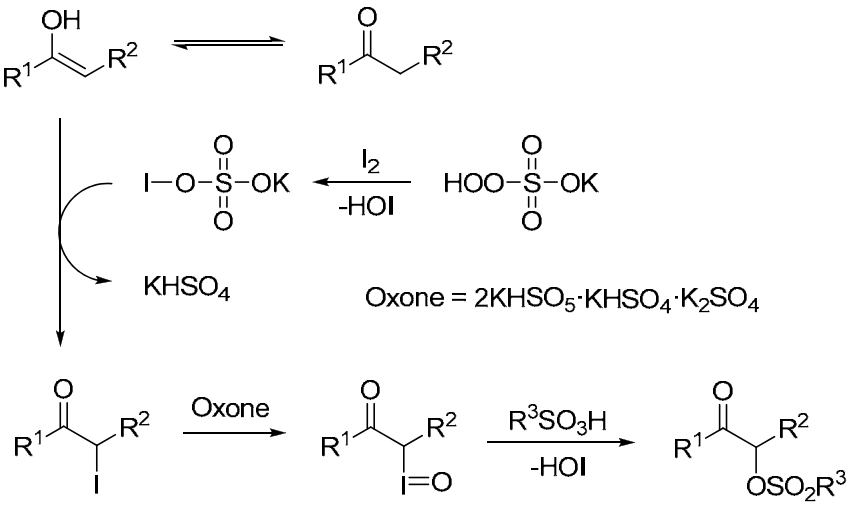

Scheme 53. Reaction path proposed by Togo's group for the oxidative α-functionalization of ketones with iodine, Oxone and a sulfonic acid.

In particular, the corresponding α-(alkylsulfonyl) ketones were obtained in good yields when using methanesulfonic acid, instead of the *p*-toluenesulfonic acid, as the *O*-nucleophile. To shed some light on the mechanism, the authors compared the reactivity of α-iodoacetophenone and α-bromoacetophenone in the reaction of formation of α-tosyloxylacetophenone under the tested conditions (treatment with Oxone and a sulfonic acid). The former gives quantitative yield of the desired product,

[126] Hu, J.; Zhu, M.; Xu, Y.; Yan, J. *Synthesis* **2012**, *44*, 1226.

while the later proved completely unreactive. Based on these observations, the authors proposed the reaction path depicted in Scheme 53, involving the α-iodination of the enol form of the ketone with a hypoiodite-sulfate species generated in the reaction of the molecular iodine with Oxone. The α-iodoketone thus formed is smoothly oxidized into a very reactive α-iodosylketone, followed by a rapid nucleophilic attack by the sulfonic acid to yield the corresponding product.

3.1.2 Supported organoiodanes for recycling purposes

As discussed above, the researchers have indeed made a big step forward by replacing stoichiometric amounts or organoiodanes with catalytic amounts of iodine reagents. However, efforts never stopped for looking superior alternative protocols which are more environmentally benign and economic. On one hand, scientists are continuing the search for new catalytic chemical routes with iodoarenes as catalysts. On the other hand, significant efforts have been made, in the case of the already developed processes, to achieve the recovery and recycling of the catalytic iodoarenes.

3.1.2.1 Recyclable iodine reagents for α-tosyloxylation of ketones

In the area of α-tosyloxylation of ketones, the Togo group[127] developed in 2001 polystyrene-supported organoiodines, such as poly[4-hydroxy(tosyloxy)iodo]styrene and poly{α-methyl[4-hydroxy(tosyloxy)iodo]styrene (Scheme 54), as recyclable stoichiometric tosyloxylation reagents. Indeed, these polymeric reagents can be recycled and showed similar reactivity in the second run. However, this protocol required a separate regeneration process to reoxidize the poly(4-iodo)styrene formed in the reaction back to the corresponding hypervalent species. What's more, a stoichiometric amount of the polymeric material is needed to achieve the corresponding transformations. This methodology was later improved by using poly(4-iodo)styrene as a supported catalyst in the presence of *m*-CPBA as terminal oxidant. It was proven that the standard linear poly(4-iodo)styrene had better reactivity than the macroporous cross-linked poly(4-iodo)styrene. The former polymer indeed could be recycled up to three times affording the α-tosyloxy products in moderate yields; however, this potentially catalytic material still should be added in stoichiometric amounts in order to achieve good results.[125]

---

[127] Abe, S.; Sakuratani, K.; Togo, H. *J. Org. Chem.* **2001**, *66*, 6174.

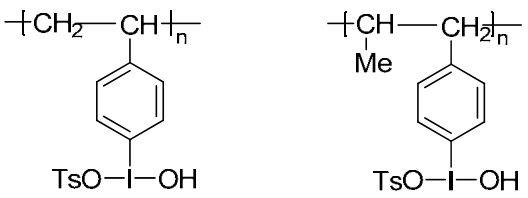

Scheme 54. Poly[4-hydroxy(tosyloxy)iodo]styrene and poly{α-methyl[4-hydroxy(tosyloxy)iodo]styrene} developed by Togo's group.

More recently, Togo's group [128] developed three novel polymer-supported iodobenzene derivatives (Scheme 55a-c) as catalysts for the α-tosyloxylation of ketones. The polystyrene polymers **b** and **c** exhibited better activity than polymer **a**. Furthermore, for polymer **c**, only 0.5 eq. (per ArI) was needed to achieve the transformation with good yields and the material could be recycled up to five times when used in with *p*-nitroacetophenone as substrate. These results are better than the ionic liquid-supported catalyst developed earlier by the same group.[129]

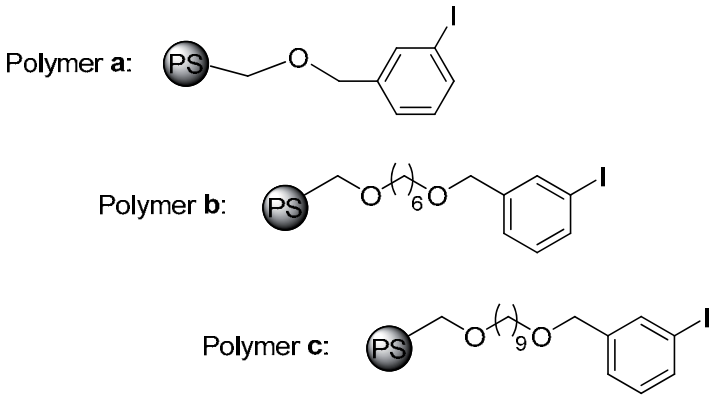

Scheme 55. Polymer-supported iodobenzene derivatives for recyclable purposes.

3.1.2.2 Relevant strategies of supported iodine reagents for recycling purposes in other oxidative transformations

In addition to the examples illustrated above, there exists a large number of polymer-supported hypervalent organoiodines products, especially for aryl-λ^3-iodanes, that can be found as recyclable catalysts or oxidants.[130] In addition, various protocols

[128] Suzuki, Y.; Togo, H. *Synthesis* **2010**, *14*, 2355.

[129] Akiike, J.; Yamamoto, Y.; Togo, H. *Synlett* **2007**, *14*, 2168.

[130] Please see, reviews: (a) Ladziata, U.; Zhdankin, V. V. *ARKIVOC* **2006**, *9*, 26. (b) Ladziata, U.; Zhdankin, V. V. *Synlett* **2007**, 527. (c) H. Togo, K. Sakuratani, *Synlett* **2002**, 1966. (c) Ochiai, M.; Miyamoto, K. *Eur. J. Org. Chem.* **2008**, 4229. Papers: (d) Sorg, G.; Mengel, A.; Jung, G.; Rademann, J. *Angew. Chem. Int. Ed.* **2001**, *40*, 4395. (e) Reed, N. N.; Delgado, M.; Hereford, K.; Clapham, B.; Janda, K. D. *Bioorg. Med. Chem. Lett.* **2002**, *12*, 2047. (f) Ochiai, M.; Miyamoto, K. *Eur. J. Org. Chem.* **2008**, 4229. (g) Lei, Z.; Denecker,

have also been investigated, from the point of view of reagent recyclability, including those based on fluorous-tagged reagents, nanoparticles with magnetic properties (*e. g.*, Fe_3O_4 and γ-Fe_2O_3 nanoparticles), hybrid silicas and others.

a) Fluorous λ³-iodanes related examples

Perfluoroalkyl tagged hypervalent aryliodanes may act as recyclable reagents based on that, upon completion of the reaction, the corresponding reduced iodine reagents can be recovered via fluorous/organic liquid/liquid separations. Gladysz and colleagues[131] prepared some diacetoxy(aryl)iodanes (Scheme 56a) containing fluorous aryl moieties through an oxidation of the corresponding aryl iodides by sodium perborate. Fluorous alkyliodanes[132] (Scheme 56b) were also prepared in the same group from the commercially available aliphatic iodides by oxidation with hydrogen peroxide. These new compounds rapidly oxidize 1,4-hydroquinones to quinones in methanol at room temperature. With the subsequent addition of a fluorous solvent, such as *n*-C_6F_{14} or $CF_3C_6F_{11}$, liquid/liquid biphasic systems were obtained, which could be separated by decantation. Quinones were isolated in high yields from the methanol phase, and the fluorinated iodides were recovered from the fluorous phase after the removal of the solvent. A reuse of these iodides required a re-oxidizing procedure.

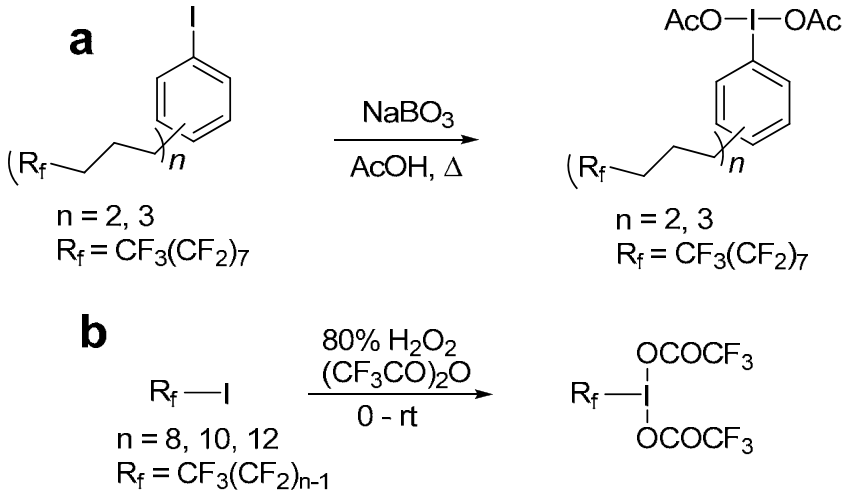

Scheme 56. Examples for the preparation of fluorous organoiodanes.

C.; Jegasothy, S.; Sherrington, D. C.; Slater, N. K. H.; Sutherland, A. J. *Tetrahedron Lett.* **2003**, *44*, 1635. (h) Chung, W.-J.; Kim, D.-K.; Lee, Y.-S. *Tetrahedron Lett.* **2003**, *44*, 9251. (i) Chung, W.-J.; Kim, D.-K.; Lee, Y.-S. *Synlett* **2005**, 2175. (j) Ladziata, U.; Willging, J.; Zhdankin, V. V. *Org. Lett.* **2006**, *8*, 167. (k) Karimov, R. R.; Kazhkenov, Z.-G. M.; Modjewski, M. J.; Peterson, E. M.; Zhdankin, V. V. *J. Org. Chem.* **2007**, *72*, 8149.

[131] Rocaboy, C.; Gladysz, J. A. *Chem. Eur. J.* **2003**, *9*, 88.

[132] Tesevic, V.; Gladysz, J. A. *Green Chem.* **2005**, *7*, 833.

b) Miscellaneous examples

Kita's group, in 2004, disclosed [133] the syntheses and applications of several interesting adamantan-based systems (Scheme 57a) as recyclable iodane reagents in various oxidative transformations. The reduced (*i.e*. iodine(I)) parent (tetraiodide) was easily separated from the reaction mixture due to its insolubility in methanol. The bis(λ^3-iodane) depicted in Scheme 57b was reactive in the vicinal halomethoxylation of olefins.[134] The reduced product, 4,4'-diiodobiphenyl, could be recovered by filtration of the precipitate formed in hexane solution and reused. Yusubov, Kirschning's and Zhdankin's groups[135] reported the syntheses of aryl-λ^3-iodanes (Scheme 57c) bearing a carboxy group at the *meta* position. Upon completion of the the reaction, the reduced poly(iodoarene) species can be separated by treatment with 5% aqueous sodium hydrogen carbonate solution or through an anion-exchange resin. A phenylsulfonate-tagged hypervalent aryl-λ^3-iodane (Scheme 57d) was also designed for recycling protocols, and the concept is based on ion exchange which is initiated by an azide-promoted S_N2 reaction at the alkyl sulfonate followed by trapping of the resulting aryl sulfonate anion, *i. e*., the reduced aryliodo species byproduct from the iodine(III)-promoted transformations, with an ion-exchange resin.[136]

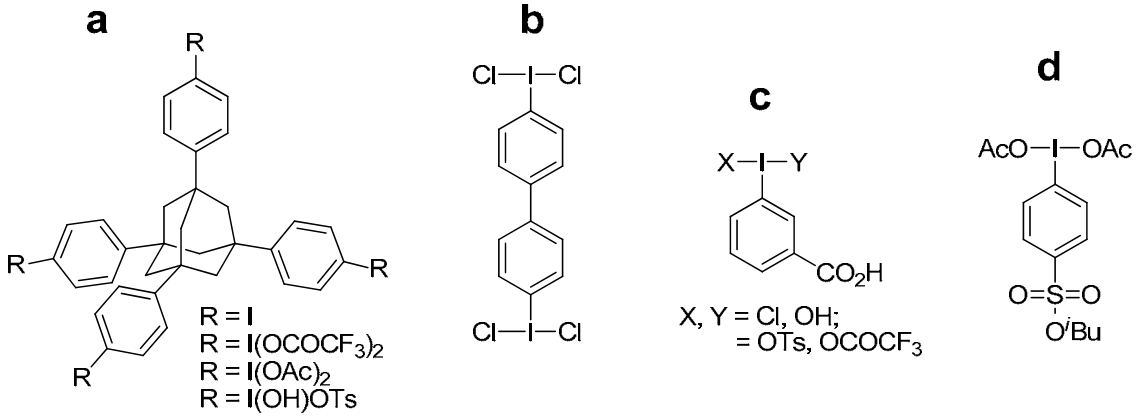

Scheme 57. Various organoiodanes for recyclable purposes

---

[133] (a) Tohma, H.; Maruyama, A.; Maeda, A.; Maegawa, T.; Dohi, T.; Shiro, M.; Morita, T.; Kita, Y. *Angew. Chem. Int. Ed.* **2004**, *43*, 3595. (b) Dohi, T.; Maruyama, A.; Yoshimura, M.; Morimoto, K.; Tohma, H.; Shiro, M.; Kita, Y. *Chem. Commun.* **2005**, 2202.

[134] Yusubov, M. S.; Drygunova, L. A.; Zhdankin, V. V. *Synthesis* **2004**, 2289.

[135] (a) Yusubov, M. S.; Gilmkhanova, M. P.; Zhdankin, V. V.; Kirschning, A. *Synlett* **2007**, 563. (b) Yusubov, M. S.; Yusubova, R. Y.; Kirschning, A.; Park, J. Y.; Chi, K.-W. *Tetrahedron Lett.* **2008**, *49*, 1506. (d) Yusubov, M. S.; Funk, T. V.; Chi, K.-W.; Cha, E.-H.; Kim, G. H.; Kirschning, A.; Zhdankin, V. V. *J. Org. Chem.* **2008**, *73*, 295.

[136] Kunst, E.; Gallier, F.; Dujardin, G.; Yusubov, M. S.; Kirschning, A. *Org. Lett.* **2007**, *9*, 5199.

Among many inorganic solids, polymeric silicon oxide is one of the most frequently used support due to its chemical, thermal and mechanical stability. Thus, in 2001, Giannis's group[137] first reported a silica gel-supported aryl-λ^5-iodane (Scheme 58a) which is particularly suitable for the oxidation of alcohols to the corresponding aldehydes and ketones under mild conditions. This method combines the advantages of silica with the advantages of IBX. Indeed, the compounds were found to be superior to the Dess-Martin reagent in terms of stability, efficiency and versatility.[138] The reduced form is easily separated by simple filtration and can be regenerated by oxidation with Oxone. Similarly, Wei and co-worker's (Scheme 58b) prepared silica supported-$PhI(OAc)_2$ as recyclable oxidant in the oxidation of a wide range of alcohols, albeit longer reaction times were needed in this case when compared with those measured for the $PhI(OAc)_2$-type species supported on γ-Fe_2O_3.[139]

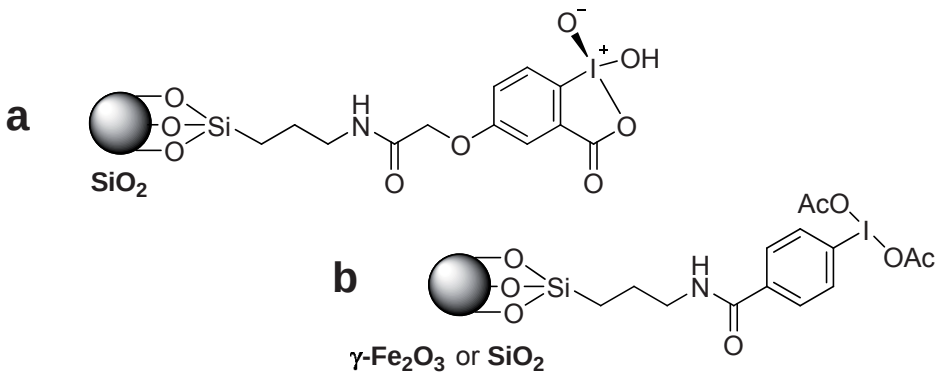

Scheme 58. Protocols developed for recycling iodanes on the basis of hybrid silica and magnetic nanoparticles

Owing to our interests in both iodoarenes as organocatalysts in oxidative C-H functionalizations and recyclable silica-supported catalysts prepared by the sol-gel methodologies,[140] we intended to develop sol-gel immobilized aryl iodides as

---

[137] Mulbaier, M.; Giannis, A. *Angew. Chem. Int. Ed.* **2001**, *40*, 4393.

[138] Frigerio, M.; Santagostino, M.; Sputore, S.; Palmisano, G. *J. Org. Chem.* **1995**, *60*, 7272.

[139] Zhu, C.; Wei, Y. *Adv. Synth. Catal.* **2012**, *354*, 313.

[140] (a) Elias, X.; Pleixats, R.; Wong Chi Man, M.; Moreau, J. J. E. *Adv. Synth. Catal.* **2006**, *348*, 751. (b) Trilla, M.; Pleixats, R.; Wong Chi Man, M.; Bied, C. *Green Chem.* **2009**, *11*, 1815. (c) Blanco, B.; Brissart, M.; Moreno-Mañas, M.; Pleixats, R.; Mehdi, A.; Reyé, C.; Bouquillon, S.; Hénin, F.; Muzart, J. *Appl. Catal. A: Gen.* **2006**, *297*, 117. (d) Monge-Marcet, A.; Pleixats, R.; Cattoën, X.; Wong Chi Man, M.; Alonso, D. A.; Almasi, D.; Nájera, C. *New J. Chem.* **2011**, *35*, 2766. (e) Elias, X.; Pleixats, R.; Wong Chi Man, M.; Moreau, J. J. E. *Adv. Synth. Catal.* **2007**, *349*, 1701. (f) Trilla, M.; Pleixats, R.; Wong Chi Man, M.; Bied, C.; Moreau, J. J. E. *Adv. Synth. Catal.* **2008**, *350*, 577. (g) Borja, G.; Pleixats, R.; Alibés, R.; Cattoën, X.; Wong Chi Man, M. *Molecules* **2010**, *15*, 5756. (h) Monge-Marcet, A.; Pleixats, R.; Cattoën, X.; Wong Chi Man, M. *J. Sol-Gel Sci. Technol.* **2013**, *65*, 93. (i) Monge-Marcet, A.; Pleixats, R.; Cattoën, X.; Wong Chi Man, M. *J. Molec. Catal. A: Chem.* **2012**, *357*, 59. (j) Monge-Marcet, A.; Cattoën, X.; Alonso, D. A.; Nájera, C.; Wong Chi Man, M.; Pleixats, R. *Green Chem.* **2012**, *14*, 1601. (k) Monge-Marcet, A.; Pleixats,

recyclable catalysts in oxidative α-tosyloxylation of ketones. Thus, we would like to give a brief introduction of organic-inorganic hybrid silica materials as follows.

3.1.3 General overview on hybrid silicas

3.1.3.1. Organic-inorganic hybrid silica materials

Hybrid silica materials are constituted by organic components with an inorganic silica skeleton. This kind of materials combines the properties of organic and inorganic components resulting in novel materials with unique properties, which frequently go beyond the sum of the individual contributions from the comprising elements. Such materials, therefore, have attracted the attention of many scientists.

Numerous organic-inorganic hybrid silica materials have been developed over the past two decades,[141] providing a great variety of applications in diverse fields such as optics,[142] electronics,[143] membranes,[144] protective coatings,[145] sensors,[146] controlled drug delivery[147] and catalysis.[148] In the area of catalysis, the immobilization of homogeneous catalysts on hybrid silica materials has been an intense research field.[149] Specially, hybrid silica-based catalysts can be easily separated from the reaction mixture, thus allowing the recovery of the catalysts. What's more, this

---

R.; Cattoën, X.; Wong Chi Man, M. *Tetrahedron* **2013**, *69*, 341. (l) Borja, G.; Monge-Marcet, A.; Pleixats, R.; Parella, T.; Cattoën, X.; Wong Chi Man, M. *Eur. J. Org. Chem.* **2012**, 3625. (m) Monge-Marcet, A.; Pleixats, R.; Cattoën, X.; Wong Chi Man, M.; Alonso, D. A.; Almasi, D.; Najera, C. *New J. Chem.* **2012**, *36*, 2647.

141 Sanchez, C.; Shea, K J.; Kitagawa. S. *Chem. Soc. Rev.* **2011**, *40*, 471.

142 (a) Carlos, L. D.; Ferreira, R. A. S.; Bermudez, V. R.; Ribeiro, S. J. L. *Adv. Mater.* **2009**, *21*, 509. (b) Tani, T.; Mizoshita, N.; Inagaki, S. *J. Mater. Chem.* **2009**, *19*, 4451.

143 (a) Zhang, Y.; Tang, Q.; Li, H.; Hu, W. *Appl. Phys. Lett.* **2009**, *94*, 203304.(b) Lu, M.; Xie, B. H.; Kang, J. H.; Chen, F. C.; Yang, Y.; Peng, Z. H. *Chem. Mater*. **2005**, *17*, 402.

144 (a) Mistry, M. K.; Choudhury, N. R.; Dutta, N. K.; Knott, R.; Shi, Z. Q.; Holdcroft, S. *Chem. Mater*. **2008**, *20*, 6857. (b) Wang, B. Q.; Li, B.; Deng, Q.; Dong, S. J. *Anal. Chem.* **1998**, *70*, 3170.

145 Zheludkevich, M. L.; Salvado, I. M.; Ferreira, M. G. S. *J. Mater. Chem*. **2005**, *15*, 5099.

146 (a) Coti, K. K.; Belowich, M. E.; Liong, M.; Ambrogio, M. W.; Lau, Y. A.; Khatib, H. A.; Zink, J. I.; Khashab, N. M.; Stoddartd, J. F. *Nanoscale* **2009**, *1*, 16. (b) Grate, J. W.; Kaganove, S. N.; Patrash, S. J.; Craig, R.; Bliss, M. *Chem. Mater.* **1997**, *9*, 1201.

147 Zhang, H.; Pan, D. K.; Zou, K.; He, J.; Duan, X. *J. Mater. Chem.* **2009**, *19*, 3069.

148 (a) Ciriminna, R.; Carà, P. D.; Sciortino, M.; Pagliaro, M. *Adv. Synth. Catal.* **2011**, *353*, 677. (b) Elias, X.; Pleixats, R.; Wong Chi Man, M. *Tetrahedron* **2008**, *64*, 6770 (c) Yin, L.; Liebscher, J. *Chem. Rev*. **2007**, *107*, 133. (d) Corma, A.; García, H. *Adv. Synth. Catal*. **2006**, *348*, 1391. (e) Hoffmann, F.; Cornelius, M.; Morell, J.; Fröba, M. *Angew. Chem. Int. Ed*. **2006**, *45*, 3216. (f) Wight, A. P.; Davis, M. E. *Chem. Rev*. **2002**, *102*, 3589. (g) De Vos, D. E.; Dams, M.; Sels, B. F.; Jacobs, P. A. *Chem. Rev*. **2002**, *102*, 3615. (h) Lindner, E.; Schneller, T., Auer, F.; Mayer, H. A. *Angew. Chem. Int. Ed.* **1999**, *38*, 2155. (i) Ying, J. Y.; Mehnert, C. P.; Wong, M. S. *Angew. Chem. Int. Ed.* **1999**, *38*, 56. (j) Moreau, J. J. E.; Wong Chi Man, M. *Coord. Chem. Rev*. **1998**, *178-180*, 1073.

149 Zamboulis, A.; Moitra, N.; Moreau, J. J. E.; Cattoën, X.; Wong Chi Man, M. *J. Mater. Chem.* **2010**, *20*, 9338.

methodology allows the possibility of performing reactions in fixed bed reactor under continuous flow process.[150]

Generally speaking, hybrid silica materials can be divided in two families depending on the interaction between the organic and the inorganic part:[151] 1) ***class I materials***, in which the organic moieties are simply entrapped or embedded in the inorganic matrix, without any interaction or, at the most, interacting with the matrix through non-covalent weak bonds such as hydrogen bond, van der Waals, hydrophobic or ionic interactions (Scheme 59a). In this case, the organic part can be separated from the inorganic skeleton by classical techniques such as extraction with organic solvents; 2) ***Class II materials***, in which the organic and inorganic components are linked through strong covalent or iono-covalent chemical bonds (Scheme 59b). Consequently, the organic moiety and inorganic matrix form a continuous phase whose components cannot be separated by classical methods.

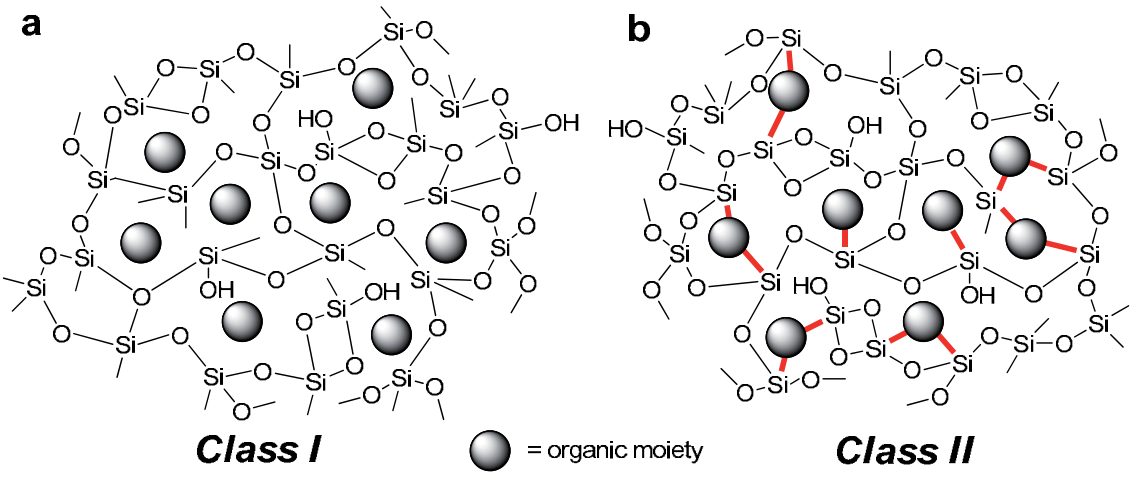

Scheme 59. Hybrid silica materials classification.

3.1.3.2. General methodologies for the preparation of hybrid silica materials

Class I materials are more often used in biology or medicine,[152] whereas in catalysis, the use of *Class I materials* is usually associated with problems of catalyst leaching, and the difficulties in controlling the loading amount of the catalyst. Thus,

---

[150] (a) Massi, A.; Cavazzini, A.; Del Zoppo, L.; Pandoli, O.; Costa, V.; Pasti, L.; Giovannini, P. P. *Tetrahedron Lett.* **2011**, *52*, 619. (b) Zhang, Z.; Qu, Y.; Wang, S.; Wang, J. *Ind. Eng. Chem. Res.* **2011**, *48*, 9083. (c) Duque, R.; Öchsner, E.; Clavier, H.; Caijo, F.; Nolan, S. P.; Mauduit, M.; Cole-Hamilton, D. J. *Green Chem.* **2011**, *13*, 1187. (d) Hintermair, U.; Gong, Z.; Serbanovic, A.; Muldoon, M. J.; Santini, C. C.; Cole-Hamilton, D. J. *Dalton Trans.* **2010**, *39*, 8501.

[151] Sanchez, C.; Ribot, F. *New J. Chem.* **1994**, *18*, 1007.

[152] Lu, J.; Liong, M.; Zink, J. I.; Tamanoi, F. *Small* **2007**, *3*, 1341.

Class II materials are preferred in this area. The most common method to prepare such materials consists in the introduction of the organic moiety by post-functionalization of a pre-formed inorganic matrix, the so-called anchoring or grafting. Alternatively, the organic fragment may also be incorporated during the formation of the inorganic network by a co-condensation synthesis using the sol-gel process.

a) Post-functionalization methods

Well defined and characterized pre-formed silicas are frequently modified with organic groups by grafting processes, involving the reaction of surface silanol groups with an organotrialkoxysilane (Scheme 60).

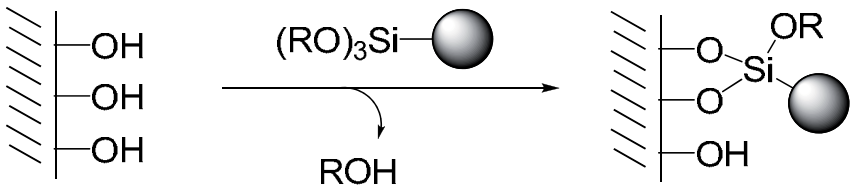

Scheme 60. Post-synthesis functionalization of a silica gel by grafting.

Surface organometallic chemistry has also been developed on the solid supports for the formation of hybrid silica materials, especially when the final material contains an organometallic species.[153] Moreover, some new methodologies for the linking of organic compounds onto solid matrices have also been developed.[154] In these cases, the organic precursors do not have to bear a trialkoxysilyl group, since the preformed solid already contains specific functional groups such as thiol, amine, azide etc., through which a covalent bond can be formed by the subsequent reaction with the grafting molecules. Scheme 61 gives three representative examples of pre-functionalized silicas. Subsequent reactions of material ***a*** (Scheme 61) with alkenes (alkene-thiol click chemistry),[154a] material ***b*** (Scheme 61) with acid derivatives[137] and material ***c*** (Scheme 61) with alkynes (azide-alkyne click chemistry),[154b-c] respectively, would afford the desired functionalized hybrid silicas.

---

[153] (a) Copéret, C.; Basset, J.-M. *Adv. Synth. Catal.* **2007**, *349*, 78. (b) Copéret, C.; Chabanas, M.; Petroff Saint-Arroman, R.; Basset, J.-M. *Angew. Chem. Int. Ed.* **2003**, *42*, 156. (c) Yermakov, Y. I.; Kuznetsov, B. N.; Zakharov, V. A. *Stud. Surf. Sci. Catal.* **1981**, *8*, 1. (d) Blanc, F.; Chabanas, M.; Copéret, C.; Fenet, B.; Herdweck, E. *J. Organomet. Chem.* **2005**, *690*, 5014.

[154] (a) Yu, P.; J. He, J.; Guo, C. X. *Chem. Commun.* **2008**, 2355. (b) Becer, C. R.; Hoogenboom, R.; Schubert, U. S. *Angew. Chem. Int. Ed.* **2009**, *48*, 4900. (c) Kolb, H. C.; Finn, M. G.; Sharpless, K. B. *Angew. Chem. Int. Ed.* **2001**, *40*, 2004.

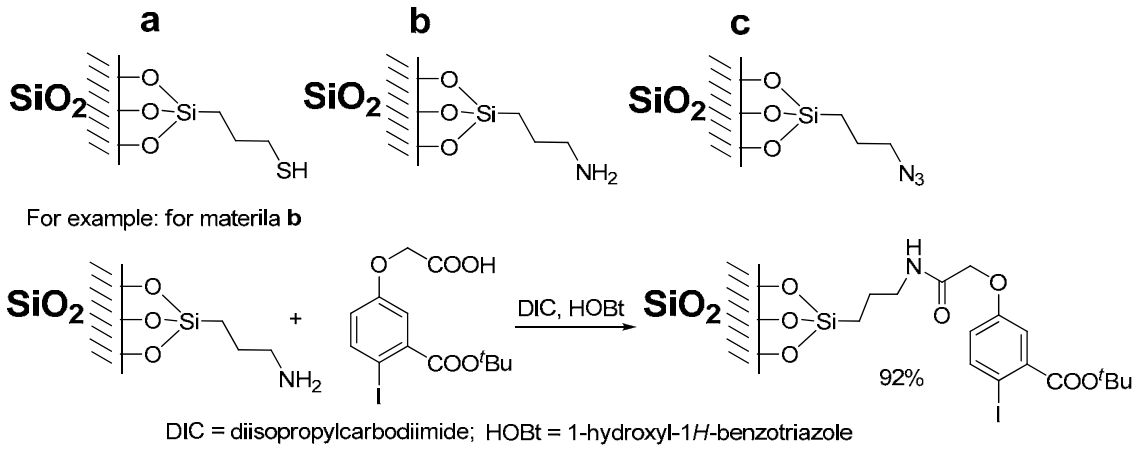

Scheme 61. Three pre-functionalized silicas and one example showing the treatment of the silica to provide the desired functionalized hybrid silica.

b) The sol-gel process[155]

This methodology allows the preparation of the hybrid silica with the organic moieties uniformly dispersed in the system. The sol-gel process can be carried out using inorganic precursors such as chlorides, nitrates or sulphates, but the most versatile methodology typically involves the use of alkoxysilanes.

The process typically starts when a tetraalkoxysilane, such as tetraethoxysilane (TEOS), is catalytically hydrolyzed in a convenient solvent (ethanol, THF, DMF...) to give colloidal silanol and siloxane species, oligomers as well as small clusters (the same thing also happens to the organic moiety bearing trialkoxysilyl groups but with a relatively slower process). These clusters condense through further siloxane bridges, then small particles, and eventually tridimensional networks that entrap the solvent to form a gel. On the macroscopic scale, gelation is the thickening of the initial solution into an elastic solid (gel) which is not fluid. This stage, however, is not the end of the process. During the so-called *aging process* of the gel, hydrolysis and condensation reactions continue, and the network stiffens restraining the flow of the pore liquid. Although the system seems virtually unchanged, polymerization, coarsening and phase transformation occur. Finally, the gel is dried and, after a thermal or mechanical treatment, the hybrid material is obtained as a powder, called xerogel.

For tetraalkoxysilanes, the nucleophilic attack of water to the silicon atom in the first step takes place through different mechanisms, depending on the catalyst used:[156]

[155] The Physics and Chemistry of Sol-Gel Processing: ed. Brinker, C. J.; Scherer, G. W. ACADEMIC PRESS: Boston, MA, 1990.

acidic, basic or nucleophilic (F^-, *N*-methylimidazole, HMPA). With an acidic catalyst, the nucleophilic attack of water (or silanol) occurs after the reversible protonation of an alkoxy group, leading to a pentacoordinate intermediate prone to lose an alcohol molecule (Scheme 62a). In the presence of hydroxide anions (basic catalysis process), a nucleophilic attack to the tetraalkoxysilane occurs through an anionic pentacoordinate intermediate, from which an alkoxide group is eliminated (Scheme 62b). Finally, in a typical nucleophilic catalytic process, an anionic pentacoordinate intermediate is generated upon the coordination of the nucleophile to the silicon centre of a tetraalkoxysilane. Water or silanol then coordinate to this intermediate and form a hexacoordinate transition state which evolves to give an alcohol, a silanol and to regenerate the catalyst (Scheme 62c). Many bases, even the hydroxide anion, can act as nucleophilic catalysts (besides as a base catalyst), although the fluoride anion is one of the most commonly used.

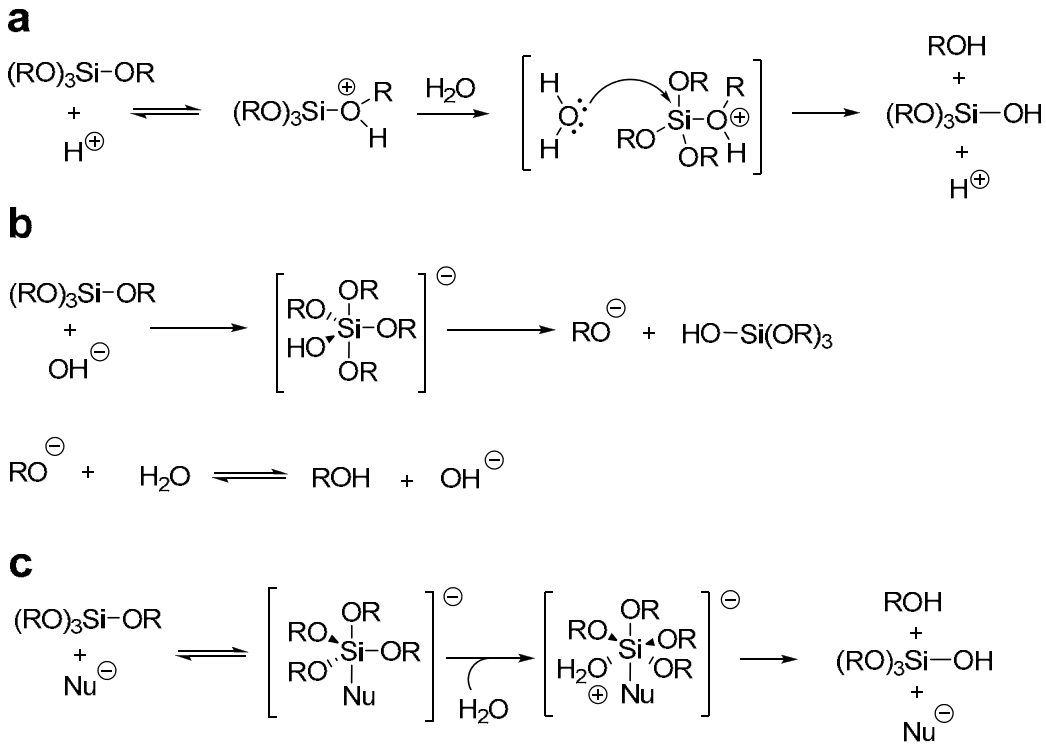

Scheme 62. Hydrolysis of tetraalkoxysilane promoted by different catalysts.

The properties of the final material, such as the porosity and the surface area, strongly depend on the experimental parameters used in the sol-gel process. Therefore any small change in temperature, solvent, concentration or catalyst can significantly affect the properties of the final hybrid silica material.

---

[156] Corriu, R. J. P.; Leclerq, D. *Angew. Chem. Int. Ed.* **1996**, *35*, 1421.

The organic moiety can be directly incorporated during the sol-gel process by co-gelification of an organotrialkoxysilane and a tetraalkoxysilane (Scheme 63a).[157] After hydrolysis and condensation, the final solid will contain organic groups dispersed in the silica matrix.[158] Alternatively, when the organic compound bears two or more trialkoxysilyl groups, the sol-gel process can be performed without the addition of tetraalkoxysilane (Scheme 63b).[159] These organosilicas are also called bridged silsesquioxanes, and are inherently homogeneous solids.[160]

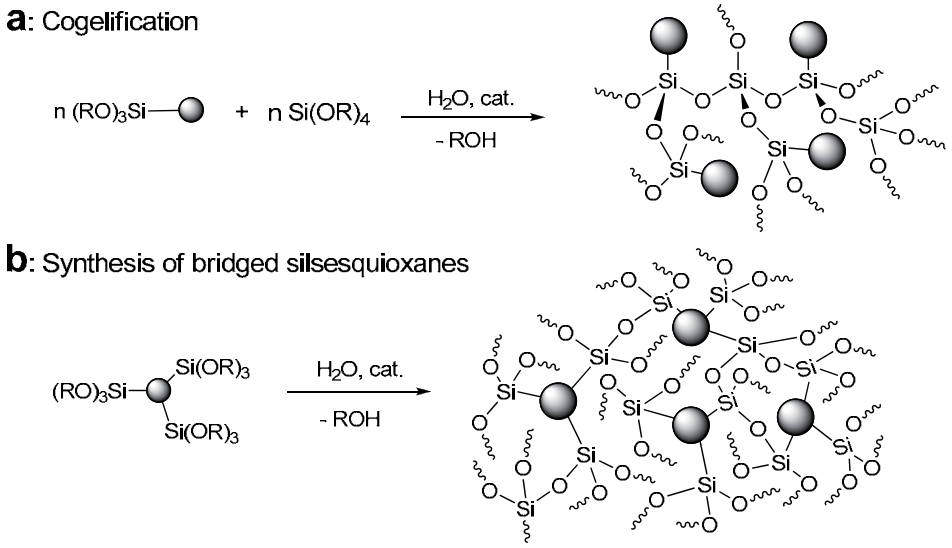

Scheme 63. Sol-gel methodologies for hybrid silica: (a) cogelification and (b) synthesis of bridged silsesquioxanes.

3.1.4 Characterization of hybrid silica materials

It is very necessary to explain the analytical techniques of hybrid silicas, because some of them are not commonly used in the general organic chemistry.[161] Chemical analyses can provide information about the concentration, and, in some cases, the structure of the incorporated organic moiety. Physical parameters, such as surface area, pore size distribution, material morphology may also be relevant in catalysis. Materials can also be classified according to their pore size in three categories: microporous (pore size < 2 nm), mesoporous (pore size 2-50 nm) and macroporous

---

[157] Monge-Marcet, A. *PhD Dissertation.* Universitat Autònoma de Barcelona, **2011**.

[158] Baney, R. H.; Itoh, M.; Sakakibara, A.; Suzuki, T. *Chem. Rev.*, **1995**, *95*, 1409.

[159] Dieudonné, P.; Wong Chi Man, M.; Pichon, B. P.; Vellutini, L.; Bantignies, J.-L.; Blanc, C.; Creff, G.; Finet, S.; Sauvajol, J.-L.; Bied, C.; Moreau, J. J. E. *Small*, **2009**, *5*, 503.

[160] (a) Corriu, R. J. P. *Eur. J. Inorg. Chem*. **2001**, 1109. (b) Loy, D. A.; Shea, K. J. *Chem. Mater*. **2001**, *13*, 3306. (c) Corriu, R. J. P. *Angew. Chem. Int. Ed*. **2000**, *39*, 1376. (d) Loy, D. A.; Shea, K. J. *Chem. Rev*. **1995**, *95*, 1431.

[161] Corma, A. *Chem. Rev.* **1995**, *95*, 559.

(pore size > 50 nm). The following is a brief summary of methods generally used for characterization of hybrid silicas.

3.1.4.1 Thermogravimetric analysis

Thermogravimetric analysis (TGA) is widely used for determining the changes in the mass of a material as a function of temperature.[162] It provides the information of thermal stability of a given material, including decomposition, moisture adsorption/desorption, etc.. In hybrid materials, it is often used to determine the loading of the organic components. In this technique, a thermogravimetric (TG) curve recorded, in which the mass is plotted as a function of temperature (T) or time (t) during an heating process. The nature of the organic moiety decides the choice of the experimental parameters like the gradient of temperature (typically 5 - 10 ºC/min) or the analysing atmosphere (air, argon).

Simultaneous Differential Scanning Calorimetry (DSC) measures both heat flow and weight changes as a function of temperature or time in a controlled atmosphere. The simultaneous measurement of these properties offers more relevant information, for instance, some endothermic or exothermic events during the testing process.

3.1.4.2 Elemental analysis

The chemical composition of hybrid silica materials can be determined by elemental analysis. The carbon, hydrogen, heteroatoms (nitrogen, sulphur, chlorine, bromine or iodine) contained in the materials can be analysed by combustion. The silicon and metals (palladium, ruthenium, rhodium, gold) are usually determined by inductively coupled plasma (ICP) atomic absorption or atomic emission analyses. Generally speaking, the experimental data is less than expected, which may be caused by the facts that some of the alkoxy groups are not hydrolyzed or some silanol groups do not condense; the discrepancy may also come from traces of high-boiling point solvent residual in the materials.

3.1.4.3 Infrared spectroscopy (IR)

Infrared spectroscopy allows the qualitative identification of functional groups present in the material, particularly those with characteristic bands, such as carbonyl, nitrile, sulfonyl, isonitrile, amine or azide groups. However, this technique is limited for

---

[162] Mansfield, E.; Kar, A.; Quinn, T. P.; Hooker, A. *Anal. Chem.* **2010**, *82*, 9977.

the cases of high percentage of organic fragment in the inorganic framework. When the ratio tetraalkoxysilane/organosilane is higher than 10, the IR spectrum is dominated by the Si-O-Si vibrations bands (around 1100 cm^{-1}), surface-adsorbed water and silanol species (3500 – 3200 cm^{-1}).[163]

3.1.4.4 ^{29}Si and ^{13}C Solid State Nuclear Magnetic Resonance (SSNMR)

The ^{29}Si-SSNMR confirms the covalent bond between silicon and the organic component and gives information about the degree of condensation in the hybrid material. During the sol-gel process, a number of silicon species is formed containing different numbers of Si-O-Si bonds (Scheme 64); these species, in turn, give signals with different chemical shifts in the ^{29}Si-SSNMR spectra, depending on the substitution pattern around the silicon atom. Thus, as shown in Scheme 64, signals are divided into four categories M, D, T and Q, whereby M represents monofunctional silicon coming from monoalkoxysilanes; D denotes the silicon species derived from dialkoxysilanes; T implies units stemming from trialkoxysilanes; and Q for those derived from tetraalkoxysilanes. In addition, numeric superindices are frequently used to indicate the degree of condensation. For instance, the superindex “0” means no condensation occured; “1” suggested only one alkoxy group has condensed; “2” implies two alkoxy groups have condensed, and so forth.

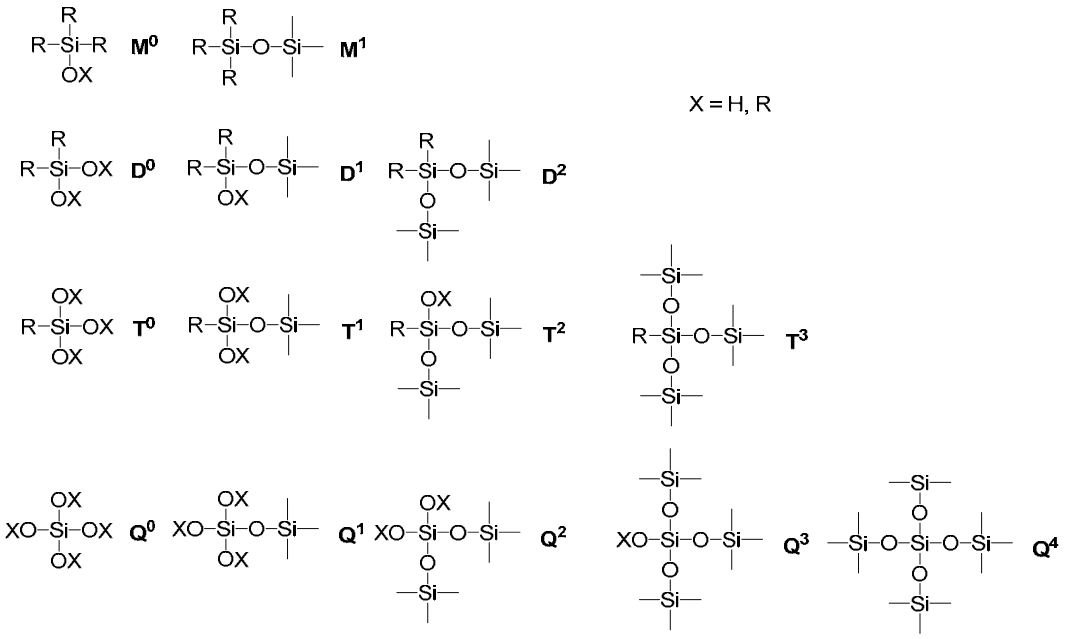

Scheme 64. Silicon environments and their corresponding label in the ^{29}Si-SSNMR.

[163] Sassi, Z.; Bureau, J. C.; Bakkali, A. *Vibrational Spectroscopy*, **2002**, *28*, 251.

In addition, the ^{13}C-SSNMR is highly useful to check for the presence and the structure of the incorporated organic moiety. Although the peaks observed are usually broad, their position tends to coincide with the peaks of the corresponding organosilane precursor, thus providing qualitative information for the identification of organic functional groups.

It should be noted that solid state ^{13}C and ^{29}Si NMR suffer from low sensitivity.[164] In fact, functionalized silicon sites T^n, in some cases, are too diluted to be readily observed in the ^{29}Si-SSNMR. Generally, for high dilution of the organic component in the hybrid material (tetraalkoxysilane/organotrialkoxysilane ratio higher than 10), the spectrum provides mainly information about the Q^n and the Si-OH sites. The ^{13}C-SSNMR suffers from similar drawbacks and, therefore for high dilution of organic component, the NMR detection of the organic moiety is far from trivial.

3.1.4.5 Surface area analysis

Gas adsorption-desorption measurements are used for determining the surface area, the average pore size and the pore volume distributions of a variety of different solid materials. Adsorption is a process in which molecules or atoms are weakly bound to the surface of a solid to form a layer at the interface. Desorption denotes the reverse process. N_2-sorption analyses are performed at 77 K from thoroughly degassed samples. The adsorption isotherm is built by adding controlled amount of nitrogen gas to the cold sample, and monitoring the corresponding equilibrium relative pressure in the surrounding environment (p/p^0, p^0 represents the saturation pressure of the nitrogen at the temperature of the measurement). When p/p^0 reaches 1, spontaneous liquefaction of N_2 occurs. Under these conditions consecutive molecular layers of nitrogen can be adsorbed on the solid surface. In a monolayer adsorption mode, all the adsorbed molecules are in contact with the sample surface. In a multilayer adsorption, the adsorption space accommodates more than one layer of molecules, therefore, not all adsorbed molecules are, in this case, in direct contact with the surface layer of the sample. The surface area of a given sample may be calculated on the basis of the adsorbed amount of nitrogen from monolayer adsorption.

The graphic representing the relationship, at constant temperature, between the amount adsorbed and the equilibrium pressure of the gas is known as the adsorption-

---

[164] Lelli, M.; Gajan, D.; Lesage, A.; Caporini, M. A.; Vitzthum, V.; Miéville, P.; Héroguel, F.; Rascón, F.; Roussey, A.; Thieleux, C.; Boualleg, M.; Veyre, L.; Bodenhause, G.; Copéret, C.; Emsley, L. *J. Am. Chem. Soc*. **2011**, *133*, 2104.

desorption isotherm.[165] In most cases, a hysteresis loop appears when adsorption and desorption curves do not coincide. In 1940, S. Brunauer, L.S. Deming, W.E. Deming and E. Teller classified isotherms in five different types. In 1985 the *International Union of Pure and Applied Chemistry* (IUPAC) expanded this classification to six types as shown in Figure 8.[166]

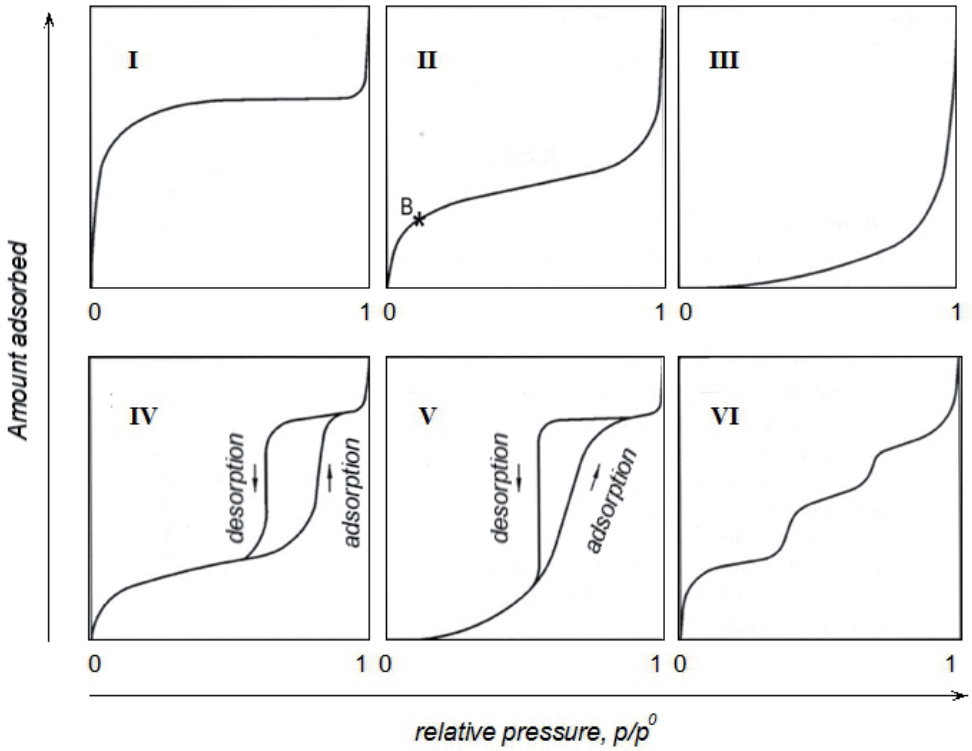

Figure 8. Different types of isotherm according to the IUPAC.

Type I isotherms are characteristic of microporous solids with relatively small external surfaces, where adsorption takes place at low relative pressure. Type II isotherms are normally obtained with non-porous or macroporous adsorbents. Some mesoporous solids also give this adsorption curve, where a monolayer adsorption is observed at low relative pressure and saturation at high relative pressure, but without hysteresis loop. The interaction between adsorbate and adsorbent is strong. Point B represents the beginning of the almost linear middle section of the isotherm. It is often taken to indicate the stage at which monolayer coverage is complete and multilayer adsorption is about to begin. The uncommon type III isotherms are observed in the systems with weak adsorbate-adsorbent interactions (for example, nitrogen on

[165] *Gas adsorption equilibria. Experimental methods and adsorptive isotherms.* Ed. Keller, J. U. SPRINGER: Boston, 2005.

[166] Sing, K. S. W.; Everett, D. H.; Haul, R. A. W.; Moscou, L.; Pierotti, R. A.; Rouquérol, J.; Siemieniewska, T. *Pure Appl. Chem.*, **1985**, *57*, 603.

polyethylene shows this profile). Because of its convex curvature over the entire range of pressure, these isotherms do not exhibit point B. Type IV isotherms are generally observed in mesoporous materials. They have a characteristic hysteresis loop, which is associated with capillary condensation taking place in mesopores, and the limiting uptake over a range of high relative pressure. Type V isotherms indicate a deviation of type IV. When a stepwise multilayer adsorption mode occurs on uniform non-porous surfaces, type VI isotherms are obtained; the sharpness of the steps depends on the system and the temperature, whereas the step height responds to the monolayer capacity of each adsorbed layer. The type VI isotherms are typically obtained with argon or krypton on graphitised carbon at liquid nitrogen temperature.

Many hybrid materials usually show adsorption isotherms which are a hybrid between types I-VI. The micropores existing in some mesoporous materials can also be recognized in type IV isotherms, resulting in a higher adsorption at low relative pressure. The hysteresis appearing in the multilayer range of isotherms is generally associated with capillary condensation in mesoporous structures. This occurs when the gas is first adsorbed in pores, where it can condense to the liquid state upon sufficient gas supply. Such hysteresis loops may exhibit different shapes classified by IUPAC in four types, with types H1 and H2 as the most frequent (Figure 9). The shapes of hysteresis loops have often been identified with specific pore structures, even though the effect of various factors on the hysteresis loop is not fully understood.

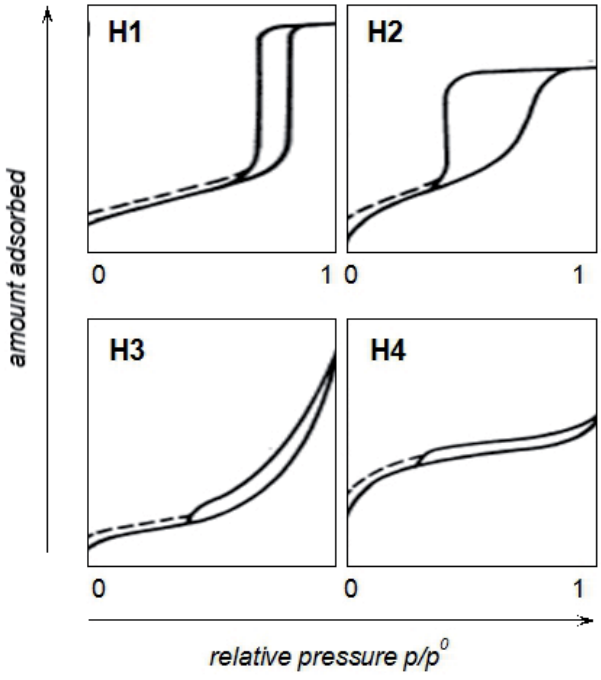

Figure 9. Types of hysteresis loops according to the IUPAC.

Type H1 has parallel adsorption and desorption branches, which is frequently observed in specific ordered mesoporous structures such as SBA-15, MCM-48 and MCM-41. Type H2 is often associated to mesoporous materials with higher disorder. Type H3 can be found in aggregates of plate-like particles with slit-shaped pores. Type IV loop is generally associated with narrow slit-like pores.

The curve shape gives information about the pore size (p/pº from the hysteresis point) and the pore volume (the area limited by adsorption and desorption curves). Several mathematical transformations have been developed to calculate the specific surface area from the adsorption isotherm data, even though the Brunauer-Emmett-Teller (BET)[167] protocol is the most widely used. However the BET method is not suitable to measure the microporous materials. The Barrett-Joyner-Halenda (BJH)[168] method is widely utilized to determine the pore size distribution.

[167] Brunauer, S.; Emmett, P. H.; Teller, E. J. *J. Am. Chem. Soc*. **1938**, *60*, 309.
[168] Barrett, E. P.; Joyner, L. G.; Halenda, P. P. *J. Am. Chem. Soc*. **1951**, *73*, 373.

3.2 Objectives

Following our interests in both recyclable silica-supported catalysts prepared by the sol-gel methodologies and iodoarenes as organocatalysts in oxidative C-H functionalizations, we intended to develop sol-gel immobilized aryl iodides as recyclable catalysts in oxidative α-tosyloxylation of ketones. Thus, we planned the following aims for this chapter 3 of part I of the thesis:

a) The preparation of bis- and monosilylated iodoarenes and their conversion to the new hybrid silica materials by sol-gel methodologies (Scheme 65).

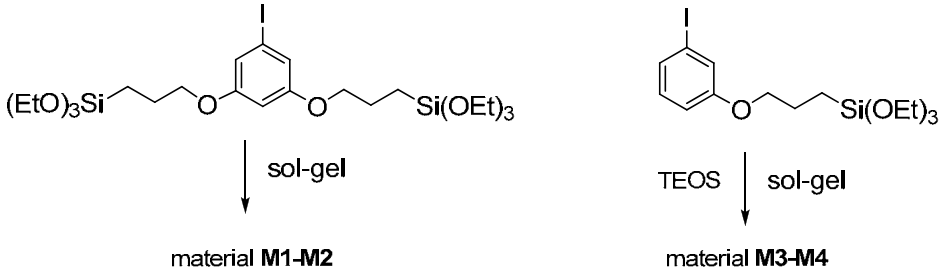

Scheme 65. Preparation of hybrid silica materials from silylated iodoarene precursors

b) The assay of all these new materials as recyclable catalysts in oxidative α-tosyloxylation of ketones (Scheme 66).

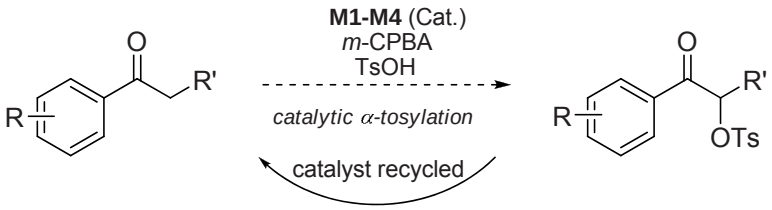

Scheme 66. Catalytic tests of hybrid silica materials in the α-tosyloxylation of ketones.

3.3 Results and Discussion

3.3.1 Preparation and characterization of hybrid silica materials M1 –M4

The synthesis of bis- and monosilylated iodoarene precursors and the hybrid silica materials derived from these precursors are summarized in Scheme 67. The bis-silylated monomer **12** was prepared from the commercially available 3,5-dimethoxyaniline through a three-step synthetic route involving a diazotization of the aniline and conversion of the diazonium salt to the corresponding iodoarene **9**,[169] followed by the deprotection of the methoxy groups to give 5-iodoresorcinol **10**[148] and the subsequent alkylation of the phenolic OH groups with (3-iodopropyl)triethoxysilane **11** derived from commercially available (3-chloropropyl)triethoxysilane (see experimental section for the synthetic details).

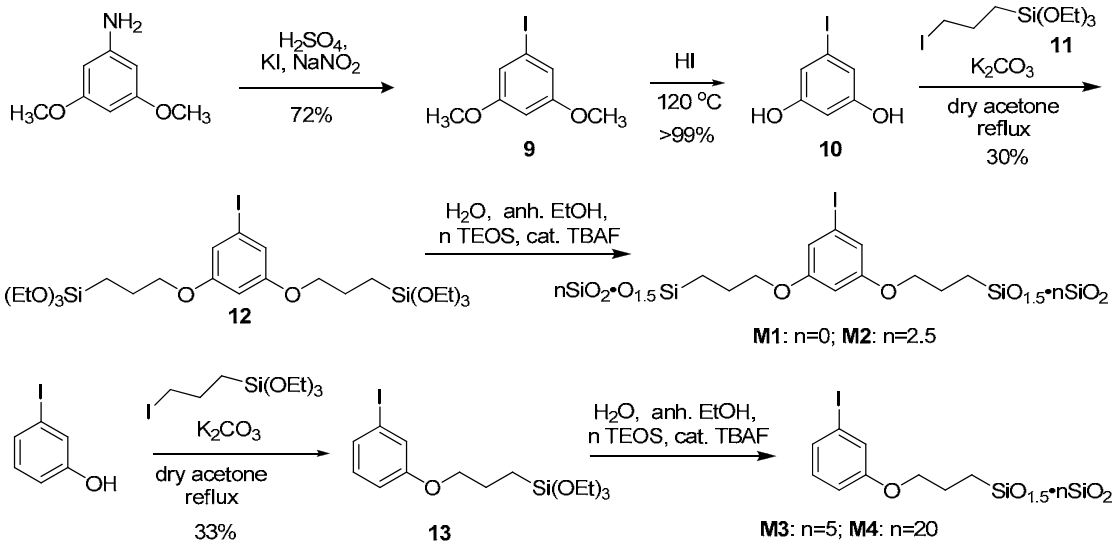

Scheme 67. Synthesis of the bis- and monosilylated precursors **12** and **13** and hybrid silica materials **M1 - M4**.

It should be noted that both the bis-silylated monomer **12** and the compound **11** are sticky oils; our attempts to remove the excess of silane **11** by distillation failed even though various conditions have been tested including the increase of distillation temperature and time. Lowering the amount of silane resulted in the formation of the mono-substituted compound as side product. Considering the relatively low isolated yield of compound **12** obtained under the present procedure (30%, chromatographic

[169] Mao, W.; Wang, T.; Zeng, H.; Wang, Z.; Chen, J.; Shen, J. *Bioorg. Med. Chem. Lett.* **2009**, *19*, 4570.

purification, see experimental part), an alternative process[170] through a hydrosilylation of an intermediate **14** derived from compound **10** was tested (Scheme 68). Despite some product **12** can be detected by NMR, we discarded this alternative protocol due to the formation of another set of hard-to-remove side products, as indicated in Scheme 68.

The monosilylated precursor **13** was obtained by the alkylation of the commercial 3-iodophenol with (3-iodopropyl)triethoxysilane **11** in refluxing acetone in the presence of potassium carbonate. Precursor **12** could either be used directly in the sol-gel reaction to yield the bridged silsesquioxane **M1** or could be co-condensed with five equiv of TEOS to yield **M2**. The monosilylated precursor **13** was co-condensed with TEOS at molar ratios of 1:5 and 1:20, providing materials **M3** and **M4**, respectively. In all cases, the sol-gel reactions were performed in anhydrous ethanol with a stoichiometric amount of water with respect to the ethoxy groups and under nucleophilic catalysis (TBAF, 1 mol% with respect to Si).[171]

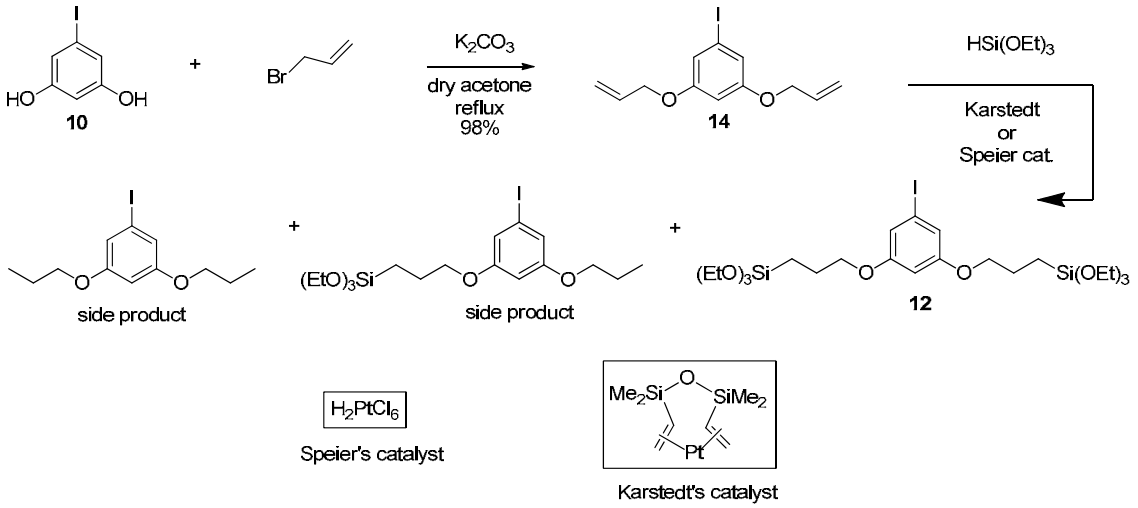

Scheme 68. An alternative synthesis of the precursor **12**.

Materials **M1-M4** were fully characterized by elemental analysis, ^{13}C and ^{29}Si SSNMR NMR, IR, thermogravimetric analysis (TGA) and N_2-sorption measurements. Some physical data of the materials are given in Table 2.

---

[170] (a) Tauk, L.; Schröder, A. P.; Decher, G.; Giuseppone, N. *Nat Chem.* **2009**, *1*, 649. (b) Behr, A.; Naendrup, F.; Obst, D. *Adv. Synth. Catal.* **2002**, *344*, 1142.

[171] Brinker, C. J.; Scherrer, G. W. Sol–gel science: the physics and chemistry of sol–gel processing, Academic Press, San Diego, 1990.

Table 2. Selected physical data for materials **M1 - M4**.[172]

Mater.	N_2 sorption measurements			TGA[b] [%]	mmol of I per gram[c]	I/Si[d] mmol/mmol	
	S_{BET} m^2/g	Uptake at saturation[a] cm^3/g STP	Microporous contribution m^2/g			Theor.	Exp.
M1	< 5	-	0	48	1.064	0.500	0.260
M2	255	48	47	63	0.646	0.143	0.075
M3	109	42	0	67	0.496	0.166	0.051
M4	124	92	0	79	0.307	0.048	0.020

[a] Amount of gas adsorbed at p/p° = 0.5. [b] Residual mass at 700 °C. [c] Determined by elemental analysis. [d] Based on the elemental analysis and ICP-OES results.

The TGA and DSC curves of **M1- M4** (see annex) showed a weight decrease of less than 5% below 250 °C, attributed to the loss of the physisorbed water and remaining uncondensed ethoxy groups. For all materials, a more significant weight loss was found in the range of 250 - 700 °C, assigned to the decomposition of the organic constituent. As expected, **M1** exhibited the highest weight loss (52%) due to the higher content of organic matter in **M1** compared with **M2 - M4.** The covalent incorporation of the organosilane in the hybrid silicas was ascertained by ^{29}Si CP-MAS solid state NMR. As shown in Figure 10, the ^{29}Si CP-MAS NMR spectra of **M1 - M4** exhibit signals between -50 and -69 ppm corresponding mainly to T^2 and T^3 species.

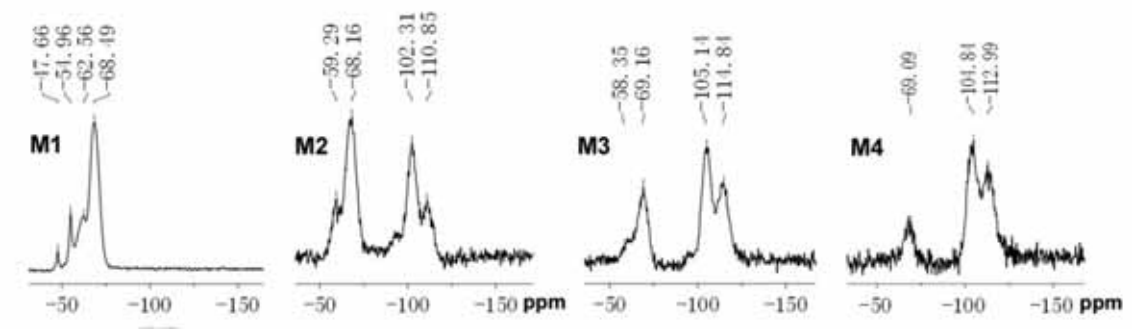

Figure 10. ^{29}Si CP-MAS solid state NMR spectra of **M1 - M4**.

Additionally, the spectra of **M2** - **M4** showed typical signals of silica environments at around -105 and -115 ppm corresponding to Q^3 and Q^4 species, respectively. To clarify,

[172] N_2 adsorption-desorption analysis was performed by Dr. Xavier Cattoën, please see experimental section for details.

the T^2, T^3, Q^3 and Q^4 species existed in **M3** and **M4** were listed as examples (Scheme 69).

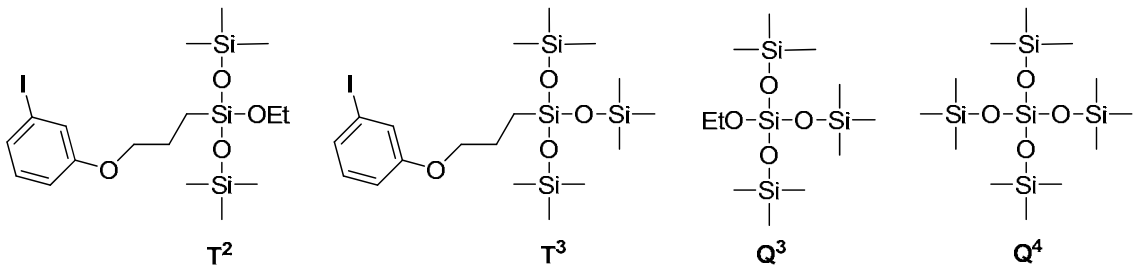

Scheme 69. The T^2, T^3, Q^3 and Q^4 species existed in **M3** and **M4**.

The incorporation of organic fragments in **M2** and **M3** was further evidenced by the ^{13}C CP-MAS solid state NMR spectra, with a typical signal at around 10 ppm attributed to CH_2-Si. The spectra of these materials and their comparison with the ^{13}C NMR solution spectra of the organic precursors **12** and **13** are shown in Figure 11.

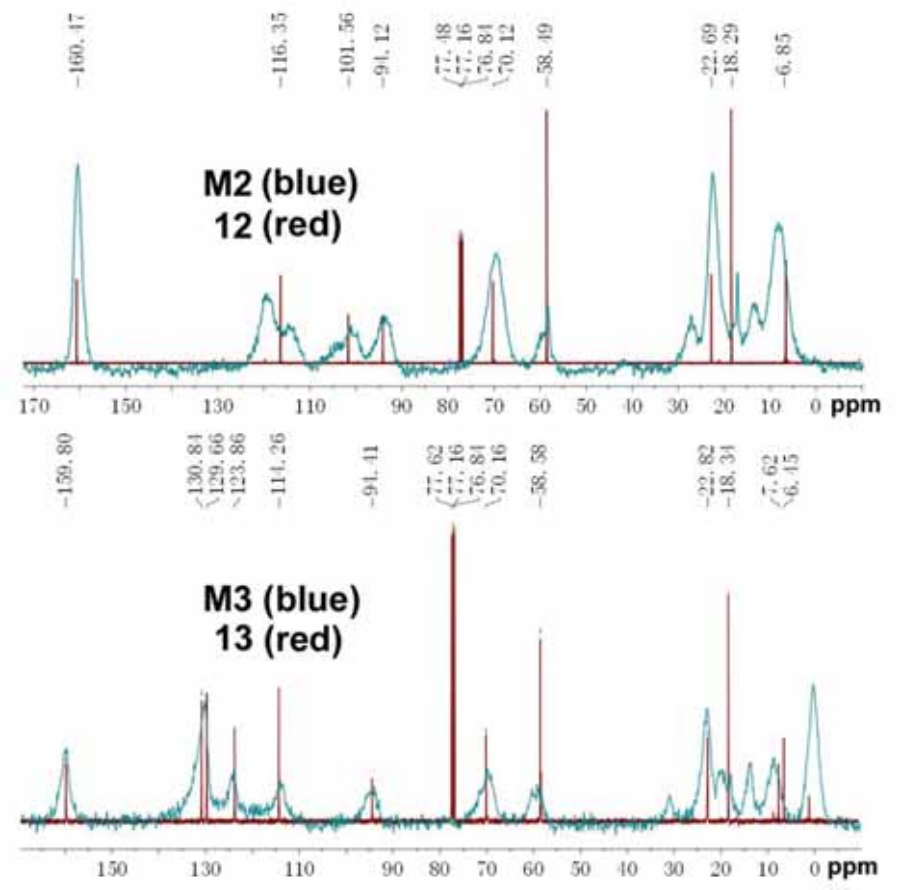

Figure 11. ^{13}C CP-MAS solid state NMR spectra of **M2** and **M3** and the ^{13}C NMR spectra of the corresponding precursors **12** and **13**.

As expected, there is a high degree of correlation between the position of the ^{13}C signals of the precursors and the corresponding hybrid silicas, with the presence of aromatic C-I carbon atom confirmed by the broad signal centered around 94 ppm. However, the observation of additional smaller signals at *ca.* 11, 24, and 59 ppm in the aliphatic C region and the splitting of some aromatic signals (101 and 116 ppm) in the case of **M1** and **M2** led us to believe that the alkyl-aryl ether tethers were partially broken during the sol-gel synthesis resulting extra signals. The consequence of this partial cleavage in the case of the mono-ethers **M3** and **M4** would be iodine content lower than expected, as was indeed observed by elemental analysis. In the case of **M1** and **M2**, the cleavage of both ether functions linking the aromatic fragment to the siloxane network is less probable, so the decrease in iodine content is less pronounced, as observed in Table 2. For the catalytic runs, the catalyst loading (*i.e.*, the loading of the ArI units) was based on material's % iodine as determined by elemental analysis.

N_2-sorption measurements are important for investigating the texture of materials. Material **M1** displayed non-detectable porosity, as was previously found for other bridged silsesquioxanes prepared in the absence of TEOS under similar conditions.[173] As shown in Figure 12, materials **M2 - M4** exhibit type II isotherms (according to IUPAC rules)[174] with a regular increase of nitrogen uptake in the range of p/p° < 0.7 and without a sharp increase that would come from a regular porous system. A slight microporous contribution (47 m^2 g^{-1}) is detected in the case of **M2**, whereas materials **M3** and **M4**, obtained from the monosilylated precursor **13**, only display porosity arising from mesopores and external surfaces. In particular, the large amount of nitrogen adsorbed at p/p° > 0.7 arises from nitrogen that condenses in the voids between particles.

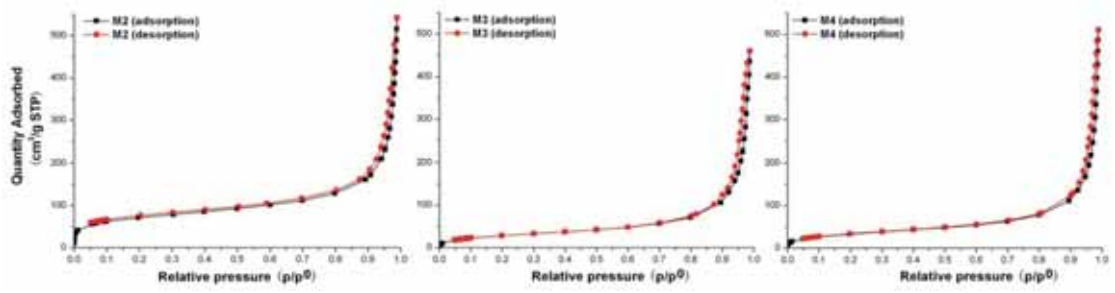

Figure 12. N_2-sorption isotherms of **M2 - M4**.

---

[173] Trilla, M.; Pleixats, R.; Wong Chi Man, M.; Bied, C. *Green Chem.* **2009**, *11*, 1815.

[174] Sing, K.S.W.; Everett, D.H.; Haul, R.A.W.; Moscou, L.; Pierotti, R.A.; Rouquerol, J.; Siemieniewska, T. *Pure Appl. Chem.* **1985**, *57*, 603.

3.3.2 Catalytic activity of the silica-supported iodoarenes M1-M4 in the α-tosyloxylation of ketones

The catalytic activity of materials **M1**-**M4** in the α-tosyloxylation of a range of ketones was then evaluated. Our initial catalytic tests were performed with propiophenone as the substrate and in the presence of *p*-toluenesulfonic acid (*p*-TsOH, 1.3 equiv), *m*-CPBA as the terminal oxidant and **M2** as the catalyst to afford α-tosyloxypropiophenone **15** (Table 3).

Table 3. Optimization of the reaction conditions with **M2** as the catalyst.

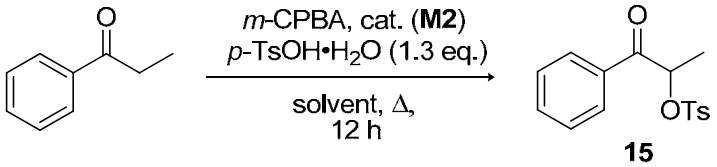

15

Entry [a]	Solvent	*m*-CPBA / eq.	**M2** / mol%	Temp. / °C	Yield / % [b]
1	acetonitrile	1.1	10	50	25
2	acetonitrile	1.1	10	65	37
3	acetonitrile	1.1	10	70	37
4	acetonitrile	2.3	10	65	69
5	acetonitrile	3.0	10	65	68
6	chloroform	2.3	10	65	0
7	toluene	2.3	10	65	4
8	acetonitrile	2.3	5	65	15
9	acetonitrile	2.3	15	65	70

[a] [substrate] = 0.2 M. [b] corrected GC yield (Ph-Ph as internal standard).

The commercially available *m*-CPBA is contaminated with varying degrees (17-33%) of water and with 10-15% of *m*-chlorobenzoic acid (*m*-CBA), depending on the commercial source. For this reason, in order to make the experiments reproducible, the commercial *m*-CPBA was dried under reduced pressure for at least 1 h prior to use, as suggested by Ochiai.[49]

A screening of different reaction conditions was performed (solvent, catalyst loading, amount of *m*-CPBA, temperature). The reaction using 10 mol% of **M2** (percentage based on ArI equivalents) in the presence of 1.1 equiv of *m*-CPBA in acetonitrile gave moderate yields (25-37%) of **15** at 50 and 65 °C (Table 3, entries 1-2), with no improvement achieved by raising the temperature to 70 °C (Table 3, entry 3). In the same solvent, the yield could be improved to 69% by raising the amount of *m*-CPBA to

2.3 eq., although higher amounts of the oxidant (3.0 eq.) had no beneficial effect (compare entries 4 and 5 of Table 3). Chloroform and toluene were also tested as solvents and proved less effective than acetonitrile (Table 3, entries 6-7). The effect of catalyst loading on the yield of the product was also investigated (Table 3, entries 8-9). As a result, the optimized reaction conditions were given as follows: 65 °C of reaction temperature, 10 mol% of catalyst, acetonitrile as solvent, 2.3 eq. of *m*-CPBA and 1.3 eq. of *p*-TsOH.

This protocol was then extended to the oxidative α-tosyloxylation of various ketones with the supported catalysts **M1**-**M4** (Table 4). The corresponding α-tosyloxyketones **15**-**22** were isolated in yields of up to 67%. As expected, the activities of the new silica-immobilized catalysts were lower than those shown by homogenous iodoarenes for this type of transformation.[124b, 175] Nevertheless, it is worthwhile to mention a certain improvement with respect to other immobilized systems,[124a] given the possibility of using just 10 mol% of the supported ArI. Materials **M1-M4** were tested as catalysts with propiophenone and *p*-bromoacetophenone as substrates (Table 4, entries 1-9). Moderate to good isolated yields of the tosylated ketones **15** and **16** were obtained for materials **M1** and **M2** derived from the bis-silylated monomer **12** (Table 4, entries 1, 2, 5 and 7), whereas **M4** displayed lower activity (23 and 19% isolated yields of **15** and **16**, respectively) (Table 4, entries 4 and 9) and material **M3** was essentially inactive under the reaction conditions (Table 4, entries 3 and 8).

The two best catalysts, **M1** and **M2,** were also tested with six other substrates: *p*-nitroacetophenone (Table 4, entries 10-12), 3-pentanone (Table 4, entries 13-14), acetophenone (Table 4, entries 15-17), *p*-methylacetophenone (Table 4, entries 18-19), *p*-chloroacetophenone (Table 4, entry 20) and 2-bromoacetophenone (Table 4, entries 21-22). The corresponding tosyloxyketones **15** - **22** were obtained in moderate isolated yields (from 18% to 58%).

To further investigate the generality of this oxidative process, two other sulfonic acids (camphorsulfonic and methanosulfonic) were also tested with 10 mol% of **M1** as the catalyst, affording the corresponding α-functionalized ketones **23** and **24** in 42% and 71% isolated yields, respectively (Table 4, entries 23-26). Notably, the material **M1** was successfully separated and reused in a second run in several cases (Table 4, entries 6, 11, 16, 22 and 25) and even in a third run (Table 4, entry 26).

---

[175] Monge-Marcet, A.; Pleixats, R.; Cattoën, X.; Wong Chi Man, M. *Catal. Sci. Technol.* **2011**, *1*, 1544

Table 4. α-Tosyloxylation of ketones using **M1-M4** as catalysts under the optimized conditions specified.

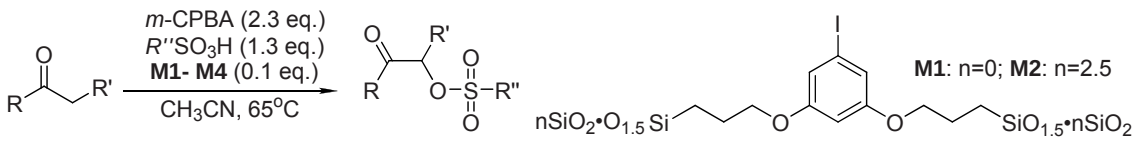

Entry[a]	Product	Cat.	Time / h	Yield[b] / %
1	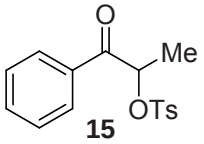 **15**	**M1**	18	47
2		**M2**	14	67
3		**M3**	27	3
4		**M4**	50	23
5	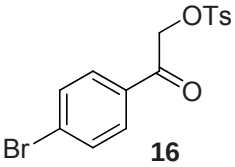 **16**	**M1**	21	60
6		**M1**	13	62[c]
7		**M2**	14	55
8		**M3**	19	5
9		**M4**	19	19
10	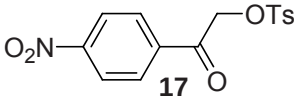 **17**	**M1**	21	35
11		**M1**	13	51[c]
12		**M2**	14	25
13	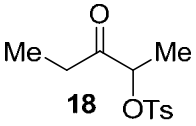 **18**	**M1**	18	24
14		**M2**	19	26
15	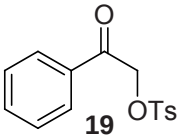 **19**	**M1**	18	43
16		**M1**	13	36[c]
17		**M2**	19	50
18	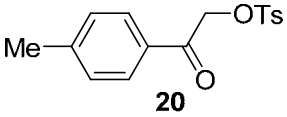 **20**	**M1**	17	21
19		**M2**	18	18
20	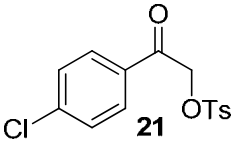 **21**	**M1**	16	54
21	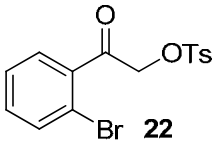 **22**	**M1**	20	58
22		**M1**	21	47[c]
23	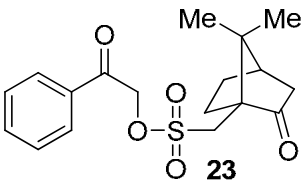 **23**	**M1**	17	42
24	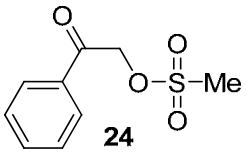 **24**	**M1**	18	71
25		**M1**	18	65[c]
26		**M1**	18	42[d]

[a] [substrate] = 0.2 M. [b] isolated yield. [c] second cycle. [d] third cycle.

3.3.3 Preparation and characterization of hybrid silica material M5

Inspired from the results reported by others with molecular iodine (I_2) and ammonium iodide in α-tosyloxylation of ketones,[125,126] we were interested in investigating the possible catalytic activity of silica supported alkyliodide, a material that can be easily obtained. Thus, a hybrid silica **M5** was prepared through the co-condensation of (3-iodopropyl)triethoxysilane **11** with 5 equivalents of TEOS as shown in Scheme 70.

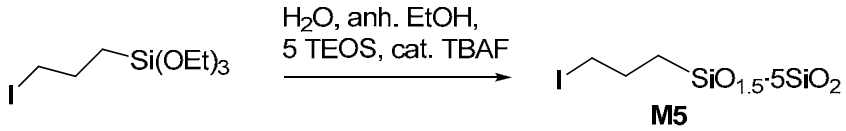

Scheme 70. Preparation of **M5**.

This material was fully characterized by N_2 sorption measurements, ^{13}C and ^{29}Si solid state NMR, IR and TGA. The BET specific surface area was found to be 319 m^2/g based on the nitrogen isotherm plots. The incorporation of the iodoalkane moiety in **M5** was evidenced by ^{13}C CP-MAS solid state NMR spectra (Figure 13a) in which the signals around 27 and 11 ppm suggested the presence of methylene signals of the $ICH_2CH_2CH_2$ fragments.

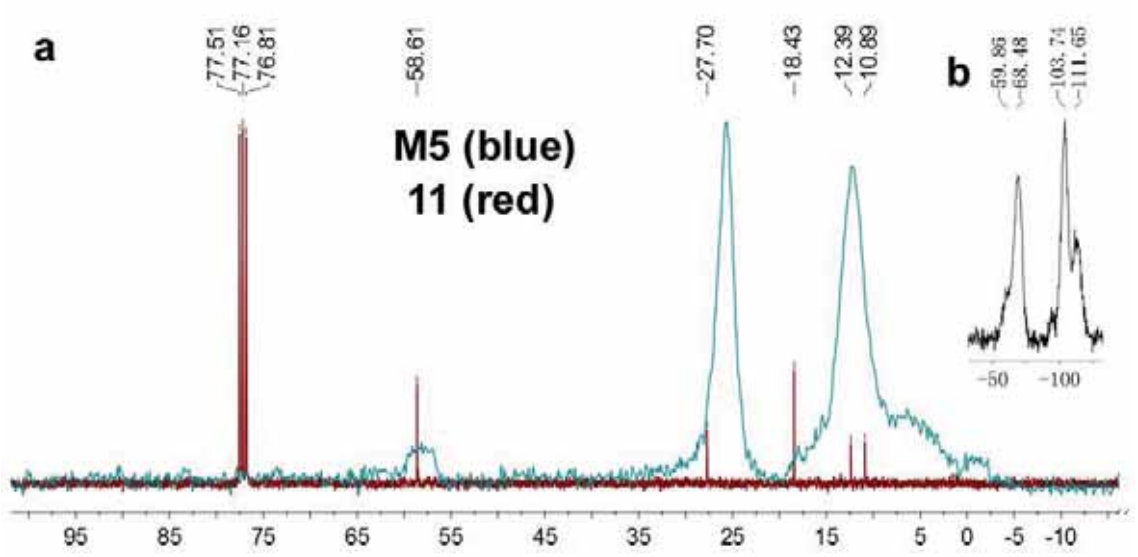

Figure 13. a) ^{13}C CP-MAS solid state NMR spectrum of **M5** and the ^{13}C NMR spectrum of the corresponding precursor **11**; b) ^{29}Si CP-MAS solid state NMR spectrum of **M5**.

The weak bands at about 58 and 18 ppm revealed the existence of some ethoxy groups stemming from the incomplete condensation of the precursor **11**. ^{29}Si solid state NMR spectrum (Figure 13b) showed signals at -68.5 (T^3), -103.7 (Q^3), -111.7 (Q^4), and

a weak T^2 signal at -59.9 ppm, which further proved the incomplete condensation. The TGA and DSC analyses (see Annex) showed curves similar to those of **M1** - **M4**. The 33% weight loss at about 700 °C, indicating the decomposition of the organic moiety, agrees very well with the theoretical value of 32%. The 9.59% iodine content, determined by elemental analysis, was lower than expected. Additional information on the characterization of **M5** can be found in the experimental section.

3.3.4 Catalytic activity of the silica-supported iodoalkane M5 in the α-tosyloxylation of ketones

The catalytic activity of material **M5** in the α-tosyloxylation of various ketones was tested as summarized in Table 5. Surprisingly, with 10% of catalyst loading, the α-tosyloxylation of propiophenone under the present optimized conditions gave a respectable isolated yield of 76% for the corresponding product **15** (Table 5, entry 1). However, attempts to recycle the catalyst resulted in a very low yield even at prolonged reaction time (27 h) (Table 5, entry 2). Notably, an excellent yield was obtained when using *p*-bromoacetophenone as substrate (Table 5, entry 3). Other substrates, such as *p*-nitroacetophenone (Table 5, entry 4) and 3-pentanone (Table 5, entry 5) were also tested, with the corresponding products obtained in moderate yields. Interestingly, it was found that the catalyst could be recycled up to three times in the α-tosyloxylation of acetophenone although a gradual decrease of catalytic activity in the successive reactions was observed (Table 5, entries 6-8). The substrate *p*-methylacetophene (Table 5, entry 9) also proved reactive with this catalyst.

Table 5. α-Tosyloxylation of ketones using **M5** as catalyst.[a]

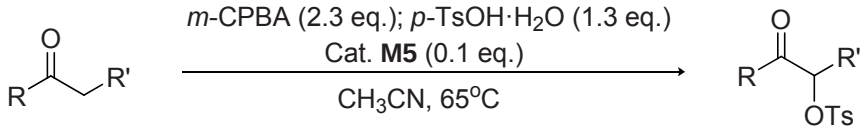

Entry	Product	Time / h	Yield[b] / %
1	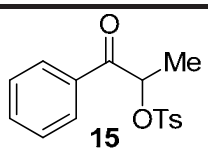 **15**	4	76
2		27	8[c]
3	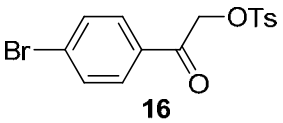 **16**	12	92
4	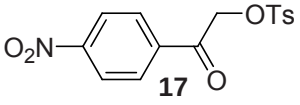 **17**	12	56

5	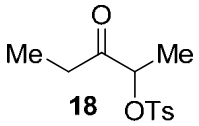 **18**	12	56
6	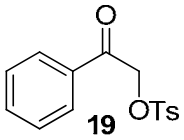 **19**	6	75
7		7	67[c]
8		7	35[d]
9	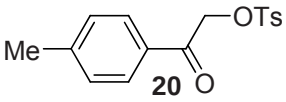 **20**	12	40

[a] [substrate] = 0.2 M. [b] Corrected GC yield (Ph-Ph as internal standard). [c] Second cycle. [d] Third cycle.

3.4 Conclusions and outlook[176]

Organic-inorganic hybrid silica materials **M1-M4** containing iodoarene moieties were synthesized by sol-gel methodologies from bis- and monosilylated precursors **12** and **13** under nucleophilic catalysis. The sol-gel process using the bis-silylated iodoarene **12** was performed with and without added TEOS (**M1**, **M2**), whereas the monosilylated monomer **13** was co-gelified with different amounts of TEOS (**M3**, **M4**). The materials were characterized by elemental analysis, ^{13}C and ^{29}Si CP-MAS solid state NMR, IR, TGA, and N_2-sorption measurements. The catalytic activity of the materials was tested in the α-tosyloxylation of ketones using *m*-CPBA as an oxidant, affording the corresponding α-tosyloxyketones **15** - **22** in moderate to good isolated yields in the case of catalysts **M1-M2**. Camphorsulfonic and methanosulfonic acids have also been successfully used for the oxidative α-functionalization of acetophenone to yield **23** and **24**. The recyclability has been investigated for **M1**, which was recovered by filtration and reused successfully in a second run for several substrates.

A hybrid silica **M5** derived from (3-iodopropyl)triethoxysilane **11** was also prepared through co-gelification with 5 equivalents of TEOS and fully characterized. Unexpectedly, although material **M5** does not contain an iodoarene but an iodoalkane fragment, it also showed catalytic activity for the α-tosyloxylation of various ketones, affording moderate to good yields of the corresponding products. We have no ideas how the **M5** works at present, however, further work (next chapter) will deal with the simple iodoalkanes, *e. g.*, iodobutane as catalyst/precatalyst in this kind of transformations.

[176] Most of this work has been published in: **Guo, W.**; Monge-Marcet, A.; Cattoën, X.; Shafir, A.; Pleixats, R. *React. Funct. Polym.* **2013**, *73*, 192.

3.5 Experimental section

3.5.1 Reagents and methods

When required (as noted in the experimental description), experiments were carried out using standard vacuum and Schlenk techniques, and the solvents were dried, distilled and degassed shortly before use following standard procedure Ethanol was distilled from Mg/I_2. Tetraethyl orthosilicate (TEOS) 98%, tetrabutylammonium fluoride (1 M solution in anhydrous THF), *m*-chloroperbenzoic acid (*m*-CPBA) (approximately 65% purity), methanesulfonic acid (99% purity) and camphorsulfonic acid (99% purity) were purchased from Aldrich and used without any further treatment; *p*-toluenesulfonic acid (*p*-$TsOH \cdot H_2O$) (98% purity) was purchased from Panreac and used as received. The silica gel for flash chromatography was a Macherey-Nagel GmbH & Co KG silica gel with a particle size of 230 – 400 mesh and a pore volume of 0.9 mL/g. The silica gel used for purifying moisture-sensitive organosilanes was dried under a nitrogen flow using a heat gun just before use.

3.5.2 Physicochemical characterization

IR data were obtained on a Bruker Tensor 27 with an ATR Golden Gate. Liquid ^{1}H and ^{13}C NMR spectra were recorded on Bruker DRX-250MHz, DPX-360MHz and AVANCE III 400 MHz instruments, and CP-MAS ^{29}Si solid state NMR spectra were recorded on a Bruker AV400WB. All NMR experiments were performed at the *Servei de Ressonància Magnètica Nuclear* of the *Universitat Autònoma de Barcelona.* ^{1}H NMR chemical shifts (δ, ppm) are referenced to the residual *protio* signal of the deuterated solvent, and the ^{13}C shifts are referenced to the ^{13}C resonance of the solvent. N_2-sorption isotherms were obtained on a Micromeritics ASAP2020 analyzer at the *Institut Charles Gerhardt in Montpellier* after degassing the materials at 55 ºC for 30 h under high vacuum. The surface areas and pore size distributions were calculated from the desorption branch by the Brunauer-Emmett-Teller (BET) transform and the Barrett–Joyner–Halenda (BJH) method, respectively. High resolution mass spectra were determined at the *Servei d'Anàlisi Química* of the *Universitat Autònoma de Barcelona* using a Bruker Daltonic MicroTOFQ spectrometer (Bremen, Germany) equipped with an ESI inlet. Elemental analyses were performed at the *Serveis Científico-Tècnics* of the *Universitat de Barcelona*, and the Si content was determined by inductively coupled plasma optical emission spectroscopy (ICP-OES) using a multichannel Perkin Elmer model Optima 3200 RL spectrometer under standard conditions. The iodine analysis was performed by combustion of the sample in an

oxygen bomb (Calorimeter IKA 5012). The formed gases were absorbed by a 0.25 M sodium hydroxide aqueous solution. The bomb was rinsed twice with deionized water that was collected and added to the sodium hydroxide aqueous solution. The combined solution was diluted to an exact volume in a volumetric flask and analyzed by HPLC (Waters 2690 model equipped with a Waters 996 photodiode array detector, IC-Pak Anion HR column). The corresponding peak was interpreted based on the calibration curve obtained from standard sodium iodide aqueous solutions. TGA analyses were performed under an argon atmosphere at the *Institut de Ciència dels Materials de Barcelona* using a NETZSCH STA 449 F1 instrument (TGA/DSC).

3.5.3 Synthesis of silylated precursors

3.5.3.1 Preparation of 1-iodo-3, 5-dimethoxybenzene, **9**

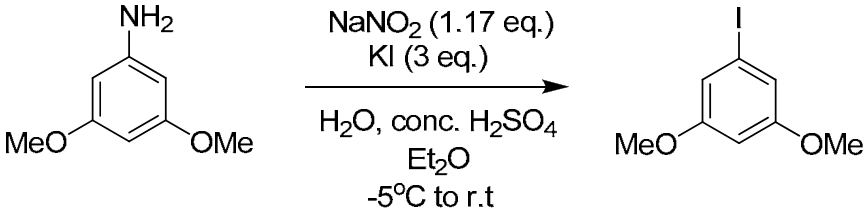

This compound was prepared following a reported procedure.[169] To a stirred solution of 3,5-dimethoxyaniline (9.15 g, 59.7 mmol) in water (100 mL) maintained at – 5 °C, concentrated H_2SO_4 (9 mL) was added dropwise, followed by the addition of a solution of $NaNO_2$ (4.85 g, 70.3 mmol) in water (20 mL). Keeping the temperature below 0 °C, the reaction mixture was stirred for 20 min, then diethyl ether was added (50 mL), followed by a dropwise addition of a solution of potassium iodide (30 g, 180.7 mmol) in water (30 mL). After the mixture was stirred at room temperature for 6 h, the layers were separated and the aqueous phase was extracted with additional diethyl ether (3 × 100 mL). The combined organic fraction was washed successively with 25% (w/v) aqueous $Na_2S_2O_3 \cdot 5H_2O$ (3 × 50 mL), 1 M HCl (1 x 100 mL) and 2 M NaOH (1 x 100 mL), then dried over anhydrous $MgSO_4$, filtered and concentrated to a brown oil. The crude mixture was purified by silica gel chromatography using hexane/ethyl acetate 95:5 (R_f = 0.56) as the eluent to yield 1-iodo-3,5-dimethoxybenzene, **9**, as a white solid; yield: 11.76 g (75%). ^{1}H NMR (250 MHz, $CDCl_3$) δ (ppm): 6.85 (d, *J* = 2.2 Hz, 2 H, *o*-ArH), 6.40 (t, *J* = 2.2 Hz, 1 H, *p*-ArH), 3.76 (s, 6 H, Me). ^{13}C NMR (62.50 MHz, $CDCl_3$) δ (ppm): 164.4, 116.1, 100.9, 94.4, 55.8. IR (ATR) *v* (cm^{-1}): 3069, 1258, 1026, 1050, 615.

3.5.3.2 Preparation of 5-iodoresorcinol, **10**

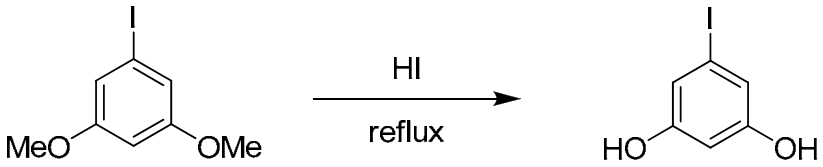

This compound was prepared following a described procedure.[169] A mixture of 1-iodo-3,5-dimethoxybenzene **9** (6.60 g, 25.0 mmol) and hydroiodic acid (45 wt%, 60 mL) was heated to reflux for 40 h. The solution was then cooled to room temperature and diluted with water (deionized, 80 mL) and diethyl ether (80 mL). The organic layer was separated and washed successively with 1 M sodium thiosulfate (3 × 60 mL) and distilled water (1 x 50 mL). The solution was dried with anhydrous $MgSO_4$, and the solvent was evaporated to afford an oil that spontaneously solidified at room temperature to give product **10** as a white solid; yield: 5.84 g (99%). ^{1}H NMR (360 MHz, DMSO-d_6) δ (ppm): 9.52 (s, 2 H), 6.57 (d, J = 1.8 Hz, 2 H), 6.20 (br s, 1 H). ^{13}C NMR (90 MHz, DMSO-d_6) δ (ppm): 159.3, 115.3, 102.4, 94.6. IR (ATR) ν (cm^{-1}): 3254, 1383, 1215, 610.

3.5.3.3 Preparation of (3-iodopropyl)triethoxysilane, **11**

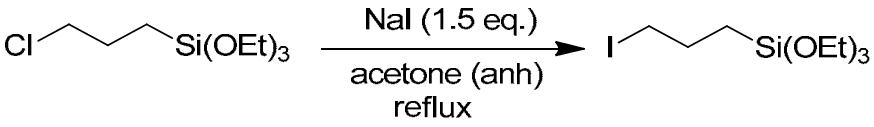

This compound was prepared following a described procedure.[177] A mixture of NaI (13.48 g, 89.9 mmol), (3-chloropropyl)triethoxysilane (15.0 mL, 1.00 g/mL, 62.3 mmol) and anhydrous acetone (50 mL) was stirred under reflux for 2 days under an argon atmosphere. At this point, the mixture was filtered and the solvent from the filtrate was evaporated under reduced pressure. The residue was triturated with dry hexane (30 mL) and once again filtered. After removal of hexane from the filtrate, the (3-iodopropyl)triethoxysilane was obtained as a pale yellow liquid; yield: 18.63 g (90%). ^{1}H NMR (250 MHz, $CDCl_3$) δ (ppm): 3.82 (q, J = 7.0 Hz, 6H, OCH_2), 3.22 (t, J = 7.0 Hz, 2H, -CH_2I), 1.99-1.87 (m, 2 H, ICH_2CH_2), 1.23 (t, J = 7.0 Hz, 9 H, CH_3), 0.79-0.66 (m, 2 H, $SiCH_2$). ^{13}C NMR (100 MHz, $CDCl_3$) δ (ppm): 58.8, 27.8, 18.6, 12.6, 11.1. IR (ATR) ν (cm^{-1}): 2972, 2884, 1073, 784, 629.

---

[177] Dubois, G.; Tripier, R.; Brandes, S.; Denat, F.; Guilard, R. *J. Mater. Chem.* **2002**, *12*, 2255.

3.5.3.4 Preparation of the bis-silylated iodoarene, **12**

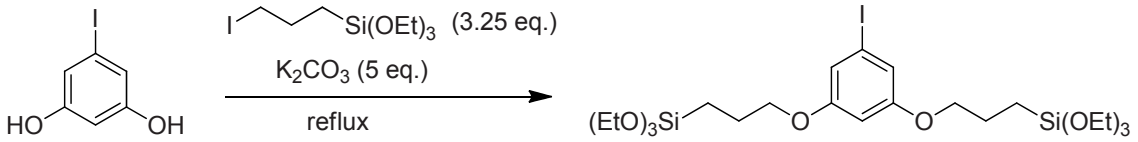

Dry acetone (20 mL) was added to a mixture of compound **10** (2.360 g, 10 mmol), K_2CO_3 (6.90 g, 50 mmol) and (3-iodopropyl)triethoxysilane **11** (10.801 g, 32.5 mmol) under a N_2 atmosphere. After refluxing for 27 h under N_2, the solvent was removed under reduced pressure and the residue was extracted with dry dichloromethane/hexane 1:4 (10 mL × 4), filtering the resulting solution after each round of extraction. The volatile fraction was removed under vacuum to afford a colorless oily residue, which was purified by silica gel chromatography (hexane/ethyl acetate 25:1 as eluent). R_f = 0.22 (silica gel, hexane/ethyl acetate 95:5). Yield of **12**: 1.93 g, 30%. ^{1}H NMR (250 MHz, $CDCl_3$) δ (ppm): 6.83 (d, *J* = 2.1 Hz, 2 H, *o*-ArH), 6.39 (m, 1 H, *p*-ArH), 3.93 – 3.77 (m, 16 H, -OCH_2), 1.88 (m, 4 H), 1.23 (t, *J* = 7.0 Hz, 18 H, -Me), 0.79 – 0.69 (m, 4 H). ^{13}C NMR (62.5 MHz, $CDCl_3$) δ (ppm): 160.3, 116.0, 101.4, 93.6, 69.9, 58.1, 22.5, 18.1, 6.3. IR (ATR) *v* (cm^{-1}): 2972, 2925, 2882, 1293, 1277, 1073, 628. HRMS (ESI): calculated for $[C_{24}H_{45}IO_8Si_2Na]^+$ (M^++Na): 667.1595; found: 667.1600.

3.5.3.5 Preparation of the monosilylated iodoarene, **13**

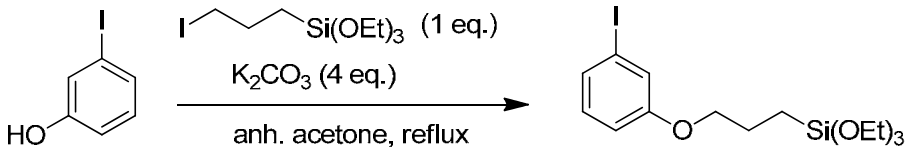

Dry acetone (20 mL) was added to a mixture of 3-iodophenol (3.30 g, 15.0 mmol), K_2CO_3 (8.29 g, 60 mmol) and (3-iodopropyl)triethoxysilane **11** (4.984 g, 15.0 mmol) under nitrogen atmosphere. The mixture was kept at reflux for 24 h under nitrogen. The organic solvent was evaporated under vacuum and the residue was extracted with dry hexane (4 x 10 mL), filtering the resulting solution after each round of extraction. The solvent was removed under reduced pressure to afford **13** as a colorless oil (2.10 g, 33% yield). ^{1}H NMR (250 MHz, $CDCl_3$) δ (ppm): 7.25-7.12 (m, 2 H), 6.98 (t, J = 8.2 Hz, 1 H), 6.85 (d, J = 7.1 Hz, 1 H), 3.96 - 3.71 (m, 8 H), 1.88 (m, *2* H), 1.23 (t, J = 7.0 Hz, 9H), 0.78 - 0.72 (t, J = 7.1 Hz, 2 H). ^{13}C NMR (62.5 MHz, $CDCl_3$) δ (ppm): 160.0, 131.0, 129.9, 124.0, 114.5, 94.7, 70.4, 58.7, 23.0, 18.6, 6.8. IR (ATR) *v* (cm^{-1}): 2967, 2883,

1584, 1259, 1075, 1015, 632. HRMS (ESI): calculated for $[C_{15}H_{25}IO_4SiNa]^+$ (M^++Na): 447.0465; found: 447.0467.

3.5.3.6 Preparation of 1,3-bis(allyloxy)-5-iodobenzene, **14**

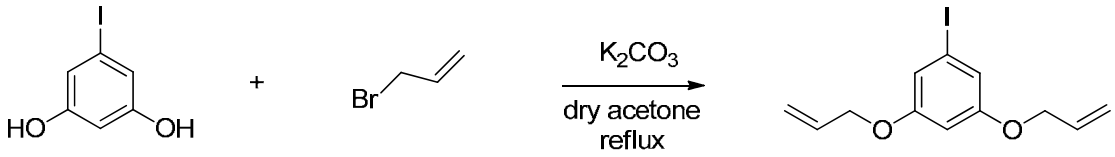

To a mixture of allyl bromide (2.420 g, 20 mmol), 1-iodo-3,5-dimethoxybenzene **9** (1.180 g, 5.0 mmol) and K_2CO_3 (3.455 g, 25 mmol) was added dry acetone (20 mL). The mixture was refluxed for 6 h under N_2 and then the cooled mixture was filtered. The filtrate was evaporated under reduced pressure to remove the volatiles affording the 1,3-bis(allyloxy)-5-iodobenzene **14** as a light green oil (1.570 g, 99%). ^{1}H NMR (250 MHz, $CDCl_3$) δ (ppm): 6.87 (d, *J* = 2.2 Hz, 2 H, ArH), 6.44 (t, *J* = 2.2 Hz, 1 H, ArH), 6.01 (m, 1 H), 5.40 (dd, *J* = 17.3, 1.5 Hz, 2 H), 5.29 (dd, *J* = 10.5, 1.3 Hz, 2 H), 4.51 – 4.43 (m, 4 H). ^{13}C NMR (62.5 MHz, $CDCl_3$) δ (ppm): 160.1, 132.8, 118.1, 116.8, 102.1, 94.1, 69.1. IR (ATR) *v* (cm^{-1}): 2962, 1591, 1569, 1019, 780, 632. HRMS (ESI): calculated for $[C_{12}H_{13}IO_2Na]^+$ (M^++Na): 338.9852; found: 338.9841.

3.5.4 Preparation of sol-gel immobilized iodoarenes and an iodoalkane

3.5.4.1 Preparation and characterization of hybrid silica material **M1**

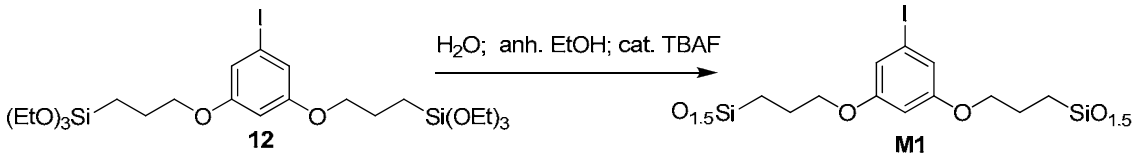

The bis-silylated compound **12** (1.665 g, 2.583 mmol) was dissolved in dry ethanol (1.8 mL). To this solution, a solution of Milli-Q water (0.28 mL, 15.49 mmol) and TBAF (30 µL, commercial 1 M in anhydrous THF) in dry EtOH (0.8 mL) was added. The final mixture was shaken vigorously for 10 s to obtain a homogenous solution and was then kept under static conditions. After 30 min, gelification was observed, and the material was aged at room temperature for 6 days. The resulting gel was pulverized, separated by filtration and washed successively with water (2 × 6 mL), EtOH (2 × 6 mL) and acetone (2 × 6 mL). The final solid was dried overnight at 55 °C under vacuum (2.0 mbar) to afford **M1** as a white solid (1.005 g). ^{13}C CP-MAS NMR (100.62 MHz) *δ* (ppm): 159.5, 118.2, 113.2, 99.9, 93.7, 68.9, 57.4, 22.2, 17.6, 7.7. ^{29}Si CP-MAS NMR (79.5

MHz) *δ* (ppm): -47.6 (T^0, 2%), -55.0 (T^1, 8%), -61.0 (T^2, 20%), -68.6 (T^3, 69%). IR (ATR) *v* (cm^{-1}): 2929, 2880, 1590, 1567, 1433, 1260, 1014 (broad), 797, 676. BET surface area: < 5 m^2/g; non-porous material. TGA: (argon, 20 to 700 ºC) residual mass 47.9%. EA calculated for $C_{12}H_{15}ISi_2O_5$ (considering complete condensation): 34.13% C, 3.58% H, 13.30% Si, 30.05% I; found: 34.7% C, 4.5% H, 11.5% Si, 13.5% I.

3.5.4.2 Preparation and characterization of hybrid silica material **M2**

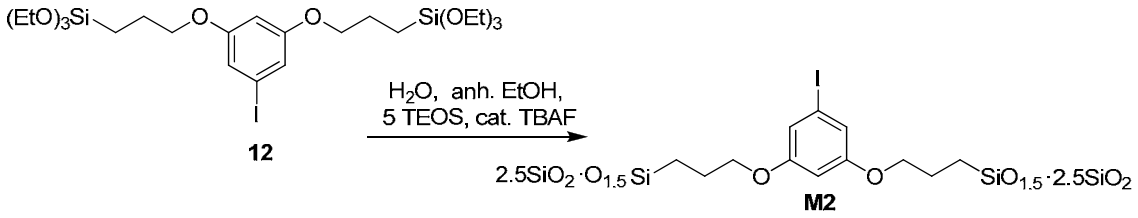

Bis-silylated compound **12** (0.410 g, 0.636 mmol) and TEOS (0.71 mL, ρ = 0.934 g/mL, 3.18 mmol) were dissolved in dry ethanol (3 mL). A solution of Milli-Q water (0.30 mL, 16.536 mmol) and TBAF (50 µL, commercial solution 1 M in anhydrous THF) in dry EtOH (0.80 mL) was then added to the first solution. The final mixture was shaken vigorously for 10 s to obtain a homogenous solution. After 10 min, a gel formed that was then aged at room temperature for 6 days. The resulting gel was pulverized, filtered and washed successively with water (2 × 6 mL), EtOH (2 × 6 mL) and acetone (2 × 6 mL). The final solid was dried overnight at 55 °C under vacuum (2.0 mbar) to afford **M2** as a white solid (0.410 g). ^{13}C CP-MAS NMR (100.62 MHz) *δ* (ppm): 160.7, 119.6, 101.7, 94.2, 69.8, 58.6, 22.8, 17.4, 8.5. ^{29}Si CP-MAS NMR (79.5 MHz) *δ*: -59.3 (T^2), -68.2 (T^3), -93.3 (Q^2), -102.3 (Q^3), -110.8 (Q^4). IR (ATR) *v* (cm^{-1}): 2944, 1592, 1438, 1050, 800, 679. BET surface area: 255 m^2/g; pore volume: 0.838 cm^3/g. TGA: (argon, 20 to 700 ºC) residual mass 59.8%. EA calculated for $C_{12}H_{15}ISi_2O_5 \cdot 5SiO_2$ (considering complete condensation): 19.94% C, 2.09% H, 27.20% Si, 17.56% I; found: 17.8% C, 2.1% H, 24.2% Si, 8.2% I.

3.5.4.3 Preparation and characterization of hybrid silica material **M3**

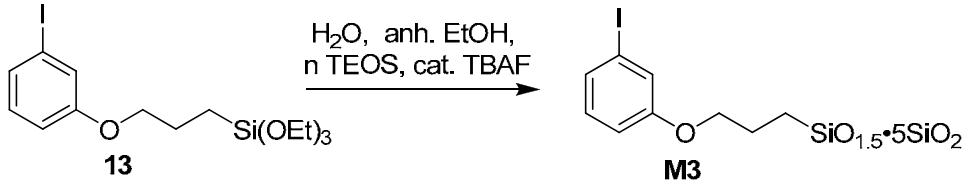

Monosilylated compound **13** (0.800 g, 1.887 mmol) and TEOS (2.10 mL, d = 0.934 g/mL, 9.4 mmol) were dissolved in dry ethanol (10 mL). Then, a solution of Milli-Q

water (0.78 mL, 43.4 mmol) and TBAF (113 µL, commercial solution 1 M in anhydrous THF) in dry EtOH (1.3 mL) was added to the first solution. The final mixture was shaken vigorously for 10 s to obtain a homogenous solution. After 15 min, a gel formed that was then aged at room temperature for 6 days. The gel obtained was pulverized, filtered off and washed successively with water (2 × 6 mL), EtOH (2 × 6 mL) and acetone (2 × 6 mL). The final solid was dried overnight at 55 °C under vacuum (2.0 mbar) to afford **M3** as a white solid (1.087 g). ^{13}C CP-MAS NMR (100.62 MHz) *δ* (ppm): 159.8, 130.2, 123.8, 113.5, 94.5, 69.6, 60.2, 58.5, 30.8, 22.9, 19.8, 17.8, 13.7, 8.7. ^{29}Si CP-MAS NMR (79.5 MHz) *δ* (ppm): -58.3 (T^2), -69.2 (T^3), -104.8 (Q^3), -114.8 (Q^4). IR (ATR) *v* (cm^{-1}): 2942, 1584, 1050, 801, 680, 654. BET surface area: 109 m^2/g; pore volume: 0.711 cm^3/g. TGA: (argon, 20 to 700 ºC) residual mass 67.1%. EA calculated for $C_9H_{10}ISiO_{2.5}{\cdot}5SiO_2$ (considering complete condensation): 17.62% C, 1.64% H, 27.46% Si, 20.68% I; found: 17.3% C, 2.2% H, 27.3% Si, 6.3% I.

3.5.4.4 Preparation and characterization of hybrid silica material **M4**

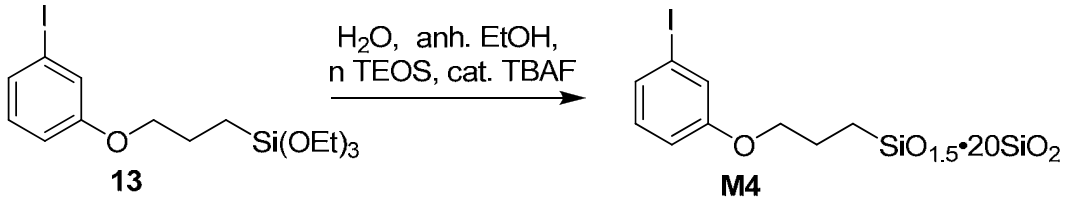

Monosilylated compound **13** (0.400 g, 0.943 mmol) and TEOS (4.2 mL, d = 0.934 g/mL, 18.9 mmol) were dissolved in dry ethanol (15 mL). Then, a solution of Milli-Q water (1.4 mL, 77.8 mmol) and TBAF (200 µL, commercial solution 1 M in anhydrous THF) in dry EtOH (4.8 mL) was added to the first solution. The final mixture was shaken vigorously for 10 s to obtain a homogenous solution. After 14 min, a gel formed that was then aged at room temperature for 6 days. Then, the gel was pulverized, filtered off and washed successively with water (2 × 6 mL), EtOH (2 × 6 mL) and acetone (2 × 6 mL). The final solid was dried overnight at 55 °C under vacuum (2.0 mbar) to afford **M4** as a white solid (1.302 g). ^{29}Si CP-MAS NMR (79.5 MHz) *δ* (ppm): -67.8 (T^3), -104.8 (Q^3), -113.0 (Q^4). IR (ATR) *v* (cm^{-1}): 2971, 1584, 1050, 800, 681. BET surface area: 124 m^2/g; pore volume: 0.790 cm^3/g. TGA: (argon, 20 to 700 ºC) residual mass 79.5%. EA calculated for $C_9H_{10}ISiO_{2.5}{\cdot}20SiO_2$ (considering complete condensation): 7.91% C, 0.74% H, 43.17%Si, 9.29% I; found: 10.1% C, 1.7% H, 44.0% Si, 3.9% I.

3.5.4.5 Preparation and characterization of hybrid silica material **M5**

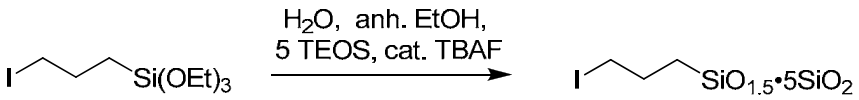

(3-Iodopropyl)triethoxysilane **11** (1.329 g, 4.0 mmol) and TEOS (4.5 mL, d = 0.934 g/mL, 20 mmol) were dissolved in dry ethanol (18 mL). Then, a solution of Milli-Q water (1.7 mL, 92.0 mmol) and TBAF (200 µL, commercial solution 1 M in anhydrous THF) in dry EtOH (6.0 mL) was added to the first solution. The final mixture was shaken vigorously for 10 s to obtain a homogenous solution. After 14 min, a gel formed that was then aged at room temperature for 6 days. Then, the gel was pulverized, filtered off and washed successively with water (3 × 6 mL), EtOH (3 × 6 mL) and acetone (3 × 6 mL). The final solid was dried overnight at 55 °C under vacuum (2.0 mbar) to afford **M5** as a white solid (1.758 g). ^{29}Si CP-MAS NMR (79.5 MHz) *δ* (ppm): -59.9 (T^2), -68.5 (T^3), -103.7 (Q^3), -111.7 (Q^4). IR (ATR) *v* (cm^{-1}): 2976, 1630, 1045, 954, 793. BET surface area: 319 m^2/g; pore volume: 0.984 cm^3/g. TGA: (argon, 20 to 700 ºC) residual mass 66.7%. EA calculated for $C_3H_6ISiO_{1.5}{\cdot}5SiO_2$ (considering complete condensation): 6.91% C, 1.16% H, 32.31%Si, 24.33% I; found: 9.59% C, 1.90% H, 29.38% Si, 9.59% I.

3.5.5 General procedure for the catalytic oxidative α-tosyloxylation of ketones and characterization of compounds

All catalytic runs were performed in screw-top sealable tubes (10 mL). To a solution of ketone (1 mmol) in CH_3CN (5 mL), *p*-toluenesulfonic acid (247 mg, 1.3 mmol), commercial available *m*-CPBA source (65% purity, 611 mg of commercial source, 2.3 mmol) and the supported catalyst (amount calculated to give 0.1 mmol of I, 10 mol% I) were added. The tube was sealed, and the mixture was stirred at 65 °C under a nitrogen atmosphere for the time indicated in Tables (Table 3, Table 4 and Table 5). For the catalyst recycling studies, the reaction mixture was filtered and the recovered catalyst was washed with acetonitrile (2 × 3 mL), further washed with diethyl ether (3 × 3 mL), dried under a vacuum and directly used in the next cycle. The IR spectra of the recovered **M1** and **M2** (see Annex) showed similar signals as the fresh materials. The filtrates were poured into a saturated aq. $NaHCO_3$ solution and extracted with $CHCl_3$ (3 × 15 mL). The combined organic layer was dried over anhydrous Na_2SO_4 and concentrated under reduced pressure. The residue was further purified by flash column chromatography on silica gel.

3.5.5.1 α-Tosyloxypropiophenone, **15**.[124a]

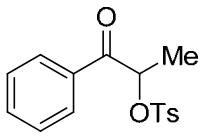

Chromatography details (EA : Hexane = 1:4, R_f = 0.34); ^{1}H NMR (360 MHz, $CDCl_3$) δ (ppm): 7.93-7.84 (m, 2H), 7.73 (d, *J* = 8.3 Hz, 2 H), 7.57 (t, *J* = 7.4 Hz, 1H), 7.43 (t, J = 7.5 Hz, 2 H), 7.24 (t, J = 8.0 Hz, 2 H), 5.77 (q, *J*= 6.9 Hz, 1 H), 2.36 (s, 3 H), 1.57 (d, *J* = 6.9 Hz, 3 H); ^{13}C NMR (90 MHz, $CDCl_3$) δ (ppm): 194.9, 145.2, 134.0, 133.8, 133.5, 129.9, 128.9, 128.8, 128.0, 77.5, 21.7, 18.8; IR (ATR) *v* (cm^{-1}): 2936, 1698 (C=O), 1577, 1356.

3.5.5.2 α-Tosyloxy-*p*-bromoacetophenone, **16**.[178]

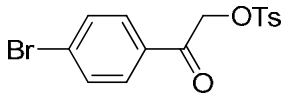

Chromatography details (EA : Hexane = 1:9, R_f = 0.15); ^{1}H NMR (360 MHz, $CDCl_3$) δ (ppm): 7.83 (d, *J* = 8.2 Hz, 2 H), 7.70 (d, *J* = 8.5 Hz, 2 H), 7.60 (d, *J* = 8.5 Hz, 2 H), 7.34 (d, *J* = 8.1 Hz, 2 H), 5.20 (s, 2 H), 2.44 (s, 3 H); ^{13}C NMR (90 MHz, $CDCl_3$) δ (ppm): 189.8, 145.6, 132.6, 132.4, 130.1, 129.7, 128.3, 69.9, 21.8; IR (ATR) *v* (cm^{-1}): 2918, 2852, 1699 (C=O), 1586, 1358, 1059.

3.5.5.3 α-Tosyloxy-*p*-nitroacetophenone, **17**.[124a]

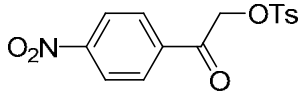

Chromatography details (EA: Hexane = 1:4, R_f = 0.30); ^{1}H NMR (360 MHz, $CDCl_3$) δ (ppm): 8.31 (d, *J* = 8.1 Hz, 2 H), 8.02 (d, *J* = 7.7 Hz, 2 H), 7.82 (d, *J* = 7.6 Hz, 2 H), 7.36 (d, *J* = 7.5 Hz, 2 H), 5.24 (s, 2 H), 2.46 (s, 3 H); ^{13}C NMR (90 MHz, $CDCl_3$) δ (ppm): 189.9, 150.9, 145.8, 138.3, 132.4, 130.2, 129.5, 128.3, 124.2, 70.1, 21.8; IR (ATR) *v* (cm^{-1}): 2950, 2858, 1708 (C=O), 1598, 1519 (NO_2), 1341 (NO_2), 1320, 848.

---

[178] Karade, N. N.; Tiwari, G. B.; Shinde, S. V.; Gampawar, S. V.; Kondre, J. M. *Tetrahedron Lett.* **2008**, *49*, 3441.

3.5.5.4 α-Tosyloxy-3-pentanone, **18**.[124a]

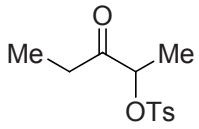

Chromatography details (EA : Hexane = 1:9, R_f = 0.11, unstable in the air); ^{1}H NMR (360 MHz, $CDCl_3$) δ (ppm): 7.81 (d, *J* = 8.3 Hz, 2 H), 7.36 (d, *J* = 7.7 Hz, 2 H), 4.85-4.76 (q, *J* = 10.8 Hz, 1 H), 2.59 (q, *J* = 7.1 Hz, 2 H), 2.46 (s, 3 H), 1.35 (d, *J* = 7.0 Hz, 3 H), 1.02 (t, *J* = 7.2 Hz, 3 H); ^{13}C NMR (90 MHz, $CDCl_3$) δ (ppm): 207.8, 145.4, 133.3, 130.1, 128.0, 80.8, 31.3, 21.8, 17.7, 7.1; IR (ATR) *v* (cm^{-1}): 1724 (C=O), 1407, 1364, 907, 632.

3.5.5.5 α–Tosyloxyacetophenone, **19**.[124a]

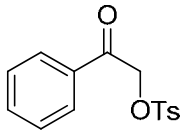

Chromatography details (EA : Hexane = 1:3, R_f = 0.36); ^{1}H NMR (250 MHz, $CDCl_3$) δ (ppm): 7.87-7.82 (m, 4 H), 7.61 (t, *J* = 7.3 Hz, 1 H), 7.46 (t, *J* = 7.6 Hz, 2 H), 7.34 (d, *J* = 8.0 Hz, 2 H), 5.26 (s, 2 H), 2.44 (s, 3 H); ^{13}C NMR (90 MHz, $CDCl_3$) δ (ppm): 190.4, 145.4, 134.3, 133.8, 132.7, 130.0, 129.0, 128.2, 128.1, 70.1, 21.8; IR (ATR) *v* (cm^{-1}): 2933, 1712 (C=O), 1596, 1449, 1356.

3.5.5.6 α-Tosyloxy-*p*-methylacetophenone, **20**.[124a]

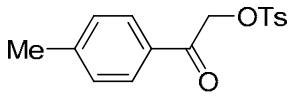

Chromatography details (EA : Hexane = 1:9, R_f = 0.11); ^{1}H NMR (360 MHz, $CDCl_3$) δ (ppm): 7.84 (d, *J* = 8.2 Hz, 2H), 7.73 (d, *J* = 8.1 Hz, 2H), 7.34 (d, *J* = 8.1 Hz, 2H), 7.25 (d, *J* = 7.5 Hz, 2H), 5.23 (s, 2H), 2.44 (s, 3H), 2.40 (s, 3H); ^{13}C NMR (90 MHz, $CDCl_3$) δ (ppm): 190.1, 145.60, 145.57, 133.0, 131.6, 130.2, 129.9, 128.44, 128.39, 70.2, 22.07, 21.98; IR (ATR) *v* (cm^{-1}): 1699 (C=O), 1345, 1170.

3.5.5.7 α-Tosyloxy-*p*-chloroacetophenone, **21**.[124a]

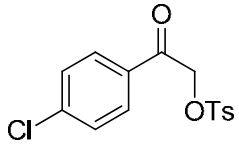

Chromatography details (EA : Hexane = 1:10, R_f = 0.44); ^{1}H NMR (360 MHz, $CDCl_3$) δ (ppm): 7.83 (d, *J* = 8.2 Hz, 2H), 7.78 (d, *J* = 8.4 Hz, 2H), 7.44 (d, *J* = 8.4 Hz, 2H), 7.35 (d, *J* = 8.0 Hz, 2H), 5.20 (s, 2H), 2.45 (s, 3H); ^{13}C NMR (90 MHz, $CDCl_3$) δ (ppm): 189.6, 145.6, 140.9, 132.6, 132.2, 130.1, 129.6, 129.4, 128.3, 70.0, 21.8; IR (ATR) *v* (cm^{-1}): 1699 (C = O), 1359, 1174, 660.

3.5.5.8 α-Tosyloxy-*o*-bromoacetophenone, **22**.[178]

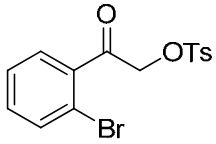

Chromatography details (EA : Hexane = 1:6, R_f = 0.28); ^{1}H NMR (360 MHz, $CDCl_3$) δ (ppm): 7.80 (d, *J* = 7.5 Hz, 2H), 7.60 (d, *J* = 7.0 Hz, 2H), 7.38 – 7.33 (m, 4H), 5.13 (s, 2H), 2.45 (s, 3H); ^{13}C NMR (90 MHz, $CDCl_3$) δ (ppm): 194.8, 145.5, 137.6, 133.9, 133.0, 132.6, 130.0, 129.8, 128.2, 127.7, 129.3, 71.2, 21.8; IR (ATR) *v* (cm^{-1}): 1721 (C = O), 1176, 1040, 633.

3.5.5.9 α-(Camphorsulfonyloxy)acetophenone, **23**.[124a]

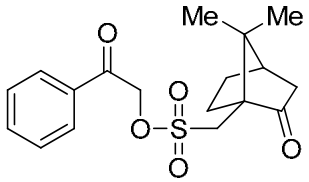

Chromatography details (EA : Hexane = 1:10, R_f = 0.40); ^{1}H NMR (360 MHz, $CDCl_3$) δ (ppm): 7.91 (d, *J* = 7.3 Hz, 2H), 7.63 (t, *J* = 7.4 Hz, 1H), 7.50 (t, *J* = 7.6 Hz, 2H), 5.53 (s, 2H, CH_2O), 3.80 (d, *J* = 15.1 Hz, 1H, C*H*HSO_2), 3.34 (d, *J* = 15.1 Hz, 1H, CH*H*SO_2), 2.48 – 2.36 (m, 2H), 2.14 – 2.06 (m, 2H), 1.95 (d, *J* = 18.5 Hz, 1H), 1.82 – 1.76 (m, 1H), 1.46 (ddd, *J* = 13.2, 9.4, 4.0 Hz 1H), 1.12 (s, 3H, CH_3), 0.90 (s, 3H, CH_3); ^{13}C NMR (90 MHz, $CDCl_3$) δ (ppm): 214.5, 190.9, 134.4, 133.8, 129.2, 128.0, 70.4, 48.6, 48.3, 42.9, 42.7, 27.1, 25.1, 19.9, 19.8; IR (ATR) *v* (cm^{-1}): 1744 (C = O), 1707 (C = O), 1171.

3.5.5.10 α-(Methanesulfonyloxy)acetophenone, **24**.[124a]

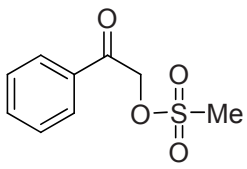

Chromatography details (EA : Hexane = 1:4, R_f = 0.20); ^{1}H NMR (360 MHz, $CDCl_3$) δ (ppm): 7.90 (d, *J* = 7.4 Hz, 2H), 7.65 (t, *J* = 7.4 Hz, 1H), 7.52 (t, *J* = 7.7 Hz, 2H), 5.52 (s, 2H), 3.29 (s, 3H); ^{13}C NMR (90 MHz, $CDCl_3$) δ (ppm): 191.2, 134.6, 133.5, 129.2, 127.9, 70.4, 39.3; IR (ATR) *v* (cm^{-1}): 1703 (C = O), 1171, 966.

Part I. Hypervalent iodine species: reagents and intermediates in oxidative processes

CHAPTER 4

Oxidative breakdown of iodoalkanes to catalytically active iodine species for the α-tosyloxylation of ketones

Chapter 4. Oxidative breakdown of iodoalkanes to catalytically active iodine species for the α-tosyloxylation of ketones

4.1 Introduction

As mentioned previously in chapter 3 of part I of this thesis, considering the close relationship between the hypervalent iodine catalysis and the classical stoichiometric applications, it is not surprising that the catalysis of α-tosyloxylation of ketones has been limited to iodoarenes (Scheme 71a). After all, with the exception of some very bulky or heavily fluorinated derivatives, hypervalent iodoalkanes are notoriously unstable,[2] making their use in stoichiometric applications unfeasible. Indeed, when generated, the $–IX_2$ moiety in such species has a leaving group ability orders of magnitude higher than that of an iodide.[25] Interestingly, few previous reports[125,126] showed the use of molecular iodine and ammonium iodide as pre-catalysts, even if the proposed mechanism still goes back to iodoarenes. In both cases they add a catalytic amount of an arene (benzene, *tert*-butylbenzene) and a stoichiometric oxidant (usually *m*-CPBA). The authors claim that, in the presence of the oxidant, catalytic amounts of iodoarenes can be formed *in situ* via the reaction of I_2 or ammonium iodide with the iodine-free arene (*e. g.*, benzene, *tert*-butylbenzene or even the reagent TsOH) present in the catalytic system (Scheme 71b), as discussed in the previous chapter of this thesis. In fact, a control reaction between TsOH (2.1 mmol) and *m*-CPBA (2.2 mmol) in the presence of molecular iodine (2.4 mmol) in a mixture of acetonitrile (3 mL) and 2,2,2-trifluoroethanol (3 mL) at 60 °C for five hours indeed provided 4-iodotoluene in 54% yield.[125] These iodoarenes would enter into the catalytic cycle shown in Scheme 71a, generating *in situ* the corresponding hypervalent iodine reagent.

It should be noted that the hypoiodite salts, instead of organo iodine species, were also proposed as true catalyst in some oxidative coupling reactions other than α-tosyloxylation of ketones.[179] During the course of our own investigation into immobilized organoiodoarenes as recyclable catalysts in the α-tosyloxylation of ketones,[176] however, the silica supported alkyliodide **M5**, in which the iodoarene is absent, was also shown to be a recyclable catalyst (Scheme 71c, see Chapter 3 of Part I of this thesis for details). Intrigued by these interesting observations, we initiated a

[179] (a) Uyanik, M.; Okamoto, H.; Yasui, T.; Ishihara, K. *Science* **2010**, *328*, 1376. (b) Li, X.; Zhou, C.; Xu, X. *ARKIVOC* **2012** (ix) 150.

project to investigate the possible catalytic activities of common iodoalkanes in this kind of transformations.

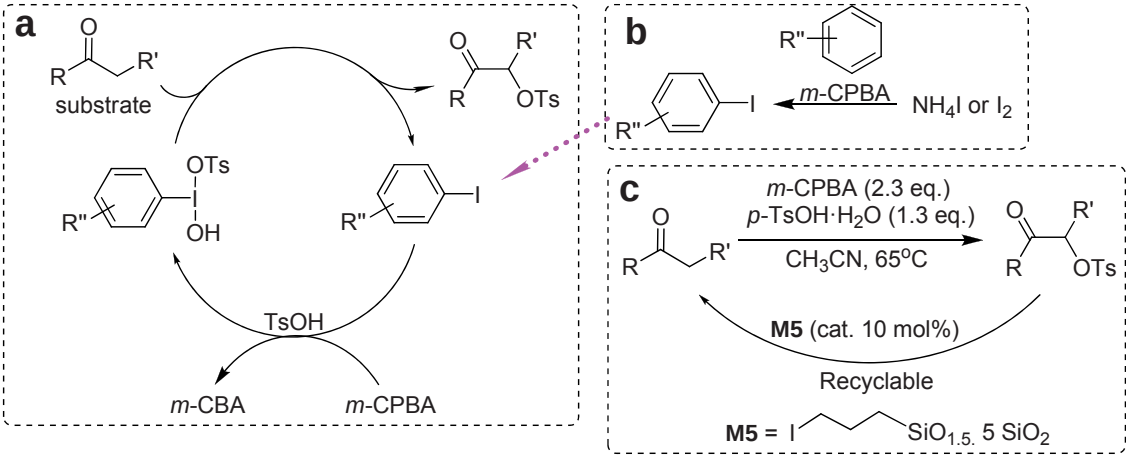

Scheme 71. Methodologies for α-tosyloxylation of ketones: a) under catalysis by iodoarenes; b) under catalysis by iodoarenes formed *in situ* from molecular iodine or iodides in the presence of an arene and an oxidant; c) under catalysis by silica supported alkyliodide **M5** (our new findings).

On the other hand, efforts have been made by several groups to develop a catalytic enantioselective variant for the preparation of α-chiral substituted ketones on the basis of chiral iodine reagents (Scheme 72).[180] Pioneering works in this field have been performed by Wirth's group,[180d,e] in terms of both chiral stoichiometric iodine reagents and iodoarene catalysts.

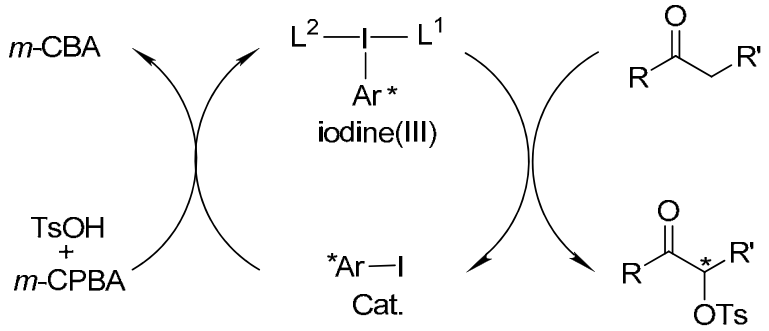

Scheme 72. Chiral iodine(III)-mediated α-tosyloxylation of ketones.

---

[180] (a) Farooq, U.; Schäfer, S.; Shah, A. A.; Freudendahl, D. M.; Wirth, T. *Synthesis* **2010**, 1023. (b) Altermann, S. M.; Richardson, R. D.; Page, T. K.; Schmidt, R. K.; Holland, E.; Mohammed, U.; Paradine, S. M.; French, A. N.; Richter, C.; Bahar, A. M.; Witulski, B.; Wirth, T. *Eur. J. Org. Chem.* **2008**, 5315. (c) Richardson, R. D.; Page, T. K.; Altermann, S. M.; Paradine, S. M.; French, A. N.; Wirth, T. *Synlett* **2007**, 538. (d) Hirt, U. H.; Schuster, M. F. H.; French, A. N.; Wiest, O. G.; Wirth, T. *Eur. J. Org. Chem.* **2001**, 1569. (e) Hirt, U. H.; Spingler, B.; Wirth, T. *J. Org. Chem.* **1998**, *63*, 7674. (f) Guilbault, A.; Basdevant, B.; Wanie, V.; Legault, C. Y. *J. Org. Chem.* **2012**, *77*, 11283.

Currently, the best enantioselectivities obtained in the catalytic enantioselective α-tosyloxylation of propiophenone with different chiral iodoarenes do not exceed 54% ee, as depicted in Scheme 73.[180f] Thus, the improvement of the enantioselectivity remains a formidable challenge with catalysts based on iodine reagents. Therefore, we were also interested in exploring the preparation of chiral α-tosyloxyketones using chiral iodoalkanes as catalysts, as outlined in the following section (4.2 objectives).

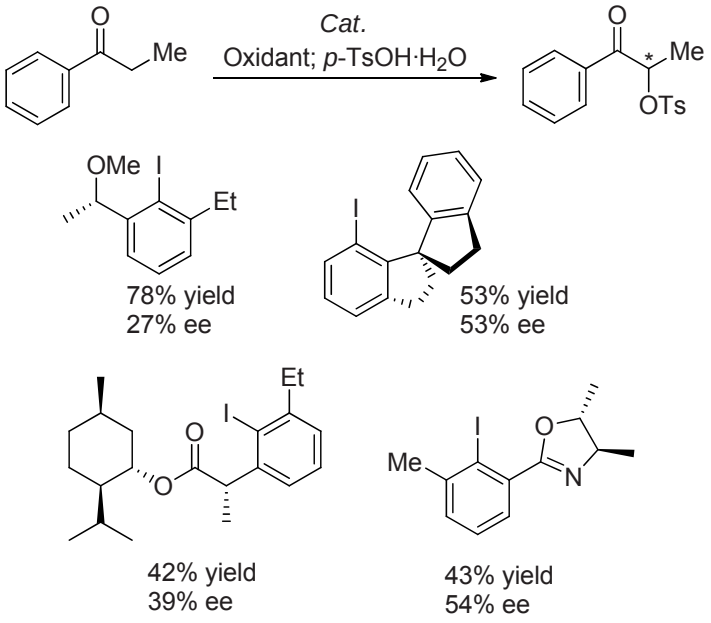

Scheme 73. The best enantioselectivities for the catalytic α-tosyloxylation of propiophenone with different chiral iodoarenes as catalysts.

4.2 Objectives

Taking into account the precedents previously mentioned, we planned the following aims for this chapter 4 of part I of the thesis:

a) The investigation of the catalytic activities of iodoalkanes in the α-tosyloxylation of various ketones (Scheme 74), with the optimization of the reaction conditions.

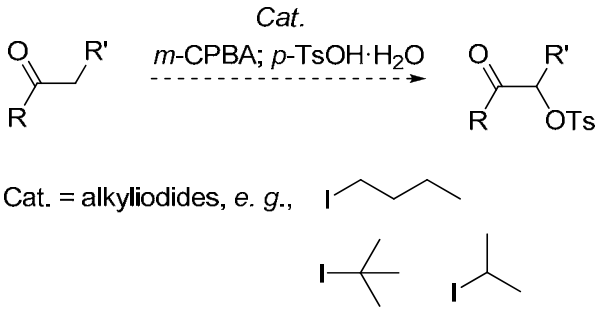

Scheme 74. α-Tosyloxylation of ketones under catalysis by iodoalkanes.

b) The assay of suitable chiral iodoalkanes for the enantioselective synthesis of α-tosyloxyketones (Scheme 75).

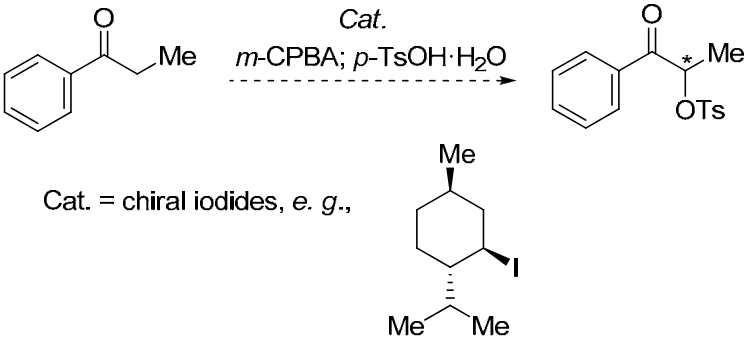

Scheme 75. α-Tosyloxylation of ketones under catalysis by chiral iodoalkanes.

c) The investigation of the evolution of the iodine species during the catalytic process.

4.3 Results and Discussion

In order to confirm the catalytic activity of the alkyl iodides RI, the performance of 2-iodobutane was compared to that of PhI in the tosyloxylation of propiophenone. We followed the procedure originally reported by Togo *et al.*[124a] with PhI as catalyst and using *m*-CPBA as a terminal oxidant. Thus, the catalytic PhI (10 mol%) performed as expected, giving a 75% yield of the α-tosyloxylated product after 10 h at 65 °C in acetonitrile. Under the same conditions, a 10 mol% loading of *sec*-BuI also proved active, affording a respectable 65% yield of the product (Scheme 76), albeit with no improvement at longer reaction times; the loss of catalytic activity with 2-iodobutane after approx. 10 h was accompanied by the precipitation of a white solid that was found to be silent by ^{1}H NMR.

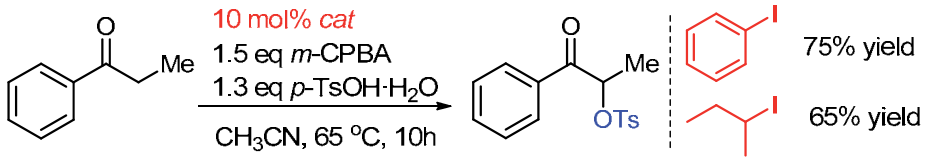

Scheme 76. Tosyloxylation of propiophenone by PhI and *sec*-BuI.

4.3.1 Optimization of the reaction conditions for the α-tosyloxylation of ketones with 2-iodobutane as potential catalyst

With the white solid aside, we first optimized the reaction conditions in order to get the best yield of the product; the performance of 2-iodobutane was examined under a range of reaction conditions (Table 6). Thus, the *m*-CPBA loading of 1.5 eq. was found to be optimal (Table 6, entries 1-5), with the best yields achieved at 50 °C, albeit at the cost of a somewhat slower reaction (compare entries 4 and 6-8). It should be noted that the commercially available *m*-CPBA is contaminated with varying degrees (17-33%) of water and with 10-15% of *m*-chlorobenzoic acid (*m*-CBA), depending on the commercial source. For this reason, in order to make the experiments reproducible, the commercial *m*-CPBA was dried under reduced pressure for at least 1 h prior to use, as mentioned in last chapter. No further improvement was observed either by changing the solvent (Table 6, entries 6 and 9-11) or by varying the catalyst loading (Table 6, entries 12-13). Notably, all reaction mixtures mentioned above went from brown to beige, followed by the appearance of a white precipitate. These results indicate that while the oxidation of the *sec*-BuI gives a catalytically active iodine species, further evolution of the catalyst to the white solid causes the catalyst deactivation.

Table 6. Optimization of the reaction conditions.[a]

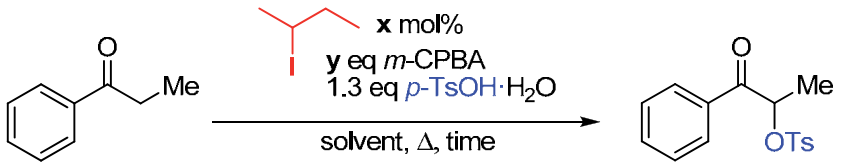

Entry	Solvent	*m*-CPBA (eq.)	2-BuI / mol%	Temp. / °C	Time[b] / h	yield[c] / %
1	CH_3CN	1.0	10	65	10	50
2	CH_3CN	1.1	10	65	10	58
3	CH_3CN	1.3	10	65	10	65
4	CH_3CN	1.5	10	65	10	74
5	CH_3CN	2.0	10	65	10	69
6	**CH_3CN**	**1.5**	**10**	**50**	**22**	**77**
7	CH_3CN	1.5	10	40	22	73
8	CH_3CN	1.5	10	75	10	45
9	Toluene	1.5	10	50	22	34
10	EtOAc	1.5	10	50	22	21
11	$CHCl_3$	1.5	10	50	22	59
12	CH_3CN	1.5	5	50	22	65
13	CH_3CN	1.5	20	50	22	69

[a] [substrate] = 0.2 M. [b] Reaction was stopped when no further evolution could be detected by GC. [c] Corrected GC yield (PhCl as internal standard).

4.3.2 Catalysis with various alkyl iodides in the α-tosyloxylation of ketones

The formation of an active tosyloxylation catalyst from alkyliodides was found to be quite general for a range of iodoalkanes tested (Table 7). Long, medium and short-chain primary iodoalkanes (Table 7, entries 1-3) all performed quite well, with a somewhat diminished yield for $C_{12}H_{25}I$ (Table 7, entry 1) likely due to its poor miscibility with CH_3CN. All three iodobutane isomers, as well as the 2-iodopropane, proved active (Table 7, entries 3-6). The amount of iodine loading from 5% to 20% did not affect the yield significantly (Table 7, entry 5). Even the use of 10% of the simple iodomethane (Table 7, entry 7) also gave a 75% yield of the isolated product. The catalyst formation was unaffected by the presence of an aromatic group (Table 7, entry 8). The similarity in the catalytic behavior between such a wide range of iodoalkanes was taken as a strong evidence that, unlike aryl iodides, the catalytic cycle employing the simple

iodoalkanes does not involve a hypervalent organoiodine reagent, but rather proceeds through a common inorganic iodine species.

Table 7. Screening of iodoalkanes as potential α-tosyloxylation catalysts.[a]

Entry	RI	yield[b] / %
1	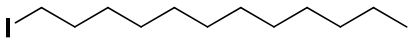	69
2	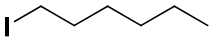	78
3	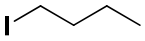	78
4	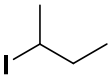	75
5		78[c] /69[d] /83[e] /86[f]
6		79
7	MeI	75
8	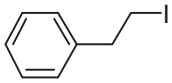	79
9	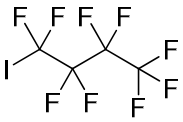	<5%
10	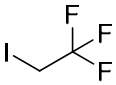	<5%
11	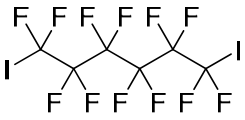	<5%
12	I_2	69/61[g]
13	NaI	77
14	KI	73
15	KBr	-

[a] [substrate] = 0.2 M. [b] Isolated yield. [c] 10% of I. [d] 5% of I. [e] 15% of I. [f] 20% of I. [g] 5% and 2.5 mol% I_2, respectively.

Interestingly, fluorinated iodoalkanes (Table 7, entries 9-11), which presumably could give a reasonably stable hypervalent species, and thus operate through an organoiodane-based catalytic cycle (such as depicted in Scheme 77), proved inactive.

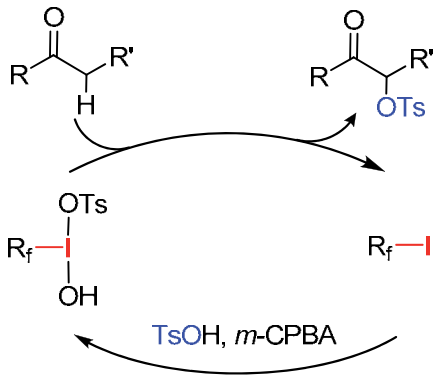

Scheme 77. A possible catalytic process in α-tosyloxylation of ketones using fluorinated iodoalkanes.

Additional experiments established that a reaction between C_4F_9I and *m*-CPBA did not lead to the formation of any white solid. A stable Koser-type iodane $C_4F_9I(OH)OTs$ was indeed prepared (Scheme 78) following a method developed by Zhdankin *et al.*, in which nonafluoro-1-iodobutane was treated with Oxone in trifluoroacetic acid and, subsequently, with TsOH in acetonitrile giving, successively, the [bis(trifluoroacetoxy)iodo]perfluorobutane **25** and [hydroxy(tosyloxy)iodo]-perfluorobutane **26**. [181] However, the reaction between propiophenone and stoichiometric amounts (1.2 eq.) of compound **26**, proved sluggish, affording only trace amounts of the corresponding tosyloxylated product after 24 h at 50 °C (see experimental section for details). The insolubility of the $C_4F_9I(OH)OTs$, **26**, in the reaction medium should also be noted. Thus, resistance to the oxidative breakdown of the fluorinated iodoalkanes, coupled to the peculiar reactivity of the corresponding hydroxytosylate reagents, such as **26**, (and, perhaps, their low solubility in CH_3CN) would all contribute to the lack of catalytic activity of such reagents.

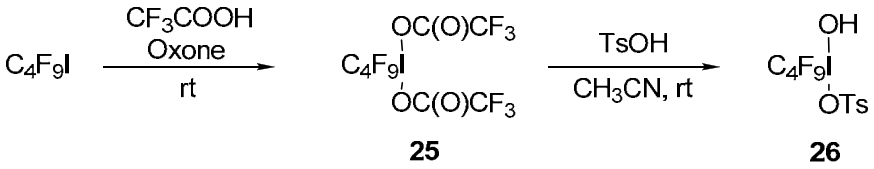

Scheme 78. The preparation of Koser-type iodane $C_4F_9I(OH)OTs$

[181] Zagulyaeva, A. A.; Yusubov, M. S., V. V. Zhdankin, *J. Org. Chem.* **2010**, *75*, 2119.

In contrast, molecular iodine and inorganic iodides, as previously reported by Togo's group,[125] also proved catalytically active (Table 7, entries 12-14) under the present conditions. In addition, the systems obtained from the *n*-, *sec*- and *tert*-BuI showed similar kinetic profiles (Figure 14), although with some differences likely due to the different reaction rates in the presence of different iodoalkanes. Interestingly, the reaction rates (especially at the initial stages of the reaction) were found to be only slightly lower than those obtained with a better studied PhI catalyst (Figure 14).

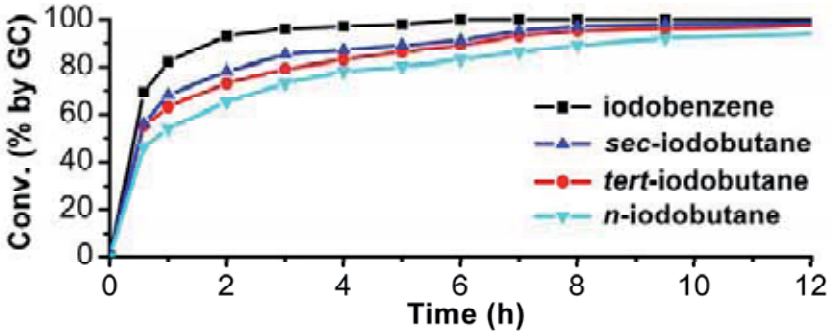

Figure 14. Kinetic profiles of the *n*-, *sec*- and *tert*-iodobutanes *vs.* that of PhI (% GC conv. of propiophenone, corrected with int. standard PhCl), conditions as in Table 7.

4.3.3 Catalysis with chiral alkyl iodides in the α-tosyloxylation of ketones

Despite the fact that the catalytic cycle might proceed through a common inorganic iodine species, we, nevertheless, proceeded to double check whether the use of a chiral iodoalkanes would result in an enantioselective α-tosyloxypropiophenone, as discussed in the introduction and objective sections. Thus, we chose to check a menthyl iodide derived from menthol, an alcohol from the natural chiral pool. However, a conversion from the commercially available (-)-menthol to an enantioenriched iodocyclohexane derivative, following a procedure reported previously,[182] was proven to be unsuccessful in this case and gave mainly the elimination product (Scheme 79).

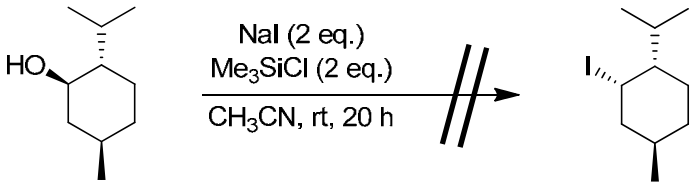

Scheme 79. Attempt for the preparation of (*1S,2S,5R*)-menthyl iodide from (-)-menthol.

[182] (a) Yamashita, M.; Soeda, Y.; Suzuki, N.; Yamada, M.; Tsunekawa, K.; Oshikawa, T.; Inokawa, S. *Bull. Chem. Soc. Jpn.* **1983**, *56*, 1871. (b) Fessner, W.; Rodriguez, M. *Angew. Chem., Int. Ed.* **1991**, *30*, 1020.

Taking into account that the nucleophilic substitution reaction from the (*1R,2S,5R*)-menthyl methanesulfonate (**27**) may be easier due to the good leaving group ability of the methanesulfonic group, the menthol was treated with methanesulfonyl chloride (MsCl) and Et_3N in CH_2Cl_2 at room temperature affording the compound **27** in 92% yield (Scheme 80).[183]

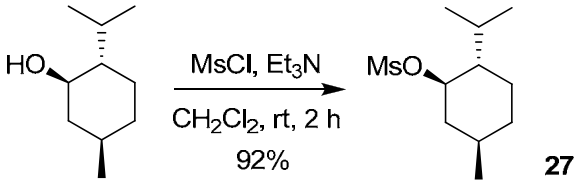

Scheme 80. Preparation of (*1R,2S,5R*)-menthyl methanesulfonate **27** from (-)-menthol.

In order to prepare an iodocyclohexane derivative, we first treated compound **27** with KI using a method reported for other substrates.[184] In this case it was ineffective and furnished a complex mixture (Scheme 81).

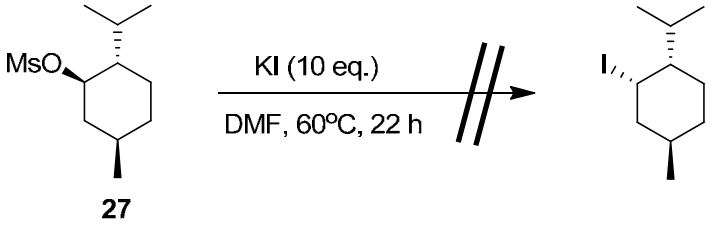

Scheme 81. Attempt to prepare (*1S,2S,5R*)-menthyl iodide from (*1R,2S,5R*)-menthyl methanesulfonate **27**.

Then we came across a method recently reported by Martin and colleagues[185] involving the addition of an iron(III) salt as a catalyst and trimethylsilyl iodide (TMSI) as the iodine source. The authors find that the stereochemical course of the reaction is governed by the substrate and by the experimental conditions. Indeed, under the conditions described by the authors, in the presence of $FeBr_3$ as a catalyst, the reaction of sulfonate **27** with TMSI in dichloromethane at room temperature for only 2 h afforded a mixture of iodocyclohexane derivatives (ratio of compounds **28** : **29** = 10 : 1) in 77% yield (Scheme 82).

---

[183] A. Sébastien.; D. Albert. *Synthesis* **2006**, 1635.

[184] Olah, G. A.; Narang, S. C.; Gupta, B. G.; Malhotra, R. *J. Org. Chem.* **1979**, *44*, 1247.

[185] For experimental details and interpretation of the proton NMR spectrum, please see experimental section and: Ortega, N.; Feher-Voelger, A.; Brovetto, M.; Padrón, J. I.; Martín, V. S.; Martín, T. *Adv. Synth. Catal.* **2011**, *353*, 963.

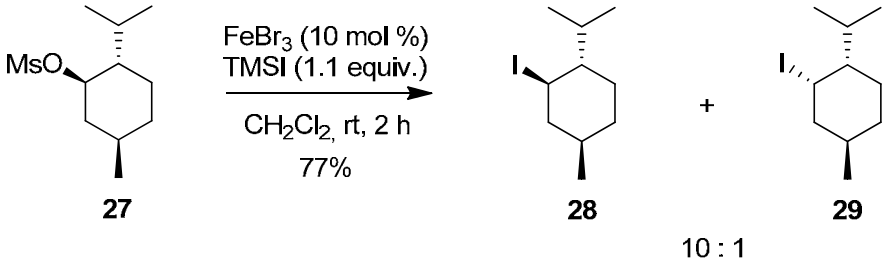

Scheme 82. Preparation of an enriched mixture of menthol-derived iodocyclohexane diastereoisomers

The nature of the major isomer was confirmed by ^{1}H NMR. For clarity, the fragments of the ^{1}H NMR spectra of the sulfonate **27** and the mixture of menthyl iodides (**28** mixed with minor **29**) are given in a stacked format (Figure 15), focusing on the protons adjacent to the iodine or the methanesulfonate group. As expected, for compounds **27** and **28**, the protons in C-1 appear as a triplet of doublets, which is in accordance with the axial position of these protons (and, thus, the equatorial position of the MsO and the I groups). Besides, the methyl from the sulfonate **27** appears as a singlet at 3.0 ppm, which is absent in the mixture of **28** and **29**.

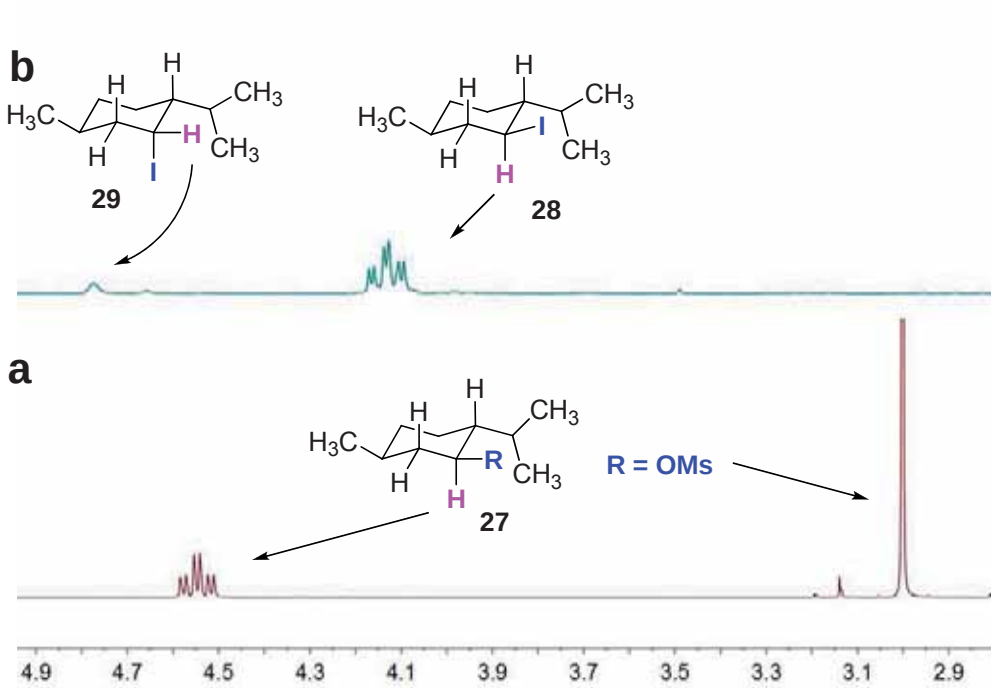

Figure 15. Fragments of the ^{1}H NMR spectra of: (a) (*1R,2S,5R*)-menthyl methanesulfonate **27;** (b) (*1R,2S,5R*)-menthyliodide **28** in the presence of small amount of **29**.

Unfortunately, although **28** was an effective catalyst to achieve the α-tosyloxylation of propiophenone in 69% yield under the optimized conditions (1.5 eq. of *m*-CPBA, 10 mol% eq. of I, 50 ^{o}C and 1.3 eq. of TsOH), no enantiomeric excess (ee) was obtained, *i. e.*, affording a racemic product (see experimental section for the HPLC traces). This result suggests that the catalytic cycle proceed through a common inorganic iodine species. At this point, we gave up the idea to achieve the enantioselective synthesis of α-tosyloxyketones with other chiral iodoalkanes.

4.3.4 Application of the new catalytic system based on iodoalkanes to the α-tosyloxylation of various substrates

In addition to its mechanistic implications, the oxidative α-tosyloxylation of ketones using iodoalkanes as catalyst precursors might offer, under certain conditions, an attractive synthetic procedure. Thus, before delving the nature of the catalytic species, we briefly tested the performance, as catalyst precursors, of the three iodobutane isomers along with KI and I_2, in the α-tosyloxylation of several additional substrates. As can be seen in Table 8, all five catalyst precursors performed quite well with the *para*-bromoacetophenone and *para*-nitroacetophenone (Table 8, entries 1-2). However, with the exception of KI, only a 30-36% yield could be achieved for the 3-pentanone (Table 8, entry 3). The substrates acetophenone (Table 8, entry 4), *para*-methylacetophenone (Table 8, entry 5) and *para*-chloroacetophenone (Table 8, entry 6) also showed effectiveness with all five catalyst precursors.

Interestingly, the catalytic activity of I_2 in this reaction was previously claimed to proceed through the *in situ* conversion of TsOH to *p*-iodotoluene in the presence of I_2 and the oxidant (*m*-CPBA). The *p*-iodotoluene would act as the true catalyst, as shown in Scheme 52 and Scheme 71b.[125] The authors argued, therefore, that an aromatic sulfonic acid is required for I_2 to be used as a pre-catalyst. A related proposal by a different group suggested that a catalytic iodobenzene was formed through the iodination of the benzene added to the reaction.[126]

However, in our hands, the 10-camphorsulfonic acid gave a modest yield (22%) of the product, with the results somewhat improved using *sec*-iodobutane (Table 8, 40%, entry 7); no aromatic solvent was used. In fact, the simplest aliphatic sulfonic acid, $MeSO_2OH$, also was coupled in good yields, using either iodobutane or molecular iodine as pre-catalysts (Table 8, 10 mol% I, entry 8). The results suggest that species other than aromatic iodides may act as catalyst in this process.

Table 8 α-Tosyloxylation of ketones with iodine sources as pre-catalysts [a]

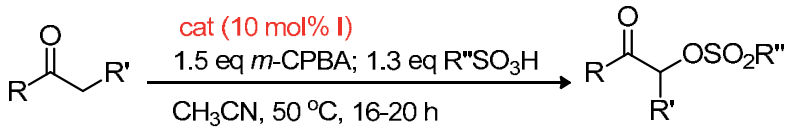

Entry[a]	Product		yield[b] / %			
					KI	I_2
1	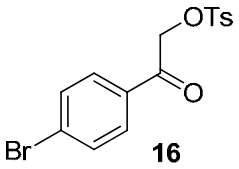 **16**	82	86	81	81	73
2	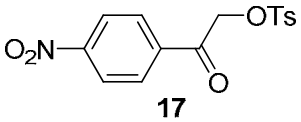 **17**	66	58	65	63	56
3	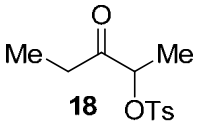 **18**	36	32	31	66	30
4	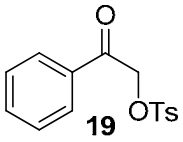 **19**	70	76	70	80	64
5	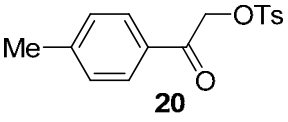 **20**	64	65	68	59	55
6	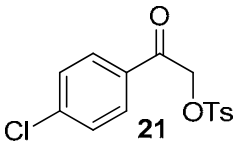 **21**	73	72	75	70	66
7	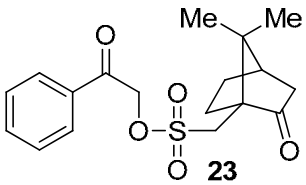 **23**	29	40	33	27	22
8	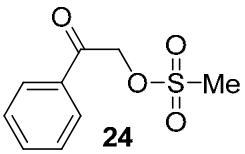 **24**	64	76	80	72	61

[a] [sub] = 0.2 M. [b] Isolated yields.

No reaction occurred when using H_2O_2 as an oxidant and propiophenone as a substrate in the presence of a catalytic amount of iodobutane (Table 9, entry 1). In the presence of *m*-CPBA as oxidant, iodine-free conditions failed to produce any desired products (Table 9, entries 2 - 3).

Table 9. Control tests for the catalytic oxidative α-tosyloxylation of ketones under the indicated conditions.

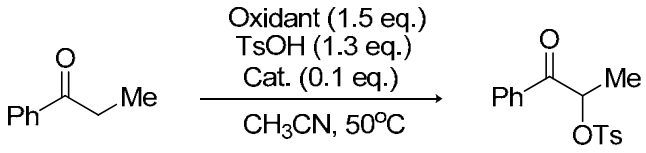

Entry[a]	Oxidant	Catalyst	Time / h	Yield[b] / %
1	H_2O_2	$I(CH_2)_3CH_3$	16	-[c]
2	*m*-CPBA	PhCl	14	-[c]
3	*m*-CPBA	-	16	-[c]

[a] [substrate] = 0.2 M. [b] Isolated yields after consumption of the starting material and GC detection of the target product. [c] The corresponding product was not detected.

As shown in Figure 16, the control tests in the absence of any iodine source failed to produce the desired products. The α-tosyloxylation of various ketones under catalysis by iodobenzene were also performed as references; notably, in some cases, (as in the α-tosyloxylation of *p*-bromoacetophenone), the newly developed catalytic system outperformed the one using catalytic iodobenzene.

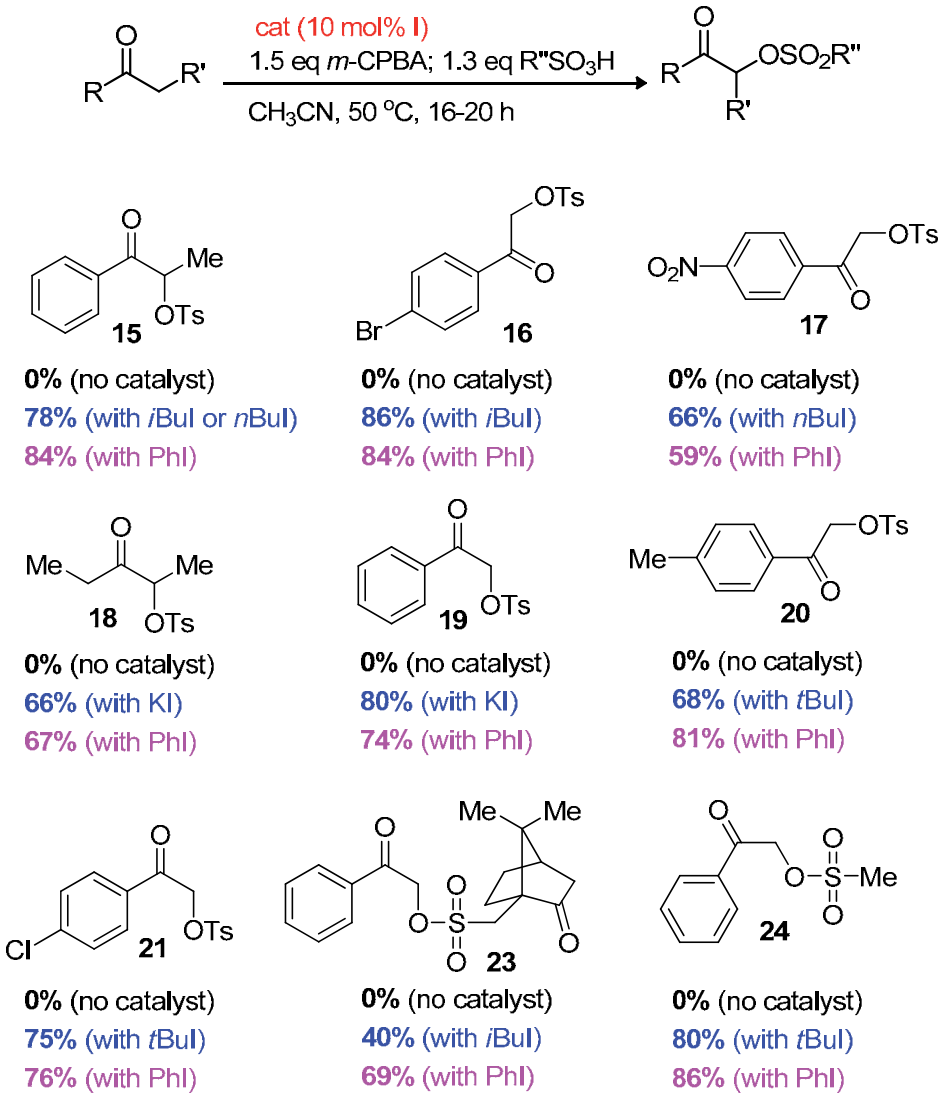

Figure 16. α-Tosyloxylation of various ketones under the optimized conditions: the control tests without catalysts, best results achieved with the newly developed iodine reagents as pre-catalysts and the reference tests with iodobenzene as catalyst.

4.3.5 Investigation of the catalyst deactivation pathways

During the course of the model α-tosyloxylation reactions, the GC peak for the iodoalkane disappeared immediately and, as mentioned above, a white solid appeared gradually. Given that the nature of the white solid might shed light upon the catalyst deactivation, the solid obtained in entry 4 of Table 7 (denoted **M6**) was separated and examined. The material was found to be insoluble in normal organic solvents but soluble in DMSO and D_2O with no informative ^1H NMR signals. To our surprise, the powder X-Ray diffraction (*p*-XRD) of **M6** produced a pattern identical to that of a

substance identified in an earlier publication[186] (ICDD card reference, 00-045-0872) as a mixed iodine oxide I_4O_9, formulated as $I(IO_3)_3$ and described as a yellow air-sensitive solid obtained through the ozonation of I_2 (Equation 1) or MeI.[187]

$$4\ I_2\ (\text{vapor}) + 6\ O_3 \longrightarrow 2\ I_4O_9 \quad (1)$$

In fact, the chemistry of inorganic iodine oxides is somewhat complex, with a variety of such oxides that have been reported, such as IO, IO_2, IO_3, IO_4, I_2O, I_2O_2, I_2O_3, I_2O_4, I_2O_5, HIO_3, I_2O_6, I_2O_7, I_2O_8, I_4O_9, etc. For some of these, however, related experimental evidences are still scant.[187a] In particular, despite the fact that several articles on the preparation of I_4O_9 (CAS Registry Number 73560-00-6) by different methods have been published,[187b-e] the corresponding characterization data are still very limited and unconvincing. Our surprise stemmed from the fact that, in spite of the coincidence of the diffraction patterns with the reported I_4O_9,[187b] the product **M6** was white and showed no sign of decomposition in air. Incidentally, a material with the same diffraction pattern could be prepared in the absence of the two substrates (ketone and *p*-TsOH) simply by oxidizing alkyl iodides (or I_2) with *m*-CPBA, as documented in Table 10 (entries 1-4). Interestingly, oxidation of KI with *m*-CPBA at 65 °C afforded KIO_3 which was recognized from the *p*-XRD analysis (Table 10, entry 5), and no reaction occurred when the oxidant was changed to H_2O_2 (Table 10, entry 6). Under the same reaction conditions, a bromoalkane was not oxidized by *m*-CPBA (Table 10, entry 7). For comparison purposes, all the relevant *p*-XRD patterns are shown in a stacked format in Figure 17.

Table 10. Preparation of **M6** from *m*-CPBA and iodoalkanes and some related control tests.[a]

Entry	Iodine species (0.5 mmol of I)	Oxidant/ 6.0 mmol	Temperature / ºC	Product	Time
1	1-iodobutane	*m*-CPBA	65	White solid	30 m
2	1-iodododecane	*m*-CPBA	65	White solid	25 m

[186] Wikjord, A.; Taylor, P.; Torgerson, D.; Hachkowski, L. *Thermochimica Acta* **1980**, *36*, 367.

[187] For a general overview, see (a) Chase, M. V. *J. Phys. Chem. Ref. Data* **1996**, *25*, 1297. For more information about I_4O_9, see: (b) Sunder, S.; Wren, J. C.; Vikis, A. C. *J. Raman Spectrosc.* **1985**, *16*, 424. (c) Vikis, A. C.; MacFarlane, R. *J. Phys. Chem.* **1985**, 89, 812 and references therein. (d) The first report on preparation of I_4O_9 from iodine vapor and ozone via ozonolysis, please see: M. Beger. *Chem. Ztg.* **1909**, *33*, 1232. (e) I_4O_9 appears in the textbook, please see: Cotton, F. A.; Wilkinson, G.; Murillo, C. A.; Bochmann, M. *Advanced Inorganic Chemistry*, 6th Ed.; John Wiley and Sons, **1999**.

3	1-iodobutane	*m*-CPBA	rt	White solid	15 h
4	I_2	*m*-CPBA	65	White solid	10 m
5	KI	*m*-CPBA	65	White solid	1 m
6	KI	H_2O_2	65	-[b]	15 h
7	1-bromohexane	*m*-CPBA	65	-[b]	15 h

[a] A mixture of the iodine species (0.5 mmol of I) and the corresponding oxidant (6.0 mol) in acetonitrile (20 mL) was stirred for the indicated time. When the reaction mixture changed to a colourless solution and a white solid precipitated, the reaction was stopped and cooled down at room temperature. The white solid was obtained by centrifugation and thoroughly washed with acetonitrile. [b] No solid appeared.

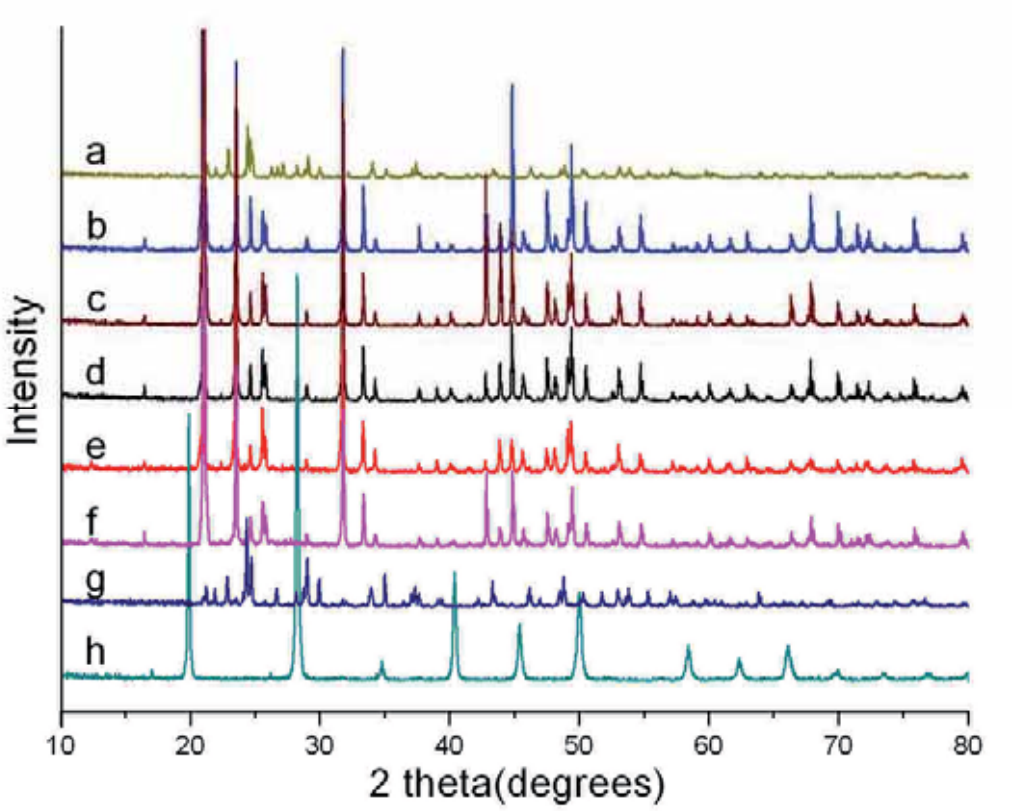

Figure 17. *p*-XRD spectra of:

(a) commercial I_2O_5 (in good agreement with ICDD card 00-052-0319);

(b) product of the reaction of iodobutane with *m*-CPBA in acetonitrile at rt;

(c) product of the reaction of molecular iodine (I_2) with *m*-CPBA in acetonitrile at rt;

(d) product of the reaction of iodobutane with *m*-CPBA in acetonitrile at 65 ºC;

(e) product of the reaction of iodobutane with *m*-CPBA in acetonitrile at 50 ºC;

(f) M6;

(g) M6 was heated at 140 ºC for 3 h under reduced pressure (in good agreement with ICDD card 00-052-0319);

(h) product of the reaction of potassium iodide with *m*-CPBA in acetonitrile at 65 ºC (in good agreement with ICDD card 00-001-0776, KIO_3).

The structure of **M6** was solved from powder x-ray diffraction data (*p*-XRD) using the cluster-based direct methods implemented in XLENS_pd6[188] and refined with RIBOLS[189] applying an unrestrained Rietveld refinement as shown in Figure 18.

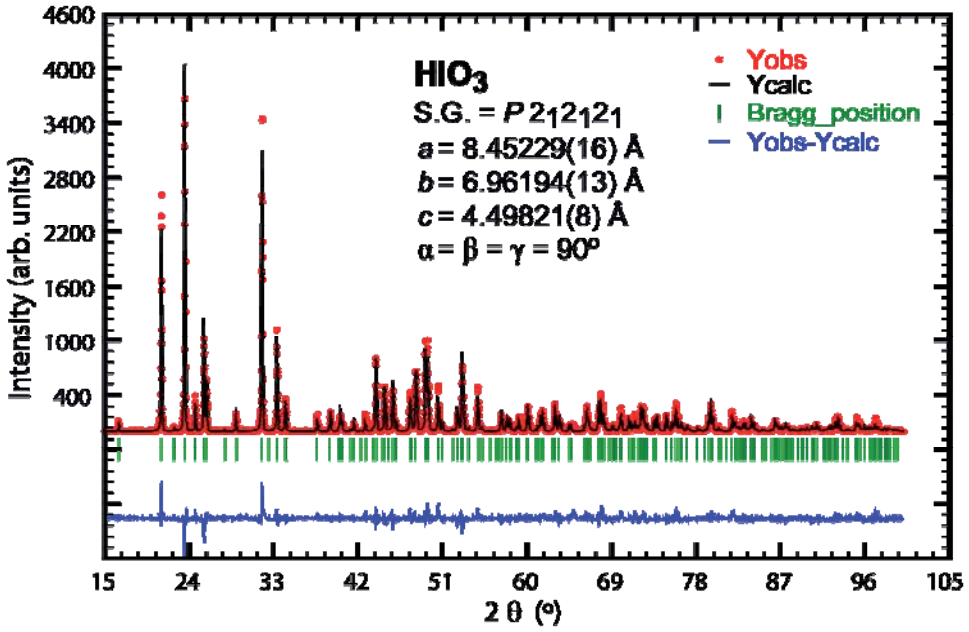

Figure 18. Observed (points), calculated (line) and difference profile (bottom) for the Rietveld refinement of **M6.**

The crystal structure of this solid **M6** (Table 11) showed that the iodine atoms form hexagonal layers parallel to the crystalline *bc* planes, with each iodine surrounded by oxygen atoms in a distorted octahedral coordination (Figure 19), and each HIO_3 molecule connected to neighbour molecules through three weak I···O interactions and the (probable) O2···O3' hydrogen bond [2.62(3) Å]. The bond lengths, bond angles and atomic coordinates are also given in Table 12, Table 13 and Table 14, respectively. In spite of the different crystal packing, bond lengths are similar to other reported HIO_3

[188] Rius, J. *Acta Crystallogr. A* **2011**, 67, 63.

[189] Rius, J. RIBOLS18 A computer program for least-squares refinement from powder diffraction data; Institut de Ciència de Materials de Barcelona (CSIC): Barcelona, Spain, 2012.

structures.[190] It should be mentioned that the task of obtaining atomic coordinates (i.e. solid state structure) for an unknown compound using powder X-ray data is far from trivial, with most structures obtained through single-crystal diffraction. In this case, the *p*-XRD analysis was performed by Dr. Oriol Vallcorba and Prof. Jordi Rius at the *Institut de Ciència dels Materials de Barcelona (ICMAB)* who are experts in this field of powder structure determination by *p*-XRD.

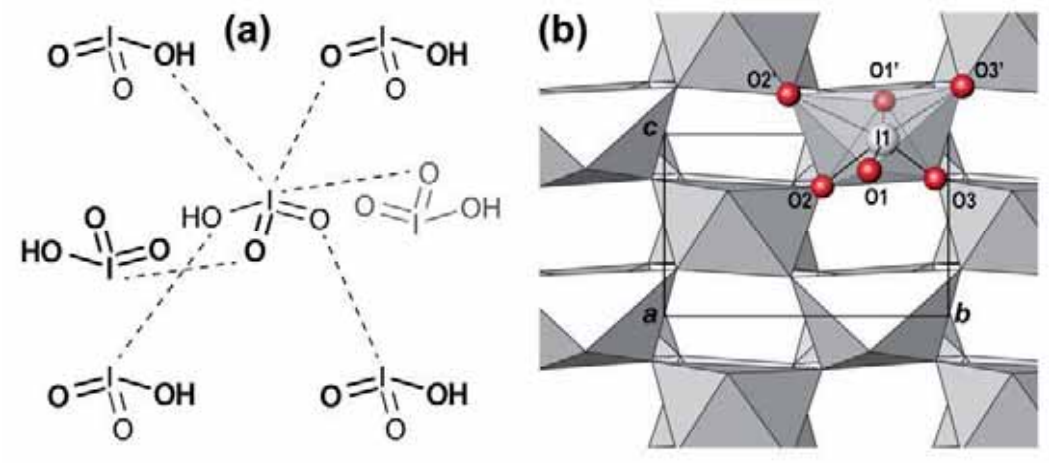

Figure 19. Crystal structure of **M6**: (a) Molecular scheme of the I-O weak interactions (dotted lines, 2.5 to 2.8 Å); (b) Packing of the distorted iodine octahedra. Iodine centres form hexagonal layers normal to *a*.

Table 11. Crystallographic data and structure refinement details for **M6**.

Molecular formula	HIO_3
Formula weight	175.9
Crystal System	Orthorhombic
Space group	$P2_12_12_1$
a (Å)	8.45229(16)
b (Å)	6.96194(13)
c (Å)	4.49821(8)
α (º)	90
β(º)	90
γ(º)	90
Volume ($Å^3$)	264.694(8)

[190] International Centre for Diffraction Data (a) Rogers, T.; Helmholtz, L. *J. Am. Chem. Soc.* **1941**, *63*, 278. (b) Garret. B. Report ORNL-1745, 1954, 97-148, Oak Ridge National Laboratory, Tennessee, USA. (c) Ståhl, K.; Szafranski, M. *Acta Crystallogr. C* **1992**, *48*, 1571.

Z	4
Calculated density (g/cm^3)	4.389
Measurement Temperature (K)	298
Radiation (wavelengths in Å)	Cu$K\alpha_{1,2}$ (1.54056; 1.54439)
F(000)	308.0
Measured 2θ range, stepsize (º)	5.00–100.00, 0.02
Rietveld refinement details:	
Profile function	Pseudo-Voigt
2θ range used	15.0–100.0
Num. of reflections	182
Data points	4250
Parameters	21
Restraints	0
R_{wp}	0.181
R_{exp}	0.107
Goodness of fit (χ)	1.692

Table 12. Bond lengths of **M6**.

Atom 1	Atom 2	distance (Å)
I1	O1	1.800(14)
I1	O1[a]	2.798(14)
I1	O2	1.990(17)
I1	O2[b]	2.721(17)
I1	O3	1.75(2)
I1	O3[c]	2.54(2)
Symmetry code: (a) -1/2+x ,3/2-y ,-Z; (b) 1/2-x, 2-y, -1/2+z; (c) 1/2-x, 1-y, -1/2+z		

Table 13. Bond angles of **M6**.

Atom 1	Atom 2	Atom 3	Angle (º)
O1	I1	O1	169.5(7)
O1	I1	O2	83.2(9)
O1	I1	O2	70.3(8)
O1	I1	O3	103.3(10)
O1	I1	O3	87.3(8)

O1	I1	O2	86.8(8)
O1	I1	O2	104.2(6)
O1	I1	O3	80.7(9)
O1	I1	O3	102.8(7)
O2	I1	O2	74.0(7)
O2	I1	O3	97.0(8)
O2	I1	O3	170.3(9)
O2	I1	O3	169.2(7)
O2	I1	O3	104.7(6)
O3	I1	O3	83.2(9)
Symmetry code: (a) -1/2+x ,3/2-y ,-Z; (b) 1/2-x, 2-y, -1/2+z; (c) 1/2-x, 1-y, -1/2+z			

Table 14. Atomic fractional coordinates of **M6**.

Atom	x/a	y/b	z/c	Occup.	B_{iso}
I1	0.2219(2)	0.7302(2)	0.0255(4)	1.00	0.02(3)
O1	0.4117(16)	0.7775(30)	0.1913(29)	1.00	0.02(3)
O2	0.1523(27)	0.9447(24)	0.2872(42)	1.00	0.02(3)
O3	0.1463(27)	0.5426(26)	0.2429(43)	1.00	0.02(3)

In order to further confirm the above conclusion, TGA, XPS and elemental analysis of **M6** were performed. As can be seen in Figure 20, the TGA graph of **M6** is similar to the one obtained from commercial HIO_3, differing only in the endothermic peak at 218 ºC, which is shifted to 132 ºC. Accordingly, heating of **M6** to 140 ºC for 3 h leads to a new material whose *p*-XRD pattern is that of iodine pentoxide, I_2O_5, the iodic acid anhydride (Figure 17g, ICDD card number 00-052-0319). In consequence, the peak at 132 ºC corresponds to the water loss from HIO_3 to give I_2O_5, consistent with the well-defined 5% weight loss; the peak at 440-450 ºC is attributed to the decomposition of the formed I_2O_5 to unidentified products. The weak interactions between the iodine atom layers in the new HIO_3 polymorph may be the cause of this easier loss of water to form I_2O_5.

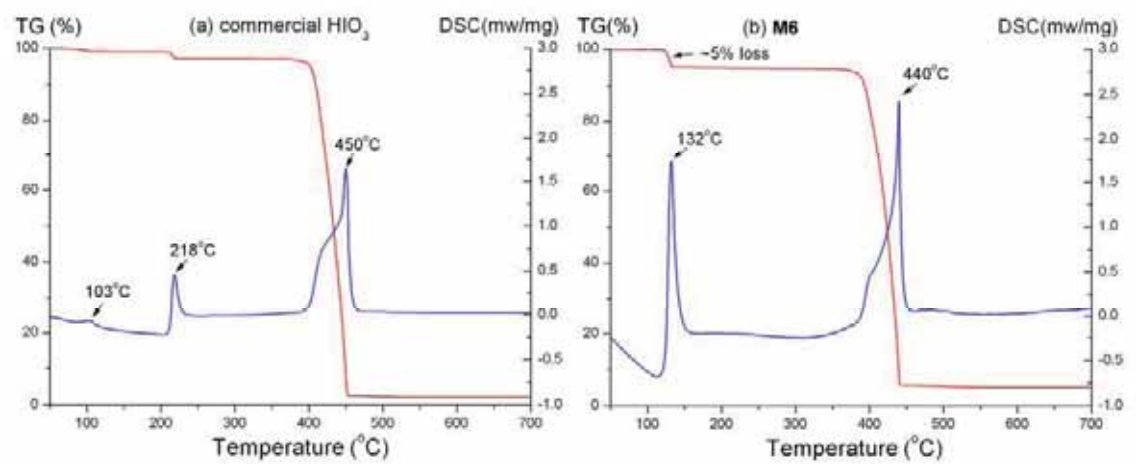

Figure 20. TGA (red) and DSC (blue) curves: (a) commercial HIO_3 and (b) **M6**.

X-ray photoelectron spectroscopy (XPS) is a form of electron spectroscopy in which a sample is irradiated with a beam of monochromatic x-ray and the energies of the resulting photoelectrons are measured. It is a very helpful technique in obtaining information about oxidation state and atomic composition of the analyzed compounds. As shown in Scheme 83, a photon with certain energy hitting the sample causes the electrons to be ejected. The information to determine the kind of elements present in the sample can be provided by measuring the kinetic energy of the ejected electrons. Keeping this in mind, we hoped to further investigate the iodine oxidation state in the above-mentioned white solid with XPS technique.

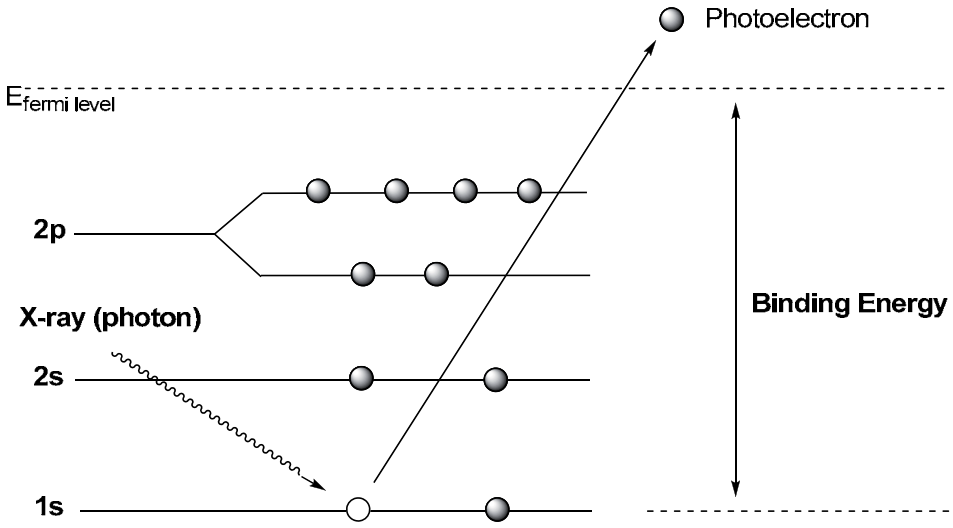

Scheme 83. Schematic representation of the x-ray photoelectron process.

Indeed, the XPS spectrum of **M6** (Figure 21) further confirmed the presence of I^{5+} species with bonding energies at 623.8 and 635.2 eV representing I $3d_{3/2}$ and I $3d_{5/2}$,

respectively, which are similar to those of the commercial HIO_3 and very different from those of I^- in KI at around 619.6 and 631.2 eV.[191] Elemental analysis results of 0.51% H and 74.32% I are close to the theoretical values of HIO_3, 0.57% H and 72.14% I, which further evidences the composition of HIO_3. Thus, we conclude that **M6** is a hitherto unreported crystal form of the iodic acid, HIO_3.[192]

On the basis of the evidences provided by this work, we put in doubt the existence of the genuine I_4O_9. The I_4O_9 structure, also denoted as $I(IO_3)_3$, previously reported by others[187b] was probably formulated due to an impurity present in this new form of HIO_3.

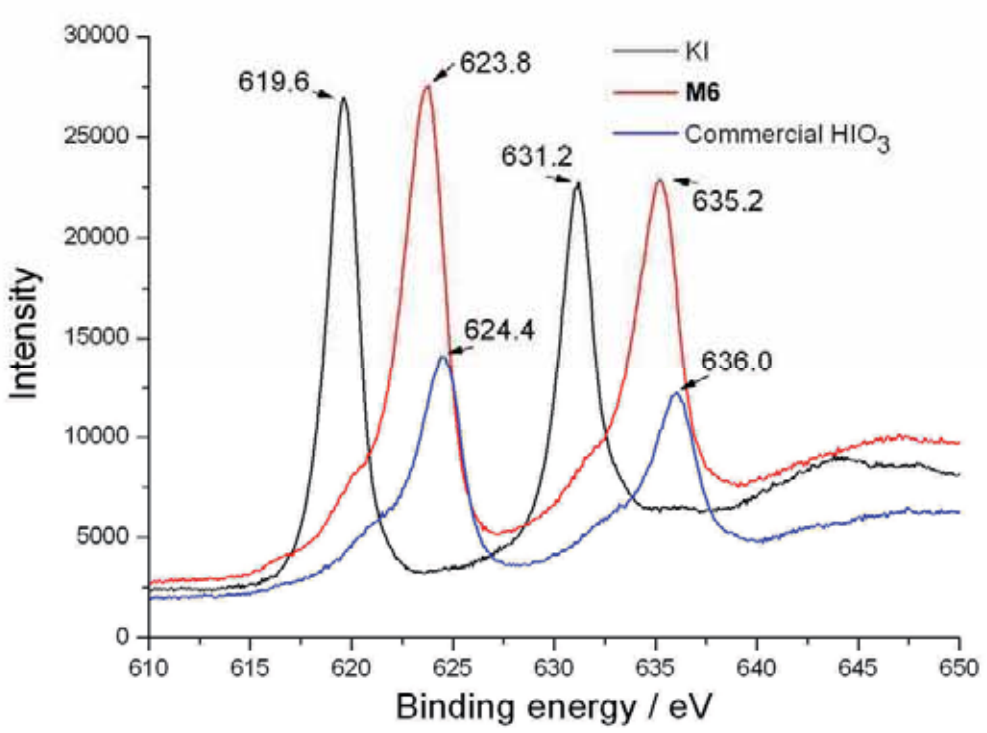

Figure 21. X-ray photoelectron spectra of potassium iodide, commercial HIO_3 and **M6** (3d regions).

Consistent with the notion that the precipitation of the white solid is symptomatic of catalyst deactivation, either the isolated **M6** or the commercially available sample of HIO_3 or its anhydride I_2O_5 showed poor reactivities in the α-tosyloxylation of propiophenone (Table 15). A while solid was also found when using catalytic amount of

---

[191] (a) Brown, M. A.; Newberg, J. T.; Krisch, M. J.; Mun, B. S.; Hemminger, J. C. *J. Phys. Chem. C* **2008**, *112*, 5520. (b) Kalita, G.; Wakita, K.; Takahashi, M.; Umeno, M. *J. Mater. Chem.* **2011**, *21*, 15209. (c) Zhang, Q., Li, Y.; Ackerman, E. A.; Gajdardziska-Josifovska M.; Li, H. *Appl. Catal. A: Gen.* **2011**, *400*, 195.

[192] (a) Checked in ICSD (2012). *Inorganic Crystal Structure Database*, release 2012/1 and ICDD (2012). *PDF-4+*. International Centre for Diffraction Data (b) Rogers, T.; Helmholtz, L. *J. Am. Chem. Soc.* **1941**, *63*, 278

KI in the reaction system, however, the diffraction pattern obtained for the solid showed it to be KIO_3 (Figure 17h) rather than the corresponding acid.

Table 15. Attempts to obtain α-tosyloxypropiophenone by using I_2O_5, commercial HIO_3 and **M6** as catalysts.

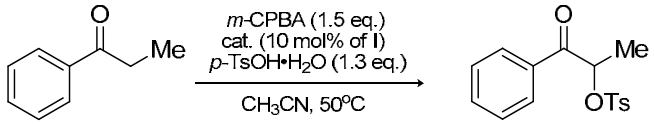

Entry[a]	Catalyst/10 mol% of I	Time/h	Yield[b]/%
1	I_2O_5	20	9
2	commercial HIO_3	20	8
3	**M6**	20	12

[a] [substrate] = 0.2 M. [b] Corrected GC yield (PhCl as internal standard).

Based on these results and the previous research[193] on related processes, we propose that an iodine (+1) and/or (+3) intermediate might be the true catalyst in cases where alkyliodides are used (Scheme 84). As previously proposed,[193] the specific species corresponding to these oxidation states might be the hypoiodite IO^- and the iodite IO_2^-. An attack of the tosylate on a transient hypervalent iodine species[194] derived from the alkyliodide would give rise to the catalytically active I^{+1} (or I^{+3}) intermediate.[195] Here, the I^{+3} (*e.g.* iodite) species could also form *via* disproportionation of I^+ to I^{+3} and I^- species. Further oxidation might then lead to the inactive I^{+5} products (*i.e.* **M6** or KIO_3), explaining the drop in the catalytic activity over time. The I^{+5} (specifically the IO_3^-) might also form as the result of the known propensity of the hypoiodite IO^- to disproportionate to iodide and iodate. The same active species may be obtained from the oxidation of iodide or molecular iodine (the initial brown color observed with alkyl iodides also indicates the formation of at least some I_2).

---

[193] (a) Uyanik, M.; Okamoto, H.; Yasui, T.; Ishihara, K. *Science* **2010**, *328*, 1376. (b) Uyanik, M.; Ishihara, K. *ChemCatChem* **2012**, *4*, 177.

[194] Alkyl tosylates have been detected by GC–MS in some cases.

[195] For a related mechanism for the oxidation of methyl iodide to the hypoiodous acid, see Asensio, G.; Andreu, C.; Boix-Bernardini, C.; Mello, R.; Gonzalez-Nunez, M. E. *Org. Lett.* **1999**, *1*, 2125.

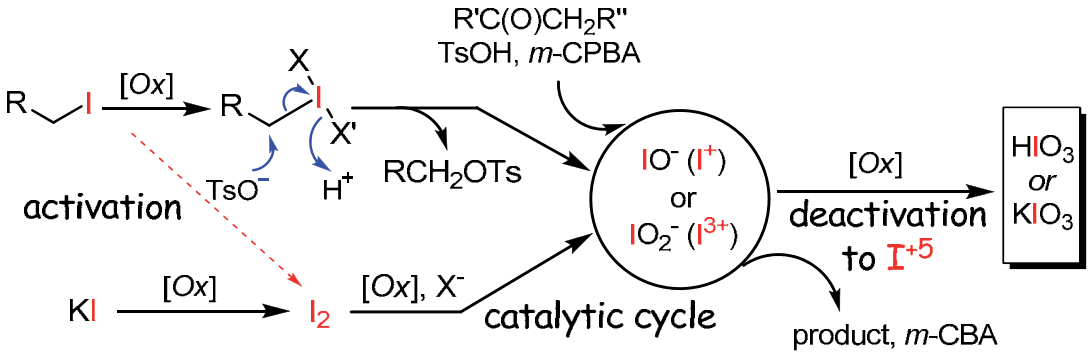

Scheme 84. Proposed evolution of the I species throughout the reaction.

4.4 Conclusions[196]

In summary, we have shown that, in addition to ArI, simple iodoalkanes can also serve as precursors to species active in the catalytic oxidative α-toxytosylation of aliphatic ketones with sulfonic acids. However, unlike the ArI, whose catalytic activity is based on the intermediacy of the $PhIX_2$ species, the iodoalkanes appear to be quickly degraded to the catalytically active inorganic iodite (and/or hypoiodite). Overoxidation and/or disproportionation of such species leads to the catalyst deactivation through the formation of a white solid identified as a previously unreported polymorph of the HIO_3 (observed as white precipitate, **M6**), or, in some cases, as KIO_3.

The coincidence between the *p*-XRD diffraction pattern of the new polymorph of HIO_3 and that for the previously reported mixed oxide I_4O_9 raises doubts as to the existence of the latter mixed valent iodine oxide species. At the very least, the diffraction pattern attributed in these earlier publications to this species was likely due to an impurity of HIO_3 present in the samples. Further investigation will be required to determine whether authentic I_4O_9 could be prepared as reported.

---

[196] **Guo, W.**; Vallcorba, O.; Vallribera, A.; Shafir, A.; Pleixats, R.; Rius, J. *ChemCatChem*, **2014**, *6*, 468.

4.5 Experimental section

4.5.1 General comments

4.5.1.1 Reagents and methods

All the reagents were purchased from Aldrich. *m*-CPBA (approximately 65% purity) was dried under high vacuum (0.25 mbar) for at least 1 h before use. The methanesulfonic acid (99% purity), camphorsulfonic acid (99% purity) and *p*-toluenesulfonic acid (*p*-TsOH·H_2O) (98% purity) were used as received without any further treatment. The silica gel for flash chromatography was a Macherey-Nagel GmbH & Co KG silica gel with a particle size of 230 – 400 mesh and a pore volume of 0.9 mL/g.

4.5.1.2 Physicochemical characterization

IR data were obtained on a Bruker Tensor 27 spectrometer with an ATR Golden Gate module with a diamond window. Liquid ^{1}H and ^{13}C NMR spectra were recorded on Bruker DRX-250MHz and DPX-360MHz instruments. All the NMR experiments were performed at the *Servei de Ressonància Magnètica Nuclear* of the *Universitat Autònoma de Barcelona.* ^{1}H NMR chemical shifts (δ, ppm) are referenced to the residual proton signal of the deuterated solvent, and the ^{13}C shifts are referenced to the ^{13}C resonance of the solvent. Elemental analyses were performed in Institute of Advanced Chemistry of Catalonia (CSIC-IQAC). The HPLC analysis was performed on a Waters 2960 instrument equipped with an UV photodiode array detector using a Dialcel Chiralpak AD-H chiral column, using hexane : isopropanol (80:20) as eluent with 1 mL/min of flow rate. TGA analyses were performed under an argon atmosphere at the *Institut de Ciència dels Materials de Barcelona* using a NETZSCH STA 449 F1 instrument (TGA/DSC). The X-ray diffraction (XRD) spectra were collected using a conventional powder X-ray diffractometer (Siemens D5000) at the *Institut de Ciència dels Materials de Barcelona*. XPS experiments were performed at the Surface Analysis Unit, *Centres Científics i Tecnològics* at the *Universitat de Barcelona* – CCiTUB. The measurements were carried out in a PHI 5500 Multitechnique System (from Physical Electronics) with a monochromatic X-ray source (Al Kα line of 1486.6 eV energy and 350 W), placed perpendicular to the analyzer axis and calibrated using the 3d5/2 line of Ag with a full width at half maximum (FWHM) of 0.8 eV. The analyzed area was a circle of 0.8 mm in diameter, and the selected resolution for the spectra was 187.5eV of pass energy and 0.8 eV/step for the general spectra, and 58.7eV of Pass Energy and 0.25

eV/step for the spectra of the different elements in the depth profile spectra. When necessary, a low energy electron gun (less than 10 eV) was used in order to discharge the surface. All measurements were made in an ultrahigh vacuum (UHV) chamber pressure between $5x10^{-9}$ and $2x10^{-8}$ torr.

4.5.2 General procedure for the catalytic oxidative α-tosyloxylation of ketones

All catalytic runs were performed in screw-top sealable tubes (10 mL). To a solution of ketone (1 mmol) in CH_3CN (5 mL), *p*-toluenesulfonic acid (247 mg, 1.3 mmol), *m*-CPBA (65% purity, 400 mg, 1.5 mmol) and the corresponding alkyl iodide (amount calculated to give 0.1 mmol of I, 10 mol% I) were added successively. The tube was sealed, and the mixture was stirred at 50°C for the time indicated in the tables. The reaction mixtures were poured into a saturated aq. $NaHCO_3$ solution and extracted with $CHCl_3$ (3 × 15 mL). The combined organic layer was dried over anhydrous Na_2SO_4 and concentrated under reduced pressure. The residue was further purified by flash column chromatography on silica gel.[197]

4.5.3 Preparation of M6

To a solution of propiophenone (0.134 g, 1 mmol) in CH_3CN (5 mL), *p*-toluenesulfonic acid (247 mg, 1.3 mmol), *m*-CPBA (65% purity, 400 mg of commercial source, 1.5 mmol) and *sec*-iodobutane (11 μL, ρ = 1.598 g/mL, 0.1 mmol) were added successively. The tube was sealed, and the mixture was stirred at 50 °C overnight. The reaction mixture was cooled down to room temperature and centrifuged with a speed of 4000 rpm for 10 min. Upon removal of the supernatant, a white solid was afforded. This solid was further washed with CH_3CN (3 × 5 mL) and dried under vacuum to give **M6** as a white powder (0.0142 g, 82%).

4.5.4 Determination of the crystal structure of HIO_3 (M6) from *p*-XRD data

These experiments were performed at the *Institut de Ciència dels Materials de Barcelona* (ICMAB) by Dr. Oriol Vallcorba and Prof. Jordi Rius.

Diffraction data of **M6** were collected on a Siemens D5000 diffractometer (45 kV, 35 mA, Bragg-Brentano geometry, secondary graphite monochromator, scintillation detector, Cu $K\alpha_{1,2}$ radiation, room temperature). The sample was mounted in a side-loaded sample holder to minimize possible preferred orientation effects. The measured

---

[197] All the spectra data of the corresponding α-tosyloxyketones have been given in Chapter 3 of Part I in this thesis.

2θ interval was 5.0-100.0º with a step size of 0.02º and a measuring time of 3s/step. The diffraction pattern was indexed with DICVOL04 and the intensities were extracted with DAjust software. The extracted intensities were introduced in the cluster-based direct methods program XLENS_PD6 which found the exact position of the iodine atoms and the approximate position of the three oxygen atoms. The obtained model underwent a final Rietveld refinement with no restraints introduced.

4.5.5 Synthesis of [bis(trifluoroacetoxy)iodo]perfluorobutane, 25[181]

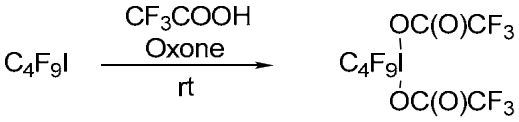

To a solution of nonafluoro-1-iodobutane (1 mL, 2.01 g/mL, 6 mmol) in trifluoroacetic acid (10 mL) was added oxone (3.689 g, 6 mmol) under stirring at room temperature. The reaction mixture was stirred at room temperature for 24 h. Upon the completion of the reaction, the solvent was evaporated under vacuum and the residue was treated with acetonitrile (20 mL). The insoluble part was washed with acetonitrile and discarded. Evaporation of the combined acetonitrile extracts under reduced pressure affording the corresponding product as a solid (2.744 g, 80%). ^{19}F NMR (376 MHz, CD_3CN) δ (ppm): -75.3 (s), -78.1 (br s), -80.4 (br s), -115.8 (br s), -125.1 (br s).

4.5.6 Synthesis of [hydroxy(tosyloxy)iodo]perfluorobutane, 26[181]

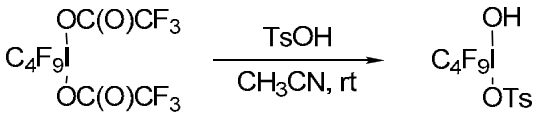

To a stirred solution of $TsOH \cdot H_2O$ (0.880 g, 4.626 mmol) in acetonitrile (20 mL) was added [bis(trifluoroacetoxy)iodo]perfluorobutane (2.116 g, 3.700 mmol) at 0 ºC. The mixture was warmed to room temperature and stirred until formation of a white precipitate. Evaporation of the solvent under reduced pressure affording the crude product. Analytical pure compound was obtained by recrystallization from acetonitrile. (1.640 g, 83%). ^{1}H NMR (400 MHz, CD_3CN/DMSO-d_6, 20:1) δ (ppm): 7.62 (d, J = 8.0 Hz, 2 H), 7.18 (d, J = 8.0 Hz, 2 H), 2.34 (s, 3 H). ^{19}F NMR (376 MHz, CD_3CN/DMSO-d_6, 20:1) δ (ppm): -80.5 (br s), -83.3 (br s), -116.3 (br, s), -125.3 (br, s).

4.5.7 α-Tosyloxylation of propiophenone with compound 26

The stoichiometric reaction between propiophenone (0.2 mmol) and [hydroxy(tosyloxy)iodo]perfluorobutane (**26**) (0.118 g, 0.22 mmol, 1.1 eq.) under the

optimized conditions (50 °C) for 24 h gave no/trace product (see the following GC spectra Figure 22). The peak at 2.47 min corresponds to the propiophenone (*i.e.* the starting material).

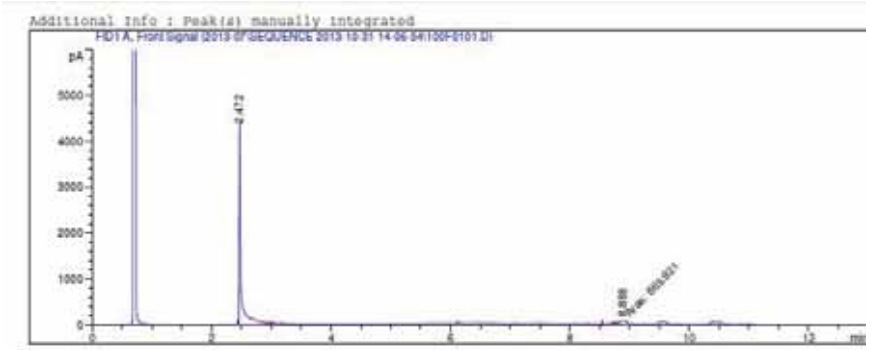

Figure 22. GC trace of the reaction mixture between propiophenone and compound **26**.

4.5.8 Synthesis of (1*R*, 2*S*, 5*R*)-2-isopropyl-5-methylcyclohexyl methanesulfonate, 27

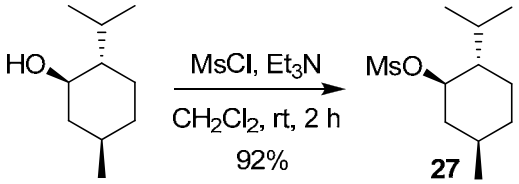

Following a previously reported procedure,[183] a solution of (-)-menthol (0.316 g, 2 mmol) in a mixture of anhydrous dichloromethane (28 mL) and triethylamine (0.84 mL, 6 mmol, d = 0.727 g/ mL) was cooled to 0°C, followed by an addition of mesyl chloride (0.31 mL, 4 mmol, d = 1.480 g/mL). The mixture was further stirred at 0 °C for 30 min and then stirred for 2 h at room temperature (GC monitoring). At this point, the mixture was filtered through a plug of silica gel, and then the filtrate was washed with sat. $NaHCO_3$ solution and dried over anhydrous sodium sulfate. After removal of the solvent, a light green oil was obtained (0.43 g, 92% yield). ^{1}H NMR (360 MHz, $CDCl_3$) δ (ppm): 4.55 (apparent td, *J* = 10.9, 4.6 Hz, 1 H), 3.00 (d, *J* = 1.4 Hz, 3 H), 2.31 – 2.21 (m, 1 H), 2.07 (dtd, *J* = 13.9, 7.0, 2.3 Hz, 1 H), 1.78 - 1.62 (m, 2 H), 1.54 - 1.27 (m, 2 H), 1.33 - 1.20 (m, 2H), 1.06 (ddd, *J* = 16.5, 13.6, 3.6 Hz, 1 H), 0.93 (dd, *J* = 6.8, 3.0 Hz, 6 H), 0.83 (d, *J* = 6.9 Hz, 3 H). ^{13}C NMR (90 MHz, $CDCl_3$) δ (ppm): 83.5, 47.6, 42.4, 39.2, 33.9, 31.8, 25.9, 23.2, 21.9, 20.9, 15.8.

4.5.9 Synthesis of (1*R*, 2*S*, 5*R*)- 2-isopropyl-5-methylcyclohexyl iodide, 28

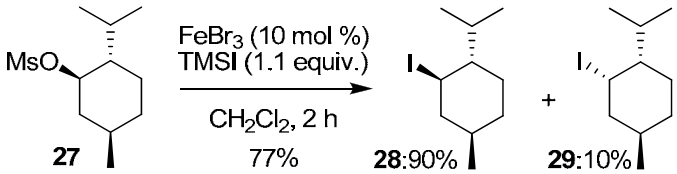

This method was adapted from a previous article.[185] To a solution of (1*R*, 2*S*, 5*R*)-2-isopropyl-5-methylcyclohexyl methanesulfonate (0.469 g, 2 mmol) in anhydrous dichloromethane (20 mL), iodotrimethylsilane (0.313 mL, 2.2 mmol, 1.406 g/mL) and iron(III) bromide (0.059 g, 0.2 mmol) were added. The mixture was stirred at room temperature under nitrogen for 2 h (GC monitoring). Then, the mixture was washed with 25% (W/V) aqueous $Na_2S_2O_3 \cdot 5H_2O$, and the aqueous phase extracted with dichloromethane. The combined organic phases were dried over anhydrous sodium sulfate, the organic solvent was removed under reduced pressure affording a mixture of (1*R*, 2*S*, 5*R*)-menthyl iodide (**28**) and (1*S*, 2*S*, 5*R*)-menthyl iodide (**29**) (ratio 10 : 1) as a light yellow oil (0.410 g, 77% yield). ^{1}H NMR (360 MHz, $CDCl_3$) δ (ppm): selected peaks for **28**, 4.13 (apparent td, *J* = 11.9, 4.0 Hz, 1 H), 2.66-2.51 (m, 1 H), 2.33 - 2.11 (m, 1 H), 0.78 - 0.59 (m, 3 H); selected peaks for **29**, 4.77 (m, 1 H); see the spectrum for other signals.

4.5.10 HPLC analysis of the α-tosyloxypropiophenone obtained with a chiral iodoalkane as pre-catalyst

This HPLC analysis corresponds to the α-tosyloxypropiophenone obtained under catalysis by the menthol-derived chiral iodoalkane (1*R*, 2*S*, 5*R*)-menthyl iodide and shows a complete lack of enantioselectivity.

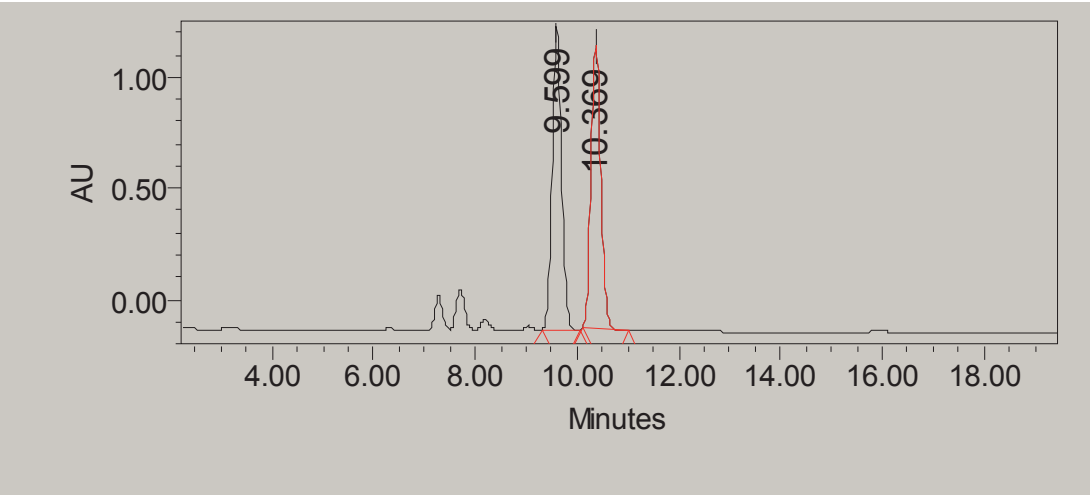

	Retention Time	Area	% Area	Height
1	9.599	17905080	50.61	1374006
2	10.369	17471331	49.39	1269060

Part II. Water-soluble metal nanoparticles (Rh, Au) in catalysis

CHAPTER 1

Introduction to metal nanoparticles: preparation, characterization and applications in catalysis

Chapter 1. Introduction to metal nanoparticles: preparation, characterization and applications in catalysis

Catalysis lies at the heart of chemical communities, both in the academic research area and in the chemical industry. In the absence of catalysts, various products which are essential to our life would not be accessible, such as fine chemicals, fibers, polymers, medicines, paints, lubricants and fuels. Homogenous catalysts are generally employed by chemists either in industrial or laboratory processes but encountering the difficulties in separating the catalyst from the final reaction mixture. Heterogeneous catalyst, at a certain extent, is desirable in order to recycle the precious catalyst. One solution strategy is immobilizing the catalyst on supports, such as inorganic oxides, polymers, etc., as discussed in the third chapter of part one in this thesis. Alternative choices were developed in recent years on the basis of transition metal NPs, taking advantage of the large surface area of the particles and their relatively high activity.

1.1 Preparation of metal nanoparticles

Metal NPs, defined as aggregates of atoms between 1 and 100 nm in size, have found application in areas as diverse as optics, magnetism, chemical sensors, as well as medicine and catalysis.[198,199] In terms of catalysis, it is usually desirable to obtain NPs with the smallest possible size, thus allowing to maximize the number of metal

---

[198] For some books on nanomaterials and NPs: (a) *Clusters and Colloids; from Theory to Applications*; Schmid, G. Ed.; VCH, Weinheim, **1994**. (b) *NPs and Nanostructured Films; Preparation, Characterization and Applications*; Fendler, J. H. Ed.; Wiley-VCH, Weinheim, **1998**. (c) *Metal NPs; Preparation, Characterization and Applications;* Feldheim, D. L., Colby Jr, A. F., Eds.; Marcel Dekker, New York, **2002**. (d) *The Chemistry of Nanomaterials; Synthesis, Properties and Applications*; vol. 1 y 2; Rao, C. N. R. ; Müller, A.; Cheetham, A. K. Eds.; Wiley-VCH, Weinheim, **2004**. (e) *NPs and Catalysis*; Astruc, D. Ed.; Wiley-VCH, Weinheim, **2008**. (f) Roucoux, A.; Philippot, K. In *Handbook of Homogeneous Hydrogenation*, De Vries, J. G.; Elsevier, C. J. Eds., **2007**, *1*, 217-256.

[199] For some reviews on the preparation, characterization, properties and applications of metal NPs, see: (a) Toshima, N.; Yonezawa, T. *New J. Chem*, **1998**, 1179. (b) Crooks, R. M.; Zhao, M.; Sun, Li; Chechik, V.; Yeung, L. K. *Acc. Chem. Res*. **2001**, *34*, 181. (c) Roucoux, A.; Schulz, J.; Patin, H. *Chem. Rev*. **2002**, *102*, 3757. (d) Kamat, P. V. *J. Phys. Chem. B* **2002**, *106*, 7729. (e) Moreno-Mañas, M.; Pleixats, R. *Acc. Chem. Res*. **2003**, *36*, 638. (f) Widegren, J. A.; Finke, R. G. *J. Molec. Catal. A: Chem*. **2003**, *191*, 187. (g) Daniel, M.-C.; Astruc, D. *Chem. Rev*. **2004**, *104*, 293. (h) B. L.; Kolesnichenko, V. L.; O'Connor, C. J. *Chem. Rev*. **2004**, *104*, 3893. (i) Astruc, D.; Lu, F.; Ruiz Aranzaes, J. *Angew. Chem. Int. Ed*. **2005**, *44*, 7852. (j) Roucoux, A. *Top. Organomet. Chem*. **2005**, *16*, 261. (k) Malik, M. A.; O'Brien, P. *Top. Organomet. Chem*. **2005**, *9*, 173. (l) *Synthesis, structure and properties of metal nanoclusters*; Wilcoxon, J. P.; Abrams, B. L. *Chem. Soc. Rev*. **2006**, *35*, 1162. (m) Starkey Ott, L.; Finke, R. G. *Coord. Chem. Rev*. **2007**, *251*, 1075. (n) Astruc, D. *Inorg. Chem*. **2007**, *46*, 1884. (o) Shan, J.; Tenhu, H. *Chem. Commun*. **2007**, 4580. (p) Durand, J.; Teuma, E.; Gómez, M. *Eur. J. Inorg. Chem*. **2008**, 3577. (q) Corma, A.; Garcia, H. *Chem. Soc. Rev*. **2008**, *37*, 2096. (r) Jain, P. K.; Huang, X.; El-Sayed, I. H.; El-Sayed, M. A. *Acc. Chem. Res*. **2008**, *41*, 1578. (s) Campelo, J. M.; Luna, D.; Luque, R.; Marinas, J. M.; Romero, A. A. *ChemSusChem* **2009**, *2*, 18. (t) Amiens, C.; Chaudret, B.; Ciuculescu-Pradines, D.; Colliere, V.; Fajerwerg, K.; Fau, P.; Kahn, M.; Maisonnat, A.; Soulanticac, K.; Philippot, K. *New J. Chem*. **2013**, *37*, 3374.

atoms on the surface. However, metal NPs are subject to facile agglomeration and the formation of the thermodynamically more stable bulk metal, with the consequent loss of the catalytic properties. This problem can be solved by the addition of a suitable protecting reagent (stabilizer) or by immobilization of the nanoclusters on a solid support. Thus, a variety of protocols have been developed, including top-down and bottom-up methodologies, as depicted in Scheme 85, to prepare stabilized and/or supported metal NPs.

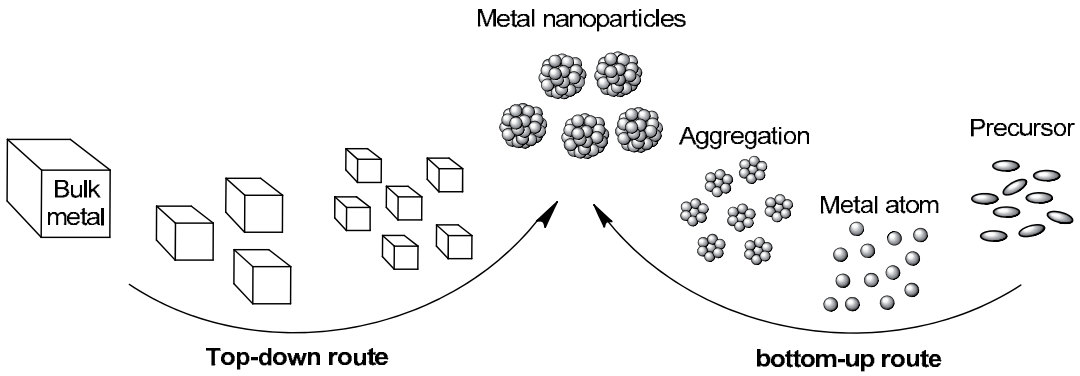

Scheme 85. Schematic illustration of preparative methods of metal NPs.

1.1.1 Stabilization of metal nanoparticles

In the presence of a protective reagent/stabilizer, the metal NPs can be suspended in liquid phase. The nature of the stabilizing reagent can control the solubility of the NPs in different media (organic, aqueous, fluorous). Based on the stabilizing agents used, the stabilization for the suspension of the metal NPs can be divided into four categories:[199c] 1) the electrostatic stabilization provided by the surface adsorbed ions; 2) the steric stabilization given by the presence of bulky compounds or materials, for instance polymers; 3) the combination of electrostatic and steric stabilization (electrosteric), provided by surfactants; 4) stabilization with a ligand. However, some authors consider that the ligands, which generally bear coordinating groups and bulky moieties, can be included into the electrosteric stabilization category.

1.1.1.1 Electrostatic stabilization

Ionic compounds such as carboxylates, halides or polyoxoanions can generate electrostatic stabilization when dissolved in aqueous solution. The adsorption of these anions and their counterions on the metal surface will generate an electrical double-layer around the particles, therefore resulting in a coulombic repulsion between the particles (Scheme 86). When the electric potential with the double layer is high enough,

the aggregation between the NPs is suppressed.[200] However, it should be noted that this stabilization is very sensitive to any factor which may disturb the double layer, *e. g.*, thermal motion.

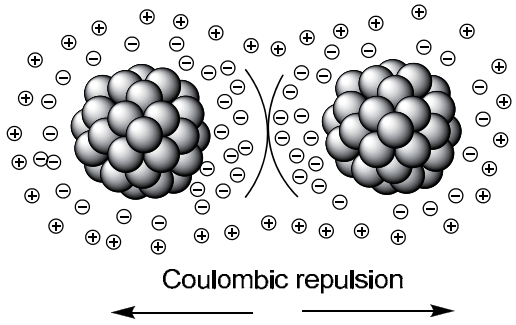

Scheme 86. Schematic representation of electrostatic stabilization of metal NPs.

1.1.1.2 Steric stabilization

Metal NPs can also be prevented from aggregation by using macromolecules like polymers or oligomers, in which the adsorption of the macromolecules at the surface of the NPs will provide a protective layer. The suspension of metal NPs can be achieved by either formation of single separate particle@macromolecule layer units (Scheme 87a) or an intercrossed network (Scheme 87b). This kind of stabilization can be explained by visualizing the approach between two NPs. When these NPs are close enough, the adsorbed molecules will be restricted in motion, which causes a decrease in entropy and thus increase in free energy. A second stabilization effect should be ascribed to the increase in concentration of adsorbed macromolecules as the protective layers begin to interpenetrate. Whereas the electrostatic stabilization is mainly utilized in aqueous systems, the steric stabilization can be used in both organic and aqueous solutions. Nevertheless, one should keep in mind that the length or the nature of the macromolecules influence the thickness of the protective layer and, thus, affect the stability of the metal NPs.

[200] (a) Goia, D. V.; Matijevic, E. *New J. Chem.* **1998**, *22*, 1203. (b) Aiken, J. D.; III; Finke, R. G. *J. Mol. Catal. A: Chem.* **1999**, *145*, 1. (c) Labib, M. E. *Colloids Surf.* **1988**, *29*, 293.

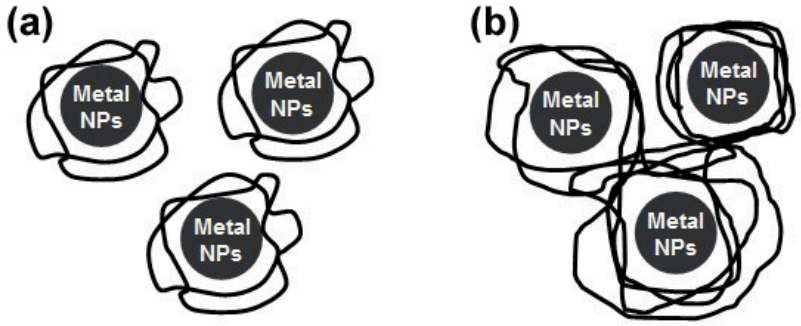

Scheme 87. The suspension of metal NPs by steric stabilization: a) through single separate particle/macromolecule layer units; b) through intercrossed network.

1.1.1.3 Electrosteric stabilization

The electrosteric stabilization combines the electrostatic and steric stabilization to maintain the metal NPs stable in solution.[201] Generally speaking, this stabilization is provided by ionic surfactants which bear a polar headgroup able to produce an electric double layer and a lypophilic long chain able to generate steric repulsion. The electrosteric stabilization can be also obtained from polyoxoanions such as the ion pair (Bu_4N^+)/polyoxoanion. The significant steric repulsion of the bulky Bu_4N^+ countercations associated with the highly charged polyoxoanion (Coulomb repulsion) provide an efficient electrosteric stability for the suspension of metal NPs.[202]

1.1.1.4 Stabilization by a ligand

Traditional ligands have also been utilized as stabilizers to prevent the aggregation of metal NPs. In these cases, the stabilization occurs by the coordination of the ligand (such as phosphines,[203] thiols,[204] amines,[205] etc) to the nanoparticle surface.

---

[201] (a) Aiken, J. D., III; Lin, Y.; Finke, R. G. *J. Mol. Catal. A: Chem.* **1996**, *114*, 29. (b) Lin, Y.; Finke, R. G. *J. Am. Chem. Soc.* **1994**, *116*, 8335.

[202] Schmid, G. *Chem. Rev.* **1992**, *92*, 1709.

[203] (a) Schmid, G.; Pfeil, R.; Boese, R.; Bandermann, F.; Meyers, S.; Calis, G. H. M.; Van Der Velden, J. W. A. *Chem. Ber.* **1981**, *114*, 3634. (b) Amiens, C.; De Caro, D.; Chaudret, B.; Bradley, J. S.; Mazel, R.; Roucau, C. *J. Am. Chem. Soc.* **1993**, *115*, 11638. (c) Duteil, A.; Schmid, G.; Meyer-Zaika, W. *J. Chem. Soc., Chem. Commun.* **1995**, 31.

[204] (a) Dassenoy, F.; Philippot, K.; Ould Ely, T.; Amiens, C.; Lecante, P.; Snoeck, E.; Mosset, A.; Casanove, M. J.; Chaudret, B. *New J. Chem.* **1998**, *22*, 703. (b) Chen, S.; Kimura, K. *J. Phys. Chem. B* **2001**, *105*, 5397.

[205] (a) Schmid, G.; Morun, B.; Malm, J. O. *Angew. Chem. Int. Ed.* **1989**, *28*, 778. (b) Schmid, G.; Maihack, V.; Lantermann, F.; Peschel, S. *J. Chem. Soc., Dalton Trans.* **1996**, 589. (c) Schmid, G.; Emde, S.; Maihack, V.; Meyer-Zaika, W.; Peschel, S. *J. Mol. Catal. A: Chem.* **1996**, *107*, 95.

1.1.2 Supports used for metal nanoparticles

1.1.2.1 Porous materials as supports

Porous materials are normally solids which have an interconnected network of pores. Many synthetic products, including metal oxides, ceramics, carbonaceous materials and membranes are porous materials. The use of porous materials with defined pore sizes as supports for metal NPs allows the formation of specific adsorption sites, creating a partition between the exterior and interior pores.[206] Besides, these kinds of materials also confine the particle growth to a particular domain and stop the particle aggregation.[207] A variety of porous materials have been utilized as the support media for the formation of metal NPs. Each support offers a set of advantages. For example, porous carbonaceous materials have been of great interest in high-temperature and high-pressure catalytic transformations.[208]

a) (Insoluble) polymers

Polymers are often used as supports for a colloidal suspension of metal NPs.[209] They have been widely utilized due to their availability and enhanced stability. Recently, some novel engineered polymers with an inorganic backbone,[210] fibers,[211] dendrimers[212] and polyvinylpyridine[213] have attracted much interest as supports. Biopolymers and biomass-related polymers also were found to offer some advantages as supports, including low toxicity, low cost, ready availability and high biocompatibility, when comparing with traditional supports.[214]

---

[206] (a) Astruc, D.; Lu, F.; Aranzaes, J. R. *Angew. Chem. Int. Ed.* **2005**, *44*, 7852. (b) Karimi, B.; Abedi, S.; Clark, J. H.; Budarin, V. *Angew. Chem. Int. Ed.* **2006**, *45*, 4776.

[207] (a) White, R. J.; Luque, R.; Budarin, V.; Clark, J. H.; Macquarrie, D. J. *Chem. Soc. Rev.* **2009**, *38*, 481. (b) Pan, X.; Bao, X. *Chem. Commun.* **2008**, 6271. (c) Karimi, B.; Abedi, S.; Clark, J. H.; Budarin, V. *Angew. Chem. Int. Ed.* **2006**, *45*, 4776.

[208] Deshpande, R. M.; Buwa, V. V.; Rode, C. V.; Chaudhari, R. V.; Mills, P. L. *Catal. Commun.* **2002**, *3*, 269.

[209] (a) Dahl, J. A.; Maddux, B. L. S.; Hutchinson, J. E. *Chem. Rev.* **2007**, *107*, 2228. (b) Park, C. M.; Kwon, M. S.; Park, J. *Synthesis* **2006**, 3790. (c) Okamoto, K.; Akiyama, R.; Yoshida, H.; Yoshida, T.; Kobayashi, S. *J. Am. Chem. Soc.* **2005**, *127*, 2125. (d) Yang, Y. C.; Luh, T. Y. *J. Org. Chem.* **2003**, *68*, 9870. (e) Ooe, M.; Murata, M.; Mizugaki, T.; Ebitani, K.; Kaneda, K. *J. Am. Chem. Soc.* **2004**, *126*, 1604. (f) Desforges, A.; Backov, R.; Deleuze, H.; Mondain-Monval, O. *Adv. Funct. Mater.* **2005**, *15*, 1689.

[210] Panziera, N.; Pertici, P.; Barazzone, L.; Caporusso, A. M.; Vitulli, G.; Salvadori, P.; Borsacchi, S.; Geppi, M.; Veracini, C. A.; Martra, G.; Bertinetti, L. *J. Catal.* **2007**, *246*, 351.

[211] Gallon, B. J.; Kojima, R. W.; Kaner, R. B.; Diaconescu, P. L. *Angew. Chem. Int. Ed.* **2007**, *46*, 7251.

[212] (a) Boisselier, E.; Diallo, A. K.; Salmon, L.; Ruiz, J.; Astruc, D. *Chem. Commun.* **2008**, 4819. (b) Garcia-Martinez, J. C.; Lezutekong, R.; Crooks, R. M. *J. Am. Chem. Soc.* **2005**, *127*, 5097. (c) Knecht, M. R.; Garcia-Martinez, J. C.; Crooks, R. M. *Langmuir* **2005**, *21*, 11981.

[213] Caporusso, A. M.; Innocenti, P.; Aronica, L. A.; Vitulli, G.; Gallina, R.; Biffis, A.; Zecca, M.; Corain, B. *J. Catal.* **2005**, *234*, 1.

[214] (a) Wei, W. L.; Zhu, H. Y.; Zhao, C. L.; Huang, M. Y.; Jiang, Y. Y. *React. Funct. Polym.* **2004**, *59*, 33. (b)

b) Carbonaceous materials

Materials related to carbon offer excellent properties as supports based on several facts 1) recent advances in this area allow the synthesis of carbon nanostructures with well-defined pore structure, *i. e.*, regular pore shape, controlled sizes and high specific surface area; 2) various protocols have been developed to modify carbon materials to act as catalysts support. These protocols include a treatment with plasma, acid or base etching as well as doping with heteroatoms or ozonolysis.[215] In particular, carbon nanotubes and graphene, were also investigated as supports for metal NPs. Their unique physical properties, combined with intrinsic morphologies, high surface area, high electrical conductivity and inherent geometry, make them stand out as supports of metal NPs for catalytic purposes.[216]

c) Metal oxides

Metal oxides offer thermal and chemical stabilities, and therefore meet the requirements for supporing metal NPs. What's more, they can be easily prepared and further functionalized for the catalytic applications. Among the metal oxides, alumina,[217] ceria,[218] zirconia[219] and titania[220] are the most frequently utilized supports. Superparamagnetic oxides Fe_3O_4[221] and γ-Fe_2O_3,[222] emerged as new materials for the

---

Zhang, X.; Geng, Y.; Han, B.; Ying, M. Y.; Huang, M. Y.; Yiang, Y. Y. *Polym. Adv. Technol.* **2001**, *12*, 642. (c) Quignard, F.; Choplin, A.; Domard, A. *Langmuir* **2000**, *16*, 9106. (d) Bandini, M.; Luque, R.; Budarin, V.; Macquarrie, D. J. *Tetrahedron* **2005**, *61*, 9860. (e) Budarin, V.; Clark, J. H.; Luque, R.; Macquarrie, D. J.; White, R. J. *Green Chem.* **2008**, *10*, 382. (f) Zhang, Z.; Wang, Z.; *J. Org. Chem.* **2006**, *71*, 7485.

215 Tasis, D.; Tagmatarchis, N.; Bianco, A.; Prato, M. *Chem. Rev*. **2006**, *106*, 1105.

216 Nanotubes as supports, please see: (a) Terrones, M. *Int. Mater. Rev.* **2004**, *49*, 325. (b) Wildgoose, G. G.; Banks, C. E.; Compton, R. G. *Small* **2006**, *2*, 182. (c) Wang, C.; Guo, S.; Pan, X.; Chen, W.; Bao, X. *J. Mater. Chem.* **2008**, *18*, 5782. Graphene as supports, please see: (d) Si, Y.; Samulski, E. T. *Chem. Mater.* **2008**, *20*, 6792. (e) Kou, R.; Shao, Y.; Mei, D.; Nie, Z.; Wang, D.; Wang, C.; Viswanathan, V. V.; Park, S.; Aksay, I. A.; Lin, Y.; Wang, Y.; Liu, J. *J. Am. Chem. Soc.* **2011**, *133*, 2541. (f) Muszynski, R.; Seger, B.; Kamat, P. V. *J. Phys. Chem. C* **2008**, *112*, 5263.

217 (a) Glaspell, G.; Hassan, H. M. A.; Elzatahry, A.; Abdalsayed, V.; El-Shall, M. S. *Top. Catal.* **2008**, *47*, 22. (b) Sandoval, A.; Gomez-Cortes, A.; Zanella, R.; Diaz, G.; Saniger, J. M. *J. Mol. Catal. A: Chem.* **2007**, *278*, 200. (c) Senkan, S.; Kahn, M.; Duan, S.; Ly, A.; Ledholm, C. *Catal. Today* **2006**, *117*, 291.

218 (a) Abad, A.; Corma, A.; Garcia, H. *Chem. Eur. J.* **2008**, *14*, 212. (b) Abad, A.; Almela, C.; Corma, A.; Garcia, H. *Chem. Commun.* **2006**, 3178. (c) Abad, A.; Concepcion, P.; Corma, A.; Garcia, H. *Angew. Chem. Int. Ed.* **2005**, *44*, 4066. (d) Yang, Y.; Saoud, K. M.; Abdelsayed, V.; Glaspell, G.; Deevi, S.; El-Shall, M. S. *Catal. Commun.* **2006**, *7*, 281.

219 (a) Moreno, J. M.; Aramendia, M. A.; Marinas, A.; Marinas, J. M.; Urbano, F. J. *Appl. Catal. B* **2007**, *76*, 34. (b) J. M. Moreno, M. A. Aramendia, A. Marinas, J. M. Marinas, F. J. Urbano, *Appl. Catal. B* **2005**, *59*, 275. (c) Cioffi, N.; Faticanti, M.; Ditaranto, N.; De Rossi, S.; Traversa, L.; Monopoli, A.; Nacci, A.; Torsi, L.; Sabbatini, L. *Curr. Nanosci.* **2007**, *3*, 121. (d) Faticanti, M.; Cioffi, N.; De Rossi, S.; Ditaranto, N.; Porta, P.; Sabbatini, L.; Bleve-Zacheo, T. *Appl. Catal. B* **2005**, *60*, 73.

220 (a) Bedford, R. B.; Singh, U. G.; Walton, R. I.; Williams, R. T.; Davis, S. A. *Chem. Mater.* **2005**, *17*, 701. (b) Hofmeister, H.; Miclea, P. T.; Steen, M.; Moerke, W.; Drevs, H. *Top. Catal.* **2007**, *46*, 11.

221 (a) Rossi, L. M.; Silva, F. P.; Vono, L. L. R.; Kiyohara, P. K.; Duarte, E. L.; Itri, R.; Landers, R.; Machado,

immobilization of metal NPs with improved separation capabilities whereby, in the presence of a magnet, the supported metal NPs can be easily separated from the final reaction mixture for next run.

Mesoporous aluminosilicates[223,224,225] have been reported to be excellent supports for metal NPs. More recently, metal phoshates[226] and metal-organic frameworks (MOFs)[227] were also investigated as supports of metal NPs.

1.1.2.2 Nonporous materials as supports

Nonporous materials can be defined as those materials without any voids or pores in their structure. Such materials can also be used as supports for the formation of metal NPs including metals, foils, glass, hard plastic and some polymers as polypropylene, polyethylene and other engineered polymers.[199s] Following the initial work by Raveendran[228] on biomaterials as supports, related investigations were pursued by others with chitosan,[229] cellulose[230] and poly(allylamine) gels as supports for the metal NPs.[231]

1.1.3 Synthetic methodologies for the preparation of metal nanoparticles

The classical protocols for the preparation of supported NPs include impregnation, co-precipitation and deposition-precipitation. The colloidal suspensions can be

---

G. *Green Chem.* **2007**, *9*, 379. (b) Jacinto, M. J.; Kiyohara, P. K.; Masunaga, S. H.; Jardim, R. F.; Rossi, L. M. *Appl. Catal. A: Mol.* **2008**, *338*, 52.

222 Please see recent reviews: (a) Polshettiwar, V.; Luque, R.; Fihri, A.; Zhu, H.; Bouhrara, M.; Basset, J. -M. *Chem. Rev.* **2011,** *111*, 3036. (b) Gijs, M. A. M.; Lacharme, F.; Lehmann, U. *Chem. Rev.* **2010**, *110*, 1518. (c) An example of paper: Mori, K.; Kanai, S.; Hara, T.; Mizugaki, T.; Ebitani, K.; Jitsukawa, K.; Kaneda, K. *Chem. Mater.* **2007**, *19*, 1249.

223 (a) Han, J.; Fang, P.; Jiang, W.; Li, L.; Guo, R. *Langmuir* **2012**, *28*, 4768. (b) Zhu, J.; Kónya, Z.; Puntes, V. F.; Kiricsi, I.; Miao, C. X.; Ager, J. W.; Alivisatos, A. P.; Somorjai, G. A. *Langmuir*, **2003**, *19*, 4396.

224 (a) Wang, D.; Xie, T.; Peng, Q.; Li, Y. *J. Am. Chem. Soc.* **2008**, *130*, 4016. (b) Pal, M.; Ganesan, V. *Langmuir* **2009**, *25*, 13264.

225 Campelo, J. M.; Lee, A. F.; Luna, D.; Luque, R.; Marinas, J. M.; Romero, A. A. *Chem. Eur. J.* **2008**, *14*, 5988.

226 Ma, Z.; Yin, H.; Overbury, S. H.; Dai, S. *Catal. Lett.* **2008**, *126*, 20.

227 (a) Müller, M.; Hermes, S.; Kähler, K.; van den Berg, M. W. E.; Muhler, M.; Fischer, R. A. *Chem. Mater.* **2008**, *20*, 576. (b) Schröder, F.; Esken, D.; Cokoja, M.; van den Berg, M. W. E.; Lebedev, O. I.; Tendeloo, G. V.; Walaszek, B.; Buntkowsky, G.; Limbach, H.-H.; Chaudret, B.; Fischer, R. A. *J. Am. Chem. Soc.* **2008**, *130*, 6119.

228 Raveendran, P.; Fu, J.; Wallen, S. L. *Green Chem.* **2006**, *8*, 34.

229 (a) Corma, A.; Concepcion, P.; Dominguez, I.; Fornes, V.; Sabater, M. J. *J. Catal.* **2007**, *251*, 39. (b) Zhu, B. W.; Lim, T. T.; Feng, J. *Chemosphere* **2006**, *65*, 1137. (c) Laudenslager, M. J.; Schiffman, J. D.; Schauer, C. L. *Biomacromolecules* **2008**, *9*, 268.

230 (a) Reddy, K. R.; Kumar, N. S.; Reddy, P. S.; Sreedhar, B.; Kantam, M. L. *J. Mol. Catal. A: Chem.* **2006**, *252*, 12. (b) Kotelnikova, N.; Vainio, U.; Pirkkalainen, K.; Serimaa, R. *Macromol. Symposia* **2007**, 254, 74.

231 Hong, Y.; Sen, A. *Chem. Mater.* **2007**, *19*, 961.

prepared by chemical reduction of transition metal salts in the presence of a suitable stabilizer, by ligand reduction and displacement from organometallics in the presence of a stabilizer, by chemical vapor deposition, by the use of microemulsions, by electrochemical reduction of a metal precursor and by thermal and photochemical decomposition. The chemical reduction of transition metal salts is the most frequently used. Another method, the reduction of ligands to release metals from organometallic complexes, is also gaining much attention.

1.1.3.1 Reduction of metal salts in the presence of a stabilizer

The reduction of metal salts in the presence of a suitable stabilizer is the most widely used method for the preparation of colloidal suspensions of transition metals. In fact, this methodology is, in general, very simple to implement and can yield metal NPs with very narrow size distributions and high yields.[199f,h]

A wide range of reducing agents have been employed for achieving metal NPs, such as hydrogen, carbon monoxide, sodium citrate, hydrazine, sodium borohydride, oxidable solvents (e.g. alcohols), etc.. In the presence of a suitable stabilizer, the metal salts (such as $HAuCl_4$, $RhCl_3$, H_2PtCl_6, H_2PdCl_4, $RuCl_3$, etc.) can be reduced to metal NPs (M^0) which can be dispersed in various solvents, affording a colloidal suspension. A variety of polymers (polyvinyl alcohol or PVA, polyvinylpyrrolidone or PVP, polyvinyl ether or PVE,…), ionic and non-ionic surfactants, oligomers, dendrimers, cyclodextrines, etc. were found to act as excellent stabilizers.[232] The earlier studies mainly focused on the preparation of various metal NPs (Pd, Rh, Pt, Au, Ir, Ag and Ru).[199c] Nowadays researchers are doing great efforts to design and synthesize new stabilizers for metal NPs for special catalytic purposes.[233]

It is well accepted that the steps for the formation of NPs by chemical reduction are: 1) the corresponding metal atoms are obtained after the reduction; 2) nucleation occurs, followed by atom aggregation to give small clusters; 3) the growth of the clusters afford the NPs and 4) the stabilizer is adsorbed, and thus the agglomeration process is stopped (Scheme 88).

---

[232] (a) Hirai, H.; Nakao, Y.; Toshima, N. *J. Macromol. Sci., Chem.* **1978**, *A12*, 1117. (b) Hirai, H.; Nakao, Y.; Toshima, N. *J. Macromol. Sci., Chem.* **1979**, *A13*, 727. (c) Borsla, A.; Wilhelm, A. M.; Delmas, H. *Catal. Today* **2001**, *66*, 389. (d) Hirai, H. *Makromol. Chem., Suppl.* **1985**, *14*, 55. (e) Hirai, H.; Nakao, Y.; Toshima, N. *Chem. Lett.* **1978**, 545. (f) Toshima, N.; Kuriyama, M.; Yamada, Y.; Hirai, H. *Chem. Lett.* **1981**, 793. (g) Komiyama, M.; Hirai, H. *Bull. Chem. Soc. Jpn.* **1983**, *56*, 2833.

[233] (a) Barbaro, P.; Dal Santo, V.; Liguori, F. *Dalton Trans.* **2010**, *39*, 8391. (b) Roy, S.; Pericas, M. A. *Org. Biomol. Chem.* **2009**, *7*, 2669. (c) Yasukawa, T.; Miyamura, H.; Kobayashi, S. *Chem. Soc. Rev.* **2014**, *43*, 1450.

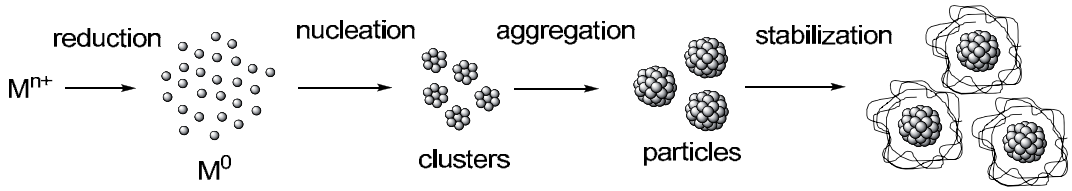

Scheme 88. Preparation of metal NPs by reduction of metal salts in the presence of a stabilizer.

1.1.3.2 Reduction and displacement of ligands from organometallic compounds

Metal NPs can also be obtained from some zerovalent organometallic complexes by reduction or displacement of ligands.[199k,199t] With this method, which has been developed by Chaudret and coworkers, Pt and Pd colloidal suspensions were prepared from the reduction of dibenzylidene ligand of $Pt(dba)_2$ (dba = dibenzylydeneacetone) and $Pd(dba)_2$ in the presence of cellulose or cellulose nitrate in THF.[234 a,b] In the presence of PVP, cellulose nitrate or cellulose acetate, Ru NPs were obtained from the hydrogenation of Ru(COD)(COT).[234c] Similarly, $Ni(COD)_2$ was utilized to prepare Ni NPs stabilized from PVP (Scheme 89).[235] Cu, Co and Au NPs stabilized by PVP were also generated with this methodology.[236]

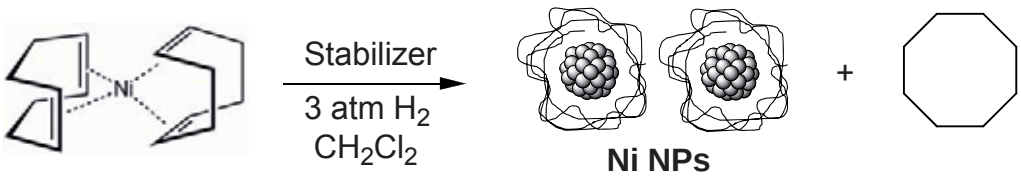

Scheme 89. Preparation of Ni NPs from $Ni(COD)_2$ by hydrogenation.

1.1.3.3 Impregnation

This protocol requires the "wetting" of the solid support with a solution of metal precursor. The metal precursor, normally a metal salt, is dissolved in the minimum amount of solvent, and this solution is added to the porous support. When the solution has filled the pores, the solvent is then removed to give a solid which is commonly

---

[234] (a) Duteil, A.; Queau, R.; Chaudret, B.; Mazel, R.; Roucau, C.; Bradley, J. S. *Chem. Mater.* **1993**, *5*, 341. (b) Bradley, J. S.; Millar, J. M.; Hill, E. W.; Behal, S.; Chaudret, B.; Duteil, A. *Faradays Discuss.* **1991**, *92*, 255. (c) Lara, P.; Philippot, K.; Chaudret, B. *ChemCatChem* **2013**, *5*, 28.

[235] (a) De Caro, D.; Bradley, J. S. *Langmuir* **1997**, *13*, 3067. (b) Ould Ely, T.; Amiens, C.; Chaudret, B.; Snoeck, E.; Verelst, M.; Respaud, M.; Broto, J. M. *Chem. Mater.* **1999**, *11*, 526.

[236] (a) De Caro, D.; Agelou, V.; Duteil, A.; Chaudret, B.; Mazel, R.; Roucau, C.; Bradley, J. S. *New J. Chem.* **1995**, *19*, 1265. (b) Osuna, J.; De Caro, D.; Amiens, C.; Chaudret, B.; Snoeck, E.; Respaud, M.; Broto, J. M.; Fert, A. *J. Phys. Chem.* **1996**, *100*, 14571.

oven-dried, subsequently submitted to calcination, and reduced if necessary. The formed metal NPs are dispersed depending on the nature of metal and support.[237]

1.1.3.4. Co-precipitation

The co-precipitation involves the simultaneous precipitation of the support and the metal NPs. A template-directed sol-gel process is frequently employed in this method. However, the presence of metal precursors in solution can often interfere with the sol-gel process, resulting in materials with undesirable properties. However, in comparison with the above-mentioned impregnation method, the metal NPs prepared by this protocol usually show narrower size distribution and better dispersion in the matrix.[238]

1.1.3.5 Precipitation-Deposition

This method was first introduced by Haruta and co-workers.[239] It involves the dissolution of the metal precursor followed by adjustment of the pH value to achieve a precipitation of the metal hydroxide, *e. g.*, $Au(OH)_3$, on the surface of the support. The hydroxide is subsequently calcined and reduced to the elemental metal.[240] Generally speaking, this protocol often gives nanomaterials with broad size distribution and it is very difficult to control the particle size. Some of the reported cases need the addition of an excess of external reductant such as $NaBH_4$, H_2 or hydrazine.[241]

1.1.3.6 Other methods

Microemulsions have been proven as an alternative for the preparation of metal NPs. This protocol takes advantage of self-assembly chemistry and generally requires the combination of water, oils and surfactant.[242] Only few reports have dealt with the formation of metal NPs by photochemical methods.[199d, 243] Chemical vapor deposition

---

[237] (a) Chen, X.; Zhu, H. Y.; Zhao, J. C.; Zheng, Z. F.; Gao, X. P. *Angew. Chem. Int. Ed.* **2008**, 47, 5353. (b) Chiang, C. W.; Wang, A.; Mou, C. Y. *Catal. Today* **2006**, *117*, 220. (c) Campelo, J. M.; Lee, A. F.; Luna, D.; Luque, R.; Marinas, J. M.; Romero, A. A. *Chem. Eur. J.* **2008**, *14*, 5988.

[238] (a) Bekyarova, E.; Kaneko, K. *Adv. Mater.* **2000**, *12*, 1625. (b) Liu, H.; Ma, D.; Blackley, R. A.; Zhou, W.; Bao, X. *Chem. Commun.* **2008**, 2677.

[239] M. Haruta, S. Tsubota, T. Kobayashi, T. Kageyama, M. J. Genet, *J. Catal.* **1993**, *144*, 175.

[240] (a) Centeno, M. A.; Portales, C.; Carrizosa, I.; Odriozola, J. A. *Catal. Lett.* **2005**, 102, 289. (b) Date, M.; Okumura, M.; Tsubota, S.; Haruta, M. *Angew. Chem. Int. Ed.* **2004**, *43*, 2129.

[241] Cushing, B. L.; Kolesnichenko, V. L.; O'Connor, C. J. *Chem. Rev.* **2004**, *104*, 3893.

[242] (a) Hoar, T. P.; Shulman, J. H. Nature **1943**, *152*, 102. (b) Eriksson, S.; Nylen, U.; Rojas, S.; Boutonnet, M. *Appl. Catal. A: Mol.* **2004**, *265*, 207. (c) Yashima, M.; Falk, L. K. L.; Palmqvist, A. E. C.; Holmberg, K. *J. Colloid Interface Sci.* **2003**, *268*, 348. (d) Ruta, M.; Semagina, N.; Minsker, L. K. *J. Phys. Chem. C* **2008**, *112*, 13635.

[243] (a) He, P.; Zhang, M.; Yang, D.; Yang, J. *Surf. Rev. Lett.* **2006**, *13*, 51. (b) Yu, K. P.; Yu, W. Y.; Kuo, M. C.; Liou, Y. C.; Chien, S. H. *Appl. Catal. B* **2008**, *84*, 112.

involves the vaporization of metals and the growth of metal NPs under high vacuum in the presence of stabilizing organic solvents.[244] Although electrochemical reduction is not widely employed, it offers several advantages: 1) the particle size can be easily controlled by changing the current intensity; 2) easy procedure of isolation of metal NPs; 3) the synthesis can often result in excellent yields.[245] A few examples of greener methods that combined physicochemical routes were also developed, with the sonoelectrochemistry and flame spray pyrolysis being the most common.[246]

Metal NPs can also be prepared via a physical route in a top-down manner (Scheme 85), *e. g.*, ball-milling protocol. However, this way generally results in metal NPs with broad particle size distribution and irreproducible catalytic activities.[247] In recent years, a variety of green protocols have been well developed including laser, microwave, sonication, plasma and supercritical fluids in the formation of supported metal NPs.[199s] It should be noted that, although these methodologies were termed as "physical routes" by some authors,[199s] chemical transformations were sometimes adopted in these procedures. Some of the main technologies are listed as follows:

a) Pulsed laser ablation

The pulsed laser ablation approach involves the vaporization of metals with a pulsed laser and subsequent controlled deposition on the surface of the support under certain conditions of temperature and pressure.[217a,248] This method does not use any chemical reagents (apart from the metal) or solvents and, therefore, is a simple and environmentally friendly synthetic route for the preparation of contamination-free metal NPs. Besides, any mixtures of metals in any composition can be turned into metal NPs. What's more, the NPs can be directly supported because they are created with a great number of dangling bonds and, thus, they are strongly adsorbed and anchored onto the supports. Most importantly, this protocol does not produce any side products and it is suitable to scale up for industrial applications. Practical experiments showed the sizes

---

[244] (a) Okumura, M.; Nakamura, S.; Tsubota, S.; Nakamura, T.; Azuma, M.; Haruta, M. *Catal. Lett.* **1998**, *51*, 53. (b) Ishida, T.; Nagaoka, M.; Akita, T.; Haruta, M. *Chem. Eur. J.* **2008**, *14*, 8456.

[245] (a) Reetz, M. T.; Helbig, W. *J. Am. Chem. Soc.* **1994**, *116*, 7401. (b) Dominguez-Dominguez, S.; Arias-Pardilla, J.; Berenguer-Murcia, A.; Morallon, E.; Cazorla-Amoros, D. *J. Appl. Electrochem.* **2008**, *38*, 259.

[246] (a) Compton, R. G.; Eklund, J. C.; Marken, F. *Electroanalysis* **1997**, *9*, 509. (b) Pollet, B. G.; Phull, S. S. Recent Developments in Electrochemistry, Vol. 4 (Ed.: Pandalai, S. G.), Transworld Research Network, Trivandrum, India, **2001**, pp. 55. (c) Liu, Y. C.; Wang, C. C.; Juang, L. C. *J. Electroanal. Chem.* **2004**, *574*, 71.

[247] Willner, I.; Mandler, D. *J. Am. Chem. Soc.* **1989**, *111*, 1330.

[248] B. Liu, Z. Hu, Y. Che, US 2008006524 A1 20080110, **2008**.

and compositions of the generated NPs can be adjusted for specific catalytic purposes.[217a,217c, 249]

b) Microwave irradiation

Microwaves have been found as an effective mean to prepare metal NPs with the advantages of short reaction time, small particle size, narrow size distribution and high purity. In this protocol, a solution of metal salts is usually employed as the metal source. The irradiation time is a critical parameter as longer reaction times lead to particle agglomeration. Generally speaking, this methodology has difficulties to control the particle size and distribution of the metal NPs on the support, but this situation is greatly improved when using a polymer as stabilizer.[250]

c) Sonication

Ultrasounds significantly enhance mass transport, reducing the thickness of the diffusion layer and enhancing the surface contact area.[251] The deposition and reduction of the metal NPs occurs almost consecutively and therefore the heating step employed in other protocols is unnecessary, which makes the preparation of supported metal NPs more environmentally friendly and energy-efficient.[252] By using this method it is also easy to achieve size control of the particles due to the acoustic cavitation phenomena, that is, the formation, growth and collapse of the produced bubbles in a liquid medium. However, this protocol sometimes requires the addition of a reducing agent to ensure the reduction of the metal NPs on the support.[253]

d) Plasma

The method of reduction by plasma has been found suitable for the preparation of supported metal NPs at room temperature. For example, dihydrogen microwave plasma and Ar-glow discharged plasma have been reported in the synthesis of a range

---

[249] Savastenko, N.; Volpp, H. R.; Gerlach, O.; Strehlau, W. *J. Nanopart. Res.* **2008**, *10*, 277.

[250] (a) Luque, R.; Budarin, V.; Clark, J. H.; Macquarrie, D. J. *Appl. Catal. B* **2008**, *82*, 157. (b) Zhu, J.; Palchik, O.; Chen, S.; Gedanken, A. *J. Phys. Chem. B* **2000**, *104*, 7344. (c) Boxall, D. L.; Lukehart, C. M. *Chem. Mater.* **2001**, *13*, 806. (d) Glaspell, G.; Fuoco, L.; El-Shall, M. S. *J. Phys. Chem. B* **2005**, *109*, 17350. (e) Mukherjee, P.; Patra, C. R.; Ghosh, A.; Kumar, R.; Sastry, M. *Chem. Mater.* **2002**, *14*, 1678. (f) Harpeness, R.; Peng, Z.; Liu, X.; Pol, V. G.; Koltypin, Y.; Gedanken, A. *J. Colloid Interface Sci.* **2005**, *287*, 678.

[251] (a) I. Haas, A. Gedanken, *Chem. Commun.* **2008**, 1795. (b) A. Gedanken, *Ultrason. Sonochem.* **2004**, *11*, 47.

[252] N. Perkas, Z. Zhong, J. Grinblat, A. Gedanken, *Catal. Lett.* **2008**, *120*, 19.

[253] (a) Li, H.; Wang, R.; Hong, Q.; Chen, L.; Zhong, Z.; Koltypin, Y.; Calderon-Moreno, J.; Gedanken, A. *Langmuir* **2004**, *20*, 8352. (b) Baranchikov, A. Y.; Ivanov, V. K.; Tretyakov, Y. D. *Russian Chem. Rev.* **2007**, *76*, 133. (c) Nagao, D.; Shimazaki, Y.; Saeki, S.; Kobayashi, Y.; Konno, M. *Colloids Surf. A* **2007**, *302*, 623. (d) Perkas, N.; Zhong, Z.; Chen, L.; Besson, A.; Gedanken, A. *Catal. Lett.* **2005**, *103*, 9.

of supported Au, Pt, Pt-Au, Pd and Ag NPs.[254] Although this technique is promising, fast and simple, the specialized and costly equipment makes its widespread use difficult.

e) Supercritical fluids

This protocol involves the dissolution of a metal precursor in a supercritical fluid and the subsequent incorporation on a support.[255] The impregnated metal precursor can be reduced to its elemental form by different approaches, such as chemical reduction by H_2 or ethanol,[254a, 256] thermal reduction[254b, 257] or thermal decomposition[254, 258] in an inert gas atmosphere. This protocol offers several advantages: 1) provides enhanced mass-transfer properties due to high diffusivities of supercritical fluids; 2) the low surface tension of supercritical fluids results in better penetration and wetting, without the problems related to structure shrinkage or pore collapse of the supports; 3) the NPs dispersion and morphology on various supports can be easily controlled by using different metal precursors and varying the reduction temperatures and chemistry.[255a] Supercritical CO_2 has been widely used for the formation of metal NPs because it is abundant, low cost, non-toxic and non-flammable.[255-257, 259]

1.2 Characterization of metal nanoparticles

The characterization of metal NPs can be performed using various instrumental techniques depending on the parameters or structural element to be determined. Only some frequently used techniques will be mentioned herein.

1.2.1 Transmission electron microscopy (TEM) and high resolution transmission electron microscopy (HRTEM)

Recent studies showed that, in some cases, the morphologies of metal NPs have great effect on the catalytic activities.[260] TEM is frequently utilized to characterize the

---

254 (a) Legrand, J. C.; Diamy, A. M.; Riahi, G.; Randriamanantenasoa, Z.; Polisset-Thfoin, M.; Fraissard, J. *Catal. Today* **2004**, *89*, 177. (b) Zou, J. J.; Zhang, Y. P.; Liu, C. J. *Langmuir* **2006**, *22*, 11388. (c) Zhu, X.; Huo, P. P.; Zhang, Y. P.; Liu, C. J. *Ind. Eng. Chem. Res.* **2006**, *45*, 8604.

255 (a) Zhang, Y.; Erkey, C. *J. Supercrit. Fluids* **2006**, *38*, 252. (b) Zhang, Y.; Kang, D.; Saquing, C.; Aindow, M.; Erkey, C. *Ind. Eng. Chem. Res.* **2005**, *44*, 4161.

256 Long, D. P.; Blackburn, J. M.; Watkins, J. J. *Adv. Mater.* **2000**, *12*, 913.

257 Saquing, C. D.; Kang, D.; Aindow, M.; Erkey, C. *Microporous Mesoporous Mater*. **2005**, *80*, 11.

258 Lee, S. S.; Park, B. K.; Byoung, S. H.; Chang, F.; Kim, H. *Chem. Mater*. **2006**, *18*, 5631.

259 Ye, X. R.; Lin, Y.; Wang, C.; Engelhard, M.; Wang, Y.; Wai, C. M. *J. Mater. Chem.* **2004**, *14*, 908.

260 (a) Mostafa, S.; Behafarid, F.; Croy, J. R.; Ono, L. K.; Li, L.; Yang, J. C.; Frenkel, A. I.; Cuenya, B. R. *J. Am. Chem. Soc.* **2010**, *132*, 15714. (b) An, K.; Somorjai, G. A. *ChemCatChem*, **2012**, *4*, 1512.

morphologies of metal NPs. In this technique, a beam of electrons is transmitted through a layer of the stabilized metal NPs deposited on a special copper grid. An image indicating the morphologies of the metal NPs is formed upon the interaction of the electrons with the specimen. HRTEM is an imaging mode of TEM that allows for direct imaging of the atomic structure of the sample. In HRTEM a virtually planar electron wave transmits a very thin specimen (thickness < 20 nm). During the transmission process, the incident electron wave is scattered or diffracted in the case of a crystal at the potentials of the atoms, and thereby the phase of the electron wave is varied. At the exit surface of the specimen an *informative* wave is formed, which carries direct and highly resolved information on the sample. The *informative* wave is magnified in the electron microscope and during this stage the wave suffers additional phase shifts due to imperfect lenses (aberrations). The image finally recorded on film plates or digital cameras is an interference pattern of the *image* wave, which contains essentially the phase contrast with all the microscopic aberrations included.[261] The preparation of the specimen depends on the nature of the sample. In our case, a small amount of the material is dissolved in a volatile solvent (1 mg/mL), and a drop of this solution is deposited on a copper grid. Upon complete evaporation, the copper grid is submitted for the analysis. The nanoparticle sizes and distribution can be obtained by measurement of a number of particles using Digital Micrograph software (Gatan, Inc.) and averaged to produce the mean diameter.

1.2.2 Electron diffraction (ED)

The technique of electron diffraction is closely related to the X-Ray diffraction, and is based on the wave nature of electrons. The method is frequently used to study the crystal structure of the metal NPs. The experiments are generally performed in a TEM instrument where the electrons are greatly accelerated in order to gain the desired energy. The periodic structure of metal NPs acts as a diffraction grating, scattering the electrons in a predictable manner. Working back from the observed diffraction patterns, the crystalline structure of the specimen (particularly the unit cell parameters) could be deduced. This allows for the diffraction pattern to be matched against known crystalline lattices, and thus confirm, in an indirect way (through a particular crystal lattice), the nanoparticle composition.

---

[261] Saxton, W.O.: Object reconstruction, In *Computer Techniques for Image Processing in Electron Microscopy* (Ed. L. Marton), Academic Press, New York (**1978**) 236.

1.2.3 Dynamic light scattering (DLS)

Dynamic light scattering (DLS) allows to determine the size distribution profile of nanoparticles. DLS measures the light scattered from a laser that passes through a colloidal solution, and by analyzing the modulation of the scattered light intensity as a function of time, the hydrodynamic size of particles and particle agglomerates can be evaluated. Larger particles diffuse slower than smaller particles and the DLS instrument measures the time dependence of the scattered light to provide a correlation function that is mathematically relevant to a particle size. DLS provides particle sizes including the stabilizing layer around the metal particle surface. The difference between the particle sizes determined by DLS and TEM are shown in Scheme 90.

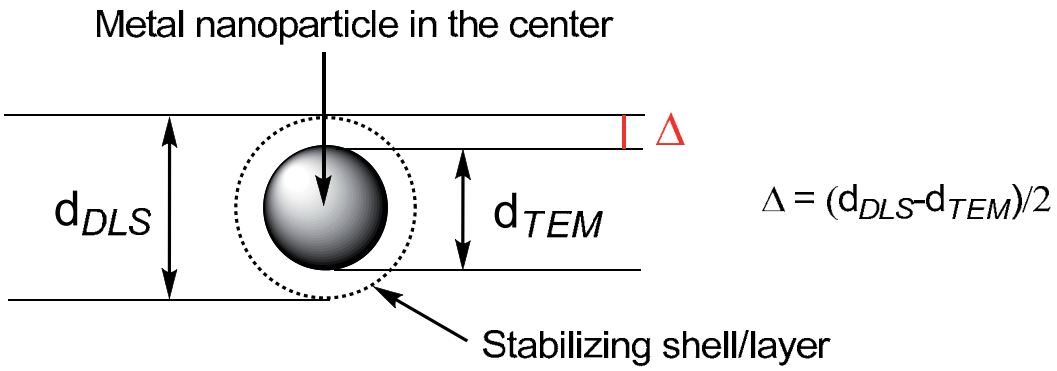

Scheme 90. Difference between the particle sizes determined by DLS and TEM

1.2.4 Energy Dispersive X-ray Spectroscopy (EDX/EDS)

EDX is a powerful tool to provide information on the composition of the samples. It is based on the detection of characteristic x-rays emitted from an element as a result of the de-excitation of core electron holes generated by a high energy electron beam. An electron from a higher binding energy level falls into the core hole and the difference in energy between the higher-energy shell and the lower energy shell is released in the form of an x-ray. Due to the quantization of electron energy levels, the emitted characteristic x-ray energies for elements will, in general, be different from element to element, with only a few spectral peaks overlapping. Even if, in some cases, the identification of one peak is ambiguous, other peaks or limited knowledge of the sample history will often allow a reasonable elemental identification of the peak. The normal electron beam of a TEM or SEM (scanning electron microscopy) can be used as the excitation source. The sample is effectively the anode of an x-ray source. The addition of an energy measuring x-ray detector with a thin, low mass element window

on a TEM/SEM enables the registration of EDS/EDX for all elements from carbon on up in atomic mass. A spectrum containing all of the characteristic x-rays emitted by the elements present in the sample will be registered, as exemplified in Figure 23.

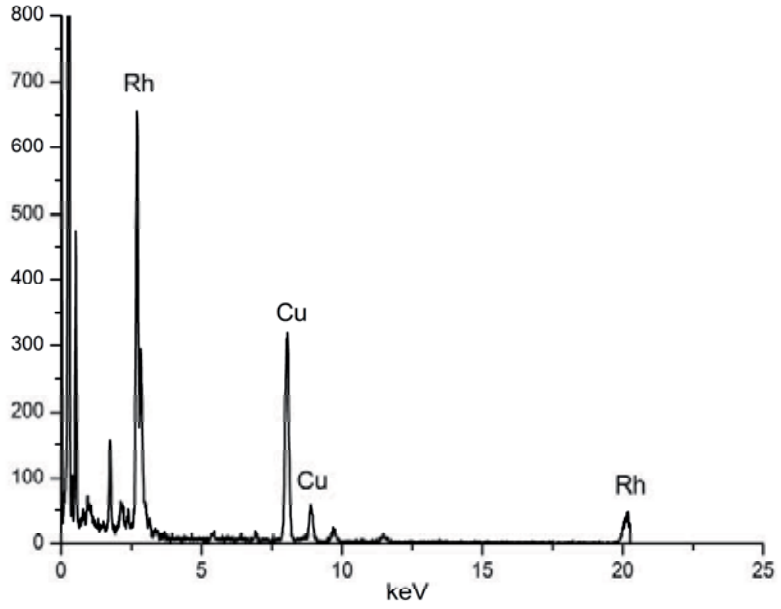

Figure 23. An example of EDX spectrum of Rh(0) NPs.

1.2.5 X-ray diffraction (XRD)

XRD is a rapid analytical technique for phase identification of metal NPs. It can further prove the results obtained from ED analysis or can be used as an alternative technique. Similar to ED, the crystalline substances act as three-dimensional diffraction gratings for x-ray wavelengths. When monochromatic x-rays pass through the sample, the interaction of the incident x-rays with the sample generates constructive interference (and a diffracted ray) if the conditions satisfy the Bragg's Law ($n\lambda = 2d\sin\theta$) (Scheme 91). This law relates the wavelength of electromagnetic radiation to the diffraction angle and the lattice spacing in a crystalline sample. These diffracted x-rays are then detected, processed and counted. By scanning the sample through a range of 2θ angles, all possible diffraction directions of the lattice could be obtained due to the random orientations of the powdered material. Conversion of the diffraction peaks to d-spacings allows identification of the sample since each kind of samples has a set of unique d-spacing values. Typically, this is achieved by comparison of these values with standard reference patterns which are stored in several databases, for instance, the International Centre for Diffraction Data (ICDD).

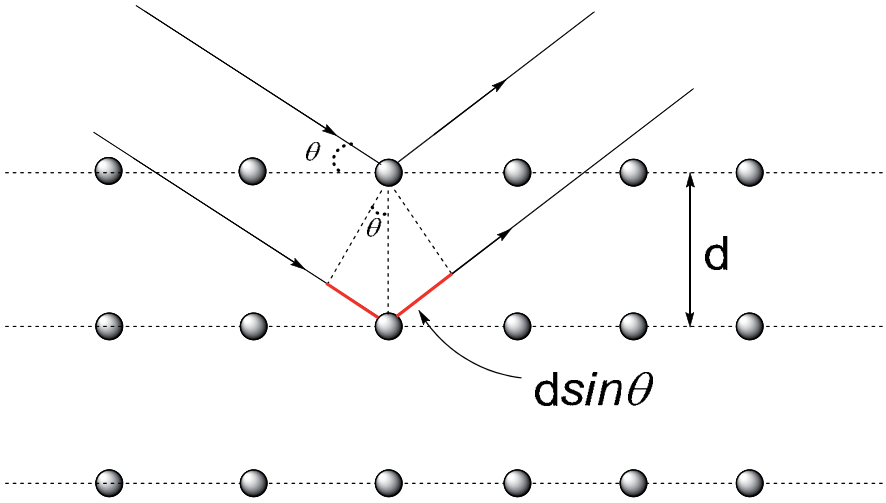

Scheme 91. Schematic of Bragg diffraction.

1.3 Catalytic applications of metal nanoparticles

Transition-metal-catalysis plays a key role as a synthetic methodology in the development of industrial processes, particularly in fine chemical production. Over the last decade, the application of transition metal NPs in catalysis has flowered, particularly those of Pd, Au, Rh, Ni, Ag, Cu, etc.. In many cases, the used nanocatalysts can be isolated and re-dissolved in organic solvents or aqueous solutions, depending on the nature of the stabilizer. In catalysis, metal NPs can exhibit great potential as recyclable catalysts. The following paragraphs, far from offering a comprehensive account of all the reported catalytic applications of metal NPs, provide an overview of the key usage of the nanocatalysts in various organic transformations.

1.3.1 Pd nanoparticles in catalysis

Palladium is one of the most versatile metals in promoting catalytic reactions, especially those involving C-C bond formation, such as Heck, Negishi, Sonogashira, Suzuki, Kumada and Stille coupling reactions (Scheme 92)[262] The preparation of either supported palladium NPs[199s] or colloidal suspensions[199e] has been extensively investigated. Notably, a great number of publications focused on Pd NPs as catalysts in Heck, Sonogashira and Suzuki couplings.[199e,199f,199n,199s, 263]

[262] Tsuji, J. Palladium Reagents and Catalysts, Wiley-VCH, Weinheim, **2004**.

[263] (a) Balanta, A.; Godard, C.; Claver, C. *Chem. Soc. Rev.* **2011**, *40*, 4973. (b) Fihri, A.; Bouhrara, M.; Nekoueishahraki, B.; Basset, J. M.; Polshettiwar, V. *Chem. Soc. Rev.* **2011**, *40*, 5181.

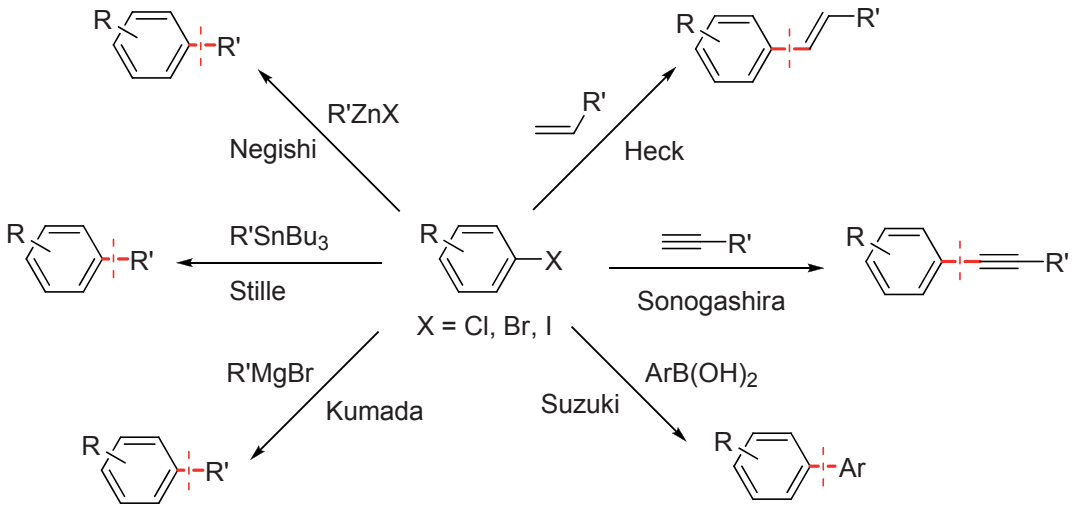

Scheme 92. Palladium catalyzed C-C bond forming reactions.

The Suzuki coupling reaction involves the coupling of aryl (or vinyl) halides with aryl boronic acids (or other boronic acid derivatives) (Scheme 92). The reports concerning the use of Pd NPs in Suzuki C-C couplings involve Pd NPs supported on magnetic NPs,[264] alumina and silica-based oxides,[265] carbonaceous materials,[266] mesoporous biopolymers,[214e] etc. or colloidal suspensions of Pd NPs stabilized by polymers, dendrimers, ionic liquids, and so forth.[211] The Heck reaction is another very important kind of C-C bond-making transformations (Scheme 92). It provides a great deal of new extended alkenes through the reaction of aryl (or vinyl) halides or triflates with alkenes. The catalytic use of Pd NPs in Heck reaction blossomed in the last two decades.[263, 264, 267] Some articles reported the usage of Pd NPs as catalysts in Sonogashira reaction (Scheme 92). The process involves the alkynylation of aryl or alkenyl halides with terminal alkynes. PVP,[268] TBAB[269] and 2-hydropropyl-α-cyclodextrin[270] have been proven to stabilize Pd NPs as active catalysts in Sonogashira reaction. Pd NPs

---

[264] (a) Y. Zhu, S. C. Peng, A. Emi, Z. Su, Monalisa, R. A. Kemp, *Adv. Synth. Catal.* **2007**, *349*, 1917. (b) P. D. Stevens, G. Li, J. Fan, M. Yen, Y. Gao, *Chem. Commun.* **2005**, 4435. (c) P. D. Stevens, J. Fan, H. M. R. Gardimalla, M. Yen, Y. Gao, *Org. Lett.* **2005**, *7*, 2085.

[265] (a) D. D. Das, A. Sayari, *J. Catal.* **2007**, *246*, 60. (b) A. Gniewek, J. J. Ziolkowski, A. M. Trzeciak, M. Zawadzki, H. Grabowska, J. Wzryszcz, *J. Catal.* **2008**, *254*, 121.

[266] A. Corma, H. Garcia, A. Leyva, *J. Mol. Catal. A: Chem.* **2005**, *230*, 97.

[267] (a) N. Erathodiyil, S. Ooi, A. M. Seayad, Y. Han, S. S. Lee, J. Y. Ying, *Chem. Eur. J.* **2008**, *14*, 3118. (b) B. Yoon, C. M. Wai, *J. Am. Chem. Soc.* **2005**, *127*, 17174.

[268] P. Li, L. Wang and H. Li, *Tetrahedron* **2005**, *61*, 8633.

[269] M. B. Thathagar, P. J. Kooyman, R. Boerleider, E. Jansen, C. J. Elsevier and G. Rothenberg, *Adv. Synth. Catal.* **2005**, *347*, 1965.

[270] Senra, J. D.; Fernando, L.; Malta, B.; da Costa, M. E. H. M.; Michel, R. C.; Aguiar, L. C. S.; Simas A. B. C.; Antunes, O. A. C. *Adv. Synth. Catal.* **2009**, *351*, 2411 and references therein.

supported on graphite oxide,[271] and metal organic framework material MOF-5[272] also showed catalytic activities in the Sonogashira coupling. Pd NPs have also found use in tandem cross-coupling and subsequent alkynes functionalization processes. As a typical example, in 2010, Ranu and co-workers[273] disclosed the one-pot reaction of 2-iodophenols and arylacetylenes resulting in benzofurans under catalysis of Pd NPs in water in the absence of any ligand (Scheme 93). Thus, the initially formed arylalkyne undergoes a Pd-catalyzed intramolecular hydrophenoxylation of the triple bond. In this research, a series of functionalized benzo[*b*]furan derivatives were prepared with high yields and the catalyst could be recycled up to 4 times.

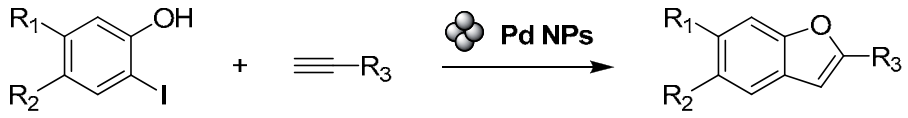

Scheme 93. Synthesis of benzo[*b*]furans catalyzed by Pd NPs through a Sonogashira reaction followed by cyclisation.

However, the homogeneous and/or colloidal nature of the active palladium species in C-C bond formation reactions is still unclear.[274] When Pd NPs are used as catalysts, the possibility of leaching and formation of soluble catalytically active species should be considered. Possible mechanisms are summarized in Scheme 94: 1) Pd NPs may act as true heterogeneous species; 2) palladium atoms could leach from the particles or an oxidative addition could occur at the surface of the particle followed by leaching of the [Pd(Ar)X] species to initiate a homogeneous catalytic cycle. It has been suggested that the leaching could be reversible.[274c-g]

Pd NPs were also proven as catalysts in a wide range of other organic transformations such as oxidations,[275] hydrogenations,[276] oxidative C-C coupling through C-H activation[277] and hydrodechlorinations.[278]

---

[271] Rumi, L.; Scheuermann, G. M.; Mulhaupt, R.; Bannwarth, W. *Helv. Chim. Acta* **2011**, *94*, 966 and references therein.

[272] Gao, S.; Zhao, N.; Shu, M.; Che, S. *Appl. Catal. A* **2010**, *388*, 196.

[273] D. Saha, R. Dey, B. C. Ranu, *Eur. J. Org. Chem.* **2010**, 6067.

[274] (a) Reetz, M. T.; de Vries, J. G. *Chem. Commun.* **2004**, 1559. (b) Durand, J.; Teuma, E.; Gomez, M. *Eur. J. Inorg. Chem.* **2008**, 3577. (c) Astruc, D. *Inorg. Chem.* **2007**, *46*, 1884. (d) Corma, A.; Das, D.; Garcia, H.; A. Leyva, *J. Catal.* **2005**, *229*, 322. (e) Sanhes, D.; Raluy, E.; Retory, S.; Saffon, N.; Teuma, E.; Gomez, M. *Dalton Trans.* **2010**, *39*, 9719. (f) de Vries, J. G. *Dalton Trans.* **2006**, 421 and references therein. (g) de Vries, A. H. M.; Parlevliet, F. J.; Schmeder-van de Vondervoort, L.; Mommers, J. H. M.; Hendrickx, H. J. W.; Walet, M. A. N. *Adv. Synth. Catal.* **2002**, *344*, 996. (h) Pacardo, D. B.; Slocik, J. M.; Kirk, K. C.; Naikb, R. R.; Knecht, M. R. *Nanoscale* **2011**, *3*, 2194.

[275] (a) Lopez-Sanchez, J. A.; Dimitratos, N.; Miedziak, P.; Ntainjua, E.; Edwards, J. K.; Morgan, D.; Carley, A. F.; Tiruvalam, R.; Kiely, C. J.; Hutchings, G. J. *Phys. Chem. Chem. Phys.* **2008**, *10*, 1921. (b) Li, F.; Zhang,

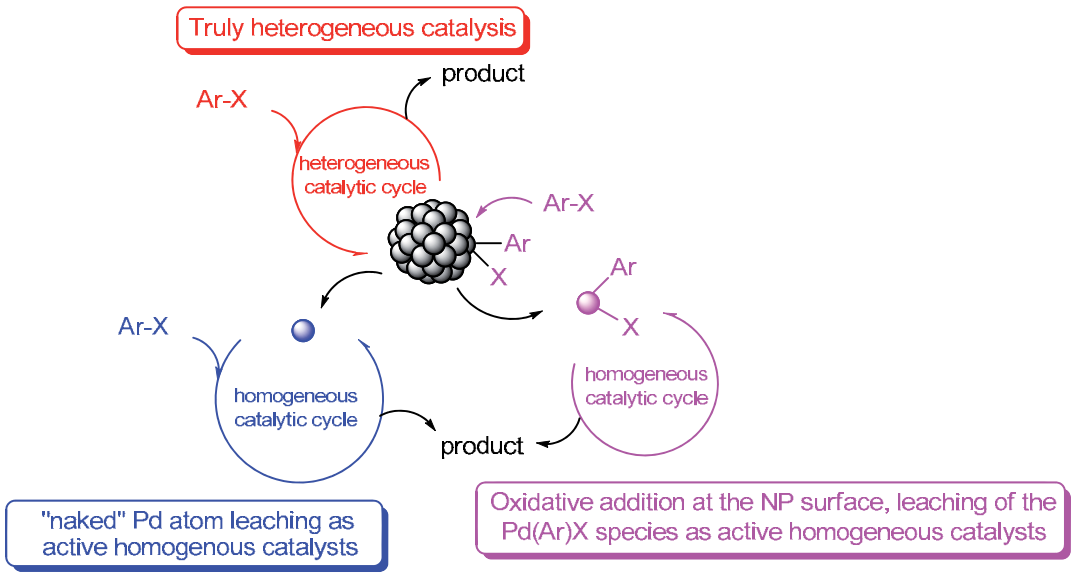

Scheme 94. Proposed mechanisms for the Pd NPs catalyzed C-C coupling reactions.

1.3.2 Au nanoparticles in catalysis

Bulk gold is a very stable metal and it is resistant to oxidation. However, Au NPs have been recognized as active and effective green catalysts in various organic reactions.[279] Needless to say, gold species other than Au NPs, *i. e.*, gold salts and complexes, also showed excellent activities in a wide range of transformations.[280] The first major discovery of the use of Au NPs in catalysis was the selective oxidation of CO to CO_2, which now can be operated at ambient conditions allowing several practical applications.[281] Following this discovery, several industrial processes were found to be

---

Q.; Wang, Y. *Appl. Catal. A: Mol.* **2008**, *334*, 217. (c) Karimi, B.; Biglari, A.; Clark, J. H.; Budarin, V. *Angew. Chem. Int. Ed.* **2007**, *46*, 7210. (d) Mori, K.; Hara, T.; Mizugaki, T.; Ebitani, K.; Kaneda, K. *J. Am. Chem. Soc.* **2004**, *126*, 10657. (e) Hara, T.; Mori, K.; Oshiba, M.; Mizugaki, T.; Ebitani, K.; Kaneda, K. *Green Chem.* **2004**, *6*, 507. (f) Behr, A.; Eilting, J.; Irawadi, K.; Leschinski, J.; Lindner, F. *Green Chem.* **2008**, *10*, 13. (g) Zhou, C. H.; Beltramini, J. N.; Fan, Y. X.; Lu, G. Q. *Chem. Soc. Rev.* **2008**, *37*, 527. (h) Newton, M. A.; Belver-Coldeira, C.; Martinez-Arias, A.; Fernandez-Garcia, M. *Nat. Mater.* **2007**, *6*, 528. (i) Li, J. J.; Xu, X. Y.; Jiang, Z.; Hao, Z. P.; Hu, C. *Environ. Sci. Technol.* **2005**, *39*, 1319.

[276] (a) Gao, Y.; Chen, C. A.; Gau, H. M.; Bailey, J. A.; Akhadov, E.; Williams, D.; Wang, H. L. *Chem. Mater.* **2008**, *20*, 2839. (b) Makowski, P.; Demir, R. C.; Antonietti, M.; Goettmann, F.; Titirici, M. M. *Chem. Commun.* **2008**, 999. (c) Takasaki, M.; Motoyama, Y.; Higashi, K.; Yoon, S. H.; Mochida, I.; Nagashima, H. *Org. Lett.* **2008**, *10*, 1601.

[277] Neal, L. M.; Hagelin-Weaver, H. E. *J. Mol. Catal. A: Chem.* **2008**, *284*, 141.

[278] (a) Liao, W.; Chen, Y. C.; Wang, J. S.; Yak, H. K.; Wai, C. M. *Ind. Eng. Chem. Res.* **2007**, *46*, 5089. (b) Wang, X.; Liang, M.; Zhang, J.; Wang, Y. *Curr. Org. Chem.* **2007**, *11*, 299. (c) Shekhar, S. C.; Murthy, J. K.; Rao, P. K.; Rao, K. S. R. *Appl. Catal. A: Mol.* **2004**, *271*, 95.

[279] (a) Daniel, M.-C.; Astruc, D. *Chem. Rev.* **2004,** *104*, 293. (b) Stratakis, M.; Garcia, H. *Chem. Rev.* **2012**, *112*, 4469.

[280] Li, Z.; Brouwer, C.; He, C. *Chem. Rev.* **2008,** *108*, 3239.

[281] (a) Haruta, M. *Catal. Today* **1997**, *36*, 153. (b) Min, B. K.; Friend, C. M. *Chem. Rev.* **2007**, *107*, 2709. (c) Coquet, R.; Howard, K. L.; Willock, D. J. *Chem. Soc. Rev.* **2008**, *37*, 2046. (d) Gong, J.; Mullins,

achieved with the Au NPs as catalysts, such as oxidation of methanol to methyl formate,[282] the preparation of raw materials for polymers production,[283] etc.. What's more, Au NPs have also found applications as catalysts in the oxidation of alcohols, hydrocarbons, aldehydes, amines, and the epoxidation of alkenes.[284] Hydrogen peroxide, an industrially valuable reagent, can also be obtained from the reaction between hydrogen and oxygen under catalysis by Au NPs.[285] Apart from the above-mentioned transformations, Au NPs have recently found numerous applications as unique catalysts in novel and unprecedented reactions. The recent achievements with Au NPs as catalysts mainly include the activation of dihydrogen, epoxides, carbonyl compounds, hydrosilanes, boron hydrides, CO_2 fixation, C-C coupling, hydrogen transfer reactions, etc..[279b, 286]

As an interesting example, Au NPs supported on a bifunctional periodic mesoporous organosilica were recently used as catalysts in the Ullmann-type couplings (Scheme 95).[287] This reaction was observed by chance when the etherification reaction between iodobenzene and phenol was attempted; instead of the corresponding ether, biphenyl was obtained, resulting from the homocoupling of iodobenzene. Further investigations have shown that the reaction is applicable to aryl iodides, but the corresponding bromides are highly unreactive.

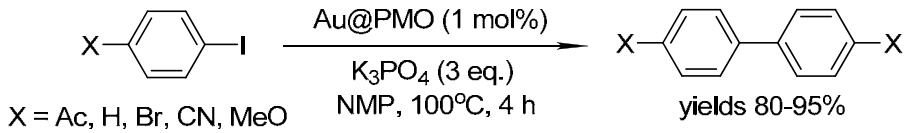

Scheme 95. Ullmann coupling of aryl iodides achieved by Au NPs.

C. B. *Acc. Chem. Res.* **2009**, *42*, 1063. (e) Lopez-Acevedo, O.; Kacprzak, K. A.; Akola, J.; Hakkinen, H. *Nature Chem.* **2010**, *2*, 329. (f) Yoshida, H.; Kuwauchi, Y.; Jinschek, J. R.; Sun, K.; Tanaka, S.;Kohyama, M.; Shimada, S.; Hatuta, M.; Takeda, S. *Science* **2012**, *335*, 317. (g) Christensen, C. H.; Norskov, J. K. *Science* **2010**, *327*, 278. (h) Ishida, T.; Haruta, M. *Angew. Chem. Int. Ed.* **2007**, *46*, 7154.

[282] Wittstock, A.; Zielasek, V.; Biener, J.; Friend, C. M.; Baumer, M. *Science* **2010**, *327*, 319.

[283] Meyer, R.; Shaikhutdinov, S. K.; Freund, H.-J. *Gold Bull.* **2004**, *37*, 72.

[284] (a) Della Pina, C.; Falletta, E.; Prati, L.; Rossi, M. *Chem. Soc. Rev.* **2008**, *37*, 2077. (b) Della Pina, C.; Falletta, E. *Catal. Sci. Technol.* **2011**, *1*, 1564. (c) Tsukuda, T.; Tsunoyama, H.; Sakurai, H. *Chem. Asian J.* **2011**, *6*, 736. (d) Della Pina, C.; Falletta, E.; Rossi, M. *Chem. Soc. Rev.* **2012**, *41*, 350.

[285] (a) Hutchings, G. J. *Chem. Commun.* **2008**, 1148. (b) Edwards, J. K.; Solsona, B.; Ntainjua, N. E.; Carley, A. F.; Herzing, A. A.; Kiely, C. J.; Hutchings, G. J. *Science* **2009**, *323*, 1037.

[286] (a) Hutchings, G. J. *Chem. Commun.* **2008**, 1148. (b) Shan, J.; Tenhu, H. *Chem. Commun.* **2007**, 4580.

[287] Karimi, B.; Esfahani, F. K. *Chem. Commun*. **2011**, *47*, 10452.

1.3.3 Rodium nanoparticles in catalysis

Compared with Pd and Au NPs, catalysis by Rh NPs is relatively less studied. The reported cases have mostly focused on hydrogenations, involving the reduction of nitroarenes, alkenes, arenes, ketones, CO hydrogenation and the reduction of various α,β-unsaturated compounds.[288] Dehalogenation of halogenoarenes, as a special case of hydrogenation, was also achieved under catalysis by Rh NPs.[289]

Hydroformylation is one of the most versatile methods for the synthesis of fine chemicals through the functionalization of C=C bonds. Some articles describe hydroformylation reactions under catalysis by Rh NPs.[290] Interestingly, the Rh NPs can even be stabilized by chiral ligands for asymmetric synthesis.[233c,291] For example, Li and co-workers[291b] prepared chiral diphosphorus ligand stabilized Rh NPs which were further immobilized on silica support (Scheme 96). The catalytic tests on asymmetric hydroformylation of styrene showed that the chirally stabilized Rh NPs indeed lead to an enantioenriched 2-phenylpropanal with 26 ee (Scheme 96).

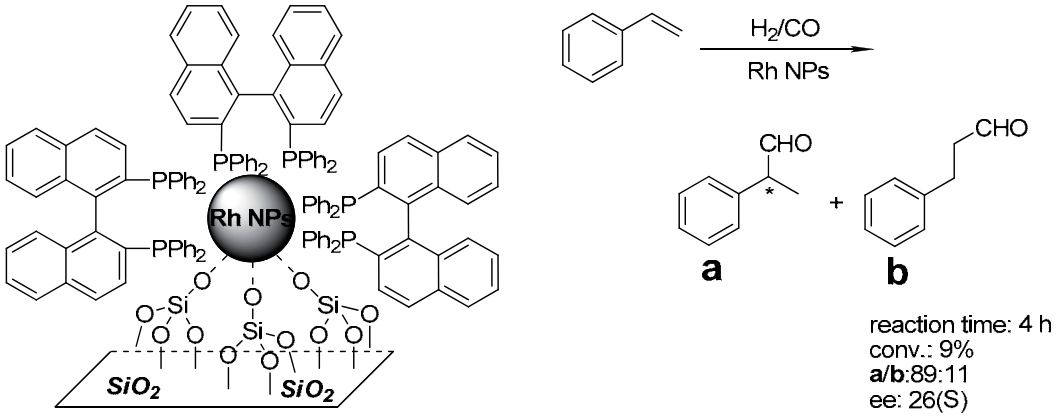

Scheme 96. Silica supported Rh NPs stabilized by chiral diphosphorus ligand.

---

[288] (a) Campelo, J. M.; Garcia, A.; Luna, D.; Marinas, J. M. *J. Catal.* **1988**, *113*, 172. (b) Evangelisti, C.; Panziera, N.; Vitulli, M.; Pertici, P.; Balzano, F.; Uccello-Barretta, G.; Salvadori, P. *Appl. Catal. A: Gen.* **2008**, *339*, 84.(c) J. A. Cabello, J. M. Campelo, A. Garcia, D. Luna, J. M. Marinas, *J. Mol. Catal.* **1993**, *78*, 249. (d) I. S. Park, M. S. Kwon, K. Y. Kang, J. S. Lee, J. Park, *Adv. Synth. Catal.* **2007**, *349*, 2039. (e) M. Ojeda, S. Rojas, M. Boutonnet, F. J. Perez-Alonso, F. J. Garcia-Garcia, J. L. G. Fierro, *Appl. Catal. A: Gen.* **2004**, *274*, 33. (f) T. Hanaoka,H. Arakawa, T. Matsuzaki, Y. Sugi, K. Kanao, Y. Abe, *Catal. Today* **2000**, *58*, 271. (g) Niembro, S.; Donnici, S.; Shafir, A.; Vallribera, A.; Buil, M. L.; Esteruelas, M. A.; Larramona, C. *New J. Chem.* **2013**, *37*, 278. (h) Bile, E. G.; Sassine, R.; Denicourt-Nowicki, A.; Launay, Franck.; Roucoux, A. *Dalton Trans*. **2011**, *40*, 6524. (i) Hubert, C.; Bile, E. G.; Denicourt-Nowicki, A.; Roucoux, A. *Green Chem.* **2011**, *13*, 1766. (j) Dykeman, R. R.; Yan, N.; Scopelliti, R.; Dyson, P. J. *Inorg. Chem.* **2011**, *50*, 717.

[289] Leger, B.; Nowicki, A.; Roucoux, A.; Rolland, J.-P. *J. Mol. Catal. A: Chem.* **2007,** *266*, 221.

[290] (a) Bruss, A. J.; Gelesky, M. A.; Machado, G.; Dupont, J. *J Mol Catal A: Chem*. **2006**, *252*, 212. (b) Giordano, R.; Serp, P.; Kalck , P.; Kihn, Y.; Schrei-ber, J.; Marhic, C. Duvail, J.-L. *Eur. J. Inorg. Chem.* **2003**, *4*, 610.

[291] (a) Axet, M. R.; Castillón, S.; Claver, C.; Philippot, K.; Lecante, P.; Chaudret, B. *Eur. J. Inorg. Chem.* **2008**, 3460. (b) Han, D.; Li, X.; Zhang, H.; Liu, Z.; Hu, G.; Li, C. *J. Mol. Catal. A: Chem*. **2008**, *283*, 15.

More recently, Rh NPs have also been used in C-C bond formation reactions, including Heck, Suzuki, Sonogashira and Stille couplings.[292] Khlobystov and colleagues[293] have recently described that Rh NPs confined in carbon nanotubes can achieve regioselective hydrosilylation of terminal alkynes. To the best of our knowledge, this is the only report of the use of Rh NPs for hydrosilylation reactions of alkynes.

1.3.4 Other metal (Pt, Ag, Ru, Ni, Cu) nanoparticles in catalysis

The Pt, Ag, Ru, Ni and Cu NPs have also shown great promise in a number of catalytic processes. Pt NPs are mainly used in hydrogenations,[294] and electrocatalytic oxidations[295] for fuel cell purposes. In 2014, Suárez, Phillipot, Chaudret and coworkers reported an efficient and selective hydrogenation of nitroaromatics catalyzed by Pt nanoparticles stabilized by NHC-type ligands.[296] Few reports also showed applications of Pt NPs in the oxidation of CO[297], alcohols[298], alkenes[299] and others.[300] It should be noted that Pt NPs are also employed in the hydrosilylation of alkynes, which will be discussed in detail in the fourth chapter of this part. Silver-based compounds have antimicrobial properties, resulting in applications in biological and/or medical domains.[301] In the area of catalysis, Ag NPs have been utilized to achieve selective oxidation of alkanes and alkenes for the preparation of valuable products such as

---

[292] (a) Kantam, M. L.; Roy, Sarabindu.; Roy, Moumita.; Sreedhar, Bojja.; Choudary, B.M.; Dec, R. L. *J. Mol. Catal. A: Chem*. **2007**, *273*, 26. (b) Guha, N. R.; Reddy, C. B.; Aggarwal, N.; Sharma, D.; Shil, A. K.; Bandna.; Das, Pralay. *Adv. Synth. Catal.* **2012**, *354*, 2911. (c) Kanuru, V. K.; Humphrey, S. M.; Kyffin, J. M. W.; Jefferson, D. A.; Burton, J. W.; Armbruster, M.; Lambert, R. M. *Dalton Trans.* **2009**, 7602. (d) Li, L.; Shi, J. *Adv. Synth. Catal*. **2008**, *350*, 667. (e) Trivedi, R.; Roy, S.; Roy, M.; Sreedhar, B.; Kantam, M. L. *New J. Chem.* **2007**, *31*, 1575.

[293] Solomonsz, W. A.; Rance, G. A.; Suyetin, M.; Torre, A. L.; Bichoutskaia, E.; Khlobystov, A. N. *Chem. Eur. J.* **2012**, *18*, 13180.

[294] (a) Savastenko, N.; Volpp, H. R.; Gerlach, O.; Strehlau, W. *J. Nanopart. Res.* **2008**, *10*, 277. (b) Molnar, E.; Tasi, G.; Konya, Z.; Kiricsi, I. *Catal. Lett.* **2005**, *101*, 159. (c) Centomo, P.; Zecca, M.; Lora, S.; Vitulli, G.; Caporusso, A. M.; Tropeano, M. L.; Milone, C.; Galvagno, S.; Corain, B. *J. Catal.* **2005**, *229*, 283. (d) Guo, G.; Qin, F.; Yang, D.; Wang, C.; Xu, H.; Yang, S. *Chem. Mater.* **2008**, *20*, 2291. (e) Rioux, R. M.; Komor, R.; Song, H.; Hoefelmeyer, J. D.; Grass, M.; Niesz, K.; Yang, P.; Somorjai, G. A. *J. Catal.* **2008**, *254*, 1. (f) Serrano-Ruiz, J. C.; Lopez-Cudero, A.; Solla-Gullon, J.; Sepfflveda-Escribano, A.; Aldaz, A.; Rodriguez-Reinoso, F. *J. Catal.* **2008**, *253*, 159. (g) Abu-Reziq, R.; Wang, D.; Post, M.; Alper, H. *Adv. Synth. Catal.* **2007**, *349*, 2145.

[295] (a) Shao-Horn, Y.; Sheng, W. C.; Chen, S.; Ferreira, P. J.; Holby, E. F.; Morgan, D. *Top. Catal.* **2007**, *46*, 285. (b) Ding, J.; Chan, K. Y.; Ren, J.; Xiao, F. S. *Electrochim. Acta* **2005**, *50*, 3131. (c) Chen, W. X.; Lee, J. Y.; Liu, Z. *Chem. Commun.* **2002**, 2588. (d) Kongkanand, A.; Kuwabata, S.; Girishkumar, G.; Kamat, P. *Langmuir* **2006**, *22*, 2392. (e) Zeng, J.; Su, F.; Lee, J. Y.; Zhou, W.; Zhao, X. S. *Carbon* **2006**, *44*, 1713.

[296] Lara, P.; Suárez, A.; Collière, V.; Philippot, K.; Chaudret, B. *ChemCatChem* **2014**, *6*, 87.

[297] Fukuoka, A.; Kimura, J. I.; Oshio, T.; Sakamoto, Y.; Ichikawa, M. *J. Am. Chem. Soc.* **2007**, *129*, 10120

[298] (a) Yamada, Y. M. A.; Arakawa, T.; Hocke, H.; Uozumi, Y. *Angew. Chem. Int. Ed.* **2007**, *46*, 704. (b) G. Maayan, R. Neumann, *Catal. Lett.* **2008**, *123*, 41.

[299] Maayan, G.; Neumann, R. *Chem. Commun.* **2005**, 4595.

[300] Koutsopoulos, S.; Johannessen, T.; Eriksen, K. M.; Fehrmann, R. *J. Catal.* **2006**, *238*, 206.

[301] (a) Sambhy, V.; MacBride, M. M.; Peterson, B. R.; Sen, A. *J. Am. Chem. Soc.* **2006**, *128*, 9798. (b) Kenawy, E. R.; Worley, S. D.; Broughton, R. *Biomacromolecules* **2007**, *8*, 1359.

epoxides and aldehydes.[302] Other applications in catalysis involved dehydrogenation of alcohols[303] and hydrogenation of dyes.[304] Supported Ru NPs were used to reduce nitrogen oxide to nitrogen[305] and to hydrogenate a variety of aromatic compounds, *e.g.*, tetralin, methyl benzoate, [306] 2-methoxycarbonylphenyl-1,2-dioxane [307] or to hydrogenate CO.[308] Ni NPs were often utilized in hydrogenation reactions, including the hydrogenation of aromatic compounds,[309] fatty acid ethyl esters and propargyl alcohols.[310] As early as the late 1970s,[311] Cu NPs were found to be active in catalysis. For example, Cu NPs supported on Al_2O_3 can be used as recyclable catalysts for the preparation of 1,2,3-triazoles by the reaction of terminal alkynes, sodium azide and alkyl/allyl halides.[312] An interesting reaction under catalysis by Cu NPs was disclosed recently, which involves the reaction of water and CO to offer CO_2 and H_2. However, this reaction is limited by the high reaction temperature employed in the procedure.[313]

1.4 Precedents in our research group

In our research group various stabilizers and supports were designed for the preparation of a variety of metal NPs including Pd, Pt, Au, Rh and Ru NPs. Some of

---

[302] Campelo, J. M.; Conesa, T. D.; Gracia, M. J.; Jurado, M. J.; Luque, R.; Marinas, J. M.; Romero, A. A. *Green Chem.* **2008**, *10*, 853.

[303] Mitsodume, T.; Mikami, Y.; Funai, H.; Mizugaki, T.; Jitsukawa, K.; Kaneda, K. *Angew. Chem. Int. Ed.* **2008**, *47*, 138.

[304] (a) Jiang, Z. J.; Liu, C. Y.; Sun, L. W. *J. Phys. Chem. B* **2005**, *109*, 1730. (b) Zhai, H. J.; Sun, D. W.; Wang, H. S. *J. Nanosci. Nanotechnol.* **2006**, *6*, 1968. (c) Bron, M.; Teschner, D.; Knop-Gericke, A.; Steinhauer, B.; Scheybal, A.; Haevecker, M.; Wang, D.; Foedisch, R.; Hoenicke, D.; Wootsch, A.; Schloegl, R.; Claus, P. *J. Catal.* **2005**, *234*, 37.

[305] (a) Shelef, M.; Gandhi, H. S. *Ind. Eng. Chem. Prod. Res. Dev.* **1972**, *11*, 393. (b) Clausen, C.; Good, M. L. *J. Catal.* **1977**, *46*, 58.

[306] Sun, C.; Peltre, M. J.; Briend, M.; Blanchard, J.; Fajerwerg, K.; Krafft, J. M.; Breysse, M.; Cattenot, M.; Lacroix, M. *Appl. Catal. A: Mol.* **2003**, *245*, 245.

[307] Marconi, G.; Pertici, P.; Evangelisti, C.; Caporusso, A. M.; Vitulli, G.; Capannelli, G.; Hoang, M.; Turney, T. W. *J. Organomet. Chem.* **2004**, *689*, 639.

[308] (a) Nijs, H.; Jacobs, P. A.; Uytterhoeven, J. B. *J. Chem. Soc. Chem. Commun.* **1979**, 180. (b) Leith, I. R. *J. Catal.* **1985**, *91*, 283.

[309] (a) Wojcieszak, R.; Zielinski, M.; Monteverdi, S.; Bettahar, M. M. *J. Colloid Interface Sci.* **2006**, *299*, 238. (b) Boudjahem, A. G.; Monteverdi, S.; Mercy, M.; Ghanbaja, D.; Bettahar, M. M. *Catal. Lett.* **2002**, *84*, 115. (c) Boudjahem, A. G.; Monteverdi, S.; Mercy, M.; Bettahar, M. M. *J. Catal.* **2004**, *221*, 325

[310] (a) Bautista, F. M.; Campelo, J. M.; Garcia, A.; Guardeno, R.; Luna, D.; Marinas, J. M. *J. Mol. Catal.* **1991**, *67*, 91. (b) Bautista, F. M.; Campelo, J. M.; Garcia, A.; Guardeno, R.; Luna, D.; Marinas, J. M. *J. Catal.* **1990**, *125*, 171.

[311] (a) Pajonk, G.; Taghavi, M. B.; Teichner, S. J. *Bull. Soc. Chim. Fr.* **1975**, 983. (b) Klvana, D.; Chaouki, J.; Kusohorsky, D.; Chavarie, C.; Pajonk, G. M. *Appl. Catal.* **1988**, *42*, 121.

[312] Kantam, M. L.; Jaya, V. S.; Sreedhar, B.; Raoa, M. M.; Choudary, B. M. *J. Mol. Catal. A: Chem.* **2006**, *256*, 273.

[313] (a) Rodriguez, J. A.; Liu, P.; Hrbek, J.; Perez, M.; Evans, J. *J. Mol. Catal. A: Chem.* **2008**, *281*, 59. (b) Rodriguez, J. A.; Liu, P.; Hrbek, J.; Evans, J.; Perez, M. *Angew. Chem. Int. Ed.* **2007**, *46*, 1329.

these nanopamerials were found active as catalysts in organic transformations, including C-C couplings, hydrosilylation of alkynes, among others.

1.4.1 Metal nanoparticles stabilized by fluorinated compounds and their use in catalysis

In the early 2000, our group entered into the area of metal NPs by chance when attempts to prepare a fluorous version of the palladium complex $Pd(dba)_2$ failed, leading instead to the formation of Pd NPs soluble in fluorinated solvents.[314] Further investigations showed that palladium NPs can also be prepared by reduction of palladium chloride in the presence of a range of compounds bearing long fluorinated carbon chains (Scheme 97) and those materials were proven to be recoverable catalysts under organic-fluorous biphasic conditions in Suzuki and Heck coupling reactions.[314b] Continuing the reseacrh on metal NPs and catalysis in our group, an extension of these preliminary findings was undertaken. Thus, various fluorinated compounds have been developed as stabilizers for the formation of Ru, Pd and Pt NPs and some of the NPs were used as catalysts in Heck, Suzuki and Sonogashira coupling reactions.[315]

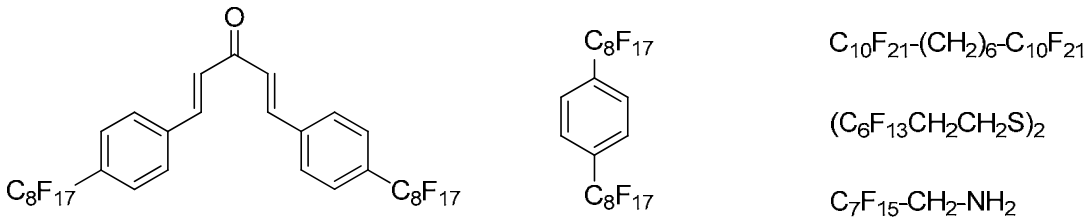

Scheme 97. Some heavily fluorinated stabilizers developed in our group for the preparation of Pd NPs.

---

[314] (a) Moreno-Mañas, M.; Pleixats, R.; Villarroya, S. *Chem. Commun.* **2002**, 60. (b) Moreno-Mañas, M.; Pleixats, R.; Villarroya, S. *Organometallics* **2001**, *20*, 4524. (c) Villarroya, S. *Doctorial thesis*, Universitat Autònoma de Barcelona, **2002**.

[315] (a) Tristany, M. *Doctorial thesis*, Universitat Autònoma de Barcelona, **2005**. (b) Tristany, M.; Courmarcel, J.; Dieudonne, P.; Moreno-Mañas, M.; Pleixats, R.; Rimola, A.; Sodupe, M.: Villarroya, S. *Chem. Mat.* **2006**, *18*, 716. (c) Moreno-Mañas, M.; Pleixats, R.; Tristany, M. *J. Fluorine Chem.* **2005**, *126*, 1435. (d) Tristany, M.; Chaudret, B.; Dieudonne, P.; Guari, Y.; Lecante, P.; Matsura, V.; Moreno-Mañas, M.; Philippot, K.; Pleixats, R. *Adv. Funct. Mat.* **2006**, *16*, 2008. (e) Tristany, M.; Moreno-Mañas, M.; Pleixats, R.; Chaudret, B.; Philippot, K.; Dieudonne, P.; Lecante, P. *J. Mater. Chem.* **2008**, *18*, 660. (f) Tristany, M.; Moreno-Manas, M.; Pleixats, R.; Chaudret, B.; Philippot, K.; Guari, Y.; Matsura, V.; Lecante, P. *New J. Chem.* **2009**, *33*, 1529. (g) Niembro, S. *Doctorial thesis*, Universitat Autònoma de Barcelona, **2010**. (h) Niembro, S.; Vallribera, A.; Moreno-Mañas, M. *New J. Chem*. **2008**, *32*, 94.

1.4.2 Fluorinated metal nanoparticles supported on silica gel and their use in catalysis

With the aim of taking advantages of the properties of silica such as thermal stability and insolubility, our group also prepared silica-supported metal NPs for developing recyclable catalysts.[316] The immobilization of metal NPs on the silica was achieved through two methodologies. One consisted in the preparation of metal NPs in the presence of compounds **a** or **b** (Scheme 98) as stabilizer, followed by treatment of the newly formed nanomaterial with fluorous silica gel (FSG). This methodology proved to be effective for the formation of Au and Pd NPs, and the corresponding materials showed excellent catalytic activities in Heck,[316a] Suzuki, [316e] Sonogashira[316c] couplings (Pd NP) and also active for some substrates in the oxidation of alcohols (Au NP). [316b]

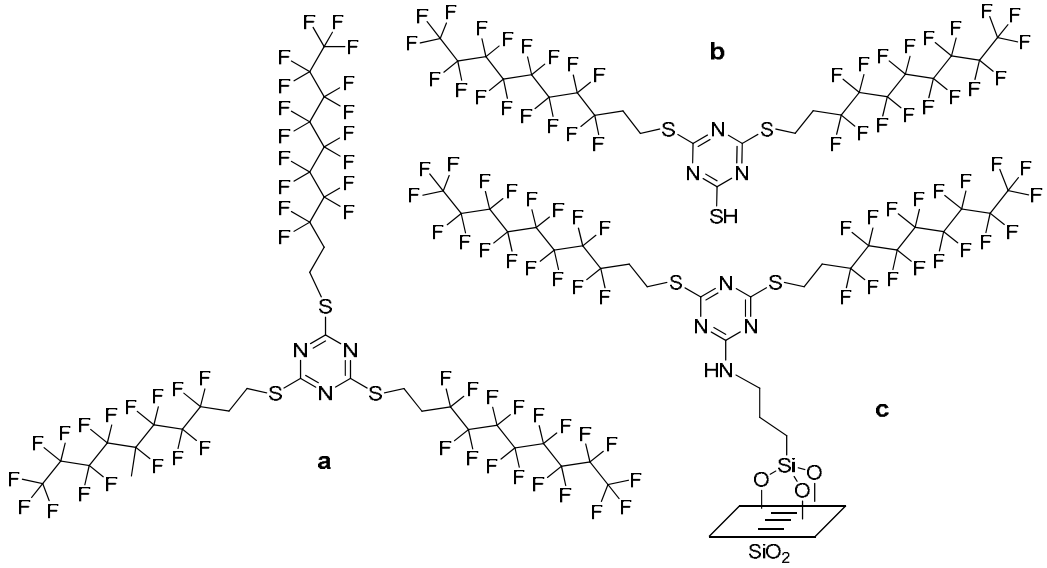

Scheme 98. Previously reported fluorous stabilizers for the formation of metal NPs.

Notably, in some cases, the catalysts could be recycled up to 15 runs without significant loss of activities.[316a] Although FSG supported metal NPs work very well in catalysis, during the reaction the materials suffered some degradation, and the analysis of the supernatant liquid obtained after a catalytic run confirmed the leaching of both metal NPs and small amounts of the fluorous stabilizer.[316a] Thus, the effort was

---

[316] (a) Bernini, R.; Cacchi, S.; Fabrizi, G.; Forte, G.; Niembro, S.; Petrucci, F.; Pleixats, R.; Prastaro, A.; Sebastián, R. M.; Soler, R.; Tristany, M.; Vallribera, A. *Org. Lett*. **2008**, *10*, 561. (b) Bernini, R.; Cacchi, S.; Fabrizi, G.; Niembro, S.; Prastaro, A.; Shafir, A.; Vallribera, A. *ChemSusChem* **2009**, *2*, 1036. (c) Bernini, R.; Cacchi, S.; Fabrizi, G.; Forte, G.; Petrucci, F.; Prastaro, A.; Niembro, S.; Shafir, A.; Vallribera, A. *Org. Biomol. Chem.* **2009**, *7*, 2270. (d) Niembro, S.; Shafir, A.; Vallribera, A.; Alibés, R. *Org. Lett*. **2008**, *10*, 3215. (e) Bernini, R.; Cacchi, S.; Fabrizi, G.; Forte, G.; Petrucci, F.; Prastaro, A.; Niembro, S.; Shafir, A.; Vallribera, A. *Green Chem.* **2010**, *12*, 150.

directed to the synthesis of organic-inorganic hybrid silica **c** (Scheme 98) in which the fluorinated stabilizer is linked covalently to the silica gel matrix.[315g, 316c-e] Indeed, this second approach leads, in some cases,[316c-e] to materials with better catalytic results in terms of recovery and reuse, when compared with the FSG supported metal NPs.

1.4.3 Metal nanoparticles stabilized with tris-imidazolium salts and their use in catalysis

The previous research experience in our group [317] on tris-imidazolium salts encouraged us to investigate their application as stabilizers in the preparation of metal NPs for catalytic purposes.[318] Thus, recently our group reported tris-imidazolium salts stabilized Pd NPs **c-Pd** (iodide salt) and **d-Pd** (tetrafluoroborate salt) depicted in Scheme 99, as catalysts for the Suzuki cross-coupling reaction.[319] Both nanomaterials were prepared in an efficient manner via the hydrogenation of $Pd(dba)_2$ at 3 atm H_2 at room temperature. The tris-iodide **c-Pd** proved to be very effective for the Suzuki coupling, producing a catalytic system tolerant of a wide range of functional groups. After some control tests, it was suggested that the catalytic activity may have a close relationship with the Pd-NHC species formed from the interaction of palladium nanoparticle surface with the imidazolium moiety. Interestingly, further investigation showed that the Pd NPs **d-Pd** are catalytically active in the hydrosilylation of internal alkynes, although this catalytic process was very sensitive to the presence of water.[320]

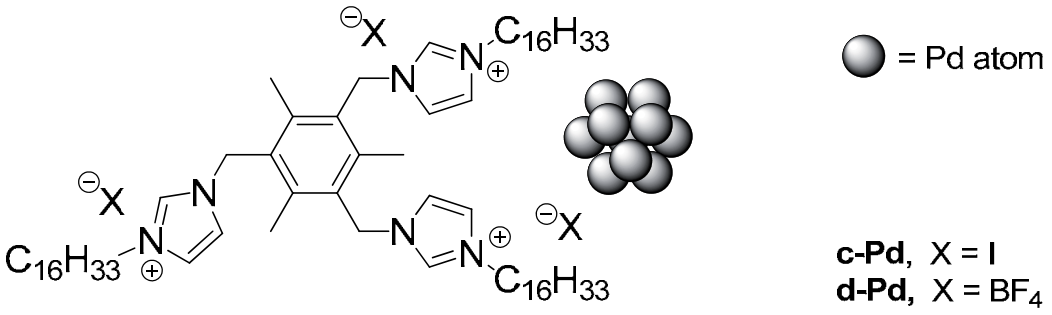

Scheme 99. Palladium NPs stabilized by tris-imidazolium salt **c-Pd** (iodide) and **d-Pd** (tetrafluororate).

---

[317] (a) Trilla, M. *Doctorial thesis*, Universitat Autònoma de Barcelona, **2008**. (b) Trilla, M.; Pleixats, R.; Parella, T.; Blanc, C.; Dieudonné, P.; Guari, Y.; Wong Chi Man, M. *Langmuir* **2008,** *24*, 259. (c) Trilla, M.; Cattoen, X.; Blanc, Ch.; Wong Chi Man, M.; Pleixats, R. *J. Mater. Chem.* **2011**, *21*, 1058.

[318] Planellas, M. *Doctorial thesis*, Universitat Autònoma de Barcelona, **2012**.

[319] Planellas, M.; Pleixats, R.; Shafir, A. *Adv. Synth. Catal.* **2012**, *354*, 651.

[320] Planellas, M.; **Guo, W.**; Alonso, F.; Yus, M.; Shafir, A.; Pleixats, R.; Parella, T. *Adv. Synth. Catal.* **2014**, *356*, 179.

1.4.4 Metal nanoparticles stabilized with PEG-tagged compounds and their use in catalysis

The nature of the stabilizing shell controls the solubility of the nanoclusters in organic, fluorous or aqueous media. With the increasing need of environmental protection, efforts have been made in the chemical communities to perform organic reactions in water, which is an environmentally benign medium of low cost and no toxicity.[321] However, most of the reported catalysts, *e. g.*, organocatalysts, supported metal NPs and hybrid silica-based catalysts, are not water soluble, which greatly decreases the opportunities of the substrate to contact the catalyst in water, and therefore this might result in long reaction time or low activity of the catalyst. In the area of catalysis by metal NPs, these problems can be solved by developing water-soluble metal NPs.

The water-soluble polymers and oligomers based on polyethylene glycol are well known (polyethylene glycols of different molecular weights are available), inexpensive, nontoxic, and nonvolatile, which make them perfect building blocks of stabilizers for the formation of water-soluble nanocatalysts. Thus, various organic entities functionalized with PEG chains have been developed as stabilizers for the syntheses of water-soluble metal NPs.[322] These kinds of PEG-tagged stabilizers lead to water-soluble but diethyl ether-insoluble nanomaterials. By taking advantage of these solubility properties, the final reaction products from the catalytic reaction can be extracted with diethyl ether, leaving the nanocatalyst-containing aqueous phase available for the next run.

Our group previously reported[323]15-membered triolefinic azamacrocycles (Scheme 100a) and star-shaped triazolic compounds (Scheme 100b), both bearing PEG chains, as stabilizers for the preparation of water-soluble metal NPs. Indeed, the Pd NPs developed in this way proved to work efficiently as recyclable catalysts in aqueous conditions in C-C bond formation reactions.[323c, 323e] However, attempts to prepare other

---

[321] (a) Layek, K., Kantam, M. L.; Shirai, M.; Nishio-Hamane, D.; Sasaki T.; Maheswaran, H. *Green Chem*. **2012**, *14*, 3164. (b) Han, J.; Guo, R. *Adv. Funct. Mater*. **2009**, *19*, 1112.

[322] Jadzinsky, P. D.; Calero, G.; Ackerson, C. J.; Bushnell, D. A.; Kornberg, R. D. *Science* **2007**, *318*, 430. (b) Pengo, P.; Polizzi, S.; Battagliarin, M.; Pasquato, L.; Scrimin, P. *J. Mater. Chem*. **2003**, *13*, 2471. (c) Foos, E. F.; Snow, A. W.; Twigg, M. E.; Ancona, M. G. *Chem. Mater*. **2002**, *14*, 2401. (d) Feng, B.; Hou, Z.; Yang, H.; Wang, X.; Hu, Y.; Li, H.; Qiao, Y.; Zhao, X.; Huang, Q. *Langmuir* **2010**, *26*, 2505. (e) Sawoo, S.; Srimani, D.; Dutta, P.; Lahiri, R.; Sarkar, A. *Tetrahedron* **2009**, *65*, 4367.

[323] (a) Serra-Muns, A. *Doctorial thesis*, Universitat Autònoma de Barcelona, **2008**. (b) Serra-Muns, A.; Soler, R.; Badetti, E.; de Mendoza, P.; Moreno-Mañas.; Pleixats, R.; Sebastián, R. M.; Vallribera, A. *New J. Chem.* **2006**, *30*, 1584. (c) Mejías, N. *Doctorial thesis*, Universitat Autònoma de Barcelona, **2011**. (d) Mejías, N.; Serra-Muns, A.; Pleixats, R.; Shafir, A.; Tristany, M. *Dalton Trans.* **2009**, 7748. (e) Mejías, N.; Pleixats, R.; Shafir, A.; Medio-Simón, M.; Asensio, G. *Eur. J. Org. Chem.* **2010**, 5090.

metal NPs, including Pt, Ru, Rh, and Au NPs, were less successful with low yields obtained with respect to the metal sources.[323c-d] Interestingly, some authors have shown that the incorporation of amino coordinating groups may improve the stabilizing ability for the formation of metal NPs.[324] Pursuing with our interest to find excellent stabilizers for the formation of water-soluble metal NPs-based catalysts, we initiated this project as outlined in the next objectives section.

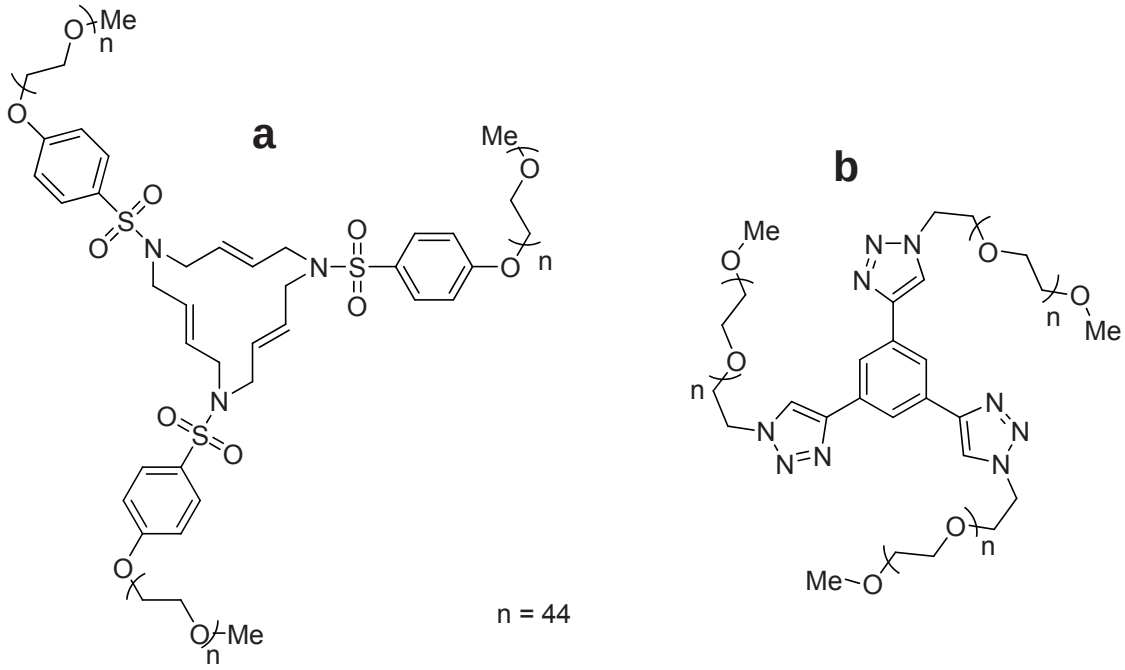

Scheme 100. PEG-tagged stabilizers developed by our group.

[324] (a) Deki, S.; Sayo, K.; Fujita, T.; Yamada, A.; Hayashi, S. *J. Mater. Chem.* **1999**, *9*, 943. (b) Iwamoto, M.; Kuroda, K.; Zaporojtch-enko, V.; Hayashi, S.; Faupel, F. *Eur. Phys. J. D* **2003**, *24*, 365.

CHAPTER 2

Objectives

Chapter 2. Objectives

A nitrogen-rich stabilizer **30** (Scheme 101) was designed to prepare water-soluble metal NPs (Rh, Au and Pd), whose catalytic activities in different organic transformations in aqueous media would be investigated. Thus, we planned the following aims for the part II of the thesis:

a) Preparation of the newly designed stabilizer **30** following the methodology previously developed by Dr. Nereida Mejias Ruiz for a related compound. The synthesis would involve an efficient click reaction via a threefold [2+3] copper-catalyzed azide-alkyne cycloaddition (Scheme 101).

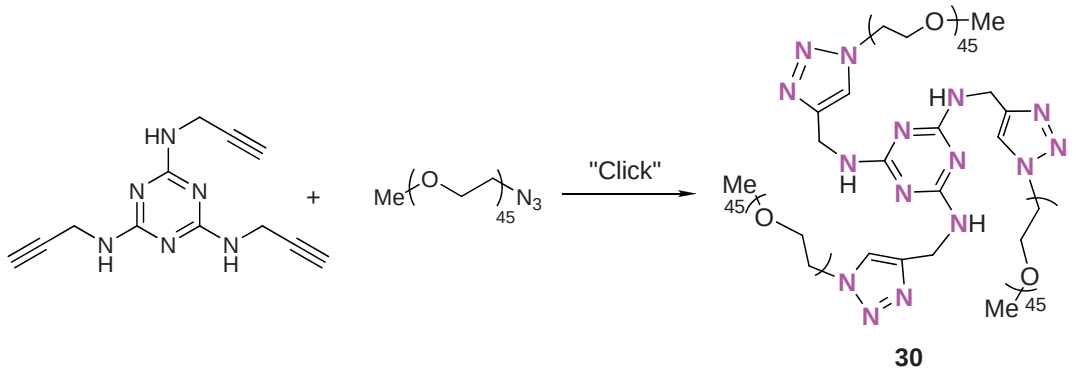

30

Scheme 101. Proposal for the preparation of PEG-tagged stabilizer **30**.

b) Development of efficient protocols for the preparation of metal NPs (Rh, Au, Pd) in the presence of the stabilizer **30**.

c) Investigation of the Rh NPs as recyclable catalysts in the hydrosilylation of alkynes; Au NPs as recyclable catalysts in oxidation reactions and in the reduction of nitroarenes in aqueous conditions; Pd NPs as recyclable catalysts in C-C coupling reactions.

Part II. Water-soluble metal nanoparticles (Rh, Au) in catalysis

CHAPTER 3

Preparation and characterization of metal nanoparticles (Rh, Au) stabilized by a nitrogen-rich polyoxyethylenated substrate

Chapter 3. Preparation and characterization of metal nanoparticles (Rh, Au) stabilized by a nitrogen-rich polyoxyethylenated substrate

3.1 Introduction of click chemistry

3.1.1 Overview of click chemistry

The concept of "click chemistry" was introduced by Sharpless[325] to describe a category of powerful, highly reliable, and selective reactions for the fast preparation of useful new products. As a special case, the Huisgen 1, 3-dipolar cycloaddition reaction of organic azides and alkynes has gained considerable attention due to the introduction in 2001 of Cu(I) catalysis by Tornøe and Meldal (Scheme 102),[326] resulting in a major improvement in both rate and regioselectivity of the reaction, as noticed by Meldal's and Sharpless's laboratories.[327]

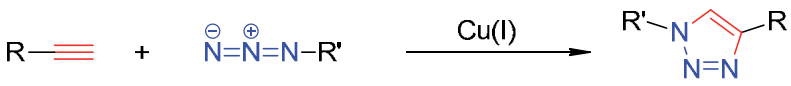

Scheme 102. Cu-catalyzed Azide-Alkyne Cycloaddition (CuAAC).

Nowadays the Cu-catalyzed Azide-Alkyne Cycloaddition (CuAAC) reactions have found significant applications in various areas such as materials, biology, medicine, etc..[328] The great success of CuAAC reaction lies in the fact that it is a quantitative, robust, highly selective and *in vivo* applicable process.[329] For chemists, the most common procedures to perform this reaction involve the use of aqueous conditions, the copper(I) species being formed from $CuSO_4$ and a reducing agent, *e. g.*, sodium

---

[325] Kolb, H. C.; Finn, M. G.; Sharpless, K. B. *Angew. Chem. Int. Ed.* **2001**, *40*, 2004.

[326] Tornøe, C.W.; Meldal, M. Peptidotriazoles: Copper(I)-catalyzed 1,3-dipolar cycloadditions on solid-phase, Peptides 2001, Proc. Am. Pept. Symp.; American Peptide Society and Kluwer Academic Publishers: San Diego, **2001**; pp 263-264.

[327] (a) Tornøe, C. W.; Christensen, C.; Meldal, M. *J. Org. Chem.* **2002**, *67*, 3057. (b) Rostovtsev, V. V.; Green, L. G.; Fokin, V. V.; Sharpless, B. K. *Angew. Chem. Int. Ed.* **2002**, *41*, 2596.

[328] See the following recent reviews and the references therein: (a) Meldal, M.; Tornøe, C. W. *Chem. Rev.* **2008**, *108*, 2952. (b) Hanni, K. D.; Leigh, D. A. *Chem. Soc. Rev.* **2010**, *39*, 1240. (c) Hoyle, C. E.; Lowe, A. B.; Bowman, C. N. *Chem. Soc. Rev.* **2010**, *39*, 1325. (d) Hua, Y.; Flood, A. H. *Chem. Soc. Rev.* **2010**, *39*, 1262.

[329] Speers, A. E.; Adam, G. C.; Cravatt, B. F. *J. Am. Chem. Soc.* **2003**, *125*, 4686. (b) Beatty, K. E.; Xie, F.; Wang, Q.; Tirrell, D. A. *J. Am. Chem. Soc.* **2005**, *127*, 14150. (c) Deiters, A.; Schultz, P. G. *Bioorg. Med. Chem. Lett.* **2005**, *15*, 1521.

ascorbate.[330] With the use of microwave heating, the reaction times were remarkably shortened to minutes with improved yields and enhanced product purities in contrast to the conventional heating methods.[331] Needless to say, a variety of non-classical methodologies were recently developed.[332] A great number of publications show that the CuBr catalyst is preferred in polymer-relevant click chemistry.[333] It is worth mentioning that copper-free conditions involving highly strained alkynes have also been pursued for applications *in vivo*.[334]

3.1.2 Mechanistic aspects of CuAAC reaction

The role of copper in the catalysis has been the subject of many disputes and revisions since the discovery of this powerful cycloaddition. An earlier proposal[335] of the mechanism based on the DFT calculations stated that the catalysis is mediated by a single copper atom in the +1 oxidation state (Scheme 103). These calculations assumed the existence of a terminal Cu-alkyne species in the transition state. Thus, the copper would first coordinated to the acetylene π-electrons, followed by an

---

330 (a) Some examples: Bakbak, S.; Leech, P. J.; Carson, B. E.; Saxena, S.; King, W. P.; Bunz, U. H. F. *Macromolecules* **2006**, *39*, 6793. (b) Helms, B.; Mynar, J. L.; Hawker, C. J.; Fre´chet, J. M. J. *J. Am. Chem. Soc.* **2004**, *126*, 15020. (c) Lee, J. W.; Kim, B. K.; Kim, H. J.; Han, S. C.; Shin, W. S.; Jin, S. H. *Macromolecules* **2006**, *39*, 2418. (d) Ornelas, C.; Ruiz Aranzaes, J.; Cloutet, E.; Alves, S.; Astruc, D. *Angew. Chem., Int. Ed.* **2007**, *46*, 872. (e) Lee, J. W.; Kim, J. H.; Kim, B. K.; Kim, J. H.; Shin, W. S.; Jin, S. H. *Tetrahedron* **2006**, *62*, 9193. (f) Ryu, E. H.; Zhao, Y. *Org. Lett.* **2005**, *7*, 1035. (g) Gou, Z.; Lei, A.; Zhang, Y.; Xu, Q.; Xue, X.; Zhang, F.; Liang, X. *Chem. Commun.* **2007**, 2491.

331 (a) Guezguez, R.; Bougrin, K.; El Akri, K.; Benhida, R. *Tetrahedron Lett.* **2006**, *47*, 4807. (b) Moitra, N.; Moreau, J. J. E.; Cattoën, X.; Wong Chi Man, M. *Chem. Commun.* **2010,** *46*, 8416. (c) Kappe, C. O. *Chem. Soc. Rev.* **2008**, *37*, 1127. (d) Caddick, S.; Fitzmaurice, R. *Tetrahedron* **2009**, *65*, 3325. (e) Appukkuttan, P.; Van der Eycken, E. *Eur. J. Org. Chem.* **2008**, 1133.

332 Kappe, C. O.; Van der Eycken, E. *Chem. Soc. Rev.* **2010**, *39*, 1280.

333 (a) Sieczkowska, B.; Millaruelo, M.; Messerschmidt, M.; Voit, B. *Macromolecules* **2007**, *40*, 2361. (b) Malkoch, M.; Thibault, R. J.; Drockenmuller, E.; Messerschmidt, M.; Voit, B.; Russell, T. P.; Hawker, C. J. *J. Am. Chem. Soc.* **2005**, *127*, 14942. (c) Binder, W. H.; Kluger, C. *Macromolecules* **2004**, *37*, 9321. (d) Bock, V. D.; Speijer, D.; Hiemstra, H.; Van Maarseveen, J. H. *Org. Biomol. Chem.* **2007**, *5*, 971. (e) Malkoch, M.; Schleicher, K.; Drockenmuller, E.; Hawker, C. J.; Russell, T. P.; Wu, P.; Fokin, V. V. *Macromolecules* **2005**, *38*, 3663. (f) Bock, V. D.; Perciaccante, R.; Jansen, T. P.; Hiemstra, H.; Van Maarseveen, J. H. *Org. Lett.* **2006**, *8*, 919. (g) Zhang, X.; Hsung, R. P.; Li, H. *Chem. Commun.* **2007**, 2420. (h) Marmuse, L.; Nepogodiev, S. A.; Field, R. A. *Org. Biomol. Chem.* **2005**, *3*, 2225. (i) Ladmiral, V.; Mantovani, G.; Clarkson, G. J.; Cauet, S.; Irwin, J. L.; Haddleton, D. M. *J. Am. Chem. Soc.* **2006**, *128*, 4823. (j) Cavalli, S.; Tipton, A. R.; Overhand, M.; Kros, A. *Chem. Commun.* **2006**, 3193. (k) Altintas, O.; Yankul, B.; Hizal, G.; Tunca, U. *J. Polym. Sci.* **2006**, *44*, 6458. (l) Zeng, Q.; Li, T.; Cash, B.; Li, S.; Xie, F.; Wang, Q. *Chem. Commun.* **2007**, 1453. (m) Zhang, X.; Li, H.; You, L.; Tang, Y.; Hsung, R. P. *Adv. Synth. Catal.* **2006**, *348*, 2437. (n) Vogt, A. P.; Sumerlin, B. S. *Macromolecules* **2006**, *39*, 5286. (o) Lutz, J. F.; Borner, H. G.; Weichenhan, K. *Macromolecules* **2006**, *39*, 6376. (p) Gao, H.; Louche, G.; Sumerlin, B. S.; Jahed, N.; Golas, P.; Matyjaszewski, K. *Macromolecules* **2005**, *38*, 8979. (q) Sumerlin, B. S.; Tsarevsky, N. V.; Louche, G.; Lee, R. Y.; Matyjaszewski, K. *Macromolecules* **2005**, *38*, 7540. (r) Hasegawa, T.; Umeda, M.; Numata, M.; Fujisawa, T.; Haraguchi, S.; Sakurai, K.; Shinkai, S. *Chem. Lett.* **2006**, *35*, 82. (s) Gao, H.; Matyjaszewski, K. *Macromolecules* **2006**, *39*, 4960.

334 Jewett, J. C.; Bertozzi, C. R. *Chem. Soc. Rev.* **2010**, *39*, 1272.

335 Himo, F.; Lovell, T.; Hilgraf, R.; Rostovtsev, V. V.; Noodleman, L.; Sharpless, K. B.; Fokin, V. V. *J. Am. Chem. Soc.* **2005**, *127*, 210.

exothermal process to give a Cu^{+}-acetylide complex. The Cu acetylide coordination to the azide is followed by rearrangement of the complex into a 6-membered metallocycle and subsequently into the copper-metallated triazole. Upon protonation or reaction with other electrophiles, the Cu-triazole complex finally releases the target triazole with the regeneration of copper catalyst.

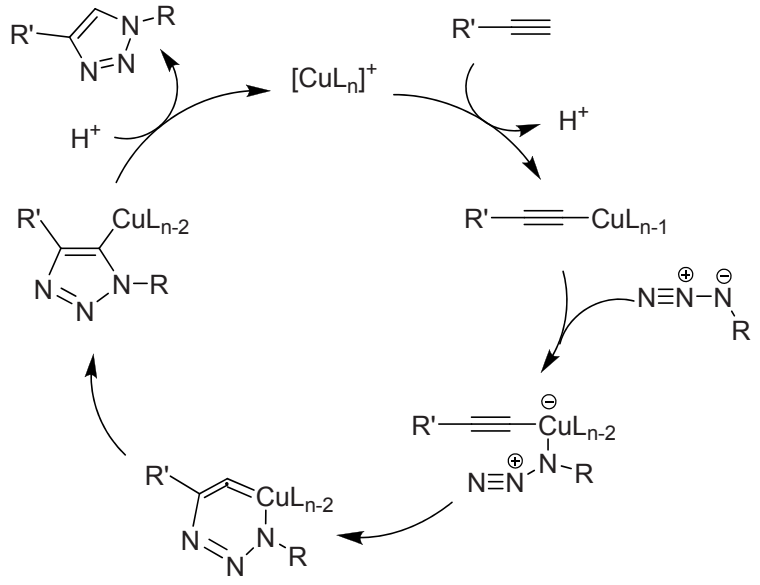

Scheme 103. Schematic showing the evolution of copper catalyst in the CuAAC.

Although this proposal was informative, new evidences suggested that more than one copper atom were more likely involved in the transition state of the reaction.[336] Thus, a revised mechanism was proposed as depicted in Scheme 104.[328a, 337] Here, after formation of the Cu^{+}-acetylide complex **b** from the intermediate π-complex **a**, the azide can coordinate to Cu(I) either *via* the carbon-linked nitrogen atom, offering intermediate **c** or through an "end-on" coordination to yield a novel *gem*-dicuprate intermediate **d**. Further steps in the cycloaddition processes provided intermediate **e** or **f**, respectively. Ring contraction of **e** and **f** produced the metallated triazole **g** which later reacts with electrophiles to release the product **h** with the regeneration of copper catalyst. This mechanistic pathway is regioselective and gives rise to the 1, 4-disubstituted triazole ring.

---

[336] (a) Bock, V. D.; Hiemstra, H.; Van Maarseveen, J. H. *Eur. J. Org. Chem.* **2006**, 51. (b) Rodionov, V. O.; Fokin, V. V.; Finn, M. G. *Angew. Chem. Int. Ed.* **2005**, *44*, 2210. (c) Straub, B. F. *Chem. Commun.* **2007**, 3868.

[337] (a) Bock, V. D.; Hiemstra, H.; Van Maarseveen, J. H. *Eur. J. Org. Chem.* **2006**, 51. (b) Rodionov, V. O.; Fokin, V. V.; Finn, M. G. *Angew. Chem. Int. Ed.* **2005**, *44*, 2210. (c) Straub, B. F. *Chem. Commun.* **2007**, 3868.

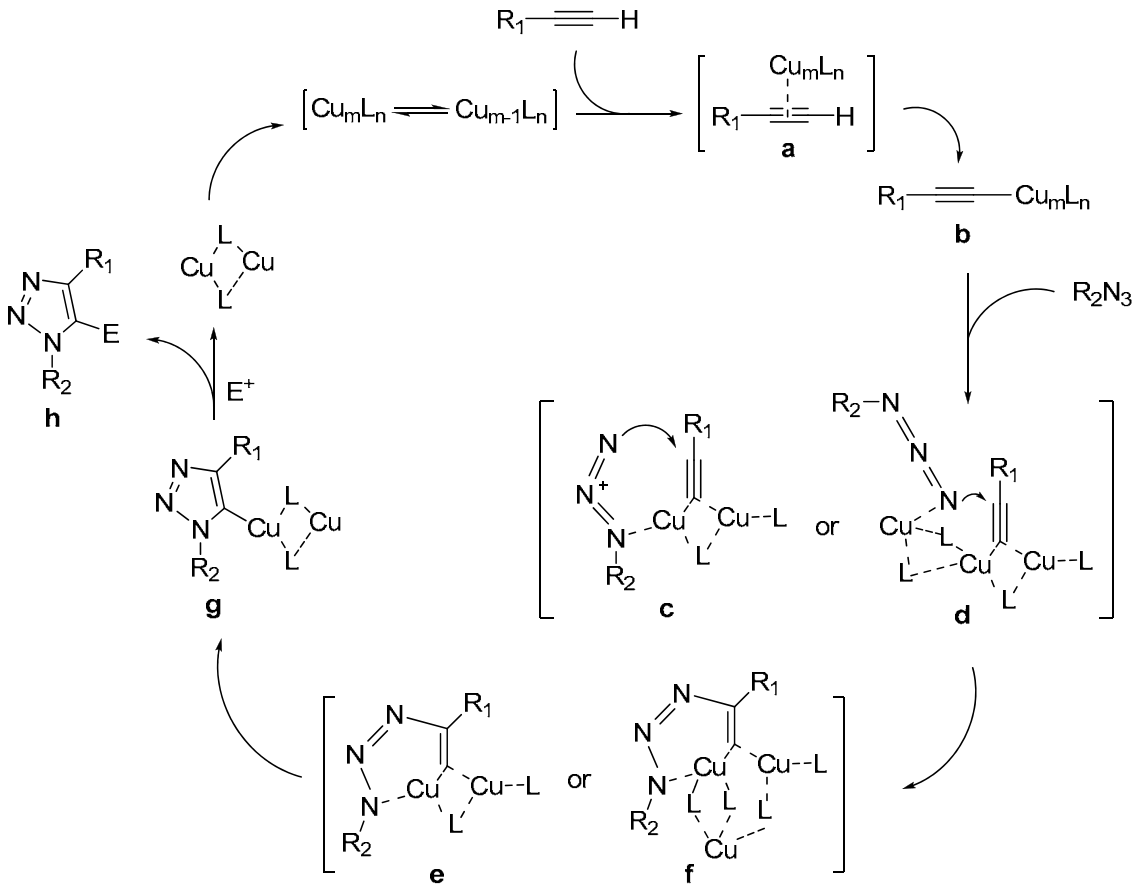

Scheme 104. Revised proposal showing the evolution of copper catalyst in the CuAAC.

3.2 Preparation of the PEG-tagged stabilizer 30 via CuAAC reaction

Dr. Nereida Mejias Ruiz, a former member of our research group, previously prepared a star-shaped triazolic compound bearing PEG chains as stabilizers for the preparation of water-soluble Pd NPs via a threefold [2+3] CuAAC reaction (Scheme 105).[323e] In this process, the alkyne partner 1,3,5-triethynylbenzene **a** (Scheme 105) was obtained in two steps from 1,3,5-tribromobenzene through 1,3,5-tris(trimethylsilylethynyl)benzene;[338] the azide **b** (Scheme 105) was prepared in two steps form a commercially available MeO-PEG-OH (average MW = 2000); the threefold copper-catalyzed 1,3-dipolar cycloaddition between the alkyne **a** (Scheme 105) and the azide **b** (Scheme 105) were performed under the standard click conditions.[339]

---

[338] (a) Uhl, W.; Bock, H. R.; Breher, F.; Claesener, M.; Haddadpour, S.; Jasper, B.; Hepp, A. *Organometallics* **2007**, *26*, 2363. (b) Weber, E.; Hecker, M.; Koepp, E.; Orlia, W.; Czugler, M.; Csöregh, I. *J. Chem. Soc. Perkin Trans. 2* **1988**, 1251. (c) Gaab, K. M.; Thompson, A. L.; Xu, J.; Martínez, T. J.; Bardeen, C. J. *J. Am. Chem. Soc.* **2003**, *125*, 9288. (d) Wright, A. T.; Zhong, Z.; Anslyn, E. V. *Angew. Chem. Int. Ed.* **2005**, *44*, 5679.

[339] (a) Rostovtsev, V. V.; Green, L. G.; Fokin, V. V.; Sharpless, K. B. *Angew. Chem. Int. Ed.* **2002**, *41*, 2596. (b) Devic, T.; David, O.; Valls, M.; Marrot, J.; Couty, F.; Férey, G. *J. Am. Chem. Soc.* **2007**, *129*, 12614.

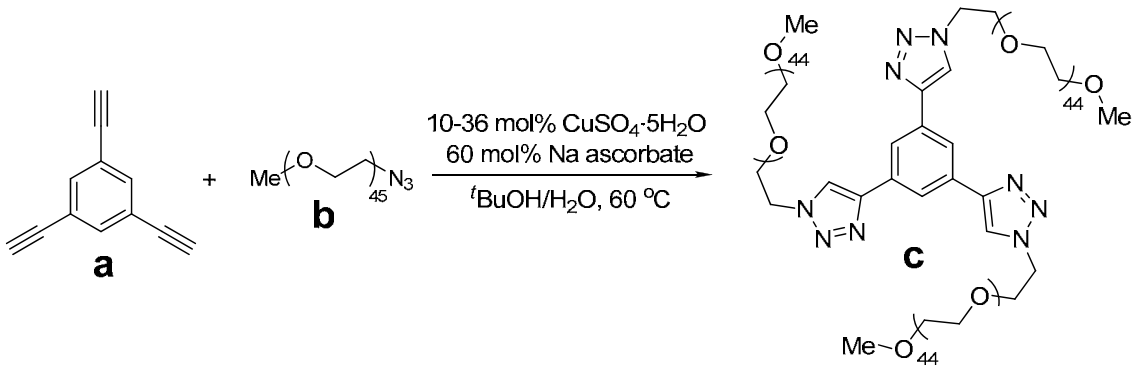

Scheme 105. Preparation of a star-shaped triazolic stabilizers via a CuAAC reaction.

Following the methodology developed by Dr. Nereida Mejias Ruiz,[323e] a commercially available MeO-PEG-OH (average MW = 2000) was treated with methanesulfonyl chloride in the presence of triethylamine to give the corresponding mesylate **31** in 94% yield (Scheme 106, see experimental section for details). The product was then allowed to react with sodium azide in dimethylformamide at 60°C overnight affording the corresponding azide **32** in quantitative yield (Scheme 106, see experimental section for details).

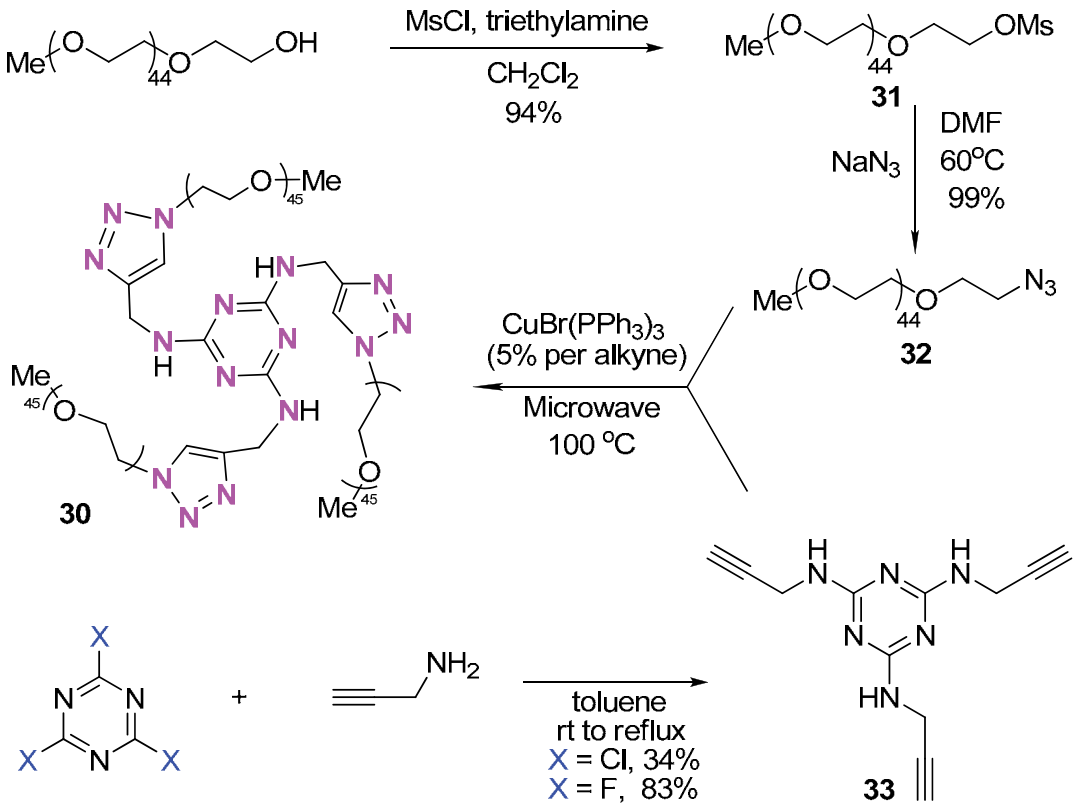

Scheme 106. Synthesis of the polyoxyethylenated substrate **30**.

The second coupling partner, 2,4,6-tris(propargylamino)-1,3,5-triazine **33** could be easily obtained in one step from the reaction of propargylamine with either cyanuric chloride or cyanuric fluoride in 43% and 83% yields, respectively (Scheme 106).[340] It should be noted that extreme caution should be taken when using the cyanuric fluoride due to its strongly unpleasant smell.

Once the trialkyne **33** and the azide **32** were prepared, we were in a position to test the target threefold copper-catalyzed 1,3-dipolar cycloaddition for the formation of the desired stabilizer **30**. We first applied the protocol used previously in our group for stabilizer **c** in Scheme 105,[323e] but it was found that, under that conditions, it is hard to get all the three alkyne branches in **33** reacted with the azide **32** resulting in materials bearing just one or two PEG chains. Further attempts involving the increase of temperature, sodium ascorbate and copper amount showed ineffectiveness. Then we found that the coupling under microwave conditions proposed by Xavier Cattoën and coworkers[331b] works well in a short reaction time. Thus, a mixture of trialkyne **33** and azide **32** (a precise molar ratio of 1 : 3) was dissolved in a mixture of THF and triethylamine (volume ratio of 1 : 1) and heated under the microwave irradiation at 100°C for 15 min in the presence of $CuBr(PPh_3)_3$ as a catalyst (Scheme 106). The reaction progress was monitored by IR analysis, with the disappearance of the absorption of the azide group ($-N_3$) at around 2099 cm^{-1} signaling the completion of the reaction.

The final product was characterized by NMR, IR and MALDI-TOF. As an example, the ^{1}H-NMR spectra of the stabilizer **30**, the mesylate **31** and azide **32** are given in a stacked mode in Figure 24. Apart from the signals corresponding to CH_2CH_2O units, the mesylate **31** showed an obvious methyl signal derived from OMs group at 3.08 ppm, which was absent in the azide **32**, and the stabilizer **30** exhibited the unique singlet of triazole at 7.72 ppm, as well as a broad band from the amino group at 4.64 ppm. Further evidence is provided by the IR spectra (Figure 25). Thus, the characteristic stretching vibration of N_3 group can be observed at 2099 cm^{-1} in the azide **32,** but is absent in the other compounds. Two weak peaks at 1571 and 1519 cm^{-1} confirmed the bending vibration of the amino functionality in stabilizer **30**, although the corresponding stretching band located around 3200-3500 cm^{-1} is weak and broad. The MALDI-TOF spectrum of compound **30** (Figure 26), showed a range of mass distributions (*m/z*) for

---

[340] M. Jarman, H. M. Coley, I. R. Judson, T. J. Thornton, D. E. V. Wilman, G. Abel.; C. J. Rutty, *J. Med. Chem.* **1993**, *36*, 4195.

$[M+H]^+$ separated by 44 D (CH_2CH_2O unit) and centered at 6161 (131 CH_2CH_2O units + the nitrogen-rich core with a mass of 366).

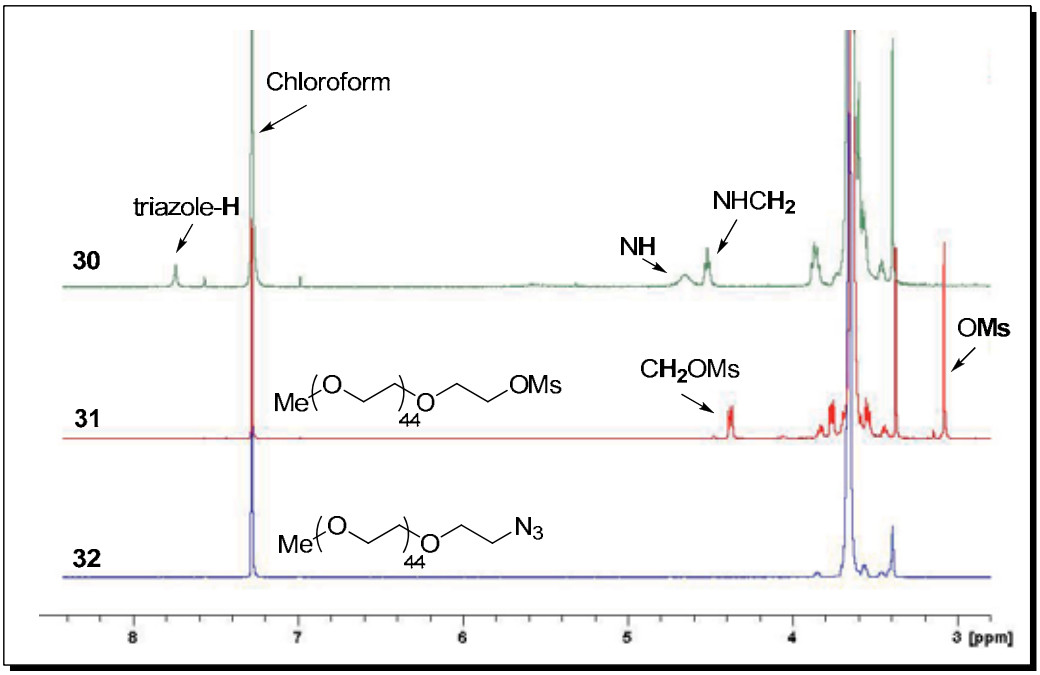

Figure 24. NMR spectra of compounds **30**, **31** and **32**.

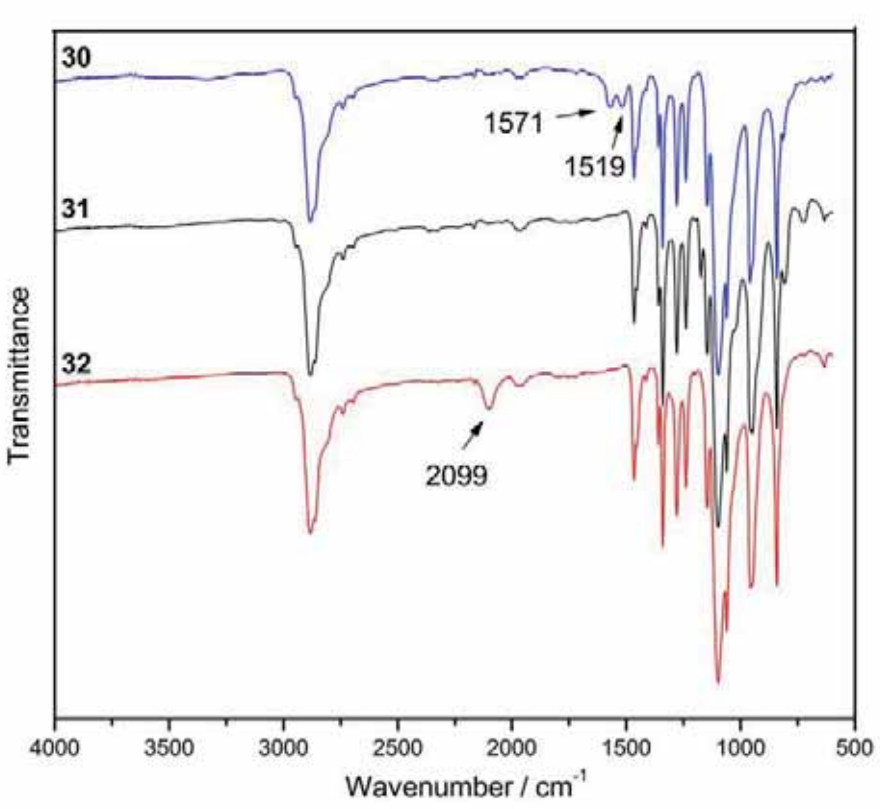

Figure 25. IR spectra of the stabilizer **30**, mesylate **31** and azide **32**.

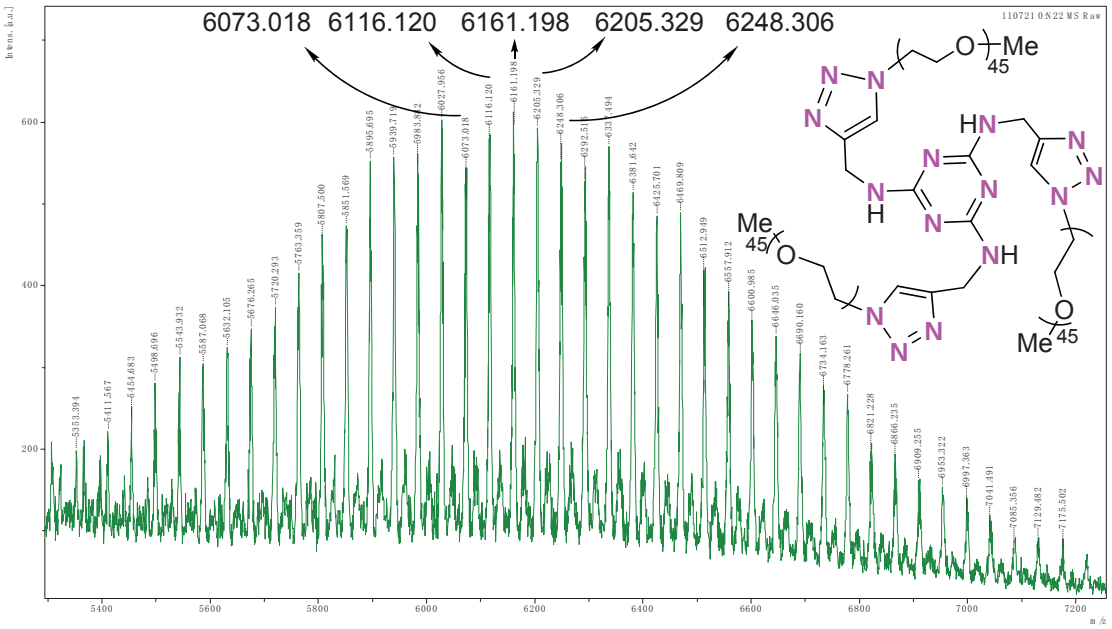

Figure 26. MALDI-TOF spectrum of the stabilizer **30**.

3.3 Preparation and characterization of rhodium nanoparticles

In the presence of the stabilizer **30**, a chemical reduction method was applied to test the stabilizing ability for the formation of Rh NPs, using $RhCl_3 \cdot 3H_2O$ as rhodium source and $NaBH_4$ as reducing reagent, as shown in equation (2). Different molar ratios L:Rh were tested, as summarized in Table 16. In all cases the reduction was performed in water at room temperature.

$$8\ RhCl_3 + 3\ NaBH_4 + 9\ H_2O \xrightarrow[rt]{\mathbf{30}} 8\ Rh + 3\ B(OH)_3 + 3\ NaCl + 21\ HCl \qquad (2)$$

Table 16. Preparation of Rh NPs stabilized with different amounts of stabilizer **30**.

Entry[a]	Rh NPs	**30** : Rh	Diameter[b] /nm	%Rh Theor.	%Rh Exper.[c]	Yield / %[d]
1	**M7**	1.00:1	1.6 ± 0.2	1.61	1.33	81
2	**M8**	0.30:1	2.1 ± 0.6	5.08	3.81	69
3	**M9**	0.10:1	8.5 ± 5.6[e]	13.84	8.43	57
4	**M10**	0.05:1	25.6 ± 5.5[e]	24.31	17.60	70
5	**M11**	0.02:1	32.3 ± 7.5[e]	44.54	34.60	76
6	-	0:1	Bulk rhodium	100	-	-

[a] Reaction conditions: [Rh] = 1 mM in water mixed with the chosen amount of stabilizer **30** was stirred overnight at room temperature with $NaBH_4$ (15 mmol per mmol of Rh) as reductant. [b] Mean diameter determined by TEM. [c] Determined by ICP. [d] Yields of the Rh NPs with respect to the rhodium added. [e] The presence of nanoflowers was observed, see text.

We first examined the formation of Rh NPs with a molar ratio of **30**/Rh = 1.00/1 (Table 16, entry 1). Thus, a Schlenk flask equipped with a magnetic stir bar was charged with the noted amount of stabilizer **30**, $RhCl_3$ and water, followed by three evacuate-refill cycles with nitrogen. It was found that, upon the dropwise addition of an aqueous solution of $NaBH_4$ via syringe at room temperature, the reaction solution immediately experienced a color change from light brown to black, suggesting the reduction from Rh(III) to Rh(0). After an overnight stirring at room temperature, the reaction mixture was filtered through a Millipore filter (no bulk rhodium was observed), the filtrate was extracted with dichloromethane and the organic solvent was evaporated, affording **M7** as a black solid. The TEM analysis gave a mean size of the Rh NPs of 1.6 nm. Considering that the amount of the stabilizer might affect the sizes, morphologies and catalytic activity of the Rh NPs, additional syntheses were performed following the same experimental procedure, but varying the ratio **30**/Rh from 0.3/1 to 0.02/1 (Table 16, entries 2-5). In all the entries, no bulk metal was found. The experimental percentage of rhodium in the nanomaterials was determined by elemental analysis (ICP). A reference test in the absence of stabilizer **30** gave a bulk rhodium precipitate (Table 16, entry 6).

The EDX spectra of **M7** and **M10** were chosen as examples for confirming the existence of rhodium element (Figure 27). Background signals derived from the copper grid used as sample holder can also be observed.

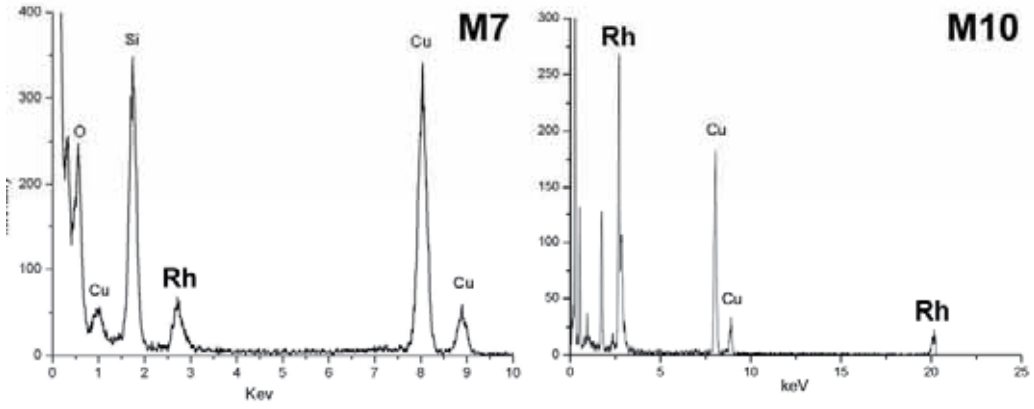

Figure 27. EDX spectra of **M7** and **M10**.

Notably, the rhodium particle sizes increased remarkably from 1.6 to 32.2 nm when the ratio of **30**/Rh decreased gradually from 1.0/1 to 0.02/1. Indeed, as summarized in Figure 28, small nanoclusters were observed when the ratio of **30**/Rh is 1.00/1, although the particles are somewhat irregular in shape. With the ratio decreasing to

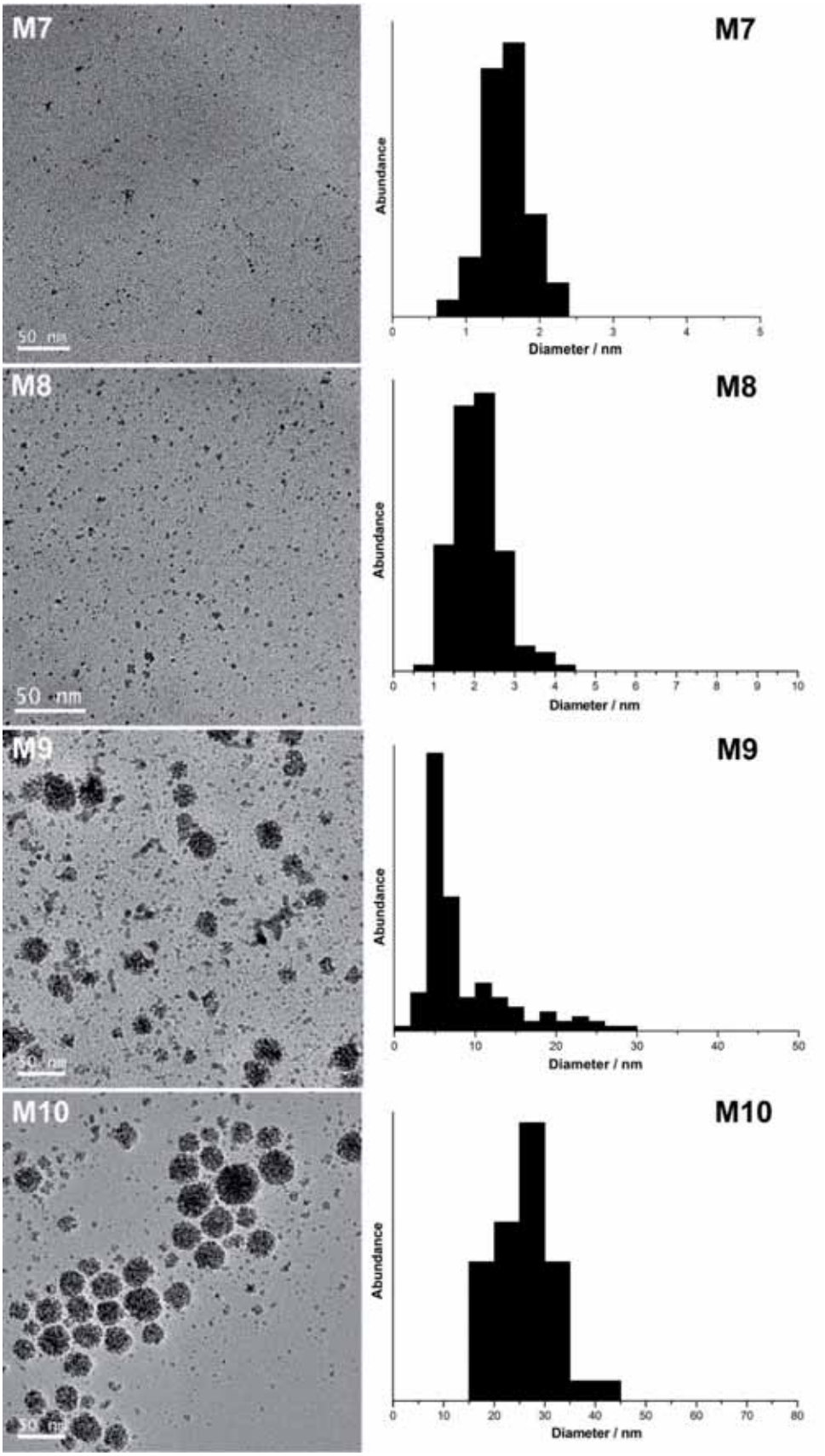

Figure 28. TEM images of **M7** (a), **M8** (b), **M9** (c) and **M10** (d), visually showing the changes in size and morphology of Rh NPs.

0.10/1, some of the nanoclusters began to aggregate yielding rhodium nanoflowers, and therefore leading to the wide size distribution. Further decrease of stabilizer (**M10**) results in the appearance of more and larger nanoflowers. Surprisingly, when the ratio is reduced to just 0.02/1, instead of bulk rhodium, almost pure nanoflowers were afforded as depicted in Figure 29a-b. HRTEM image of a chosen "nanoflower" was registered, clearly showing the different lattice planes as shown in Figure 29c. The statistic measurement gave a mean size of 32 nm for the nanoflowers of **M11** with a quite narrow size distribution (Figure 29d). The electron diffraction of a chosen single flower of **M11** confirmed the face-centered cubic (fcc) pattern of Rh(0) species (Figure 30).

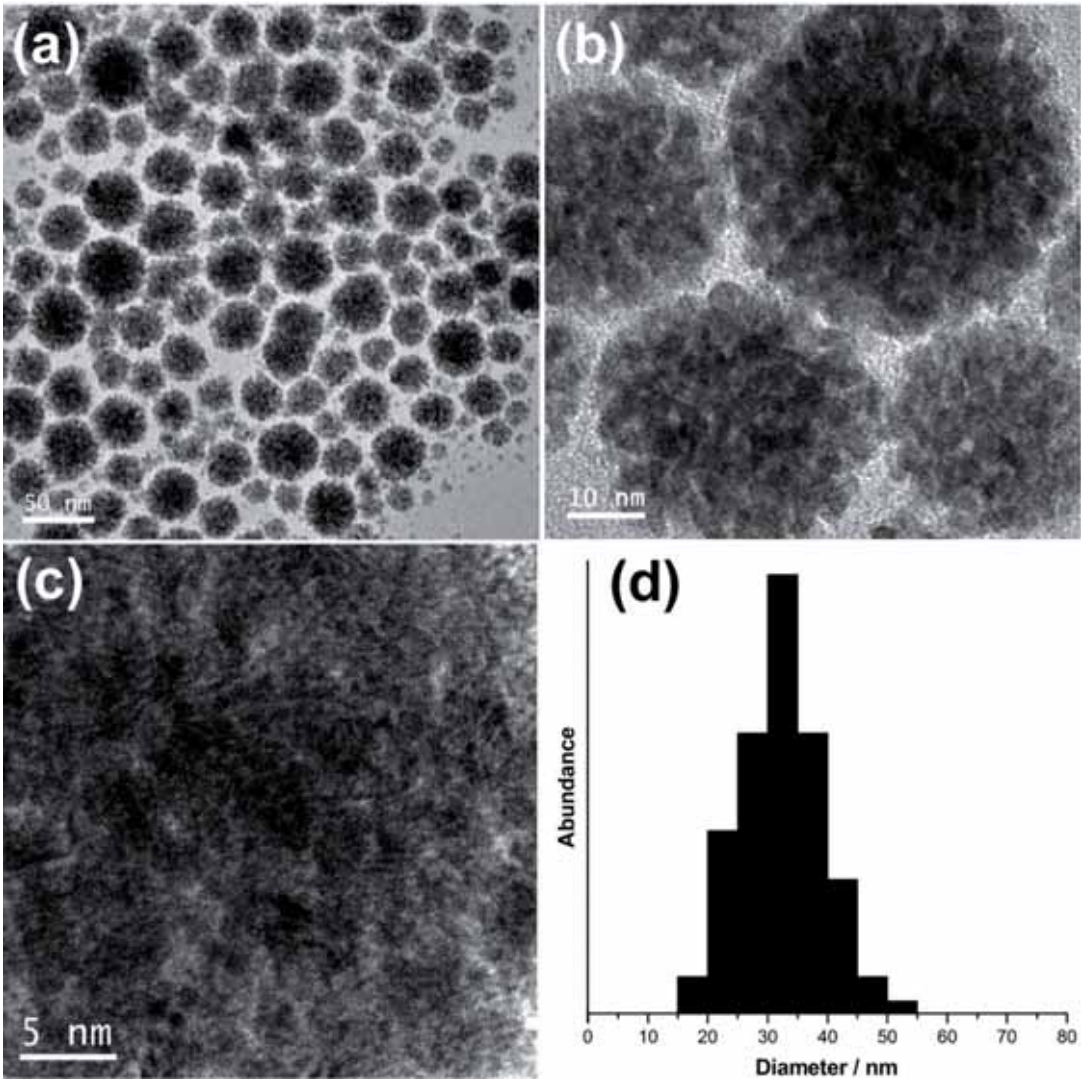

Figure 29. TEM images of **M11** under different magnification (a-b), HRTEM image of one chosen flower (c), and the size distribution of **M11** (d).

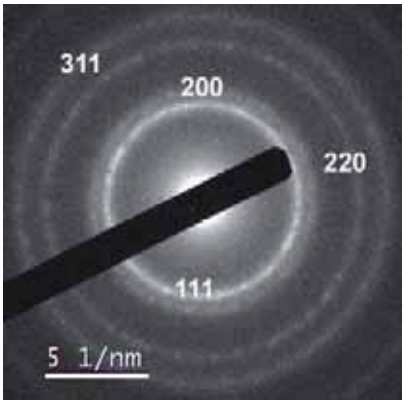

Crystal plane h k l	d_{hkl} (nm) Experimental	Theoretical[a]
(1 1 1)	0.2187	0.2196
(2 0 0)	0.1892	0.1902
(2 2 0)	0.1322	0.1345
(3 1 1)	0.1130	0.1147

[a]Corresponding the fcc Rh(0).[323d]

Figure 30. ED spectrum of **M11** and the corresponding lattice planes information.

The X-ray diffraction analysis was expected to offer further structural information of the stabilized Rh NPs. Thus, *p*-XRD patterns of **M8**, **M9**, **M10**, **M11** and the reference of commercially available PEG-2000 were collected and are given in Figure 31.

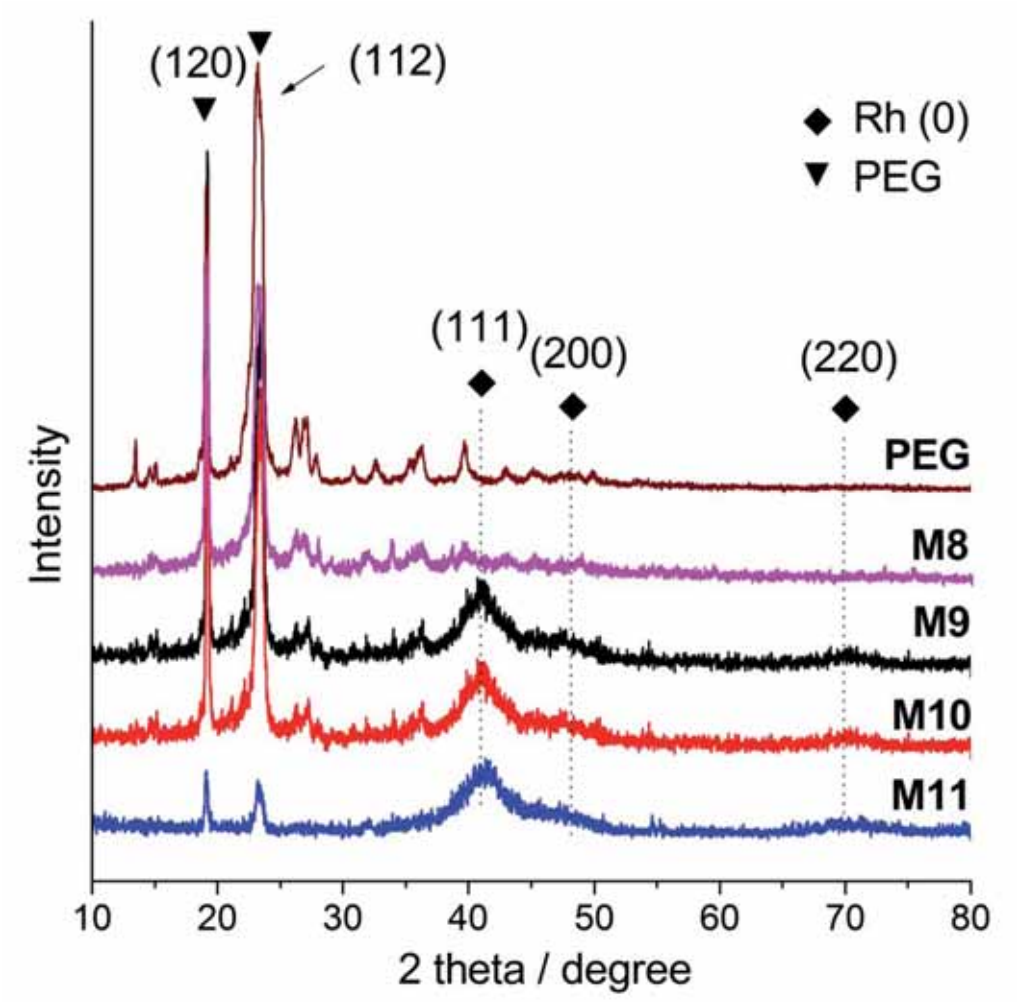

Figure 31. *p*-XRD patterns of PEG-2000, **M8**, **M9**, **M10** and **M11**.

The broad peaks at around 2θ = 41, 48 and 70° correspond to the fcc rhodium(0) planes of (111), (200) and (220), respectively.[341] In addition, two sharper peaks at 2θ = 19 and 23° were also observed in all the nanomaterials. A careful check in the ICDD database suggested that these peaks match very well with the (120) and (112) planes of PEG.[342] Thus, commercially available PEG-2000, the starting material for the preparation of stabilizer **30**, was analyzed as a reference further confirming the assignments as marked in Figure 31. No significant signals derived from Rh(0) were observed in **M7** due to its low rhodium content.

3.4 Stabilized gold nanoparticles

3.4.1 Preparation and characterization

A similar experimental procedure was followed to test the stabilizing ability of the compound **30** for the formation of Au NPs. Thus, a chemical reduction method was employed using $HAuCl_4 \cdot 3H_2O$ as the source of gold. This salt was treated with $NaBH_4$ in water at room temperature (Equation 3). The different experiments performed are summarized in Table 17.

$$8\ HAuCl_4 + 3\ NaBH_4 + 9\ H_2O \xrightarrow[rt]{\mathbf{30}} 8\ Au\ (0) + 3\ B(OH)_3 + 3\ NaCl + 29\ HCl \quad (3)$$

Table 17. Preparation of Au NPs stabilized by different amounts of **30**.

Entry[a]	**30** : Au	Diameter/nm[b]	% Au/Theor.	% Au/Exper.[c]	Yield/%[d]	Ref.
1	2.00 : 1	1.1 ± 0.2	1.54	1.26	68	**M12**
2	1.00 : 1	1.3 ± 0.3	2.33	1.91	76	**M13**
3	0.70 : 1	1.5 ± 0.3	4.27	3.66	83	**M14**
4	0.50 : 1	1.7 ± 0.4	6.23	5.21	84	**M15**
5	0.30 : 1	2.1 ± 0.3	9.43	8.21	85	**M16**
6	0.20 : 1	2.4 ± 0.5	13.60	10.86	78	**M17**
7	0.10 : 1	3.0 ± 0.5	24.10	17.41	71	**M18**
8	0.07 : 1	3.3 ± 0.8	31.12	19.40	61	**M19**
9	0.04 : 1	4.4 ± 1.6[e]	44.17	37.30	76	**M20**
10	0.01 : 1	tadpole morphology[f]	75.98	56.80	75	**M21**
11	0 : 1	bulk gold	100.0	-	-	**-**

[341] The diffraction data is consistent with the ICDD card 04-001-0093.

[342] The diffraction data is consistent with the ICDD card 00-049-2095.

[a] [Au] = 0.6 mM, 6 mmol of $NaBH_4$ was used with respect to 1 mmol of Au in all cases. [b] Mean diameter determined by TEM. [c] Determined by ICP. [d] Yields of the Au NPs with respect to the gold added. [e] It is a hybrid of spherical Au NPs and tadpole-like Au NPs, herein only the spherical NPs were taken into account. [f] Irregular tadpole-like Au NPs were observed.

A molar ratio of **30**/Au = 2 was first chosen in the reduction process. As expected, upon addition of an aqueous solution of $NaBH_4$, the reaction solution immediately experienced a color change from light yellow to black, with no precipitate of bulk gold being observed after stirring overnight. Then, the reaction mixture was filtered through a Millipore filter, the filtrate was extracted with dichloromethane and the organic solvent was evaporated, affording **M12** as a black solid. TEM analysis confirmed that the NPs were spherical and well dispersed. As shown in Table 17 (Entry 1), the measurement of more than 250 particles gave a mean size of 1.1 nm. The yield with respect to the initial amount of added Au was 68% on the basis of the elemental analysis (ICP), which constitutes a significant improvement with respect to the results obtained from other stabilizers previously developed in our research group.[318, 323c, 323d]

Theoretically, metal NPs with such a small size and narrow size distribution should give good performances in catalysis, because smaller particles result in higher surface areas and, therefore, they should present better catalytic activities. However, after our results with Rh NPs, we were also interested in investigating if and how the amount of the stabilizer would affect the size and morphology of the Au NPs. Actually, the size and morphology of NPs have been reported to play a key role in the activity for some catalytic systems.[343] Besides, too much stabilizer may also lead to low catalytic activity of the metal NPs.[344]

Thus, a careful screening of the ratio **30**/Au under the present reaction conditions was performed as documented in Table 17 (entries 1 - 10). It was observed that when the ratio of **30**/Au was gradually decreased from 1 to 0.07 (Table 17, entries 2 - 8), spherical and well dispersed gold NPs **M13** – **M19** were obtained, the particle size gradually increasing from 1.3 ± 0.3 to 3.3 ± 0.8 nm. These results clearly indicate that the size of the spherical Au NPs is controllable by simply varying the ratio of **30**/Au, which is consistent with our research on Rh NPs.

[343] (a) Chimentao, R. J.; Medina, F.; Sueiras, J. E.; Fierro, J. L. G.; Cesteros, Y.; Salagre, P. *J. Mater. Sci.* **2007**, *42*, 3307. (b) Chimentao, R. J.; Kirm, I.; Medina, F.; Rodriguez, X.; Cesteros, Y.; Salagre, P.; Sueiras, J. E. *Chem. Commun.* **2004**, 846.

[344] (a) Liu, L.; Sun, G.; Wang, C.; Yang, J.; Xiao, C.; Wang, H.; Ma, D.; Kou, Y. *Catal. Today* **2012**, *183*, 136. (b) Yan, N.; Yuan, Y.; Dyson, P. J. Dalton Trans. **2013**, *42*, 13294. (c) Barkhuizen, D.; Mabaso, I.; Viljoen, E.; Welker, C.; Claeys, M.; van Steen, E.; Fletcher, J. C. Q. *Pure Appl. Chem.* **2006**, *78*, 1759.

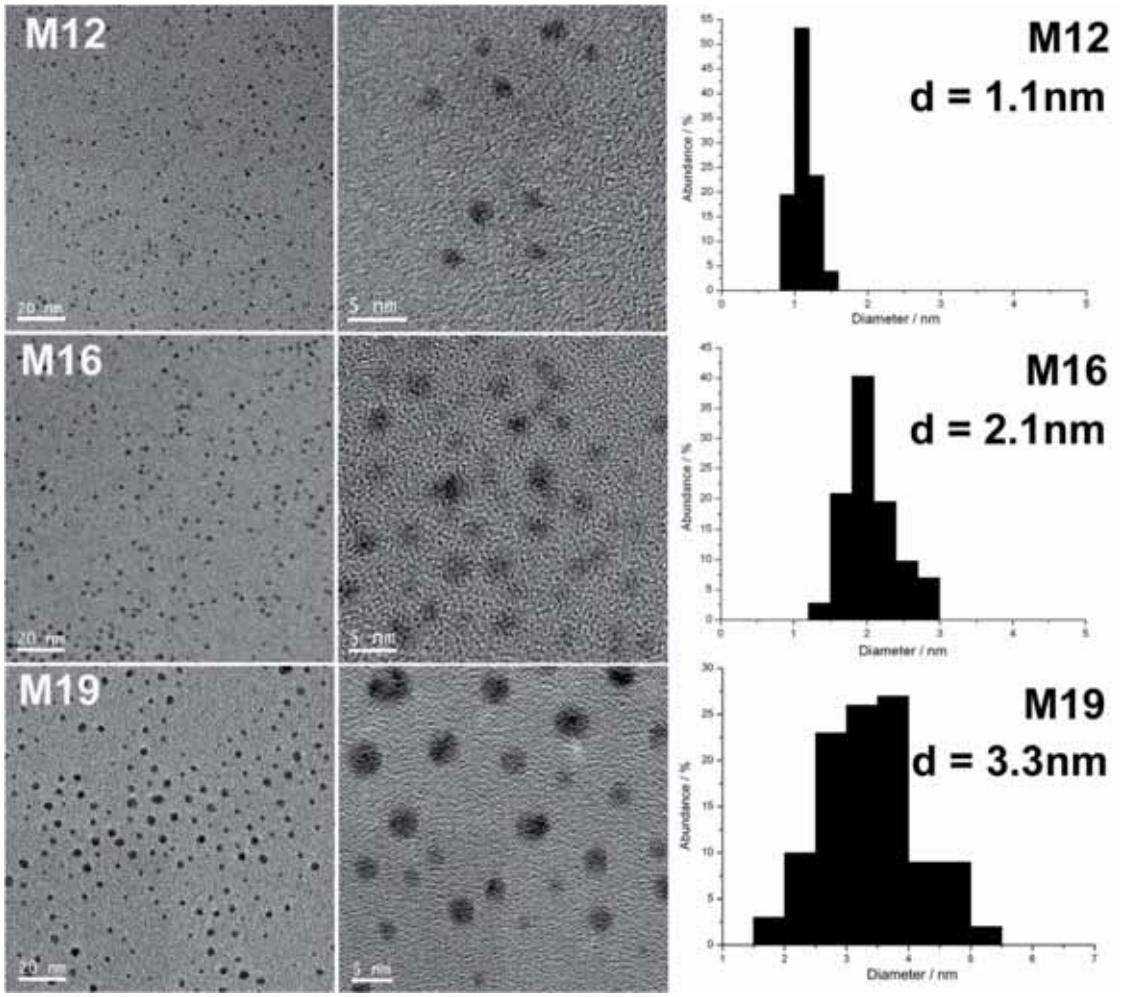

Figure 32. TEM, HRTEM images and the corresponding size distributions of the materials **M12**, **M16** and **M19**.

In order to visualize the size and morphology changes of the Au NPs with different amounts of stabilizer, selected TEM and HRTEM images and the corresponding size distributions of the materials **M12**, **M16** and **M19** are given in Figure 32. As shown, **M19** exhibited wider size distributions than **M12** and **M16**. The obtained Au NPs are significantly smaller and better dispersed as compared with those stabilized by PEG-tagged dendrimers or the simple PEGlated 1, 2, 3-triazole ligand derived from click chemistry reported in the literature.[345] Since the size of the Au NPs is generally determined by the relative rates between nucleation and particle growth, the formation of smaller Au NPs when using higher amounts of stabilizer can be ascribed to the more significant suppression of the growth of the Au nuclei by the stabilizer. The EDX

[345] (a) Zhao, P.; Li, N.; Salmon, L.; Liu, N.; Ruiz, J.; Astruc, D. *Chem. Commun*. **2013**, *49*, 3218. (b) Boisselier, E.; Diallo, A. K.; Salmon, L.; Ornelas, C.; Ruiz, J.; Astruc, D. *J. Am. Chem. Soc.* **2010**, *132*, 2729.

spectrum of **M17** is given in figure 33 showing the presence of the gold signal along with the background peaks attributed to the copper grid.

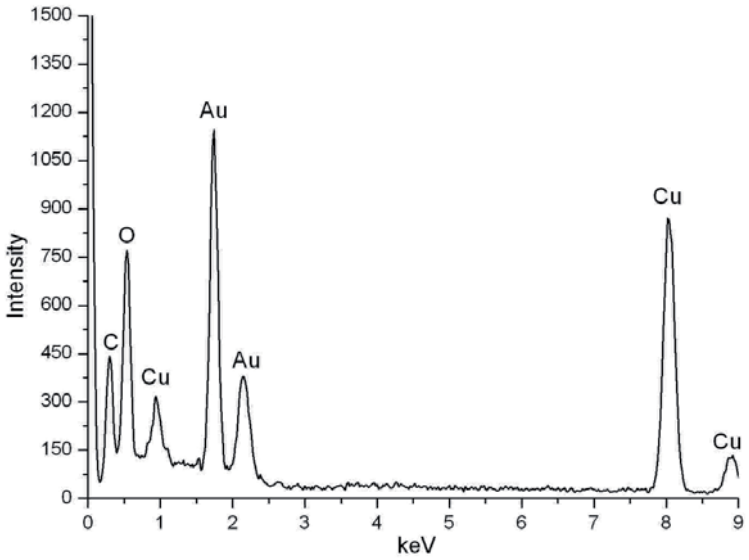

Figure 33. EDX spectrum of **M17**.

When the ratio of **30**/Au was further decreased to 0.04/1 (Table 17, entry 9), a hybrid Au NPs **M20** consisting in a mixture of spheres and "tadpoles" was observed (Figure 34). Interestingly, the use of only 0.01 eq. of stabilizer **30** (Table 17, entry 10) did not lead to the precipitation of bulk metal, but to the formation of Au NPs **M21** with a predominant tadpole-like morphology (Figure 34).

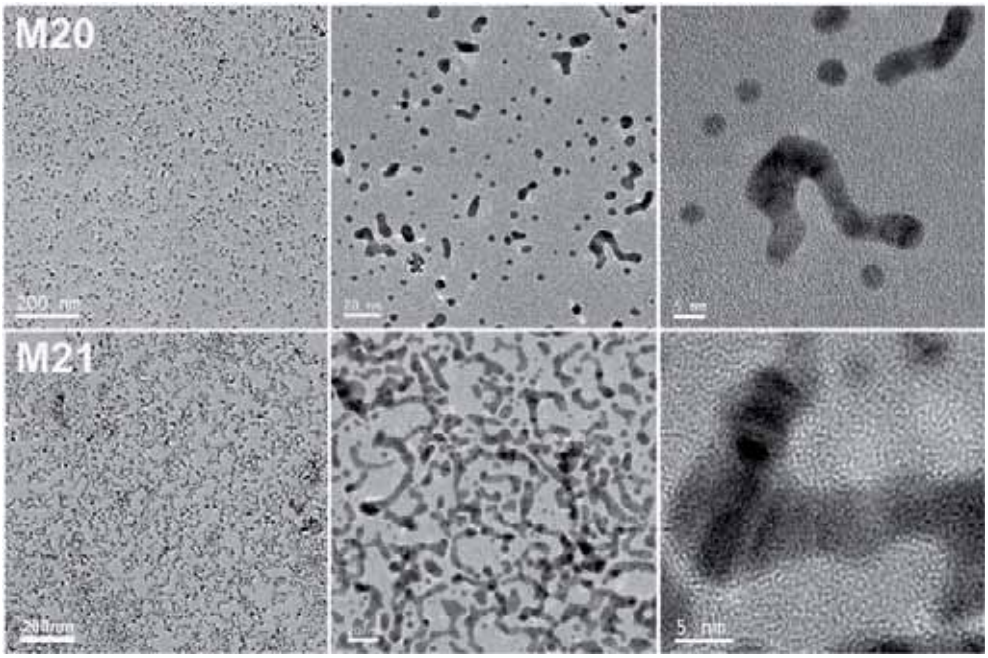

Figure 34. TEM images of **M20** and **M21** under different magnifications, and the corresponding HRTEM images.

The elemental analysis (ICP) of **M21** gave a value of 56.80% Au, although lower than the theoretical value of 75.98% (Table 17). Electron diffraction of the Au NPs provided structural information. Thus, as can be seen in Figure 35, the experimental interplanar distances of **M21** extracted with Gatan Software were very close to the theoretical values corresponding to a face-centered cube (fcc) gold structure.

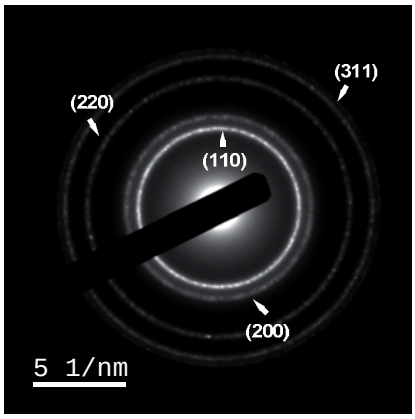

Crystal plane h k l	d_{hkl} (nm) Experimental	Theoretical[a]
(1 1 1)	0.2327	0.2355
(2 0 0)	0.2040	0.2039
(2 2 0)	0.1426	0.1442
(3 1 1)	0.1209	0.1230

[a]Corresponding the fcc Au(0).[323d]

Figure 35. ED pattern of **M21**.

A control reaction in the absence of any stabilizer led to bulk metal precipitation (Table 17, entry 11). An alternative protocol involving methanol in basic medium as reducing reagent of tetrachloroauric acid (Equation 4) failed for the formation of Au NPs in the presence of the polyoxyethylenated stabilizer.

$$2\ HAuCl_4 + 3\ CH_3OH + 8\ NaOH \xrightarrow[rt]{L} 2\ Au\ (0) + 8\ H_2O + 3\ H_2CO + 8\ NaCl \quad (4)$$

With the Au NPs in hand, the water solubility was tested by adding 2 mg of the selected materials into 1 mL of water. After the mixture was well stirred, the materials were found to be completely soluble in water as depicted in Figure 36a. Further structural investigation was conducted by registering the UV-Vis spectra of the materials **M12**-**M21** in THF (Figure 36b). When the particle sizes are bigger than 2 nm (**M16**-**M21**), we can see clearly the appearance of a broad shoulder at 450-600 nm representing the localized surface plasmon resonance (LSPR).[346] This absorption shows an appreciably red shift with the decreasing of the ratio **L**/Au from 0.30/1 to 0.01/1, which can be ascribed to the gradual size increase as reported by others.[347]

---

[346] The basis of LSPR can be found in the following text.

[347] (a) Sanchez-Gaytan, B. L.; Qian, Z.; Hastings, S. P.; Reca, M. L.; Fakhraai, Z.; Park, S.-J. *J. Phys. Chem. C* **2013**, *117*, 8916. (b) Qiao, Y., Chen, H.; Lin, Y.; Huang, J. *Langmuir* **2011**, *27*, 11090.

However, for the materials **M12**-**M15**, whose sizes are smaller than 2 nm, the LSPR band was not clearly observed, in good agreement with others' research.[348]

The *p*-XRD patterns (Figure 36c) of the selected three samples **M16**, **M17** and **M18** showed two intense peaks in the range of 2θ = 15 - 25° representing the crystalline planes (120) and (112) of the PEG-tagged stabilizer, as was the case for the Rh NPs. Four weak diffraction bands appeared in range from 2θ = 40° to 80°, which were assigned to the (111), (200), (220) and (311) planes[349] of fcc gold crystals, respectively. These data fit well with the ED analysis (Figure 35).

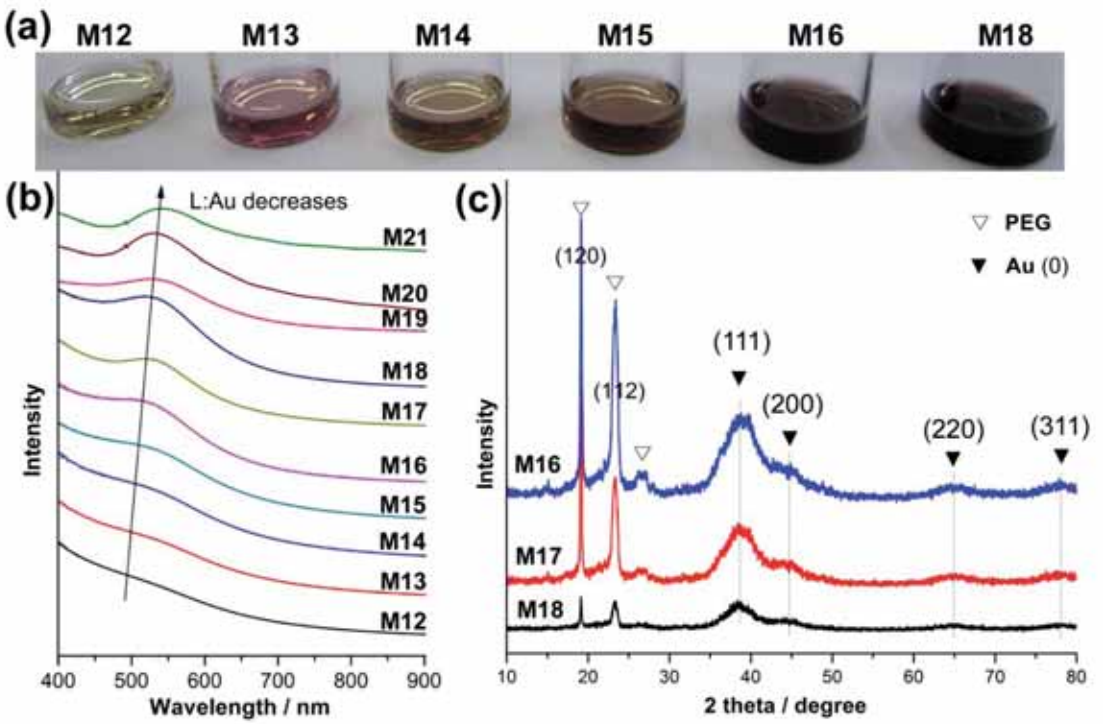

Figure 36. (a) Optical photographs of Au NPs (2 mg) in H_2O (1 mL); (b) Absorption spectra of the Au NPs in THF (0.2 mM of Au) and (c) *p*-XRD patterns of selected Au NPs.

3.4.2 Evaluation of the gold nanoparticles as refractive index sensors

Distinct physical and chemical attributes make Au NPs excellent scaffolds for a variety of sensors in chemical and biological areas.[350] One of the most interesting properties of Au NPs is the occurrence of LSPR, which corresponds to the collective

[348] Oh, E., Susumu, K.; Goswami, R.; Mattoussi, H. *Langmuir* **2010**, *26*, 7604

[349] The diffraction data is consistent with the ICDD card 04-001-2616.

[350] (a) Saha, K.; Agasti, S. S.; Kim, C.; Li, X.; Rotello, V. M. *Chem. Rev.* **2012**, *112*, 2739. (b) Mayer, K. M.; Hafner, J. H. *Chem. Rev.* **2011**, *111*, 3828.

excitation of surface electrons upon absorption of light. Such excitation results in electronic cloud oscillation against the restoring force of positive nuclei at the frequency of the absorbed radiation (Scheme 107).[351] This resonance is found to be very sensitive to the refractive index of the interfacial region. Thus, a great deal of sensors are designed on the basis of the change in LSPR absorption of Au NPs.[350b] The simplest sensing of LSPR-active Au NPs is to detect the changes in the refractive index of their environment through shifts in the LSPR peak wavelength.

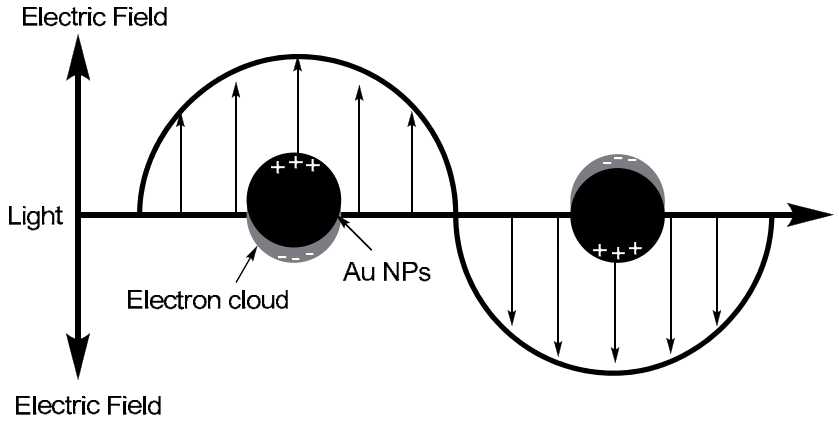

Scheme 107. Schematic illustration of LSPR of Au NPs showing the displacement of the electron charge cloud relative to the nuclei.

As a separate but related research of our Au NPs, **M18** was chosen as representative nanomaterial to investigate the ability of gold NPs to act as a refractive index sensing. Thus, **M18** was dissolved in a series of solvents with covering a range of refractive index values at a concentration of 0.2 mmol Au/L. Specifically, the experiments were conducted in carbon disulfide (n = 1.627), toluene (n = 1.496), chloroform (n = 1.447), *t*-butanol (n = 1.399) and water (n = 1.333). The absorbance spectra of the five samples (Figure 37A) showed that, by increasing the refractive index from 1.333 to 1.627, the maximum absorbance of the samples experiences a notable gradual red shift from 526 nm to 541 nm, indicating that Au NPs could, indeed, be used as sensors of the refractive index. As can be seen from Figure 37B, there is an approximate linear correlation between the LSPR peak wavelength and the medium refractive index, in good agreement with results reported by for other classes of Au nanoparticles.[352]

---

[351] (a) Stewart, M. E.; Anderton, C. R.; Thompson, L. B.; Maria, J.; Gray, S. K.; Rogers, J. A.; Nuzzo, R. G. *Chem. Rev.* **2008**, *108*, 494. (b) Love, J. C.; Estroff, L. A.; Kriebel, J. K.; Nuzzo, R. G.; Whitesides, G. M. *Chem. Rev.* **2005**, *105*, 1103. (c) Willets, K. A.; Van Duyne, R. P. *Ann. Rev. Phys. Chem.* **2006**, *58*, 267.

[352] Mayer, K. M.; Lee, S.; Liao, H.; Rostro, B. C.; Fuentes, A.; Scully, P. T.; Nehl, C. L.; Hafner, J. H. *ACS Nano* **2008**, *2*, 687.

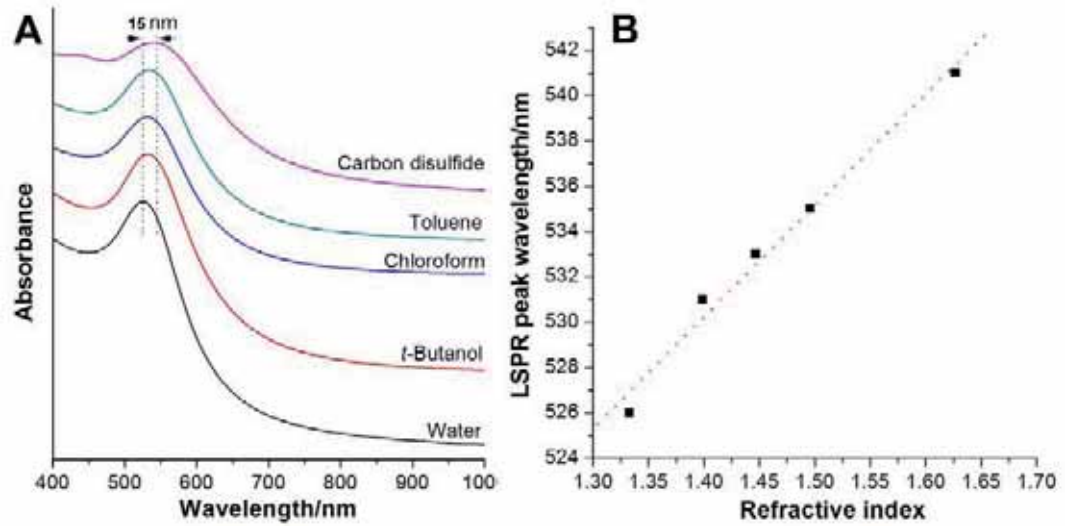

Figure 37. A) Optical absorbance of **M18** with concentration of 0.2 mM gold in carbon disulfide, toluene, chloroform, *t*-butanol and water and B) Plotting the peak wavelength versus refractive index, showing the approximately linear correlation.

3.5 Attempts to prepare palladium nanoparticles

Inspired by our fruitful results on Rh and Au NPs, we envisaged the preparation of water soluble Pd NPs *via* the hydrogenation of $Pd(dba)_2$ in the presence of stabilizer **30** (method of reduction and displacement of ligand from an organometallic compound) (Scheme 108). Actually, this protocol has been successfully proven in our group for the formation of Pd NPs with various types of stabilizers.[318, 323b] Thus, a Fischer-Porter apparatus equipped with a magnetic stir bar was charged with a solution of stabilizer **30** and $Pd(dba)_2$ (**30**/Pd = 2/1 or 1/1) in THF and we performed three evacuate-refill cycles with hydrogen. The resulting solution was stirred overnight at room temperature under 3 atm of hydrogen. A clear pale yellow solution was obtained, indicating the failure for the formation of Pd NPs. Further investigation was not performed in this thesis.

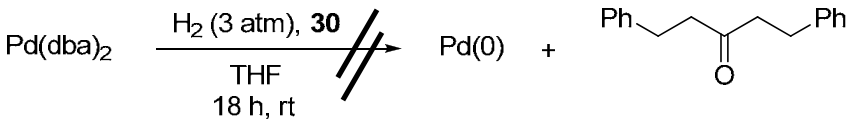

Scheme 108. Attempt for the preparation of Pd NPs *via* hydrogenation of $Pd(dba)_2$ in the presence of stabilizer **30**.

3.6 Conclusions

A nitrogen-rich polyoxyethylenated substrate **30** was designed and synthesized on

the basis of a threefold [2+3] CuAAC click reaction. It was successfully used as stabilizer for the formation of water-soluble metal nanoparticles (Rh, Au) by the chemical reduction method. It was found that by varying the molar ratio **30**/Rh, we can achieve size and morphology controllable Rh NPs, with morphology ranging from small clusters to “nanoflowers”. A similar phenomenon was also found for the formation of Au NPs, with morphologies varying from small spheres to “nanotadpoles”, with the nanoparticle sizes determined by the proportion of the of stabilizer employed in the synthesis. The newly prepared nanomaterials were fully characterized by TEM, ED, *p*-XRD, UV-vis and elemental analysis (ICP). The Au NPs were successfully tested as refractive index sensors. The hydrogenation of $Pd(dba)_2$ in the presence of **L** failed to afford Pd NPs.

3.7 Experimental section

3.7.1 General remarks

Water Milli-Q was used in the preparation and purification of compounds and nanoparticles. All NMR measurements were carried out at the *Servei de Ressonància Magnètica Nuclear* of the *Universitat Autònoma de Barcelona*. NMR spectra were recorded on Bruker Avance250 (250 MHz) and Avance360 (360 MHz) spectrometers. Infrared spectra were recorded using a Bruker Tensor 27 instrument equipped with an ATR Golden Gate cell and a diamond window. MALDI-TOF spectrum was recorded using dithranol as the matrix on a MALDI-TOF UltrafleXtreme (Bruker Daltonics) at the *Institut de Biotecnologia i Biomedicina* in *Universitat Autònoma de Barcelona*. ICP measurements of gold and rhodium content were carried out at the *Serveis Científico-Tècnics* of the *Universitat de Barcelona (SCT-UB)* with a multichannel Perkin–Elmer instrument, model Optima 3200 RL. The powder X-ray diffraction (*p*-XRD) patterns were collected using a conventional powder X-ray diffractometer (Siemens D5000) at the *Institut de Ciència dels Materials de Barcelona*. The absorption spectra of the Au NPs were registered in a HP 8453 UV-VIS spectrophotometer at the *Servei d'Anàlisi Química (SAQ)* of the *Universitat Autònoma de Barcelona.* Transmission electron microscopy (TEM), High resolution transmission electron microscopy (HRTEM) and electron diffraction (ED) analyses were performed at the *Servei de Microscopia of the Universitat Autonoma de Barcelona*, using a JEOL JEM-2010 model at 200 kV. The click chemistry is performed in a microwave *CEM discover* reactor.

3.7.2 Synthesis of compound 31[323c,e]

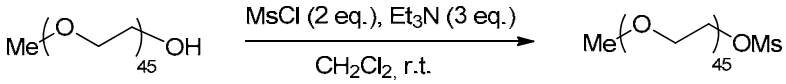

Commercial MeO-PEG-OH (average n = 44; 10.0 g, 5 mmol) was dried at 80°C overnight under vacuum. Then, the material was dissolved in anhydrous CH_2Cl_2 (140 mL), followed by addition of triethylamine (2.1 mL, 1.53 g, 15.1 mmol). The mixture was cooled to 0°C, and methanesulfonyl chloride (0.8 mL, 1.184 g, 10.2 mmol) was added dropwise while stirring for 15 min. After the addition of all the reagents, the stirring was continued at the same temperature for an additional 15 min, then at room temperature for 5 h. After that, the reaction mixture was filtered through a plug of silica gel, and the plug was washed with CH_2Cl_2. The solvent was evaporated, and the oily residue was triturated with diethyl ether to yield the target compound as a white solid, which was isolated by filtration, washed and dried under vacuum (9.646 g, 94%). ^{1}H NMR (360

MHz, $CDCl_3$) δ (ppm): 4.38 - 4.36 (m, 2H, C**H**$_2$OMs), 3.77-3.75 (m, 2H, C**H**$_2$CH$_2$OMs), 3.63 (m, 174, C**H**$_2$ of PEG chain), 3.55-3.53 (m, 2H, CH_2), 3.37 (s, 3H, OC**H**$_3$), 3.08 (s, 3H, SO_2C**H**$_3$).

3.7.3 Synthesis of compound 32[323c,e]

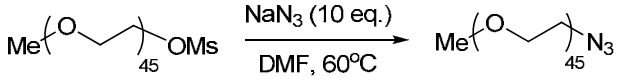

Sodium azide (1.034 g, 15.75 mmol) was added to a solution of compound **31** (3.275 g, 1.57 mmol) in dimethylformamide (200 mL), and the mixture was stirred at 60°C for 25 h. The solvent was evaporated at reduced pressure, and the residue was partitioned between CH_2Cl_2 and water. The organic phase was dried with anhydrous sodium sulfate. After removal of solvent, diethyl ether was added to the residue resulting in the precipitation of the target compound as a white solid, which was filtered, further washed with ether and dried under vacuum (3.147 g, 99%). ^{1}H NMR (360 MHz, $CDCl_3$) δ (ppm): 3.37-3.40 (m, 5H, OC**H**$_3$ and C**H**$_2$), 3.53-3.84 (m, 178H, C**H**$_2$). IR (ATR) *v* (cm^{-1}): 2882 (CH_2), 2099 (N_3), 1466, 1340, 1098.

3.7.4 Synthesis of 2,4,6-tris(propargylamino)-1,3,5-triazine, 33[340]

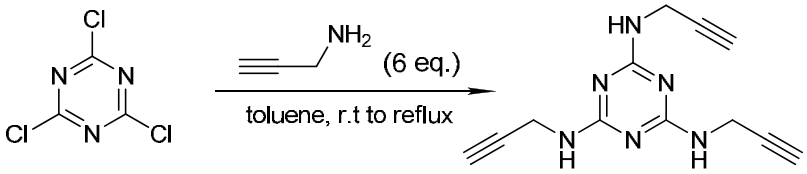

Synthesis from cyanuric chloride. To a stirred suspension of cyanuric chloride (1.840 g, 10 mmol) in dry toluene (50 mL) was added dropwise, during 5 minutes, propargylamine (3.30 g, 60 mmol). The mixture was heated under reflux for 20 h; at this point the mixture was filtered while hot. The solid, which separated on cooling, was removed by filtration, the filtrate was concentrated, and the residue was recrystallized from boiling water to give a light yellow product (1.009 g, 42%); m.p. = 127 - 129°C (lit:[340] 125-127°C); MS (ESI) *m/z* $C_{12}H_{12}N_6$ [M+H]$^+$: 241.1; ^{1}H NMR (360 MHz, DMSO) δ (ppm): 7.13 (s, 3H), 3.98 (s, 6H), 2.98 (s, 3H); ^{13}C NMR (360 MHz, DMSO, δppm): 165.35, 82.38, 72.21, 29.29. IR (ATR) *v* (cm^{-1}): 3456 (NH), 3382, 3282, 1624, 1503, 1405, 1160.

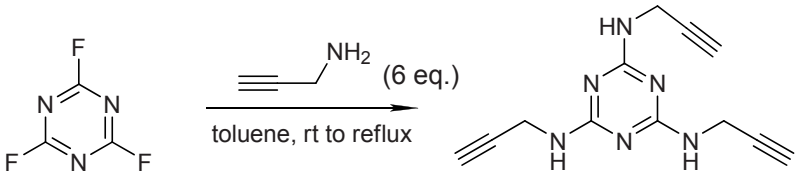

Synthesis from cyanuric floride. To a stirred suspension of cyanuric floride (0.675 g, 5 mmol) in dry toluene (30 mL) was added dropwise, during 5 minutes, propargylamine (1.8 mL, ρ = 0.86 g/mL, 30 mmol). The reaction mixture was heated under reflux overnight and then filtered hot, the filtrate was cooled down to room temperature affording a light yellow product, which was filtered, washed and dried (1.001 g, 83%).

3.7.5 Synthesis of $Cu(PPh_3)_3Br$[353]

To boiling methanol (30 mL) was added slowly triphenylphosphine (4.460 g, 17 mmol). After the complete dissolution of triphenylphosphine, $CuBr_2$ (1.117 g, 5 mmol) was added in small portions. No special precautions were taken for the exclusion of air. Upon addition of the copper bromide, a white precipitate formed. When the addition was finished, the contents were stirred for 30 min and the flask was allowed to cool to room temperature. The reaction mixture was then filtered through a Buchner funnel and the white residue was washed repeatedly with ethanol and then with diethyl ether. The resultant white solid was dried under vacuum to give $Cu(PPh_3)_3Br$ (4.360 g, 87% yield, m.p. = 169 - 172°C, lit:[353] 164-166°C).

3.7.6 Synthesis of the stabilizer 30

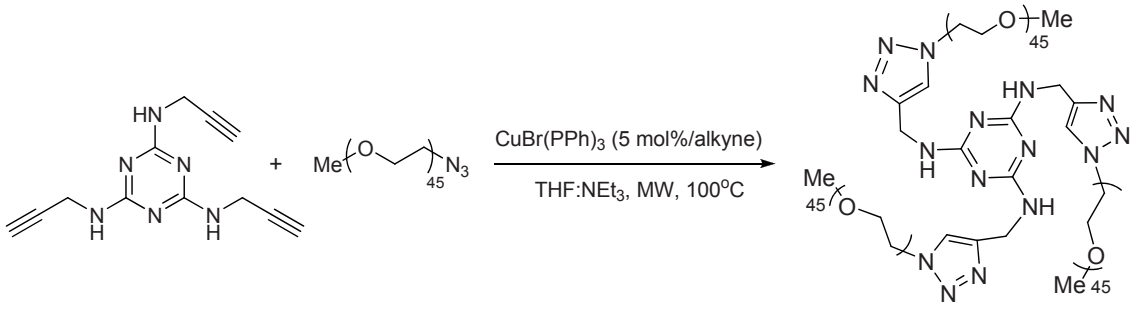

In a microwave tube, to a stirred solution of the azide **32** (182 mg, 0.09 mmol), the alkyne **33** (7 mg, 0.03 mmol), $[CuBr(PPh_3)_3]$ (0.0045 mmol, 4 mg, 5 mol% / alkyne

[353] Allen, D. V.; Venkataraman, D. *J. Org. Chem.* **2003**, *68*, 4590.

function) in THF (1.5 mL) was added triethylamine (1.5 mL), and the tube was then sealed. After 15 min under microwave irradiation at 100°C (maximum power = 200 W), the reaction mixture was allowed to cool and the solvents were removed under vacuum affording a yellow solid. The solid was then suspended in water, and the insoluble part was removed by centrifugation. After the removal of water, the stabilizer **30** was afforded as a light yellow solid (175 mg, 92% yield). ^{1}H NMR (360 MHz, $CDCl_3$) δ (ppm): 7.72 (s, 3H, triazole-**H**), 4.64 (broad s, 3H, N**H**), 4.50 (t, J = 5.0 Hz, 6H, NHC**H**$_2$), 3.85-3.82 (m, 6H, C**H**$_2$), 3.64-3.53 (m, 520H, C**H**$_2$ of PEG chains), 3.48-3.41 (m, 6H, C**H**$_2$), 7.72 (s, 9H, OC**H**$_3$); MALDI-TOF MS: *m/z* range for $[M + H]^+$ from 5411 (114 CH_2CH_2O units +nitrogen-rich core) to 7175 (154 CH_2CH_2O units + nitrogen-rich core), separated from 44 D (CH_2CH_2O unit); the most intense peak at 6161 (131 CH_2CH_2O units + nitrogen-rich core); IR (ATR, neat) *v* (cm^{-1}): 2882, 1571, 1519, 1466, 1098, 959.

3.7.7 Typical procedure for the preparation of rhodium nanoparticles (M9, Table 16, entry 3)

M9: To a solution of the stabilizer **30** (187 mg, 0.03 mmol) and rhodium trichloride trihydrate (79 mg, 0.30 mmol) in water (260 mL) was added dropwise a solution of 0.1 M sodium borohydride in water (45 mL, 4.5 mmol of $NaBH_4$) under protection of N_2. The mixture was stirred at room temperature overnight, and then was filtered through a Milli-Pore filter. The filtrate was extracted with dichloromethane (6 × 20 mL) and the organic phase was dried over anhydrous sodium sulfate. After the removal of the solvent, Rh NPs were obtained as a black powder (210 mg, Rh % = 8.43%, 57% yield with respect to the rhodium used). See Table 16 (main text) for the variations tested using this general this procedure.

3.7.8 Typical procedure for the preparation of gold nanoparticles (M16, Table 17, entry 5)

M16: To a solution of the stabilizer **30** (112 mg, 0.018 mmol) and hydrogen chloroaurate(III) trihydrate (24 mg, 0.06 mmol) in water (100 mL) was added dropwise via syringe (over 2 min) a solution of 0.1 M sodium borohydride (3.6 mL, 0.36 mmol of $NaBH_4$) under protection of N_2. The mixture was stirred at room temperature overnight, and then was filtered through a Milli-Pore filter. The filtrate was extracted with dichloromethane (6 × 20 mL) and the organic phase was dried over anhydrous sodium sulfate. After the removal of the solvent, Au NPs were obtained as a black powder (122 mg, Au % = 8.21%, 85% yield with respect to the gold used).

3.7.9 Evaluation of the gold nanoparticles as refractive index sensors

Samples of Au NPs **M18** were dissolved in carbon disulfide (2 mL), toluene (2 mL), chloroform (2 mL), *t*-butanol (2 mL) and water (2 mL), respectively, to form homogenous solutions with concentrations of 0.2 mM of Au. Subsequently, the absorption spectra of all the solutions were collected on the UV-vis spectrometer. The absorption maxima were then plotted *vs* the solvent's refractive index.

Part II. Water-soluble metal nanoparticles (Rh, Au) in catalysis

CHAPTER 4

Catalytic applications of metal nanoparticles (Rh, Au) stabilized by a nitrogen-rich polyoxyethylenated substrate

Chapter 4. Catalytic applications of metal nanoparticles (Rh, Au) stabilized by a nitrogen-rich polyoxyethylenated substrate

4.1 Rhodium nanoparticles as catalysts in the hydrosilylation of alkynes

4.1.1 Introduction to hydrosilylation of alkynes

The hydrosilylation reaction consists of the addition of a Si-H bond across an unsaturated chemical bonds. Thus, the hydrosilylation of alkenes and alkynes produces alkyl- and vinylsilanes, while that of aldehydes and ketones offers the corresponding silyl ethers. This class of reactions was discovered by Sommer and coworkers[354] in 1947, when they performed the reaction between trichlorosilane and 1-octene, in the presence of diacetyl peroxide, to yield a 46% of *n*-octyltrichlorosilane. Later investigations showed that various organic compounds with unsaturated bonds could be subjected to similar transformations, as summarized in Scheme 109.[355]

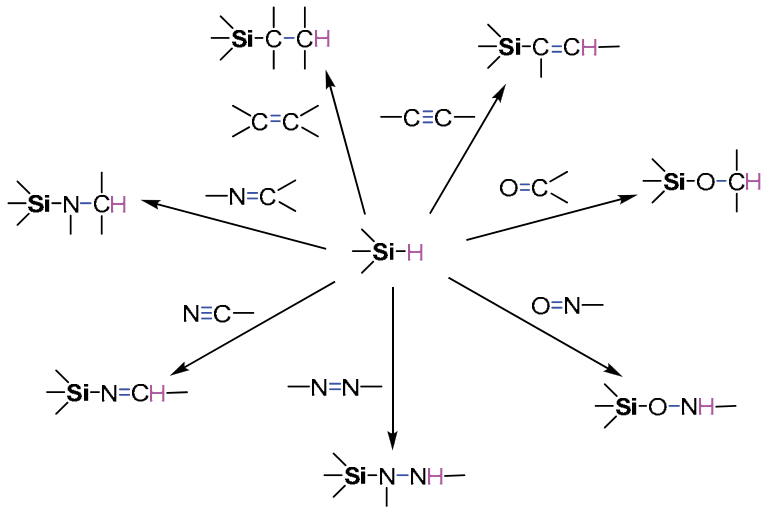

Scheme 109. Hydrosilylation of different compounds with unsaturated bonds.

As a specific case, the transition-metal catalyzed hydrosilylation of alkynes represents the most straightforward and convenient route for the preparation of vinylsilanes, and, ideally, occurs with 100% atom efficiency.[356] The resulting

---

[354] Sommer, L. H.; Pietrusza, E. W.; Withmore, F. C. *J. Am. Chem. Soc.* **1947**, *69*, 188.

[355] "Hydrosilylation: A Comprehensive Review on Recent Advances" B. Marciniec (ed.), Advances in Silicon Science, Springer Science, **2009**.

[356] (a) Ojima, I.; Li, Z.; Zhu, J. in: The Chemistry of Organosilicon Compounds; (Eds.: Z. Rappoport, Y. Apeloig), Wiley-VCH, Weinheim, **1998**, Vol. 2, pp 1687-1792. (b) Marciniec, B.; Maciejewski, H.; Pietraszuk, C.; Pawluc, P. in: Hydrosilylation: A Comprehensive Review on Recent Advances, Advances in

organosilicon reagents are versatile building blocks in a number of synthetic processes, and therefore the reaction has drawn much attention worldwide. Thus, one of the major applications of vinylsilanes is in the transition metal-catalyzed formation of C-C bonds by reaction with aryl halides.[357] Other examples of reactions involving vinylsilanes include the protodesilylation[358] to produce the corresponding alkene and the Tamao-Fleming oxidation[359] to generate the carbonyl derivatives. In general, vinylsilanes exhibit reactivity similar to that of certain organometallic vinyl derivatives, but may offer advantages in terms of cost, low molecular weight, low toxicity and high chemical stability.

Thus, the importance of the hydrosilylation of alkynes in organic synthesis is difficult to overestimate. Challenges remain, however, in achieving this transformation in a regio- and/or stereoselective manner. Depending on the kind of alkyne (terminal, symmetric internal, asymmetric internal) used, the addition of a Si-H bond can lead to a number of regio- and/or stereoisomeric vinyl silanes (Scheme 110). The development of recyclable catalysts, in particular those active in hydrosilylation reaction is another interesting topic, due to the increasing need of green and sustainable chemistry.

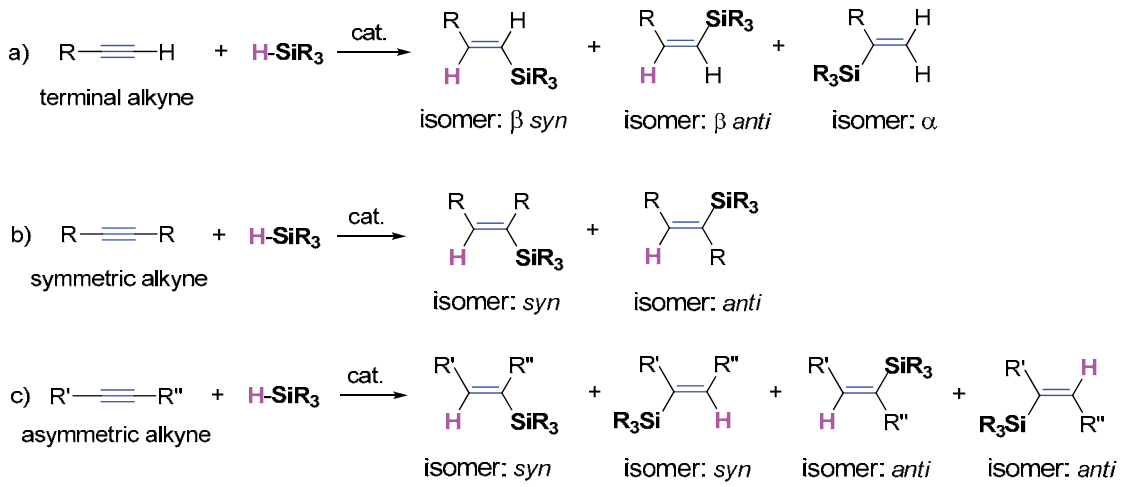

Scheme 110. Possible isomers in the hydrosilylation of different kinds of alkynes.

Silicon Science Series, (Ed.: B. Marciniec), Springer, Berlin, Heidelberg, **2009**, Vol. 1, Chapter 2.

[357] For some recent reviews on the palladium-catalyzed cross-coupling of organosilicon reagents, see: (a) Nakao, Y.; Hiyama, T. *Chem. Soc. Rev.* **2011**, *40*, 4893. (b) Sore, H. F.; Galloway, W. R. J. D.; Spring, D. R. *Chem. Soc. Rev.* **2012**, *41*, 1845.

[358] Trost, B. M.; Ball, Z. T.; Joge, T. *J. Am. Chem. Soc.* **2002**, *124*, 7922.

[359] (a) Tamao, K.; Ishida, N.; Tanaka, T.; Kumada, M. *Organometallics* **1983**, *2*, 1694. (b) Fleming, I.; Henning, R.; Plaut, H. *J. Chem. Soc., Chem. Commun.* **1984**, 29.

4.1.1.1 Various protocols for the hydrosilylation of alkynes

Most commonly, platinum-based catalysts are used for the addition of silanes to unsaturated C-C bonds.[360] Of these, the chloroplatinic acid (Speier's catalyst),[360a,b] and the olefin-stabilized Karstedt's catalyst (Scheme 111) have traditionally been the two catalysts of choice for this transformation.[360c,d]

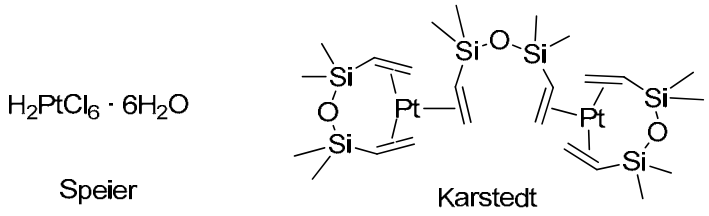

Scheme 111. Platinum catalysts for hydrosilylation reactions.

More recently, ruthenium complexes exemplified in Scheme 112, despite being generally less reactive, have also become popular in alkyne hydrosilylation due to their high levels of stereoselectivity.[361] Thus, the regio- and stereochemistry of the metal-catalyzed alkyne hydrosilylation is known to be controlled by the nature of the catalyst. Terminal acetylenes tend to be far more reactive in this process, although certain systems, including the Trost's ruthenium catalyst,[361g] do perform well with the more challenging internal alkynes.

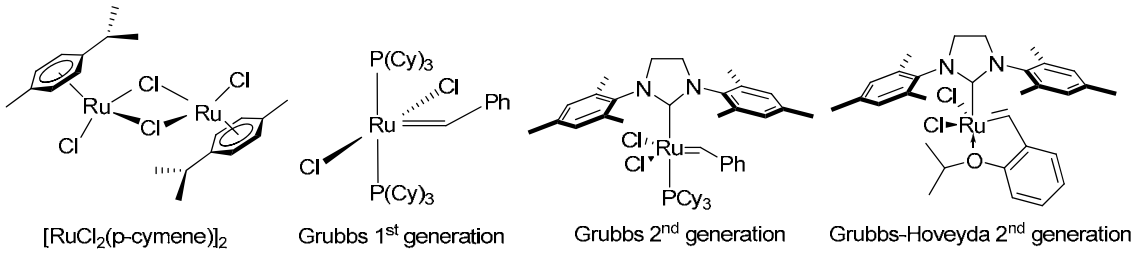

Scheme 112. Ruthenium complexes applied for the hydrosilylation of alkynes.

---

[360] (a) Speier, J. L.; Webster, J. A.; Barnes, H. H. *J. Am. Chem. Soc.* **1957**, *79*, 974. (b) Chandra, G.; Lo, P. Y.; Hitchcock, P. B.; Lappert, M. F. *Organometallics* **1987**, *6*, 191. (c) Karstedt, B. D. U.S. Patent 3 775 452, **1973**. (d) Stein, J.; Lewis, L. N.; Gao, Y.; Scott, R. A.; *J. Am. Chem. Soc.* **1999**, *121*, 3693. (e) Rooke, D. A.; Ferreira, E. M. *Angew. Chem. Int. Ed.* **2012**, *51*, 3225.

[361] For the early work, see: a) Esteruelas, M. A.; Herrero, J.; Oro, L. A. *Organometallics* **1993**, *12*, 2377. For later work, see: (b) Na, Y.; Chang, S. *Org. Lett.* **2000**, *2*, 1887. (c) Maifeld, S. V.; Tran, M. T.; Lee, D. *Tetrahedron Lett.* **2005**, *46*, 105. (d) Menozzi, C.; Dalko, P. I.; Cossy, J. *J. Org. Chem.* **2005**, *70*, 10717. (e) Arico, C. S.; Cox, L. R. *Org. Biomol. Chem.* **2004**, *2*, 2558. (f) Trost, B. M.; Ball, Z. T. *J. Am. Chem. Soc.* **2001**, *123*, 12726. (g) Trost, B. M.; Ball, Z. T. *J. Am. Chem. Soc.* **2005**, *127*, 17644.

It is worth mentioning that rhodium complexes were also found as catalysts for the hydrosilylation of internal alkynes.[362] As a separate but related research, Albrecht and coworkers[363] have just published their results applying NHC-Rh catalysts for the hydrosilylation of ketones affording the corresponding silyl ethers.

In order to achieve regio- and/or stereocontrol and, presumably, also recycling of the precious catalysts, platinum species have been immobilized on diverse organic polymers.[364] It is found that control of the stereochemical outcome of the hydrosilylation is indeed possible by the choice of suitable solvent and donor functions present within the polymer matrix;[364a] platinum nanoparticle-decorated polyaniline exhibits excellent catalytic properties toward hydrosilylation of substituted aryl alkynes;[364b] however, in these two cases, the authors did not report the recyclability of the platinum catalysts. In order to develop recyclable platinum catalyst in hydrosilylation of alkynes, efforts have been directed, among other solutions, to supporting the platinum on carbon,[365] magnesium oxide[366] and γ-alumina. However, thus far all proved less than ideal.[367] Promisingly, the platinum nanoparticles supported on silica[368] and titania[369] could be reused although the yield of the catalytic runs decreased notably after the fourth cycle. It is worth noting that platinum impregnated on magnetite was recently developed as recyclable catalyst, with the ability of being reused up to 9 times without significant loss of activity.[370] Interestingly, Khlobystov and co-workers just disclosed their results on applying the hollow graphitized carbon nanofibers as nanoscale reactors for the hydrosilylation of terminal alkynes, in which the specific π-π interaction between the aromatic reactants and the aromatic nanofiber channel promotes the formation of the (*E*)-isomer of the β-addition product under catalysis by Rh NPs.[371]

---

362 (a) Sanada, T.; Kito, T.; Mitani, M.; Mori, A. *Adv. Synth. Catal.* **2006**, *348*, 51. (b) Field, L. D.; Ward, A. J. *J. Organomet. Chem.* **2003**, *681*, 91.

363 Monney, A.; Albrecht, M. *Chem. Commun.* **2012**, 48, 10960.

364 (a) Hagio, H.; Sugiura, M.; Kobayashi, S. *Synlett* **2005**, 813. (b) Shih, H.-H.; Williams, D.; Mack, N. H.; Wang, H.-L. *Macromolecules* **2009**, *42*, 14.

365 Chauhan, M.; Hauck, B. J.; Keller, L. P.; Boudjouk, P. *J. Organomet. Chem.* **2002**, *645*, 1 and literature quoted therein.

366 Ramírez-Oliva, E.; Hernandez, A.; Martínez-Rosales, J. M.; Aguilar-Elguezabal, A.; Herrera-Perez, G.; Cervantes, J. *ARKIVOC* **2006**, *v*, 126.

367 Polizzi, C.; Caporusso, A. M.; Vitulli, G.; Salvatori, P.; Pasero, M. *J. Mol. Catal.* **1994**, *91*, 83.

368 (a) Brook, M. A.; Ketelson, H. A.; LaRonde, F. J.; Pelton, R. *Inorg. Chim. Acta* **1997**, *264*, 125. (b) Jimenez, R.; Martínez-Rosales, J. M.; Cervantes, J. *Can. J. Chem.* **2003**, *81*, 1370.

369 Alonso, F.; Buitrago, R.; Moglie, Y.; Ruiz-Martínez, J.; Sepulveda-Escribano, A.; Yus, M. *J. Organomet. Chem.* **2011**, *696*, 368.

370 Cano, R.; Yus, M.; Ramon. D. J. *ACS Catal*. **2012**, *2*, 1070.

371 Solomonsz, W. A.; Rance, G. A.; Suyetin, M.; La Torre, A.; Bichoutskaia, E.; Khlobystov, A. N. *Chem. Eur. J.* **2012**, *18*, 13180.

4.1.1.2 Mechanistic aspects

A number of publications discussed the catalytic mechanism for the hydrosilylation of alkynes.[371,372] The mechanism generally accepted nowadays, originally proposed for classical platinum catalysts by Chalk and Harrod,[372a] and later modified by Crabtree and Ojima, is often referred to as Crabtree-Ojima cycle (Scheme 113).[372b,c]

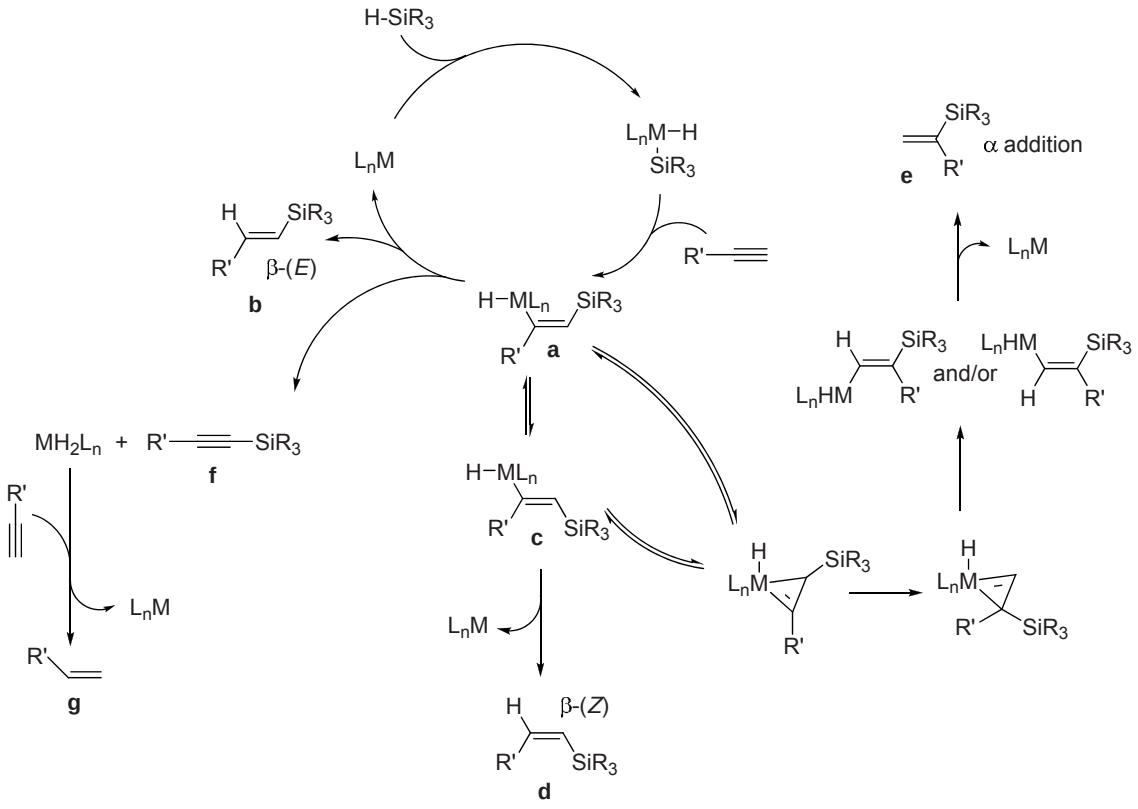

Scheme 113. Mechanism proposed for the metal-catalyzed hydrosilylation of alkynes.

The catalytic cycle begins with oxidative addition of Si-H to the metal complex (ML_n), followed by a *syn*-insertion of the alkyne into the M-Si bond affording an intermediate **a**, from which the β-(*E*) vinylsilane **b** is obtained by a reductive elimination (Scheme 113). However, alternatively, the intermediate **a** can relieve steric *cis*-repulsion within the olefinic system between the metal-containing group and the silyl group *via* double bond isomerization to form intermediate **c** (Scheme 113). With a reductive elimination process, the intermediate **c** releases the metal giving the β-(*Z*) product **d** (Scheme 113). Furthermore, the η^1-vinylmetal intermediates, either **a** or **c,** could be transformed into

[372] (a) Chalk, A. J.; Harrod, J. F. *J. Am. Chem. Soc.* **1965**, *87*, 16. (b) Tanke, R. S.; Crabtree, R. H. *J. Am. Chem. Soc.* **1990**, *112*, 7984. (c) Ojima, I. In *The Chemistry of Organic Silicon Compounds;* Patai, *S.;* Rappoport, Z. Eds.; Wiley: New York, **1989**, **p** 1479. (d) Lewis, L. N.; Stein, J.; Gao, Y.; Colborn, R. E.; Hutchins, G. *Platinum Metals Rev.* **1997**,*41*, 66. (e) Lewis, L. N.; Uriarte, R. J. *Organometallics* **1990**, *9*, 621.

an η^2 form, which experiences a rearrangement and subsequent opening to give a new η^1-vinylmetal intermediate with either *cis* or *trans* stereochemistry.[372c] This explains the formation of the α addition product **e** by reductive elimination from this new η^1-vinylmetal intermediate (Scheme 113). It was also suggested that intermediate **a** can also undergo metal hydride β-elimination, resulting in the formation of the dehydrogenative product **f** and along with a metal dihydride species (MH_2), the reaction of which with the terminal alkyne would give rise to the alkene **g** (Scheme 113). Incidentally, the multiple reaction paths, with the divergent outcomes shown in Scheme 113 were used by Khlobystov and co-workers[371] to rationalize the variety of products obtained during the hydrosilylation runs catalyzed by Rh species confined within carbon nanotubes (CNT). Interestingly, the relative ratio of the products **b**, **d**, **g**, **e** and **f** was found to be affected by confinement effects.

4.1.1.3 Precedents in our research group

We have recently[318,320] developed an efficient and stereoselective *syn* addition of silanes to internal alkynes, providing (*E*)-vinylsilanes in excellent yields, by the use of Pd NPs stabilized by tris-imidazolium tetrafluoroborates as catalysts under a dry inert atmosphere. Fair to good regioselectivities have been achieved in the case of asymmetric alkynes. The addition of controlled amounts of water to the silylation mixture promotes the oxidative hydrolysis of silanes with the concomitant formation of dihydrogen, leading to a competitive process of transfer hydrogenation of the alkynes to the (*Z*)-alkenes or the corresponding alkanes depending on the amount of water and the nature of the acetylenic substrates (Scheme 114). To the best of our knowledge, this is the first report of Pd NPs involved in hydrosilylation reactions of internal alkynes, substrates that are much less reactive than the terminal acetylenes and which have received less attention in the literature.[373]

[373] Results related to this topic are not included in this manuscript. Althought I coauthored this work, the corresponding article is added in the annex. My main contributions to the research involved: 1) to repeat the procedures to prepare the Pd NPs (see article annex, Scheme 1); 2) to repeat some reactions previously performed by Dr. Marc Planellas (see article annex, Table 1, entries 9-11; Table 6, entries 3-4); 3) to broaden the reaction scope to 1-methoxy-4-(phenylethynyl)benzene and 1-methyl-3-(phenylethynyl)benzene including the preparation of the corresponding asymmetric alkynes as starting substrates (see article annex, Table 4, entries 3 and 5); 4) to help to design and perform reactions for the confirmation of the formation of hydrogen in the hydrogenation process (see article annex, footnote 24); 5) to draft the electronic supporting information of the manuscript. All the research involved in this article has been performed during my PhD student stage.

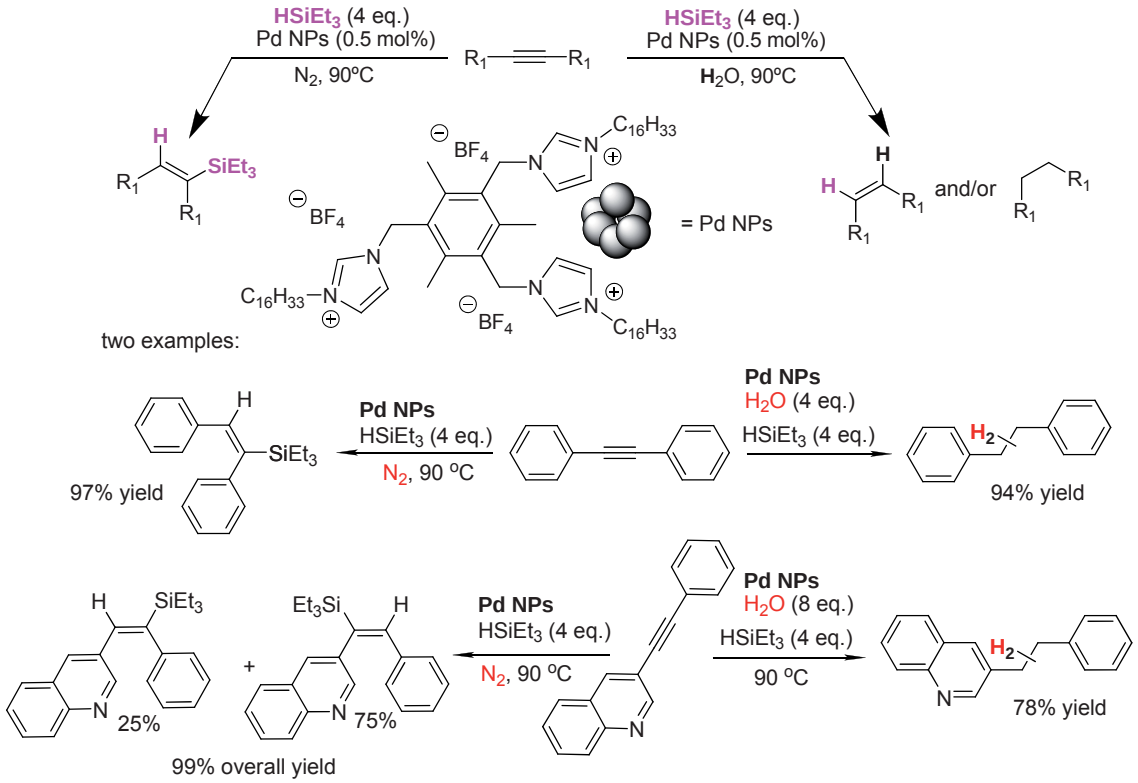

Scheme 114. Hydrosilylation and hydrogenation of internal alkynes under catalysis by Pd NPs stabilized by tris-imidazolium tetrafluoroborates.

4.1.2 Results and Discussion

4.1.2.1 Preparation of internal alkynes as starting materials

The Sonogashira reaction is frequently used for the preparation of internal alkynes.[374] The classical Sonogashira reaction employs a palladium/copper catalyst to form a new C-C bond between a terminal alkyne and an aryl or vinyl halide and the proposed mechanism is shown in Scheme 115a.[374h] The palladium-based cycle (cycle A) begins with the oxidative addition of the aryl halide to the coordinatively unsaturated PdL_n species formed in the pre-activation step. The $[L_nPd(II)R^1X]$ adduct is then transformed into the acetylide species $[L_nPd(II)\ R^1(C{\equiv}CR^2)]$ after transmetalation with a copper acetylide formed in the copper-based cycle (cycle B, Scheme 115a). A base,

[374] (a) Sonogashira K. *J. Organomet. Chem*. **2002**, *653*, 46. (b) Sonogashira, *K. In Handbook or Organopalladium Chemistry for Organic Synthesis*, vol. 1, p 493. Negishi, E. Ed.; John Wiley & Sons: New York, **2002**. (c) Negishi, E.; Anastasia, L. *Chem Rev*. **2003**, *103*, 1979. (d) Jutand, A. *Pure Appl. Chem*. **2004**, *76*, 565. (e) Alacid, E.; Alonso, D. A.; Botella, L.; Nájera, C.; Pacheco, M. C. *Chem. Rec*. **2006**, *6*, 117. (f) Doucet, H.; Hierso, J. -C. *Angew. Chem. Int. Ed*. **2007**, *46*, 834. (g) Chinchilla, R.; Nájera, C. *Chem. Rev*. **2007**, *107*, 874. (h) Chinchilla, R.; Nájera, C. *Chem. Soc. Rev*. **2011**, *40*, 5084. (i) Evano, G.; Blanchard , N.; Toumi, M. *Chem. Rev*. **2008**, *108*, 3054. McGlacken, G. P.; Fairlamb, I. J. S. *Eur. J. Org. Chem*. **2009**, 4011.

either organic or inorganic, is thought to assist in the copper acetylide formation via deprotonation of the acidified copper π-alkyne complex.[374h] The Pd catalyst is regenerated in cycle A by a reductive process offering the desired alkyne.

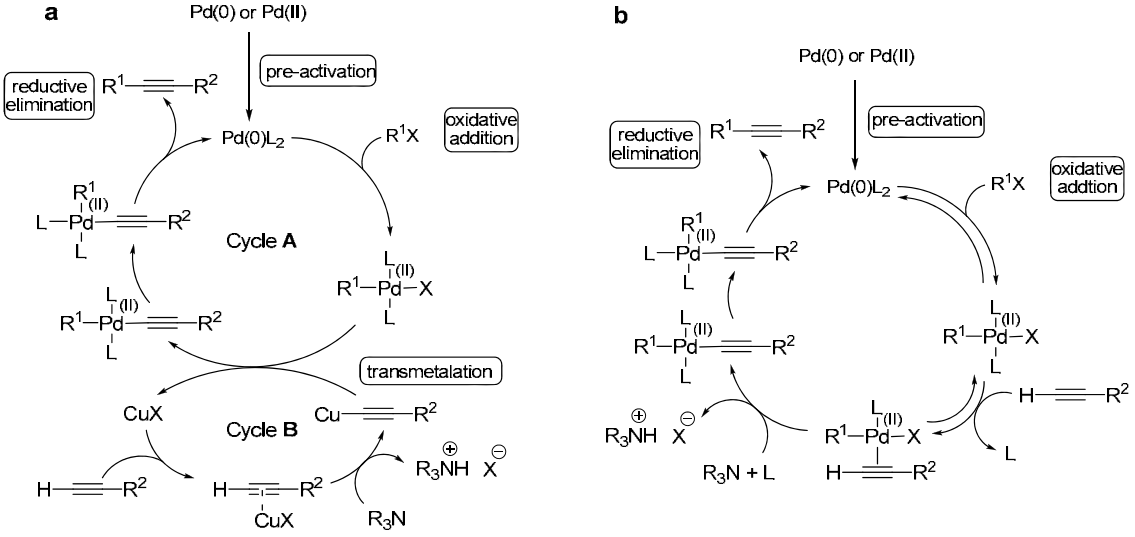

Scheme 115. Mechanism of the Sonogashira reaction: a) under catalysis by palladium and copper; b) under catalysis by palladium.

It should be noted that, in some cases, the incorporation of copper catalyst can induce the homocoupling of the terminal alkynes, thus leading to low yields of the desired internal alkynes.[375] Alternative protocols for copper-free Sonogashira coupling reactions have been developed recently, with good results obtained.[376] The suggested catalytic cycle (Scheme 115b) starts by the oxidative addition of the aryl halide to the catalytic species $[Pd(0)L_2]$. The next step is a reversible π-coordination of the alkyne to the Pd center to give an alkyne-Pd(II) complex where the acetylenic proton becomes more acidic, thus facilitating its removal by the base, leading to the η^1 alkyne-metal complex. The target internal alkyne is released from the $[Pd(II)R^1(C \equiv CR^2)L_2]$ complex after a reductive elimination process, with the regeneration of catalyst $[Pd(0)L_2]$.

Interestingly, improving upon the classical two-step process, Grieco and co-workers[377] prepared some internal alkynes in one pot, through *in situ* deprotection of trimethylsilylethynylene-added intermediates, following a palladium/copper procedure,

---

375 Siemsen, P.; Livingston, R. C.; Diederich, F. *Angew. Chem. Int. Ed.* **2000**, *39*, 2632.

376 See this article and the references therein: Shi, S.; Zhang, Y. *Synlett* **2007**, 1843.

377 Mio, M. J.; Kopel, L. C.; Braun, J. B.; Gadzikwa, T. L.; Hull, K. L.; Brisbois, R. G.; Markworth, C. J.; Grieco, P. A. *Org. Lett.* **2002**, *4*, 3199.

by the reaction of (trimethylsilyl)acetylene with aryl iodides in the presence of an amidine base (DBU), $PdCl_2(PPh_3)_2$, CuI and a substoichiometric amount of water. We followed this protocol to prepare some symmetric alkynes, as summarized in Table 18.

Table 18. Preparation of symmetric internal alkynes following the Sonogashira method developed by Grieco and co-workers.[a]

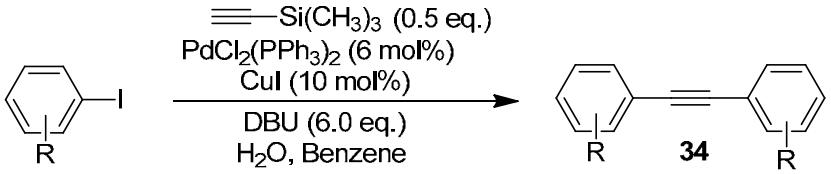

Entry	temperature / ºC	Product		Yield / %[b]
1	60	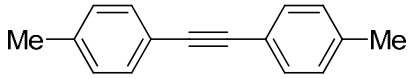	**34a**	91
2	60	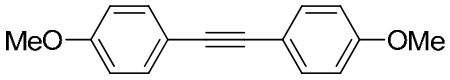	**34b**	54
3	rt	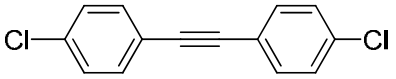	**34c**	57
4	rt	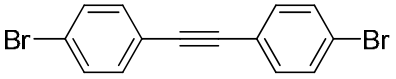	**34d**	63
5	rt	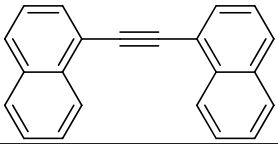	**34e**	62

[a] All reactions were stirred overnight in the absence of light with a 0.2 M solution of aryl halide in benzene using 6 mol% $PdCl_2(PPh_3)_2$, 10 mol% CuI, 6.0 eq. of DBU, 40 mol% water, and 0.5 eq. of (trimethylsilyl)acetylene (all relative to 1 eq. of aryl halide). [b] Isolated yield.

Generally, the aryl iodides with electron-donating groups (methyl, methoxy) are less reactive in the C-C cross-coupling in comparison to those with electron-withdrawing groups, such as chloro and bromo substituents. Indeed, following Grieco's procedure,[377] the coupling reactions with *p*-methyiodobenzene and *p*-methoxyiodobenzene as substrates were performed at 60 ºC (Table 18, entries 1-2) affording the corresponding symmetric alkynes **34a** and **34b** in yields similar to those obtained by Grieco *et al*. On the other hand, in our hands the syntheses of 1,2-bis(4-chlorophenyl)ethyne **34c** (Table 18, entry 3) and 1,2-bis(4-bromophenyl)ethyne **34d** (Table 18, entry 4) (performed at room temperature) afforded the isolated yields in 57% and 63%, far below the reported 89% and 99%. When 1-iodonaphthalene was used as substrate, a 62% isolated yield of **34e** was obtained from the reaction at room temperature.

Dr. Marc Planellas in our group previously prepared asymmetric internal alkynes[318,320] employing a copper-free Sonohashira protocol developed by Zhang *et al.*[376] (Table 19, entries 1-5). This method uses NaOH as a base and $Pd(OAc)_2$ as a catalyst, and provided a variety of internal alkynes bearing either electron-donating groups or electron-withdrawing groups with excellent isolated yields. Following the same procedure, the internal alkynes 1-nitro-4-(phenylethynyl)benzene (Table 19, entry 6) and 1,2-di(thiophen-3-yl)ethyne (Table 19, entry 7) were prepared as part of this doctoral work.

Table 19. Sonogashira coupling between aryl halides and terminal alkynes under catalysis by $Pd(OAc)_2$.[a]

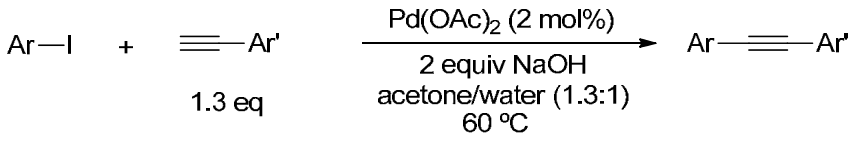

Entry	iodoarene	Ar'	Product	Yield (%)[b]
1[c]	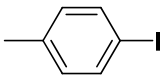	Ph	**35a** 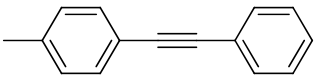	85
2[c]	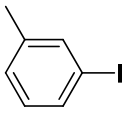	Ph	**35b** 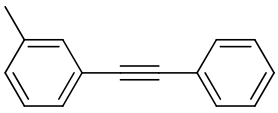	84
3[c]	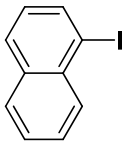	Ph	**35c** 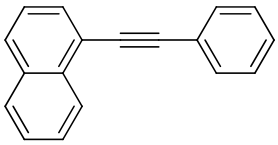	91
4[c,d]	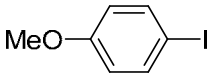	Ph	**35d** 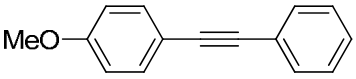	71
5[c]	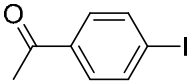	Ph	**35e** 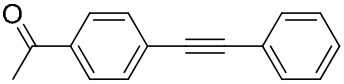	71
6	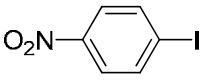	Ph	**35f** 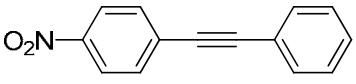	51
7	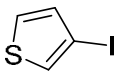	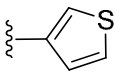	**35g** 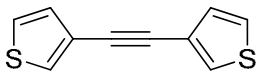	73

[a] Monitoring of the reaction by GC; 1.3 eq. of terminal alkyne used with respect to aryl halide. [b] Isolated yield. [c] Internal alkynes prepared by Marc Planellas.[318,320] [d] This process was repeated in this thesis.

4.1.2.2 Hydrosilylation of symmetric internal alkynes by Rh nanoparticles

With the Rh NPs **M7**-**M11** in hand, hydrosilylation of diphenylacetylene with Et_3SiH was chosen as the model reaction to test the Rh NPs as catalysts under a range of conditions (Table 20). An excess of silane (4 eq.) was utilized, given that neat silane was previously found to be the best reaction medium in the case of the hydrosilylation catalyzed by Pd NPs in our group.[320] Thus, diphenylacetylene was treated with neat triethylsilane in the presence of **M11** (0.5 mol% Rh) as catalyst at 90 ºC under inert atmosphere overnight. We were delighted to see that, after complete conversion of the alkyne (gauged by GC), the corresponding *syn*-addition product **36a** was selectively obtained in quantitative yield (Table 20, entry 1).

Table 20. Optimization of the reaction conditions for the hydrosilylation of diphenylacetylene with triethylsilane under Rh NPs catalysis.

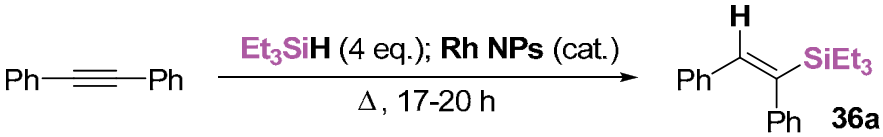

Entry[a]	Cat.	mol% Rh	Solvent / mL	T / ºC	Conv. / %	Yield / %[b]
1[c]	**M11**	0.5	-	90	>99	99
2	**M11**	0.5	-	60	>99	99
3	**M11**	0.5	-	40	19[d]	17[d]
4[e]	**M11**	0.1	-	60	>99	99 (TON = 990)
5	**M11**	0.5	H_2O/0.036	60	>99	99
6[f]	**M11**	0.5	-	60	>99	99
7[f]	**M11**	0.5	EtOH / 1	60	>99	99
8[f]	**M11**	0.5	$CHCl_3$ / 1	60	>99	99
9[f]	**M10**	0.5	-	60	>99	99
10[f]	**M9**	0.5	-	60	0	-
11[f]	**M8**	0.5	-	60	0	-
12[f]	**M7**	0.5	-	60	0	-
13[f]	-	-	-	60	0	-

[a] Performed in closed vessels (15 mL) with 0.5 mmol of alkyne and $HSiEt_3$ (0.320 mL, 2 mmol). [b] Isolated yield. [c] Experiments of entries 1-5 were performed under dry N_2 atmosphere. [d] Determined by GC with undecane as internal standard. [e] Performed with 6.0 mmol scale. [f] Experiments of entries 6-13 were performed without any special precautions with respect to air and moisture.

To our delight, lowering the reaction temperature to 60 ºC led to full conversion and complete selectivity towards the (*E*)-(1, 2-diphenylvinyl)triethylsilane (**36a**) product

(Table 20, entry 2). However, further decreasing the temperature to 40 ºC gave only 19% of conversion after 20 h. (Table 20, entry 3). Notably, the reaction with only 0.1 mol% Rh was also successful, resulting in full conversion and selectivity (Table 20, entries 4). In this case, the turnover number (TON) was calculated to reach a value of 990 (moles of product /moles of catalyst used). We also wondered whether the addition of water to the reaction mixture would lead to the formation of the hydrogenated product, as previously observed using Pd NPs.[320] Thus, an analogous experiment with the addition of water (2 mmol, 4 eq.) was performed using the new Rh catalyst under inert atmosphere (Table 20, entry 5). However, unlike the Pd-based protocol, no hydrogenated product could be detected, leading, once again, to a 99% yield of the hydrosilylation product, indicating that the behavior of this catalytic system is different from that of Pd NPs. The reaction in the absence of the N_2 atmosphere protection (Table 20, entry 6) proved also effective. What's more, the addition of other solvents such as ethanol or chloroform did not have any deleterious effect (Table 20, entries 7-8). The catalytic activity of the Rh NPs **M10** was found to be similar to that of **M11** (Table 20, entry 9). Surprisingly, no conversion was observed when the catalyst was changed to **M9**, **M8** or **M7** (Table 20, entries 10-12). This may be attributed to higher content of stabilizer present in **M7-M9**, resulting in lower catalytic activities, which is in concordance with other reports.[378] A control experiment also showed that no hydrosilylation took place in the absence of any catalyst (Table 20, entry 13).

In an attempt to broaden the scope of the catalytic hydrosilylation, we also tested a nitrile and a ketone as substrates. The Rh NPs **M11** showed no activity under the optimized conditions, *i. e.*, 4 eq. of silane and 60 ºC, for the hydrosilylation of benzonitrile and acetophenone (Scheme 116). This lack of activity showed that the catalysts have potential to reduce alkynes bearing other potentially reducible groups.

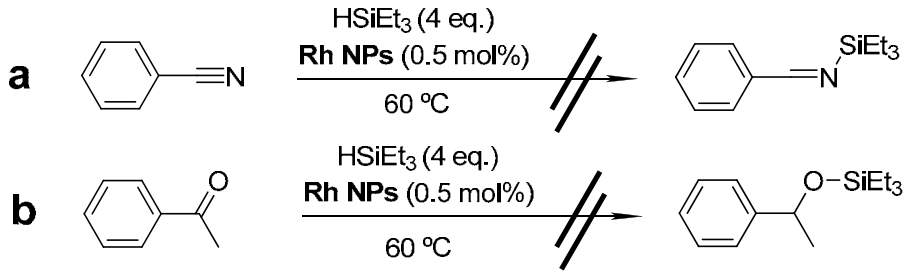

Scheme 116. Attempts failed for the hydrosilylation of benzonitrile (a) and acetophenone (b).

[378] (a) Liu, L.; Sun, G.; Wang, C.; Yang, J.; Xiao, C.; Wang, H.; Ma, D.; Kou, Y. *Catal. Today* **2012**, *183*, 136. (b) Yan, N.; Yuan, Y.; Dyson, P. J. *Dalton Trans.* **2013**, *42*, 13294. (c) Barkhuizen, D.; Mabaso, I.; Viljoen, E.; Welker, C.; Claeys, M.; van Steen, E.; Fletcher, J. C. Q. *Pure Appl. Chem.* **2006**, *78*, 1759.

Considering the good results obtained with the alkynes under catalysis by Rh NPs, we wanted to compare our system with other commercial rhodium catalysts, including rhodium on alumina, dirhodium tetraacetate and rhodium trichloride. As listed in Scheme 117, all the three rhodium catalysts worked very well in the hydrosilylation of diphenylacetylene providing quantitative yields of hydrosilylation products under the optimized conditions. Nonetheless, our rhodium nanoparticles are still attractive due to their recyclability and water solubility.

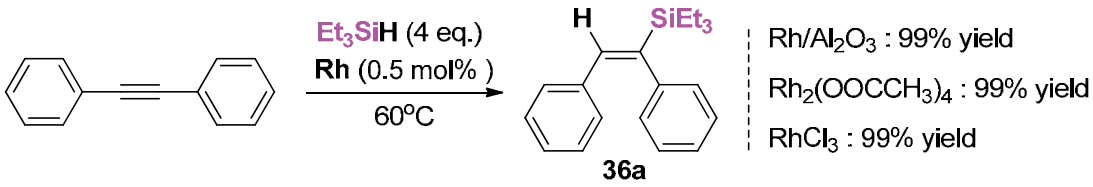

Scheme 117. Hydrosilylation of diphenylacetylene with commercial rhodium catalysts.

The product **36a** can be distinguished from its *anti*-addition isomer employing selective 1D NOE NMR experiments. A 3D model shows that the distances between the vinyl proton and the CH_2 and/or CH_3 of the ethyl group are relatively short for the (*E*)-(1,2-diphenylvinyl)triethylsilane **36a** and, therefore, a NOE effect would be expected. However, for its (*Z*) isomer, the distances are at the limit or even too long to observe the NOE effect. As can be seen in Figure 38, a NOE effect was indeed observed in the methylene and methyl signals when irradiating the signal of vinylic proton at 6.8 ppm, confirming the *syn*-addition configuration.

Having established Rh NPs **M10** and **M11** as the best catalysts, **M11** was chosen as the representative to achieve the hydrosilylation of a variety of symmetrical internal alkynes (Table 21) under the optimized conditions (0.5 mol% Rh, 4 eq. of silane, 60ºC). This catalyst proved to be highly efficient and selective, furnishing the corresponding diaryl (*E*)-alkenylsilanes in excellent yields for substrates bearing either electron-donating or electron-withdrawing substituents in the *para* position of the Ar groups (Table 21, entries 1-5). Efficient hydrosilylation was also achieved for the symmetric bis-naphthyl and bis-thienyl alkynes (Table 21, entries 6-7). Non-aromatic substrates were also successfully tested (Table 21, entries 8-9). Only in one case (Table 21, entry 2), about 8% of the *anti*-addition product was detected by GC. It should be noted that the hydrosilylation reactions of *p*-methoxy, *p*-chloro and *p*-bromo substituted diphenylacetylene (Table 21, entries 3-5) were not accomplished at 60ºC, but worked

very well when the temperature was increased to 90ºC, which may be due to the higher melting points of the substrates resulting in insolubility in the reaction system.[377,379]

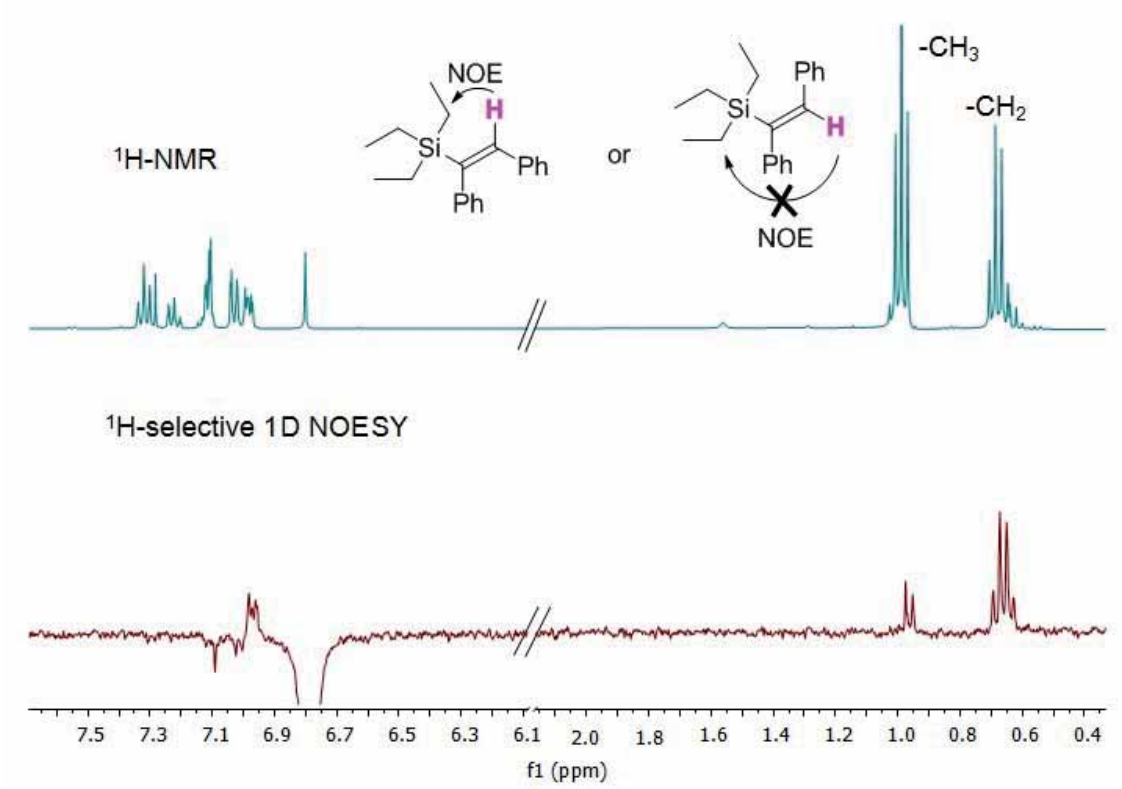

Figure 38. Compound **36a** was distinguished from its *anti*-addition isomer with NOESY NMR experiments.[320]

Next, the hydrosilylation of diphenylacetylene with other silanes was examined under the same conditions. The reactions with triethoxysilane and triphenylsilane (Table 21, entries 10-11) also proceeded with high stereoselectivity, albeit a longer reaction time was required for the full consumption of the starting alkynes. Under these conditions, the corresponding *syn*-addition products were isolated with quantitative yields. For the reactions involving volatile silanes (Table 21, entries 1-10), the work-up consisted in filtering the reaction mixture through a pipette with a short plug of silica-gel using hexane as eluent, and then removing the solvent and excess reagent by evaporation under an air flow, to afford a product that did not require any further purification.

[379] Alkynes of **36c**, **36d** and **36e** possess melting points of 142 °C, 179 °C and 186 °C, respectively, which are significantly higher than those of 61 °C of **36a**, 136 °C of **36b**, 125 °C of **37** and 96 °C of **38** (see experimental section for details).

Table 21. Hydrosilylation of symmetric alkynes under catalysis by Rh NPs **M11**.

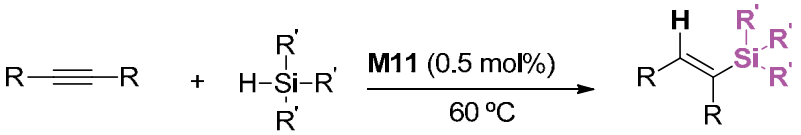

Entry[a]	Product	Time / h	Yield / %[b]
1	**36a**: R" = H	15	99
2[c]	**36b**: R" = Me	19	94
3[d]	**36c**: R" = OMe	21	97
4[d]	**36d**: R" = Cl	20	97
5[d]	**36e**: R" = Br	19	95
6	**37**	19	93
7	**38**	6	97
8	**39**	40	96
9	**40**	20	99
10	**41a**: R'= OEt	36	99
11[e]	**41b**: R'= Ph	36	99

[a] Performed in closed vessels (15 mL) with 0.5 mmol of alkyne and 2.0 mmol of silane. [b] Isolated yield. [c] About 8% of *anti* addition product was detected by GC. [d] Performed at 90 ºC. [e] Chromatographic purification needed to remove the excess of silane.

Before turning to the hydrosilylation of asymmetric alkynes, the recyclability of the Rh NPs **M11** was investigated. The stabilizer bears three PEG-chains, making the Rh NPs insoluble in diethyl ether. Therefore, the hydrosilylation product can be extracted with diethyl ether from the reaction mixture, leaving the catalyst of Rh NPs insoluble to be used for the next run. Thus, the hydrosilylation of diphenylacetylene catalyzed by **M11** was chosen as the model to check the recyclability of the Rh NPs. The recycling procedure and the results obtained are shown in Table 22. Specifically, once the reaction is completed (Table 22a), diethyl ether was added to the reaction mixture and then it was centrifuged at 4000 rpm for 10 minutes (Table 22b). The supernatant was

transferred and filtered through a short silica-gel plug (Table 22c) affording the oily product (Table 22d) after the removal of the solvent under an air flow. The catalyst remaining in the reaction vessel was ready for the next run. Promisingly, the catalyst can be recycled for 6 times with quantitative isolated yields and without any loss of activity. The 7th reusage gave a lower yield of 80% under the same reaction time with the recovery of 20% of starting material. This last result should be ascribed to the loss of some catalyst during the work-up.

Table 22. The recyclability assay of **M11** for the hydrosilylation of diphenylacetylene.

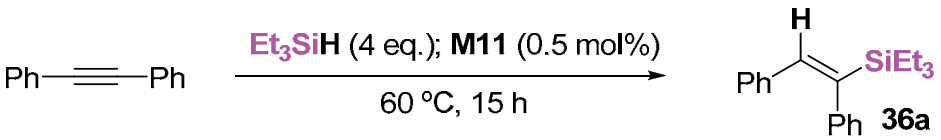

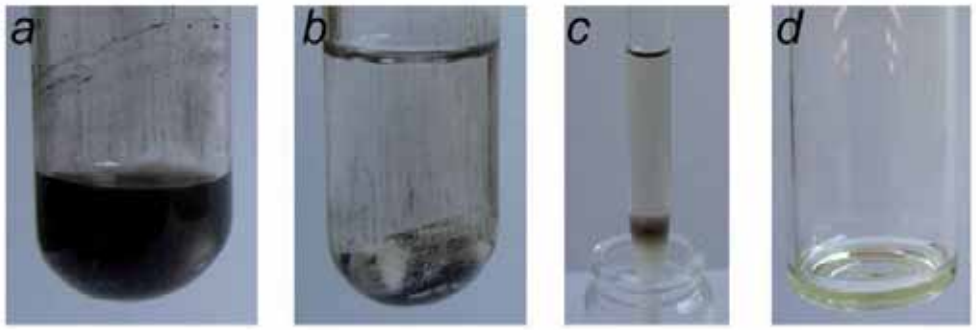

Cycle	1st	2nd	3rd	4th	5th	6th	7th
Yield / %^{e}	99	99	99	99	99	99	80^{f}

^{a} Reaction mixture after stirred 15 h. ^{b} Et_2O was added to the reaction mixture and it was centrifuged for 10 minutes at 4000 rpm. ^{c} The supernatant was transferred to a pipette filled with a small plug of silica gel. ^{d} The filtrate after removal of solvents and extra silane afforded the oily product. ^{e} Isolated yields. ^{f} Corrected GC yield with undecane as internal standard.

4.1.2.3 Hydrosilylation of unsymmetric alkynes by rhodium nanoparticles

Next, the nanocatalyst **M11** was used in the hydrosilylation of various unsymmetric internal alkynes (Table 23). In this case, four different vinylsilanes could be envisaged, with two stereoisomers (*syn* and *anti* addition) possible for each of the two regioisomeric forms. Although the expected *syn* preference might reduce this number to two, a reasonable degree of regioselectivity would only be possible for substrates with the two sides clearly differentiated.

Table 23. Hydrosilylation of unsymmetric diarylalkynes under catalysis by **M11**[a].

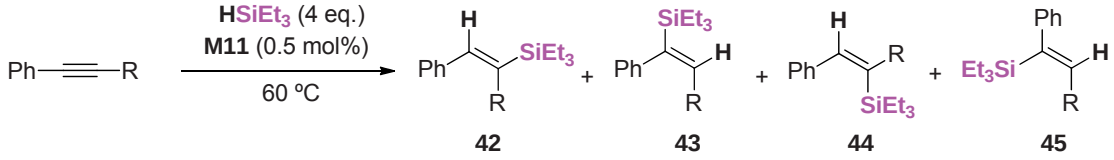

Entry	R	Time (h)	Products[b]	Yield (%)[c]
1	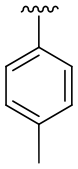	58	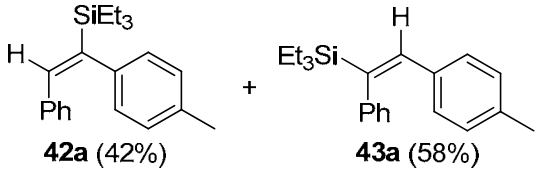 **42a** (42%) + **43a** (58%)	99
2	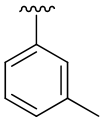	20	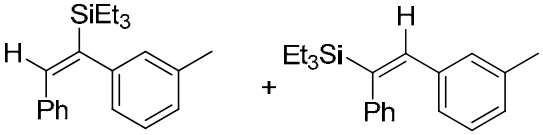 **42b** (45%) + **43b** (55%)	99
3	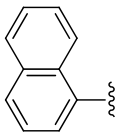	60	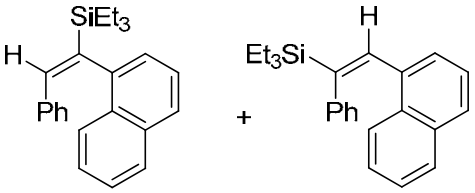 **42c** (88%) + **43c** (12%)	99
4	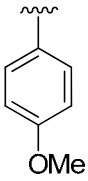	30	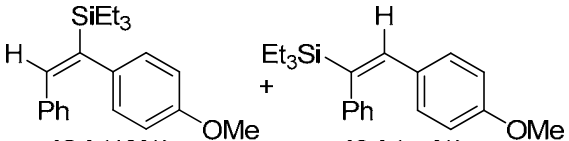 **42d** (43%) + **43d** (57%)	99
5[d]	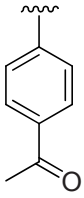	20	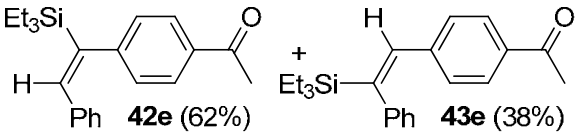 **42e** (62%) + **43e** (38%)	99
6[d,e,f]	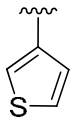	14	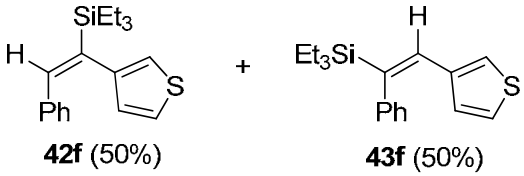 **42f** (50%) + **43f** (50%)	99

7[d]	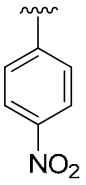	30	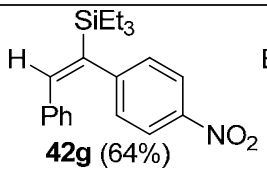 **42g** (64%) + 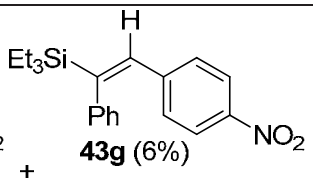 **43g** (6%) 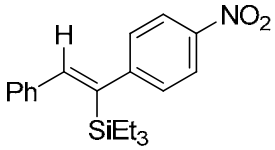 **44g** (20%) 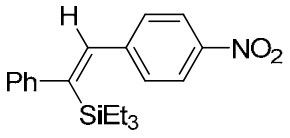 **45g** (10%)	76

[a] Performed in closed vessels (15 mL) with 0.5 mmol of alkyne under air. [b] The structural assignment of the isomers was performed by NMR techniques and the ratio was determined by GC. [c] Isolated yield. [d] An isomerisation process takes place by standing in the air for some days. [e] Difficult to assign the signals of the two isomers by NMR techniques. [f] The starting alkyne, 3-(phenylethynyl)thiophene, was prepared by Marc Planellas.[318]

We started with the hydrosilylation of unsymmetric diaryl alkynes (Table 23, entries 1-7) prepared by Dr. Marc Planellas with the described method as mentioned in Section 4.1.2.1. Indeed, as previously observed in our group for the Pd catalysis,[320] in most cases the reactions (Table 23, entries 1-6) afforded a mixture of two *syn* regioisomeric vinylsilanes, although with a remarkably respectable selectivity for the substrate bearing a phenyl and 1-naphthyl substituents (Table 23, entry 3). In agreement with the previous finding,[320] a 62:38 mixture of the two regioisomers **42e** and **43e** was obtained in entry 5, suggesting an electron-withdrawing effect of the acetyl group on the regioselectivity. As an exception, the hydrosilylation of the substrate bearing a nitro substituent (Table 23, entry 7) gave a mixture of the four different products **42g**, **43g**, **44g** and **45g** with a lower overall isolated yield of 76%, with a predominant percentage of 64% of the *syn* regioisomer **42g**. It should be noted that the isolated mixture of the *syn* addition products **42e** and **43e** (Table 23, entry 5) experienced a spontaneous isomerization upon standing at room temperature for several days, leading to four isomers being recognized by the GC analysis and 2D NMR techniques (see Annex). A similar phenomenon occurred to the mixture of **42f** and **43f** (Table 23, entry 6). In this case, however, using the NMR techniques is very difficult to assign the signals of the four isomers formed after the isomerization. In light of these observations, care was taken to analyze the product distribution immediately upon completion of the reaction, since the initially formed mixture of the two *syn* addition regioisomers can, in some cases, undergo a slow isomerization to a thermodynamic mixture of all 4 possible isomers.

In Figure 39 a representative example of the GC chromatogram trace of a fresh reaction mixture is shown, corresponding to entry 2 of Table 23. It could be seen that the starting alkyne, located at about 5 min was fully consumed resulting in the quantitative formation of regioisomers **42b** and **43b** together with traces of side products derived from the triethylsilane (triethylsilanol and $Et_3SiOSiEt_3$). All of the side products including the excess triethylsilane can be removed by evaporation under the air flow.

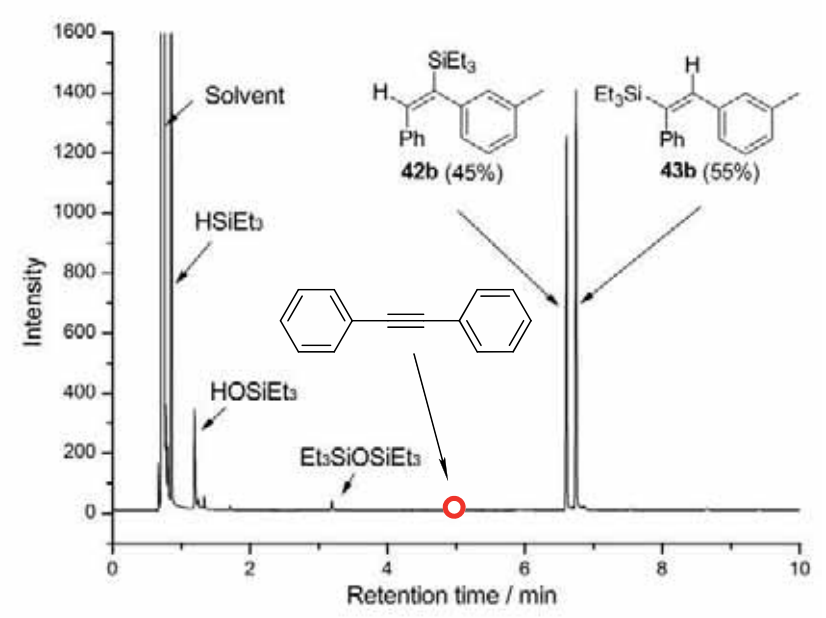

Figure 39. GC chromatogram traces of the fresh reaction mixture of entry 2 in Table 23.

Then we moved to differentiated unsymmetric alkynes (Table 24) and we assayed first an alkyne bearing an alkyl and aryl substituent. Selective *syn* addition took place in the reaction of triethylsilane with (prop-1-yn-1-yl)benzene, giving a 45:55 mixture of **46a** and **47a** (Table 24, entry 1). Then two substrates bearing alkyl substituents and functional groups were tested under the present reaction conditions (Table 24, entries 2-3). For 5-decyn-1-ol, preliminary experiments showed that the silylation took place both at the alkyne and the hydroxyl groups, furnishing a complex mixture. Thus, another test with more triethylsilane (6 eq.) led to a mixture of the two regioisomers **46b** and **47b** (ratio about 50:50 from GC). It was impossible to assign univocally the signals to each one of the isomers by 2D NMR techniques (see annex). This finding is very different from our previous results[320] with Pd NPs as catalysts (Scheme 118). Thus, with the reactions run using Pd NPs no alkyne hydrosilylation had taken place, giving, instead a formally hydrogenated *Z*-alkene product, presumably due to the hydrogen formed during alcohol silylation. In the present case, with Rh NPs, either the

hydrosilylation of the triple carbon-carbon bond occurs first or the hydrogen produced in the reaction of hydroxyl group with triethylsilane does not give the hydrogenation product under our conditions (Scheme 118).

Table 24. Hydrosilylation of differentiated unsymmetric alkynes under catalysis by **M11**.[a]

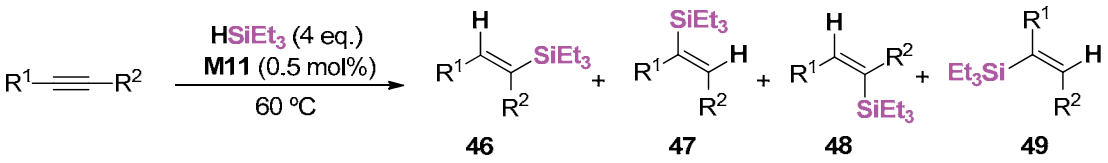

Entry	R^1, R^2	Time (h)	Products[b]	Yield (%)[c]
1	Ph, Me	30	**46a** (45%) + **47a** (55%)	95
2 [d]	^{n}Bu, $(CH_2)_4OH$	37	**46b** (50%) + **47b** (50%)	95
3	COOMe, Pentyl	55	**46c** (14%) + **47c** (58%) + **48c** (14%) + **49c** (14%)	69
4	Cy, H	33	**46d** (42%) + **47d** (40%) + **48d** (18%)	84

[a] Performed in closed vessels (15 mL) with 0.5 mmol of alkyne under air. [b] The structural assignment of the isomers was performed by NMR techniques and the ratio was determined by GC. [c] Isolated yields. [d] 6 eq. of triethylsilane was utilized; difficult to assign the signals for the two isomers by NMR techniques.

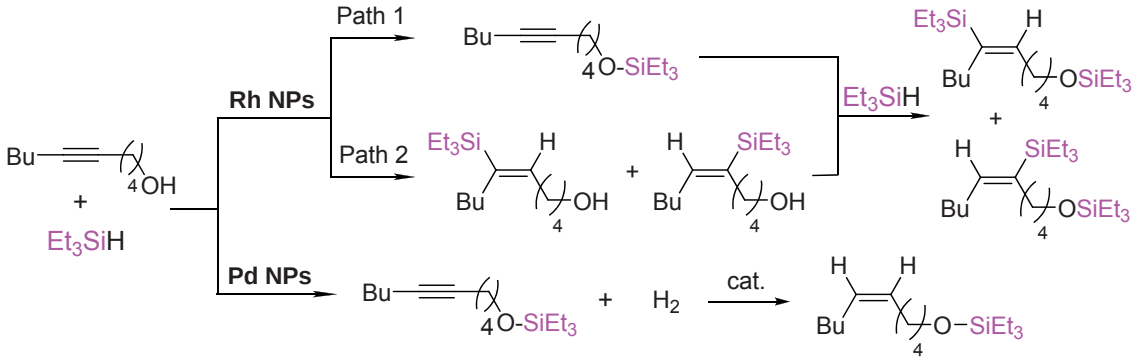

Scheme 118. Different evolution of 5-decyn-1-ol under catalysis by Rh NPs and Pd NPs.

The reaction between methyl 2-octynoate and triethylsilane (Table 24, entry 3) was relatively regio- and stereoselective, with the major product **47c** (58%) arising from the *syn* addition that placed the triethylsilyl moiety closer to the electron-withdrawing ester group; equal amounts (14%) of the other isomers **46c**, **48c** and **49c** were observed by ^{1}H NMR and GC (see Annex). Thus, we obtained a ratio of 72:28 with respect to syn/anti addition (stereochemistry) and a 72:28 with respect to regiochemistry, in favour of the isomers with the silyl group placed gem to the ester group. The terminal alkyne ethylnylcyclohexane also proved reactive under the present reaction conditions, affording a mixture of three isomers **46d**, **47d** and **48d,** the syn addition being also predominant (Table 24, entry 4). It's worth noting that the terminal acetylenes did not react with silanes under Pd NPs catalysis.[318,320] In addition, the hydrosilylation of some 1,3-diynes was carried out under analogous conditions (0.5 mol% Rh, excess triethylsilane, 60 ºC) (Table 25).

Table 25. Hydrosilylation of symmetric 1,3-diynes.[a]

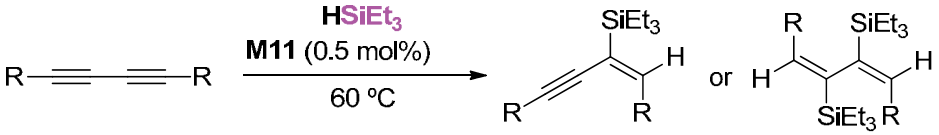

Entry	R	$HSiEt_3$[b]	Time (h)	Products	Yield (%)[c]
1	^{t}Bu	4	20	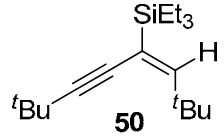 **50**	95
2	^{n}Bu	6	20	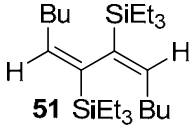 **51**	98

[a] Performed in closed vessels (15 mL) with 0.5 mmol of alkyne under air. [b] mol of silane per mol of 1,3-diyne. [c] Isolated yield.

When four moles of silane with respect to the diyne were used (2 moles per mole of each triple bond) the hydrosilylation of a sterically crowded 2,2,7,7-tetramethylocta-3,5-diyne afforded exclusively the monohydrosilylation product **50** (Table 25, entry 1). Under the same conditions (4 mol of silane with respect to diyne), the hydrosilylation of the less sterically demanding dodeca-5,7-diyne gave a mixture of mono- and dihydrosilylation products (not reported in table 25). For this reason the reaction was repeated with 6 mol of silane per mol of diyne, affording only the dihydrosilylation product **51** in an almost quantitative yield (Table 25, entry 2). This phenomenon should be ascribed to a pronounced steric effect, which has also been observed by others with Pt NPs as catalysts.[370]

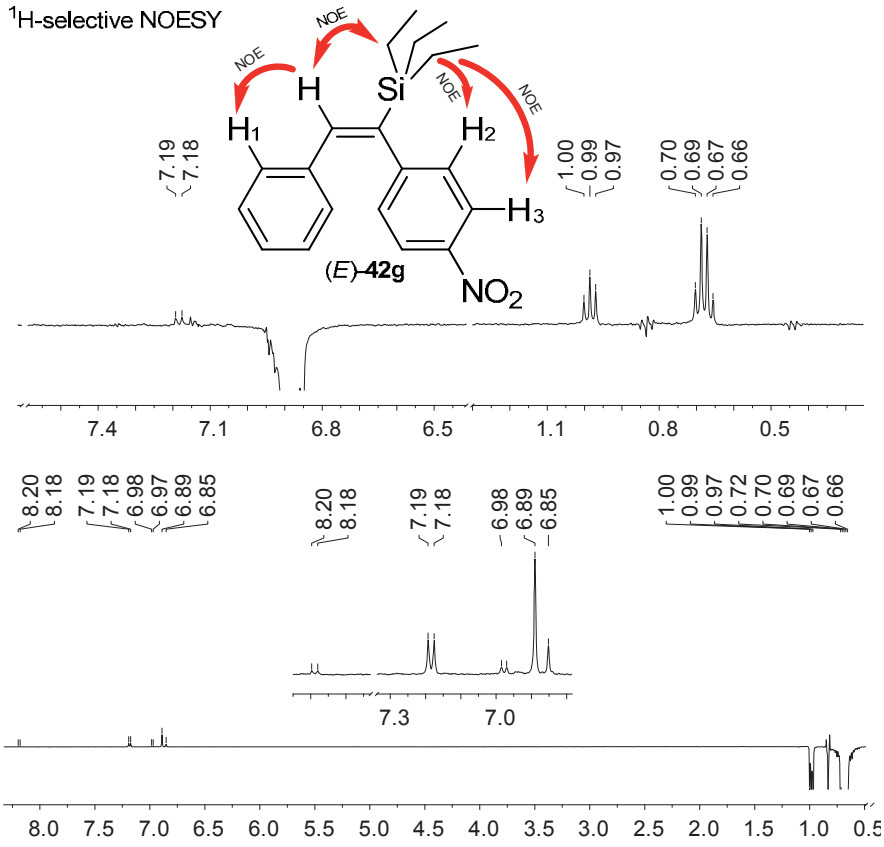

Figure 40. ^{1}H selective NOESY spectra for compound **42g**.

Structural characterization of all compounds (Tables 21, 23 and 24) included two-dimensional NMR techniques (COSY, HSQC, HMBC and NOESY experiments). The stereoselectivity of the reaction was studied by determining the relative (*E*)/(*Z*) configuration of the corresponding trisubstituted double bonds. This assignment was made by determining the through-space NOE effects, mainly on the olefinic proton and,

if necessary, was further confirmed by measuring the long-range proton-carbon and proton-silicon coupling constants using the selHSQMBC method.[318,320, 380] The regioselectivity of the process was studied by using chemical shifts assignment and NOE effects obtained from HMBC and NOESY spectra, respectively. For instance, in the case of the (*E*)-isomer **42g**, a NOE effect can be clearly observed (Figure 40) between the vinyl proton resonating at 6.89 ppm and the ethyl group. The NOE between the vinyl proton and the proton H_1 on the phenyl group resonating at 7.19 ppm is also visible, although the signal is very weak. As can also be seen from Figure 40, selective irradiation of the ethyl at 0.68 ppm yields a nice NOE effect at 6.89 ppm (vinylic proton). Additionally the NOE between the ethyl group and the aromatic protons H_2 at 7.19 ppm and H_3 at 8.19 ppm are notable as well. The correlation peaks between the vinylic proton and the related ^{13}C were perfectly observable in the 2D HSQC and 2D HMBC spectra as shown in Figure 41.

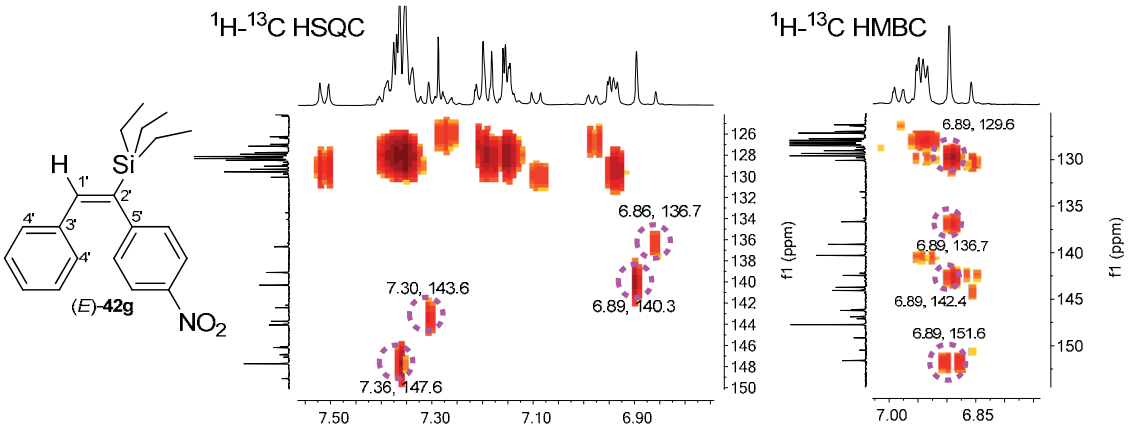

Figure 41. 2D ^{1}H-^{13}C HSQC and 2D ^{1}H-^{13}C HMBC spectra of a mixture containing **42g**, **43g**, **44g** and **45g** (Table 23, entry 7).

The coupling of vinylic proton (6.89 ppm) of **42g** and the carbon 1' to which it is attached, resonating at 140.3 ppm, was circled in the HSQC spectrum. The same has been done for the other three isomers **43g**, **44g** and **45g** present in the mixture of entry 7 of Table 23. The HMBC data successfully gave the correlations between the vinylic proton and carbons separated by two and three bonds, *i. e.*, couplings with carbons 2', 3', 4' and 5'. A large value of 12.5 Hz measured between the vinylic proton (6.89 ppm) of **42g** and the carbon resonating at 151.6 ppm confirmed the *trans* relationship between them, and therefore, this carbon is assigned to carbon 5' on the ipso *para*-

[380] Gil, S.; Espinosa, J. F.; Parella, T. *J. Magn. Reson.* **2011**, *213*, 145.

nitrosubstituted phenyl group. Actually, the deshielding effect due to the appearance of the electron-withdrawing nitro group also lead us to conclude that carbon 5' should appear at lower field comparing with the other ones mentioned above.

4.2 Gold nanoparticles as catalysts in the reduction of nitroarenes

4.2.1 Introduction

Nitroarenes are among the most common organic pollutants existing either in agricultural or industrial waste waters because they are widely used as building blocks in many areas such as dyes, pesticides, explosives and as organic solvents.[381] As a special example, 4-nitrophenol is a notorious pollutant due to its carcinogenicity and other health risks in humans, exhibiting excellent solubility and stability in water. Therefore, the U. S. Environmental Protection Agency listed it on its "Priority Pollutant List". Thus, from environmental point of view, the reduction process of nitroarenes is favourable. On the other hand, the anilines, which can be obtained from the reduction of nitroarenes, are very important industrial raw materials.[382] Promisingly, it has been found that metal nanoparticles can catalyze the reduction of nitroarenes by $NaBH_4$ to yield the corresponding anilines.[383] Thus, great efforts have recently[383, 384] been dedicated to the development of protocols for the conversion of nitroarenes to the corresponding anilines. Moreover, some researchers[321] found that this kind of transformations can be performed in water with carefully designed catalysts based on metal nanoparticles which are really environmentally benign, of low toxicity and low cost. The catalytic activity of nanoparticles is found to be strongly dependent on the active atoms at the surface, which are frequently related to the specific surface area, surface structure and the edges of the nanocatalysts.[385] It should be noted that most of

---

[381] (a) Kearney, P. C.; Kaufman, D. D. *Herbicides: Chemistry, Degradation and Mode of Action*, Marcel Dekker, Inc., New York, **1976**. (b) McCormick, N. G.; Feeherry, F. E.; Levinson, H. S. *Appl. Environ. Microbiol.* **1976**, *31*, 949.

[382] (a) Rode, C. V.; Vaidya, M. J.; Jaganathan, R.; Chaudhari, R. V. *Chem. Eng. Sci.* **2001**, *56*, 1299. (b) Komatsu, T.; Hirose, T. *Appl. Catal. A*: *Gen.* **2004**, *276*, 95. (c) Rode, C. V.; Vaidya, M. J.; Chaudhari, R. V. *Org. Process Res. Dev.* **1999**, *3*, 465.

[383] (a) Panigrahi, S.; Basu, S.; Praharaj, S.; Pande, S.; Jana, S.; Pal, A.; Ghosh, S. K.; Pal, T. *J. Phys. Chem. C* **2007**, *111*, 4596. (b) Pradhan, N.; Pal, A.; Pal, T. *Colloids Surf. A* **2002**, *196*, 247. (c) Mei, Y.; Sharma, G.; Lu, Y.; Ballauff, M. *Langmuir* **2005**, *21*, 12229.

[384] (a) Yuan, J.; Schacher, F.; Drechsler, M.; Hanisch, A.; Lu, Y.; Ballauff, M.; Muller, A. H. E. *Chem. Mater.* **2010**, *22*, 2626. (b) Gao, Y.; Ding, X.; Zheng, Z.; Cheng, X.; Peng, Y. *Chem. Commun.* **2007**, 3720. (c) Lin, F.-H.; Doong, R.-A. *J. Phys. Chem. C* **2011**, *115*, 6591. (d) Lu, W.; Ning, R.; Qin, X.; Zhang, Y.; Chang, G.; Liu, S.; Luo, Y.; Sun, X. *J. Hazard. Mater.* **2011**, *197*, 320. (e) Fang, X.; Ma, H.; Xiao, S.; Shen, M.; Guo, R.; Cao, X.; Shi, X. *J. Mater. Chem.* **2011**, *21*, 4493. (f) Lara, P.; Suarez, A.; Colliere, V.; Philippot, K.; Chaudret, B. *ChemCatChem* **2014**, *6*, 87.

[385] (a) Zeng, J.; Zhang, Q.; Chen, J.; Xia, Y. *Nano Lett.* **2010**, *10*, 30. (b) Mahmoud, M. A.; Saira, F.; El-Sayed, M. A. *Nano Lett.* **2010**, *10*, 3764. (c) Lee, H.; Habas, S. E.; Kweskin, S.; Butcher, D.; Somorjai, G. A.;

the previously reported metal nanocatalysts[383,384] are water-insoluble, which greatly decreased the opportunities of the reactants to contact with the catalyst in aqueous media and, thus, it may result in the requirement of longer reaction times and/or higher reaction temperatures. Keeping these ideas in mind, we planned to test the activity and recyclability of our water-soluble gold nanocatalysts in the reduction of nitroarenes to anilines in water. It should also be noted that this reaction is simply one of the many potential applications of gold nanoparticles, and our research has been limited to the reaction described below simply for lack of time to conduct additional tests.[386]

4.2.2 Mechanistic aspects

The exact mechanism of the reduction of nitro compounds under catalysis by metal nanoparticles is still not fully explored. Following the steps of Zhang[387] and Wunder,[388] Kantam[321a] proposed a probable surface reduction mechanism (Scheme 119) when using supported Au NPs and sodium borohydride as the catalytic system.

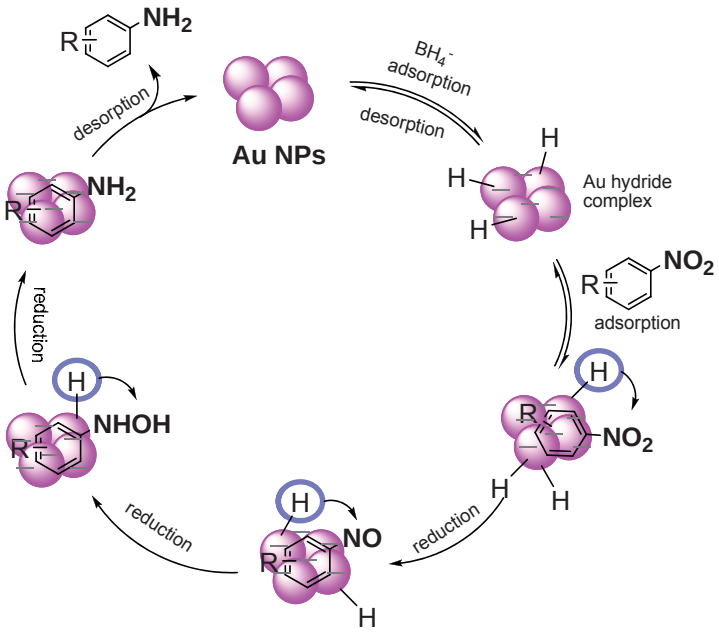

Scheme 119. Proposed mechanism for the reduction of nitroarenes to anilines by sodium borohydride catalyzed by Au NPs.

Yang, P. *Angew. Chem. Int. Ed.* **2006**, *45*, 7824. (d) Narayanan, R.; El-Sayed, M. A. *J. Am. Chem. Soc.* **2004**, *126*, 7194.

386 Takale, B. S.; Bao, M.; Yamamoto, Y. *Org. Biomol. Chem.* **2014**, *12*, 2005.

387 Zhang, H.; Li, X.; Chen, G. *J. Mater. Chem.* **2009**, *19*, 8223.

388 Wunder, S.; Polzer, F.; Lu, Y.; Mei, Y.; Ballauff, M. *J. Phys. Chem. C* **2010**, *114*, 8814.

Initially, the borohydride anions in aqueous media are adsorbed onto the surface of the Au NPs and react to offer a gold hydride species; this is followed by the adsorption of the nitroarene in a reversible fashion. Once the substrates and reductant are chemically adsorbed on the Au NPs, a hydrogen transfer process occurs between the gold hydride complex and the nitroarenes. Thereafter, two probable routes, direct or condensation route, may be involved on the basis of Haber's observation (Scheme 120).[389]

In the direct route (Scheme 120), the nitroarene is reduced to the nitroso compound, which undergoes further reduction to yield the hydroxylamine. Finally, the hydroxylamine is reduced to the corresponding anilines. The condensation route (Scheme 120) involves the condensation of a nitroso molecule with hydroxylamine affording the azoxy compound, which is reduced consecutively to azo, hydrazo and the final desired product.

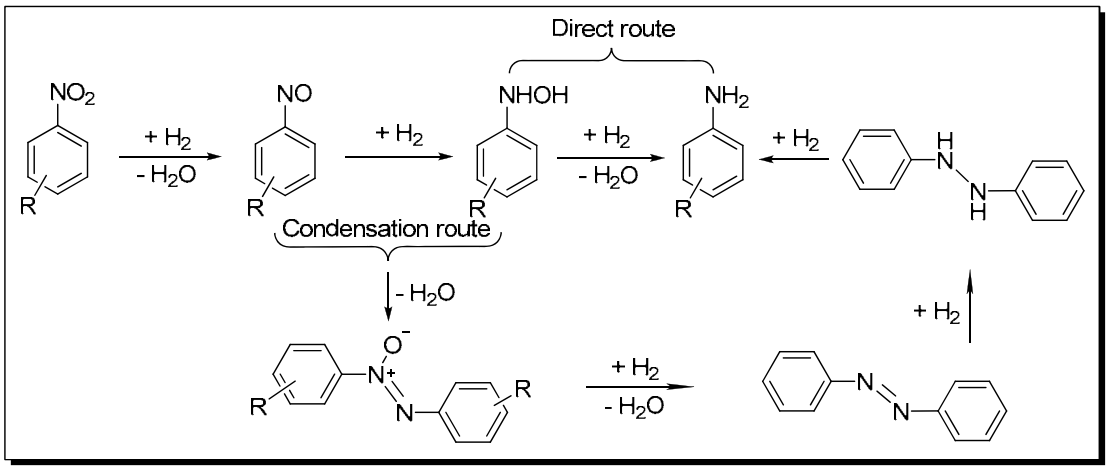

Scheme 120. Reaction pathways proposed for the reduction of nitroarenes to the corresponding anilines.

4.2.3 Optimization of the catalytic conditions

The sodium borohydride was chosen as the reducing reagent in this work. A first reaction was carried out with nitrobenzene as model compound, 0.5 mol% of Au (**M16**) and a reported[321a] amount of sodium borohydride of 50 mol per mol of substrate, using water as solvent (Table 26, entry 1). To our delight, the control by TLC showed that in only 1 h at room temperature, the starting material was consumed. Taking into account that the stabilized Au NPs are water-soluble but insoluble in diethyl ether, the reaction

[389] Haber, F.; Elektrochem. Z. *Angew. Phys. Chem.* **1898**, *22*, 506.

mixture was extracted with diethyl ether affording the pure aniline **52** in a quantitative yield (GC analysis). When decreasing the sodium borohydride to 35 mol/mol of nitrobenzene (Table 26, entry 2), the reaction still worked perfectly albeit at the cost of a somewhat slower reaction. Keeping the amount of sodium borohydride constant (35 mol/mol of nitrobenzene), the reaction time didn't change significantly on lowering the loading of catalyst to 0.3 mol% (Table 26, entry 3). Attempts of further decreasing the amount of sodium borohydride gave a lower yield of 78% in a considerable longer reaction time (Table 26, entry 4). As reference experiments, gold free conditions didn't give the expected product (Table 26, entries 5-6) which clearly proved the need of the catalyst. No reaction occurred in the absence of $NaBH_4$ (Table 26, entry 7). It is worth noting that all the reactions mentioned above were performed without any special precaution in water under air at room temperature. Thus, the optimized reaction conditions are summarized as follows: 35 mol/mol of substrate of $NaBH_4$, 0.30 mol% of Au nanocatalyst in water at room temperature.

Table 26. Optimization of the reaction conditions.[a]

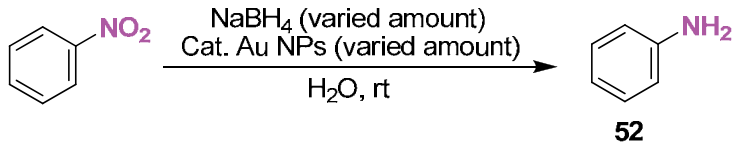

52

Entry	Cat. / mol %[b]	$NaBH_4$ / mol per mol of substrate	Time / h[c]	Yield / %
1	**M16**/0.5	50	1.0	99[d]
2	**M16**/0.5	35	1.5	99[d]
3	**M16**/0.3	35	1.5	99[d]
4	**M16**/0.3	20	6.0	78[e]
5	stabilizer **30**/0.3	50	3.0	-
6	-	50	3.0	-
7	**M16**/0.3	-	3.0	-

[a] To a well stirred mixture of nitrobenzene (1.0 mmol) and the given amount of $NaBH_4$ in water (10 mL) was added the given amount of catalyst at room temperature. [b] Calculated according to the ICP analysis results for gold in **M16**. [c] TLC monitoring. [d] Isolated yield, the product was directly extracted from the reaction mixture with diethyl ether, further purification is unnecessary. [e] Corrected yield by GC.

4.2.4 Reusability and catalytic tests with various substrates

Under the optimized conditions, the reaction scope was extended to several different nitroarenes, using **M16** as the representative gold catalyst (Table 27). The catalytic system was found to be tolerant of the presence of electron-withdrawing and

electron-donating substituents on the aromatic ring. We first investigated the reusability of **M16** in the reduction of nitrobenzene. Thus, once the reaction was deemed complete (by GC, Table 27, entry 1), the final product **52** was extracted with diethyl ether leaving the Au NPs in the aqueous phase ready for next run. Four consecutive cycles were performed (Table 27, entries 1-4), giving a respectable isolated yield of 78% in the fourth run.

Table 27. Reduction of nitroarenes catalyzed by Au NPs.[a]

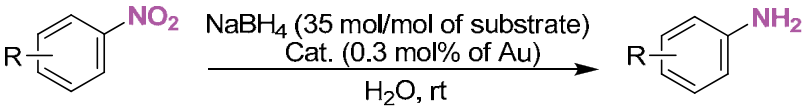

Entry[a]	Substrate	Product	Cat.	Conv /%	Time[b]	Yield /%[c]
1	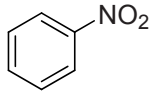	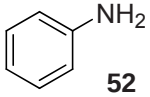 **52**	**M16**	> 99	1 h	99[d]
2			**M16**	> 99	1.5 h	88[e]
3			**M16**	94	2 h	86[f]
4			**M16**	87	5 h	78[g]
5	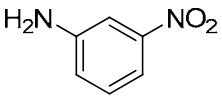	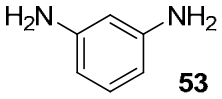 **53**	**M16**	> 99	35 min	99
6	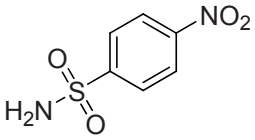	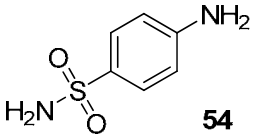 **54**	**M16**	> 99	48 min	99
7	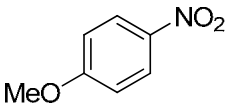	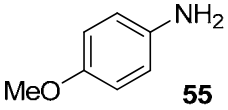 **55**	**M16**	> 99	3 h	98
8[h]	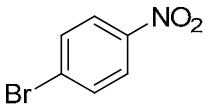	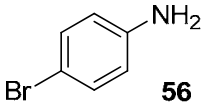 **56**	**M16**	> 99	2 h	72
9	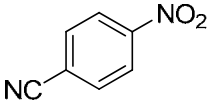	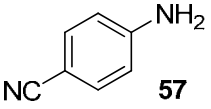 **57**	**M16**	> 99	1.5 h	89
10	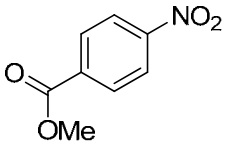	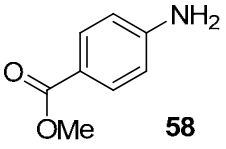 **58**	**M16**	> 99	1.5 h	82
11	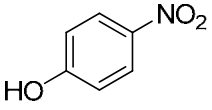	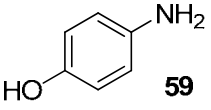 **59**	**M16**	> 99	11 min	99
12			**M20**	> 99	16 min	99
13			**M12**	> 99	22 min	99

[a] To a well stirred mixture of nitroarene (1.0 mmol) and $NaBH_4$ (35 mol/mol of substrate) in water (10 mL) at room temperature the catalyst was added (0.3 mol%). [b] TLC monitoring. [c] Isolated yield. [d-g] Consecutive cycles with the same batch of catalyst. [h] Trace amount of dehalogenated product was detected.

The catalyst was also very effective for the reduction of 3-nitroaniline and 4-nitrobenzenesulfonamide to the corresponding products **53** and **54** with quantitative yields in very short reaction times (Table 27, entries 5-6). *p*-Methoxynitrobenzene gave an excellent yield of *p*-methoxyaniline **55** albeit at a longer reaction time (Table 27, entry 7). The reduction of *p*-bromonitrobenzene furnished *p*-bromoaniline **56** in 72% isolated yield, even though some dehalogenated product was detected (Table 27, entry 8). The catalytic system was also able to reduce chemoselectively the *p*-nitrobenzonitrile and methyl *p*-nitrobenzoate, yielding the corresponding anilines **57** and **58** in 89% and 82% isolated yields, respectively (Table 27, entries 9-10), the –CN and –COOMe groups remained unaltered under the reaction conditions.

More impressively, the reduction of *p*-nitrophenol was finished in only 11 min, affording *p*-aminophenol **59** in quantitative yield (Table 27, entry 11). This reaction was later on used as a model to investigate the catalytic activities of other Au NPs **M12** and **M20**, systems with nanoparticle sizes and morphologies different from those of **M16** (Table 27, entries 12-13). As expected, **M20** showed lower activity compared with **M16** which should be ascribed to the higher particle size and, consequently, lower number of active sites on the surface. However, the catalysis utilizing **M12** needed the longest reaction time (22 minutes) which might be assigned to the excess of stabilizer that wrapped the particle surface causing a drop in catalytic activity.

4.3 Conclusions

The rhodium nanoflowers stabilized by a nitrogen-rich polyoxyethylenated substrate were efficient catalysts for the stereoselective *syn*-hydrosilylation of internal alkynes with silanes affording mainly (*E*)-vinylsilanes in almost quantitative yields under solvent-free conditions. Some degree of regioselectivity was obtained with some differentiated unsymmetric alkynes. The corresponding products can be directly extracted with diethyl ether and the insoluble Rh nanoflowers then reused in the next run. The recyclability tests showed that the rhodium nanoflowers could be recycled up to 6 times without any loss of activity. The Au NPs stabilized by the same substrate were effective catalysts for the reduction of nitroarenes to the corresponding anilines with sodium borohydride as reducing agent in water at room temperature. The catalysts could also be recycled up to four runs.

4.4 Experimental section

4.4.1 General remarks

Commercial reactants were purchased from Aldrich and the other non-commercial ones were prepared according to literature methods as described below. Water Milli-Q was used in the preparation and purification of compounds and materials. All NMR measurements were carried out at the *Servei de Ressonància Magnètica Nuclear* of the *Universitat Autònoma de Barcelona*. NMR spectra were recorded on Bruker Avance250 (250 MHz), Avance360 (360 MHz), Avance400 (400 MHz) or Avance500 (500 MHz) spectrometers. Two-dimensional COSY, HSQC, HMBC and selective 1D NOESY (mixing time of 500 ms) experiments were recorded under routine conditions. Proton-carbon and proton-silicon coupling constants were measured from ^{1}H-^{13}C and ^{1}H-^{29}Si selHSQMBC experiments. A 20 ms Gaussian-shaped pulses were used for ^{1}H-selective refocusing of the excited olefinic protons. Data were acquired and processed as described in the original publication.[390] Routine gas chromatographic analyses were accomplished using an Agilent Technologies 7890 A GC system equipped with an Agilent HP-5 column (30 m × 0.32 mm × 0.25 μm). High resolution mass spectra were determined at the *Servei d'Anàlisi Química* of the *Universitat Autònoma de Barcelona* using a Bruker Daltonic MicroTOFQ spectrometer (Bremen, Gemany) equipped with an ESI inlet. Alugram® SIL G/UV$_{254}$ sheets (Macherey–Nagel) were used for thin-layer chromatography. Column chromatography was carried out using SDS brand silica gel with a grain size of 35 - 70 μm and a pore size of 60 Å.

4.4.2 Preparation of internal alkynes

4.4.2.1 Preparation of 1,2-bis(4-methylphenyl)ethyne, **34a**[377]

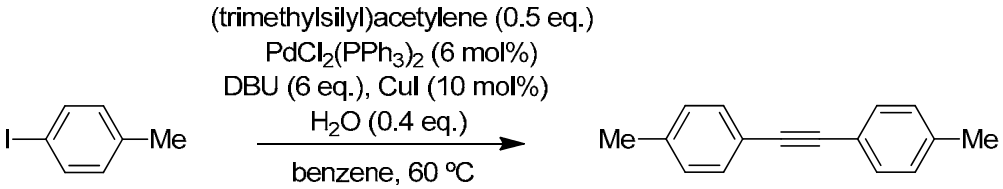

To a mixture of *p*-iodotoluene (654 mg, 3 mmol), $PdCl_2(PPh_3)_2$ (126 mg, 6 mol%) and CuI (57 mg, 10 mol%) in benzene (15 mL), DBU (2.7 mL, ρ=1.018 g/mL, 18 mmol) and ice-chilled (trimethylsilyl)acetylene (208 μL, 1.5 mmol) were added under N_2 atmosphere, followed by the addition of H_2O (21 μL, 0.4 eq.). The reaction mixture was

[390] Gil, S.; Espinosa, J. F.; Parella, T. *J. Magn. Reson.* **2011**, *213*, 145.

stirred at 60°C in the dark overnight (GC monitoring). Upon completion of the reaction, 1M HCl (45 mL) was poured into the crude mixture, which was then extracted with chloroform (3 × 45 mL). The organic layer was dried over anhydrous Na_2SO_4, and the solvent was removed under reduced pressure. The crude product was purified by silica gel column chromatography using hexane as eluent, to give a cotton-like solid (280 mg, 91%; R_f = 0.40); ^{1}H NMR (400 MHz, $CDCl_3$) δ (ppm): 7.41 (d, *J* = 8.0 Hz, 4H), 7.15 (d, *J* = 7.9 Hz, 4H), 2.36 (s, 6H); ^{13}C NMR (101 MHz, $CDCl_3$) δ (ppm): 138.3, 131.6, 129.2, 120.5, 89.0, 21.6.

4.4.2.2 Preparation of 1, 2-bis (4-methoxyphenyl) ethyne, **34b**[377]

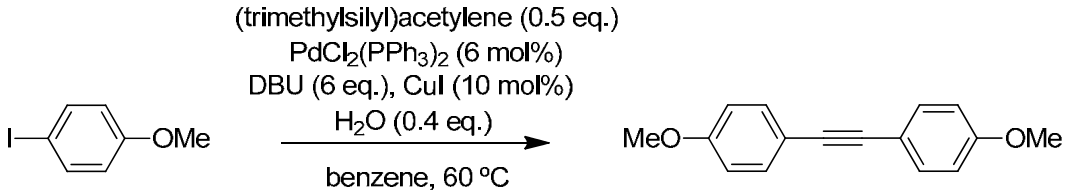

Prepared according to the reported method but with small modifications: To a mixture of *p*-iodoanisole (234 mg, 1 mmol), $PdCl_2(PPh_3)_2$ (42 mg, 6 mol%) and CuI (19 mg, 10 mol%) in benzene (5 mL), DBU (897 µL, ρ=1.018 g/mL, 6 mmol) and ice-chilled (trimethylsilyl)acetylene (69 µL, 0.5 mmol) were added under N_2 atmosphere, followed by the addition of H_2O (7 µL, 0.4 eq.). The reaction mixture was stirred at 60°C in the dark overnight (GC monitoring). Upon completion of the reaction, 1M HCl (15 mL) was poured into the crude mixture and then it was extracted with chloroform (3 × 15 mL). The organic layer was dried over anhydrous Na_2SO_4, and the solvent was removed under reduced pressure. The crude product was purified by silica gel column chromatography using hexane/ethyl acetate (50:1) as eluent, to give a white crystalline solid (64 mg, 54%; R_f = 0.44); ^{1}H NMR (400 MHz, $CDCl_3$) δ (ppm): 7.45 (d, *J* = 8.7 Hz, 4H), 6.87 (d, *J* = 8.7 Hz, 4H), 3.83 (s, 6H); ^{13}C NMR (101 MHz, $CDCl_3$) δ (ppm): 159.5, 133.0, 115.9, 114.1, 88.1, 55.4.

4.4.2.3 Preparation of 1,2-bis(4-chlorophenyl) ethyne, **34c**[377]

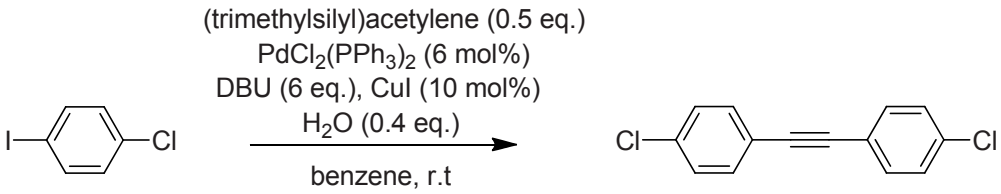

To a mixture of *p*-iodochlorobenzene (238 mg, 1 mmol), $PdCl_2(PPh_3)_2$ (42 mg, 6 mol%) and CuI (19 mg, 10 mol%) in benzene (5 mL), DBU (897 µL, ρ=1.018 g/mL, 6 mmol) and ice-chilled (trimethylsilyl)acetylene (69 µL, 0.5 mmol) were added under N_2 atmosphere, followed by the addition of H_2O (7 µL, 0.4 eq.). The reaction mixture was stirred at room temperature in the dark overnight (GC monitoring). Upon completion of the reaction, 1M HCl (15 mL) was poured into the crude mixture and then it was extracted with chloroform (3 × 15 mL). The organic layer was dried over anhydrous Na_2SO_4, and the solvent removed under reduced pressure. The crude product was purified by silica gel column chromatography using hexane as eluent, to give a yellow powder (70 mg, 57%; R_f = 0.51); ^{1}H NMR (360 MHz, $CDCl_3$) δ (ppm): 7.45 (d, *J* = 8.4 Hz, 4H), 7.33 (d, *J* = 8.4 Hz, 4H); ^{13}C NMR (101 MHz, $CDCl_3$) δ (ppm): 134.7, 133.0, 128.9, 121.6, 89.3.

4.4.2.4 Preparation of 1,2-bis(4-bromophenyl)ethyne, **34d**[377]

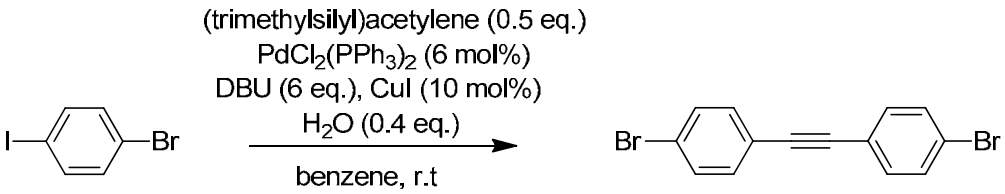

To a mixture of *p*-iodobromobenzene (707 mg, 2.5 mmol), $PdCl_2(PPh_3)_2$ (105 mg, 6 mol%) and CuI (48 mg, 10 mol%) in benzene (12 mL) DBU (2.2 mL, ρ=1.018 g/mL, 15 mmol) and ice-chilled (trimethylsilyl)acetylene (173 µL, 1.25 mmol) were added under N_2 atmosphere, followed by the addition of H_2O (18 µL, 0.4 eq.). The reaction mixture was stirred at room temperature in the dark overnight (GC monitoring). Upon completion of the reaction, 1M HCl (20 mL) was poured into the crude mixture and then it was extracted with chloroform (3 × 20 mL). The organic layer was dried over anhydrous Na_2SO_4, and the solvent removed under reduced pressure. The crude product was purified by silica gel column chromatography using hexane as eluent, to give a yellow powder (264 mg, 63%; R_f = 0.63); ^{1}H NMR (360 MHz, $CDCl_3$) δ (ppm): 7.49 (d, *J* = 8.3 Hz, 4H), 7.38 (m, 4H); ^{13}C NMR (90 MHz, $CDCl_3$) δ (ppm): 133.1, 131.8, 122.9, 122.0, 89.6.

4.4.2.5 Preparation of 1,2-di(naphthalen-1-yl)ethyne, **34e**[377]

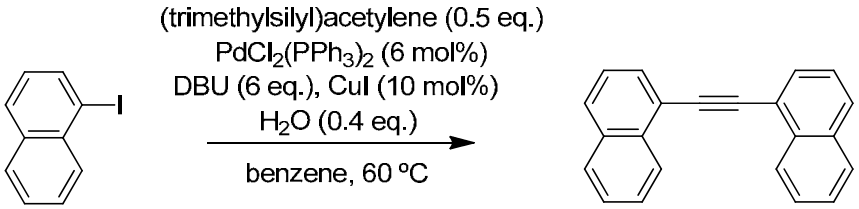

To a mixture of 1-iodonaphthalene (146 µL, ρ = 1.74 g/mL, 1 mmol), $PdCl_2(PPh_3)_2$ (42 mg, 6 mol%) and CuI (19 mg, 10 mol%) in benzene (5 mL), DBU (897 µL, ρ=1.018 g/mL, 6 mmol) and ice-chilled (trimethylsilyl)acetylene (69 µL, 0.5 mmol) were added under N_2 atmosphere, followed by the addition of H_2O (7 µL, 0.4 eq.). The reaction mixture was stirred at room temperature in the dark overnight (GC monitoring). Upon completion of the reaction, 1M HCl (15 mL) was poured into the crude mixture and then it was extracted with chloroform (3 × 15 mL). The organic layer was dried over anhydrous Na_2SO_4, and the solvent was removed under reduced pressure. The crude product was purified by silica gel column chromatography using hexane as eluent, to give an off-white powder (86 mg, 62%; R_f = 0.23); ^{1}H NMR (400 MHz, $CDCl_3$) δ (ppm): 8.57 (d, *J* = 8.3 Hz, 2H), 7.92-7.88 (m, 6H), 7.64 (t, *J* = 7.3 Hz, 2H), 7.59-7.49 (m, 4H) ^{13}C NMR (101 MHz, $CDCl_3$) δ (ppm): 133.4, 120.7, 129.0, 128.5, 127.0, 126.6, 126.4, 125.5, 121.2, 92.6.

4.4.2.6 Preparation of 1,2-di(thiophen-3-yl)ethyne, **34f**[391]

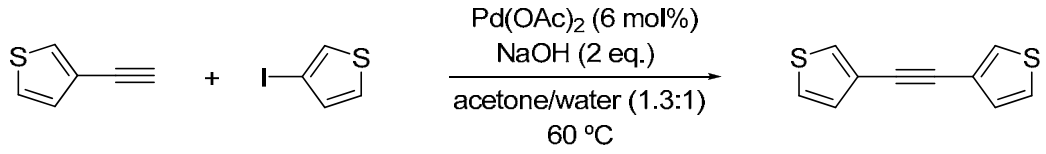

A mixture of 3-iodothiophene (305 µL, ρ = 2.06 g/mL, 3.0 mmol), 3-ethynylthiophene (385 µL, ρ = 1.09 g/mL, 3.9 mmol), $Pd(OAc)_2$ (13.5 mg, 0.06 mmol), NaOH (240 mg, 6.0 mmol) in acetone (12 mL) and H_2O (9 mL) was stirred at 60 °C in a closed vessel for 18 h (100% conv. GC). Afterwards, the reaction solution was cooled to room temperature and extracted with Et_2O (4x10 mL), the organic layer was dried over Na_2SO_4, the solvent was evaporated under reduced pressure and the residue was purified by flash column chromatography: silica gel, hexane: ethyl acetate (100:1 → 50:1) to give white crystalline needles (350 mg, 61%; R_f = 0.26). ^{1}H NMR (400 MHz, $CDCl_3$) δ (ppm): 7.50 (dd, *J* = 2.8, 0.8 Hz, 2H), 7.30 (dd, *J* = 4.9, 3.0 Hz, 2H), 7.18 (dd, *J* = 5.0, 0.8 Hz, 2H); ^{13}C NMR (101 MHz, $CDCl_3$) δ (ppm): 129.9, 128.6, 125.5, 122.3, 84.2.

[391] Martin, C. J.; Gil, B.; Perera, S. D.; Draper, S. M. *Eur. J. Org. Chem.* **2011**, 3491.

4.4.2.7 Preparation of 1-nitro-4-(phenylethynyl) benzene, **35f**[392]

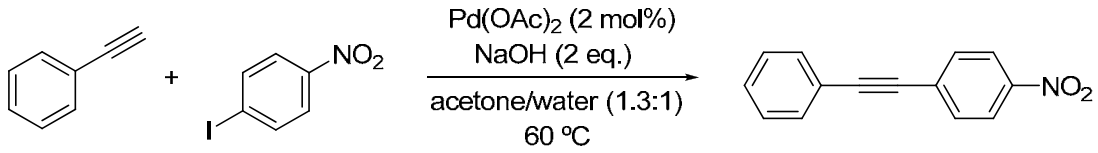

A mixture of *p*-iodonitrobenzene (747 mg, 3.0 mmol), phenylacetylene (430 µL, ρ = 0.93 g/mL, 3.9 mmol), $Pd(OAc)_2$ (13.5 mg, 0.06 mmol), NaOH (240 mg, 6.0 mmol) in acetone (12 mL) and H_2O (9 mL) was stirred at 60°C in a closed vessel for 3 h (100% conv., GC). The reaction solution was cooled to room temperature and extracted with Et_2O (4 × 10 mL), the organic layer was dried over Na_2SO_4, the solvent was evaporated under reduced pressure and the residue was purified by flash column chromatography on silica gel, eluting with hexane/ethyl acetate (4:1) to give a yellow solid (342 mg, 51%; R_f = 0.58); ^{1}H NMR (400 MHz, $CDCl_3$) δ (ppm): 8.23 (d, *J* = 8.7 Hz, 2H), 7.67 (d, *J* = 8.7 Hz, 2H), 7.57-7.55 (m, 2H), 7.40-7.39 (m, 3H); ^{13}C NMR (101 MHz, $CDCl_3$) δ (ppm): 147.1, 132.4, 132.0, 130.4, 129.4, 128.7, 123.8, 122.3, 94.9, 87.7.

4.4.3 Hydrosilylation of alkynes under catalysis by rhodium nanoparticles

4.4.3.1 General procedure for the hydrosilylation of internal alkynes by rhodium nanoparticles

To a mixture of alkynes (0.5 mmol) and **M11** (0.5 mol% Rh, 0.7 mg) triethylsilane (2 mmol) was added into a screw-top sealable tube and then the stirred mixture was heated at 60 °C overnight until total conversion of the alkyne (GC monitoring). The final reaction mixture was extracted with ether and filtered through a plug of silica-gel eluting with hexane and the solvent was removed under an air flow to afford the corresponding hydrosilylation product.

4.4.3.2 (*E*)-(1, 2-diphenylvinyl)triethylsilane, **36a**[320]

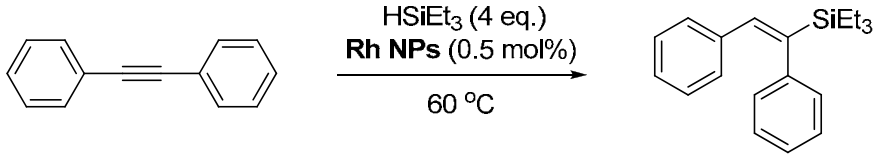

Following the general procedure for the hydrosilylation, diphenylacetylene (89 mg, 0.5 mmol), was allowed to react with triethylsilane (320 µL, ρ = 0.73 g/mL, 2 mmol) at

[392] Mao, J.; Wu, M.; Xie, G.; Ji, S. *Adv. Synth. Catal.* **2009**, *351*, 2101.

60°C for 15 h (GC monitoring). Light yellow oil (146 mg, 99%); ^{1}H NMR (360 MHz, $CDCl_3$) δ (ppm): 7.29 (t, *J* = 7.6 Hz, 2H), 7.20 (t, *J* = 7.1 Hz, 1H), 7.14-7.05 (m, 3H), 7.04-6.90 (m, 4H), 6.76 (s, 1H), 0.95 (t, *J* = 7.9 Hz, 9H), 0.64 (q, *J* = 7.9 Hz, 6H). ^{13}C NMR (101 MHz, $CDCl_3$) δ (ppm): 144.2, 143.3, 138.9, 137.5, 129.7, 128.8, 128.0, 127.4, 127.1, 125.7, 7.5, 2.9.

4.4.3.3 (*E*)-(1,2-di-*p*-tolylvinyl)triethylsilane, **36b**

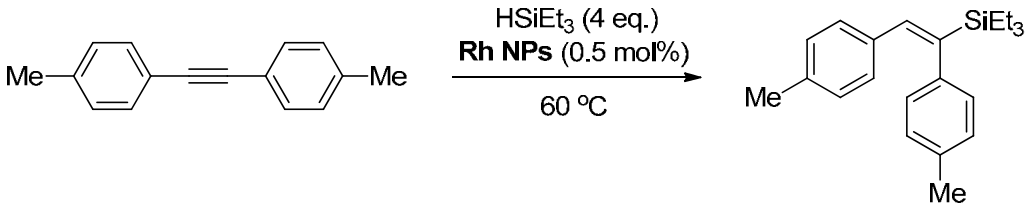

Following the general procedure for the hydrosilylation, 1,2-di-*p*-tolylethyne (103 mg, 0.5 mmol), was allowed to react with triethylsilane (320 µL, ρ = 0.73 g/mL, 2 mmol) at 60°C for 19 h (GC monitoring). Colorless oil (152 mg, 94%); ^{1}H NMR (400 MHz, $CDCl_3$) δ (ppm): 7.09 (d, *J* = 7.7 Hz, 2H), 6.92-6.85 (m, 6H), 6.71 (s, 1H), 2.35 (s, 3H), 2.23 (s, 3H), 0.95 (t, *J* = 7.9 Hz, 9H), 0.62 (q, *J* = 7.9 Hz, 6H); ^{13}C NMR (101 MHz, $CDCl_3$) δ (ppm): 143.0, 140.3, 138.8, 136.8, 134.9, 131.6, 129.6, 129.5, 128.7, 127.3, 21.34, 21.27, 7.5, 2.9; HRMS (ESI) *m*/*z* calcd for $C_{22}H_{30}SiNa$ $[M+Na]^+$: 345.2009, found: 345.2019.

4.4.3.4 (*E*)-(1,2-bis(4-methoxyphenyl)vinyl)triethylsilane, **36c**

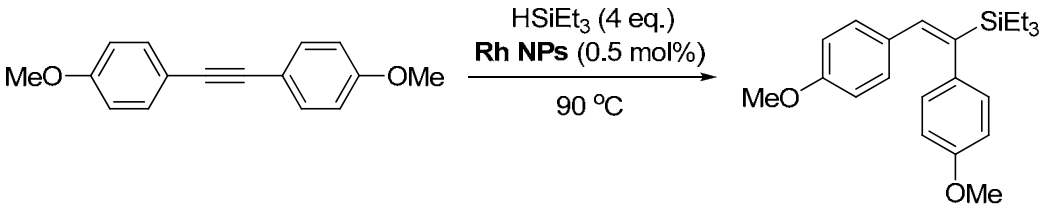

Following the general procedure for the hydrosilylation, 1,2-bis(4-methoxyphenyl)ethyne (119 mg, 0.5 mmol), was allowed to react with triethylsilane (320 µL, ρ = 0.73 g/mL, 2 mmol) at 90°C for 21 h (GC monitoring). Colorless oil (172 mg, 97%); ^{1}H NMR (400 MHz, $CDCl_3$) δ (ppm): 6.91 (two doublets overlapped, *J* = 6.9 Hz, 4H), 6.86 (d, *J* = 8.6 Hz, 2H), 6.69 (s, 1H), 6.64 (d, *J* = 8.7 Hz, 2H), 3.82 (s, 3H), 3.73 (s, 3H), 0.95 (t, *J* = 7.9 Hz, 9H), 0.62 (q, *J* = 7.9 Hz, 6H); ^{13}C NMR (101 MHz, $CDCl_3$) δ (ppm): 158.6, 157.7, 141.1, 138.6, 135.7, 131.0, 130.6, 128.6, 114.3, 113.5, 55.30, 55.27, 7.5, 3.0; HRMS (ESI) *m*/*z* calcd for $C_{22}H_{30}O_2SiNa$ $[M+Na]^+$: 377.1907, found: 377.1917.

4.4.3.5 (*E*)-(1,2-bis(4-chlorophenyl)vinyl)triethylsilane, **36d**

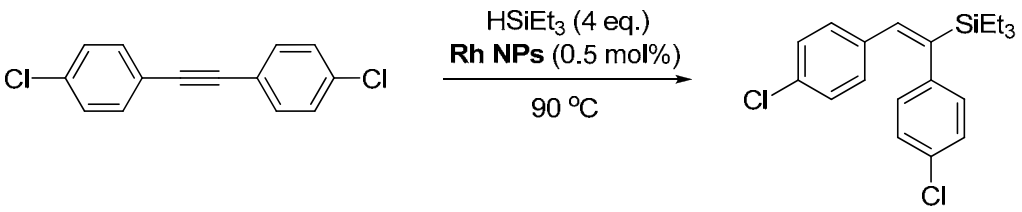

Following the general procedure for the hydrosilylation, 1,2-bis(4-chlorophenyl)ethyne (124 mg, 0.5 mmol), was allowed to react with triethylsilane (320 µL, ρ = 0.73 g/mL, 2 mmol) at 90°C for 20 h (GC monitoring). Light yellow oil (176 mg, 97%); ^{1}H NMR (400 MHz, $CDCl_3$) δ (ppm): 7.28-7.26 (2H, d overlapped with $CDCl_3$), 7.08 (d, *J* = 8.5 Hz, 2H), 6.92-6.86 (m, 4H), 6.73 (s, 1H), 0.95 (t, *J* = 7.9 Hz, 9H), 0.63 (q, *J* = 7.9 Hz, 6H); ^{13}C NMR (101 MHz, $CDCl_3$) δ (ppm): 144.0, 141.4, 138.3, 135.7, 133.0, 131.8, 130.8, 129.1, 128.8, 128.3, 7.4, 2.9; EA calculated for $C_{20}H_{24}Cl_2Si$: 66.10% C, 6.66% H, found: 66.19% C, 6.96% H.

4.4.3.6 (*E*)-(1,2-bis(4-bromophenyl)vinyl)triethylsilane, **36e**[370]

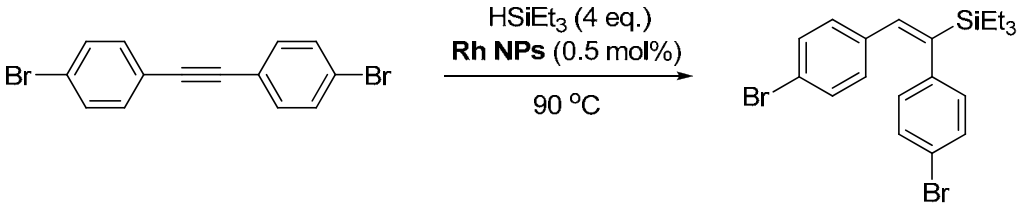

Following the general procedure for the hydrosilylation, 1,2-bis(4-bromophenyl)ethyne (118 mg, 0.5 mmol), was allowed to react with triethylsilane (320 µL, ρ = 0.73 g/mL, 2 mmol) at 90°C for 19 h (GC monitoring). Light yellow oil (215 mg, 95%); ^{1}H NMR (400 MHz, $CDCl_3$) δ (ppm): 7.42 (d, *J* = 8.3 Hz, 2H), 7.24 (d, *J* = 8.5 Hz, 2H), 6.84 (d, *J* = 8.3 Hz, 2H), 6.81 (d, *J* = 8.5 Hz, 2H), 6.71 (s, 1H), 0.94 (t, *J* = 7.9 Hz, 9H), 0.63 (q, *J* = 7.9 Hz, 6H); ^{13}C NMR (101 MHz, $CDCl_3$) δ (ppm): 144.2, 141.9, 138.2, 136.1, 132.1, 131.3, 131.1, 129.1, 121.3, 119.8, 7.42, 2.84.

4.4.3.7 (*E*)-(1,2-di(naphthalen-1-yl)vinyl)triethylsilane, **37**

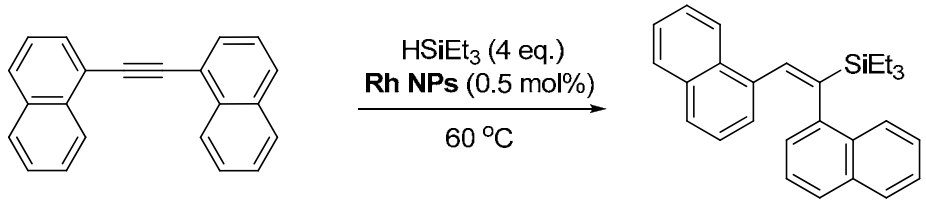

Following the general procedure for the hydrosilylation, 1,2-di(naphthalen-1-yl)ethyne (139 mg, 0.5 mmol), was allowed to react with triethylsilane (320 µL, ρ = 0.73 g/mL, 2 mmol) at 60°C for 19 h (GC monitoring). Colourless sticky oil (183 mg, 93%); ^{1}H NMR (360 MHz, $CDCl_3$) δ (ppm): 8.23 (d, *J* = 8.4 Hz, 1H), 7.92 (d, *J* = 8.3 Hz, 1H), 7.76-7.73 (m, 3H), 7.60-7.49 (m, 2H), 7.49-7.46 (m, 2H), 7.36 (t, *J* = 7.4 Hz, 1H), 7.31-7.27 (m, 2H), 7.05 (d, *J* = 7.0 Hz, 1H), 6.92-6.86 (m, 2H), 1.00 (t, *J* = 7.8 Hz, 9H), 0.71 (q, *J* = 7.8 Hz, 6H); ^{13}C NMR (90 MHz, $CDCl_3$) δ (ppm): 144.4, 140.6, 138.7, 134.7, 133.6, 133.5, 131.9, 131.5, 128.7, 128.3, 127.4, 126.3, 126.2, 126.1, 125.9, 125.60, 125.56, 125.52, 125.4, 125.2, 124.6, 124.1, 7.6, 3.6; HRMS (ESI) *m*/*z* calcd for $C_{28}H_{30}SiNa$ $[M+Na]^+$: 417.2009, found: 417.1998.

4.4.3.8 (*E*)-(1, 2-di(thiophen-3-yl)vinyl)triethylsilane, **38**[320]

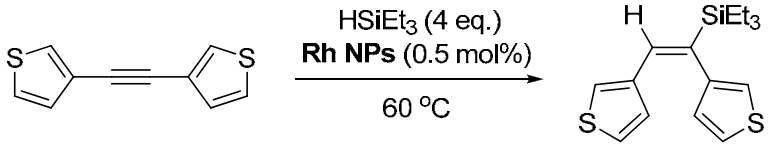

Following the general procedure for the hydrosilylation, 1,2-di(thiophen-3-yl)ethyne (95 mg, 0.5 mmol), was allowed to react with triethylsilane (320 µL, ρ = 0.73 g/mL, 2 mmol) at 60°C for 6 h (GC monitoring). Colorless oil (149 mg, 97%); ^{1}H NMR (400 MHz, $CDCl_3$) δ (ppm): 7.37-7.35 (m, 1H), 7.07-7.05 (m, 1H), 6.88-6.87 (m, 1H), 6.83-6.80 (m, 3H), 6.56-6.54 (m, 1H), 0.98 (t, *J* = 7.9 Hz, 9H), 0.67 (q, 7.8 Hz, 6H). ^{13}C NMR (101 MHz, $CDCl_3$) δ (ppm): 143.2, 139.6, 137.2, 134.3, 128.3, 128.0, 125.8, 125.0, 124.7, 118.9, 7.5, 2.8.

4.4.3.9 (*E*)-5-triethylsilyl-5-decene, **39**[320]

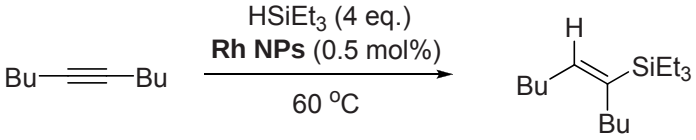

Following the general procedure for the hydrosilylation, 5-decyne (69 mg, 0.5 mmol), was allowed to react with triethylsilane (320 µL, ρ = 0.73 g/mL, 2 mmol) at 60°C for 40 h (GC monitoring). Colorless oil (122 mg, 96%); ^{1}H NMR (360 MHz, $CDCl_3$) δ (ppm): 5.65 (t, *J* = 6.8 Hz, 1H), 2.11-2.03 (m, 4H), 1.34-1.25 (m, 8H), 0.92-0.88 (m, 15H), 0.57 (q, *J* = 7.8 Hz, 6H); ^{13}C NMR (101 MHz, $CDCl_3$) δ (ppm): 142.0, 137.3, 32.6, 32.1, 29.9, 28.3, 23.4, 22.6, 14.23, 14.20, 7.6, 3.3.

4.4.3.10 (*E*)-(1,4-dimethoxybut-2-en-2-yl)triethylsilane, **40**[370]

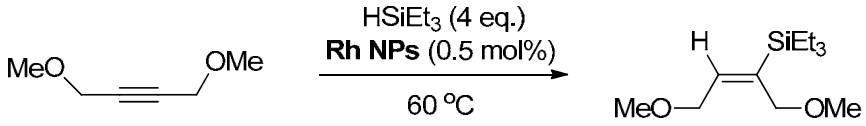

Following the general procedure for the hydrosilylation, 1,4-dimethoxy-2-butyne (57 mg, 0.5 mmol), was allowed to react with triethylsilane (320 µL, ρ = 0.94 g/mL, 2 mmol) at 60°C for 20 h (GC monitoring). Colorless oil (114 mg, 99%); ^{1}H NMR (360 MHz, $CDCl_3$) δ (ppm): 5.95 (t, *J* = 5.5 Hz, 1H), 4.09 (d, *J* = 5.5 Hz, 2H), 3.99 (s, 2H), 3.35 (s, 3H), 3.28 (s, 3H), 0.92 (t, *J* = 7.9 Hz, 9H), 0.62 (q, *J* = 7.8 Hz, 6H); ^{13}C NMR (90 MHz, $CDCl_3$) δ (ppm): 140.4, 139.7, 31.9, 30.7, 23.0, 14.3, 7.7, 4.1.

4.4.3.11 (*E*)-(1,2-diphenylvinyl)triethoxysilane, **41a**[320]

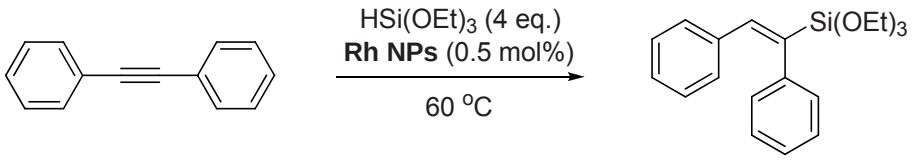

Following the general procedure for the hydrosilylation, diphenylacetylene (89 mg, 0.5 mmol), was allowed to react with triethoxysilane (370 µL, ρ = 0.89 g/mL, 2 mmol) at 60°C for 36 h (GC monitoring). Colorless oil (170 mg, 99%); ^{1}H NMR (360 MHz, $CDCl_3$) δ (ppm): 7.29-7.25 (signal overlapped with $CDCl_3$, 2H), 7.21-7.16 (m, 4H), 7.12-7.11 (m, 3H), 7.04-7.03 (m, 2H), 3.83 (q, *J* = 7.0 Hz, 6H), 1.20 (t, *J* = 7.0 Hz, 9H); ^{13}C NMR (90 MHz, $CDCl_3$) δ (ppm): 142.6, 140.8, 137.1, 137.0, 130.0, 128.6, 128.4, 128.0, 127.6, 126.6, 58.9, 18.3.

4.4.3.12 (*E*)-(1,2-diphenylvinyl)triphenylsilane, **41b**[370]

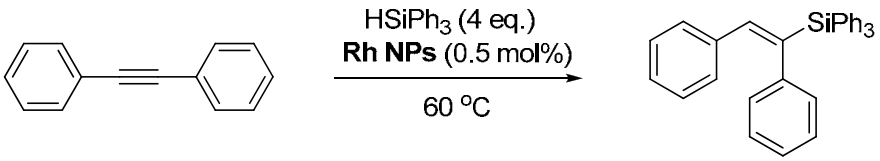

Following the general procedure for the hydrosilylation, diphenylacetylene (89 mg, 0.5 mmol), was allowed to react with triphenylsilane (520 mg, 2 mmol) at 60°C for 36 h (GC monitoring). White powder (217 mg, 99%); ^{1}H NMR (250 MHz, $CDCl_3$) δ (ppm): 7.48-7.39 (m, 9H), 7.35-7.30 (m, 6H), 7.14-7.10 (m, 6H), 7.02 (s, 1H), 6.99-6.95 (m, 2H), 6.90-6.88 (m, 2H); ^{13}C NMR (101 MHz, $CDCl_3$) δ (ppm): 143.5, 142.0, 141.2, 137.3, 136.7, 134.0, 129.9, 129.7, 128.6, 128.5, 128.1, 127.9, 127.7,127.6, 126.1.

4.4.3.13 (*E*)-Triethyl(1-phenyl-2-(*p*-tolyl)vinyl)silane, **43a**[320]

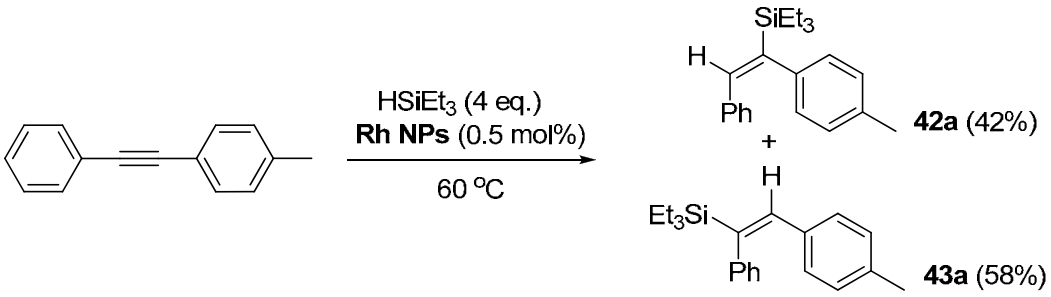

Following the general procedure of the hydrosilylation, 1-methyl-4-(phenylethynyl)benzene (96 mg, 0.5 mmol), was allowed to react with triethylsilane (320 µL, ρ = 0.73 g/mL, 2 mmol) at 60 °C for 58 h (100% conv. GC, mixture of regioisomers **42a**:**43a** = 42:58). Light yellow oil (153 mg, 99%). Some spectroscopic data of the mixture: ^{1}H NMR (360 MHz, $CDCl_3$) δ (ppm), 2.35 (s, 3H, -C**H**$_3$, minor), 2.23 (s, 3H, -C**H**$_3$, major) (for other signals see spectrum).

4.4.3.14 (*E*)-Triethyl(1-phenyl-2-(*m*-tolyl)vinyl))silane, **43b**[320]

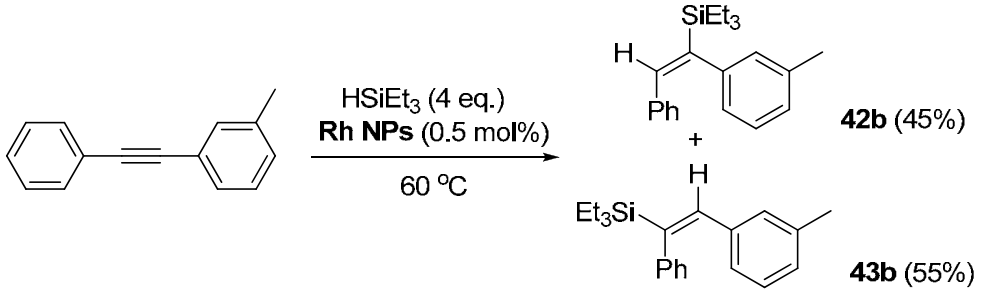

Following the general procedure of the hydrosilylation, 1-methyl-3-(phenylethynyl)benzene (96 mg, 0.5 mmol), was allowed to react with triethylsilane (320 µL, ρ = 0.73 g/mL, 2 mmol) at 60°C for 20 h (100% conv. GC, mixture of regioisomers **42b**:**43b** = 45:55). Colourless oil (153 mg, 99%). Some spectroscopic data of the mixture: ^{1}H NMR (360 MHz, $CDCl_3$) δ (ppm): 2.31 (s, 3H, -C**H**$_3$, minor), 2.16 (s, 3H, -C**H**$_3$, major) (for other signals see spectrum).

4.4.3.15 (*E*)-Triethyl(1-(naphthalen-1-yl)-2-phenylvinyl) silane, **42c**.[320]

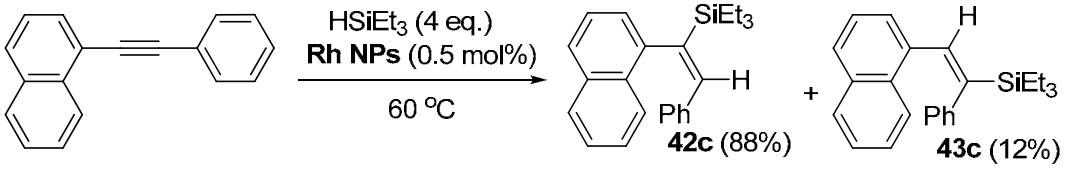

Following the general procedure of the hydrosilylation, 1-(phenylethynyl)naphthalene (114 mg, 0.5 mmol), was allowed to react with triethylsilane (320 µL, ρ = 0.73 g/mL, 2 mmol) at 60°C for 60 h (100% conv. GC, mixture of regioisomers **42c**:**43c** = 88:12). Yellow oil (171 mg, 99%). Spectroscopic data for the main product **42c**: ^{1}H NMR (360 MHz, $CDCl_3$) δ (ppm): 7.89 (d, *J* = 8.4 Hz, 1H, Ar-**H**), 7.84 (d, *J* = 8.2 Hz, 1H, Ar-**H**), 7.73 (d, *J* = 8.2 Hz, 1H, Ar-**H**), 7.43 (t, *J* = 7.6 Hz, 2H, Ar-**H**), 7.37-7.30 (m, 1H, Ar-**H**), 7.10 (d, *J* = 7.0 Hz, 1H, Ar-**H**), 7.05 (s, 1H, C=C**H**-), 7.00-6.95 (m, 3H, Ar-**H**), 6.87-6.86 (m, 2H, Ar-**H**), 0.91 (t, *J* = 7.8 Hz, 9H, -$CH_2C\mathbf{H}_3$), 0.60 (q, *J* = 7.9 Hz, 6H, -C$\mathbf{H}_2CH_3$). ^{13}C NMR (90 MHz, $CDCl_3$) δ (ppm): 142.2, 141.0, 140.2, 140.1, 137.4, 133.9, 130.8, 129.2, 128.4, 128.1, 128.0, 127.3, 126.1, 126.0, 125.9, 125.7, 123.7, 7.5, 3.3.

4.4.3.16 (*E*)-Triethyl(2-*p*-methoxyphenyl-1-phenylvinyl)silane, **43d**[320]

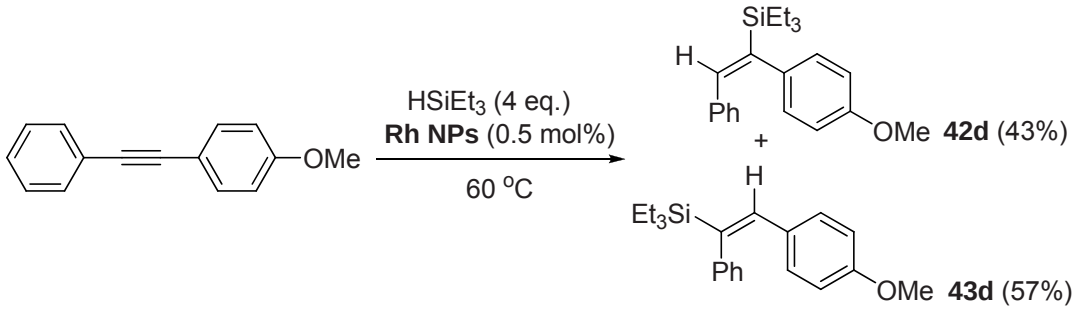

Following the general procedure for the hydrosilylation, 1-methoxy-4-(phenylethynyl)benzene (104 mg, 0.5 mmol), was allowed to react with triethylsilane (320 µL, ρ = 0.73 g/mL, 2 mmol) at 60°C for 40 h (100% conv. GC, mixture of regioisomers **42d**:**43d** = 43:57). Pale yellow oil (161 mg, 99%). Some spectroscopic data of the mixture: ^{1}H NMR (360 MHz, $CDCl_3$) δ (ppm): 3.81 (s, 3H, OC$\mathbf{H}_3$ minor isomer), 3.72 (s, 3H, OC$\mathbf{H}_3$, major isomer) (for other signals see the spectrum).

4.4.3.17 (*E*)-1-(4-(2-phenyl-1-(triethylsilyl)vinyl)phenyl)ethanone, **42e**[320]

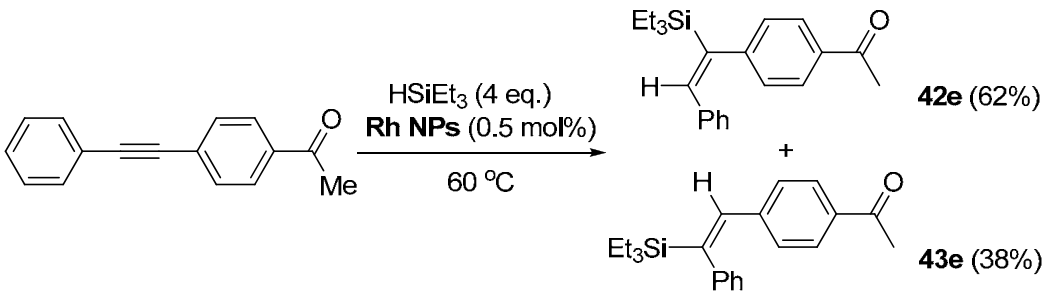

Following the general procedure for the hydrosilylation, 1-(4-(phenylethynyl)phenyl)ethanone (110 mg, 0.5 mmol), was allowed to react with triethylsilane (320 µL, ρ = 0.73 g/mL, 2 mmol) at 60°C for 18 h (100% conv. GC, initial mixture of regioisomers **42e**:**43e** = 62:38**;** E/Z isomerization of each isomer occurs upon standing). Yellowish liquid (167 mg, 99%). Selected spectroscopic data for the main product **42e**: ^{1}H NMR (360 MHz, $CDCl_3$) δ (ppm), 7.90 (d, *J* = 8.1 Hz, 2H, Ar-**H**), 7.11-7.08 (m, 5H, Ar-**H**), 6.95-6.93 (m, 2H, Ar-**H**) 6.81 (s, 1H, =C**H**), 2.61 (s, 3H, -COC**H**$_3$), 0.95 (t, *J* = 7.8 Hz, 9H, -CH_2C**H**$_3$), 0.66 (q, *J* = 7.8 Hz, 6H, -C**H**$_2$$CH_3$).

4.4.3.18 (*E*)-(2-phenyl-1-(thiophen-3-yl)vinyl)triethylsilane, **42f**

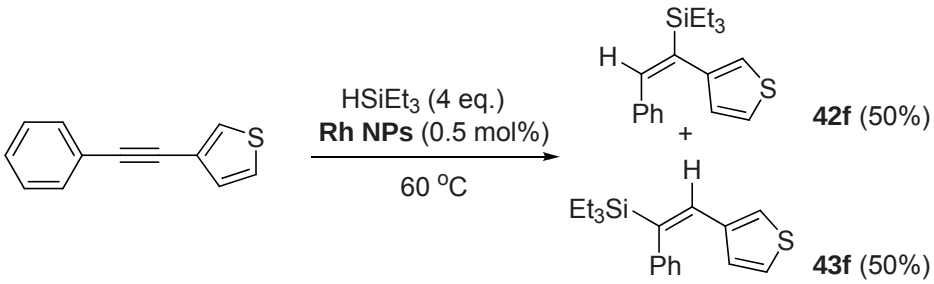

Following the general procedure for the hydrosilylation, 3-(phenylethynyl)thiophene (92 mg, 0.5 mmol), was allowed to react with triethylsilane (320 µL, ρ = 0.73 g/mL, 2 mmol) at 60°C for 14 h (100% conv. GC, initial mixture of regioisomers **42f**:**43f** = 50:50; E/Z isomerization of each isomer occurs upon standing in the air for some days). Colourless liquid (149 mg, 99%). Some spectroscopic data for the mixture, ^{1}H NMR (500 MHz, $CDCl_3$) δ (ppm): 0.98-0.93 (-Si(CH_2C**H**$_3$)$_3$), 0.69-0.61 (-Si(C**H**$_2$$CH_3$)$_3$); see the spectra for other related signals; HRMS (ESI) *m*/*z* calcd for $C_{18}H_{24}SSiNa$ $[M+Na]^+$: 323.1260, found: 323.1267.

4.4.3.19 (*E*)-(1-(4-nitrophenyl)-2-phenylvinyl)triethylsilane, **42g**[393]

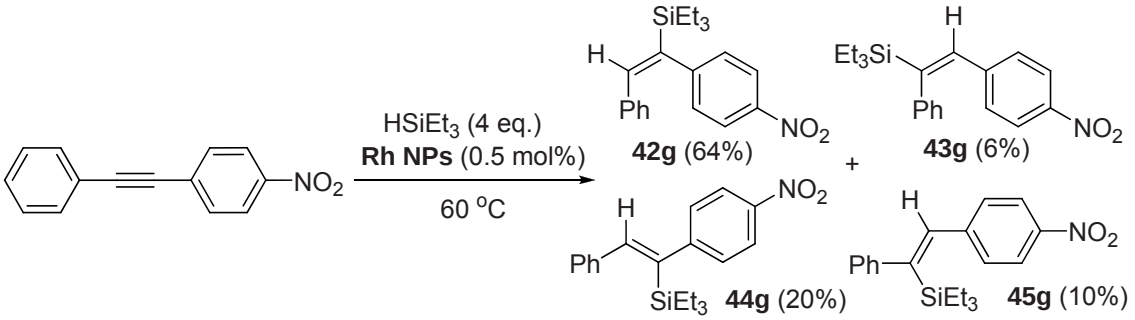

[393] Hamze, A.; Provot, O.; Alami, M.; Brion, J.-D. *Org. Lett.* **2005**, *25*, 5625.

Following the general procedure for the hydrosilylation, 1-nitro-4-(phenylethynyl)benzene (112 mg, 0.5 mmol), was allowed to react with triethylsilane (320 µL, ρ = 0.73 g/mL, 2 mmol) at 60°C for 30 h (100% conv. GC; mixture of isomers **42g**:**43g**:**44g**:**45g** = 64:6:20:10). Yellow liquid (129 mg, 76%). Some selected spectroscopic data for the mixture: ^{1}H NMR (500 MHz, $CDCl_3$), (**42g**) 6.89 (s, =C**H**); (**43g**) 6.86 (=C**H**); (**44g**) 7.36 (=C**H**); (**45g**) 7.30 (=C**H**), and see the spectra for other signals.

4.4.3.20 (*E*)-triethyl(1-phenyl-1-propenyl)silane, **47a**[320]

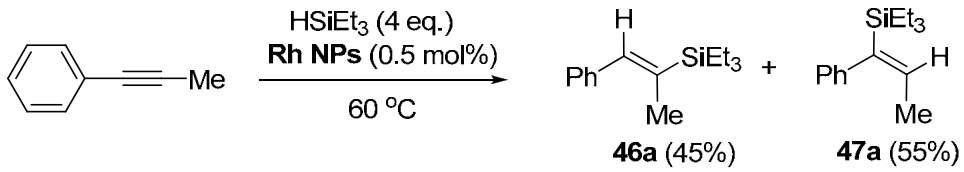

46a (45%) **47a** (55%)

Following the general procedure for the hydrosilylation, 1-phenyl-1-propyne (63 µL, ρ = 0.93 g/mL, 0.5 mmol) was allowed to react with triethylsilane (320 µL, ρ = 0.73 g/mL, 2 mmol) at 60°C for 30 h (100% conv. GC, mixture of regioisomers **46a**:**47a** = 45:55). Pale yellow liquid (110 mg, 95%). Some selected spectroscopic data for the mixture: ^{1}H NMR (500 MHz, $CDCl_3$) δ (ppm), (**46a**) 6.72 (s, =C**H**), 1.95 (s, -C**H$_3$**); (**47a**) 6.95 (d, *J* = 7.9 Hz, Ar-**H**), 6.08 (q, *J* = 6.5 Hz, =C**H**), 1.59 (d, *J* = 6.7 Hz, -C**H$_3$**).

4.4.3.21 (*E*)-Triethyl((5-(triethylsilyl)dec-5-en-1-yl)oxy)silane, **46b**

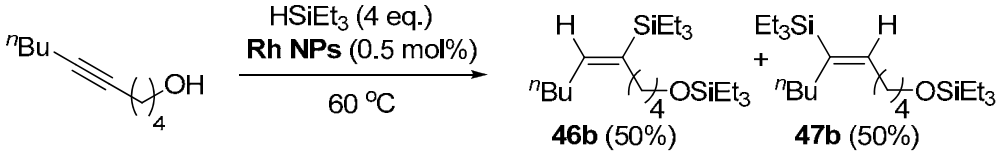

46b (50%) **47b** (50%)

Following the general procedure for the hydrosilylation, dec-5-yn-1-ol (90 µL, ρ = 0.86 g/mL, 0.5 mmol) was allowed to react with triethylsilane (480 µL, ρ = 0.73 g/mL, 3 mmol) at 60°C for 37 h (100% conv. GC, mixture of regioisomers **46b**:**47b** = 50:50). Pale yellow liquid (182 mg, 95%). Some selected spectroscopic data for the mixture: ^{1}H NMR (500 MHz, $CDCl_3$) δ (ppm), 5.68-5.64 (two triplets overlapped, 2H, =C**H**), 3.62-3.59 (two triplets overlapped, 2H, -OC**H$_2$**); HRMS (ESI) *m*/*z* calcd for $C_{22}H_{48}OSi_2Na$ $[M+Na]^+$: 407.3136, found: 407.3147.

4.4.3.22 (*E*)-methyl 2-(triethylsilyl)oct-2-enoate, **47c**

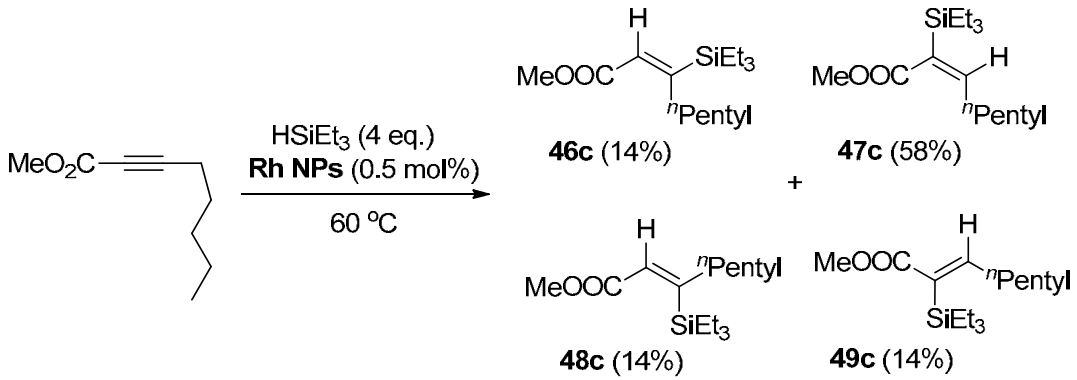

Following the general procedure for the hydrosilylation, methyl oct-2-ynoate (167 µL, ρ = 0.92 g/mL, 1 mmol) was allowed to react with triethylsilane (320 µL, ρ = 0.73 g/mL, 2 mmol) at 60°C for 55 h (100% conv. GC, mixture of isomers **46c**:**47c**:**48c**:**49c** = 14:58:14.14). Colorless oil (188 mg, 69%). Some selected spectroscopic data for the mixture: ^{1}H NMR (500 MHz, $CDCl_3$) δ (ppm), (**47c**) 6.08 (t, *J* = 7.1 Hz, 1H, =C**H**), 3.70 (s, 3H, COOC**H**$_3$); (**46c**) 5.97 (=C**H**); (**48c**) 6.31 (=C**H**); (**49c**) 7.11 (=C**H**); HRMS (ESI) *m*/*z* calcd for $C_{15}H_{30}O_2SiNa$ $[M+Na]^+$: 293.1907, found: 293.1911.

4.4.3.23 (*E*)-(2-cyclohexylvinyl)triethylsilane, **46d**[394]

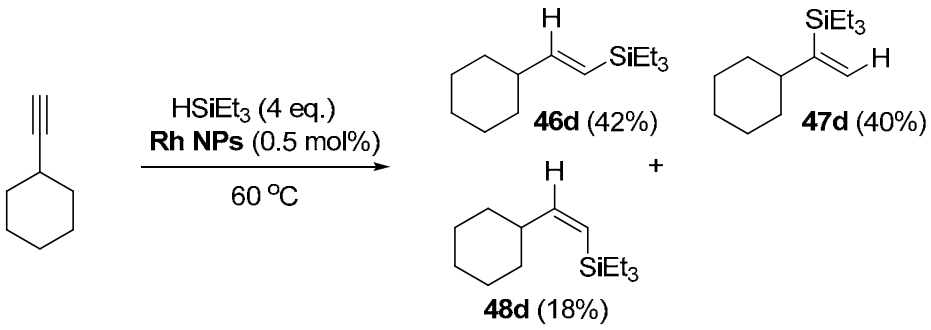

Following the general procedure for the hydrosilylation, ethynylcyclohexane (108 mg, 1 mmol), was allowed to react with triethylsilane (640 µL, ρ = 0.73 g/mL, 4 mmol) at 60°C for 33 h (100% conv. GC, mixture of isomers **46d**:**47d**:**48d** = 42:40:18). Colorless oil (189 mg, 84%). Some selected spectroscopic data of the mixture: ^{1}H NMR (500 MHz, $CDCl_3$) δ (ppm), (**46d**) 5.97 (m, 1H, SiCH=C**H**), 5.47 (m, SiC**H**=CH); (**47d**) 5.29 and 5.57 (SiC=C**H**$_2$); (**48d**) 6.18 (m, SiCH=C**H**), 5.26 (m, SiC**H**=CH), and see spectrum for other signals.

---

[394] Sridevi, V. S.; Fan, W. Y.; Leong, W. K. *Organometallics* **2007**, *26*, 1157.

4.4.3.24 (*E*)-Triethyl(2,2,7,7-tetramethyloct-3-en-5-yn-4-yl)silane, **50**[370]

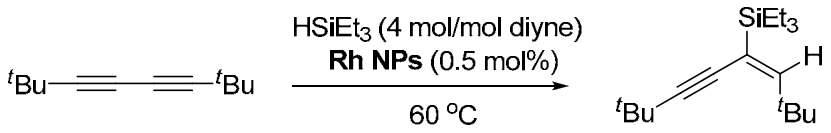

Following the general procedure for the hydrosilylation, 2,2,7,7-tetramethylocta-3, 5-diyne (81 mg, 0.5 mmol) was allowed to react with triethylsilane (320 µL, ρ = 0.73 g/mL, 2 mmol) at 60°C for 20 h (GC monitoring). Colorless oil (132 mg, 95%); ^{1}H NMR (400 MHz, $CDCl_3$) δ (ppm): 5.86 (s, 1H), 1.24 (s, 9H), 1.20 (s, 9H), 0.95 (t, *J* = 7.9 Hz, 9H), 0.63 (q, *J* = 7.9 Hz, 6H). ^{13}C NMR (101 MHz, $CDCl_3$) δ (ppm): 159.0, 119.0, 108.5, 79.1, 35.8, 31.1, 29.9, 28.6, 7.5, 3.1.

4.4.3.25 (5*Z*, 7*Z*)-dodeca-5,7-diene-6,7-diylbis(triethylsilane), **51**[370]

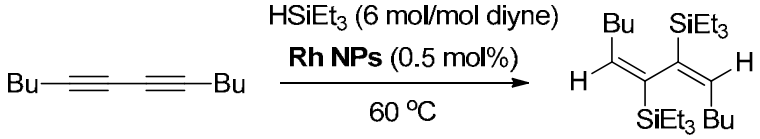

Following the general procedure for the hydrosilylation, dodeca-5,7-diyne (81 mg, 0.5 mmol), was allowed to react with triethylsilane (480 µL, ρ = 0.73 g/mL, 3 mmol) at 60°C for 20 h (GC monitoring). Colourless sticky oil (193 mg, 98%); ^{1}H NMR (250 MHz, $CDCl_3$) δ (ppm): 5.60 (t, *J* = 6.6 Hz, 2H), 1.99-1.88 (m, 4H), 1.34-1.26 (m, 8H), 0.94 (t, *J* = 7.8 Hz, 24H), 0.57 (q, *J* = 7.3 Hz, 12H); ^{13}C NMR (90 MHz, $CDCl_3$) δ (ppm): 140.4, 139.7, 31.9, 30.7, 23.0, 14.3, 7.7, 4.1.

4.4.4 Reduction of nitroarenes under catalysis by gold nanoparticles

4.4.4.1 General procedure for the reduction of nitroarenes by gold nanoparticles

To a well stirred mixture of chosen introarene (1.0 mmol) and sodium borohydride (1.324 g, 35 mmol) in distilled water (10 mL) in a small vial, **M16** (0.3 mol% Au, 0.007 g) was added and the mixture was stirred at room temperature. Upon completion of the reaction (monitored by TLC), the reaction mixture was extracted with diethyl ether. The organic layer was dried over anhydrous Na_2SO_4 and then the solvent was evaporated under reduced pressure, affording the corresponding product which was pure in most cases. When some impurities were detected by TLC analysis, the crude product was purified by flash chromatography on silica-gel using mixtures of ethyl acetate/hexane as eluent.

4.4.4.2 Aniline, **52**[321a]

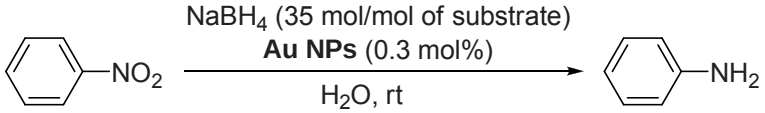

Following the general procedure, *p*-nitrobenzene (0.123 g, 1.0 mmol) reacted with sodium borohydride (1.324 g, 35 mmol) in the presence of gold catalyst **M16** (0.3 mol% Au, 0.007 g) to afford aniline **52** as a yellow oil (93 g, 99%). ^{1}H NMR (360 MHz, $CDCl_3$) δ (ppm): 7.19-7.14 (t, *J* = 7.8 Hz, 2 H), 6.79-6.75 (t, *J* = 7.4 Hz, 1 H), 6.70 (d, J = 7.4Hz, 2 H), 3.52 (s, 2H); ^{13}C NMR (90 MHz, $CDCl_3$) δ (ppm): δ 146.4, 129.4, 118.7, 115.2.

4.4.4.3 *m*-Phenylenediamine, **53**[321a]

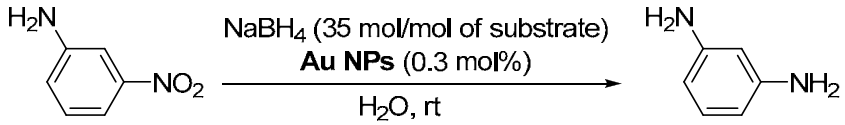

Following the general procedure, *m*-nitroaniline (0.138 g, 1.0 mmol) reacted with sodium borohydride (1.324 g, 35 mmol) in the presence of gold catalyst **M16** (0.3 mol% Au, 0.007 g) to afford *m*-phenylenediamine **53** as a liquid (0.107 g, 99%). ^{1}H NMR (360 MHz, $CDCl_3$) δ (ppm): 6.97-6.92 (t, *J* = 7.8 Hz, 1H), 6.13-6.03 (d, *J* = 7.9 Hz, 2 H), 6.02 (s, 1H), 3.53 (s, 4H); ^{13}C NMR (90 MHz, $CDCl_3$) δ (ppm): δ 147.6, 130.3, 106.1, 102.0.

4.4.4.4 *p*-Aminobenzenesulfonamide, **54**

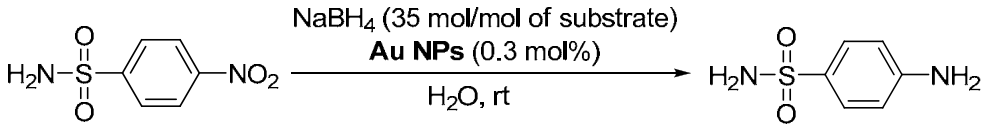

Following the general procedure, *p*-nitrobenzenesulfonamide (0.202 g, 1.0 mmol) reacted with sodium borohydride (1.324 g, 35 mmol) in the presence of gold catalyst **M16** (0.3 mol% Au, 0.007 g) to afford *p*-aminobenzenesulfonamide **54** as a white solid (0.170 g, 99%). ^{1}H NMR (360 MHz, $(CD_3)_2SO$) δ (ppm): 7.44 (d, *J* = 8.5 Hz, 2H), 6.84 (s, 2H), 6.58 (d, *J* = 8.5 Hz, 2H), 5.79 (s, 2H); ^{13}C NMR (90 MHz, $(CD_3)_2SO$) δ (ppm): 151.9, 130.2, 127.4, 112.4.

4.4.4.5 *p*-Methoxyaniline, **55**[321a]

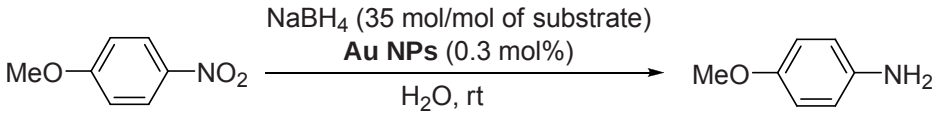

Following the general procedure, 1-methoxy-4-nitrobenzene (0.153 g, 1.0 mmol) reacted with sodium borohydride (1.324 g, 35 mmol) in the presence of gold catalyst **M16** (0.3 mol% Au, 0.007 g) to afford *p*-methoxyaniline **55** as a white solid (0.121 g, 98%). ^{1}H NMR (400 MHz, $CDCl_3$) δ (ppm): 6.75 (d, 2 H, *J* = 8.4 Hz), 6.65 (d, 2 H, *J* = 8.4 Hz), 3.75 (s, 3 H), 3.40 (s, 2 H); ^{13}C NMR (100 MHz, $CDCl_3$) δ (ppm): 152.9, 140.0, 116.5, 114.9, 55.8.

4.4.4.6 *p*-Bromoaniline, **56**[321a]

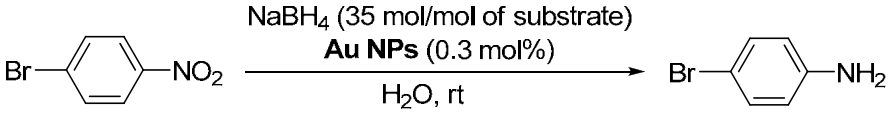

Following the general procedure, 1-bromo-4-nitrobenzene (0.201 g, 1.0 mmol) reacted with sodium borohydride (1.324 g, 35 mmol) in the presence of gold catalyst **M16** (0.3 mol% Au, 0.007 g) to afford *p*-bromoaniline **56** as a white solid (0.124 g, 72%). ^{1}H NMR (400 MHz, $CDCl_3$) δ (ppm): 7.23 (d, 2 H, *J* = 8.6 Hz), 6.56 (d, 2 H, *J* = 8.6 Hz), 3.65 (s, 2 H); ^{13}C NMR (100 MHz, $CDCl_3$) δ (ppm): 145.6, 132.2, 116.9, 110.4.

4.4.4.7 *p*-Aminobenzonitrile, **57**[321a]

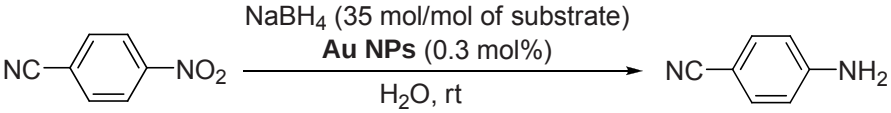

Following the general procedure, *p*-nitrobenzonitrile (0.148 g, 1.0 mmol) reacted with sodium borohydride (1.324 g, 35 mmol) in the presence of gold catalyst **M16** (0.3 mol% Au, 0.007 g) to afford *p*-aminobenzonitrile **57** as a white solid (0.106 g, 89%). ^{1}H NMR (400 MHz, $CDCl_3$) δ (ppm): 7.41 (d, 2 H, *J* = 8.4 Hz), 6.64 (d, 2 H, *J* = 8.5 Hz), 4.41 (s, 2 H); ^{13}C NMR (100 MHz, $CDCl_3$) δ (ppm): 150.7, 133.9, 120.3, 114.6, 100.2.

4.4.4.8 Methyl *p*-aminobenzoate, **58**[321a]

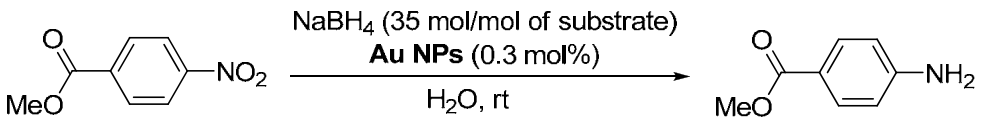

Following the general procedure, *p*-nitrobenzoate (0.181 g, 1.0 mmol) reacted with sodium borohydride (1.324 g, 35 mmol) in the presence of gold catalyst **M16** (0.3 mol% Au, 0.007 g) to afford methyl *p*-aminobenzoate **58** as a white solid (0.124 g, 82%). ^{1}H NMR (400 MHz, $CDCl_3$) δ (ppm): 7.85 (d, 2 H, *J* = 8.6 Hz), 6.64 (d, 2 H, *J* = 8.6 Hz), 4.04 (s, 2 H), 3.85 (s, 3 H); ^{13}C NMR (100 MHz, $CDCl_3$) δ (ppm): 167.3, 151.0, 131.7, 119.8, 113.9, 51.7.

4.4.4.9 *p*-Aminophenol, **59**[321a]

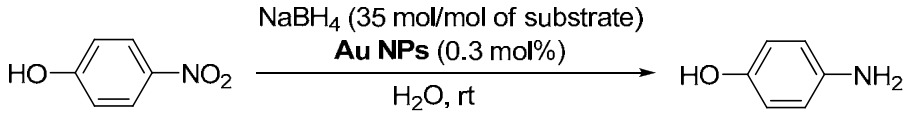

Following the general procedure, *p*-nitrophenol (0.139 g, 1.0 mmol) reacted with sodium borohydride (1.324 g, 35 mmol) in the presence of gold catalyst **M16** (0.3 mol% Au, 0.007 g) to afford methyl *p*-aminophenol **59** as a white solid (0.108 g, 99%). ^{1}H NMR (360 MHz, $(CD_3)_2SO$) δ (ppm): 8.45 (broad s, 1 H), 6.46-6.41 (m, 4 H), 4.35 (s, 2 H); ^{13}C NMR (90 MHz, $(CD_3)_2SO$) δ (ppm): 148.4, 140.6, 115.6, 115.2.

Summary and general conclusions

In the present Thesis, two research lines have been pursued. The first one is centered to the applications of hypervalent iodine species in oxidative C-C and C-O bond-forming processes (Part I of the Thesis). The second research line is concerned with the development of recyclable catalysts based on water-soluble metal nanoparticles (Rh and Au) (Part II of the Thesis).

Part 1. In Chapter 1 of Part I a general overview of the structure, preparation and reactivity of hypervalent iodine reagents is presented.

Kita had reported that hypervalent organoiodane PIFA, upon activation with $BF_3{\cdot}Et_2O$, can induce the intermolecular oxidative dehydrogenative arene-arene coupling. Our group previously performed a direct oxidative four-component coupling involving binaphthalene and arenes. As an extension of that work, we have investigated the Kita-type direct dehydrogenative arylation protocol in the arylation of the linear ter- and quaternaphthalenes using the PIFA/$BF_3{\cdot}Et_2O$ system. It was found that, in contrast to the reactions performed in our group using naphthalene and binaphthalene, the arylation of higher oligonaphthalenes has led predominantly to the double-arylation products. Still, moderate yields of the larger octiarenes could be obtained in some cases from ternaphthalene. This is a noteworthy result, in that it constitutes a direct oxidative metal-free assembly of four unfunctionalized building block molecules. The interest in practical syntheses of such large oligonaphthalenes lies in their optoelectronic properties relevant in the design of solar cells or OLED devices. Small quantities of the formal dimerization/arylation products for both of ternaphthalene and quaternaphthalene have also been detected, representing the one-pot assembly of a linear deciarene. (Part I, Chapter 2)

Hypervalent species can also promote C-O couplings. A stoichiometric amount of Koser's reagent, PhI(OH)(OTs), has been used previously to achieve α-tosyloxylation of ketones. This process was improved with applying a catalytic amount of aryl iodides in the presence of terminal oxidants, whereby the iodine (III) reagent is generated *in situ*. Based on our interest in hybrid silica as recyclable catalyst, hybrid silica materials containing iodoarene moieties have been synthesized in this thesis by sol-gel methodologies from bis- and monosilylated precursors under nucleophilic catalysis. The sol-gel processes were performed with and without added TEOS. The materials were fully characterized by elemental analysis, ^{13}C and ^{29}Si CP-MAS solid state NMR, IR, TGA, and N_2-sorption measurements. The catalytic activity of the materials was tested in the α-tosyloxylation of ketones using *m*-CPBA as a terminal oxidant, affording

the corresponding α-tosyloxyketones in moderate to good isolated yields in some cases. Camphorsulfonic and methanosulfonic acids have also been successfully used for the oxidative functionalization of acetophenone. The recyclability has also been investigated and it was found that some of the materials can be recovered by filtration and reused successfully in a second run for several substrates (Part I, Chapter 3)

In a related research, we have found that, in addition to ArI, simple iodoalkanes can also be active in the catalytic oxidative α-tosyloxylation of aliphatic ketones. However, whereas with ArI the catalytic activity is based on the intermediacy of the $PhIX_2$ species, in the presence of the oxidant (*m*-CPBA) the iodoalkanes appear to be quickly degraded to the catalytically active inorganic iodite (and/or hypoiodite). Overoxidation and/or disproportionation of such species leads to the catalyst deactivation through the formation of a white solid identified as a previously unreported polymorph of the HIO_3 (Part I, Chapter 4).

Part 2. Metal nanoparticles can be prepared through various protocols and have found significant applications in catalysis. The topic is overviewed in some detail in Chapter 1 of Part II, including the preparation, characterization and catalytic applications in a great deal of organic transformations.

Following with our group's interest on the use of metal nanoparticles in catalysis, we present in this thesis water-soluble metal nanoparticles (Au and Rh) stabilized by a new nitrogen-rich PEG-tagged substrate as recyclable catalysts in different organic reactions. As described in the objective section (Chapter 2 of Part II), the stabilizer was prepared by a three-fold copper-catalyzed [3+2] cycloaddition (CuACC, "click" chemistry). The metal NPs were prepared in an efficient manner *via* the reduction of the corresponding chloride salts ($HAuCl_4$, $RhCl_3$) in the presence of the stabilizer using $NaBH_4$ as reducing agent in water at room temperature. It was found that varying the ratio of stabilizer to rhodium, the morphology of Rh NPs could be varied in a controlled fashion, affording particles ranging from small clusters to larger "nanoflowers". Similar phenomena have also been found for the formation of Au NPs with morphologies varying from small spheres to nanotadpoles. The newly prepared nanomaterials were fully characterized by TEM, ED, *p*-XRD, UV-vis and elemental analysis. The preparation of stabilizer and the stabilized nanoparticles are the subject of Chapter 3 of Part II.

The flower-like Rh NPs proved to be very effective to catalyze the stereoselective hydrosilylation of alkynes with silanes affording (*E*)-vinylsilanes in almost quantitative yields under solvent-free conditions. For the reactions involving volatile silanes, *e. g.*,

triethylsilane, the work-up consisted in extracting the reaction mixture with ether and then filtering the extract through a short plug of silica gel with hexane as eluent; upon evaporating the solvent and excess reagent under an air flow, the pure product was afforded without any further purification. The corresponding products can be extracted with diethyl ether and separated from the catalyst, because the stabilized Rh NPs are insoluble in ether. Thus, the Rh nanocatalysts have been recycled up to 7 times without any loss of activity. The Au NPs were found to be efficient and recyclable catalysts for the selective reduction of various nitroarenes to the corresponding anilines in water at room temperature. All the catalysis results with Rh and Au NPs are described in Chapter 4 of Part II.

Formula index

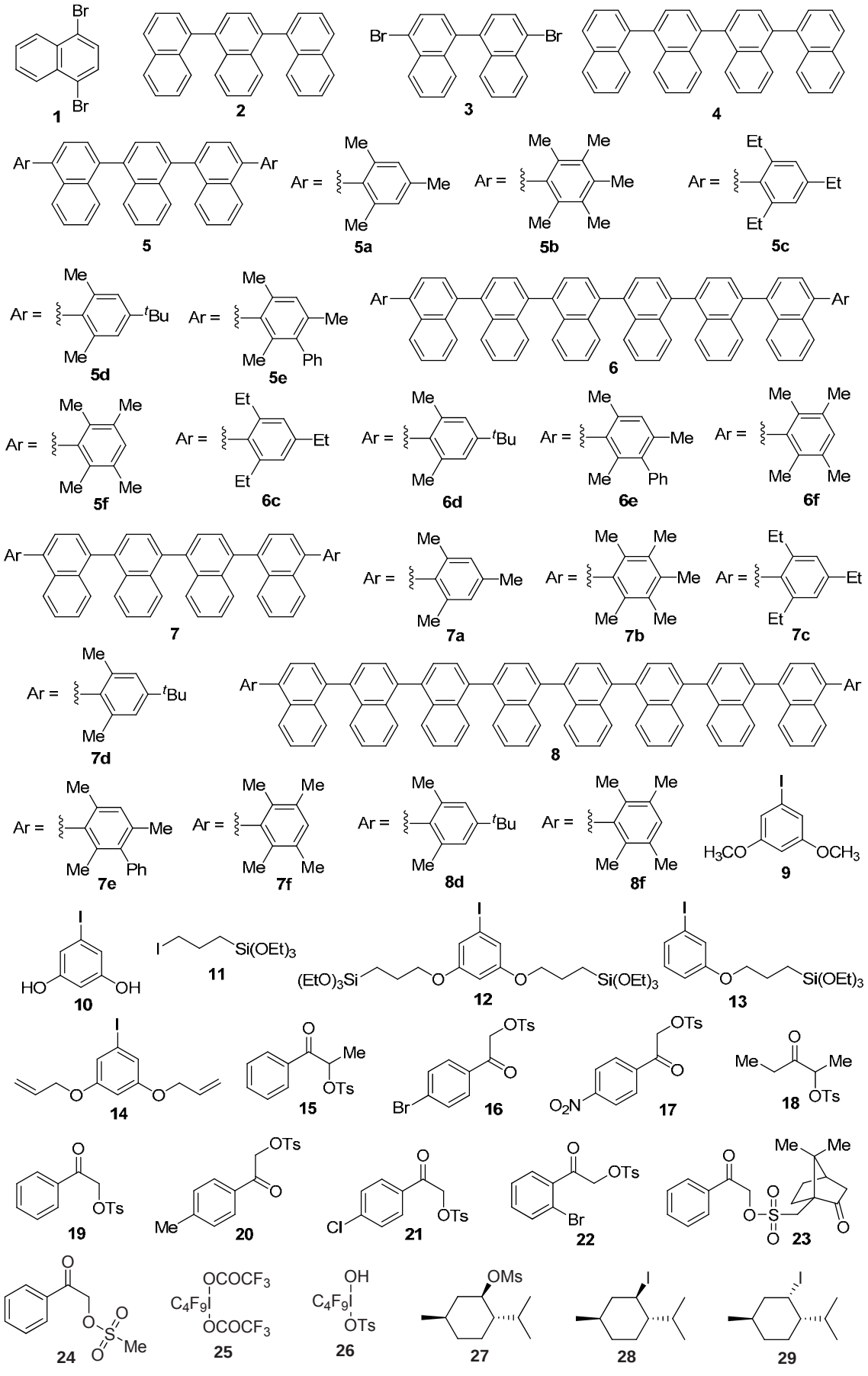

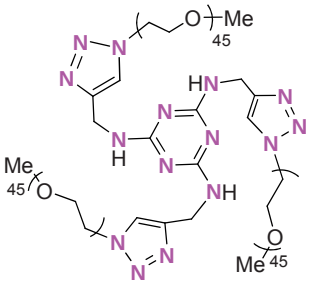

30

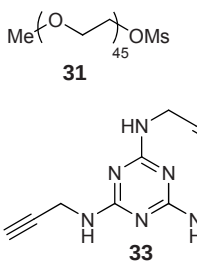

31

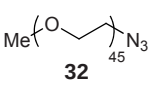

32

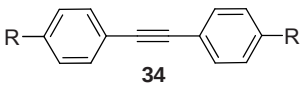

34

34a : R = Me **34c** : R = Cl

34b : R = OMe **34d** : R = Br

33

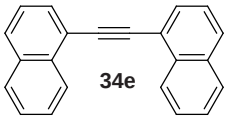

34e

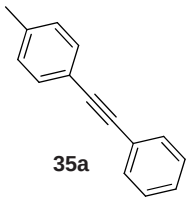

35a

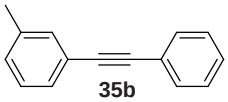

35b

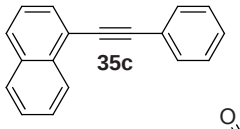

35c

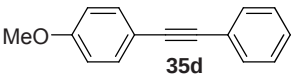

35d

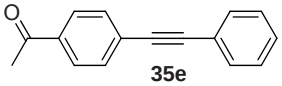

35e

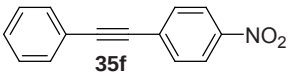

35f

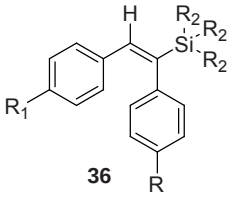

36

36a : R_1 = H, R_2 = Et

36b : R_1 = Me, R_2 = Et

36c : R_1 = OMe, R_2 = Et

36d : R_1 = Cl, R_2 = Et

36e : R_1 = Br, R_2 = Et

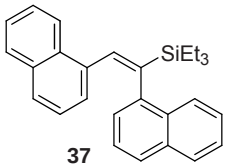

37

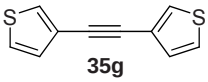

35g

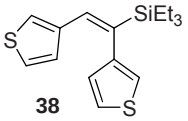

38

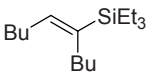

39

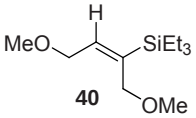

40

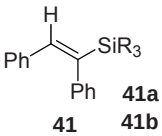

41

41a : R = OEt

41b : R = Ph

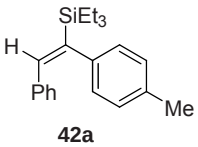

42a

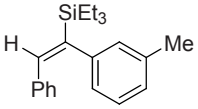

42b

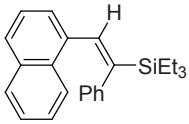

42c

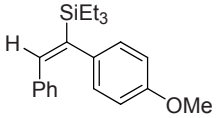

42d

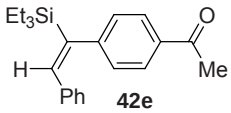

42e

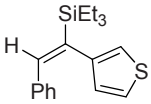

42f

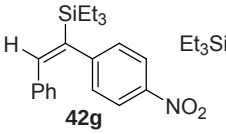

42g

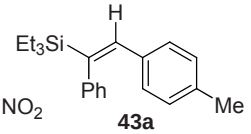

43a

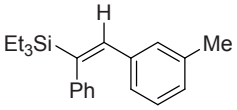

43b

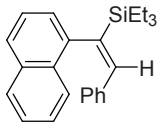

43c

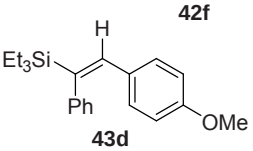

43d

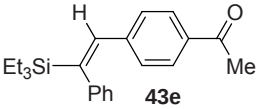

43e

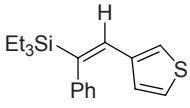

43f

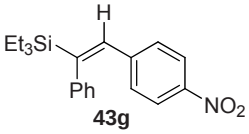

43g

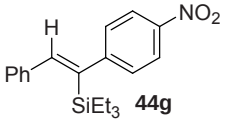

44g

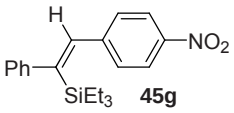

45g

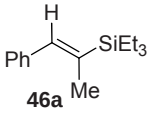

46a

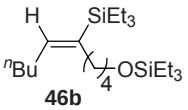

46b

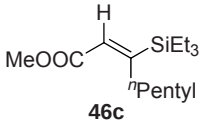

46c

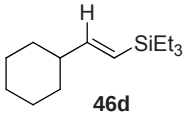

46d

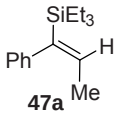

47a

47b

47c

47d

48c

48d

49c

50

51

52

53

54

55

56

57

58

59

Materials

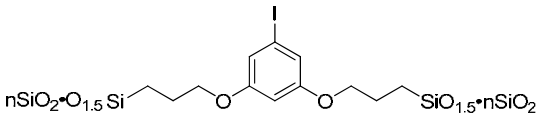

M1: n=0
M2: n=2.5

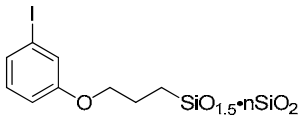

M3: n=5
M4: n=20

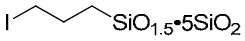

M5

M6

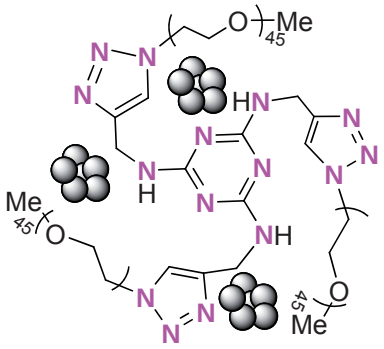

 = **Rh NPs** or **Au NPs**

Rh NPs :

M7 : Rh / **L** = 1.0 / 1

M8 : Rh / **L** = 0.3 / 1

M9 : Rh / **L** = 0.1 / 1

M10 : Rh / **L** = 0.05 / 1

M11 : Rh / **L** = 0.02 / 1

Au NPs :

M12 : Au / **L** = 2.0 / 1

M13 : Au / **L** = 1.0 / 1

M14 : Au / **L** = 0.7 / 1

M15 : Au / **L** = 0.5 / 1

M16 : Au / **L** = 0.3 / 1

M17 : Au / **L** = 0.2 / 1

M18 : Au / **L** = 0.1 / 1

M19 : Au / **L** = 0.07 / 1

M20 : Au / **L** = 0.04 / 1

M21 : Au / **L** = 0.01 / 1

ANNEX I

Co-authored publication:

***Adv. Synth. Catal.* 2014, *356*, 179-188.**

Advanced Synthesis & Catalysis

DOI: 10.1002/adsc.201300641

Hydrosilylation of Internal Alkynes Catalyzed by Tris-Imidazolium Salt-Stabilized Palladium Nanoparticles

Marc Planellas,[a] Wusheng Guo,[a] Francisco Alonso,[b] Miguel Yus,[b] Alexandr Shafir,[a,*] Roser Pleixats,[a,*] and Teodor Parella[a,c]

[a] Departament de Química, Universitat Autònoma de Barcelona, Cerdanyola del Vallès, 08193 Barcelona, Spain
Fax: (+34)-93-581-2477; phone: (+34)-93-581-2067; e-mail: Alexandr.Shafir@uab.cat or Roser.Pleixats@uab.cat

[b] Departamento de Química Orgánica, Facultad de Ciencias and Instituto de Síntesis Orgánica (ISO), Universidad de Alicante, Apdo. 99, 03080 Alicante, Spain

[c] Servei de Ressonància Magnètica Nuclear, Universitat Autònoma de Barcelona, Cerdanyola del Vallès, 08193-Barcelona, Spain

Received: July 22, 2013; Revised: October 4, 2013; Published online: January 13, 2014

Supporting information for this article is available on the WWW under http://dx.doi.org/10.1002/adsc.201300641.

Abstract: Palladium nanoparticles stabilized with tris-imidazolium tetrafluoroborates catalyze the stereoselective hydrosilylation of internal alkynes in a dry inert atmosphere to give (*E*)-vinylsilanes in excellent yields. In the presence of controlled amounts of water a transfer hydrogenation reaction takes place with the formation of (*Z*)-alkenes or the corresponding alkanes.

Keywords: alkynes; hydrosilylation; imidazolium salts; nanoparticles; palladium; transfer hydrogenation

Introduction

The transition metal-catalyzed hydrosilylation of alkynes represents the most straightforward and convenient route for the preparation of vinylsilanes. This transformation proceeds with 100% atom efficiency,[1] and the resulting organosilicon reagents are versatile building blocks in a number of synthetic processes. Some examples of reactions involving vinylsilanes include protodesilylation[2] to produce the corresponding alkene, the Hiyama cross-coupling[3] with vinyl and aryl halides, as well as the Tamao–Fleming oxidation[4] to generate the carbonyl derivatives. In general, vinylsilanes exhibit reactivity similar to that of certain organometallic vinyl derivatives, but may offer advantages in terms of cost, low molecular weight, low toxicity, functionality tolerance and high chemical stability. Platinum-based catalysis is the most usual choice for the addition of silanes to unsaturated C–C bonds,[5] most famously chloroplatinic acid (Speier's catalyst),[5a,b] and olefin-stabilized Karstedt's catalyst.[5c,d] More recently, ruthenium complexes, despite being generally less reactive, have also become popular in alkyne hydrosilylation due to their high levels of stereoselectivity.[6] Thus, the regio- and stereochemistry of the metal-catalyzed alkyne hydrosilylation is known to be controlled by the nature of the catalyst. Terminal acetylenes tend to be far more reactive in this process, although certain systems, including Trost's ruthenium catalyst,[6g] do perform well with the more challenging internal alkynes.

Our own work on C–C bond formation catalyzed by Pd nanoparticles led us to explore the preparation of vinylsilanes using the same class of catalyst. We found only few reports dealing with the addition of silanes to acetylenic compounds catalyzed by metal nanoparticles. In one instance, the regioselective hydrosilylation of terminal alkynes was recently achieved[7] with supported rhodium,[7a] rhodium-platinum[7a] and gold nanoparticles;[7b] in addition, the hydrosilylation of internal alkynes and diynes has been described with platinum deposited on titania[8a,b] and on magnetite.[8c] Although palladium nanoparticles (Pd_{np}) have found widespread applications as catalysts, mainly in hydrogenation, oxidation and cross-coupling reactions,[9] little attention has been paid to their use in the hydrosilylation reactions of unsaturated hydrocarbons. Thus, while there are few examples describing their use in the hydrosilylation of enals, enones,[10] and styrene,[11] to the best of our knowledge they have never been reported as catalysts in the hydrosilylation of alkynes. In fact, even discrete Pd complexes are quite uncommon in this process, with some examples appearing in the past years.[12]

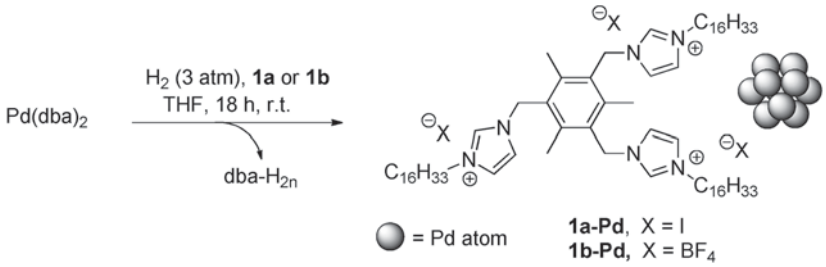

Scheme 1. Preparation of Pd_{np} *via* hydrogenation of $Pd(dba)_2$.

Recently, our group reported[13] a family of palladium nanoparticles (Pd_{np}) stabilized by tris-imidazolium salts that were active as catalysts in Suzuki–Miyaura cross couplings. We describe herein our results on the hitherto unreported hydrosilylation of internal alkynes catalyzed by this family of palladium catalysts. We also report a competitive process of transfer hydrogenation of alkynes achieved by replacing the neat silane with a silane/water mixture.

Results and Discussion

Full details on catalyst preparation are reported in our earlier publication (Scheme 1).[13] Briefly, the tris-imidazolium-stabilized nanoparticles were prepared following the organometallic approach developed by Chaudret and co-workers,[14] consisting in the reduction and subsequent displacement of a ligand from a zerovalent organometallic precursor. In our case, a THF solution of $Pd(dba)_2$[15] was stirred overnight under 3 atm of hydrogen in the presence of the corresponding stabilizer (**1a** or **1b**, Pd:L = 1:1), affording palladium nanoparticles **1a-Pd** and **1b-Pd** with a mean diameter of 2.9–4.2 nm in good yields.

Hydrosilylation of diphenylacetylene with Et_3SiH was chosen as the model substrate combination, and both **1a-Pd** and **1b-Pd** were tested as catalyst under a range of conditions (Table 1).

After an extensive testing, it was found that neat silane (4 equiv.) was the best reaction medium. Thus, treatment of the model symmetrical alkyne with neat triethylsilane in the presence of 5 mol% of the iodide salt **1a-Pd** at 90 °C under an inert atmosphere for 19 h gave complete conversion of the alkyne with good selectivity for the *syn* addition product (*E*)-**2** (entry 1,

Table 1. Optimization of the reaction conditions for the hydrosilylation of diphenylacetylene with triethylsilane under Pd_{np} catalysis.[a]

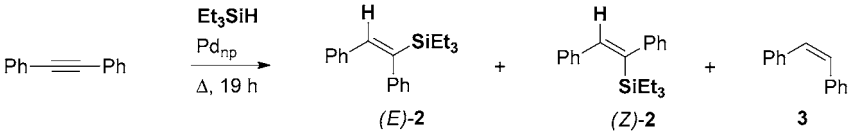

Entry	Catalyst	mol% Pd	Equiv. Silane[b]	Temperature [°C]	Conversion [%][c]	Yield of (*E*)-**2** [%][c]	Ratio (*E*)-**2**:(*Z*)-**2**:**3**
1	**1a-Pd**	5	4	90	100	95	93:7:0
2	**1a-Pd**	1	4	90	72	67	67:21:12
3	**1a-Pd**	0.5	4	90	67	64	75:17:8
4	**1b-Pd**	5	4	90	100	99	100:0:0
5	**1b-Pd**	1	4	90	100	97	100:0:0
6	**1b-Pd**	0.5	4	90	100	97	**100:0:0**
7	**1b-Pd**	0.25	4	90	100	98	**100:0:0**
8[d]	**1b-Pd**	0.5	4	90	100	56	51:0:49
9	**1b-Pd**	0.5	4	25	30	18	100:0:0
10	**1b-Pd**	0.5	2	90	79	66	96:0:4
11[e]	**1b-Pd**	0.5	1	90	4	1	–
12	–	–	4	90	0	0	–

[a] Performed in closed vessels (45 mL) in a multireactor, with 0.5 mmol of alkyne under dry N_2 atmosphere.
[b] Used as solvent.
[c] % Yield/conversion determined by GC (*n*-$C_{11}H_{24}$ as internal standard).
[d] Reaction under air atmosphere.
[e] THF was added (0.25 mL).

Table 2. Hydrosilylation of symmetric alkynes by **1b-Pd$_{np}$**.[a]

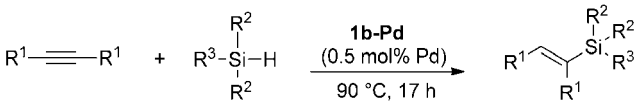

Entry	R^1	R^2, R^3	Product	Yield (%)[b]
1	Ph	Et, Et	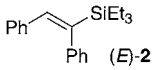 (*E*)-**2**	97
2	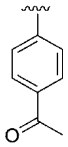	Et, Et	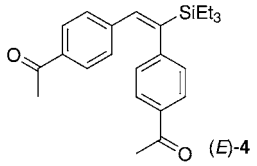 (*E*)-**4**	97
3		Et, Et	 (*E*)-**5**	99
4	Bu	Et, Et	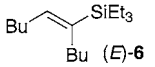 (*E*)-**6**	60[c]
5	Ph	OEt,OEt	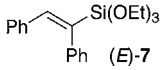 (*E*)-**7**	99
6	Ph	Ph, Ph	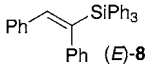 (*E*)-**8**	86
7[d]	Ph	Ph, H	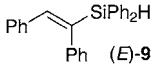 (*E*)-**9**	78

[a] In closed vessels (45 mL) with 1 mmol alkyne, 4 mmol triethylsilane under dry nitrogen.
[b] Isolated yield. The conversion was complete in all entries.
[c] Lower yield due to evaporation.
[d] 1 mmol of alkyne and 2 mmol of silane, reaction time = 170 h.

Table 1). However, incomplete conversions and lower selectivities were achieved upon decreasing the catalyst loading, with the stereoisomeric vinylsilane (*Z*)-**2** (*anti* addition) and (*Z*)-stilbene (**3**) formed as by-products (entries 2 and 3, Table 1). To our delight, analogous experiments with the tetrafluoroborate catalyst **1b-Pd** gave full conversion and complete selectivity for the vinylsilane (*E*)-**2** with catalyst loading down to 0.25 mol% Pd (entries 4–7, Table 1). When the reaction with 0.5 mol% of **1b-Pd** took place under air, the chemoselectivity dropped to about 50% in favor of the semihydrogenation product **3** (entry 8, Table 1). These experiments established **1b-Pd** as the best catalyst for the hydrosilylation, and showed that an inert atmosphere was crucial for achieving high chemoselectivity. A lower yield of (*E*)-**2** was obtained at 25 °C (entry 9, Table 1). Using less silane resulted in incomplete conversion and the formation of traces of **3** (entry 10, Table 1). An experiment with a stoichiometric amount of silane in THF as solvent was unsuccessful (entry 11, Table 1). Control experiments showed that the reaction did not occur in the absence of catalyst (entry 12). For comparison, other palladium sources, such as $Pd(dba)_2$, $Pd(OAc)_2$ and $Pd(PPh_3)_4$, were tested as catalysts and poorer results were achieved in terms of conversion and selectivity.

Having established nanoparticles **1b-Pd** as the best catalyst, the optimized conditions (0.5 mol% Pd, 4 equiv. of silane, 90 °C) were then applied to the hydrosilylation of some symmetrical internal alkynes with triethylsilane (entries 1–4, Table 2). This catalyst proved to be highly efficient and selective, furnishing the corresponding (*E*)-alkenylsilanes (entries 1–3, Table 2) in excellent yields, with the carbonyl groups of (*E*)-**4** unaltered under the reaction conditions. For the non-aromatic substrate (entry 4), the reduced yield was attributed to some loss in the isolation process due to higher volatility. For the reactions involving volatile silanes, the work-up consisted in filtering the reaction mixture through a short plug of silica gel with hexane as eluent and evaporating the solvent and excess reagent under an air flow, to afford a product that did not require any further purification.

Next, the hydrosilylation of diphenylacetylene with other silanes was examined under the same conditions. The reactions with triethoxysilane and triphenylsilane (entries 5 and 6, Table 2) proceeded with high stereoselectivity, affording the corresponding (*E*)-vi-

Table 3. Hydrosilylation of differentiated unsymmetric alkynes.[a]

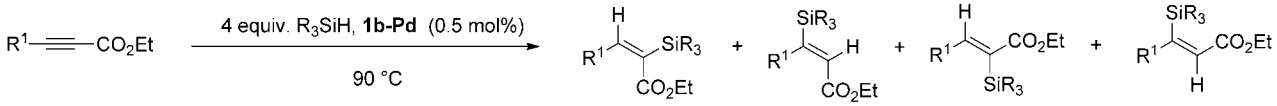

Entry	Yield [%][b]	Products and % selectivity[c]			
1	85	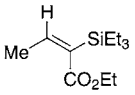	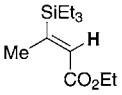	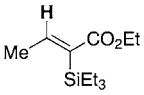	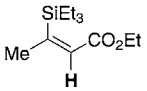
		(*E*)-**10**, 85%	(*E*)-**11**, 4%	(*Z*)-**10**, 11%	---
2	95	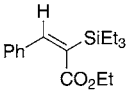	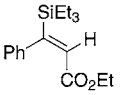	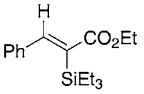	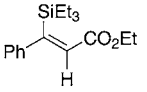
		(*E*)-**12**, 70%	(*E*)-**13**, 16%	(*Z*)-**12**, 9%	(*Z*)-**13**, 5%
3	99	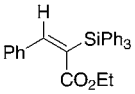	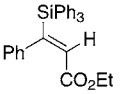	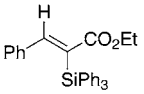	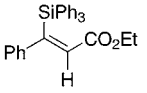
		(*E*)-**14**, 55%	(*E*)-**15**, 45%	---	---

[a] Reactions performed in closed vessels (45 mL) with 0.72 mmol alkyne, 2.88 mmol triethylsilane under N_2 for 15–22 h.
[b] Isolated yield of the mixture of vinylsilanes; complete conversion in all entries.
[c] Determined by GC.

nylsilanes **7** and **8** in good isolated yields. In the case of the diphenylsilane (Ph_2SiH_2, entry 7), 2 mmol of this reagent were used for 1 mmol of alkyne and a longer reaction time was required for the full consumption of the starting alkyne. Under these conditions, the monoaddition product (*E*)-**9** was isolated in 78% yield (entry 7, Table 2). Once again, in all cases the only product detected arose from the *syn* addition of the Si–H bond across the carbon-carbon triple bond, as determined by the selective NOE experiments.

Next, the nanocatalyst **1b-Pd** was used in the hydrosilylation of asymmetrical internal alkynes (Table 3). In this case, four different vinylsilanes could be envisaged, with two stereoisomers (*syn* and *anti* addition) possible for each of the two regioisomeric forms. Although the expected *syn* preference might reduce this number to two, a reasonable degree of regioselectivity would only be possible for substrates with the two sides clearly differentiated.

Indeed, the reaction between ethyl 2-butynoate and triethylsilane was highly regio- and stereoselective, with the major product (*E*)-**10** arising from the *syn* addition that placed the triethylsilyl moiety *gem* to the electron-withdrawing ester group; only minor amounts of the *anti* addition compound (*Z*)-**10** and traces of the regioisomer (*E*)-**11** were observed by ^{1}H NMR (entry 1, Table 3). A similar α-directing effect of the electron-withdrawing groups in the addition of silanes to internal triple bonds has been previously reported by other groups.[12b,16] The selectivity decreased somewhat in the case of the ethyl 3-phenylpropiolate, although the *syn* addition and α regioselectivity were nevertheless predominant [product (*E*)-**12**, entry 2, Table 3]. However, the use of triphenylsilane with the latter alkyne substrate led to a lower regioselectivity, giving a 55:45 mixture of the two *syn* regioisomers (*E*)-**14** and (*E*)-**15** (entry 3, Table 3). In substrates lacking such a directing group (Table 4), differentiation could be observed for an alkyne bearing one alkyl and one aryl substituents. Thus, selective *syn* addition with high regioselectivity took place in the reaction of triethylsilane with prop-1-yn-1-ylbenzene, giving an 88:12 mixture of (*E*)-**16** and (*E*)-**17** (entry 1, Table 4). In general, unsymmetrical diarylalkynes gave mixtures of the two *syn* regioisomeric vinylsilanes (entries 3–7, Table 4), although the selectivity could be improved by introducing 1-naphthyl or 3-quinolyl substituents (entries 6 and 7). However, in entry 2, a 76:24 mixture of the two stereoisomers (*E*)-**18** and (*Z*)-**18** was obtained, and only a trace amount of the *syn* regioisomeric compound (*E*)-**19** was detected by ^{1}H NMR (see the Supporting Information). The high regioselectivity can be attributed to the electron-withdrawing effect of the acetyl group. In addition, we were able to prepare enyne (*E*)-**30** in 95% isolated yield from the *syn* monohydrosilylation of the corresponding symmetric diyne (entry 8, Table 4).

Interestingly, terminal alkynes, such as phenylacetylene, proved unreactive under the reaction conditions. We traced this lack of reactivity to a poisoning effect exerted by this substrate on the catalyst. In fact, addition of phenylacetylene was found to halt the otherwise efficient hydrosilylation of diphenylacetylene.

Table 4. Hydrosilylation of unsymmetric alkynes.[a]

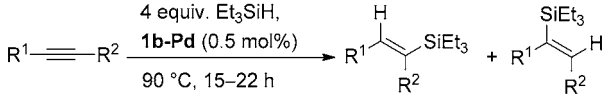

Entry	Products	Ratio[b]	Yield [%][c]
1	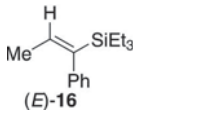 (*E*)-**16** (*E*)-**17**	88:12	96
2	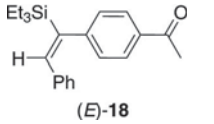 (*E*)-**18** (*Z*)-**18**	76:24	98[d]
3[e]	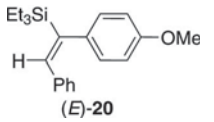 (*E*)-**20** (*E*)-**21**	33:67	90
4	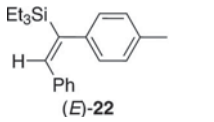 (*E*)-**22** (*E*)-**23**	42:58	99
5	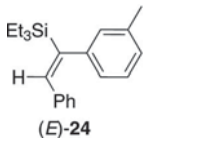 (*E*)-**24** (*E*)-**25**	46:54	99
6	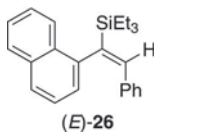 (*E*)-**26** (*E*)-**27**	94:6	96
7	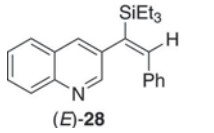 (*E*)-**28** (*E*)-**29**	75:25	99
8	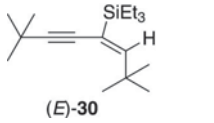 (*E*)-**30**	–	95

[a] Performed in closed vessels (45 mL) with 0.72 mmol alkyne, 2.88 mmol Et_3SiH and 0.5 mol% of Pd under N_2.
[b] Determined by GC.
[c] Isolated yield of the mixture of vinylsilanes. Complete conversion in all entries.
[d] Trace amount of regioisomeric *syn* addition product (*E*)-**19** was detected by GC and ^1H NMR.
[e] Reaction time = 40 h.

Although no further experiments were conducted, it is possible that the formation of Pd σ-alkynyl species is responsible for catalyst deactivation.

Structural characterization of all compounds included two-dimensional NMR techniques (COSY, HSQC, HMBC and NOESY experiments). The stereoselectivity of the reaction was studied by determining the relative (*E*)/(*Z*) configuration of the corresponding trisubstituted double bonds. This assignment was further confirmed by measuring the long-range proton-carbon and proton-silicon coupling constants using the selHSQMBC method[17] and determining the through-space NOE effects mainly on the olefinic proton. For instance, in the case of the (*E*)-**14** isomer, a large coupling of 15.4 Hz was measured between the olefinic proton and the carbonyl carbon, confirming their relative *trans* disposition. On the other hand, a large value of 11.1 Hz was measured between the olefinic proton and the *ipso* aromatic carbon resonating at 140.9 ppm in (*E*)-**15**, also confirming the *trans* relationship between phenyl group and the olefinic proton. The three-bond $^1H,^{29}Si$ coupling constant was also used for unambiguous determination of double bond configuration. As a general trend, values around 7–8 Hz were measured when the olefinic proton and the silicon atom are in a relative *cis* configuration, whereas larger values around 11 Hz were measured in *trans* dispositions. The regioselectivity of the process was studied by using chemical shift assignments and NOE contacts obtained from HMBC and NOESY spectra, respectively. The deshielding effects observed for the chemical shifts of olefinic carbons in the β position with respect to the ester group in isomers of entries 1–3 of Table 3, allow us a tentative determination of the α or β position of the silane group. For instance, whereas the olefinic carbon (=C–H) resonates at 147.5 ppm in (*E*)-**14**, this carbon appears at higher field (133.1 ppm) in the corresponding regioisomer (*E*)-**15**. In other isomers from entries 1–7 of Table 4, chemical shift differences of olefinic carbons are not so evident and the concerted use of HMBC and NOE data was successfully applied to elucidate the structure of each regioisomer (see the Supporting Information).

As mentioned above, the failure to employ an inert atmosphere (dry N_2) led to a decrease in the selectivity, giving a vinylsilane/alkene mixture (entry 8, Table 1). After some experimentation, we found that this was a general trend and that the formation of the semihydrogenated products was due to the moisture present in the air atmosphere. We thought we could take advantage of this observation and to perform the selective transfer hydrogenation of alkynes by the addition of controlled amounts of water to the alkyne-silane reaction mixture

The preliminary experiments with added water confirmed this assumption (*vide infra*). Presumably, dihydrogen is formed *in situ* from the reaction of the silane with water, which would also give rise to the corresponding silanol. Indeed, silanol and disiloxane (from the co-condensation of silanol) were the main side products in the hydrosilylation reactions performed under an air atmosphere. The related hydrogen production by the hydrolytic or alcoholytic oxida-

Table 5. Hydrogenation of internal alkynes using triethylsilane/water under Pd_{np} catalysis.[a]

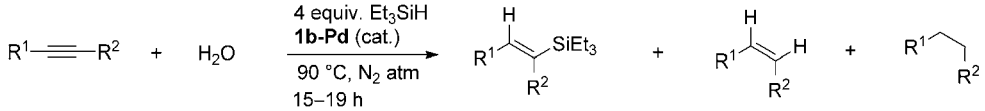

Entry	R^1, R^2	Alkyne:H_2O[b]	Products	Ratio[c]	Conversion (yield [%])[d]
1	Ph, Ph	1:1	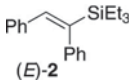 (*E*)-**2**  **3**	83:17	100
2	Ph, Ph	1:3	 **3** 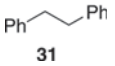 **31**	–	100
3	Ph, Ph	1:4	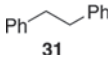 **31**	–	100 (94)
4	Ph, CO_2Et	1:3	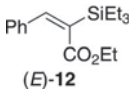 (*E*)-**12**	–	100
5	Ph, CO_2Et	1:4	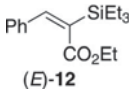 (*E*)-**12** 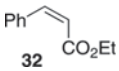 **32**	29:71	100
6	Ph, CO_2Et	1:8	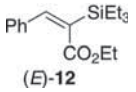 (*E*)-**12** 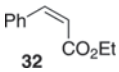 **32**	6:94	100 (62)
7	3-quinolyl, Ph	1:8	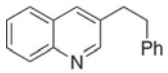 **33**	–	100 (78)

[a] *Reaction conditions:* 1 (or 0.5) mmol alkyne, 4 (or 2) mmol triethylsilane, 0.005 (or 0.025) mmol Pd (and the corresponding amount of water) in a closed vessel (45 mL) under dry nitrogen atmosphere at 90 °C.
[b] Mmol alkyne/mmol water.
[c] Ratio of products determined by GC.
[d] GC conversion. Isolated yield in parentheses.

tion of silanes is a hot topic that has received considerable attention in the recent literature.[18] Thus, the reaction has been reported to take place in the presence of catalysts such as metal NPs (silver,[18a] gold,[18b–e] Pd,[18f,g] Ni[18h]) as well as transition metal complexes (rhenium,[18i] iridium,[18j,k] ruthenium,[18l–o] and zinc[18p]). Hydrogenation of unsaturated carbon-carbon bonds with the system silane-water under palladium(II) acetate catalysis had also been previously described.[19] Oxidative cycloaddition of 1,1,3,3-tetramethyldisiloxane to terminal alkynes[20] and oxidative hydrolysis of 1,2-disilanes,[21] both under catalysis by Au/TiO_2 NP, also proceed with concomitant evolution of hydrogen gas. Selective semireduction of alkynes has also been recently accomplished with silane/alcohol under copper catalysis.[22] Although Pd/C-induced catalytic transfer hydrogenation of several types of substrates with triethylsilane has also been reported,[23] no discussion about the origin of the hydrogen atoms was included.

Our preliminary results for the transfer hydrogenation of internal alkynes with triethylsilane/water catalyzed by **1b-Pd** are summarized in Table 5. The amount of water required for the semi to full hydrogenation was highly dependent on the nature of the alkyne substrate. Thus, in the case of the diphenylacetylene, the addition of 1 mmol of water per mmol of alkyne gave a mixture of vinylsilane (*E*)-**2** and *cis*-stilbene **3**, with the hydrosilylation still predominating (entry 1, Table 5). Increasing the amount of water to 3 mmol water/mmol alkyne led to the suppression of the formation of the silylated product, but afforded a mixture of alkene **3** and 1,2-diphenylethane, **31** (entry 2, Table 5). Finally, a quantitative yield of the same fully hydrogenated alkane (**31**) was isolated when a 4:1 water/alkyne ratio was employed (entry 3, Table 5). In contrast, for ethyl phenylpropynoate the addition of three equivalents of water still produced an almost exclusive formation of the hydrosilylated product (*E*)-**12**. Selective hydrogenation in this case required eight mmol of water/mmol of alkyne to give the corresponding *cis*-alkene **32**, whereas with four equivalents of water a mixture of both products was observed (entries 4–6, Table 5). Finally, while we were unable to selectively semihydrogenate the 3-(phenylethynyl)quinoline, the fully hydrogenated compound **33** was isolated when using 8 mmol of water per mmol of alkyne (entry 7, Table 5).

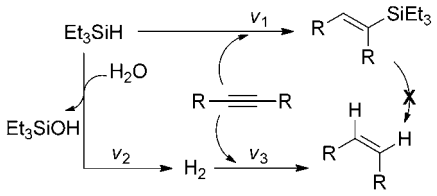

Scheme 2. Competitive hydrosilylation and transfer hydrogenation of internal alkynes.

The hypothesis of formation of semi-hydrogenated products through protodesilylation of the intermediate vinylsilanes was discarded as compound (*E*)-**2** was recovered unaffected after being subjected to the conditions of entry 2 of Table 5. This indicates that the hydrosilylation (rate v_1) and transfer hydrogenation processes (rates v_2 and v_3) occur in a competing fashion, with the relative rates (and thus the outcome) dependent on the amount of water added (Scheme 2).

The origin of each of the two hydrogen atoms of the *in situ* formed dihydrogen molecule[24] was probed using D_2O. For this purpose, the reaction corresponding to entry 6 of Table 5 was repeated with D_2O (Table 6, entries 1 and 2). Under these conditions, the use of D_2O caused the reaction to proceed more slowly and to give a mixture with the vinylsilane as the major product. Since the rate of the hydrosilylation v_1 would be unaffected by the change, this outcome indicates a strong kinetic isotope effect in the putative hydrogenation rates v_2 or v_3 (or both), diminished with respect to v_1. A partial selectivity towards the hydrogenated product could be achieved by further increasing the amount of D_2O (entries 3 and 4, Table 6). Thus, for a molar ratio alkyne:D_2O of 1:15, a mixture of the vinylsilane (*E*)-**12**, the *cis*-alkene **32** and alkane **34** was achieved (entry 3), whereas with a ratio of 1:20 the alkane **34** was the major product isolated (Table 6, entry 4). The ^{1}H NMR spectrum of the fully reduced compound **34** obtained with D_2O (see the Supporting Information) showed two methylene resonances at 2.6 and 2.9 ppm, but with an integrated intensity of 1 H each, instead of the 2 H expected for the fully *protio* species. This observation indicates that: a) about 50% of the newly incorporated H atoms proceed from water; and b) the deuterium incorporation takes place indiscriminately at both ends of the unsaturated bond. This was confirmed by recording the corresponding ^{2}H NMR spectrum (see the Supporting Information).

One possibility for the statistical 50% deuterium incorporation into **34** is the hydrogenation with two HD molecules to give exactly 2 D/molecule. However, bulk **34** could also simply consist of a mixture of isotopomers arising from indiscriminate hydrogenation with a fully (or partially) scrambled HH/HD/DD mixture. Focusing on the initial addition of dihydrogen to the alkyne, the reaction with the pure HD would give two monodeuterated regioisomers (Scheme 3, A). On

Table 6. The effect of using D_2O in the hydrosilylation/hydrogenation manifold with **1b-Pd**.[a,b]

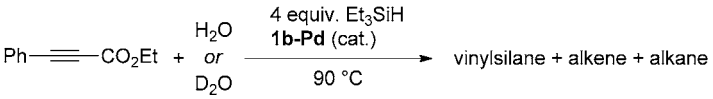

Entry	Water (equiv.)[c]	Products			Ratio	Conversion (yield [%])[d]
1[e]	H_2O (8)	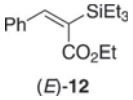 (*E*)-**12**	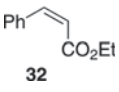 **32**		6:94	100 (62)
2	D_2O (8)	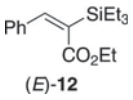 (*E*)-**12**	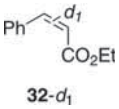 **32**-d_1		>95:5	75[f]
3	D_2O (15)	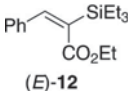 (*E*)-**12**	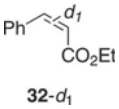 **32**-d_1	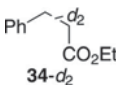 **34**-d_2	43:45:12	100
4	D_2O (20)		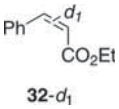 **32**-d_1	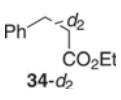 **34**-d_2	10:90	100 (80)

[a] Conditions are the same as in Table 5.
[b] Product ratio determined by GC.
[c] This refers to mmol water per mmol alkyne.
[d] GC conversion. Isolated yield in parentheses.
[e] Entry taken from Table 5.
[f] Approximate value.

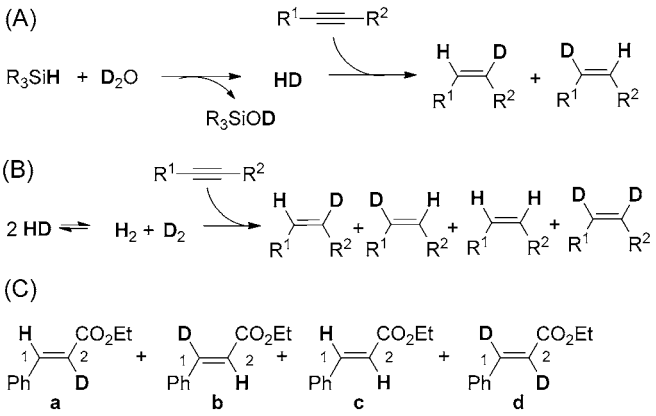

Scheme 3. Products of the transfer hydrogenation of internal asymmetric alkynes using D_2O. (A): without HD scrambling; (B): with HD scrambling; (C): the four *trans* olefins obtained as side-products for the case of ethyl phenylpropiolate.

the other hand, hydrogenation with a scrambled isotope mixture would yield four isotopomers (Scheme 3, B).

Here, our analysis was aided by the fact that some of the semihydrogenated *cis* alkene **32**-d_1 (minor product, entry 4, Table 6) had partially isomerized to its *trans* isomer during work-up, and that the olefinic ^{1}H NMR resonances (two H in *trans*) for this new species were well discernible from the rest of the signals in the mixture containing **34**-d_2 as major product. Characteristically, each olefinic resonance appeared as a combination of a triplet with a small $J_{H,D}$ (2.4 Hz) nestled within a large J doublet (16 Hz) for the *trans* H,H coupling (see Figure 1). Thus, the two large doublets correspond to the H,H product, while each of the triplets (coupling to D, S = 1) belongs respectively to each of the two H,D isotopomers; the presence of the fully deuterated form is deduced from the missing integral intensities. Based on the signal pattern and integration (Figure 1, see also the Supporting Information), the product was confirmed as a statistical mixture of isomers (a, b and c, 25% each, Scheme 3, C), with the "invisible" dideuterated isotopomer d accounting for the remaining 25%. This was confirmed by recording the corresponding ^{2}H NMR spectrum (see the Supporting Information).

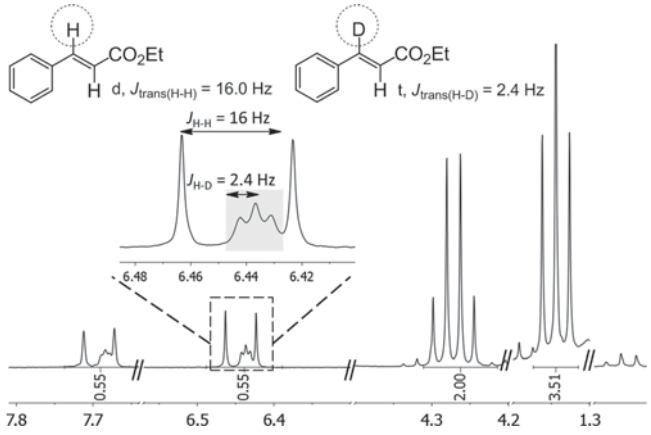

Figure 1. A fragment of the ^{1}H NMR spectrum of *trans*-**32**-d_1 (minor component; major component not shown for clarity).

Conclusions

We have developed an efficient and stereoselective *syn* addition of silanes to internal alkynes, providing (*E*)-vinylsilanes in excellent yields, by the use of palladium nanoparticles stabilized by tris-imidazolium tetrafluoroborates as catalyst under a dry inert atmosphere. Fair to good regioselectivities have been achieved in the case of asymmetric alkynes. To the best of our knowledge, this is the first report of palladium nanoparticles involved in hydrosilylation reactions of internal alkynes, substrates that are much less reactive than the terminal acetylenes and which have received less attention in the literature. The addition of controlled amounts of water to the silylation mixture promotes the oxidative hydrolysis of silanes with the concomitant formation of dihydrogen, leading to a competitive process of transfer hydrogenation of the alkynes to the (*Z*)-alkenes or the corresponding alkanes depending on the amount of water and the nature of the acetylenic substrates.

Experimental Section

Hydrosilylation of Diphenylacetylene with Triethylsilane by Pd_{np} (Entry 1, Table 2); Typical Procedure

Diphenylacetylene (178 mg, 1 mmol) and catalyst **1b-Pd** (0.5 mol% Pd) were weighed into a screw-top sealable tube. The system was subjected to three evacuate-refill cycles with dry nitrogen. Triethylsilane (640 μL, $\rho = 0.73\ g\,mL^{-1}$, 4 mmol) was added under nitrogen atmosphere. The reaction was left under stirring at 90 °C until total conversion of the alkyne (GC monitoring). The mixture was filtered through a plug of silica-gel eluting with hexane and the solvent was removed under air to afford the (*E*)-(1,2-diphenylvinyl)triethylsilane, (*E*)-**2**, as a yellowish liquid; yield: 287 mg (97%). ^{1}H NMR (400 MHz, $CDCl_3$): $\delta = 7.30$ (t, $J =$ 7.2 Hz, 2H, Ph-*H*), 7.20 (t, $J = 7.2$ Hz, 1H, Ph-*H*), 7.12–7.07 (m, 3H, Ph-*H*), 7.03–7.01 (m, 1H, Ph-*H*), 7.00–6.94 (m, 3H, Ph-*H*), 6.78 (s, 1H, SiC=C*H*), 0.97 (t, $J = 7.8$ Hz, 9H, $-CH_2CH_3$), 0.65 (q, $J = 8$ Hz, 6H, $-CH_2CH_3$); ^{13}C NMR (101 MHz, $CDCl_3$): $\delta = 144.2$, 143.3, 138.9, 137.6, 129.7, 128.7, 128.0, 127.4, 127.1, 125.7, 7.5, 2.9; MS: $m/z = 294.1$ (M^+).

Supporting Information

The Supporting Information contains details of the experimental procedures and characterization of compounds along with copies of all ^{1}H and ^{13}C NMR spectra.

Acknowledgements

We acknowledge financial support from MICINN of Spain (Projects CTQ2007-65218, CTQ2009-07881, CTQ2012-32436 and CTQ2011-24151), Consolider Ingenio 2010 (Project CSD2007-00006), Generalitat Valenciana (PROMETEO/2009/039), Generalitat de Catalunya (project SGR2009-1441) and FEDER. A. Shafir was supported through a Ramón y Cajal contract from the MEC of Spain.

References

[1] a) I. Ojima, Z. Li, J. Zhu, in: *The Chemistry of Organosilicon Compounds*; (Eds.: Z. Rappoport, Y. Apeloig), Wiley-VCH, Weinheim, **1998**, Vol. 2, pp 1687–1792; b) B. Marciniec; H. Maciejewski, C. Pietraszuk, P. Pawluc, in: *Hydrosilylation: A Comprehensive Review on Recent Advances*, *Advances in Silicon Science Series*, (Ed.: B. Marciniec), Springer Verlag, Berlin, Heidelberg, **2009**, Vol. 1, Chapter 2.

[2] B. M. Trost, Z. T. Ball, T. Jöge, *J. Am. Chem. Soc.* **2002**, *124*, 7922–7923.

[3] For some recent reviews on the palladium-catalyzed cross-coupling of organosilicon reagents, see: a) Y. Nakao, T. Hiyama, *Chem. Soc. Rev.* **2011**, *40*, 4893–4901; b) H. F. Sore, W. R. J. D. Galloway, D. R. Spring, *Chem. Soc. Rev.* **2012**, *41*, 1845–1866.

[4] a) K. Tamao, N. Ishida, T. Tanaka, M. Kumada, *Organometallics* **1983**, *2*, 1694–1696; b) I. Fleming, R. Henning, H. Plaut, *J. Chem. Soc. Chem. Commun.* **1984**, 29–31.

[5] a) J. L. Speier, J. A. Webster, H. H. Barnes, *J. Am. Chem. Soc.* **1957**, *79*, 974–979; b) G. Chandra, P. Y. Lo, P. B. Hitchcock, M. F. Lappert, *Organometallics* **1987**, *6*, 191–192; c) B. D. Karstedt, U.S. Patent 3,775,452, **1973**; d) J. Stein, L. N. Lewis, Y. Gao, R. A. Scott, *J. Am. Chem. Soc.* **1999**, *121*, 3693–3703.

[6] For the early work, see: a) M. A. Esteruelas, J. Herrero, L. A. Oro, *Organometallics* **1993**, *12*, 2377–2379. For later work, see: b) Y. Na, S. Chang, *Org. Lett.* **2000**, *2*, 1887–1889; c) S. V. Maifeld, M. T. Tran, D. Lee, *Tetrahedron Lett.* **2005**, *46*, 105–108; d) C. Menozzi, P. I. Dalko, J. Cossy, *J. Org. Chem.* **2005**, *70*, 10717–10719; e) C. S. Aricó, L. R. Cox, *Org. Biomol. Chem.* **2004**, *2*, 2558–2562; f) B. M. Trost, Z. T. Ball, *J. Am. Chem. Soc.* **2001**, *123*, 12726–12727; g) B. M. Trost, Z. T. Ball, *J. Am. Chem. Soc.* **2005**, *127*, 17644–17655.

[7] a) W. A. Solomonsz, G. A. Rance, M. Suyetin, A. La Torre, E. Bichoutskaia, A. N. Khlobystov, *Chem. Eur. J.* **2012**, *18*, 13180–13187; b) A. Psyllaki, I. N. Lykakis, M. Stratakis, *Tetrahedron* **2012**, *68*, 8724–8731.

[8] a) F. Alonso, R. Buitrago, Y. Moglie, J. Ruiz-Martínez, A. Sepúlveda-Escribano, M. Yus, *J. Organomet. Chem.* **2011**, *696*, 368–372; b) F. Alonso, R. Buitrago, Y. Moglie, A. Sepúlveda-Escribano, M. Yus, *Organometallics* **2012**, *31*, 2336–2342; c) R. Cano, M. Yus, D. J. Ramón, *ACS Catal.* **2012**, *2*, 1070–1078.

[9] a) A. Roucoux, J. Schulz, H. Patin, *Chem. Rev.* **2002**, *102*, 3757–3778; b) M. Moreno-Mañas, R. Pleixats, *Acc. Chem. Res.* **2003**, *36*, 638–643; c) A. Balanta, C. Godard, C. Claver, *Chem. Soc. Rev.* **2011**, *40*, 4973–4985; d) *Nanoparticles and Catalysis*, (Ed.: D. Astruc), Wiley-VCH, Weinheim, **2008**.

[10] M. Benohoud, S. Tuokko, P. M. Pihko, *Chem. Eur. J.* **2011**, *17*, 8404–8413.

[11] M. Tamura, H. Fujihara, *J. Am. Chem. Soc.* **2003**, *125*, 15742–15743.

[12] a) D. Motoda, H. Shinokubo, K. Oshima, *Synlett* **2002**, 1529–1531; b) Y. Sumida, T. Kato, S. Yoshida, T. Hosoya, *Org. Lett.* **2012**, *14*, 1552–1555; c) H. Zhou, C. Moberg, *Org. Lett.* **2013**, *15*, 1444–1447.

[13] M. Planellas, R. Pleixats, A. Shafir, *Adv. Synth. Catal.* **2012**, *354*, 651–662.

[14] K. Philippot, B. Chaudret, *Organometallic Derived Metals, Colloids and Nanoparticles*, in: *Comprehensive Organometallic Chemistry III*, (Eds.: R. H. Crabtree, M. P. Mingos), Elsevier, **2007**, Vol. 12, Chapter 12–03, pp 71–99.

[15] a) M. F. Rettig, P. M. Maitlis, *Inorg. Synth.* **1990**, *28*, 110–113.

[16] D. A. Rooke, E. M. Ferreira, *Angew. Chem.* **2012**, *124*, 3279–3284; *Angew. Chem. Int. Ed.* **2012**, *51*, 3225–3230.

[17] S. Gil, J. F. Espinosa, T. Parella, *J. Magn. Reson.* **2011**, *213*, 145–150.

[18] a) T. Mitsudome, S. Arita, H. Mori, T. Mizugaki, K. Jitsukawa, K. Kaneda, *Angew. Chem.* **2008**, *120*, 8056–8058; *Angew. Chem. Int. Ed.* **2008**, *47*, 7938–7940; b) T. Mitsudome, A. Noujima, T. Mizugaki, K. Jitsukawa, K. Kaneda, *Chem. Commun.* **2009**, 5302–5304; c) N. Asao, Y. Ishikawa, N. Hatakeyama, Menggenbateer, Y. Yamamoto, M. Chen, W. Zhang, A. Inoue, *Angew. Chem.* **2010**, *122*, 10291–10293; *Angew. Chem. Int. Ed.* **2010**, *49*, 10093–10095; d) W. Li, A. Wang, X. Yang, Y. Huang, T. Zhang, *Chem. Commun.* **2012**, *48*, 9183–9185; e) M. Yan, T. Jin, Y. Ishikawa, T. Minato, T. Fujita, L.-Y. Chen, M. Bao, N. Asao, M.-W. Chen, Y. Yamamoto, *J. Am. Chem. Soc.* **2012**, *134*, 17536–17542; f) K. Shimizu, T. Kubo, A. Satsuma, *Chem. Eur. J.* **2012**, *18*, 2226–2229; g) M. Jeon, J. Han, J. Park, *ChemCatChem* **2012**, *4*, 521–524; h) K. Shimizu, K. Shimura, N. Imaiida, A. Satsuma, *J. Mol. Catal. A: Chem.* **2012**, *365*, 50–54; i) E. A. Ison, R. A. Corbin, M. M. Abu-Omar, *J. Am. Chem. Soc.* **2005**, *127*, 11938–11939; j) Y. Lee, D. Seomoon, S. Kim, H. Han, S. Chang, P. H. Lee, *J. Org. Chem.* **2004**, *69*, 1741–1743; k) D.-W. Wang, D-Sh. Wang, Q.-A. Chen, Y.-G. Zhou, *Chem. Eur. J.* **2010**, *16*, 1133–1136; l) M. Lee, S. Ko, S. Chang, *J. Am. Chem. Soc.* **2000**, *122*, 12011–12012; m) E. Choi, C. Lee, Y. Na, S. Chang, *Org. Lett.* **2002**, *4*, 2369–2371; n) K. Mori, M. Tano, T. Mizugaki, K. Ebitani, K. Kaneda, *New. J. Chem.* **2002**, *26*, 1536–1538; o) S. T. Tan, J. W. Kee, W. Y. Fan, *Organometallics* **2011**, *30*, 4008–4013; p) W. Sattler, G. Parkin, *J. Am. Chem. Soc.* **2012**, *134*, 17462–17465; q) M. Jeon, J. Han, J. Park, *ACS Catal.* **2012**, *2*, 1539–1549.

[19] J. M. Tour, J. P. Cooper, S. L. Pendalwar, *J. Org. Chem.* **1990**, *55*, 3452–3453.
[20] I. N. Lykakis, A. Psyllaki, M. Stratakis, *J. Am. Chem. Soc.* **2011**, *133*, 10426–10429.
[21] C. Gryparis, M. Stratakis, *Chem. Commun.* **2012**, *48*, 10751–10753.
[22] A. M. Whittaker, G. Lalic, *Org. Lett.* **2013**, *15*, 1112–1115.
[23] P. K. Mandal, J. S. McMurray, *J. Org. Chem.* **2007**, *72*, 6599–6601.
[24] Formation of HD from a mixture of Et_3SiH, D_2O and **1b-Pd** in C_6D_6 at 333 K was detected by ^1H NMR as a 1:1:1 signal at 4.43 ppm ($J_{H,D} = 42.7$ Hz) (see the Supporting Information). The chemical shift and coupling constant are in agreement with the reported values for HD in toluene-d_8, see: J. Y.-C. Chen, A. A. Martí, N. J. Turro, K. Komatsu, Y. Murata, R. G. Lawler, *J. Phys. Chem. B* **2010**, *114*, 14689–14695.

ANNEX II

Spectral and other characterization data

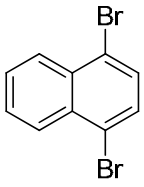

, **1**

^{1}H NMR (360 MHz, $CDCl_3$)

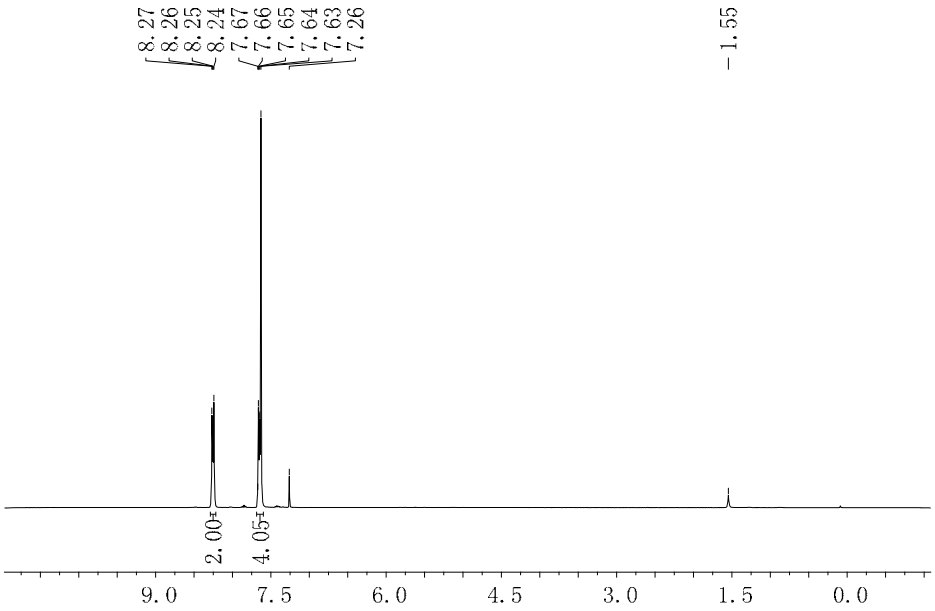

^{13}C NMR (90 MHz, $CDCl_3$)

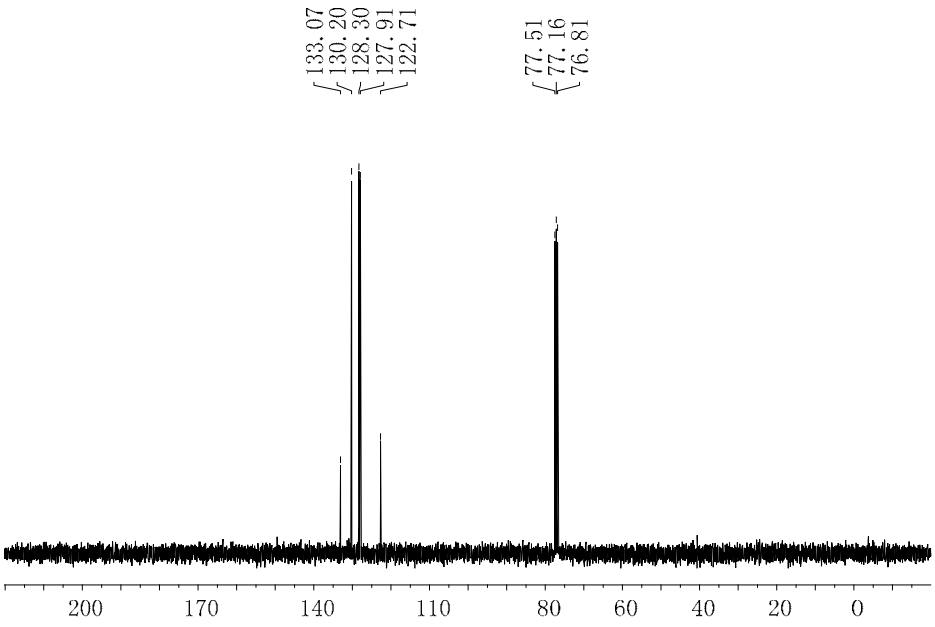

IR (ATR) *v* (cm^{-1})

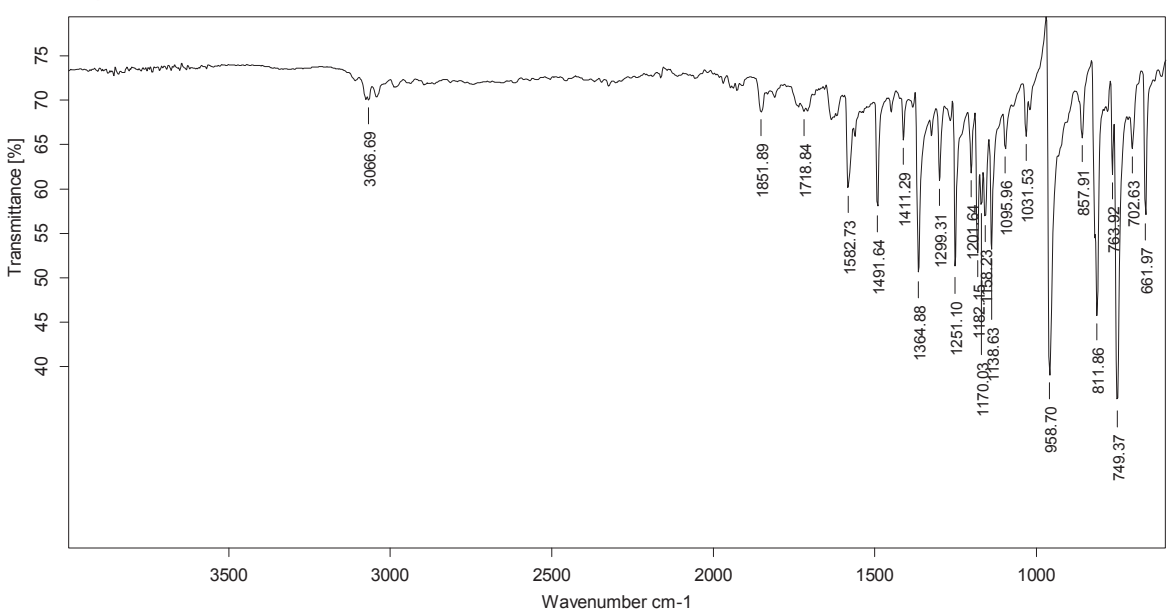

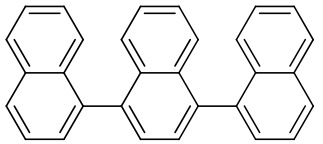

, **2**

^{1}H NMR (250 MHz, $CDCl_3$)

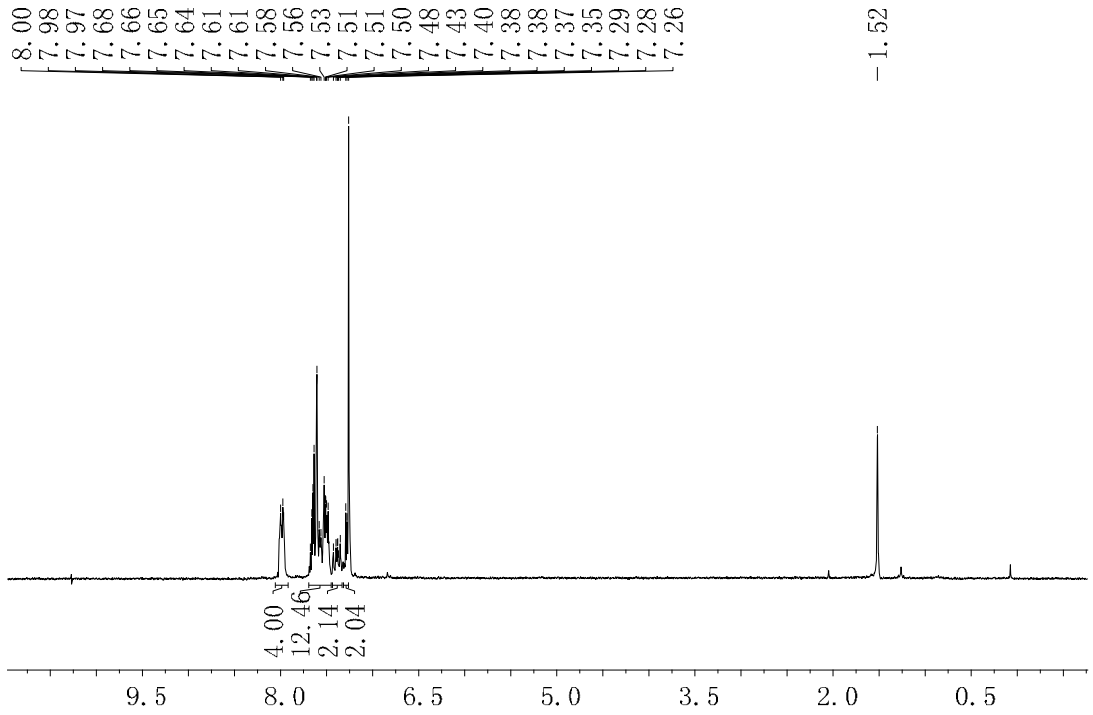

^{13}C NMR (90 MHz, $CDCl_3$)

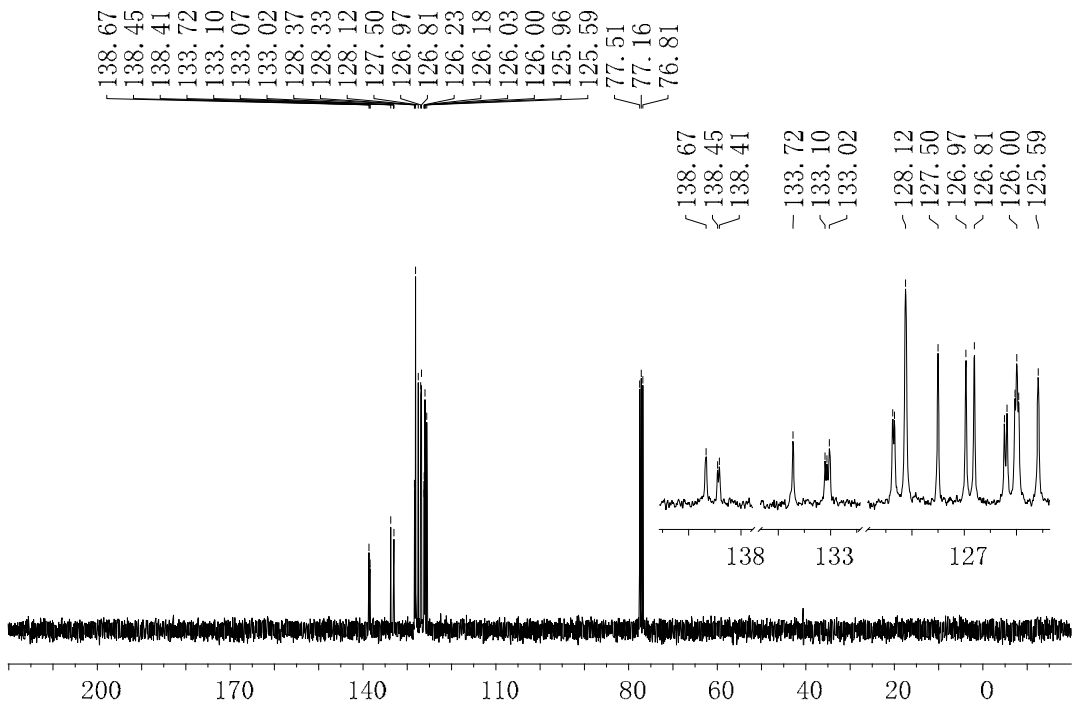

IR (ATR) *v* (cm^{-1})

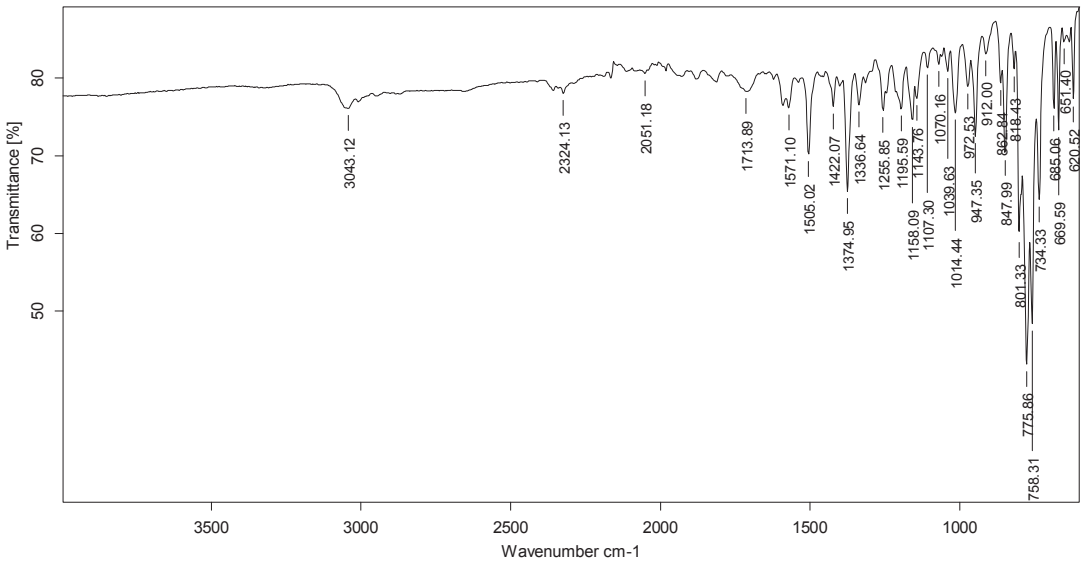

MALDI-TOF spectrum

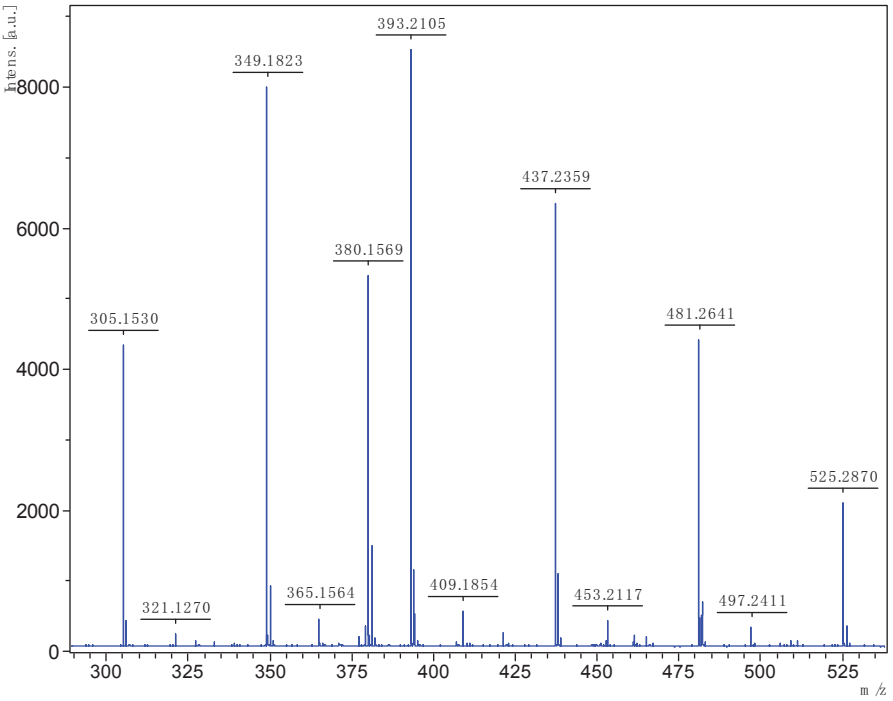

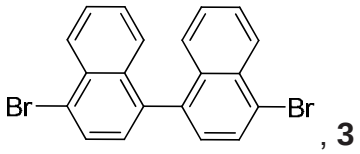

, **3**

^{1}H NMR (360 MHz, $CDCl_3$)

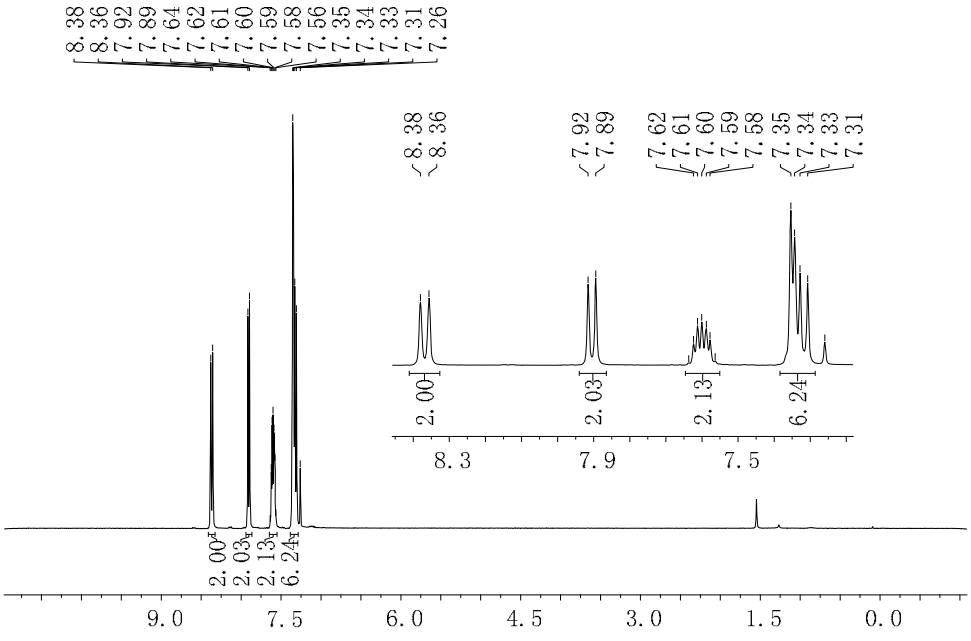

^{13}C NMR (90 MHz, $CDCl_3$)

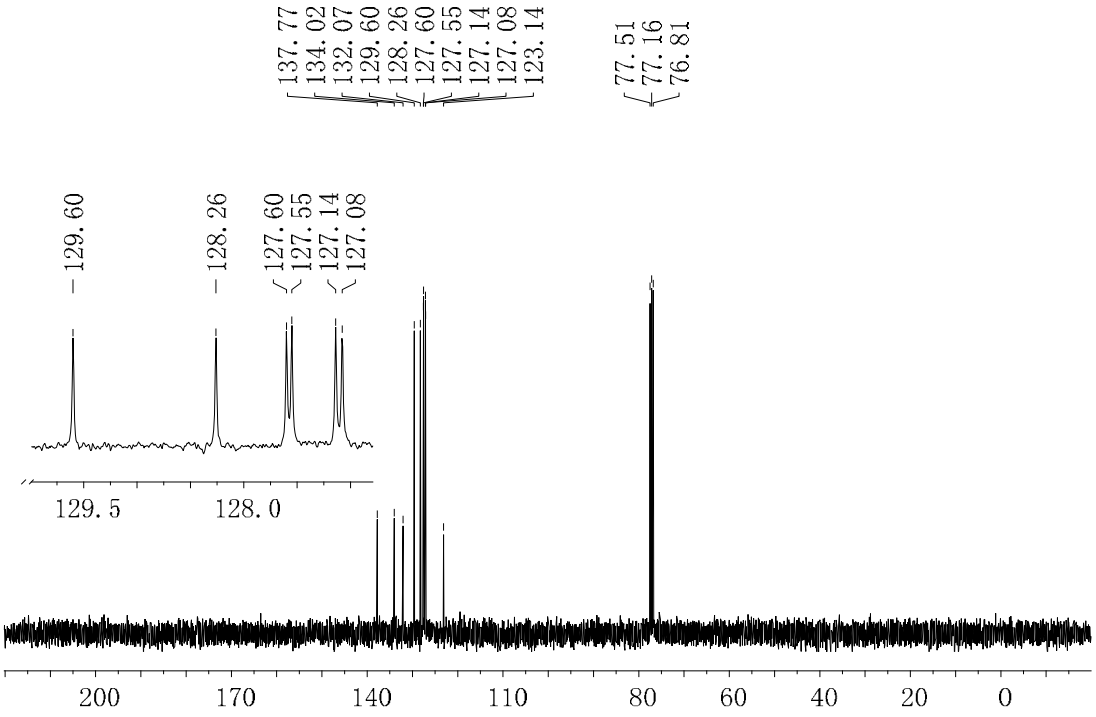

IR (ATR) *v* (cm^{-1})

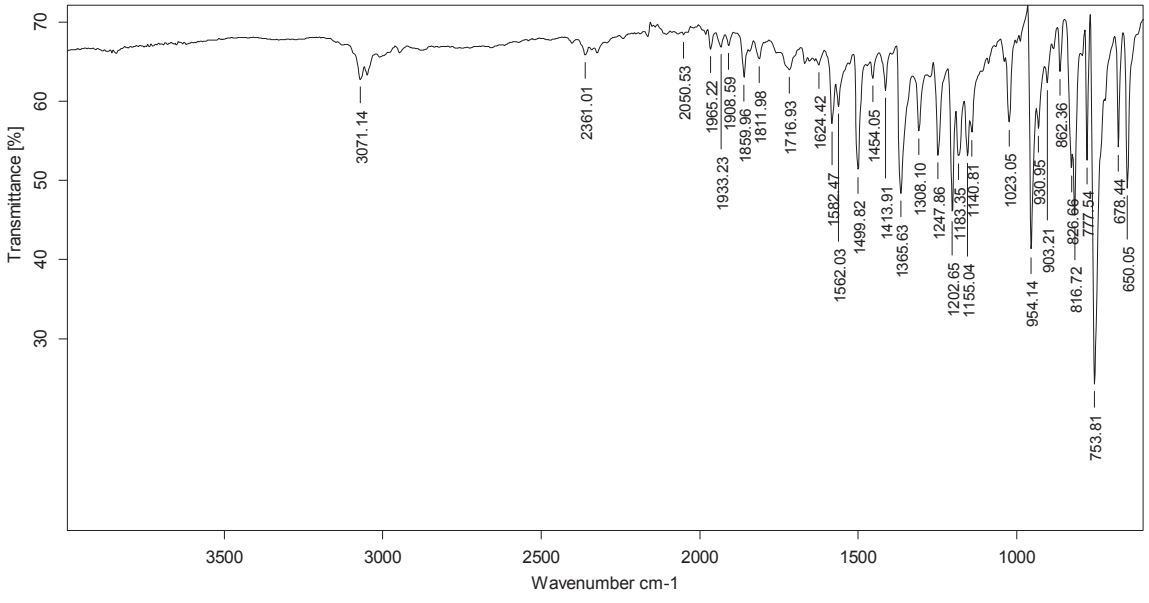

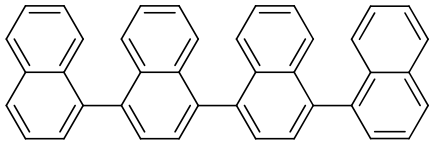

, **4**

^{1}H NMR (250 MHz, $CDCl_3$)

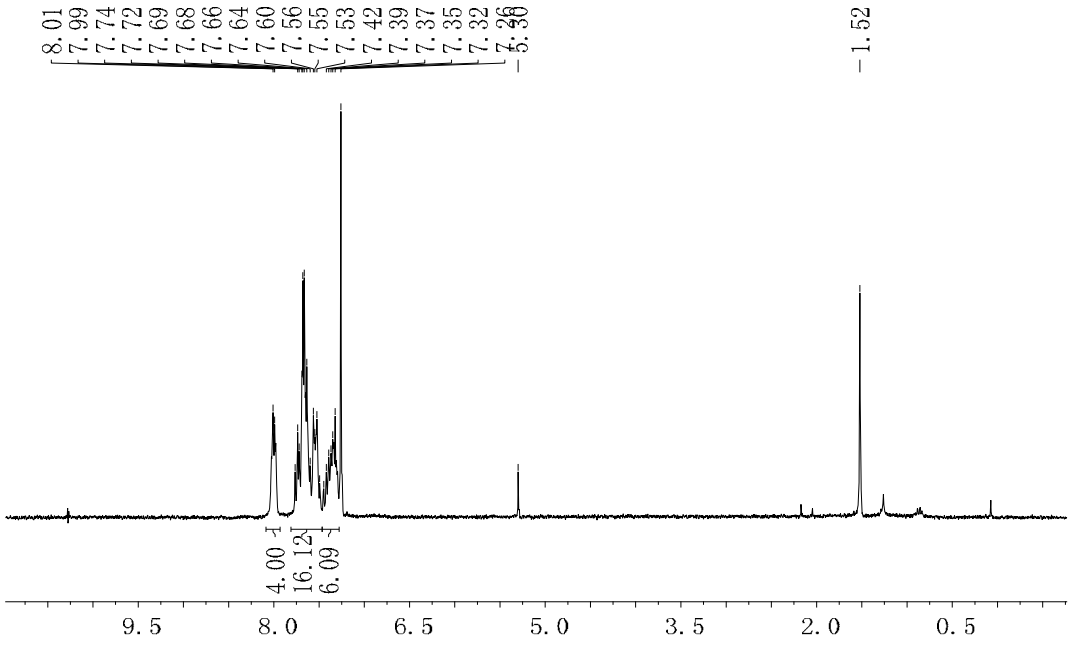

13

C NMR (90 MHz, $CDCl_3$)

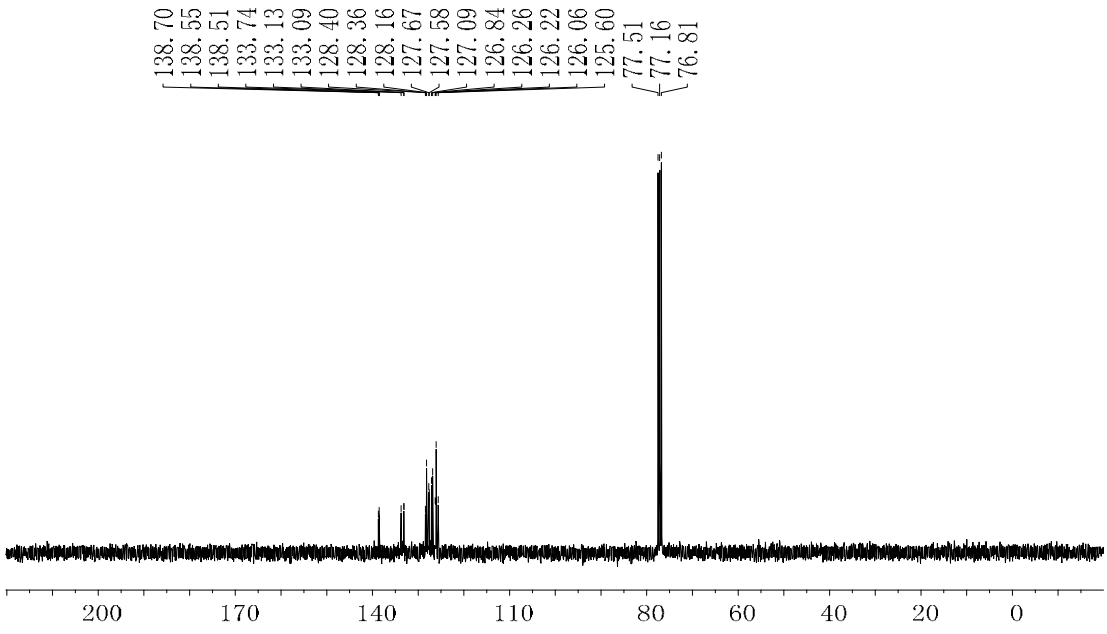

IR (ATR) ν (cm^{-1})

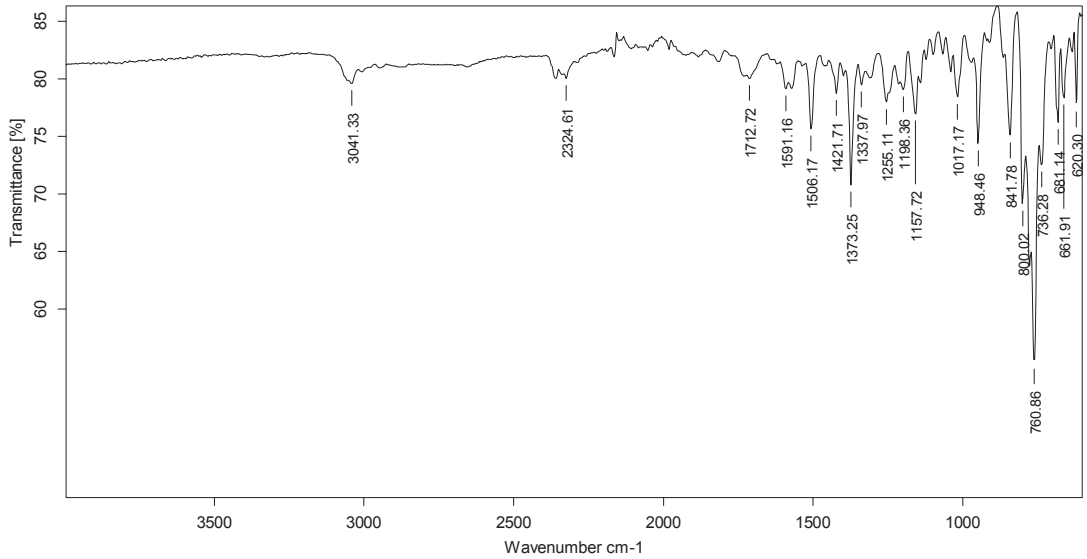

Maldi-TOF spectrum

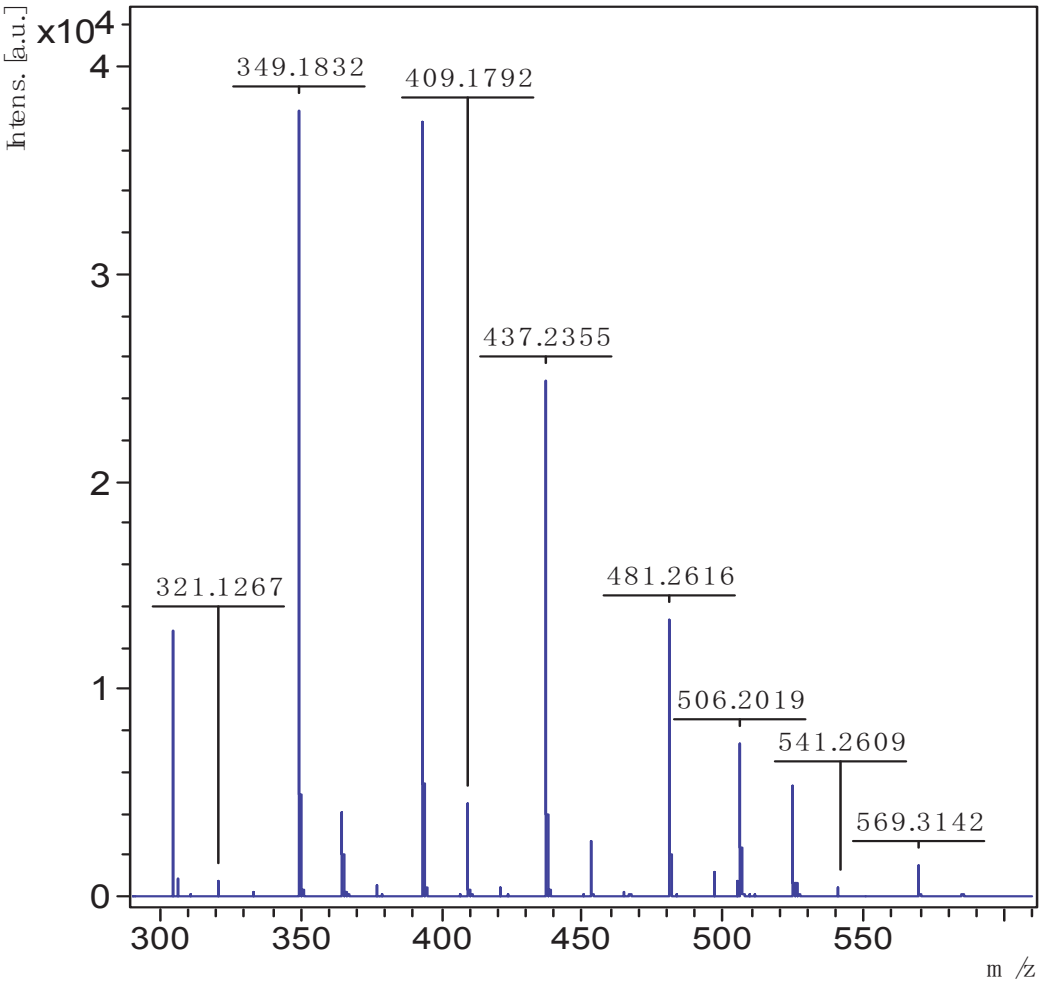

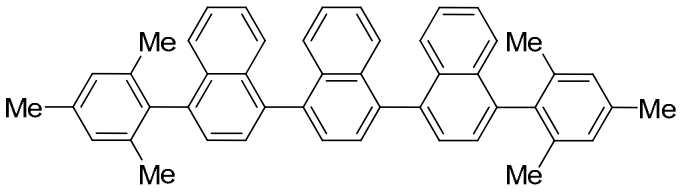

, **5a**

^{1}H NMR (360 MHz, $CDCl_3$)

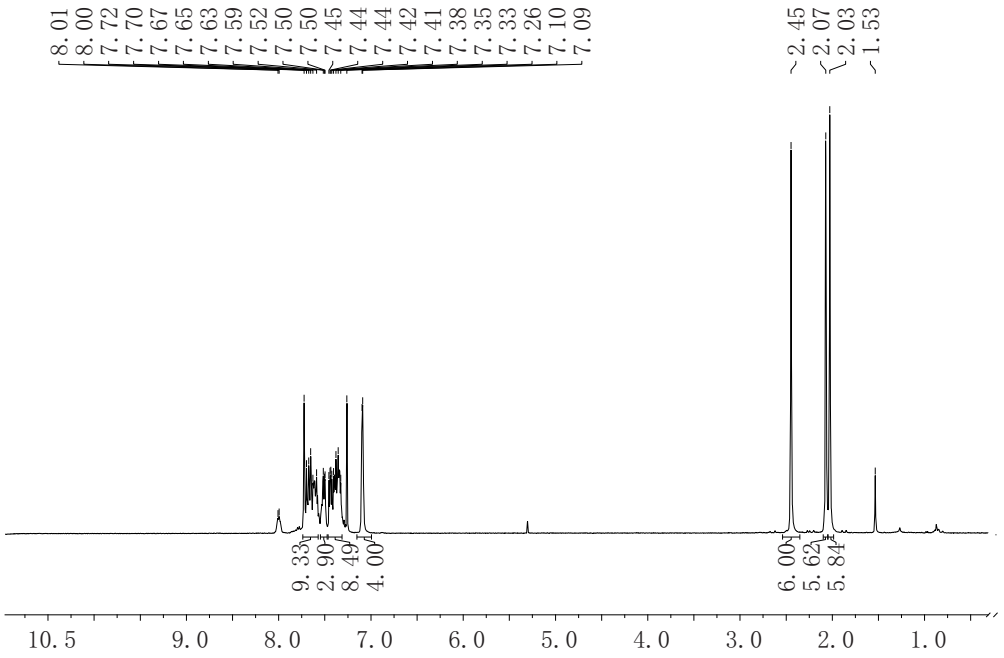

^{13}C NMR (90 MHz, $CDCl_3$)

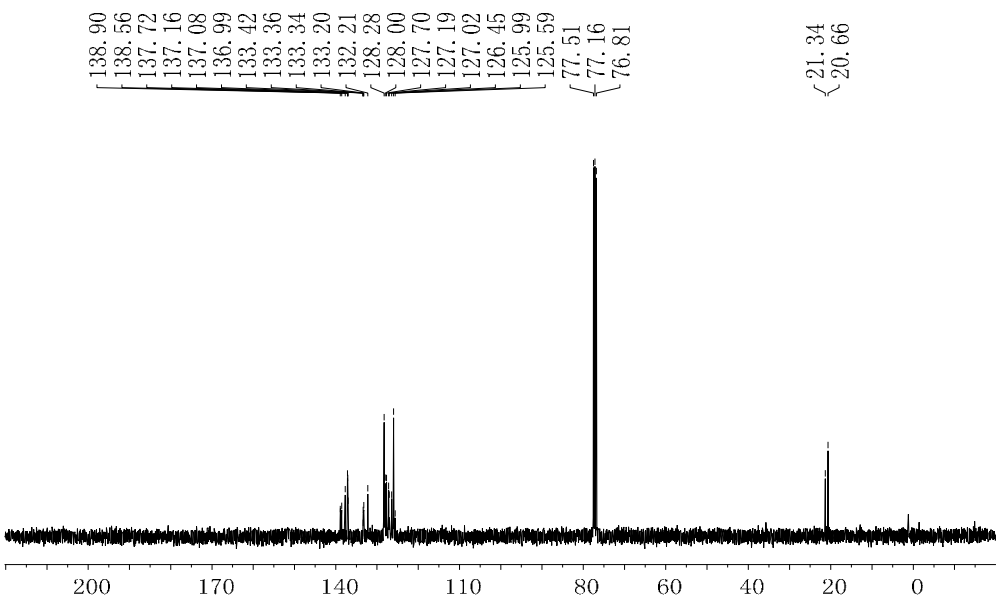

IR (ATR) ν (cm^{-1})

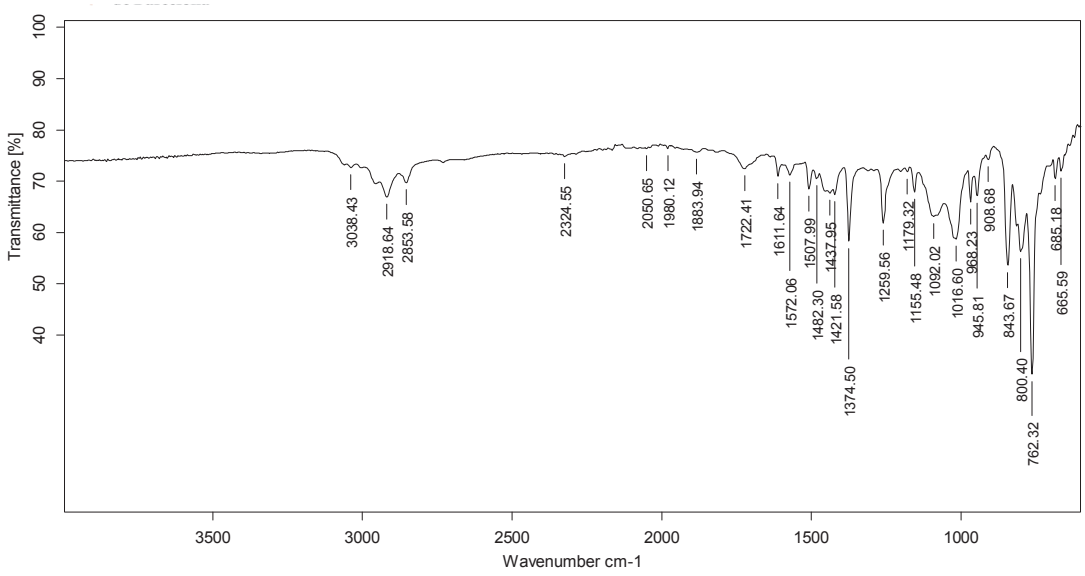

Maldi-TOF spectrum

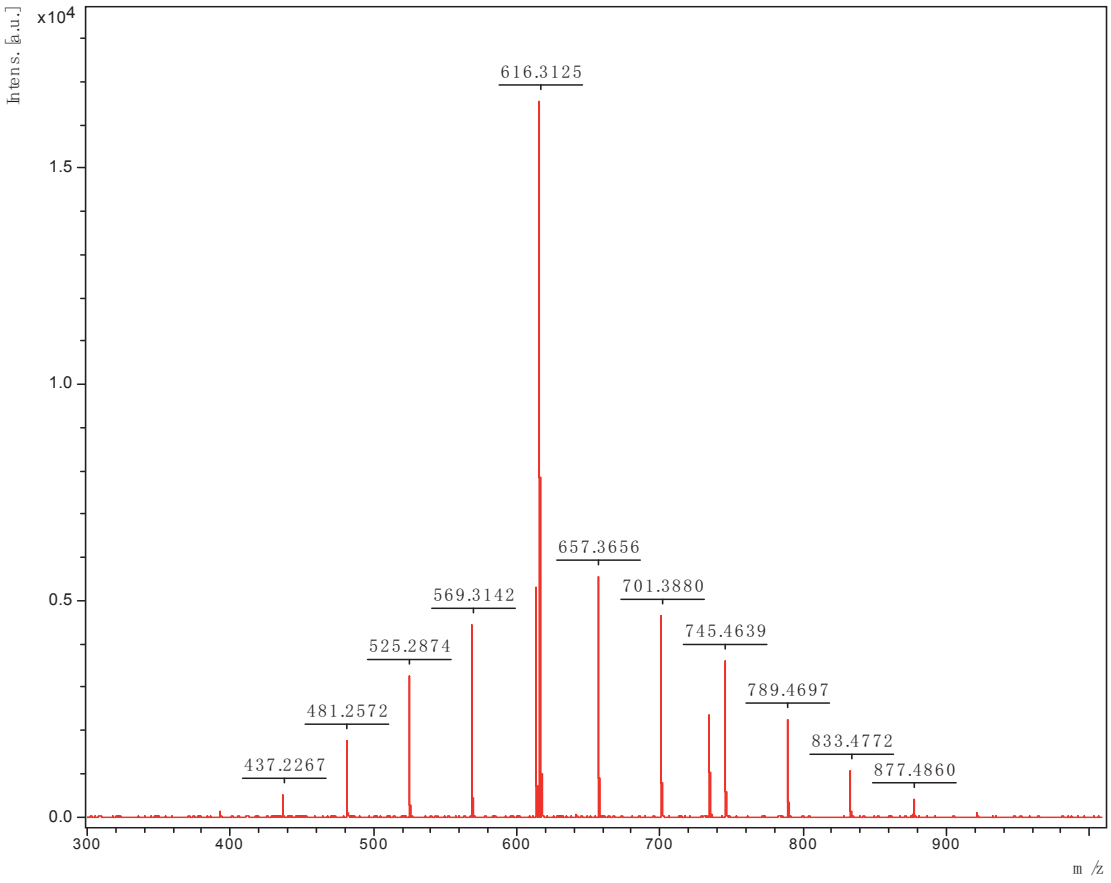

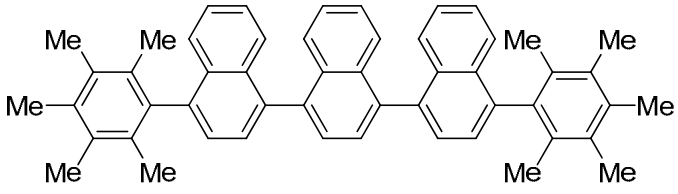

, **5b**

^{1}H NMR (360 MHz, $CDCl_3$)

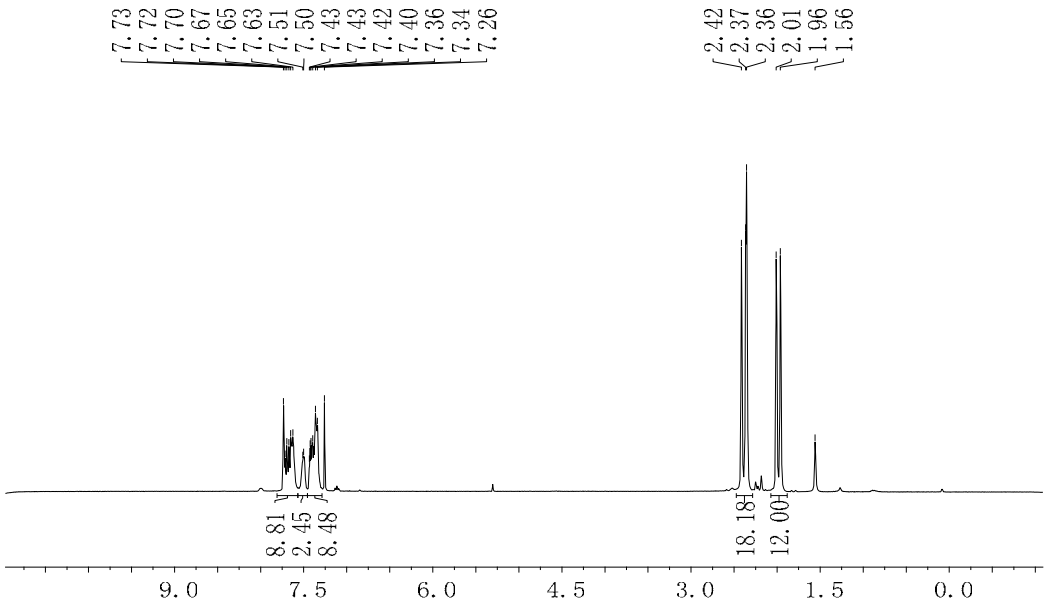

^{13}C NMR (90 MHz, $CDCl_3$)

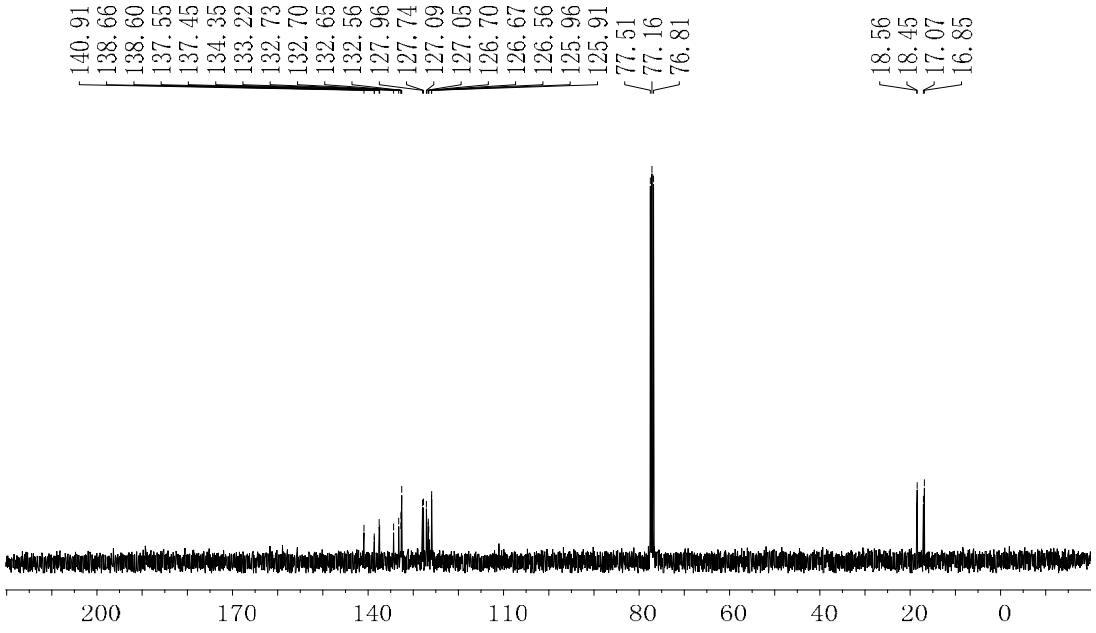

IR (ATR) ν (cm^{-1})

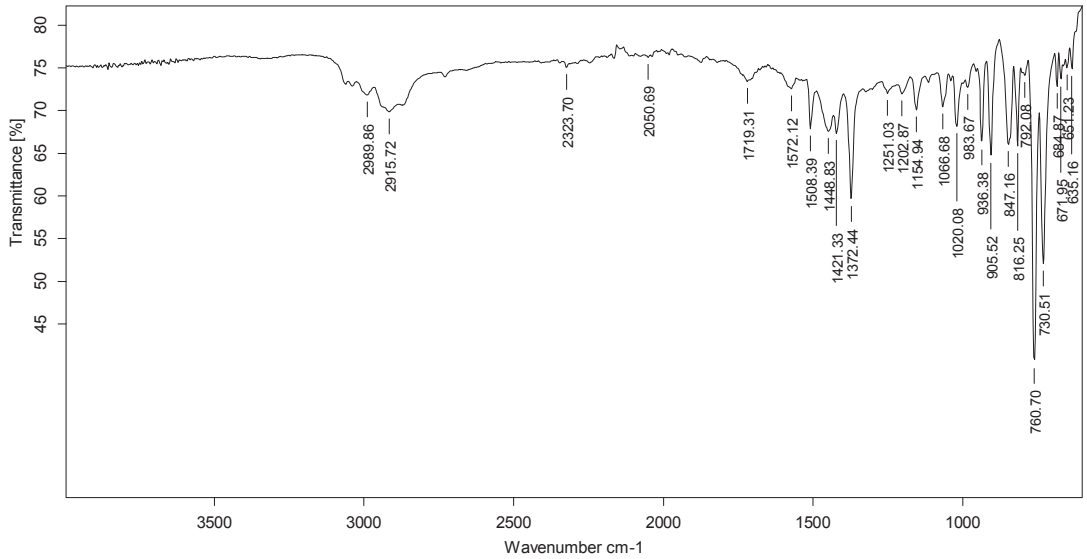

MALDI-TOF spectrum

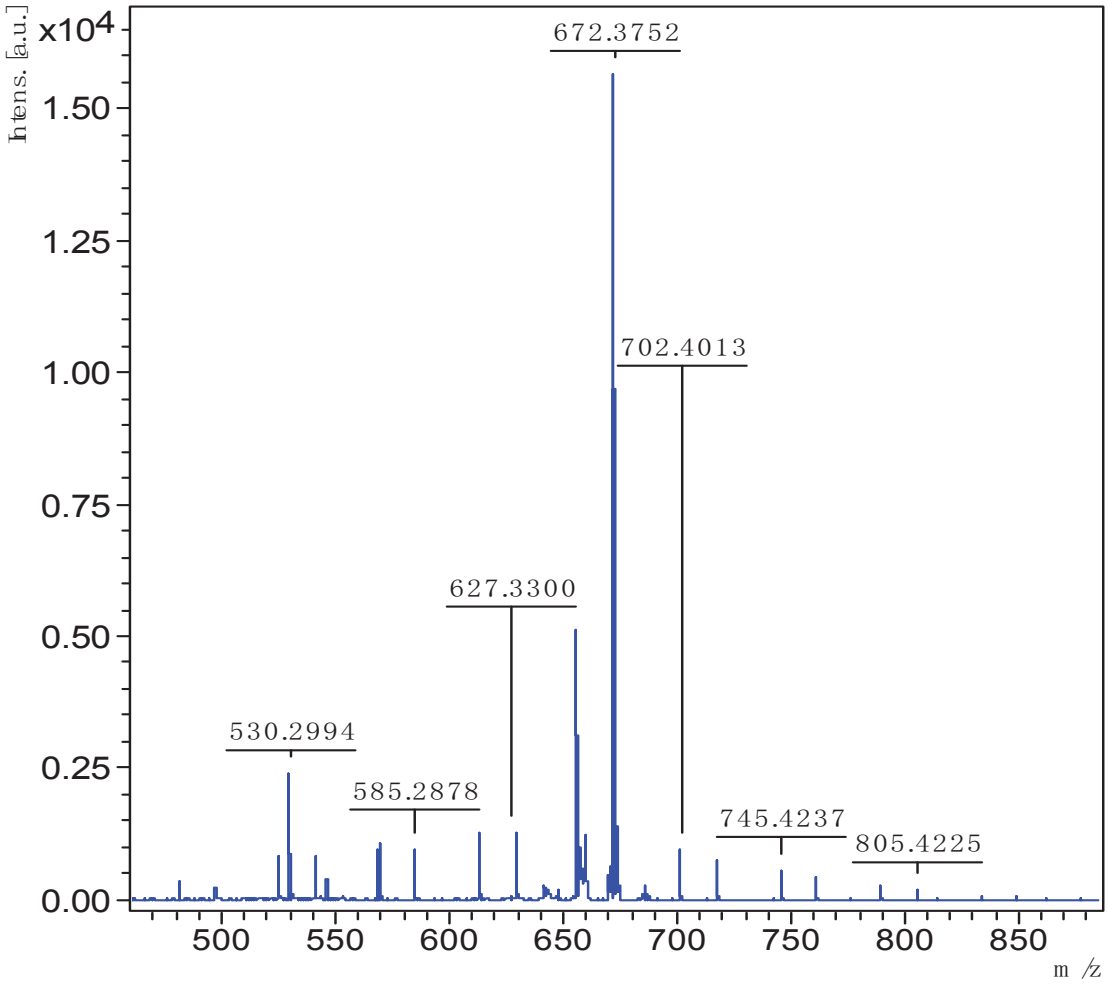

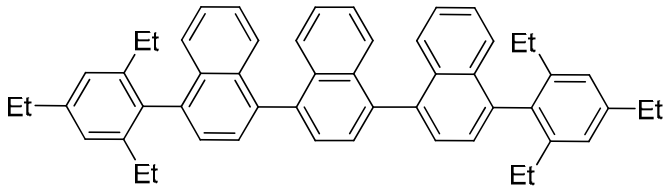

, **5c**

^{1}H-NMR (360 MHz, $CDCl_3$)

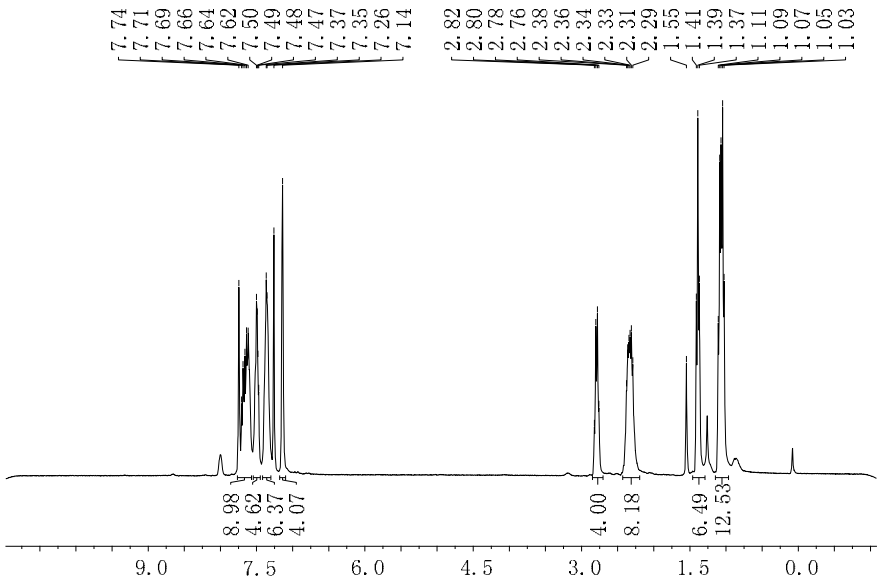

^{13}C NMR (62.5 MHz, $CDCl_3$)

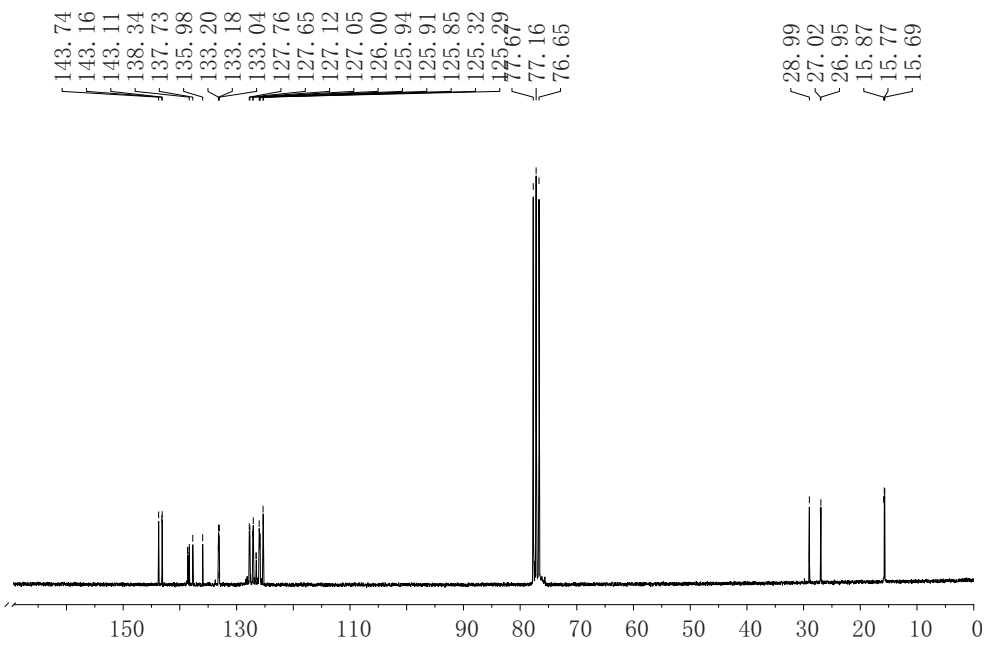

IR (ATR) ν (cm^{-1})

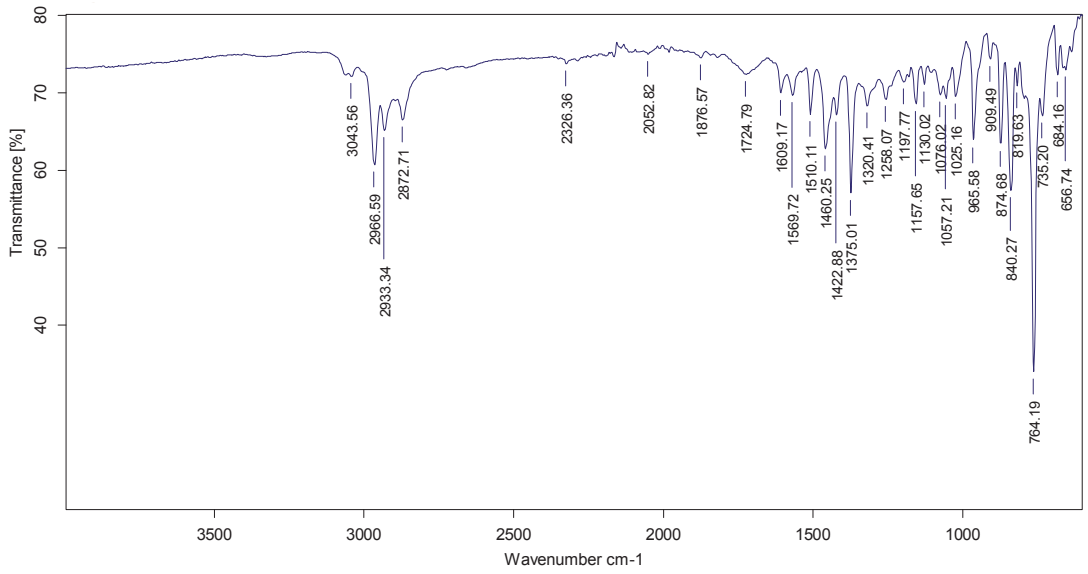

MALDI-TOF spectrum

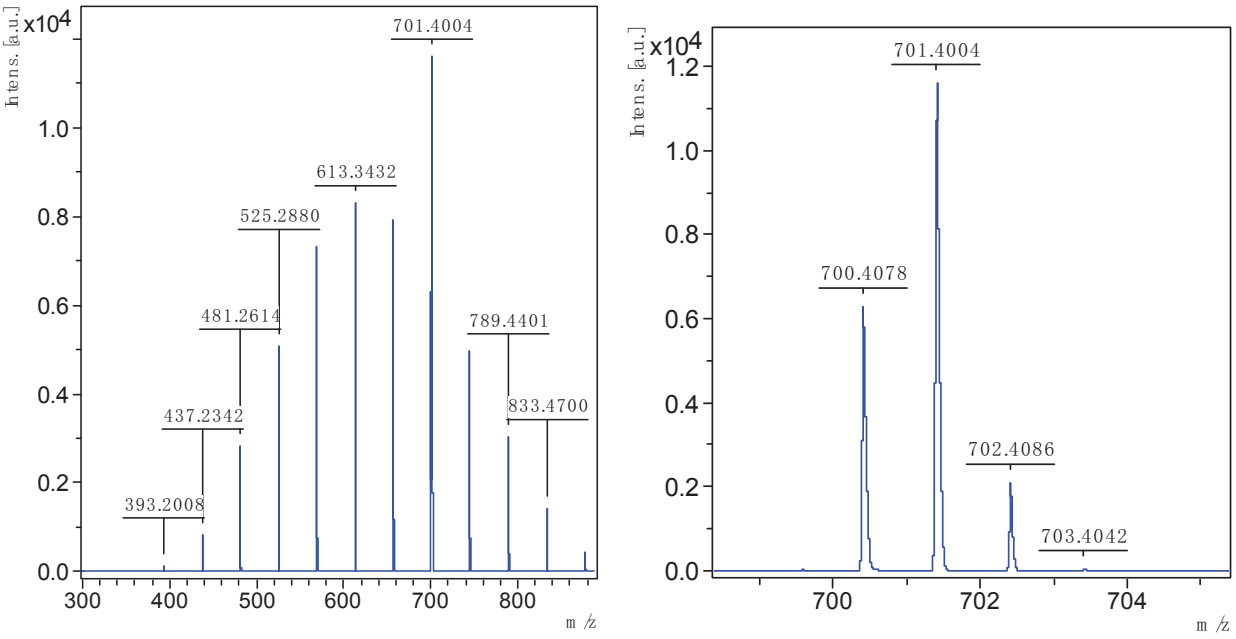

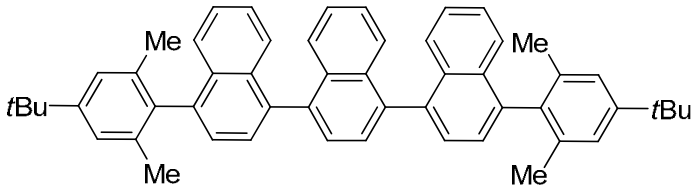

, **5d**

^{1}H NMR (360 MHz, $CDCl_3$)

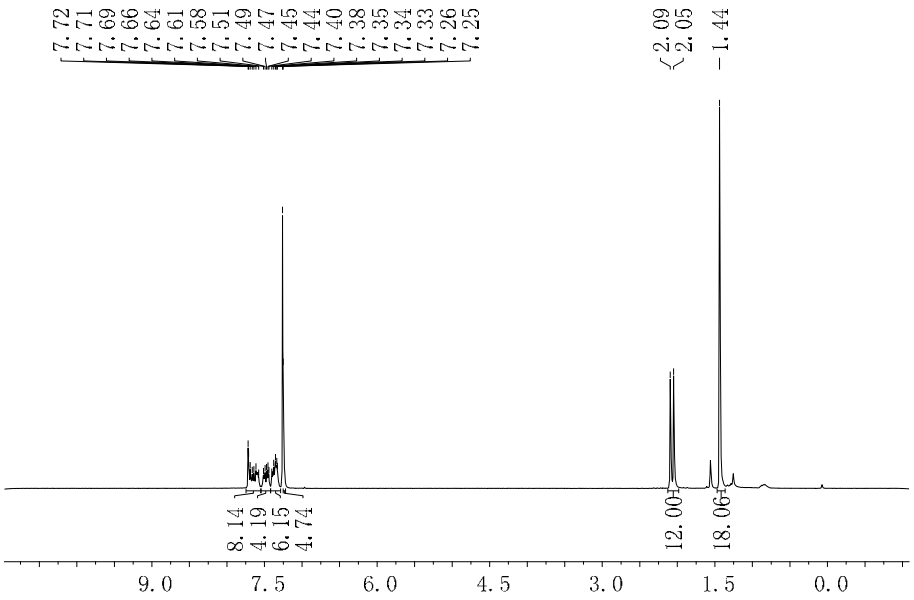

^{13}C NMR (90 MHz, $CDCl_3$)

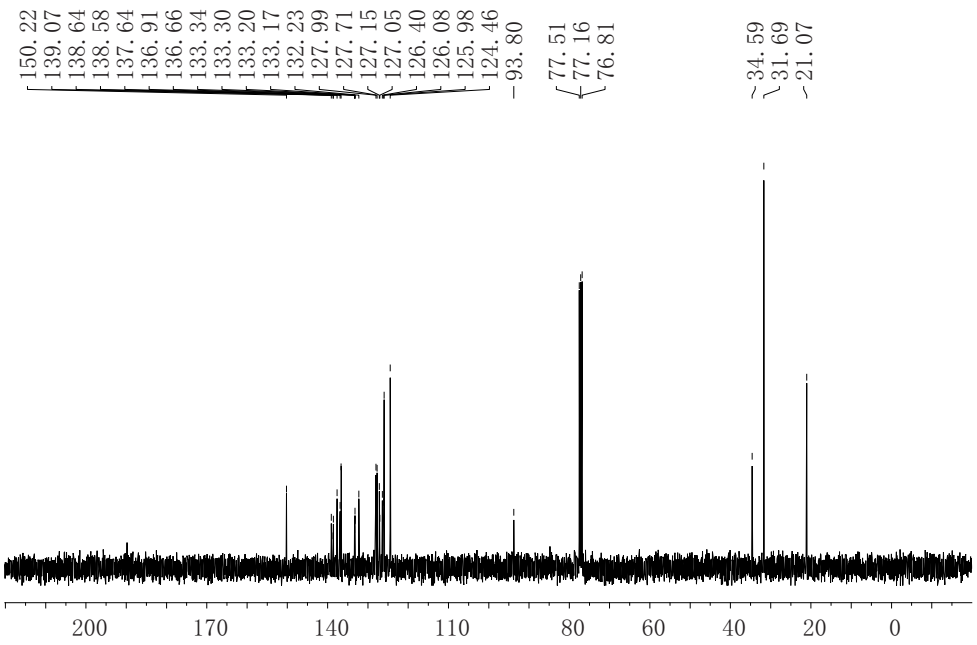

IR (ATR) ν (cm^{-1})

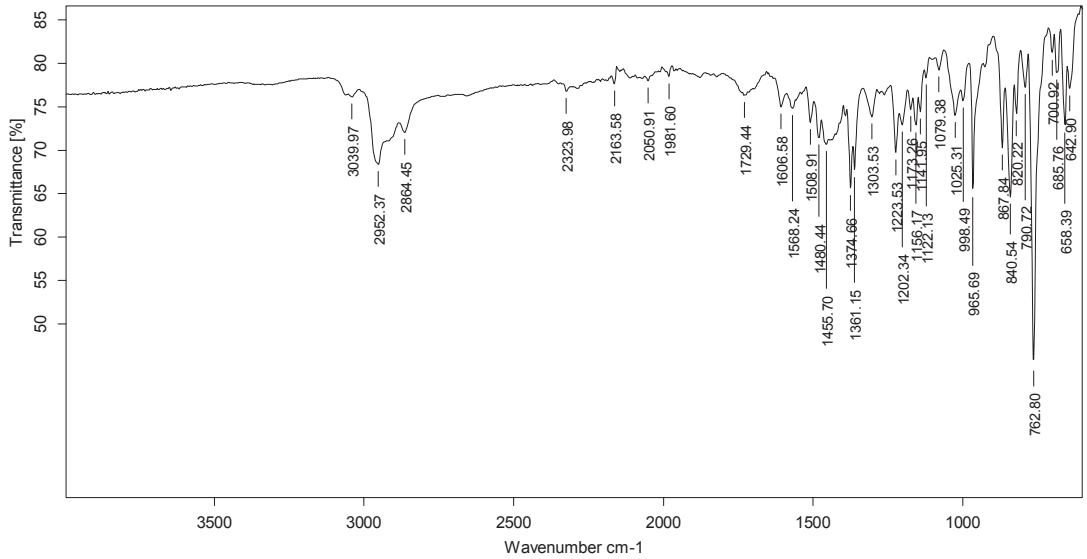

MALDI-TOF spectrum

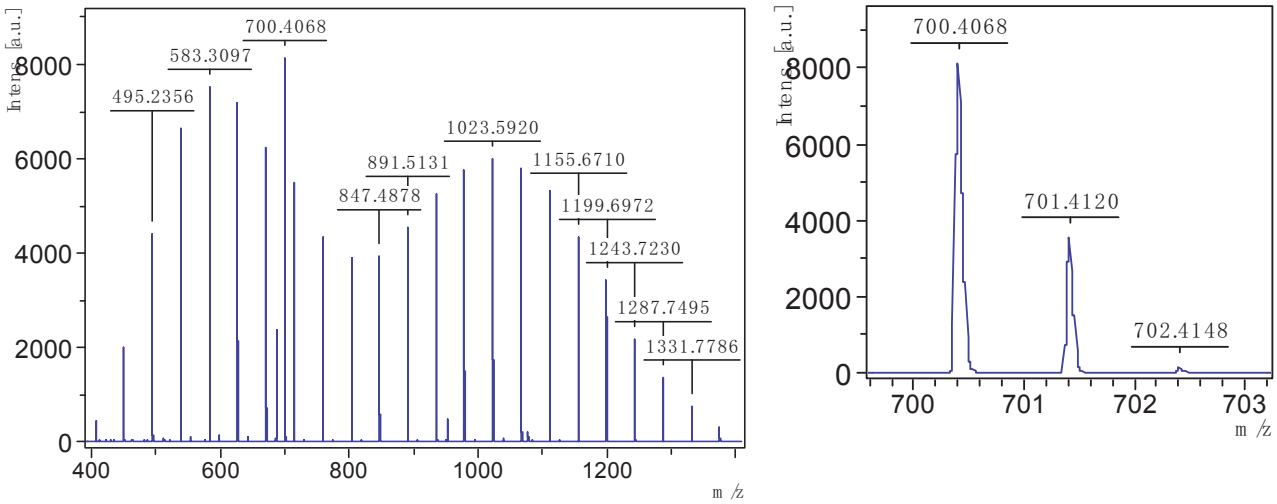

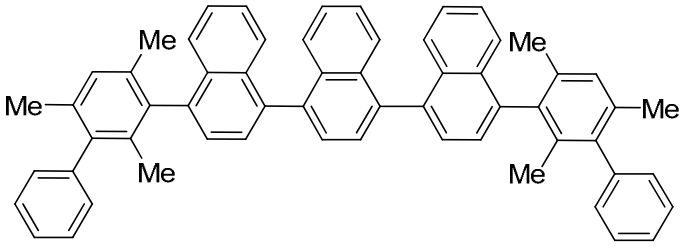

, **5e**

^{1}H-NMR (360 MHz, $CDCl_3$)

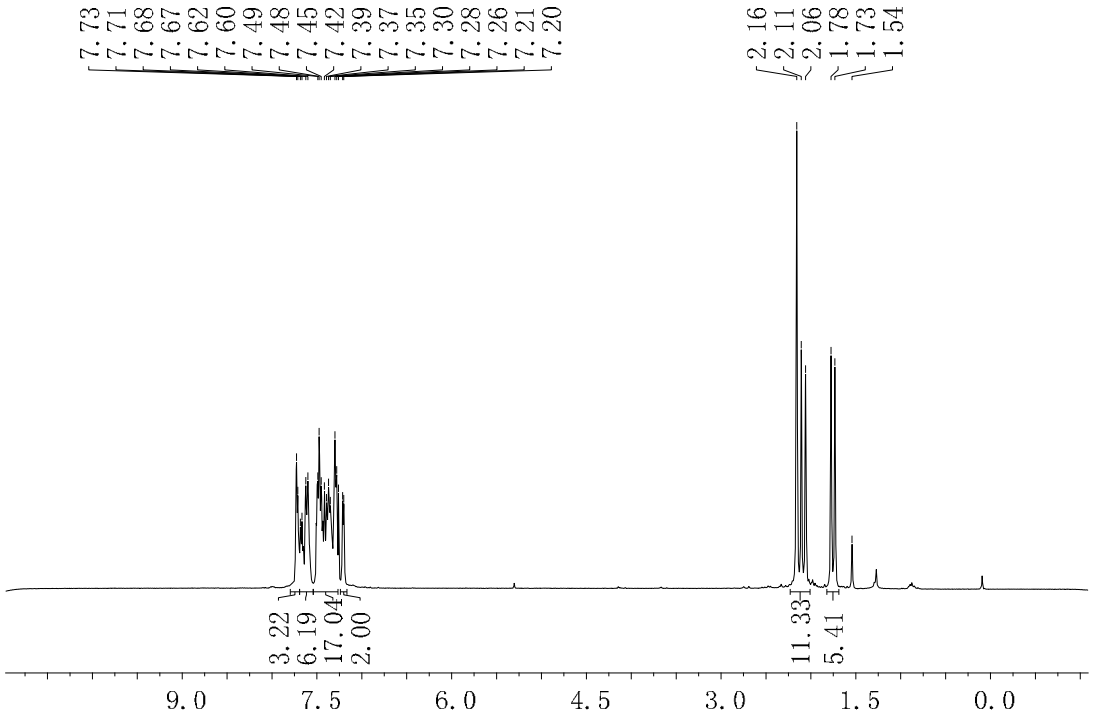

^{13}C NMR (90 MHz, $CDCl_3$)

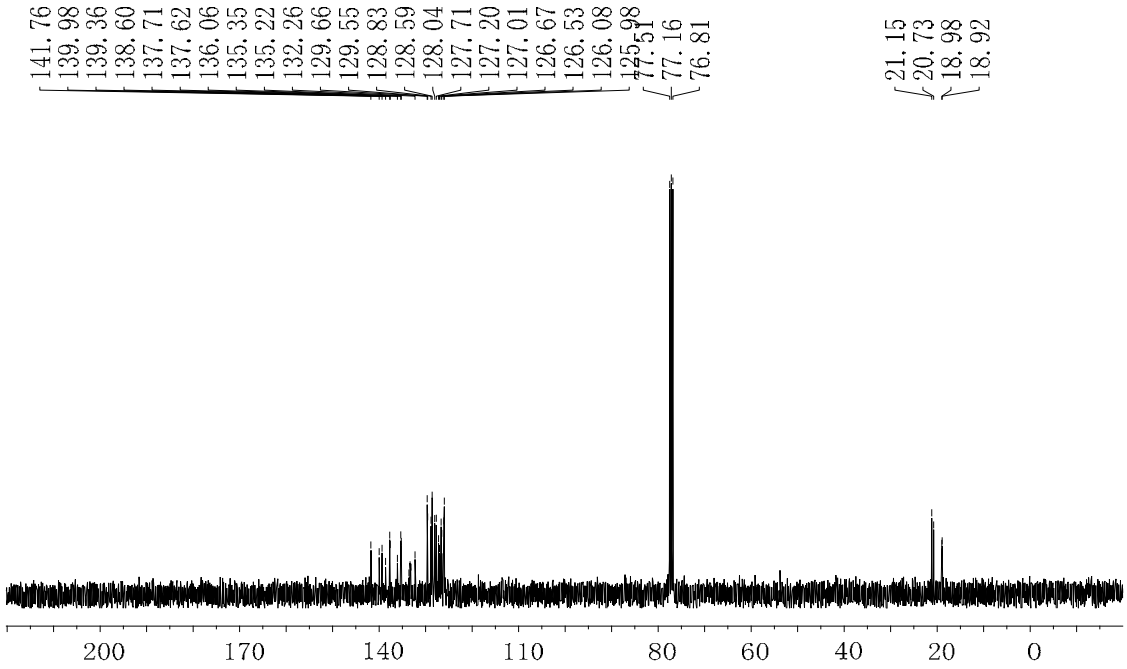

IR (ATR) ν (cm^{-1})

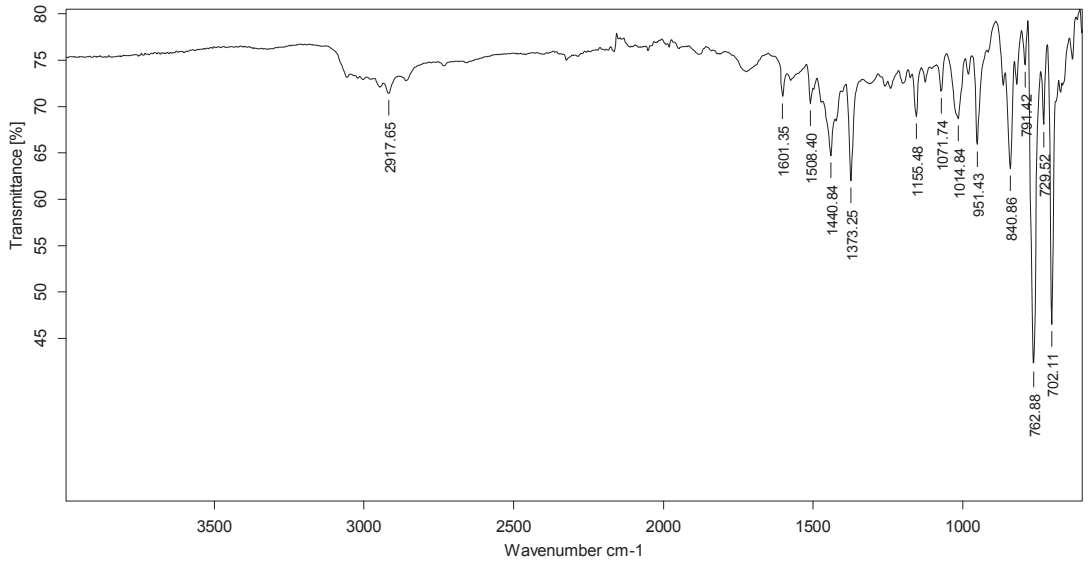

MALDI-TOF spectrum

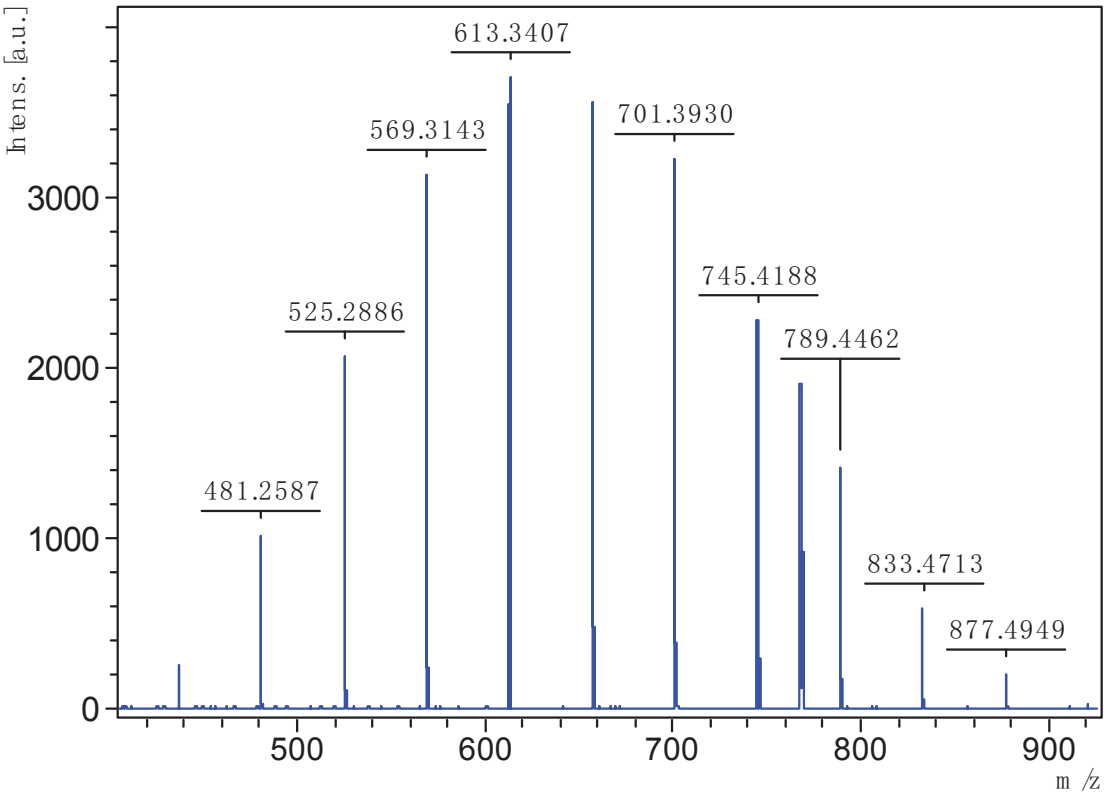

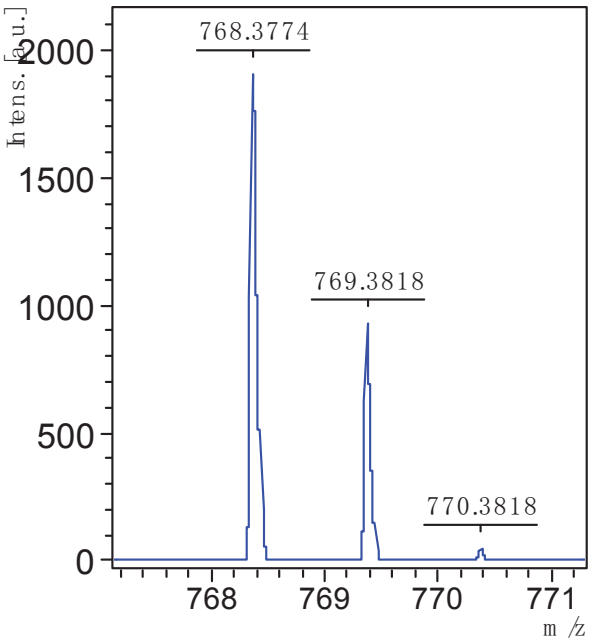

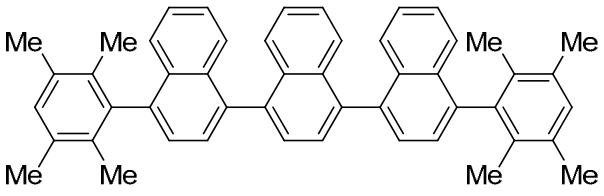

, **5f**

^{1}H NMR (360 MHz, $CDCl_3$)

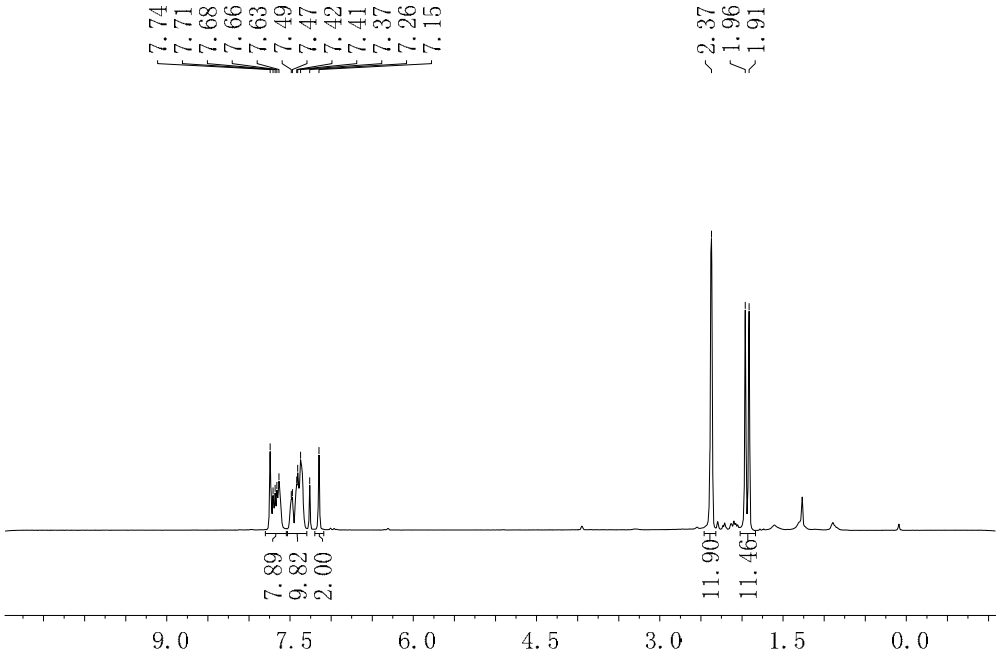

^{13}C NMR (90 MHz, $CDCl_3$)

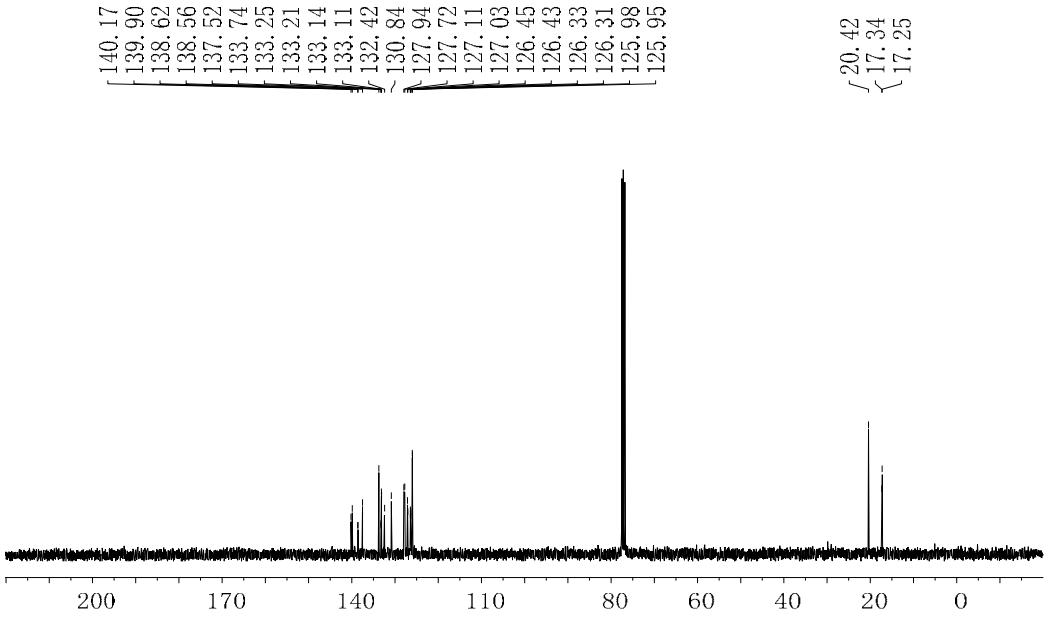

IR (ATR) ν (cm^{-1})

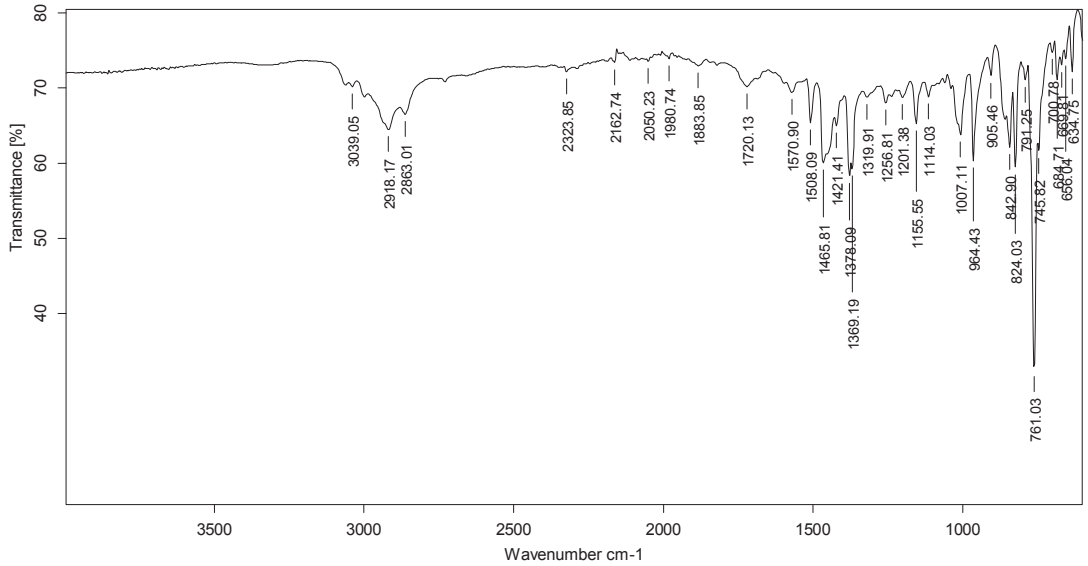

MALDI-TOF spectrum

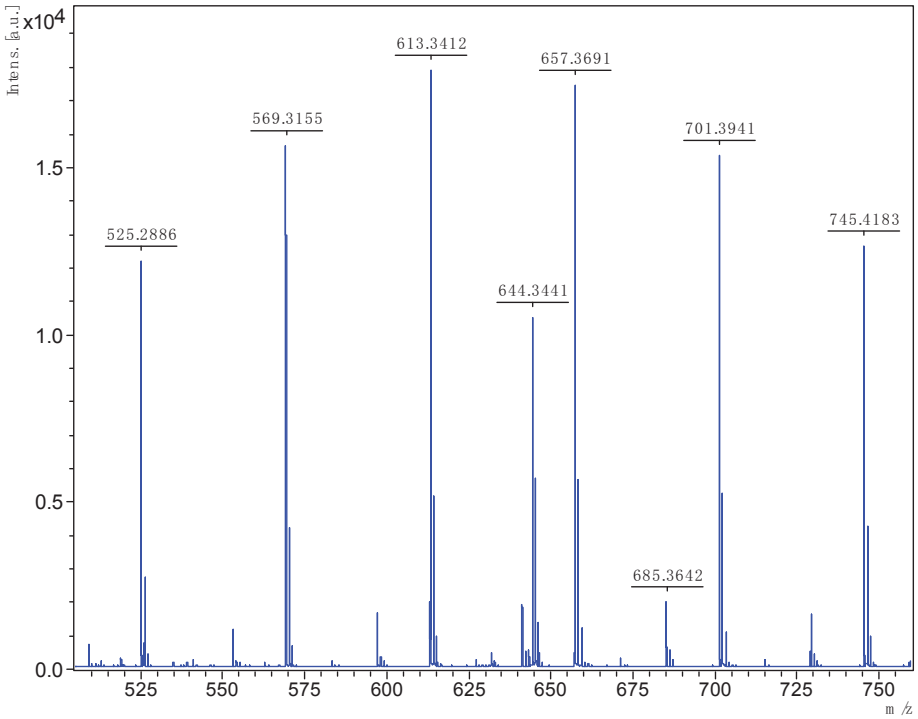

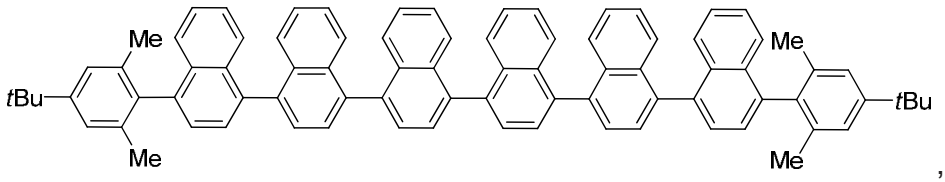

,6d

^{1}H NMR (360 MHz, $CDCl_3$)

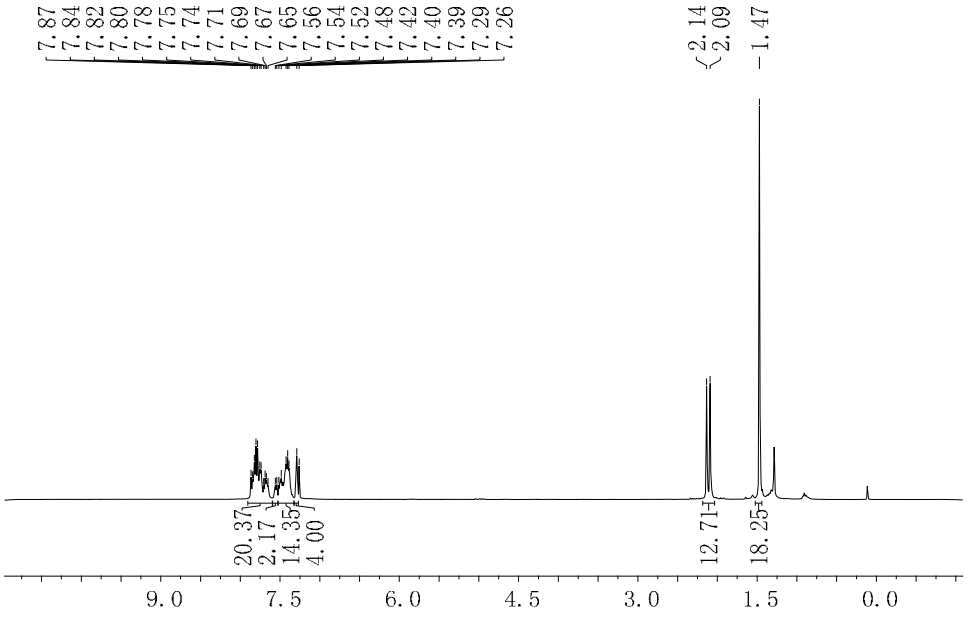

^{13}C NMR (90 MHz, $CDCl_3$)

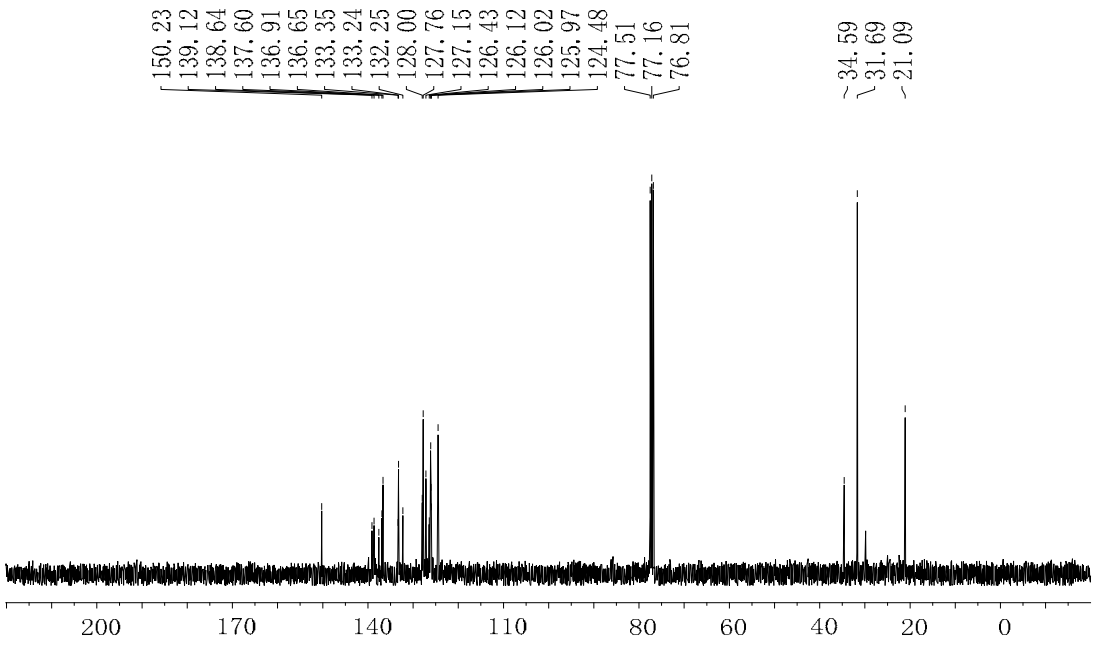

IR (ATR) ν (cm^{-1})

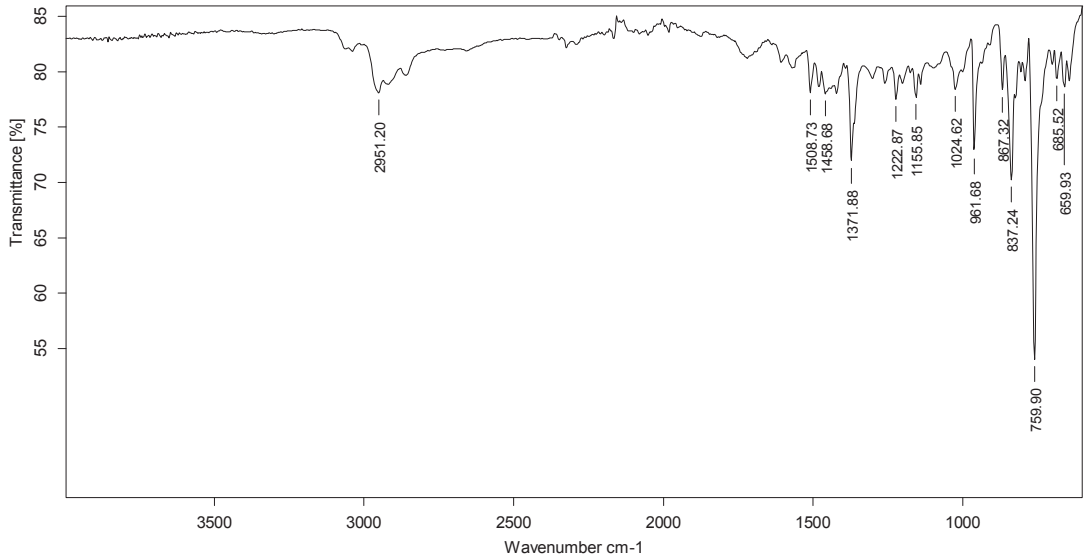

MALDI-TOF spectrum, 6d

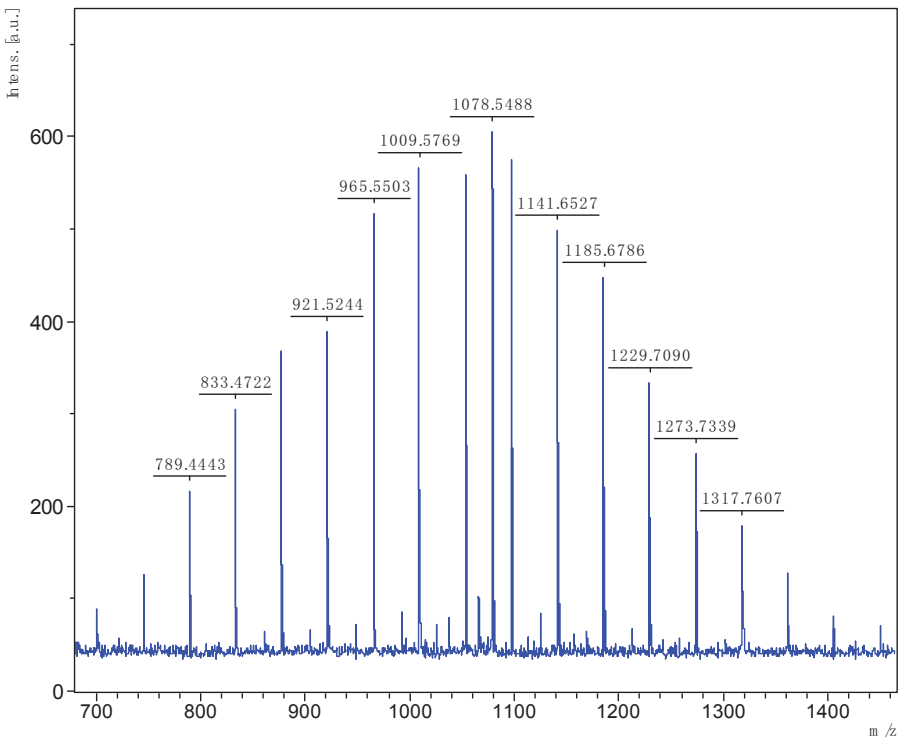

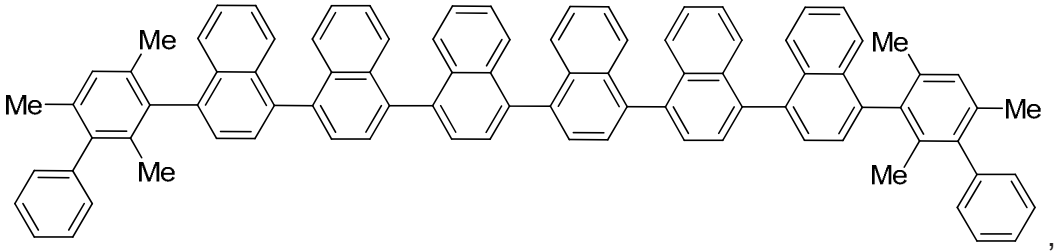

, **6e**

^{1}H NMR (360 MHz, $CDCl_3$)

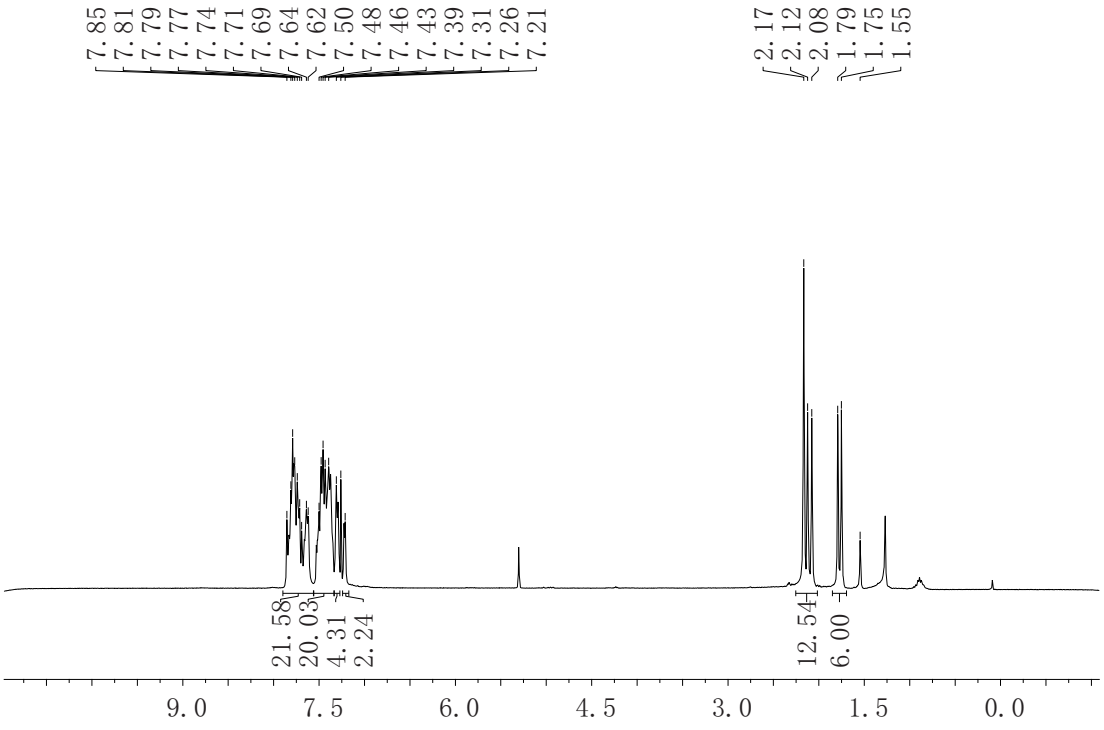

^{13}C NMR (90 MHz, $CDCl_3$)

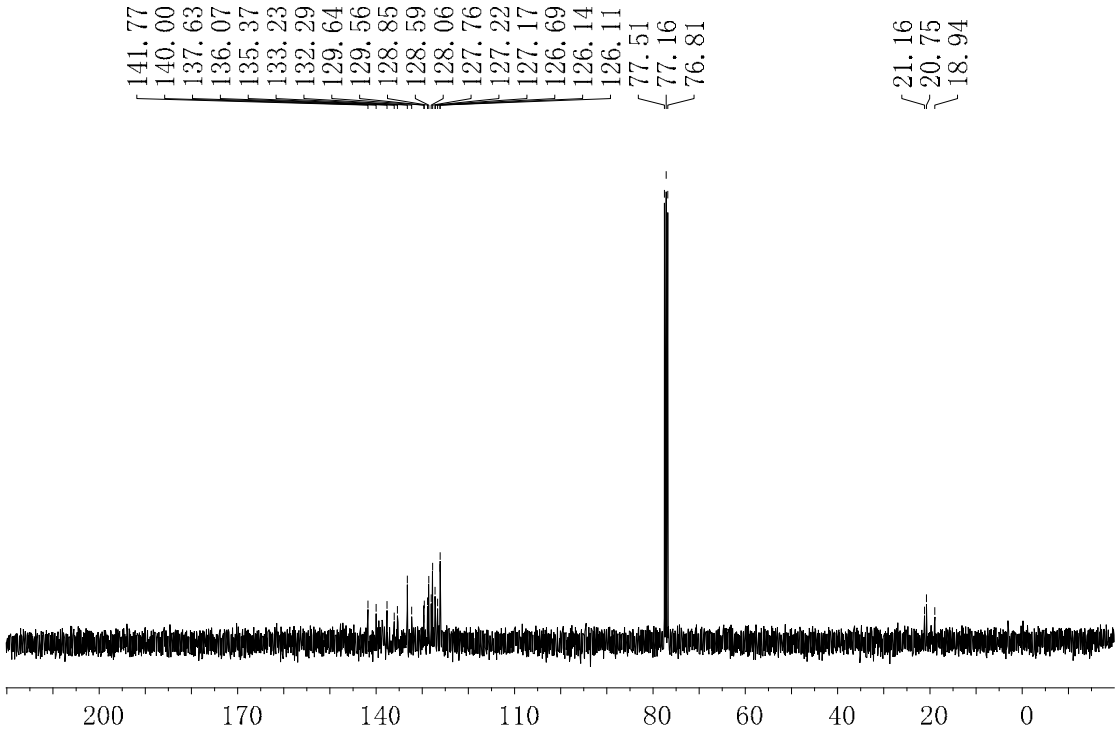

IR (ATR) *v* (cm^{-1})

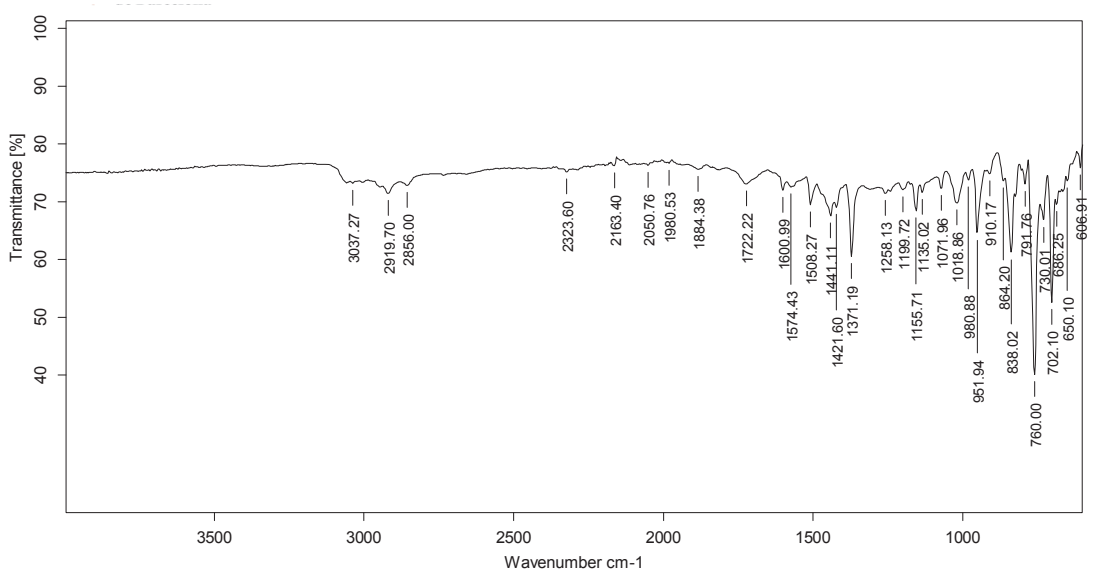

MALDI-TOF spectrum

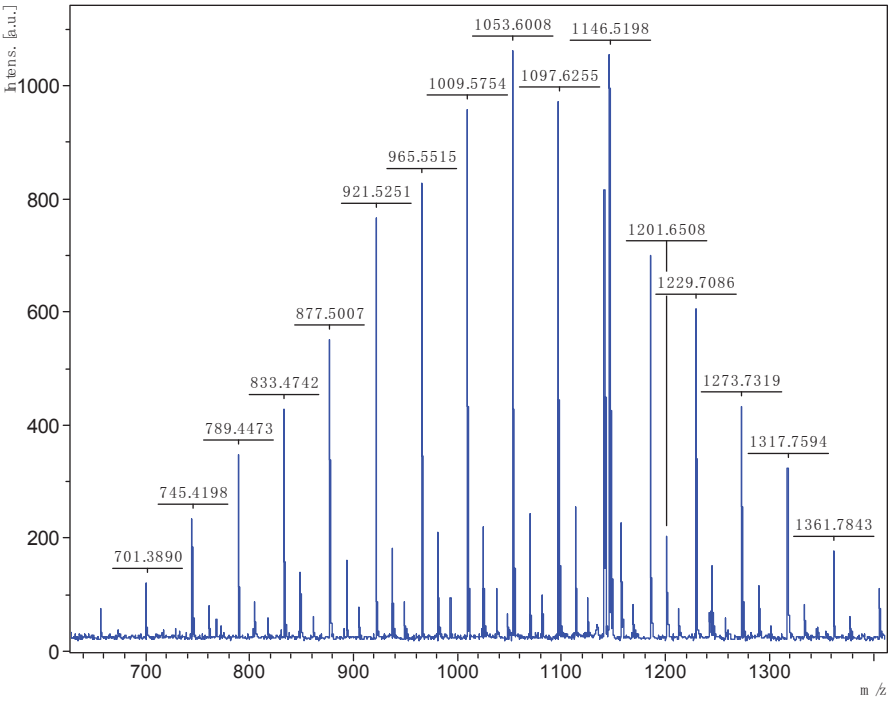

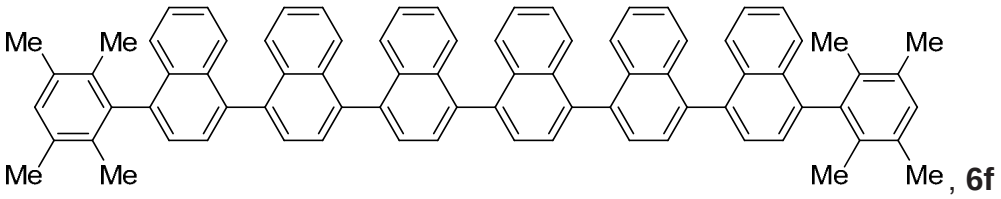

6f

^{1}H NMR (360 MHz, $CDCl_3$)

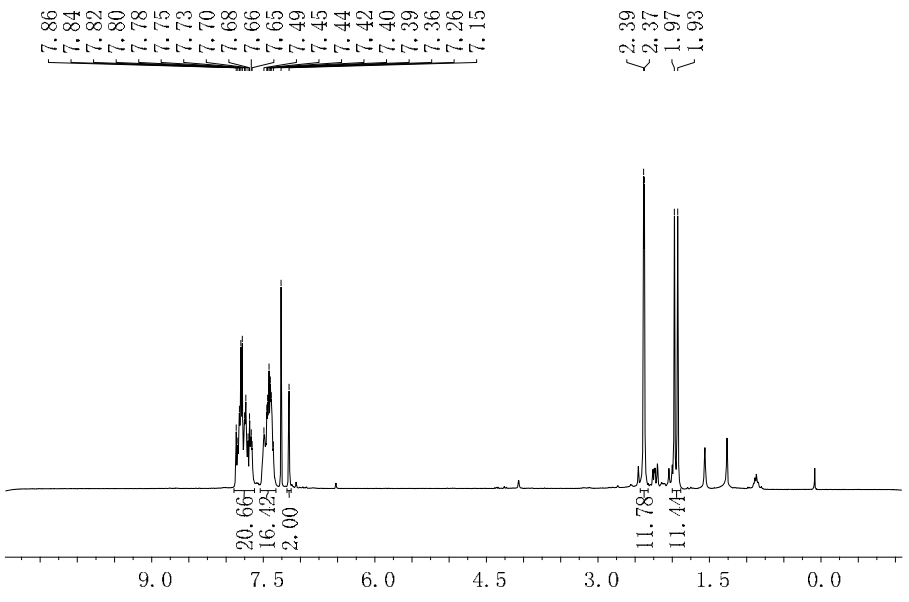

^{13}C NMR (62.5 MHz, $CDCl_3$)

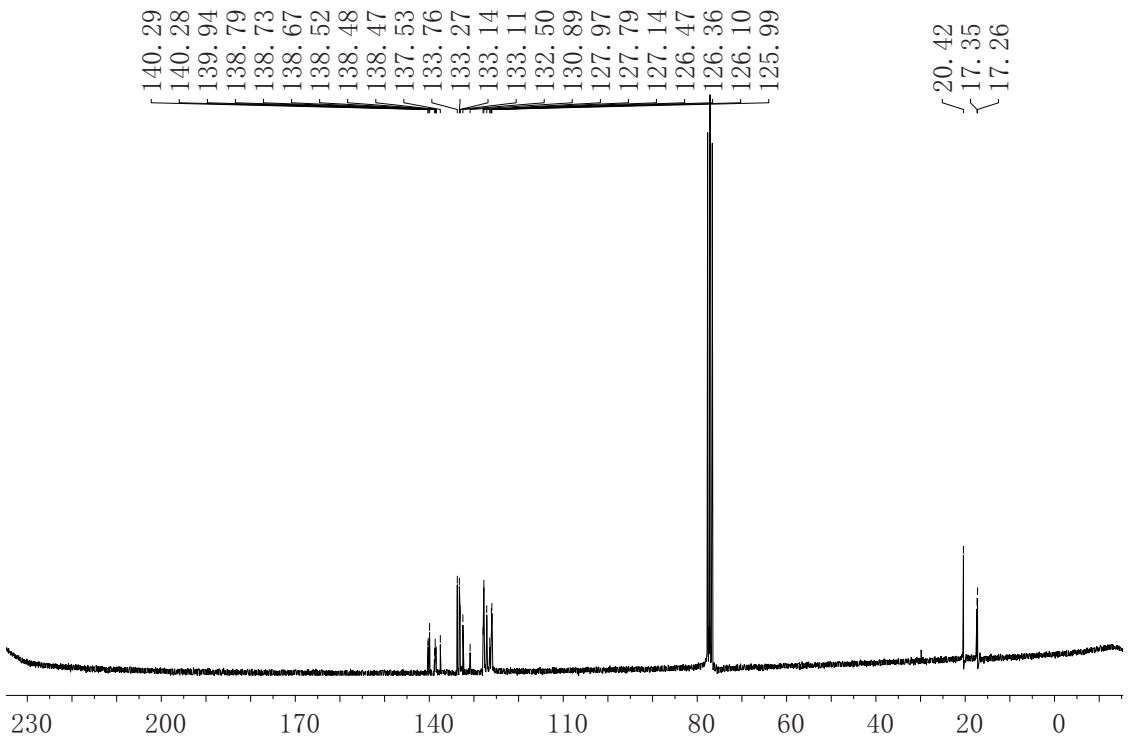

IR (ATR) ν (cm^{-1})

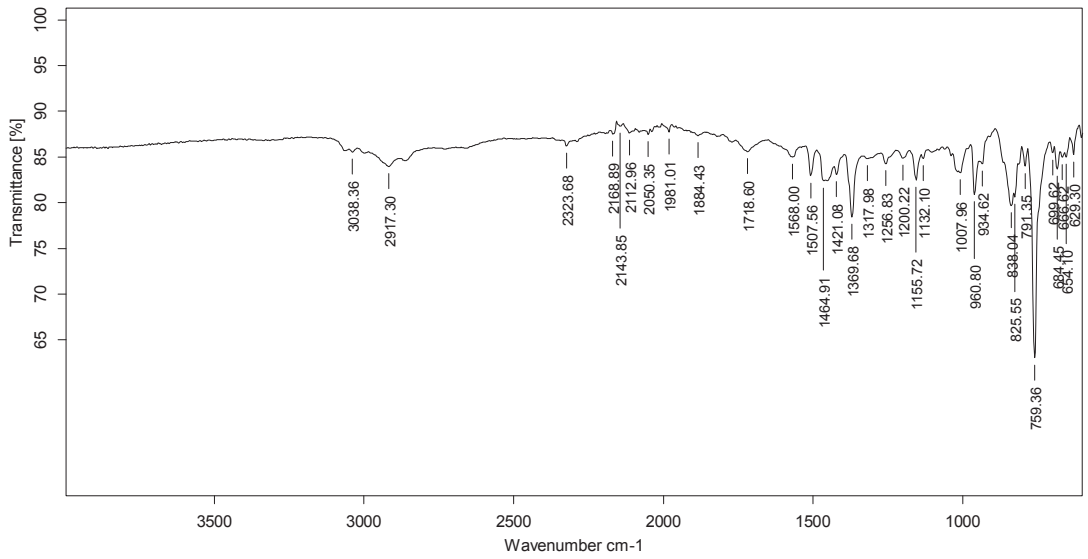

MALDI-TOF spectrum

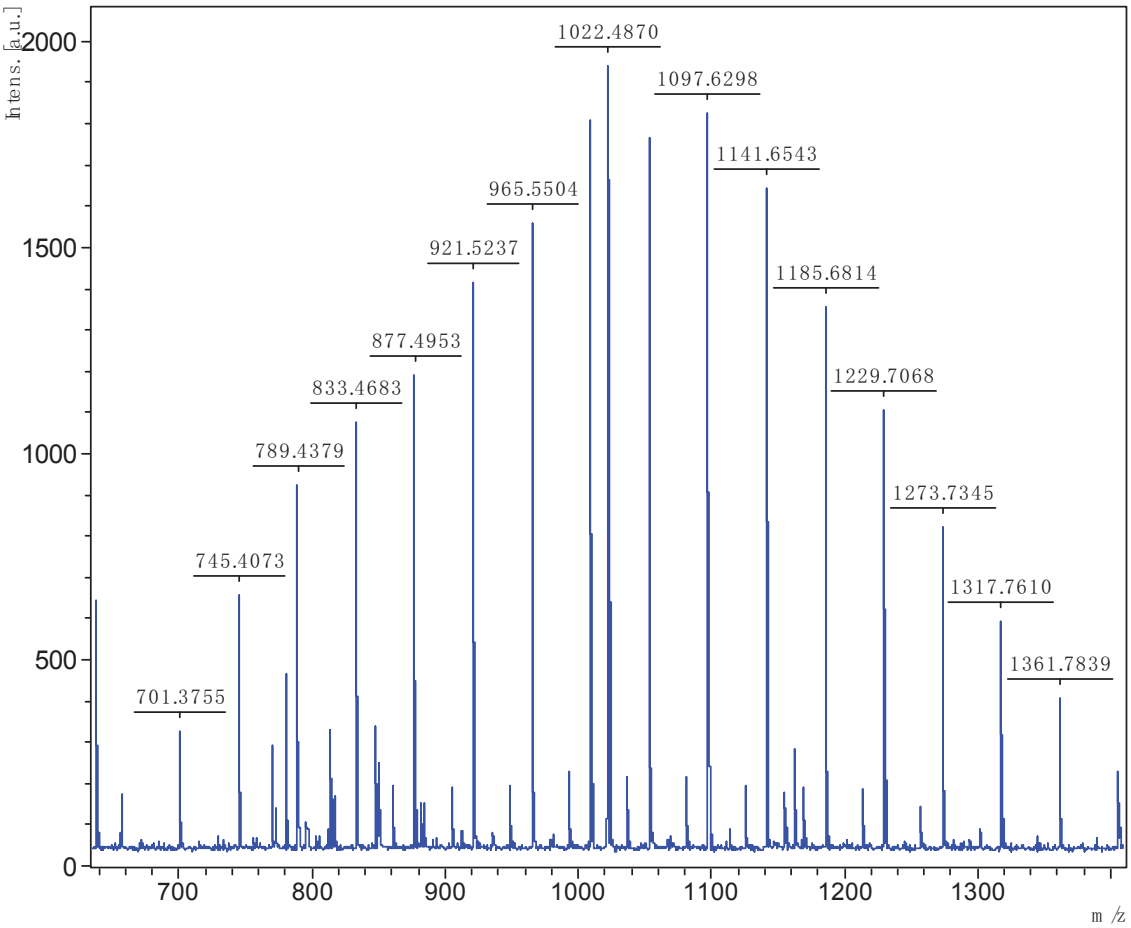

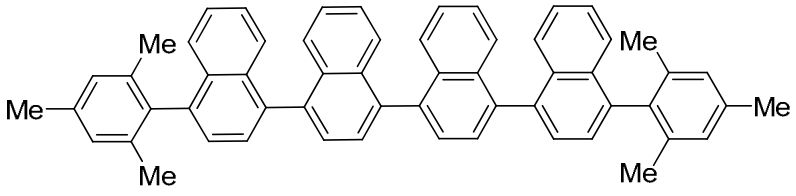

, **7a**

^{1}H-NMR (360 MHz, $CDCl_3$)

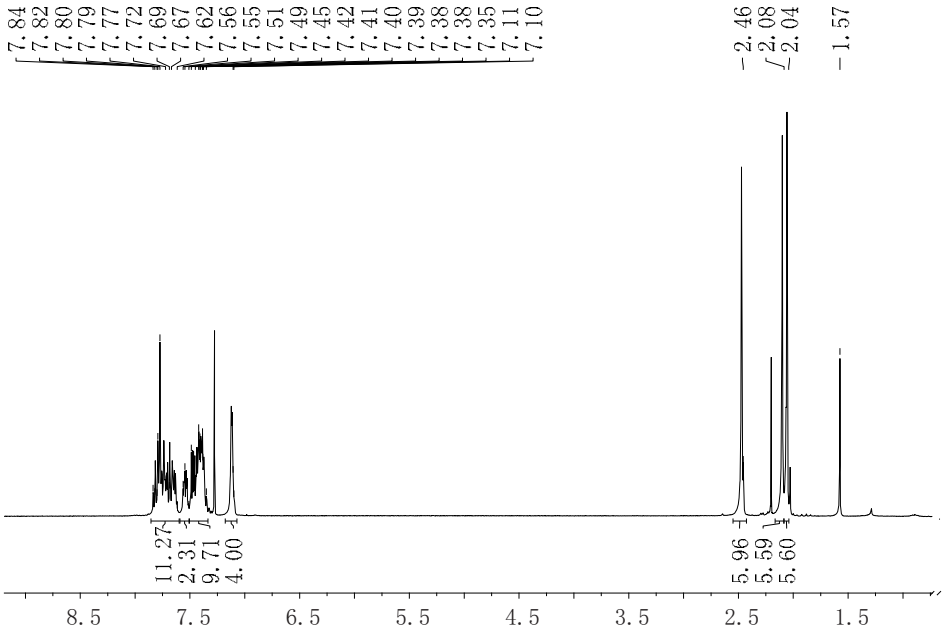

^{13}C NMR (101 MHz, $CDCl_3$)

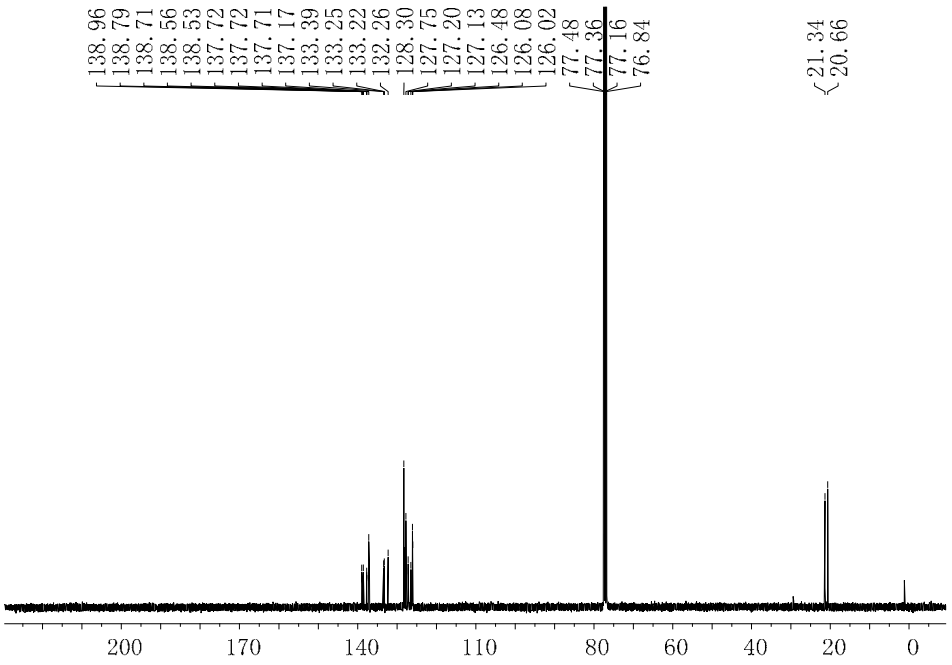

IR (ATR) ν (cm^{-1})

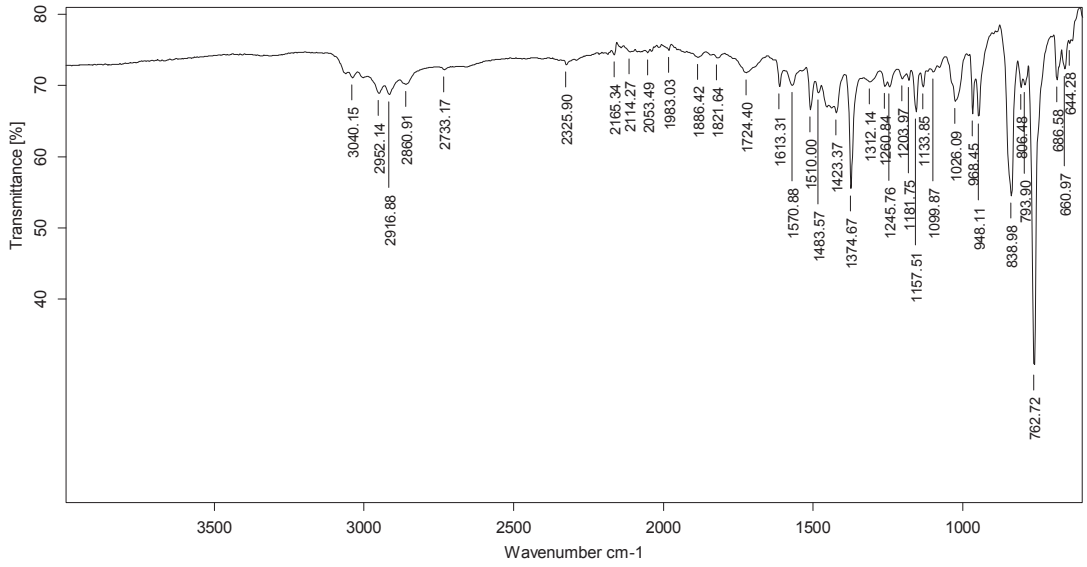

MALDI-TOF spectrum

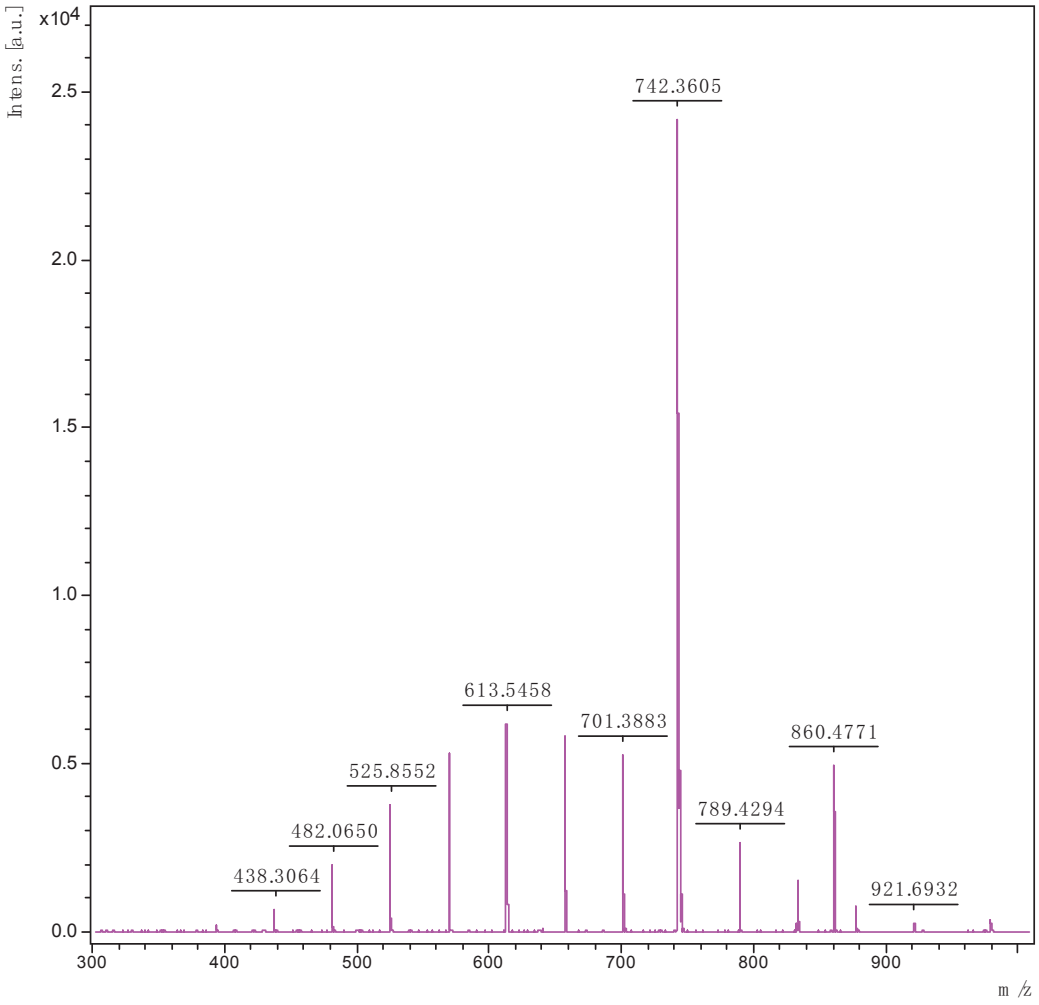

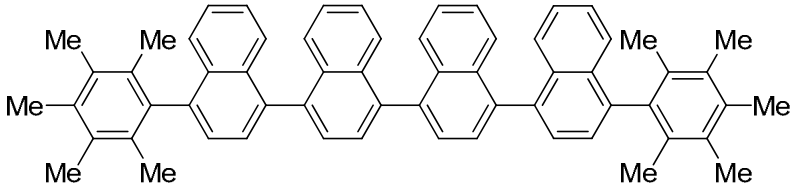

, **7b**

^{1}H-NMR (360 MHz, $CDCl_3$)

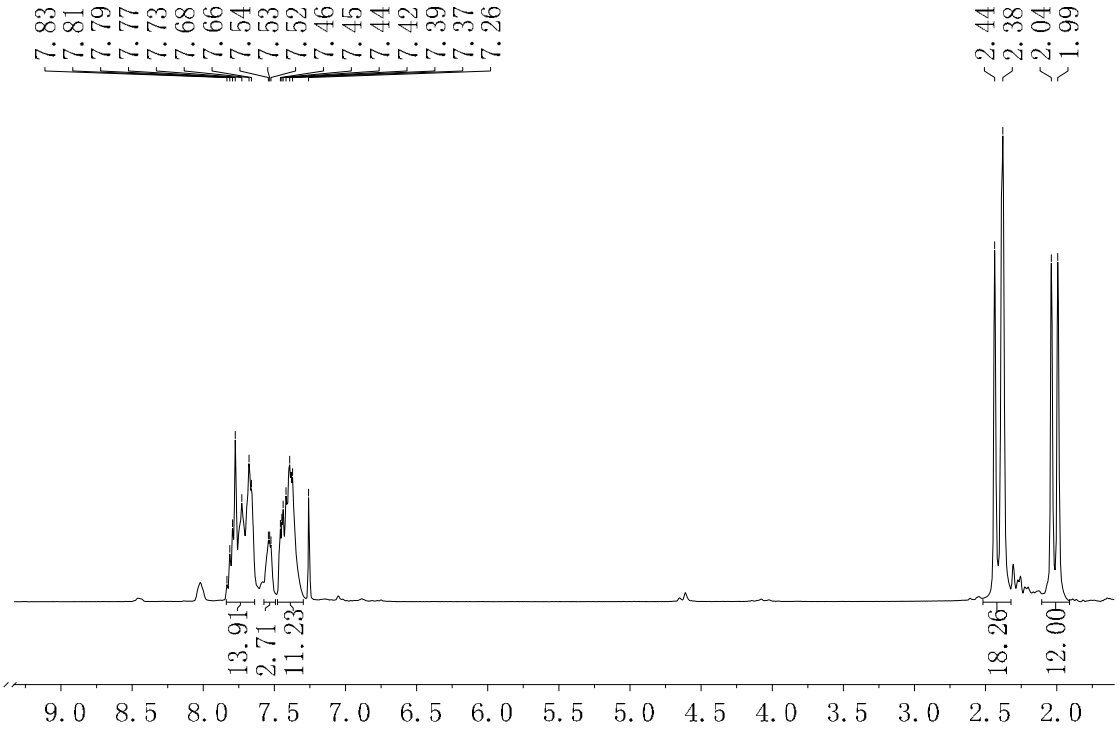

^{13}C NMR (62.5 MHz, $CDCl_3$)

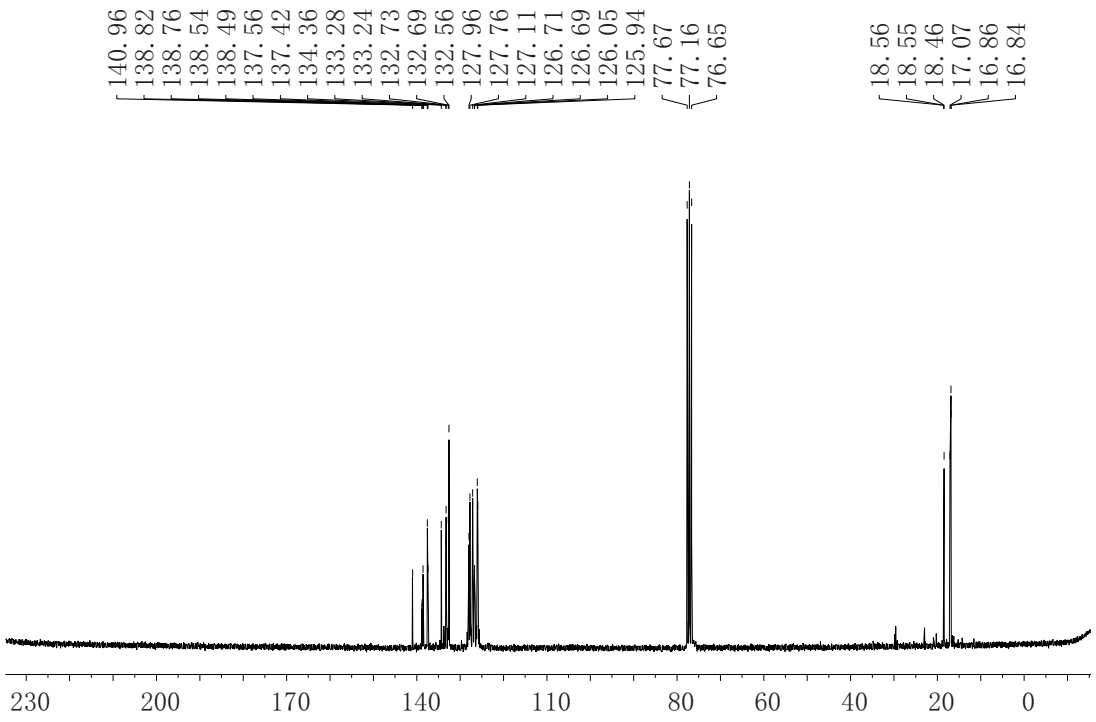

IR (ATR) *v* (cm^{-1})

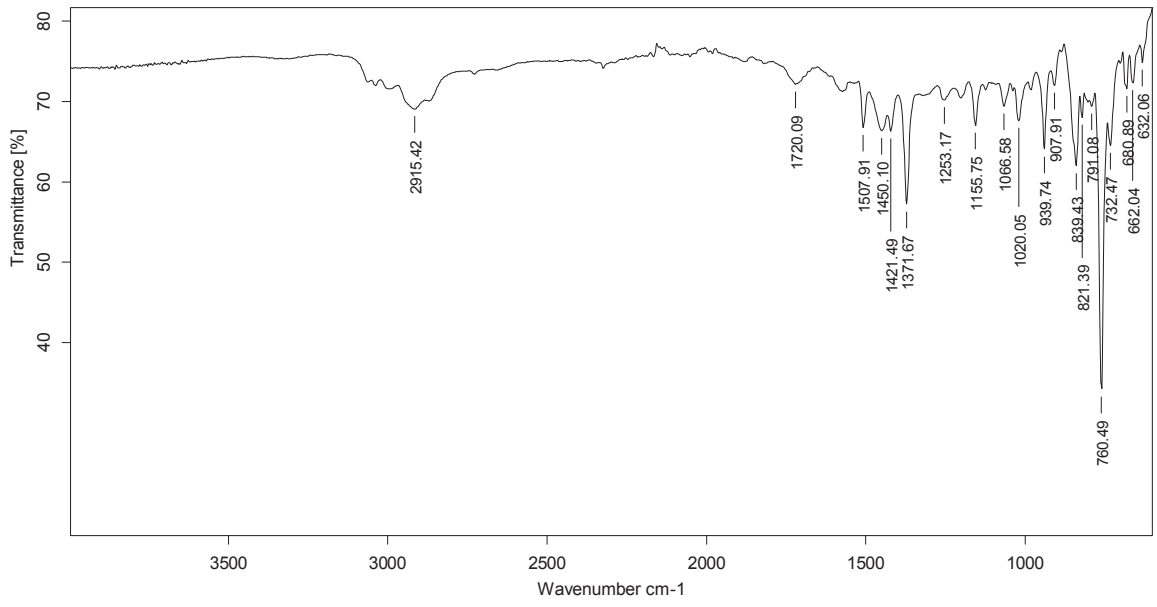

MALDI-TOF spectrum

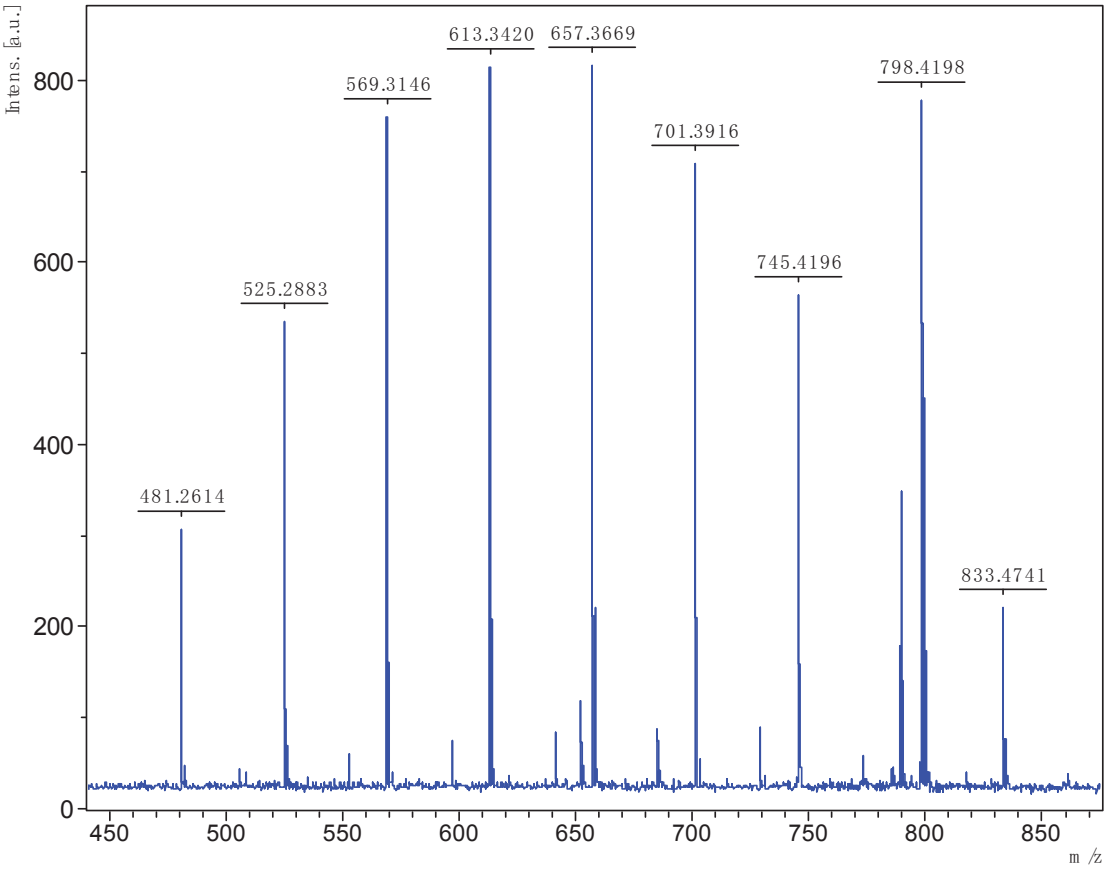

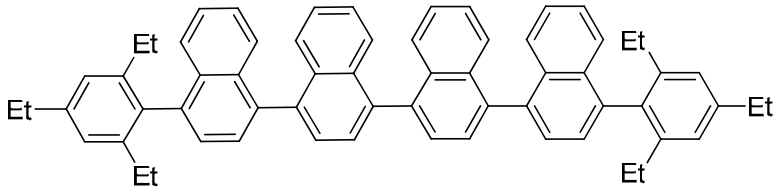

, **7c**

^{1}H-NMR (360 MHz, $CDCl_3$)

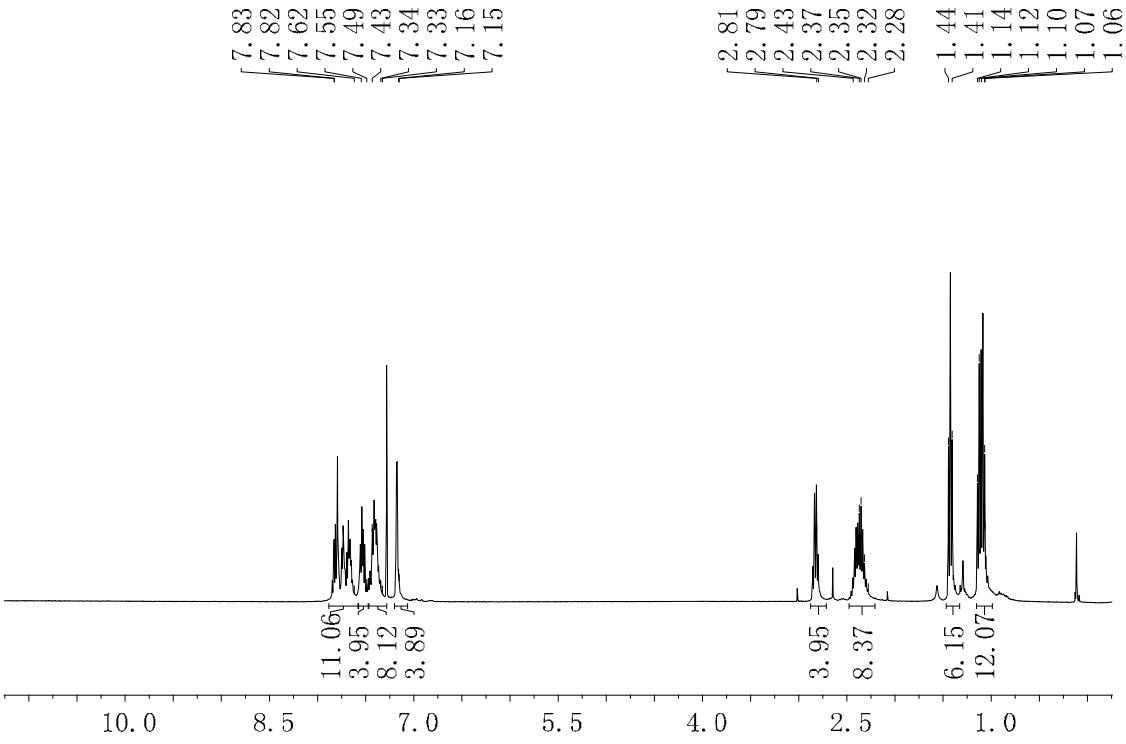

^{13}C NMR (62.5 MHz, $CDCl_3$)

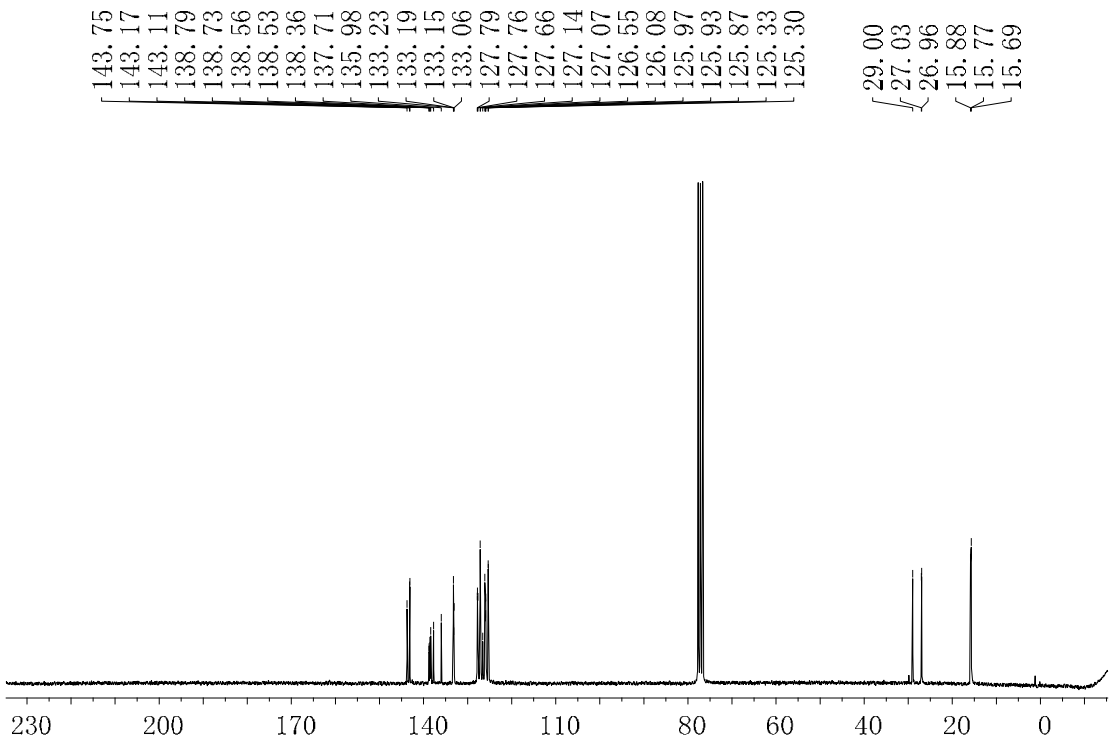

IR (ATR) *v* (cm^{-1})

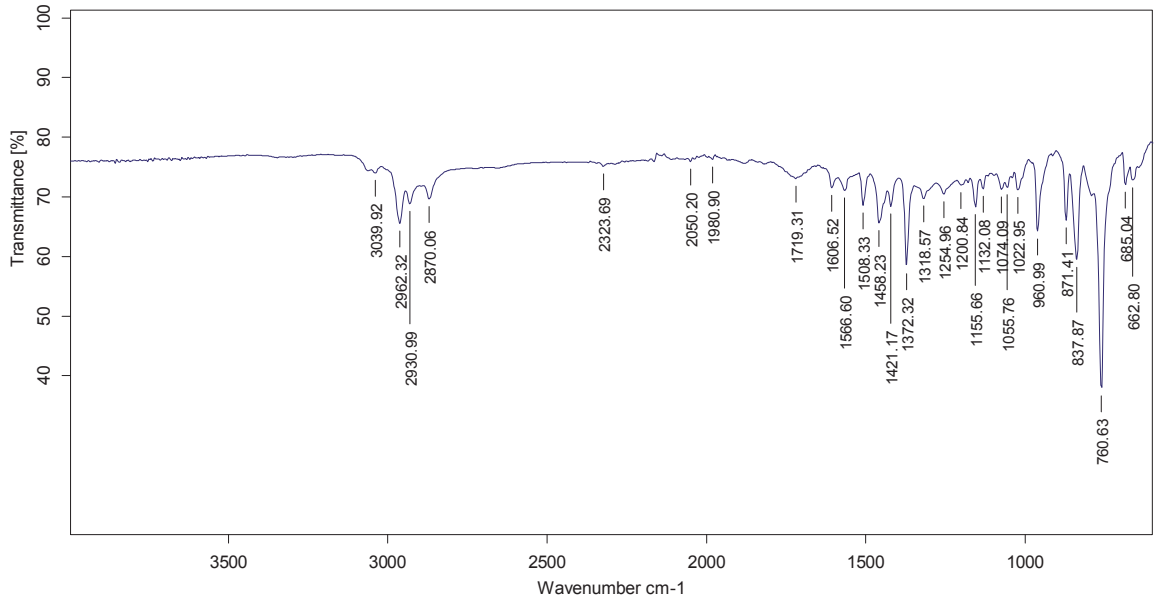

MALDI-TOF spectrum

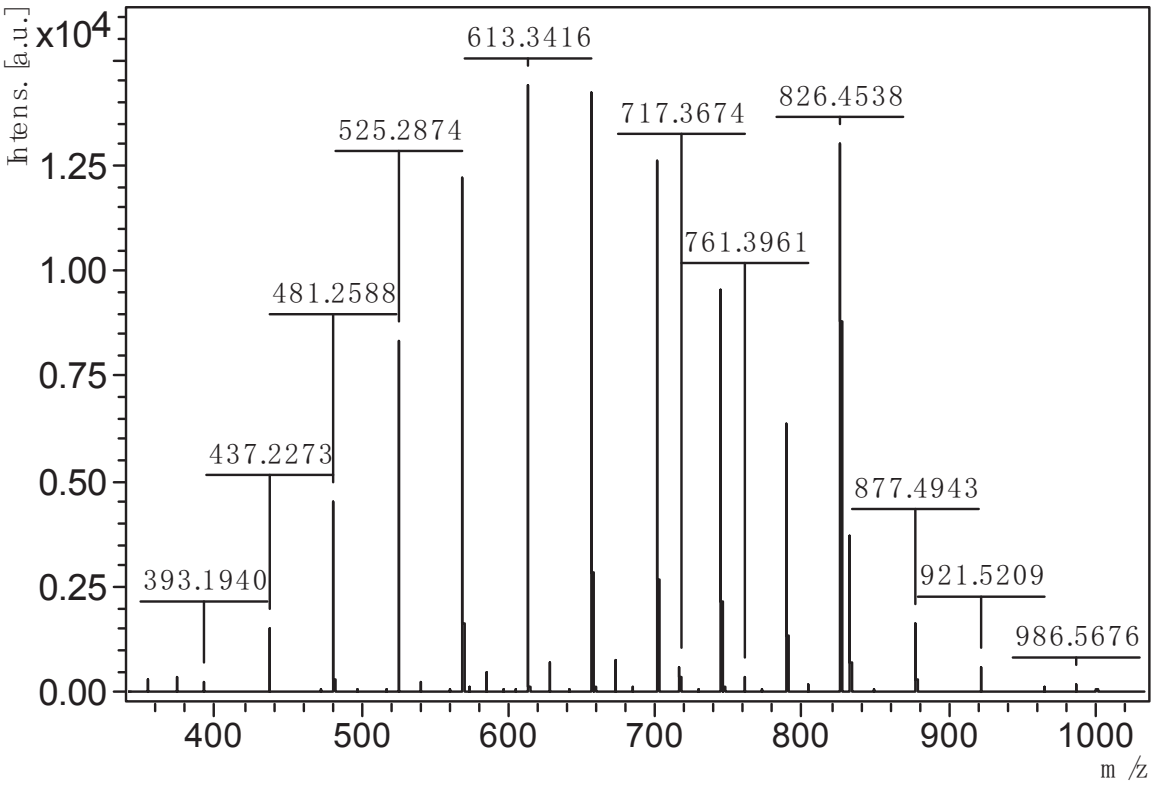

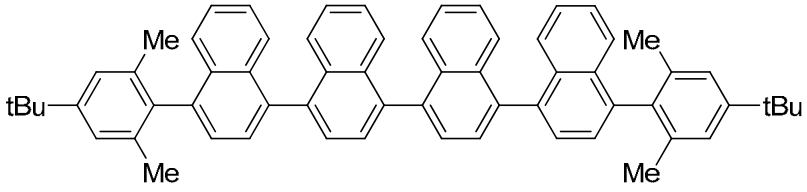

, **7d**

^{1}H-NMR (360 MHz, $CDCl_3$)

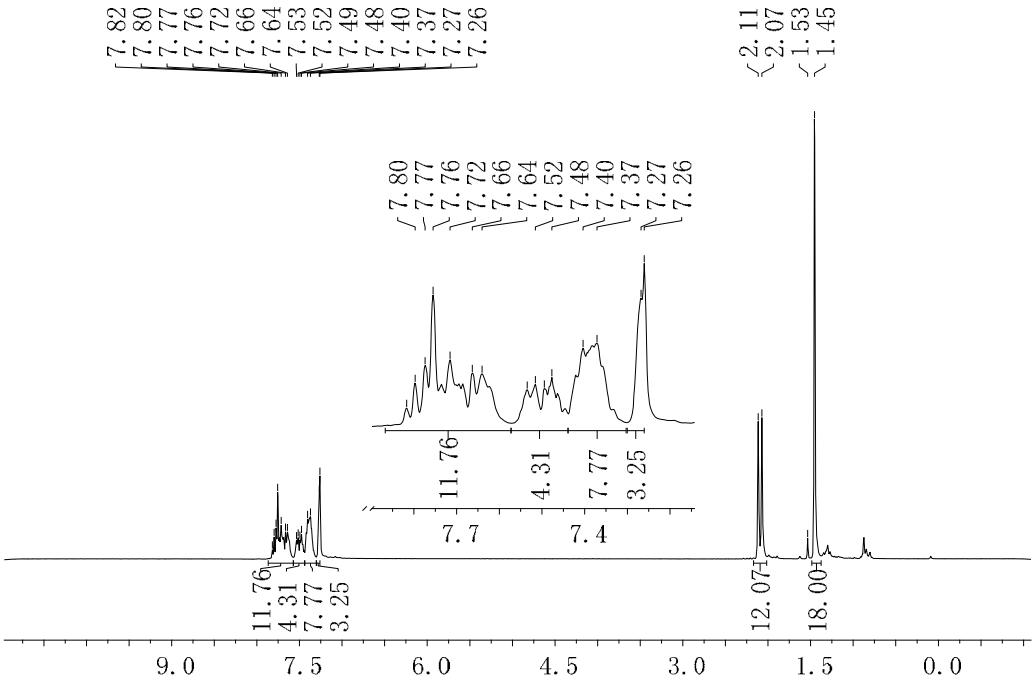

^{13}C-NMR (90MHz, $CDCl_3$)

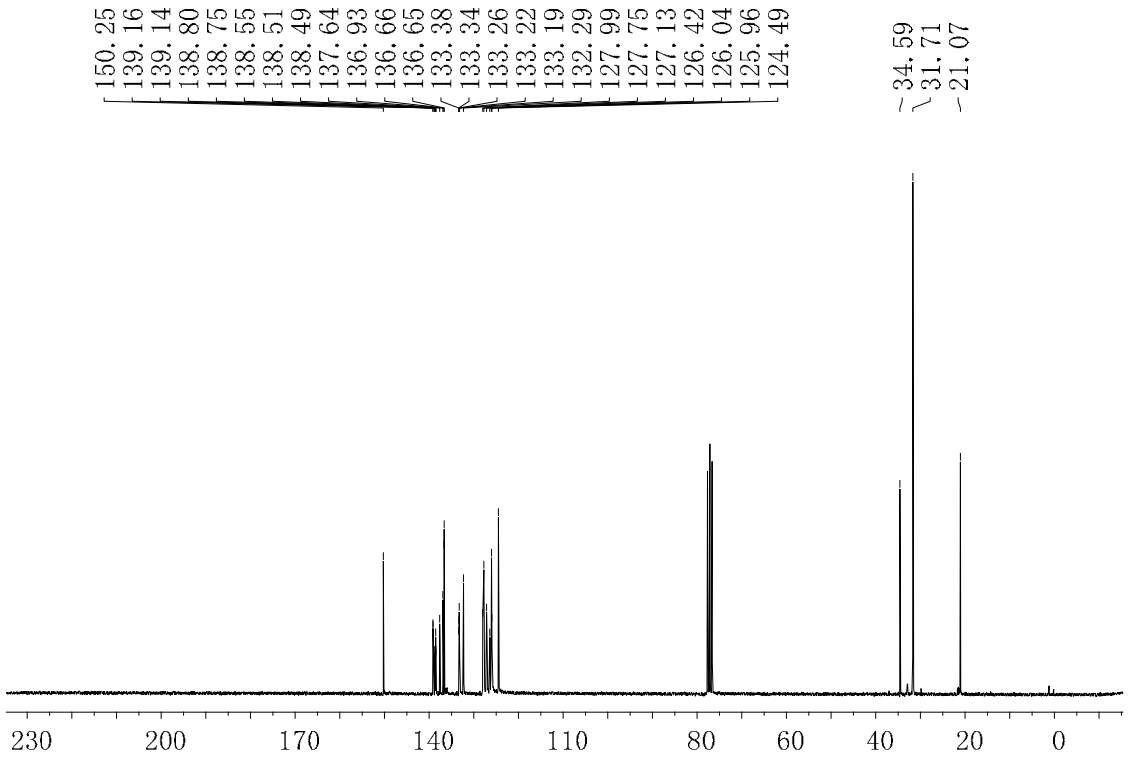

IR (ATR) ν (cm^{-1})

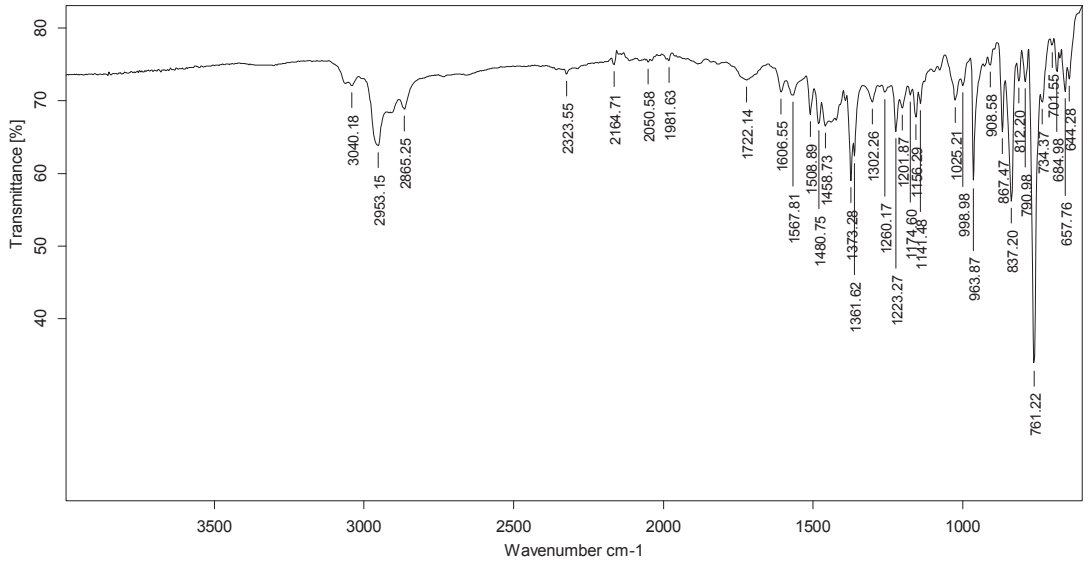

MALDI-TOF spectrum

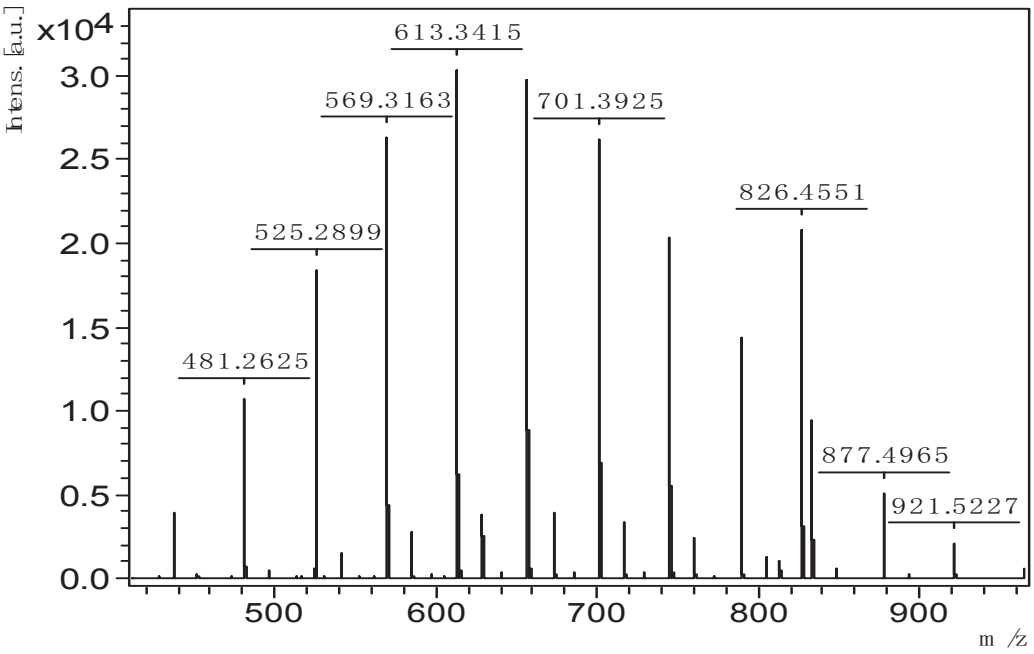

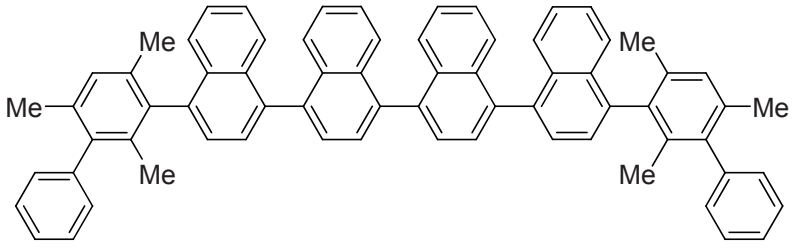

, **7e**

^{1}H NMR (360 MHz, $CDCl_3$), 4e

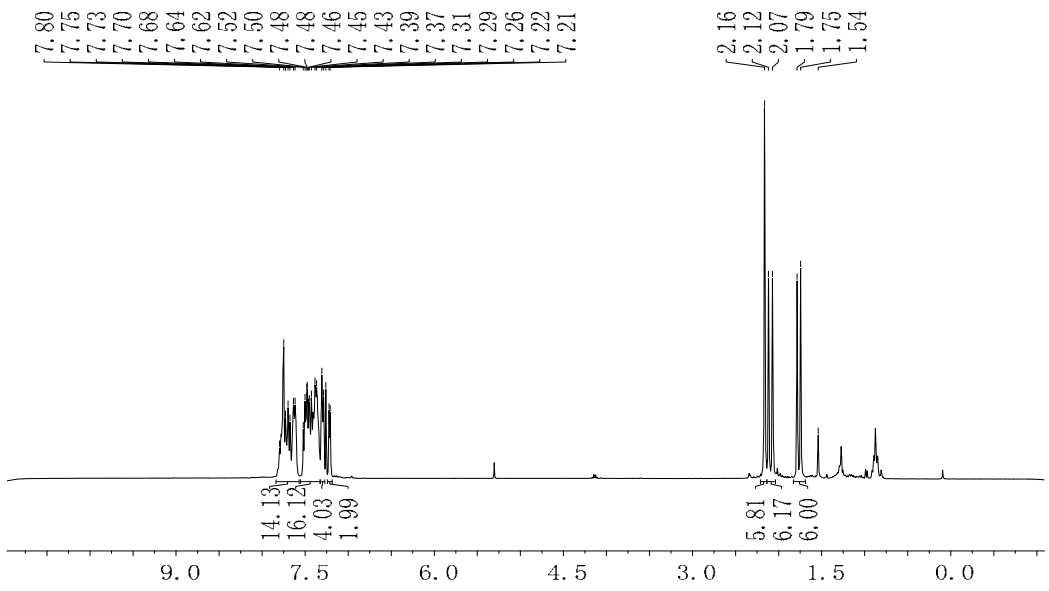

^{13}C NMR (90 MHz, $CDCl_3$)

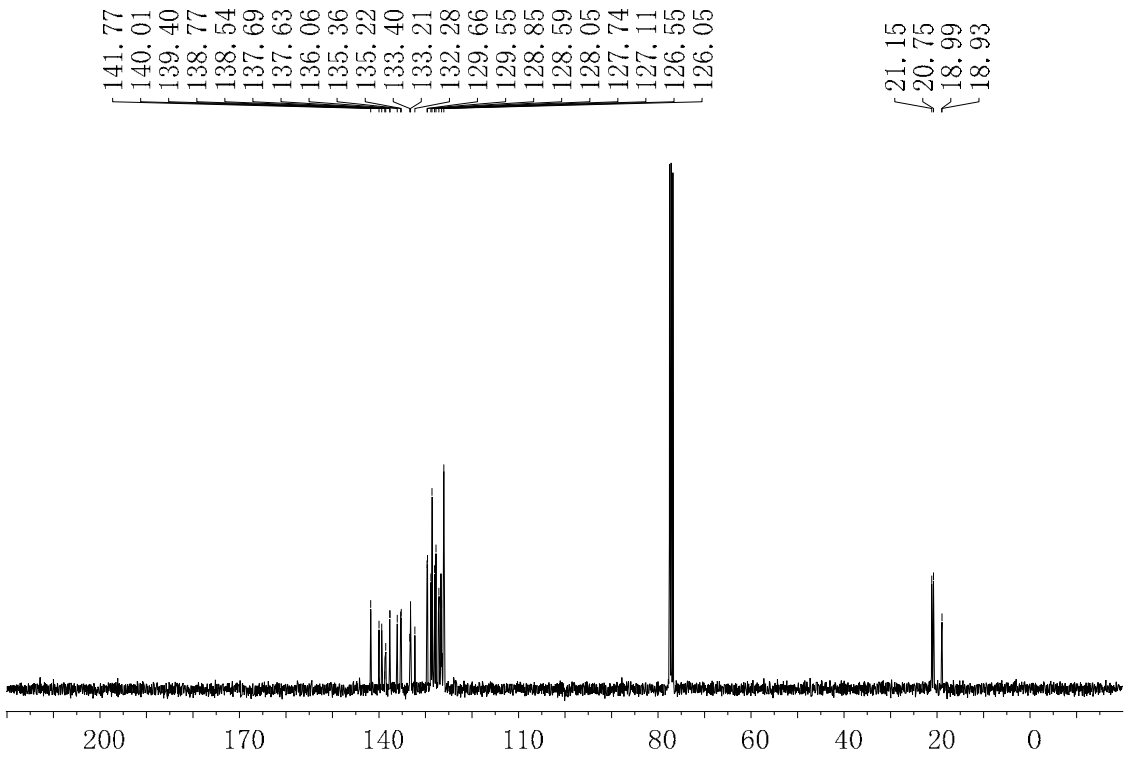

IR (ATR) *v* (cm^{-1})

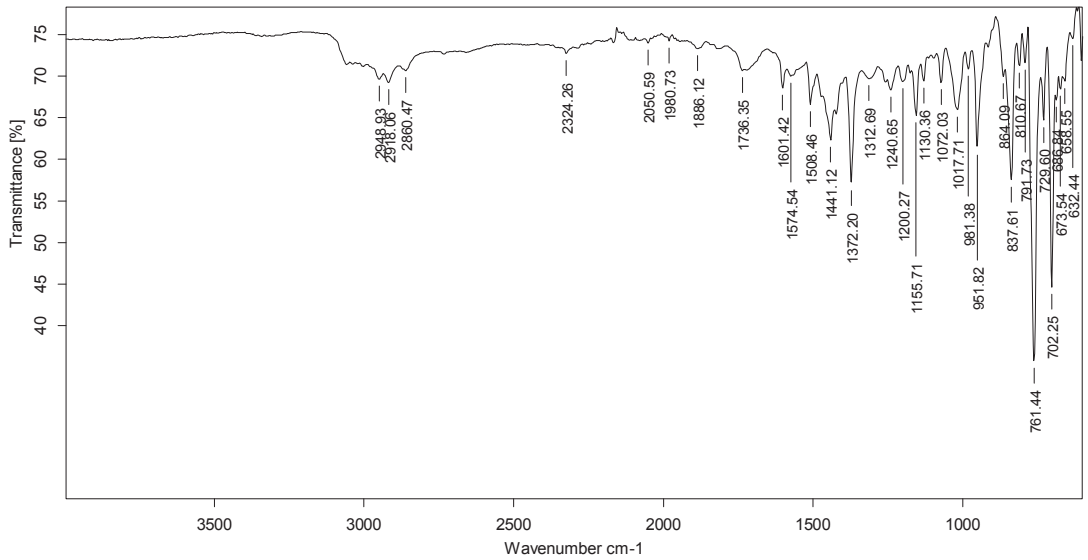

MALDI-TOF spectrum

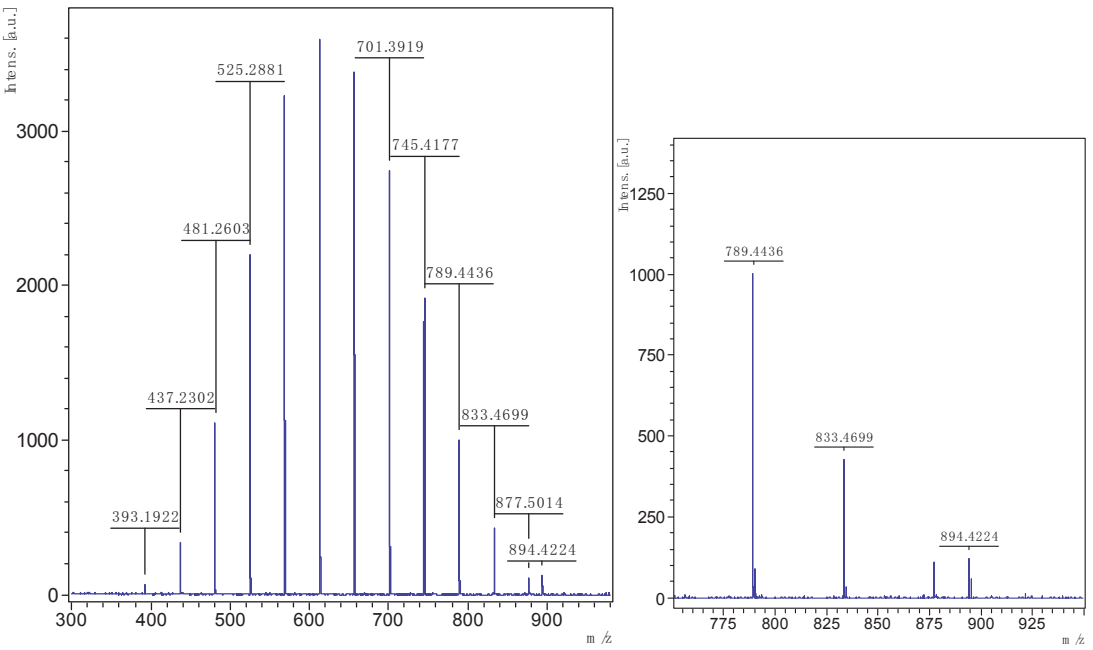

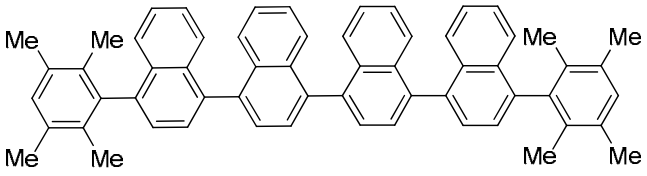

, **7f**

^{1}H-NMR (360 MHz, $CDCl_3$)

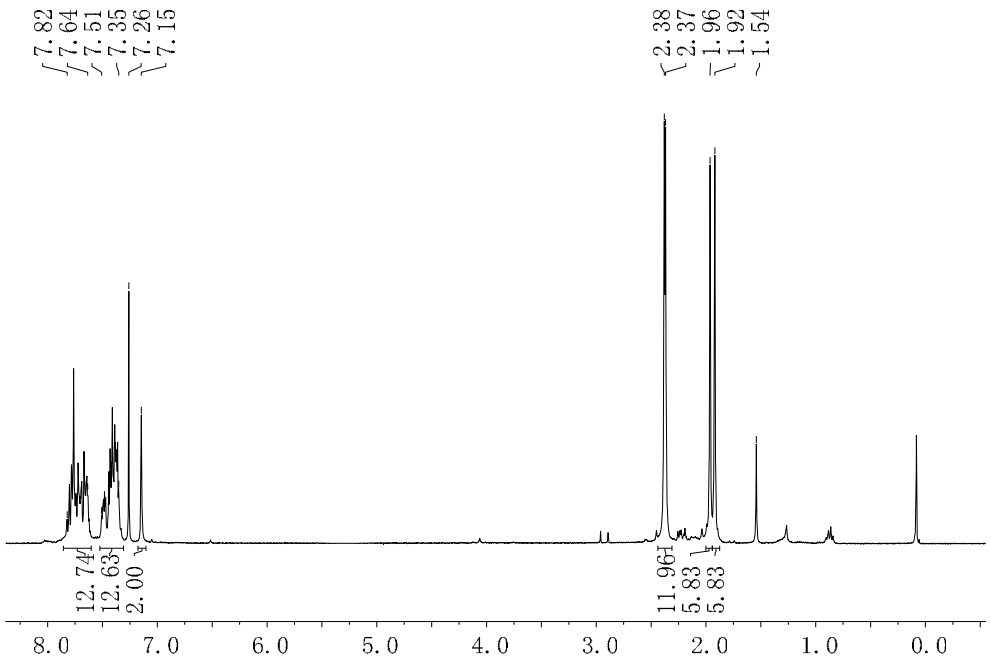

^{13}C NMR (90 MHz, $CDCl_3$)

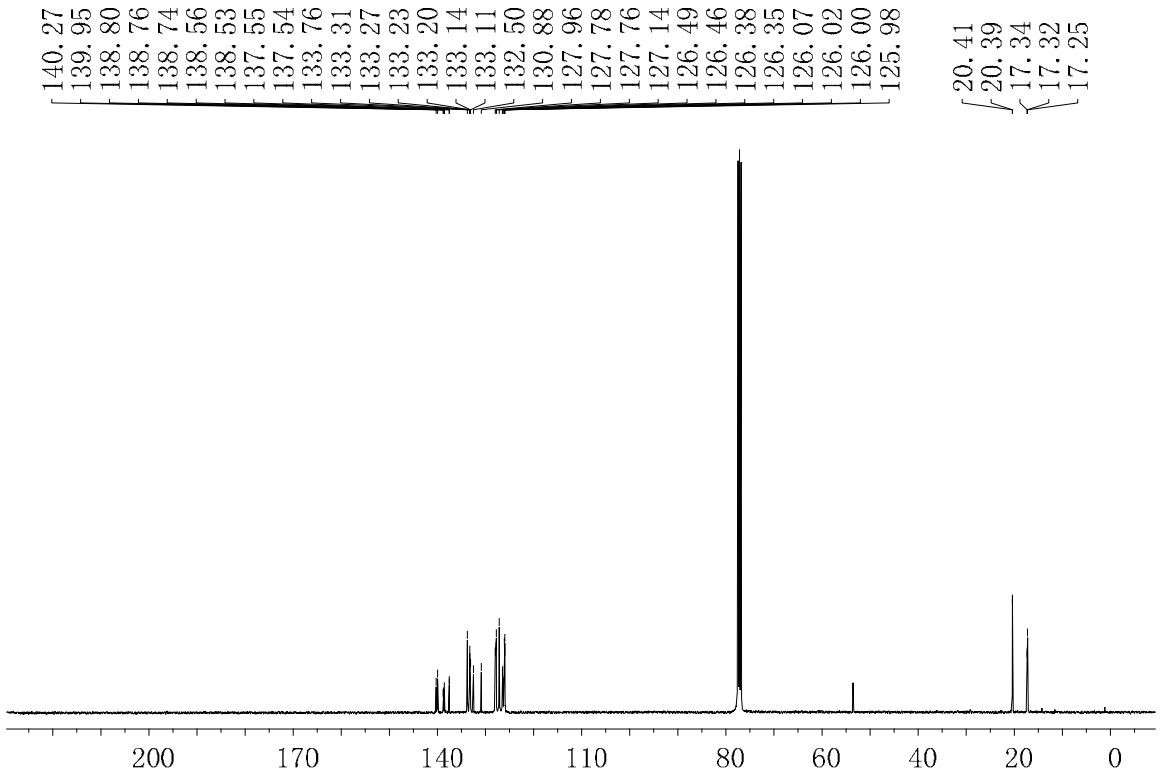

IR (ATR) *v* (cm^{-1})

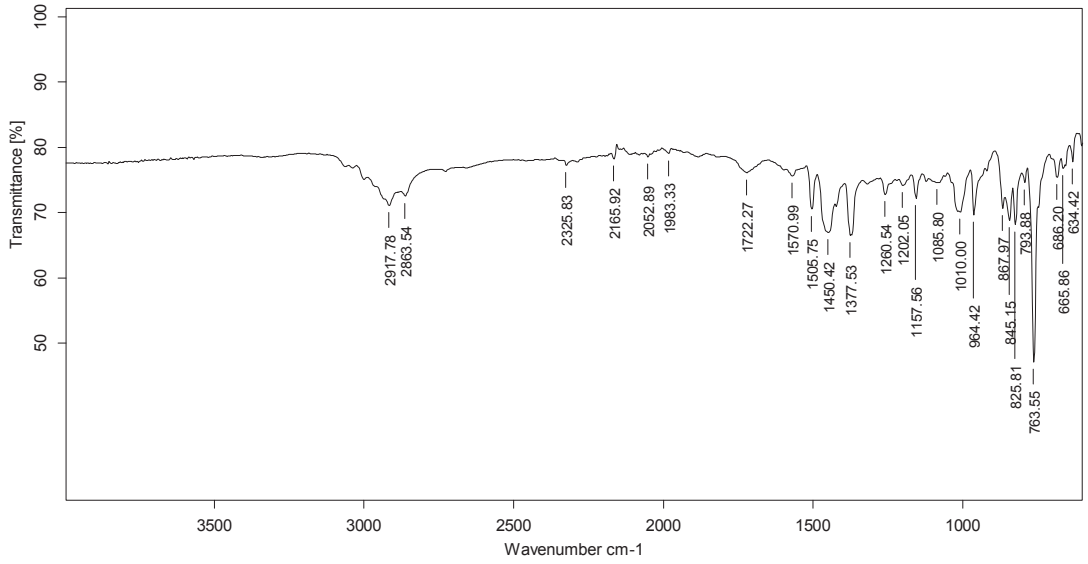

MALDI-TOF spectrum

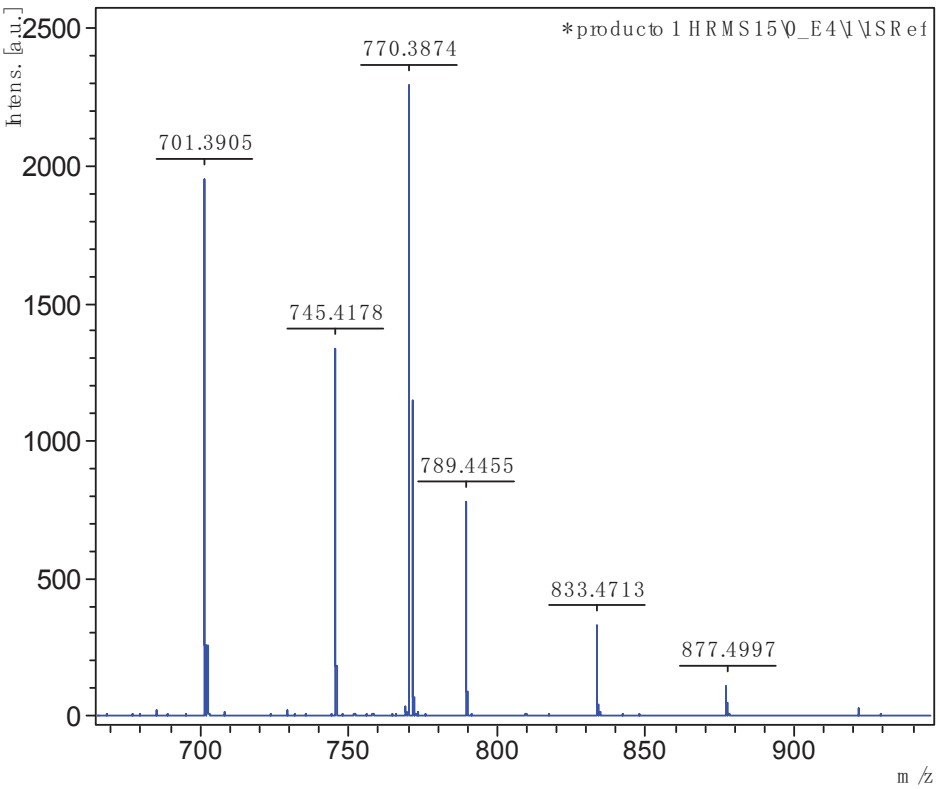

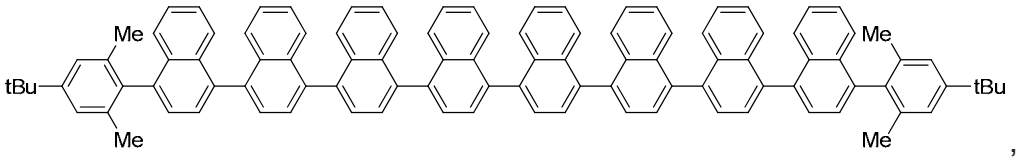

, 8d

MALDI-TOF spectrum

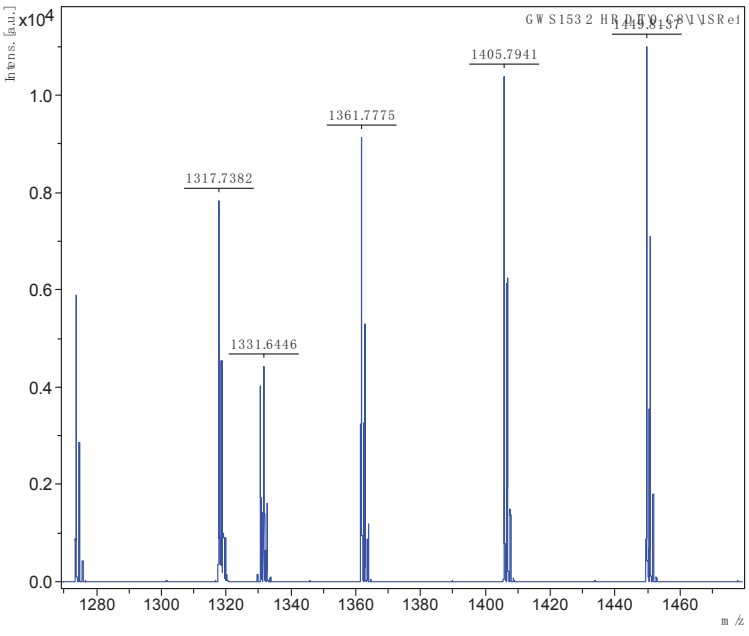

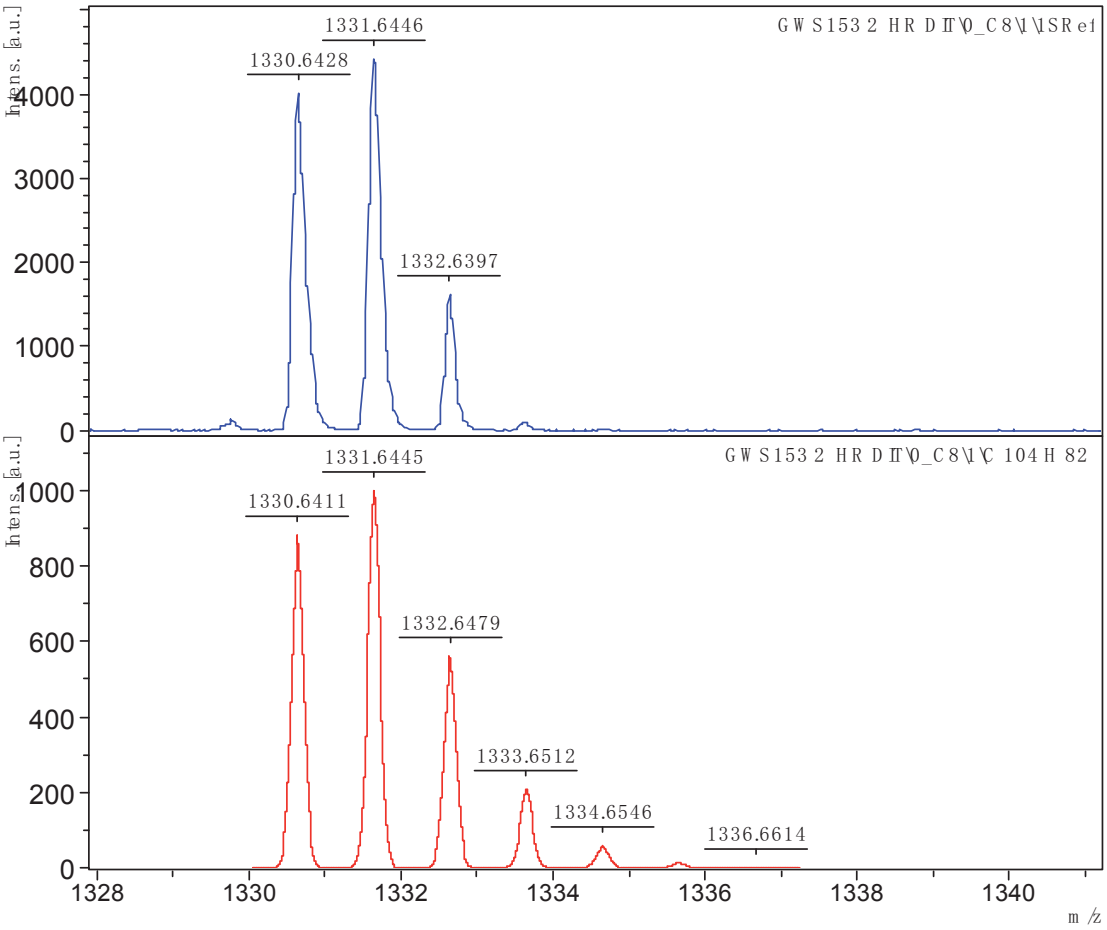
Intens. [a.u.]
1331.6446
1330.6428
1332.6397
4000
3000
2000
1000
0
Intens. [a.u.]
1331.6445
1330.6411
1332.6479
1333.6512
1334.6546
1336.6614
1000
800
600
400
200
0
1328
1330
1332
1334
1336
1338
1340
m/z

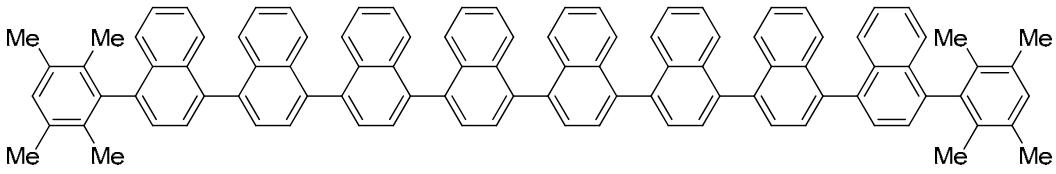

8f

^{1}H NMR (360 MHz, $CDCl_3$)

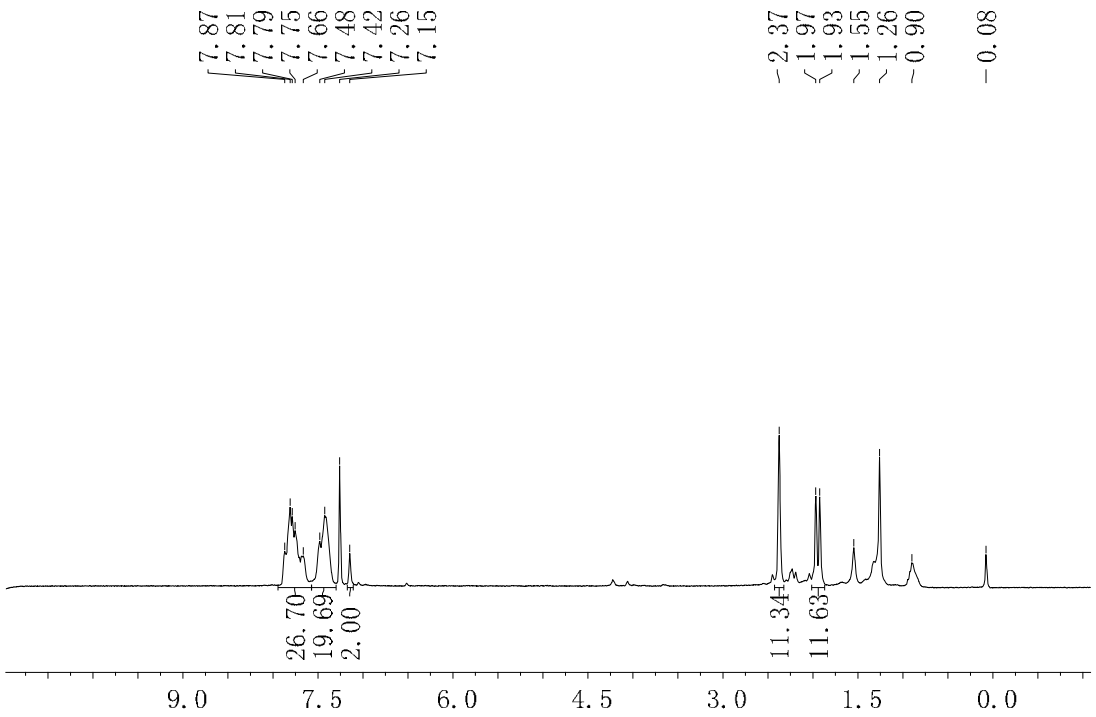

MALDI-TOF spectrum

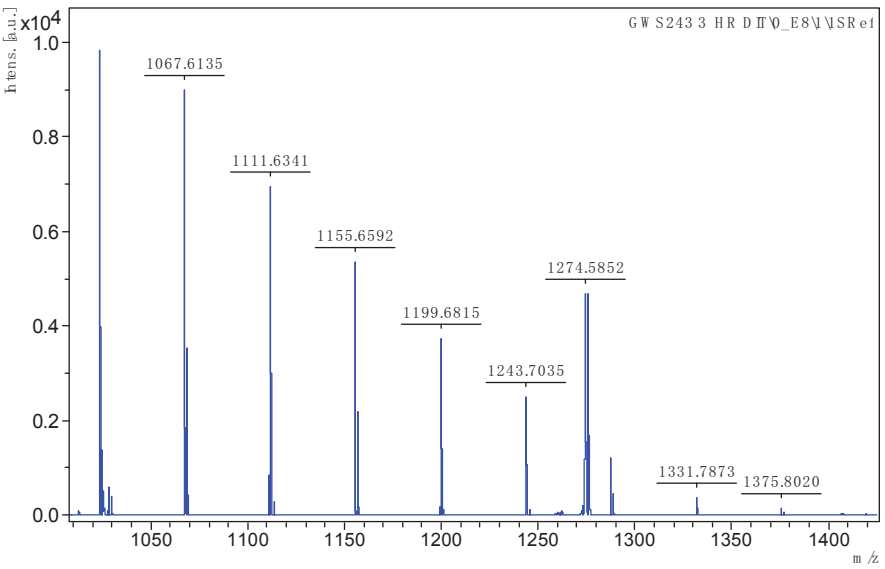

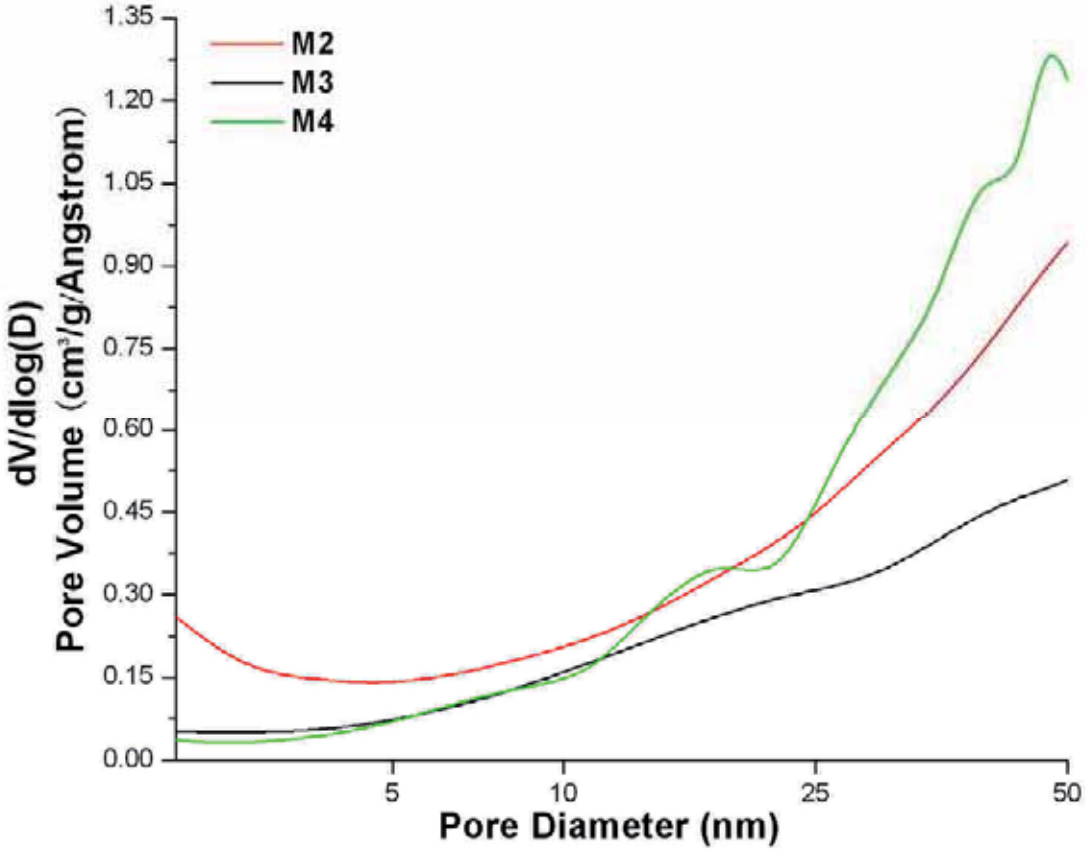

Figure. S1 Pore size distribution of **M2**-**M4**.

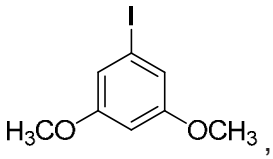

, **9**

^{1}H NMR (250 MHz, $CDCl_3$)

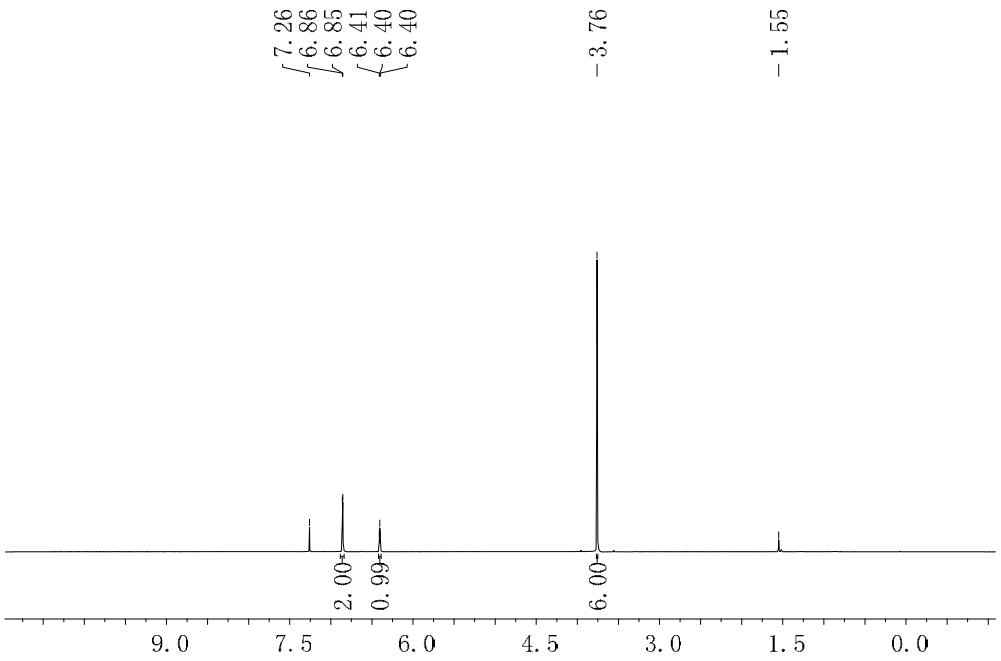

^{13}C NMR (90MHz, $CDCl_3$)

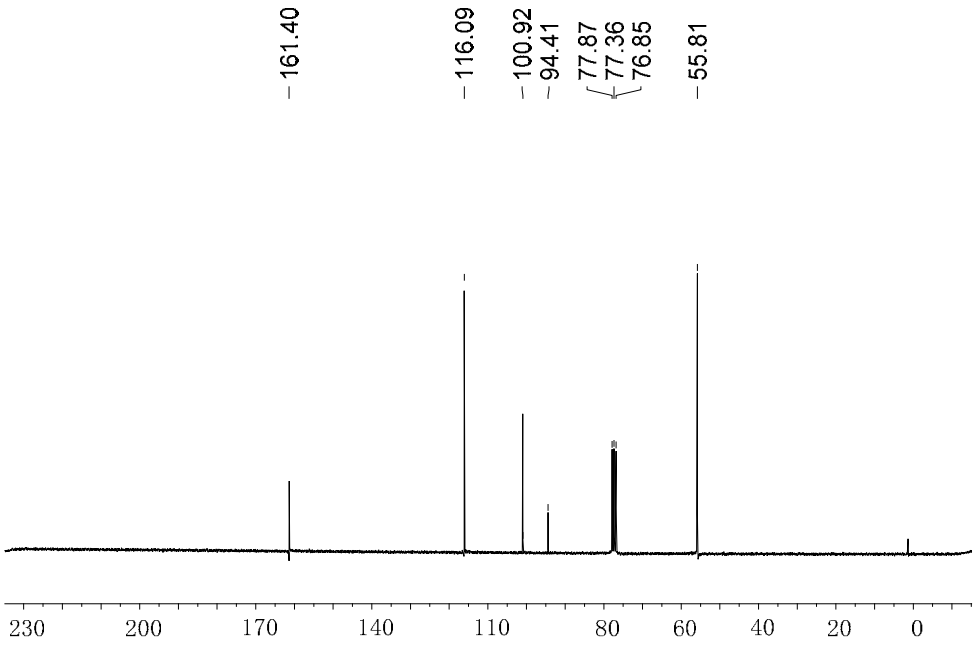

IR (ATR) *v* (cm^{-1})

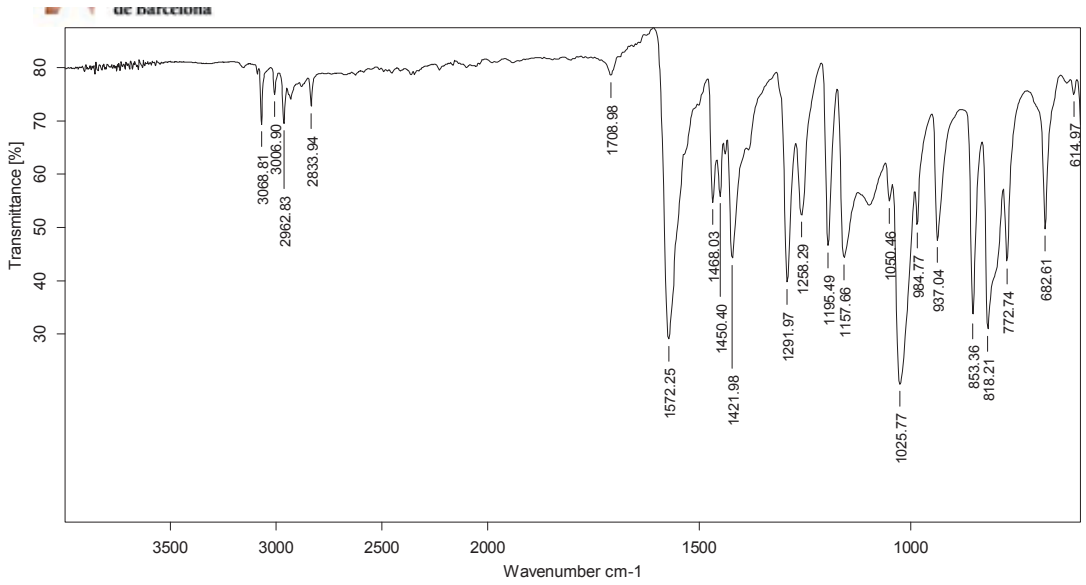

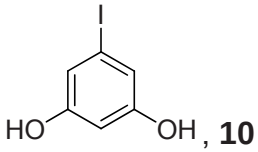

, **10**

^{1}H NMR(360 MHz, DMSO-d_6)

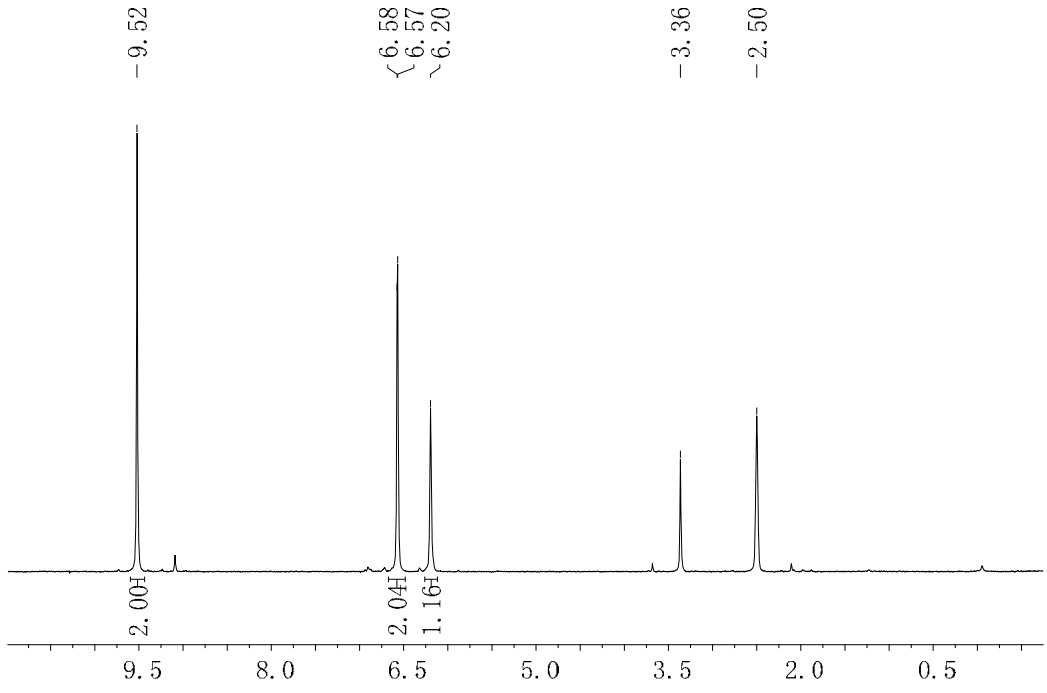

^{13}C NMR (90MHz, DMSO-d_6)

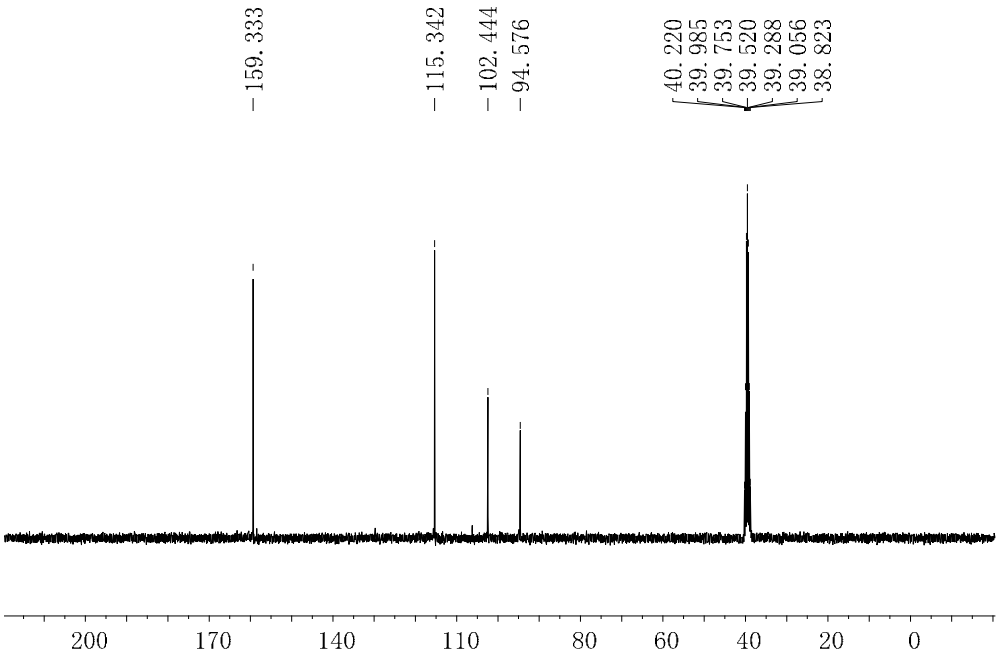

IR (ATR) *v* (cm^{-1})

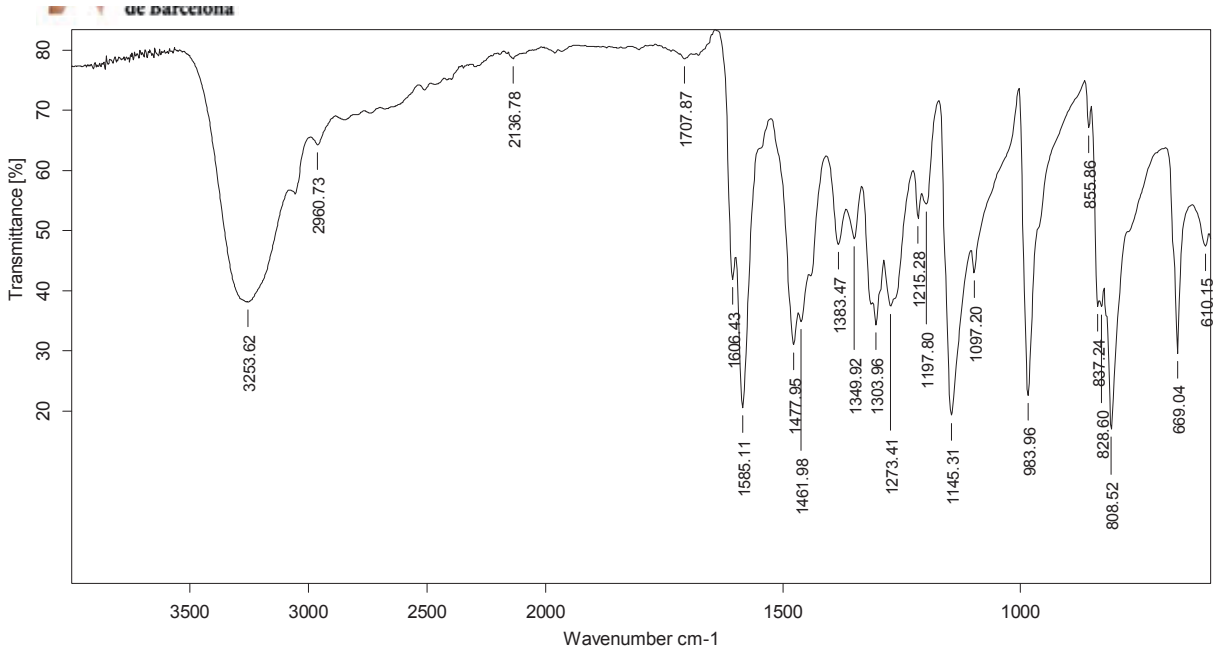

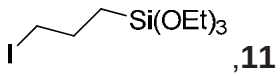

,11

^{1}H NMR (250 MHz, $CDCl_3$)

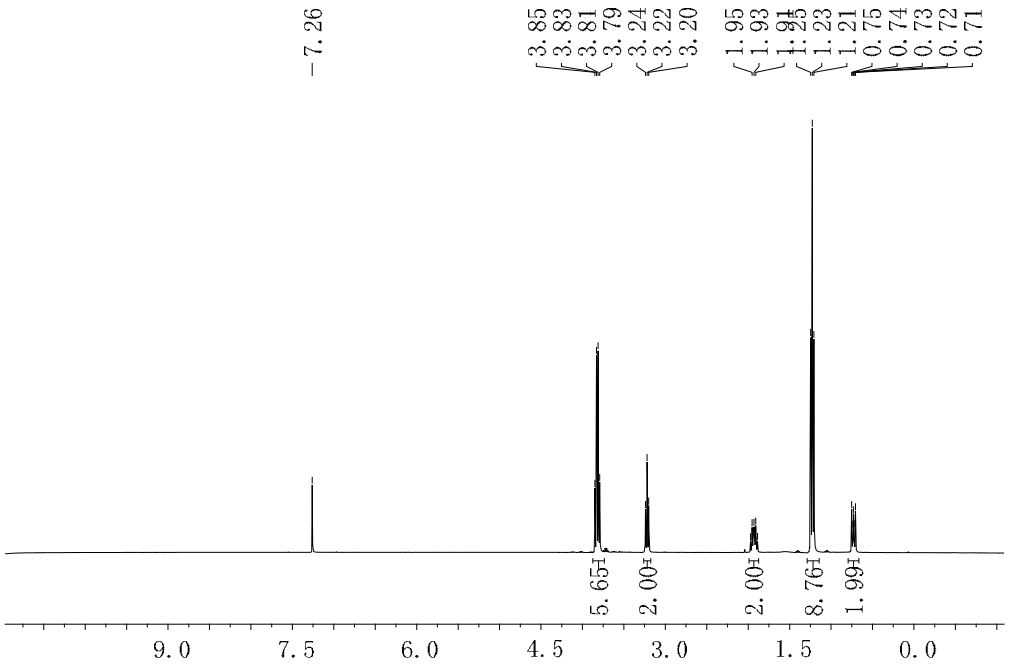

^{13}C NMR (100MHz, $CDCl_3$)

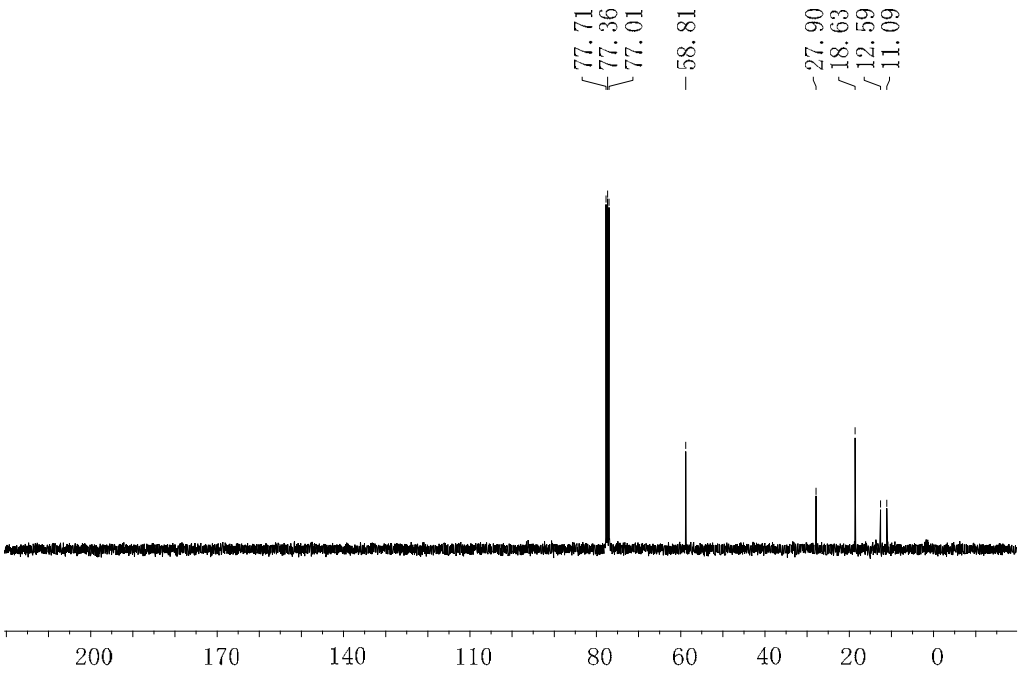

IR (ATR) ν (cm^{-1})

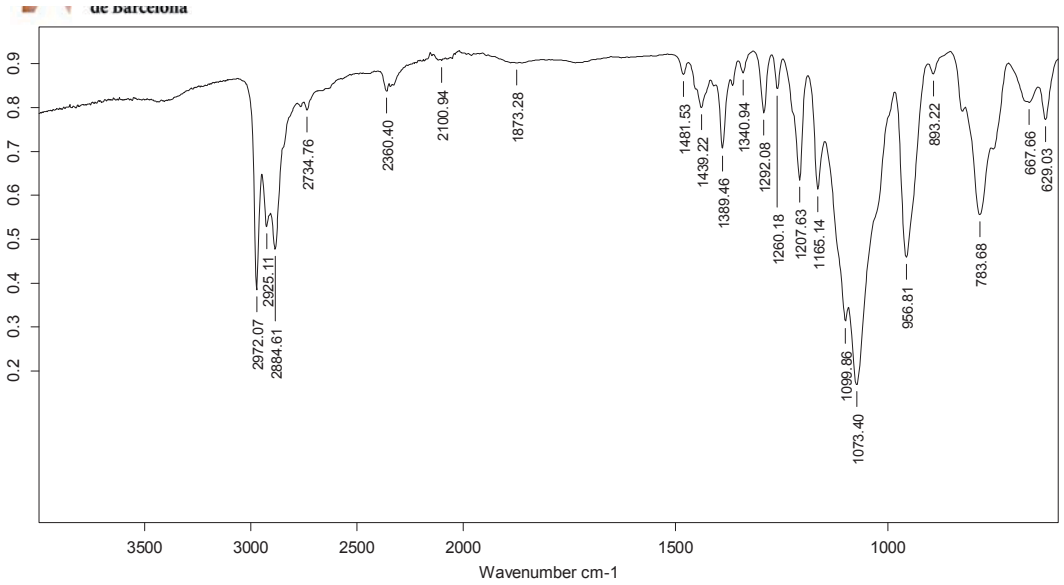

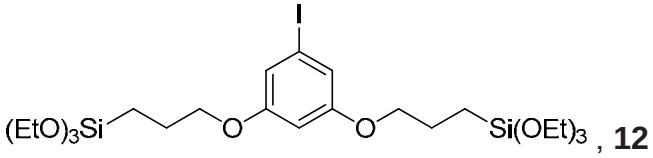

, **12**

^{1}H NMR (250 MHz, $CDCl_3$)

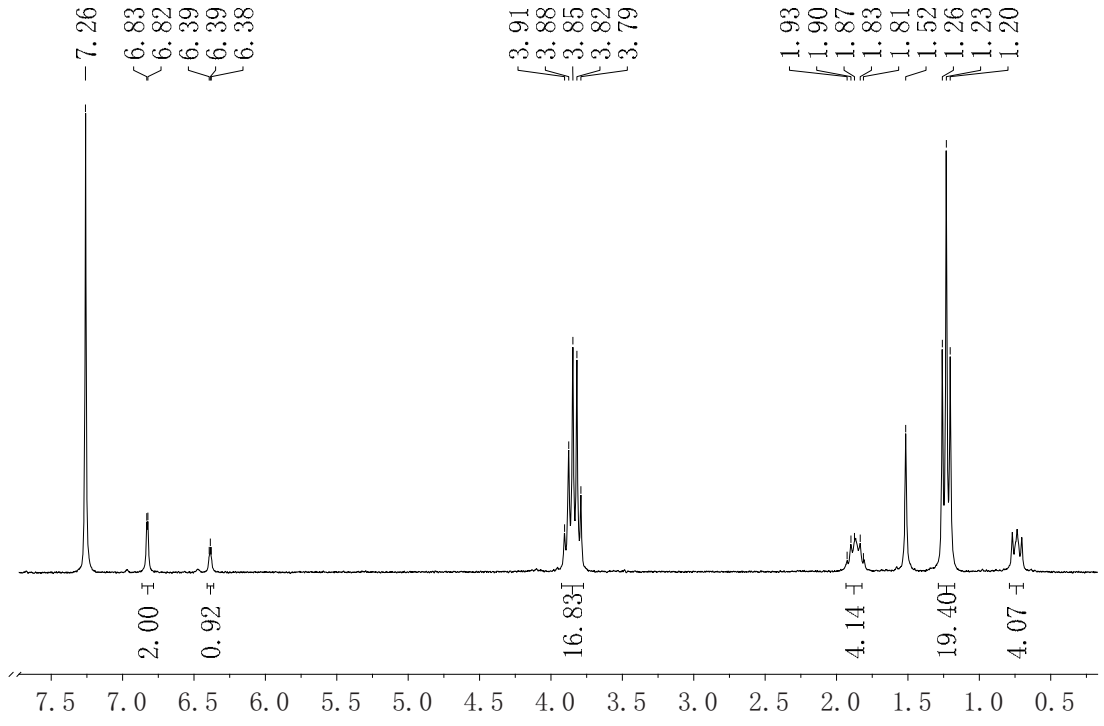

^{13}C NMR (62.5 MHz, $CDCl_3$)

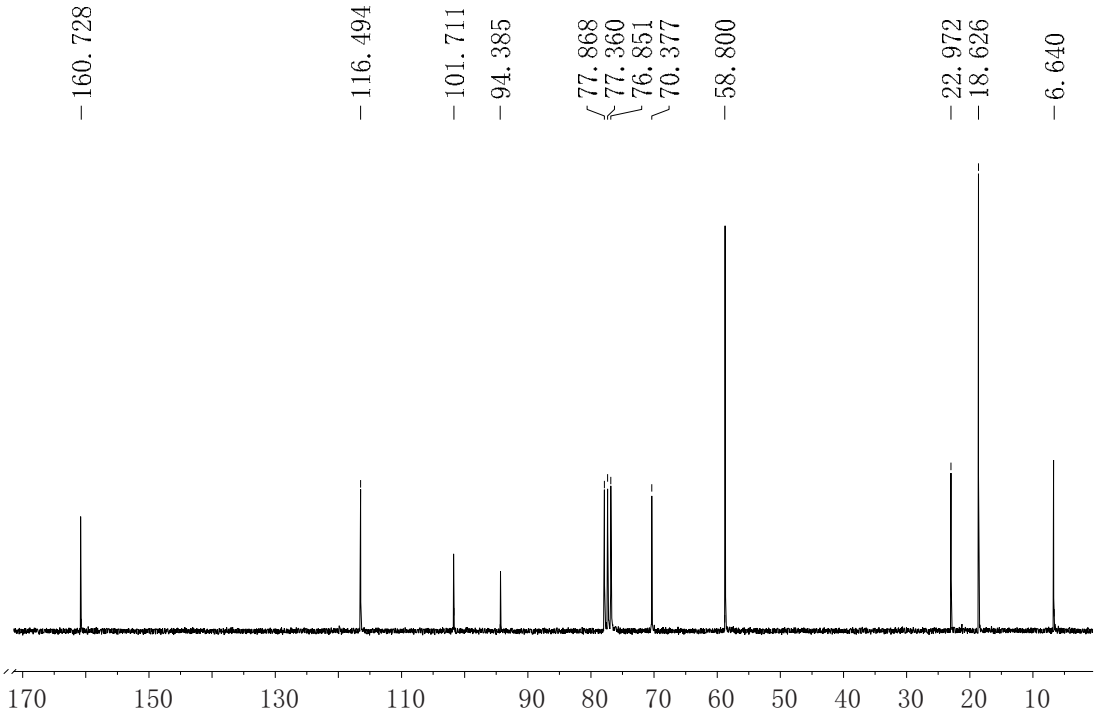

COSY ^{1}H-^{1}H

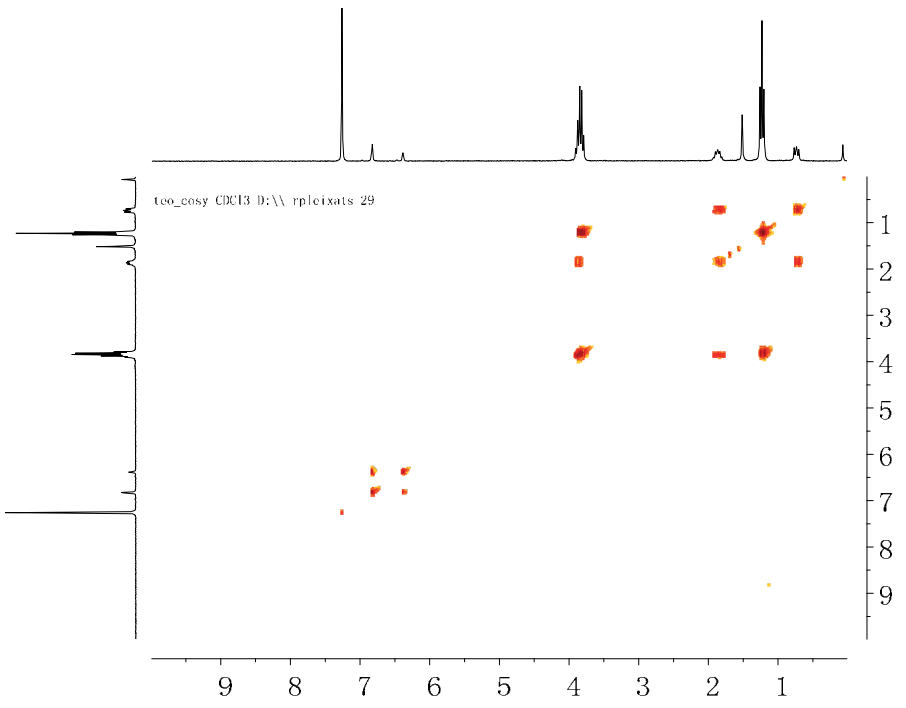

HSQCedited ^{1}H-^{13}C

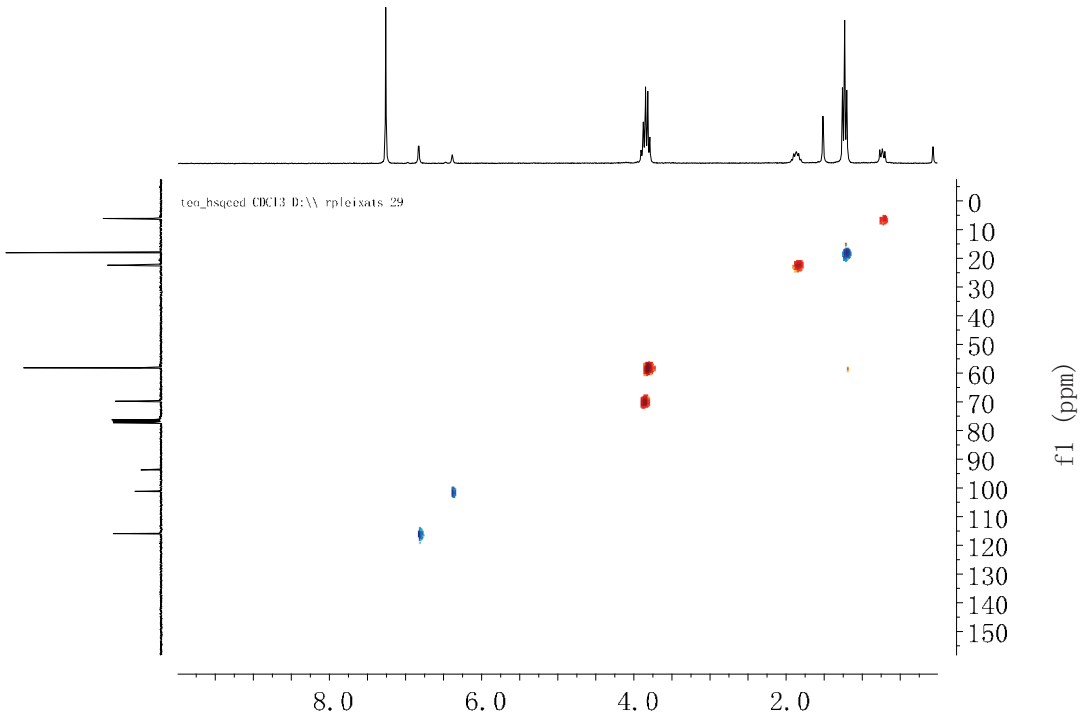

IR (ATR) *v* (cm^{-1})

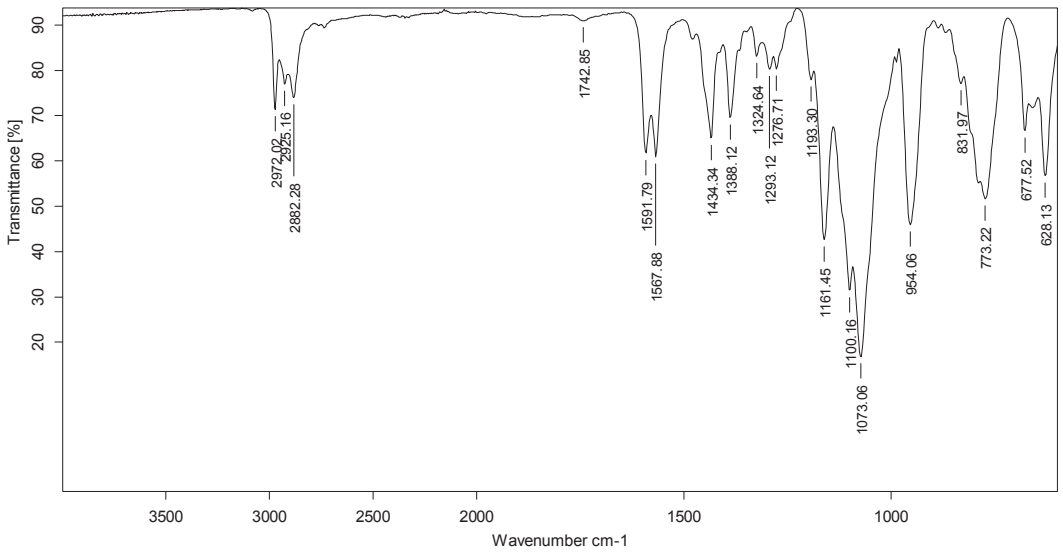

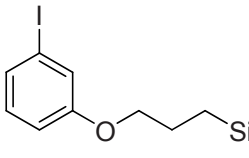

, **13**

^{1}H NMR (250 MHz, $CDCl_3$)

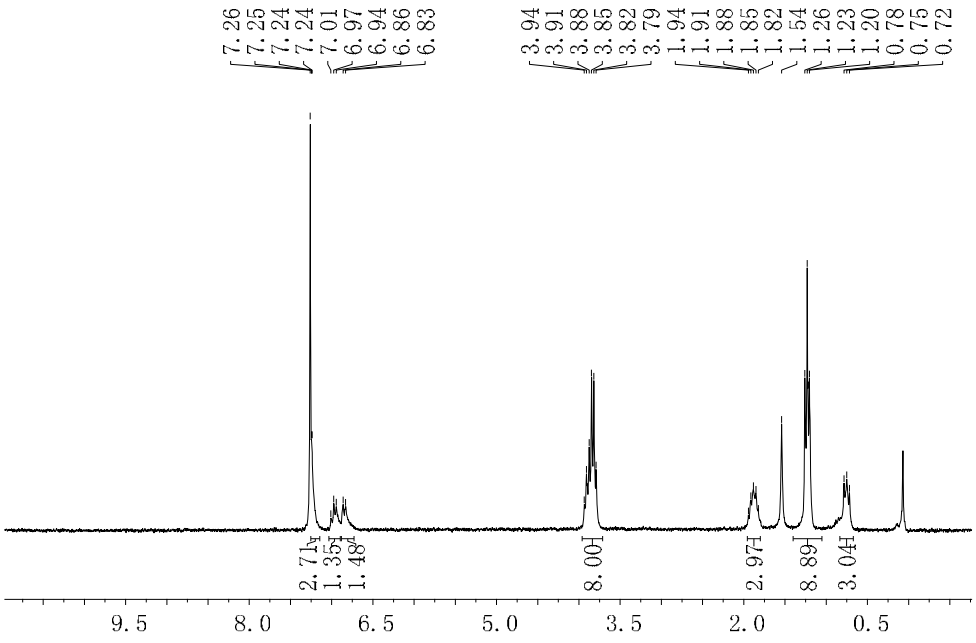

^{13}C NMR (62.5 MHz, $CDCl_3$)

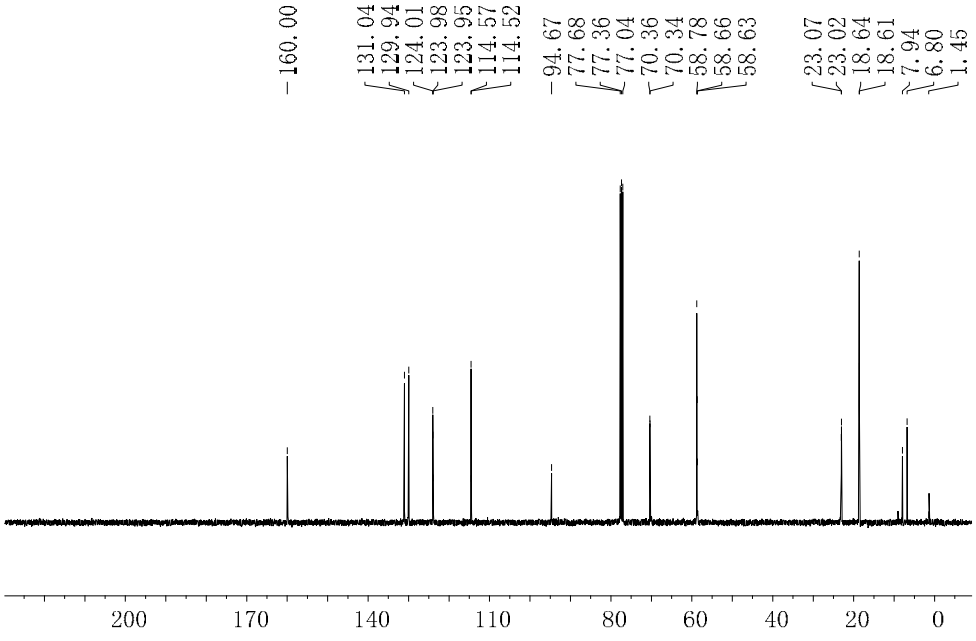

IR (ATR) *v* (cm^{-1})

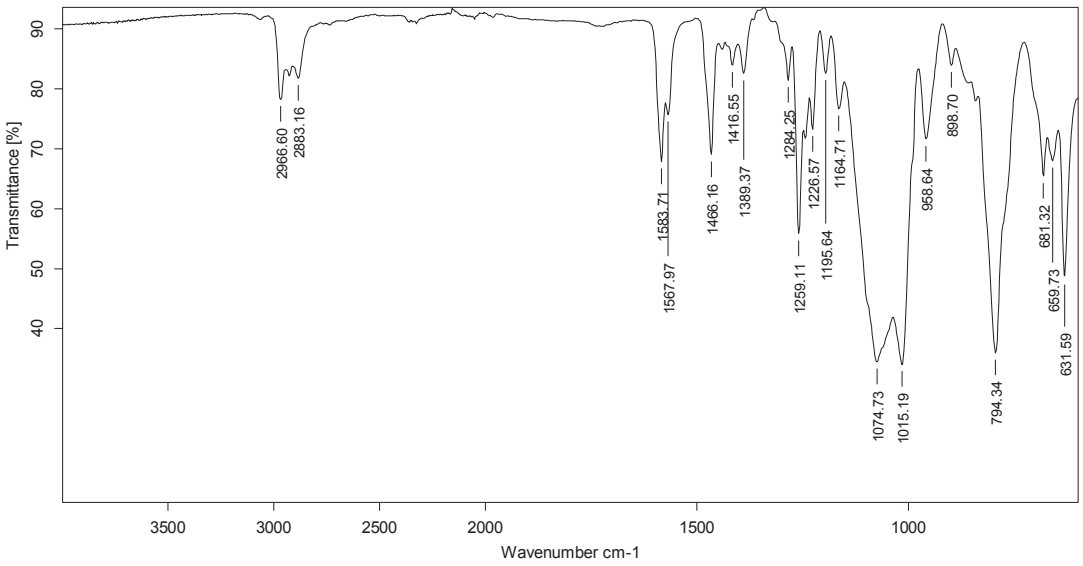

HSQCedited ^{1}H-^{13}C

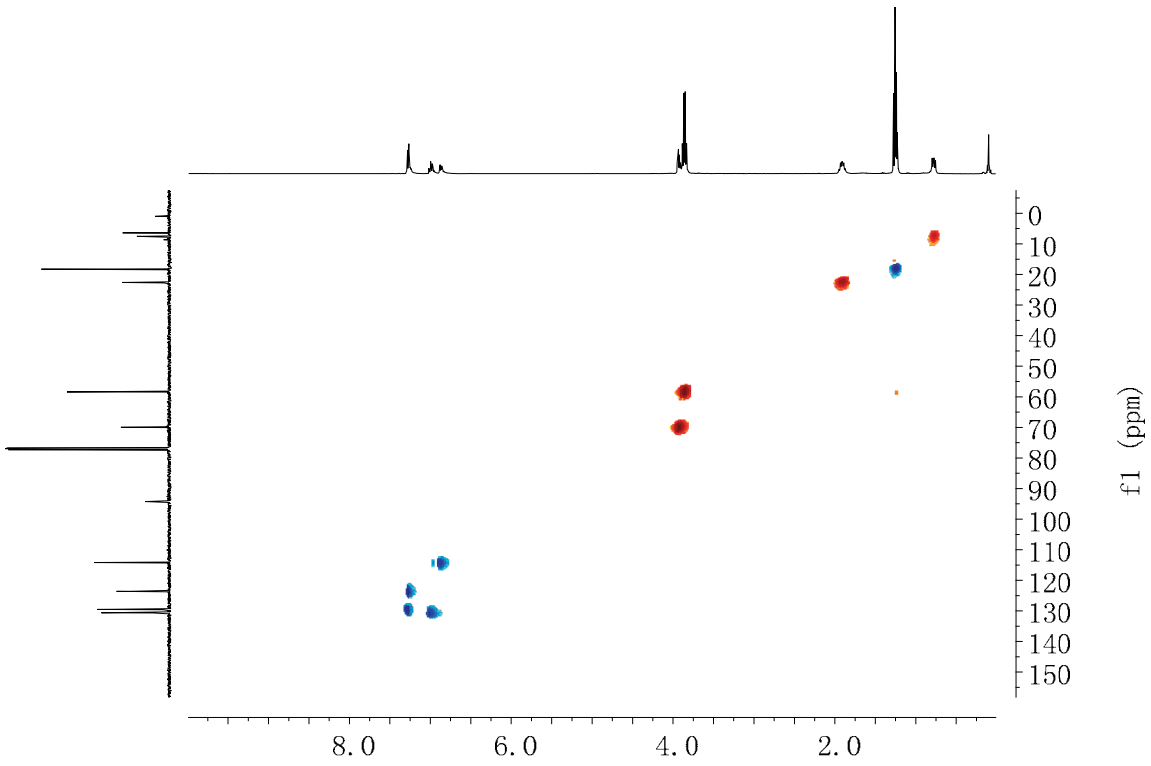

COSY ^{1}H-^{13}H

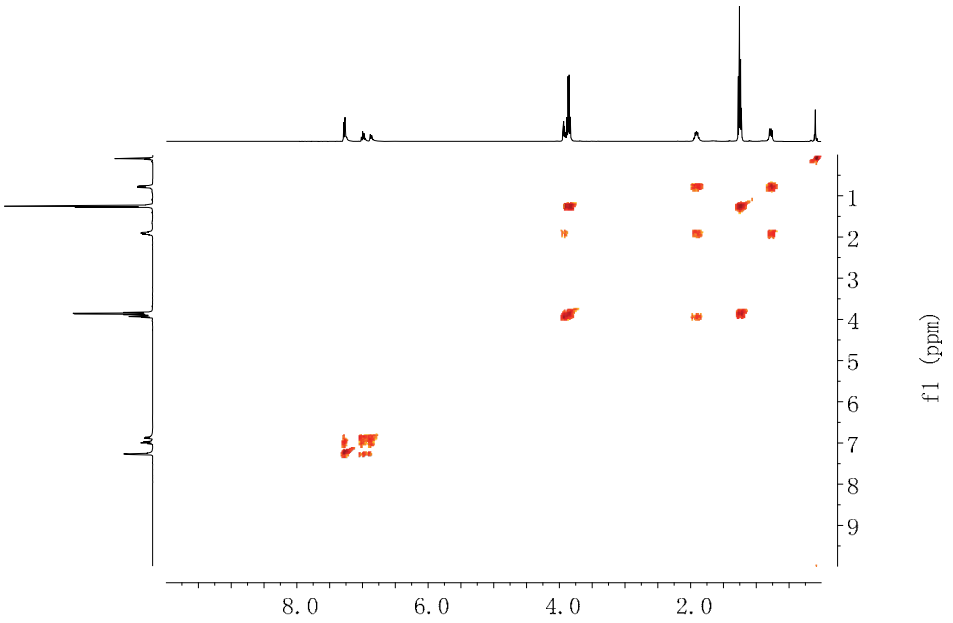

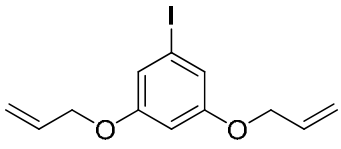

, **14**

^{1}H NMR (360 MHz, $CDCl_3$)

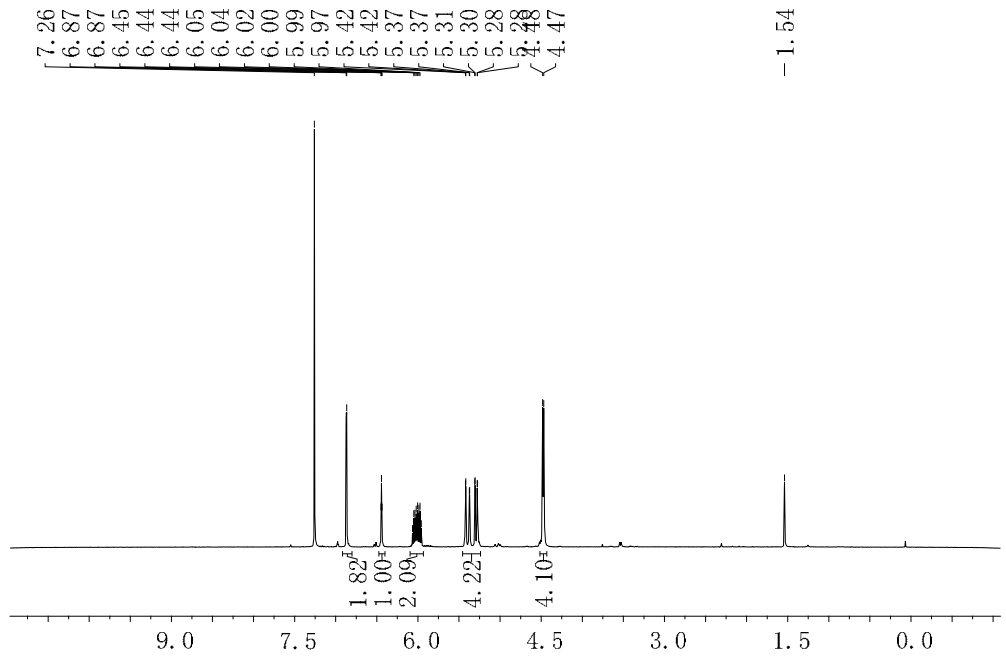

^{13}C NMR (360 MHz, $CDCl_3$)

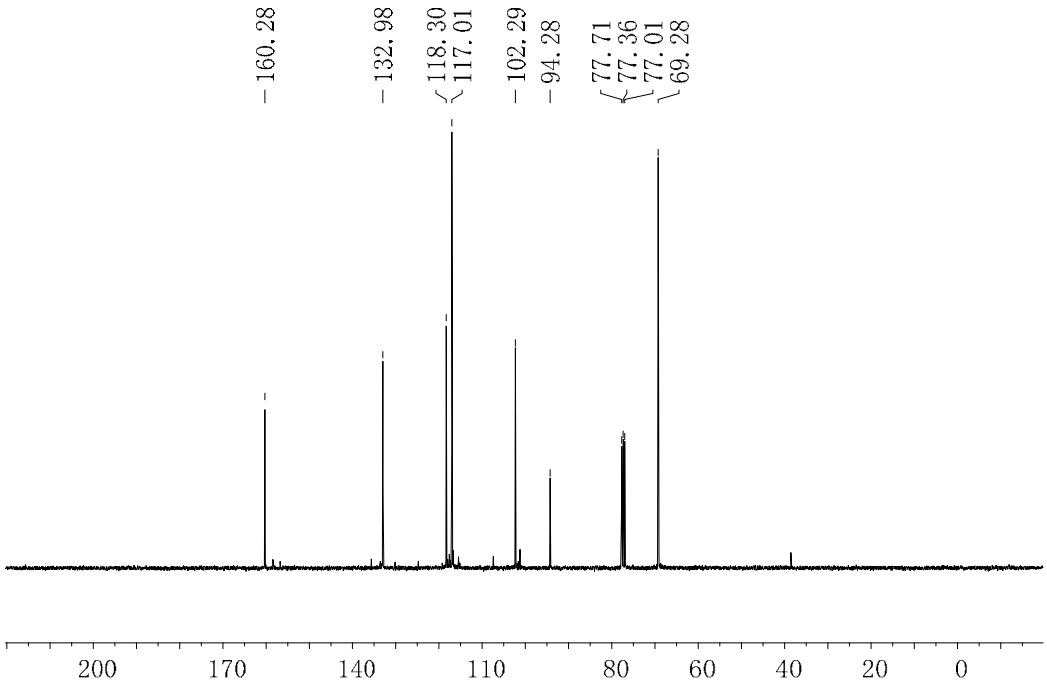

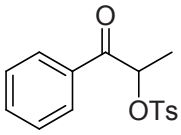

, **15**

^{1}H NMR (360 MHz, $CDCl_3$)

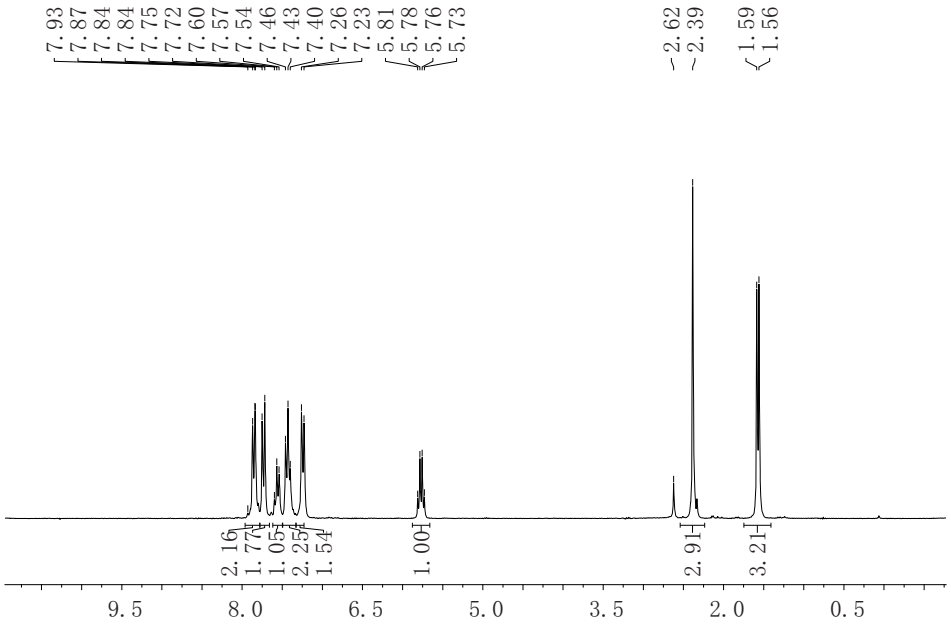

^{13}C NMR (90 MHz, $CDCl_3$)

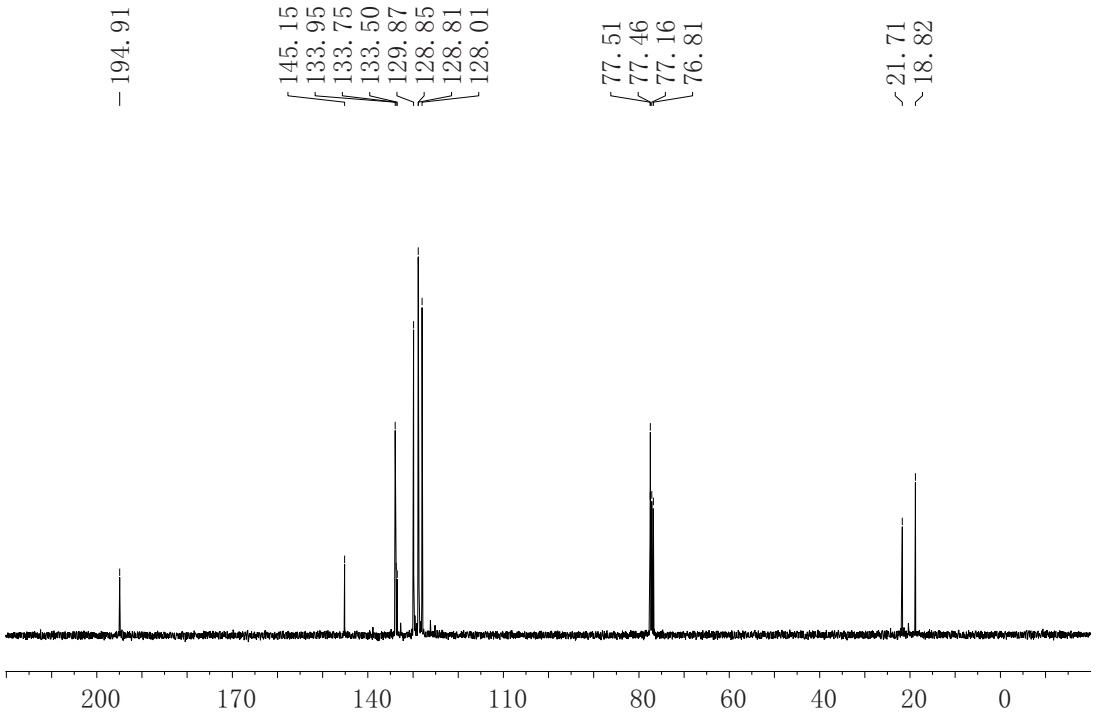

IR (ATR) *v* (cm^{-1})

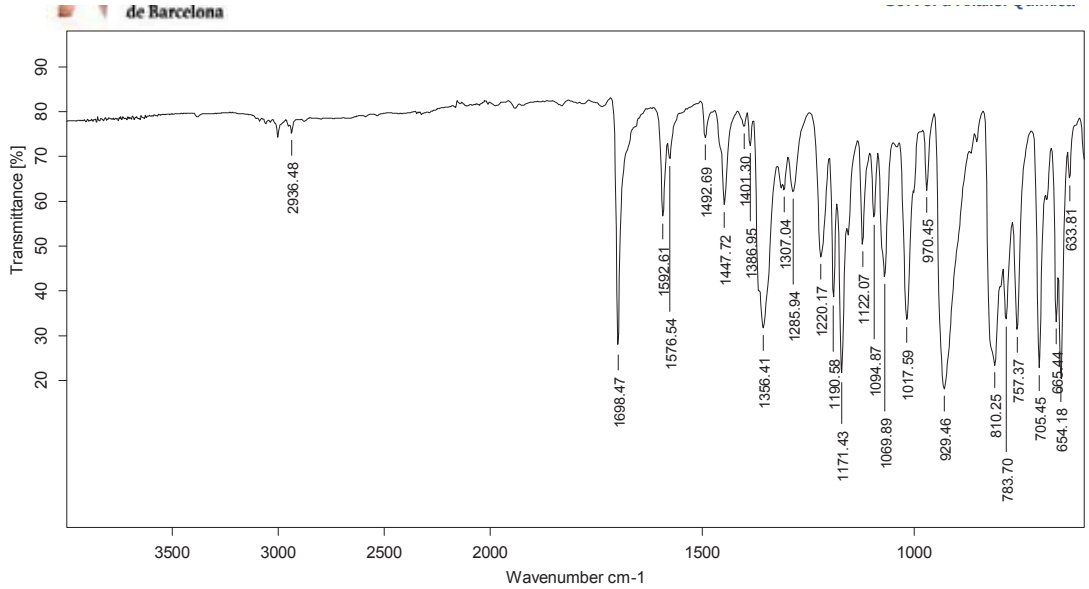

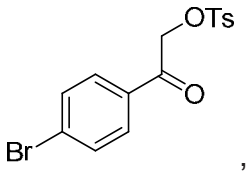

, **16**

^{1}H NMR 360 MHz, $CDCl_3$)

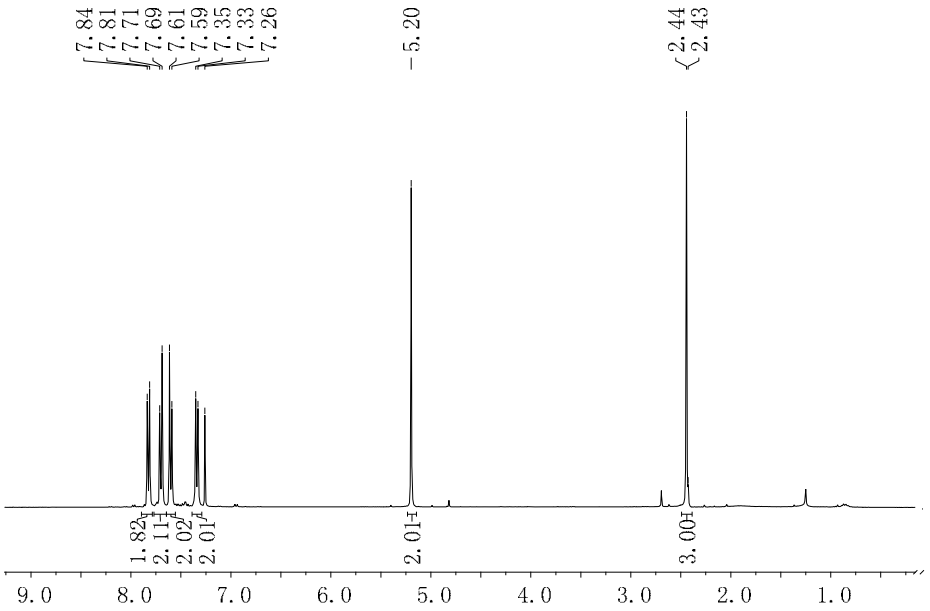

^{13}C NMR (90 MHz, $CDCl_3$)

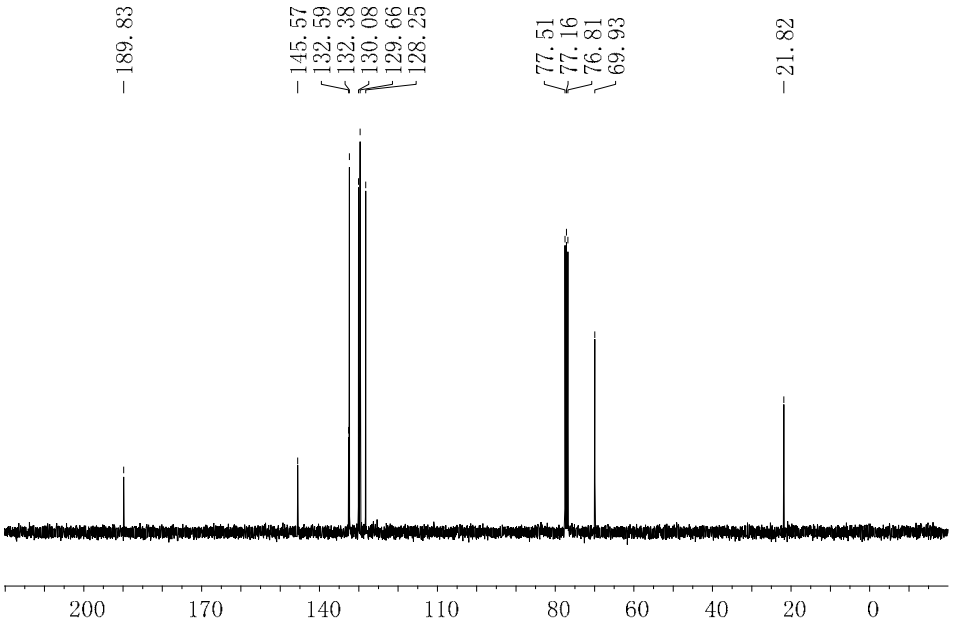

HSQCedited ^{1}H-^{13}C

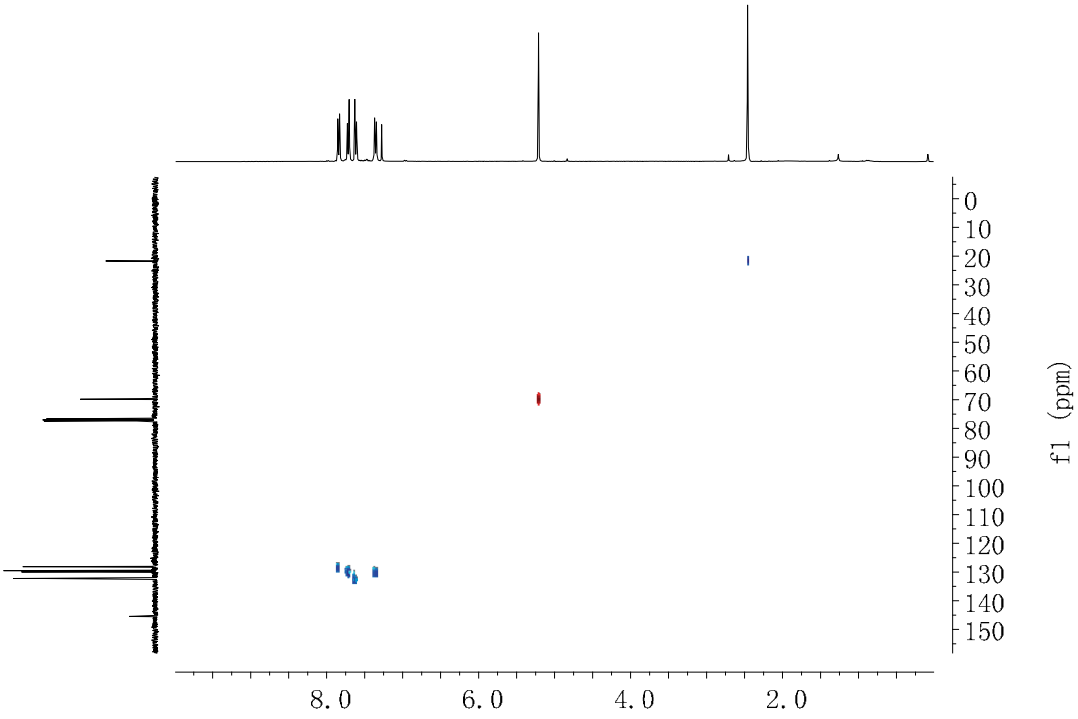

IR (ATR) ν (cm^{-1})

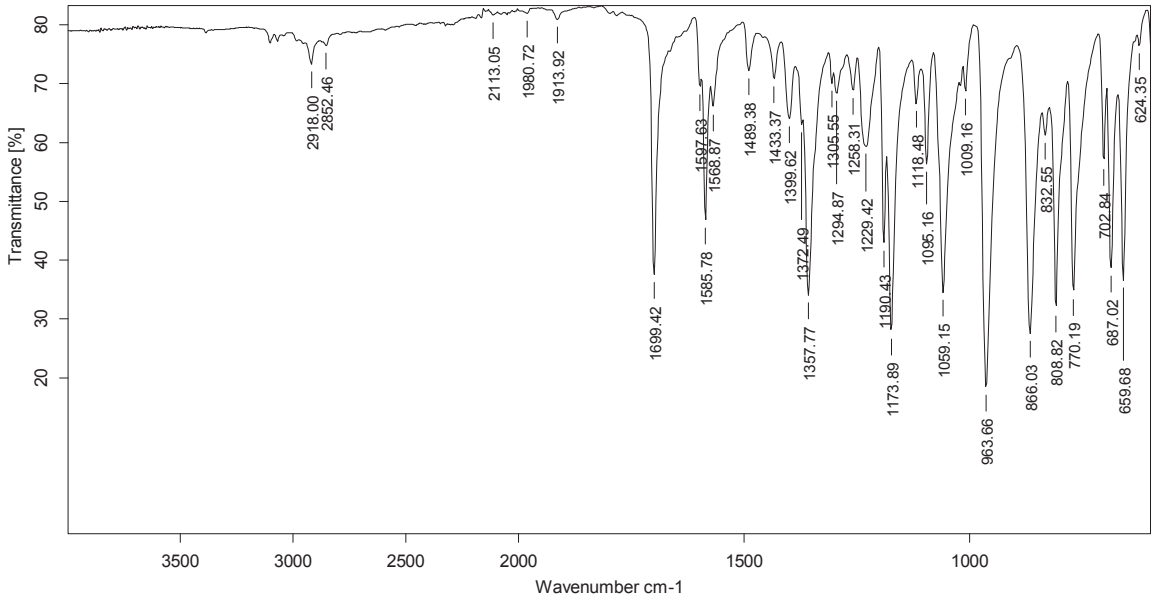

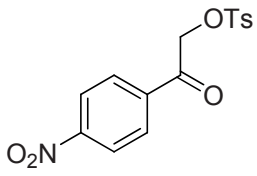

, **17**

^{1}H NMR (360 MHz, $CDCl_3$)

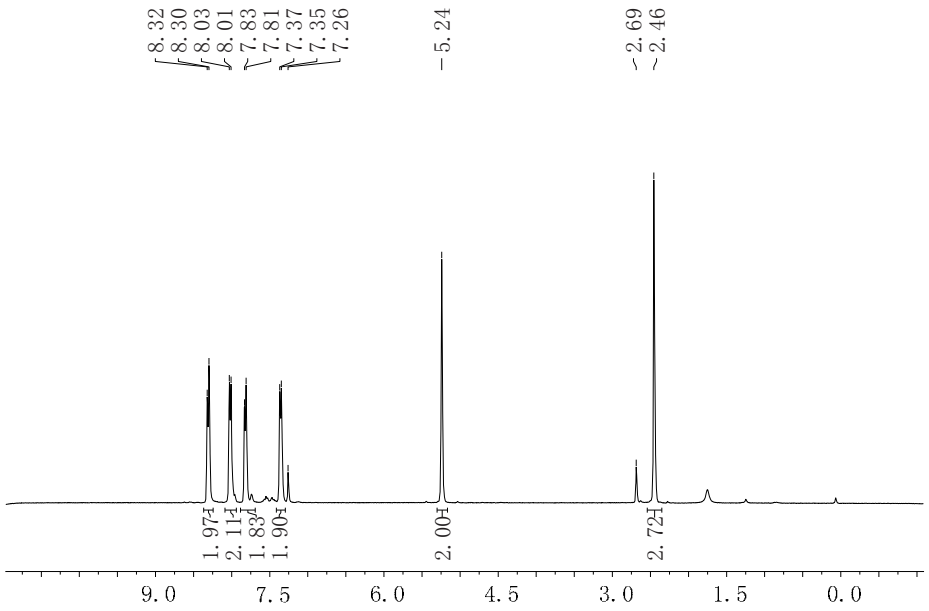

^{13}C NMR (90 MHz, $CDCl_3$)

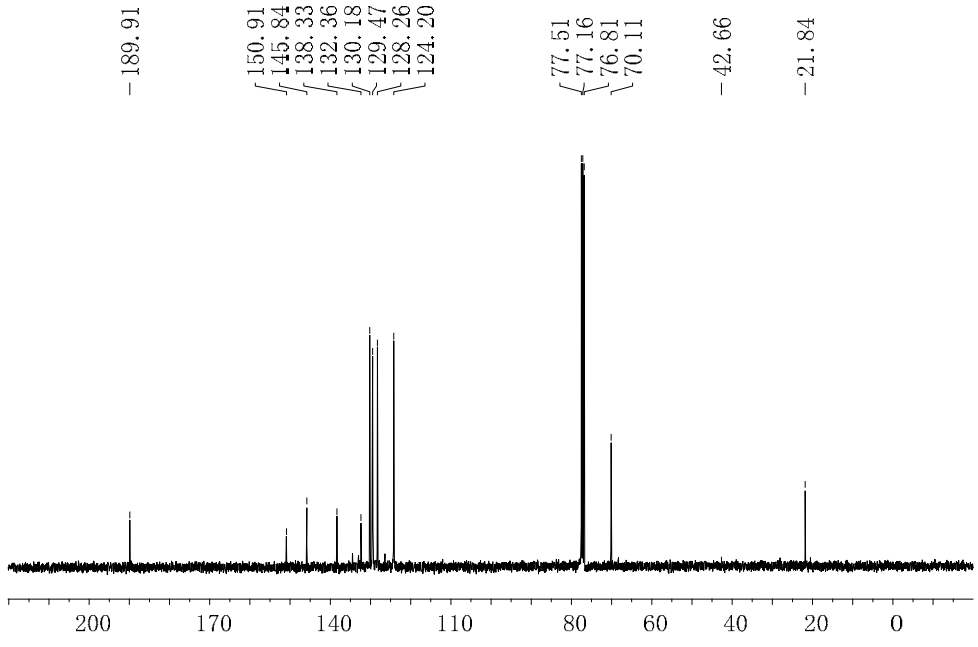

IR (ATR) *v* (cm^{-1})

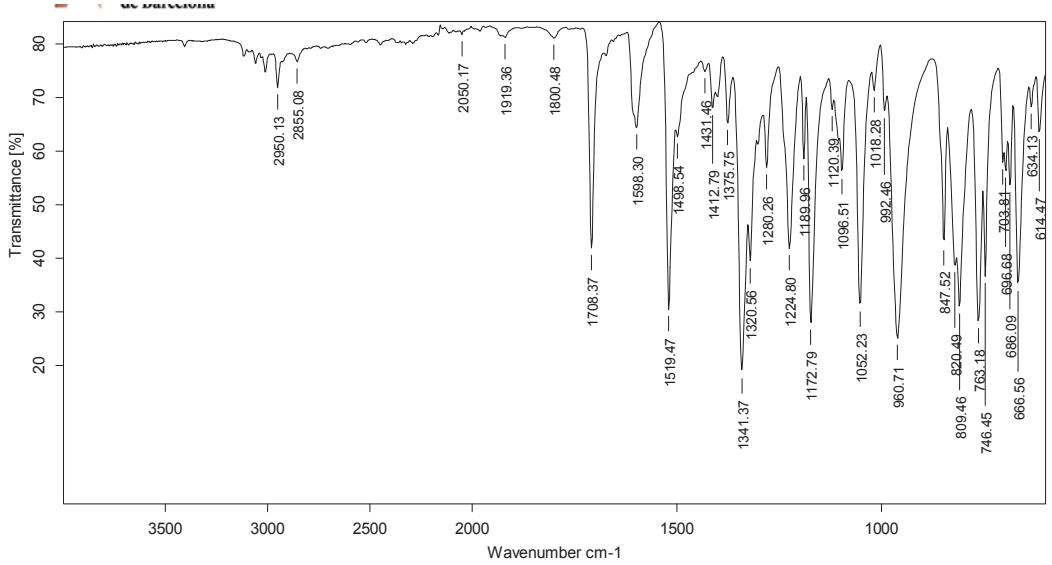

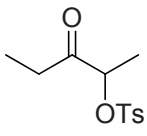

OTs , **18**

^{1}H NMR 360 MHz, $CDCl_3$)

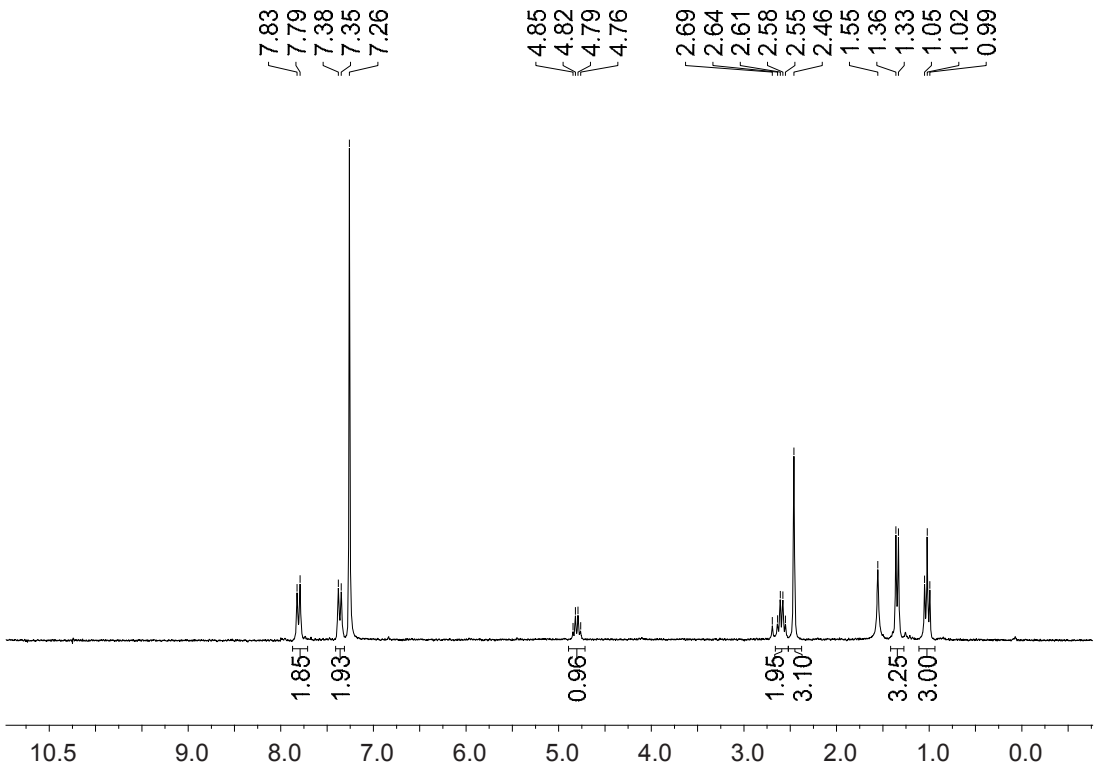

^{13}C NMR (90 MHz, $CDCl_3$)

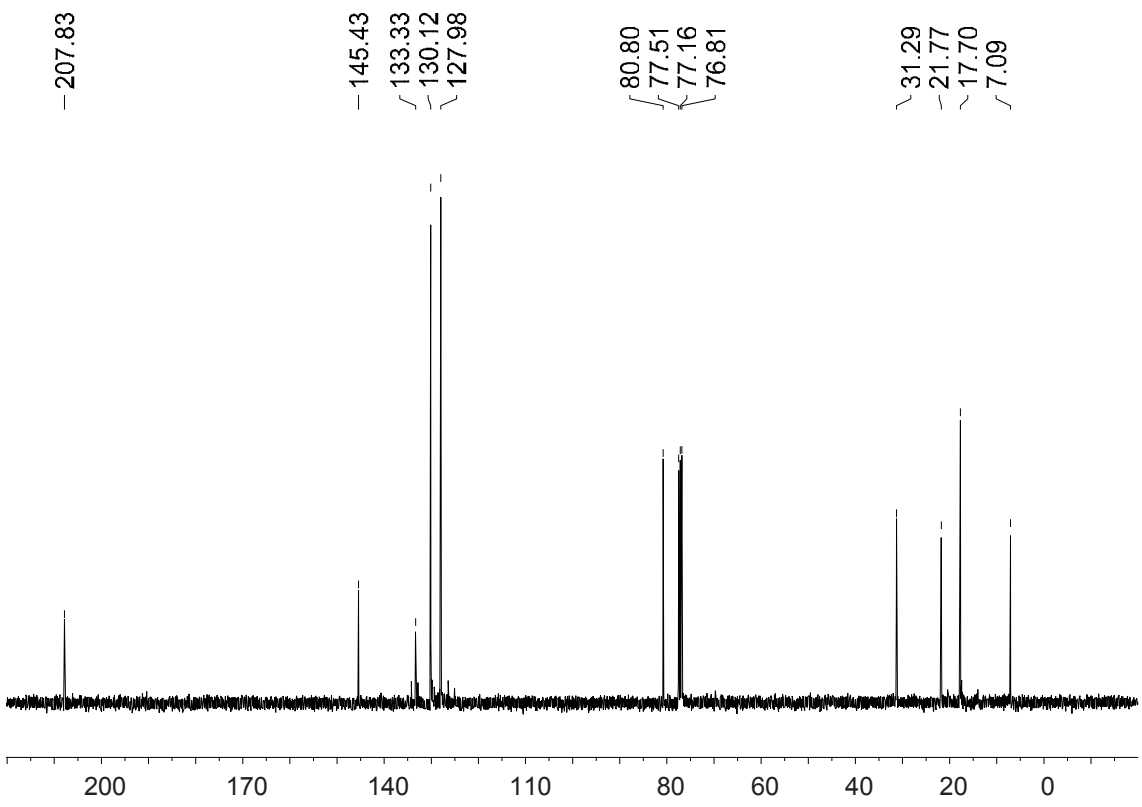

IR (ATR) *v* (cm^{-1})

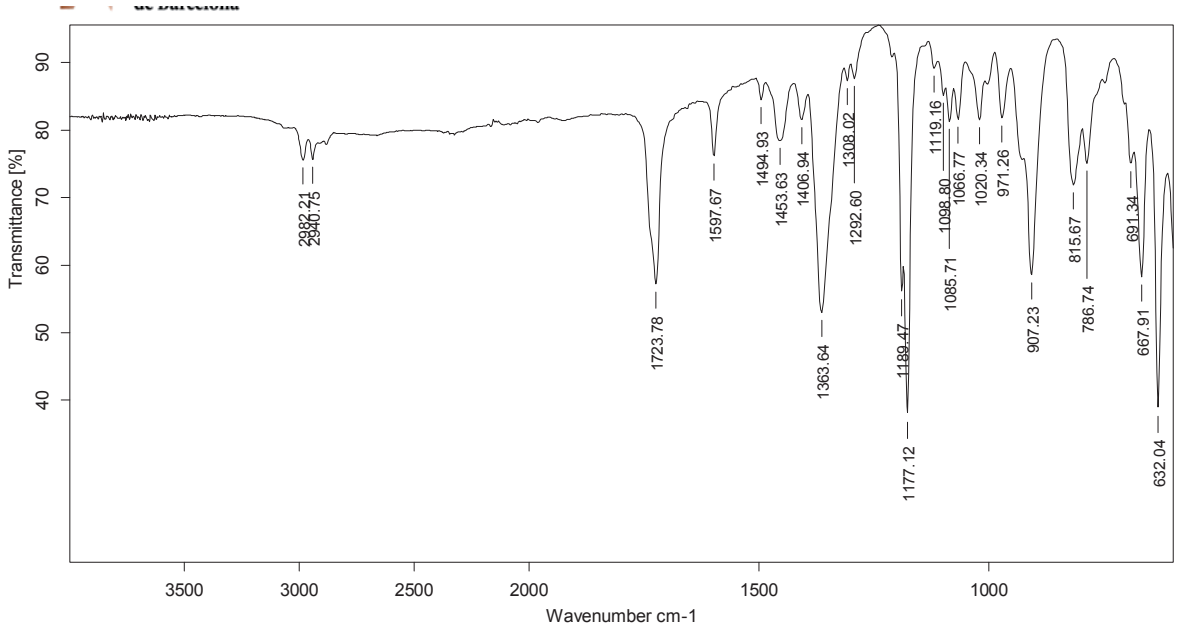

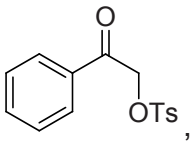

, **19**

^{1}H NMR (250 MHz, $CDCl_3$)

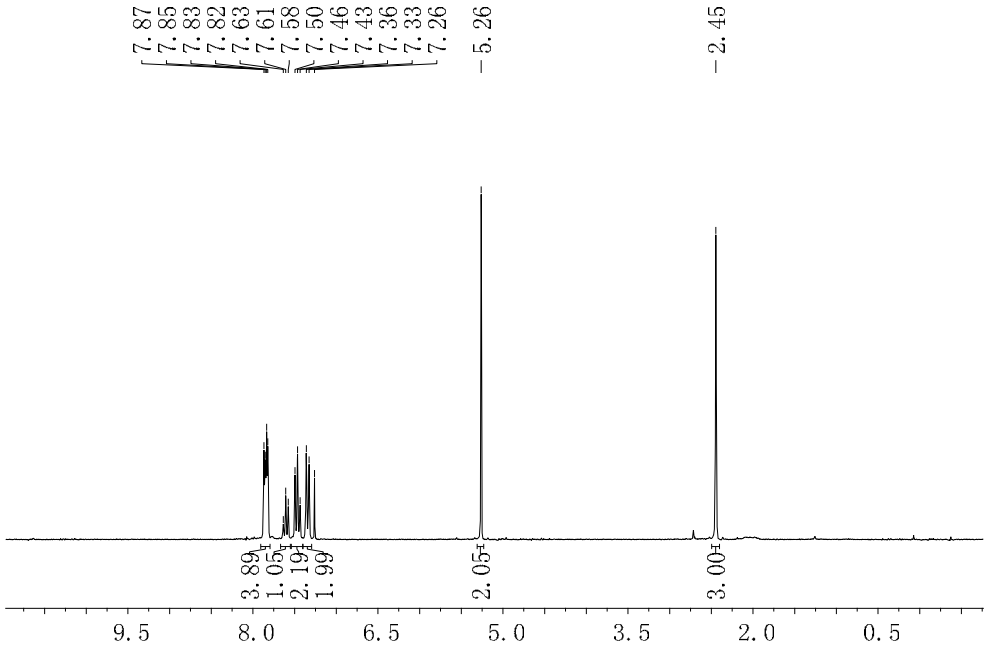

^{13}C NMR (90 MHz, $CDCl_3$)

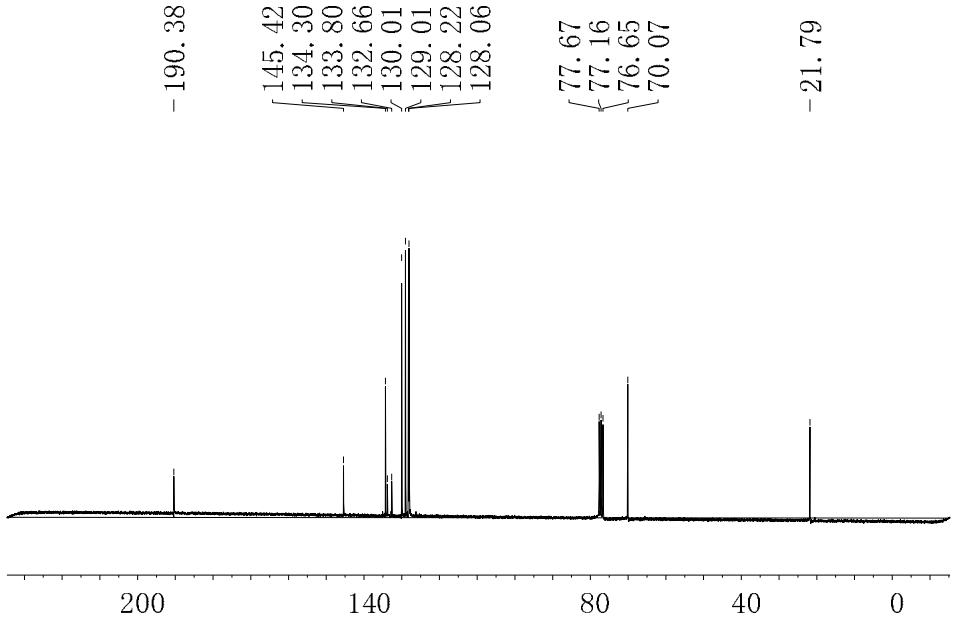

IR (ATR) *v* (cm^{-1})

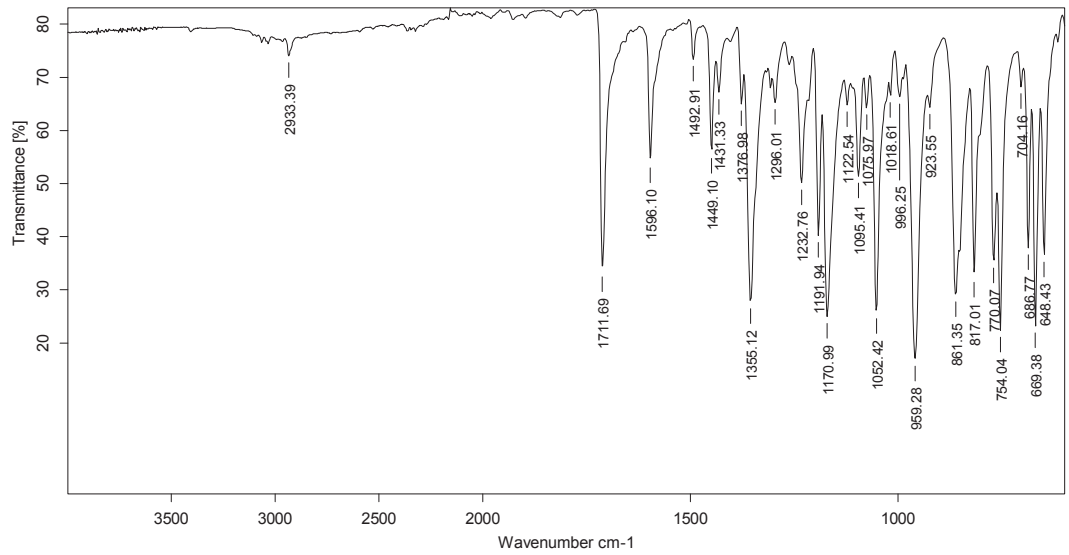

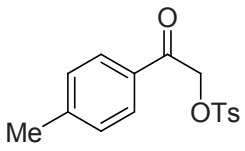

, **20**

^{1}H NMR (360 MHz, $CDCl_3$)

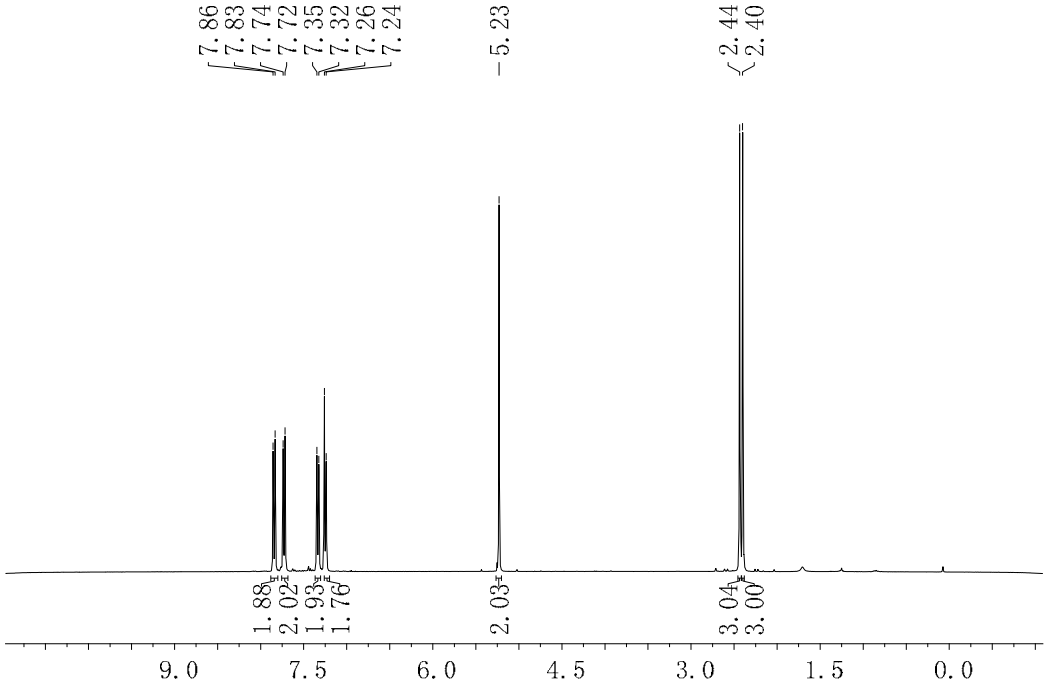

^{13}C NMR (90 MHz, $CDCl_3$)

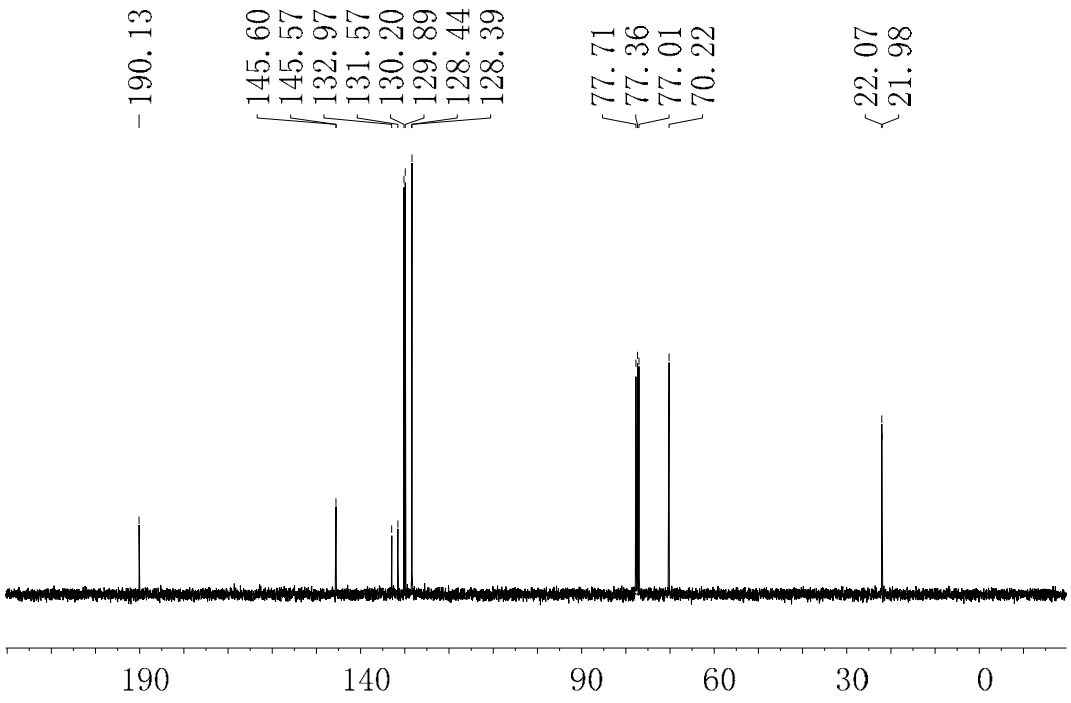

IR (ATR) *v* (cm^{-1})

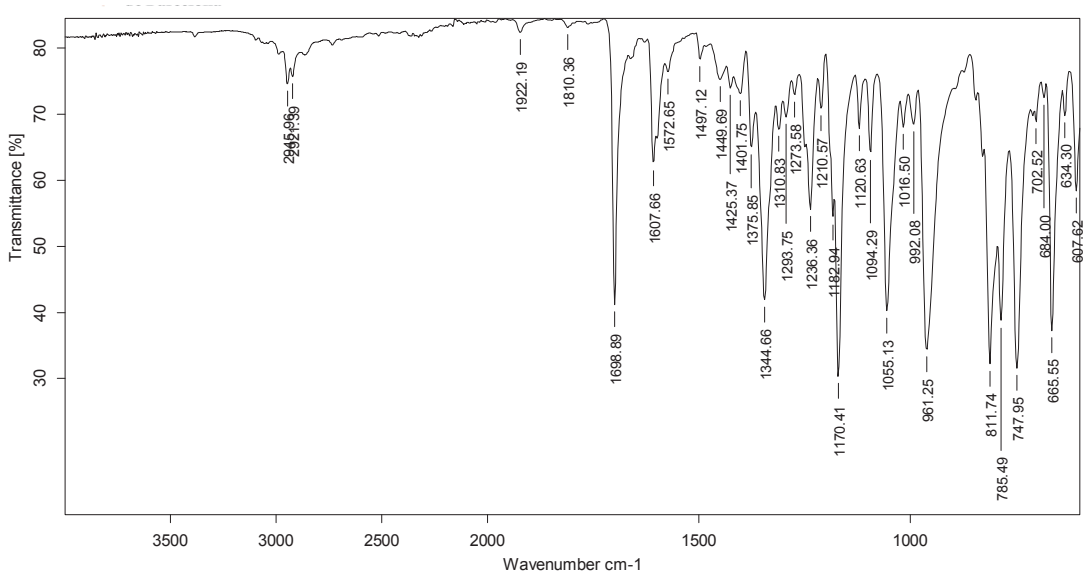

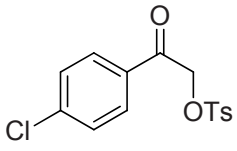

, **21**

^{1}H NMR (360 MHz, $CDCl_3$)

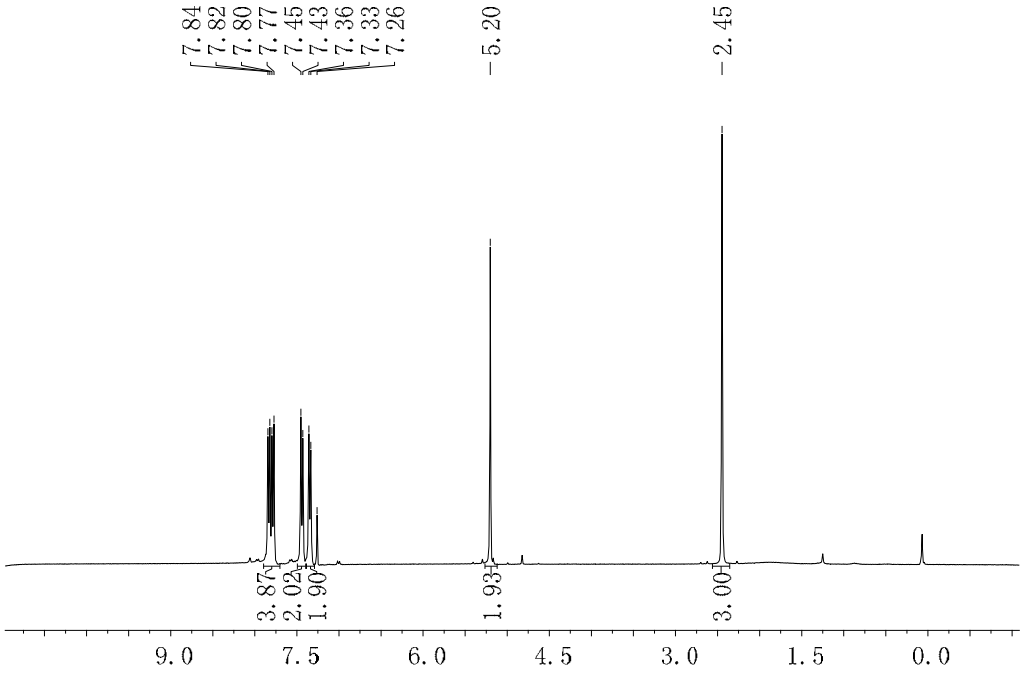

^{13}C NMR (90 MHz, $CDCl_3$)

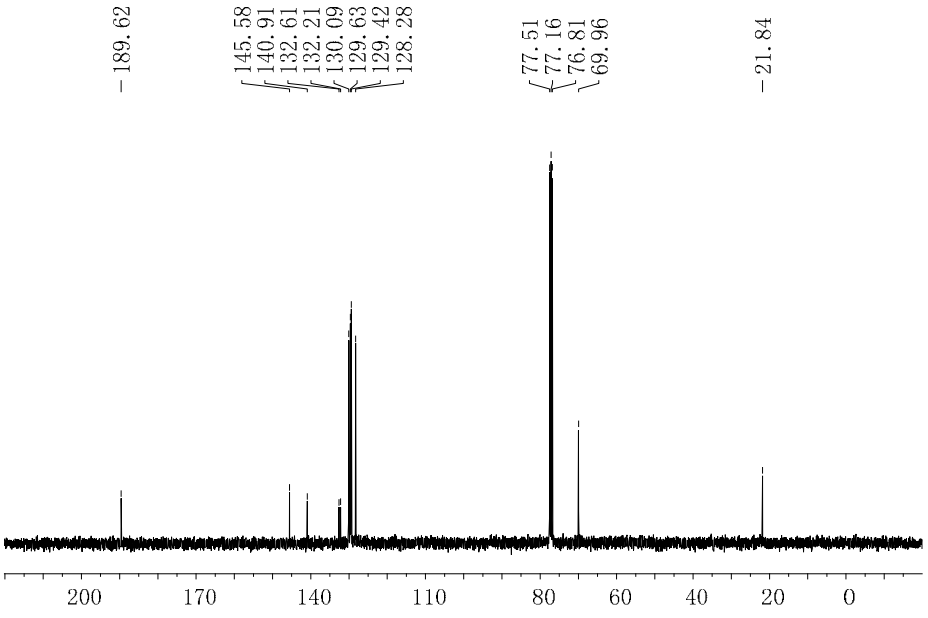

IR (ATR) *v* (cm^{-1})

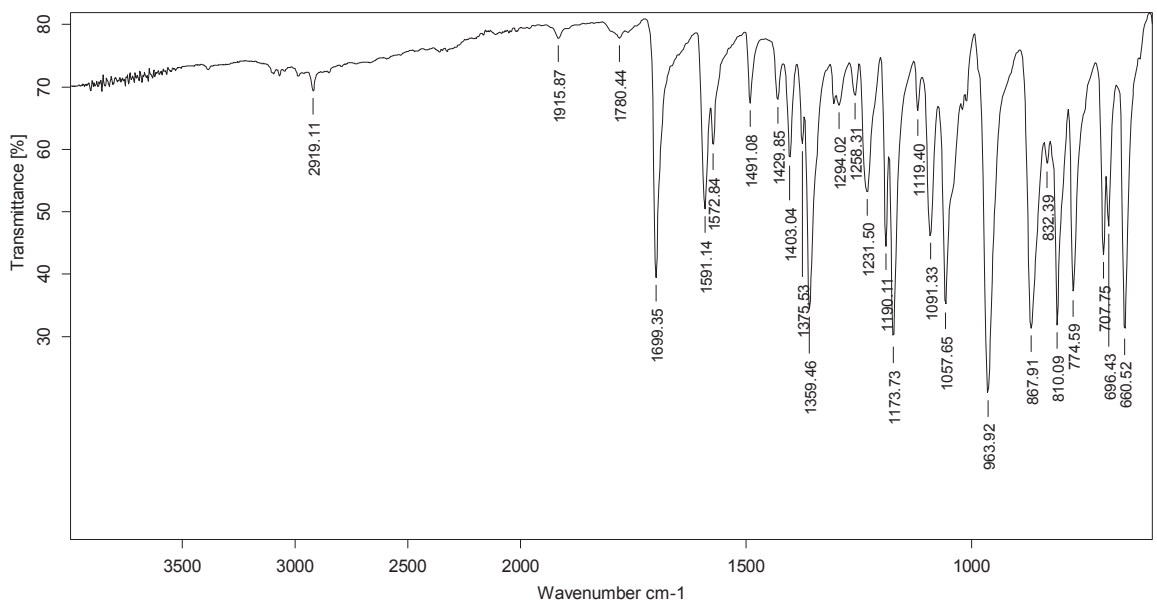

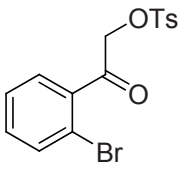

, **22**

^{1}H NMR (360 MHz, $CDCl_3$)

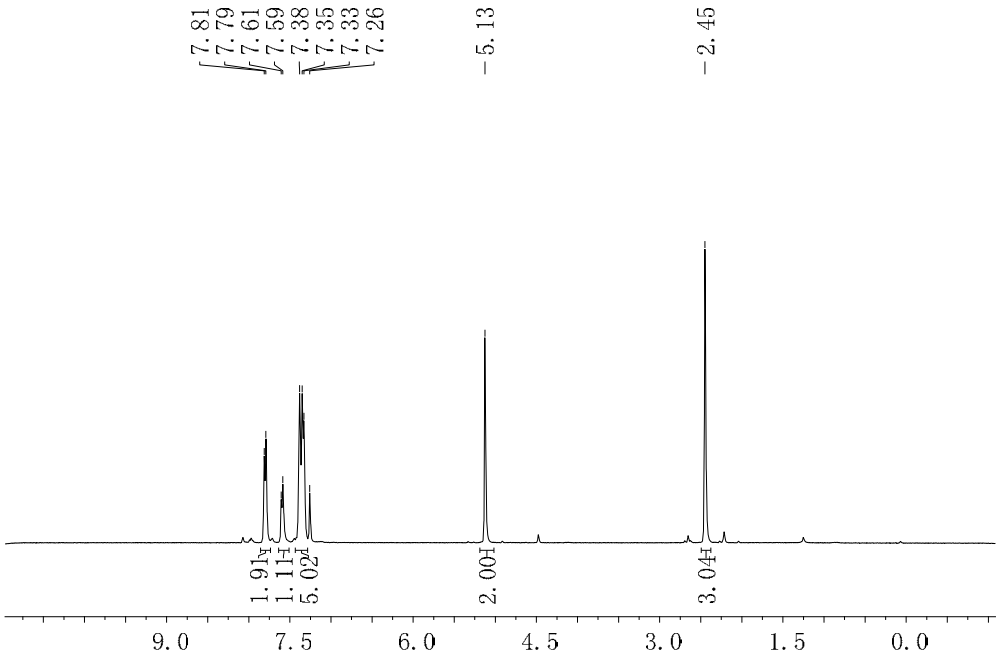

^{13}C NMR (90 MHz, $CDCl_3$)

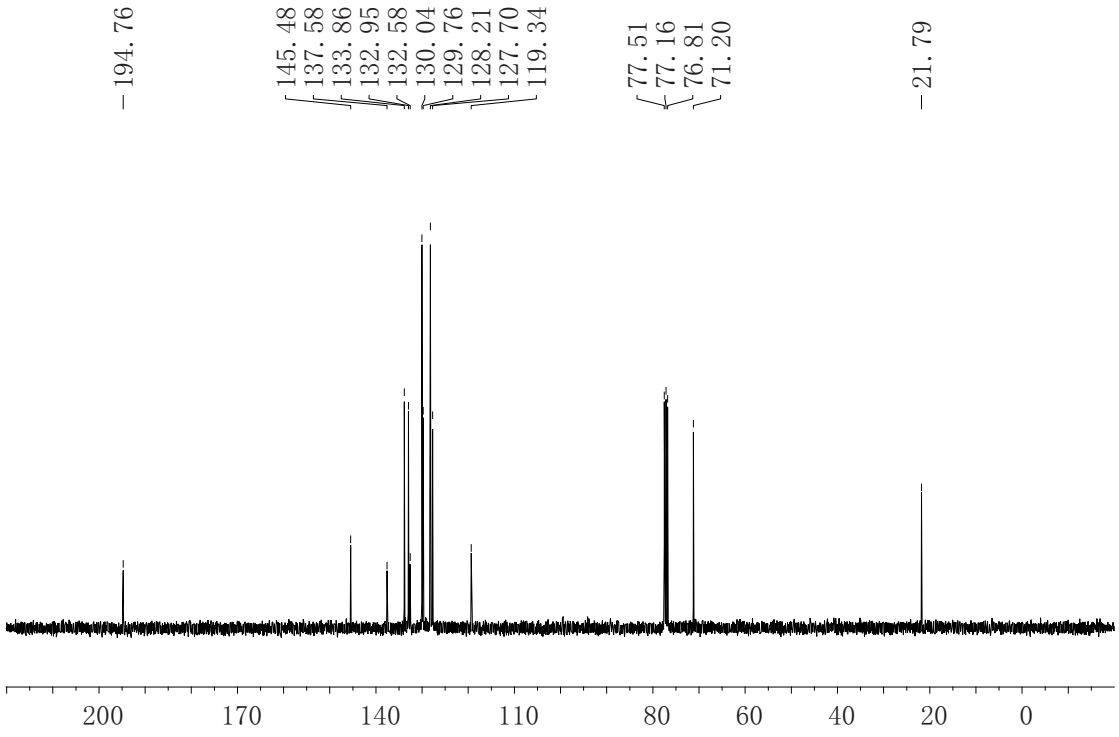

IR (ATR) ν (cm^{-1})

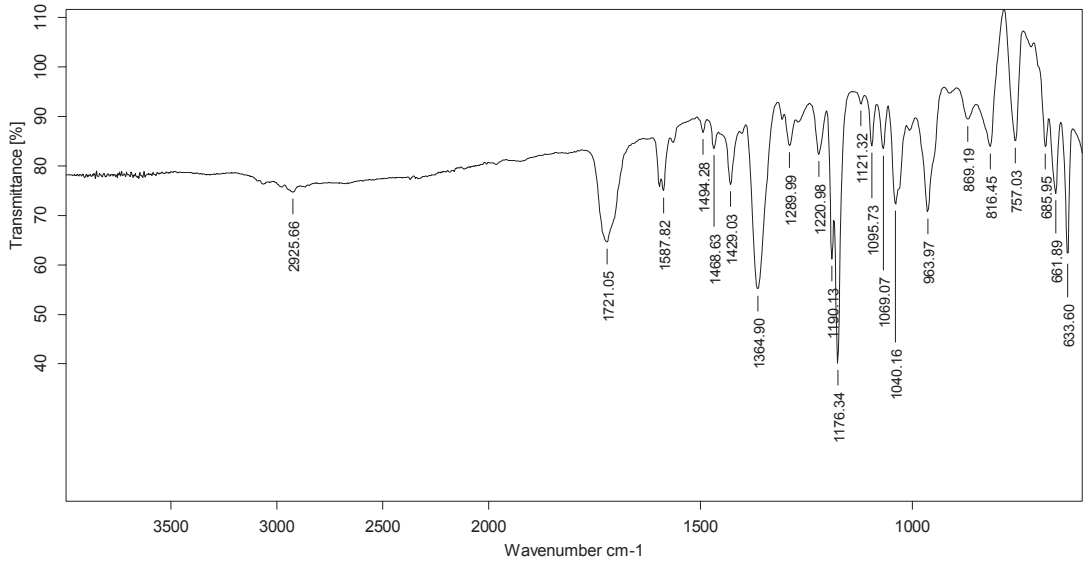

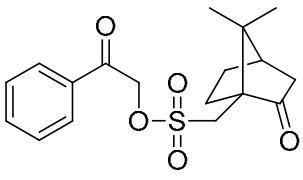

, **23**

^{1}H NMR (360 MHz, $CDCl_3$)

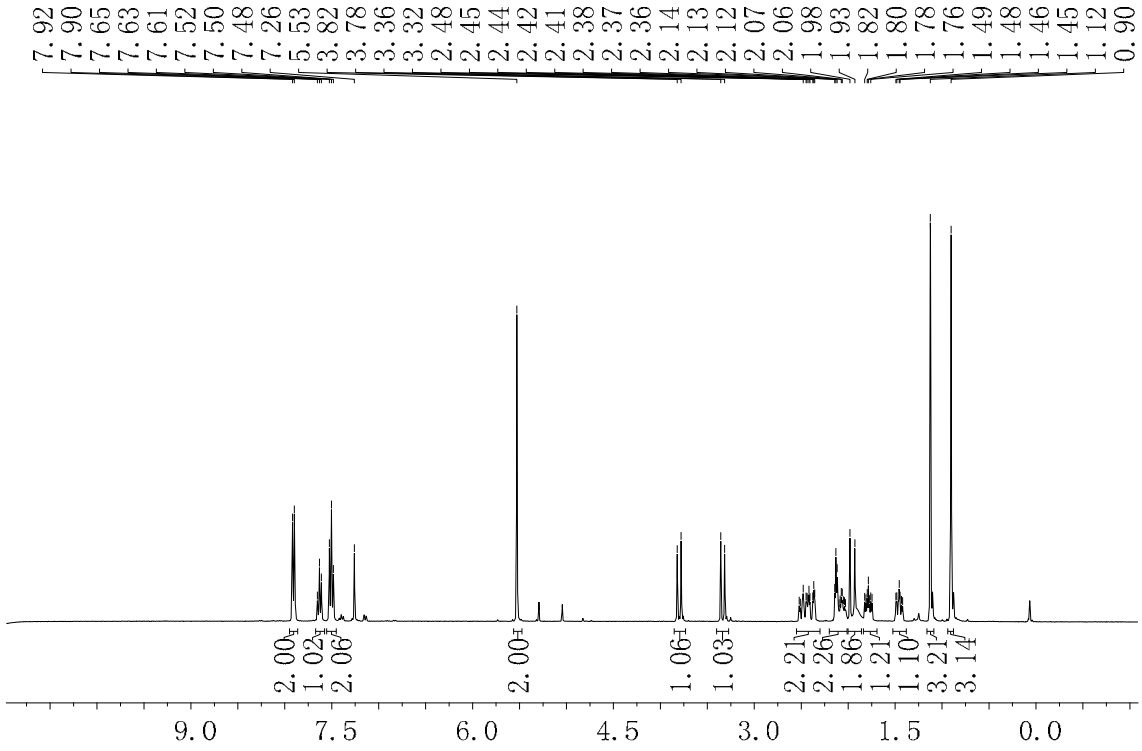

^{13}C NMR (90 MHz, $CDCl_3$)

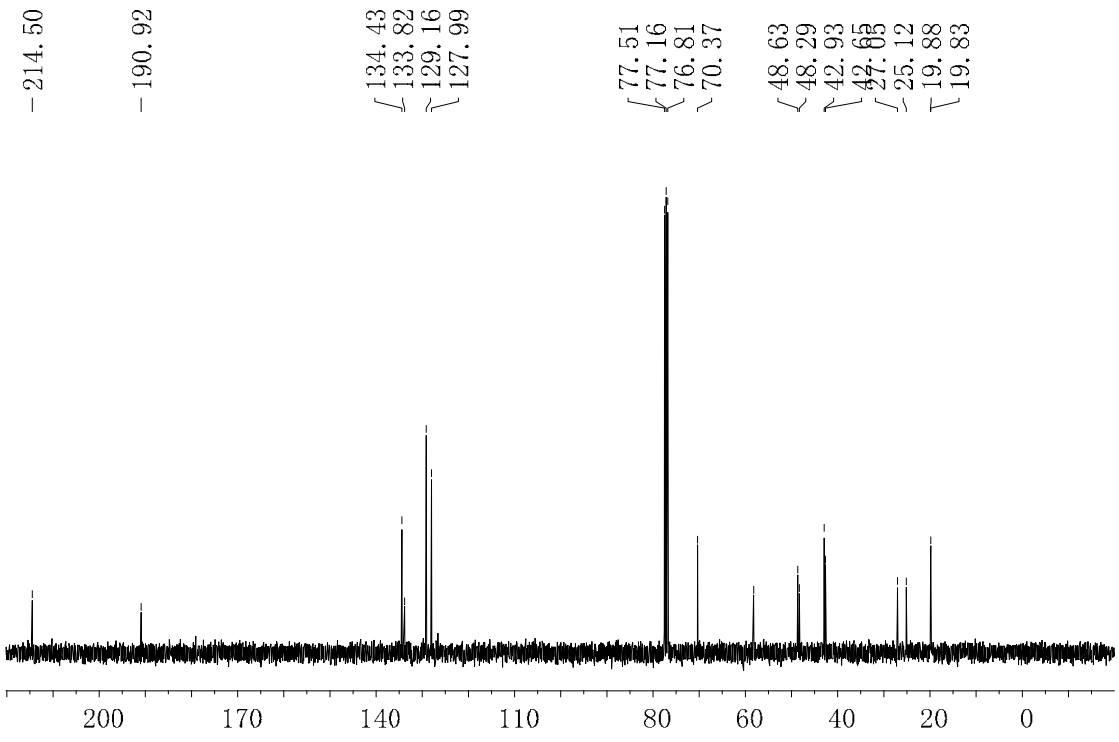

IR (ATR) ν (cm^{-1})

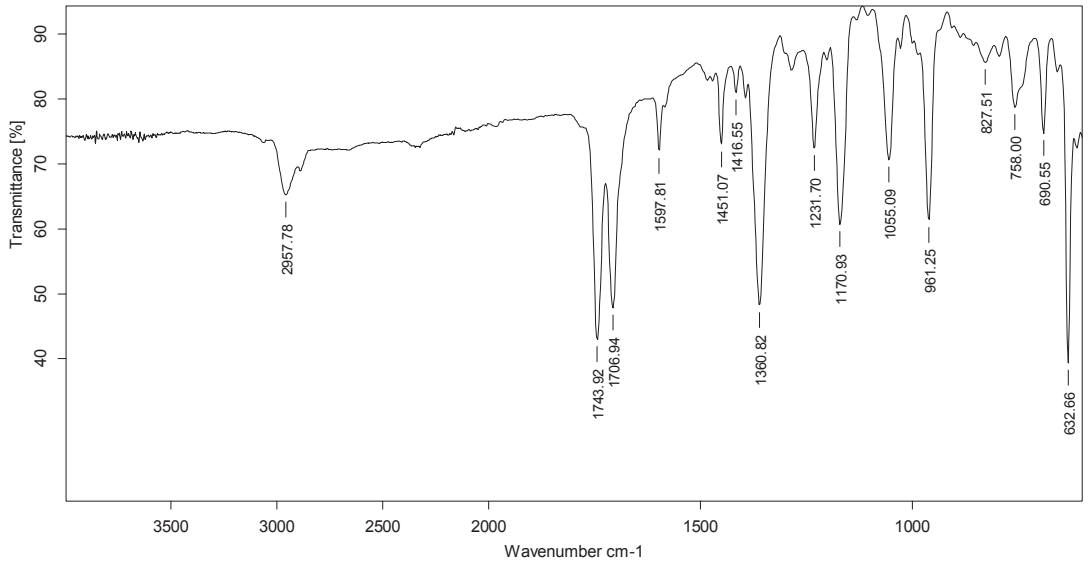

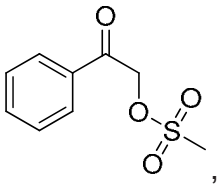

, **24**

^{1}H NMR (360 MHz, $CDCl_3$)

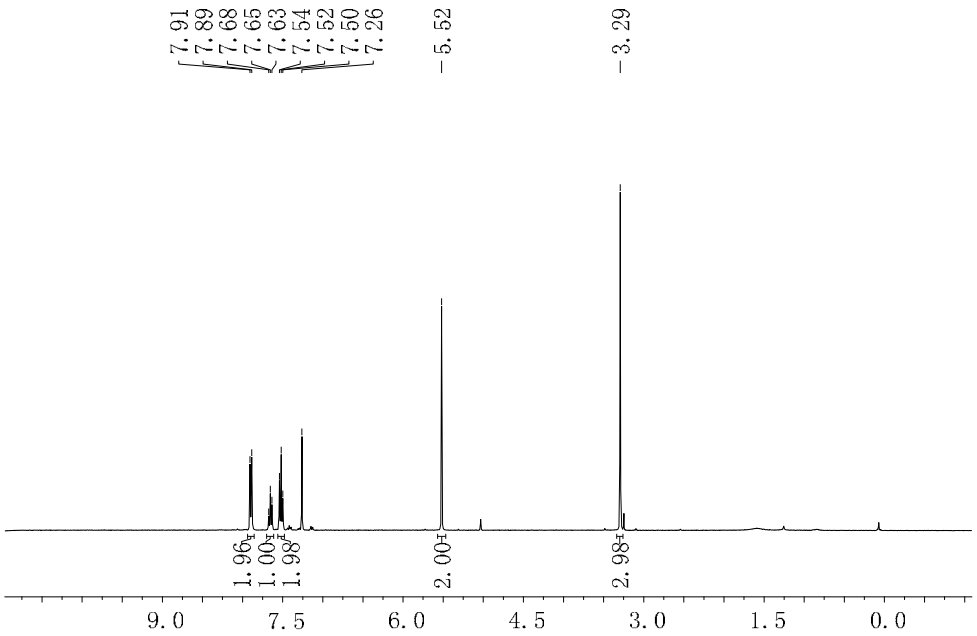

^{13}C NMR (90 MHz, $CDCl_3$)

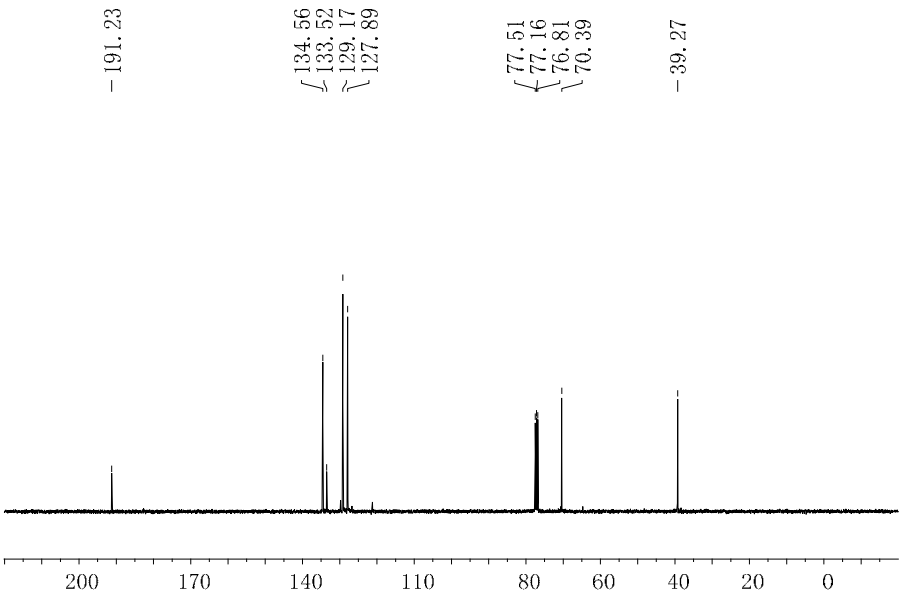

IR (ATR) ν (cm^{-1})

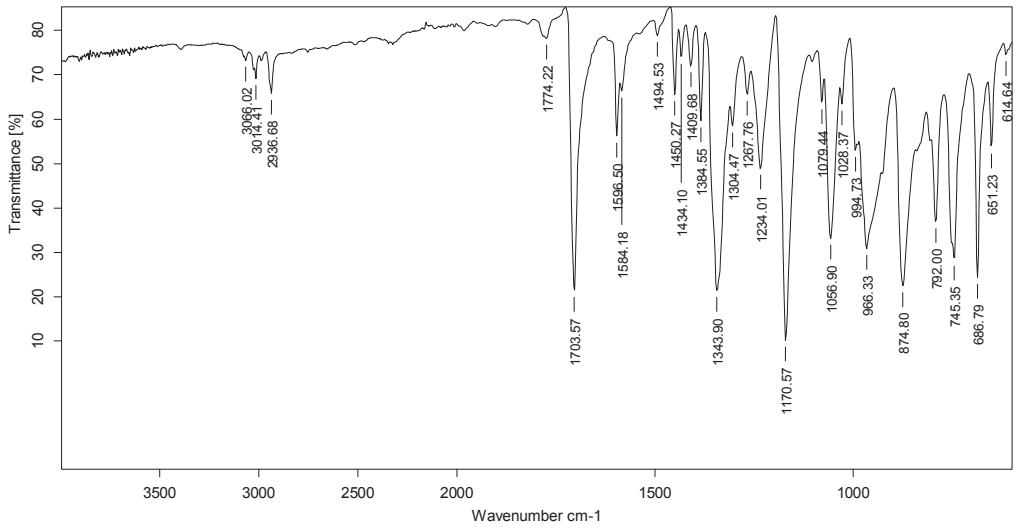

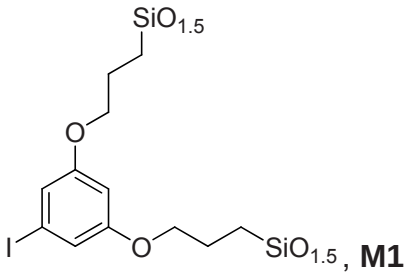

, **M1**

^{13}C solid state NMR

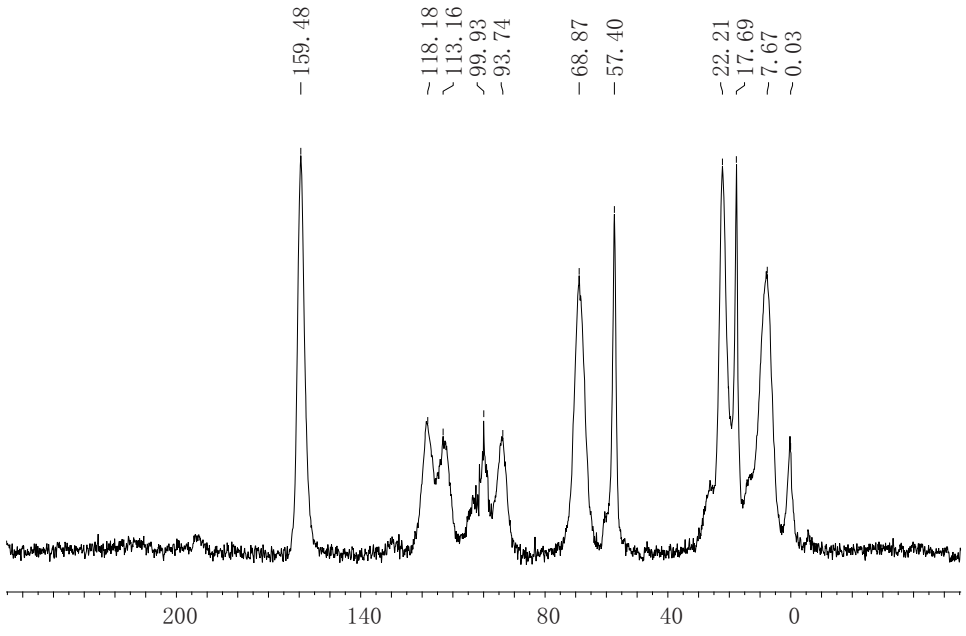

IR (ATR) *v* (cm^{-1})

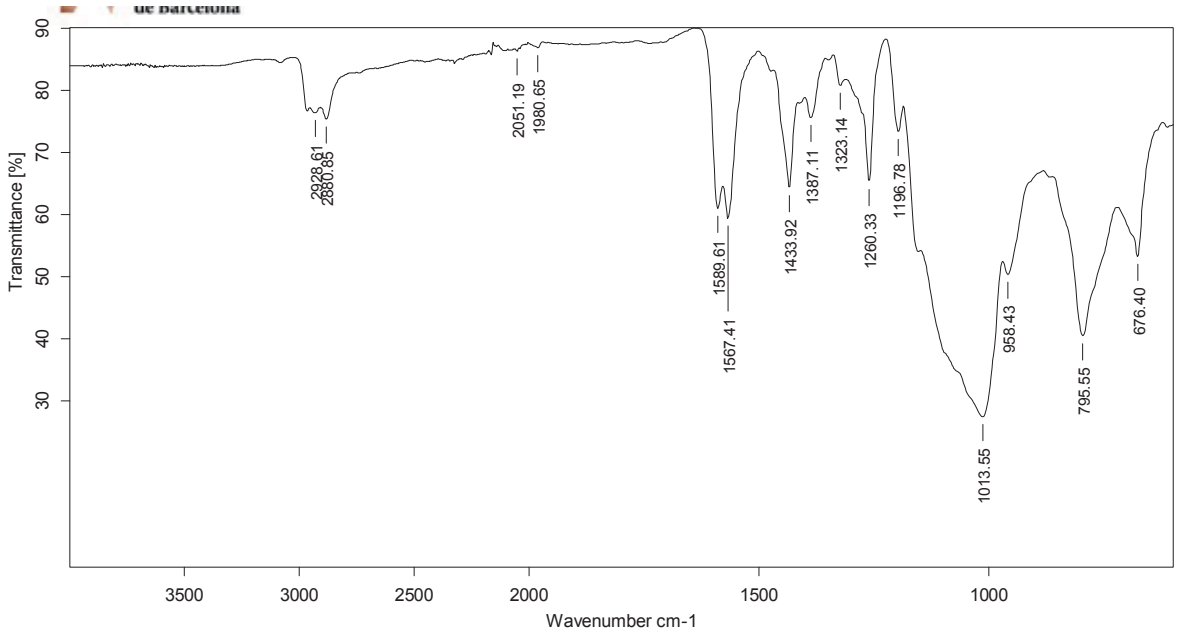

TG and DSC analyses

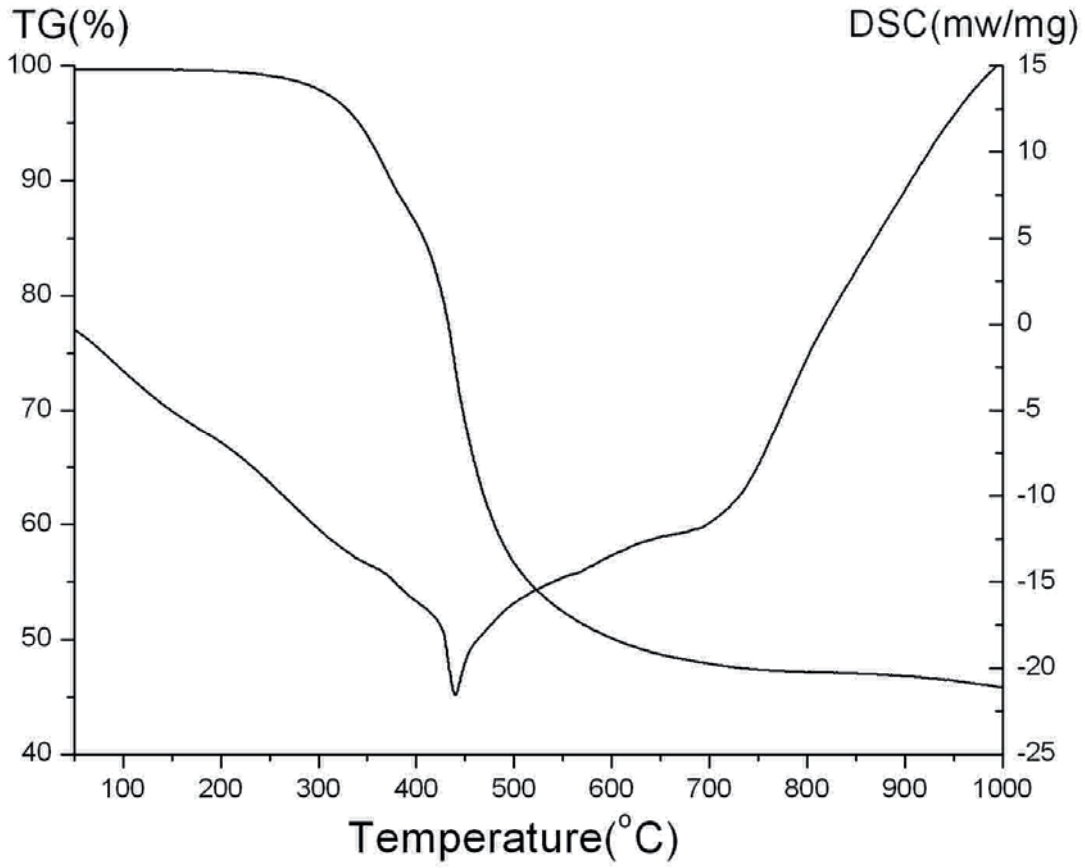

IR spectrum of the recovered **M1** (ATR) *v* (cm^{-1})

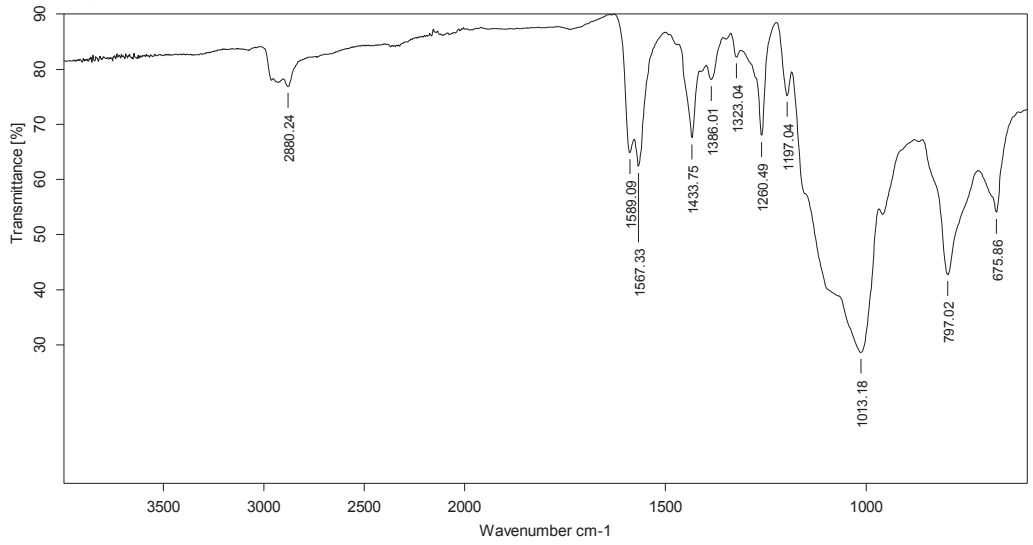

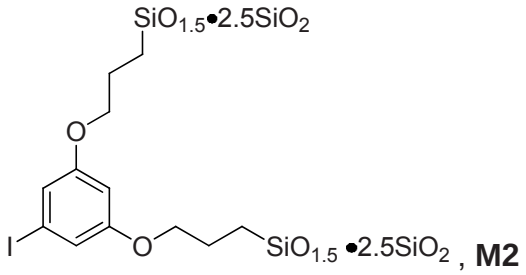

, **M2**

^{13}C solid state NMR

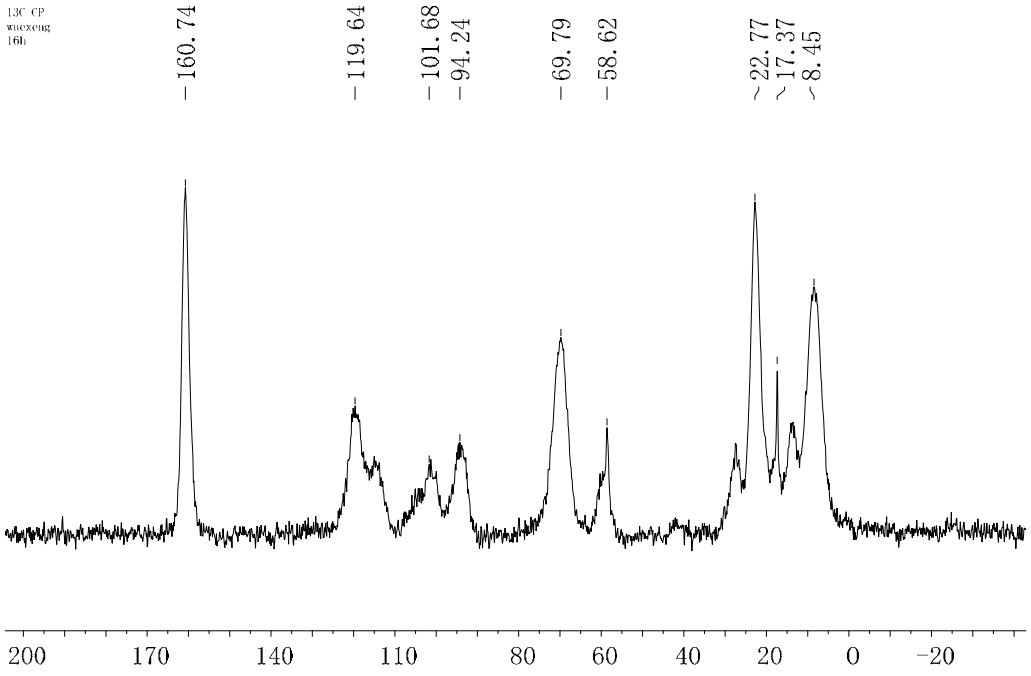

IR (ATR) *v* (cm^{-1})

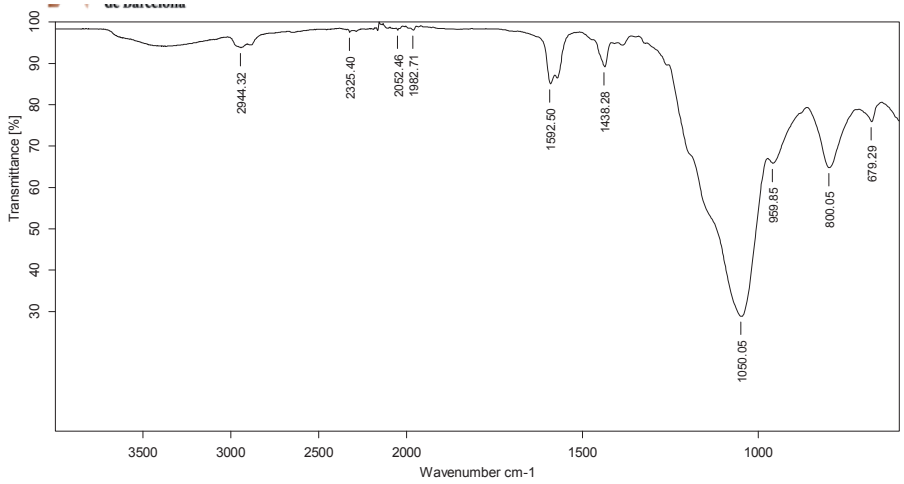

TG and DSC analyses

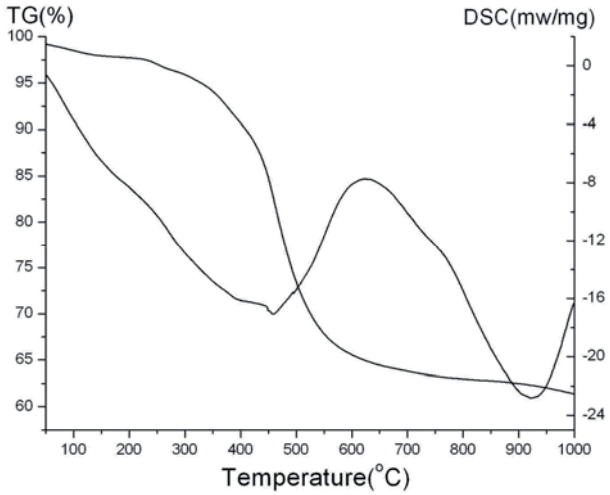

IR spectrum of the recovered **M2** (ATR) *v* (cm^{-1})

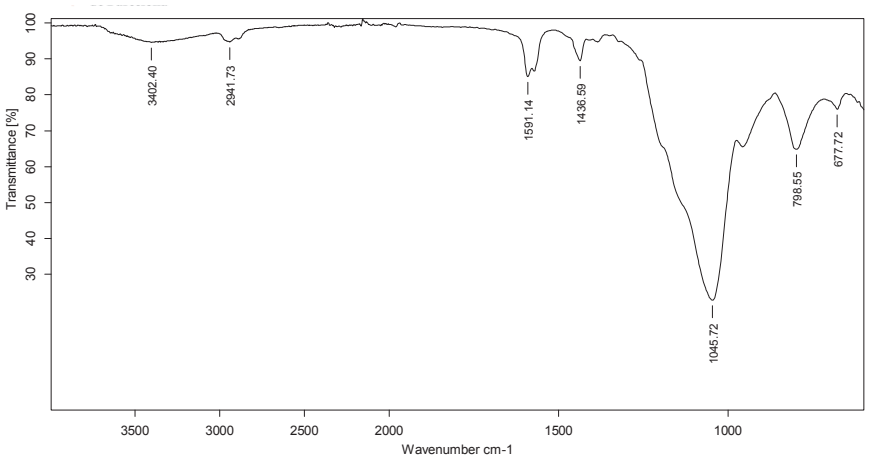

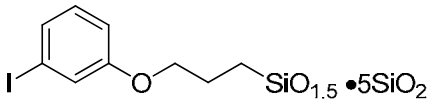

, **M3**

^{13}C solid state NMR

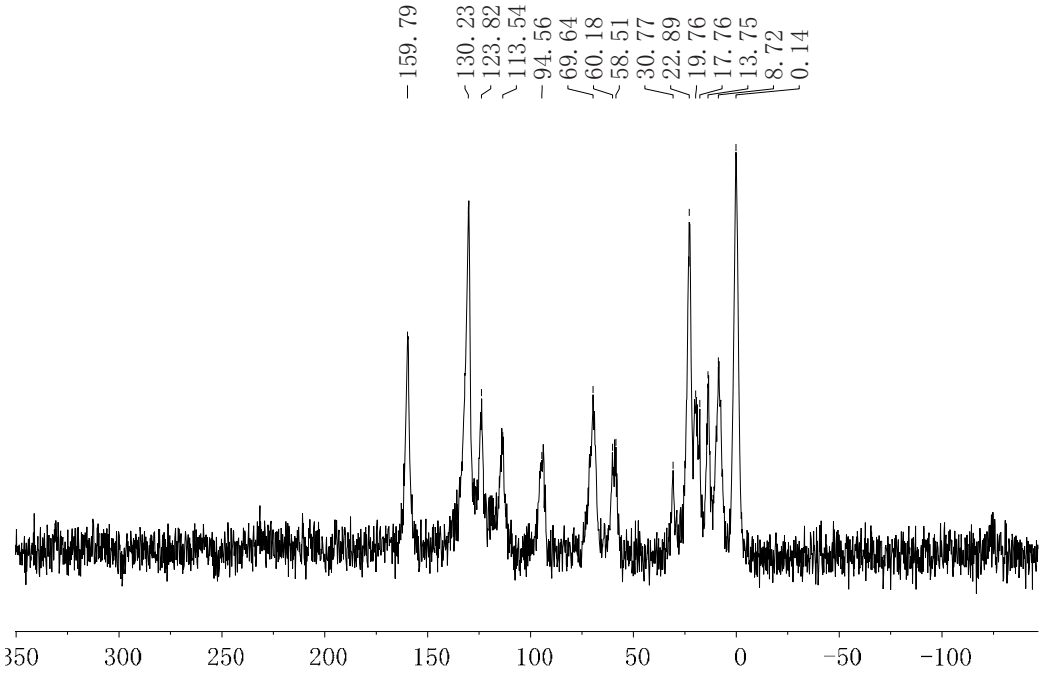

IR (ATR) *v* (cm^{-1})

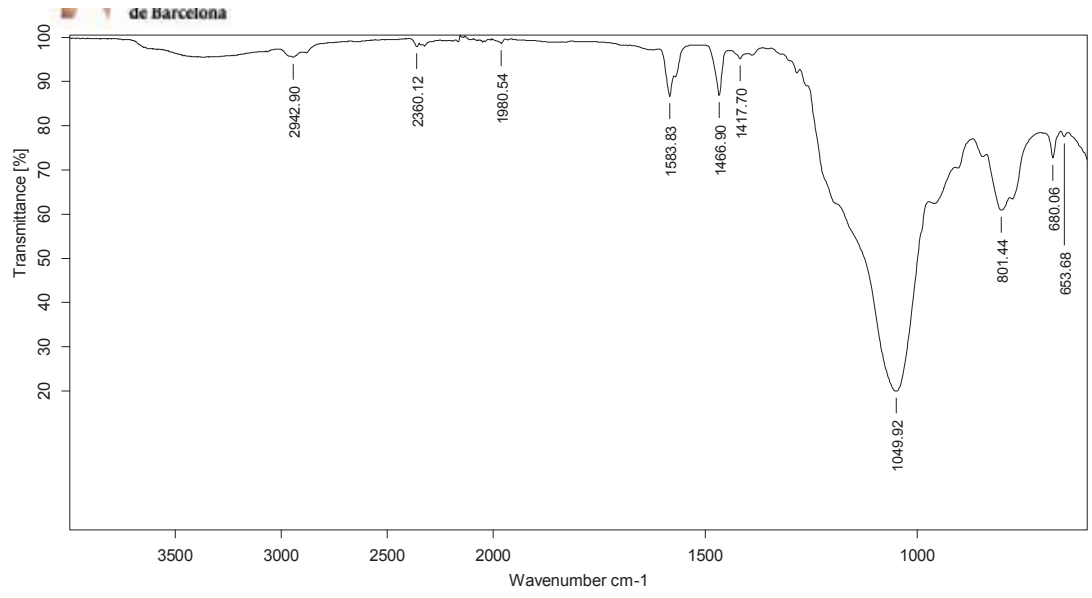

TG and DSC analyses

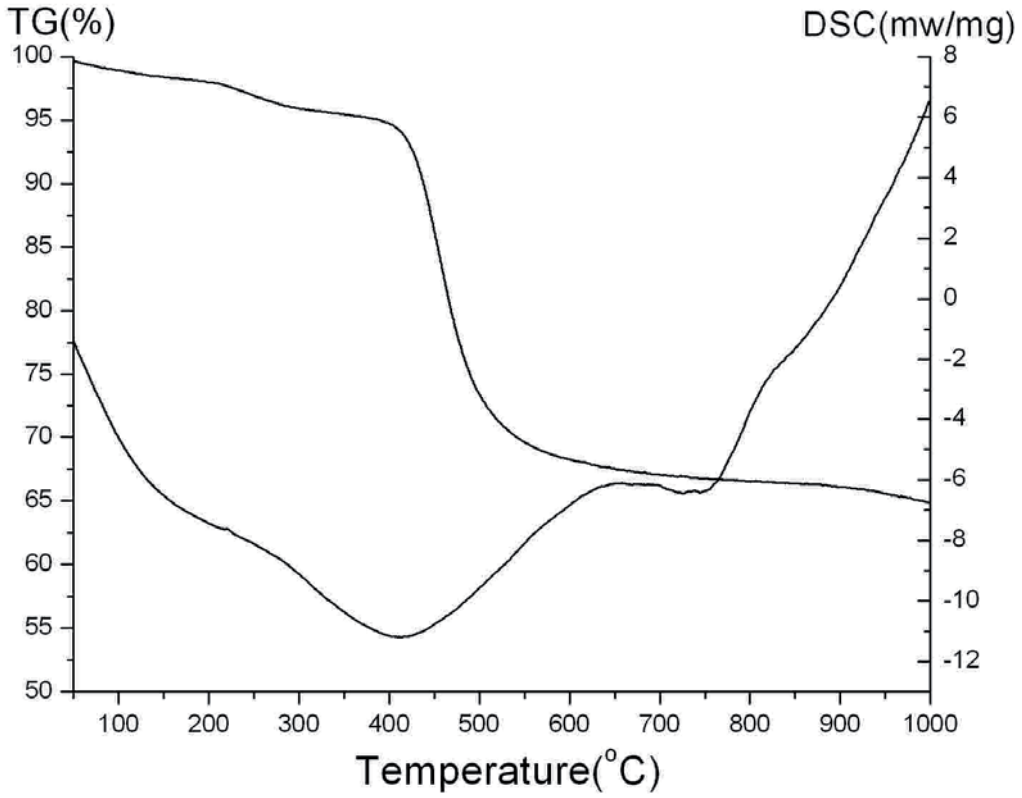

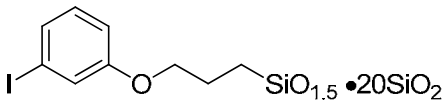

, **M4**

IR (ATR) *v* (cm^{-1})

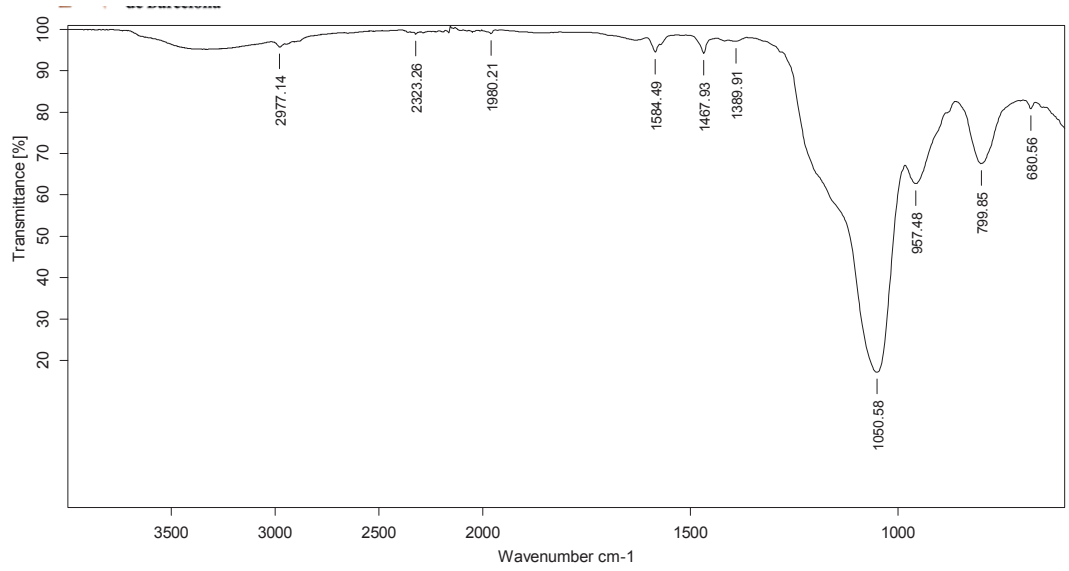

TG and DSC analyses

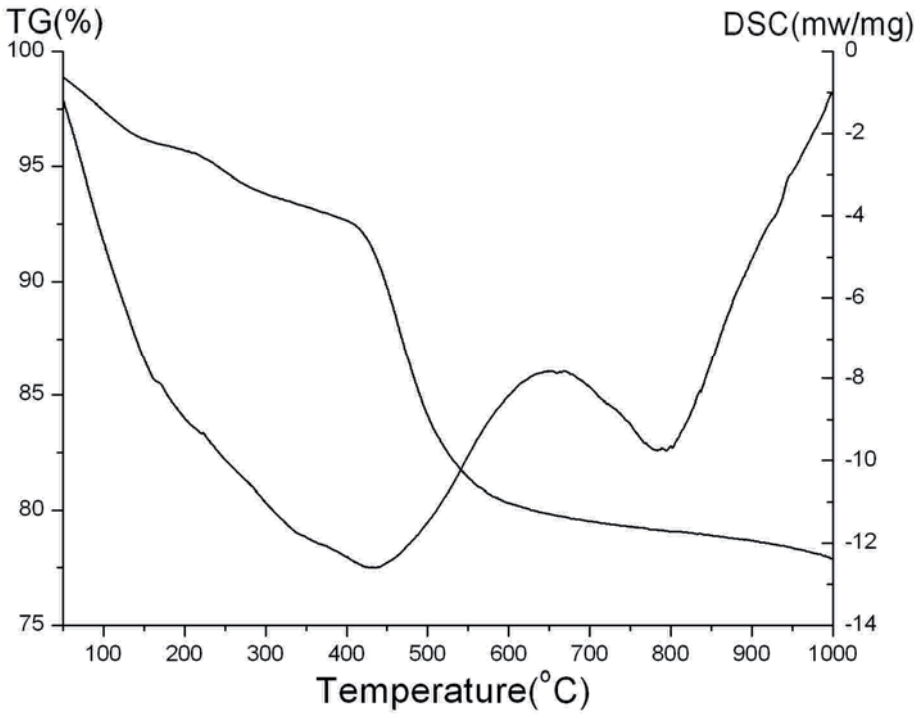

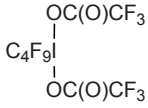

, **25**

^{19}F NMR ((376 MHz, CD_3CN)

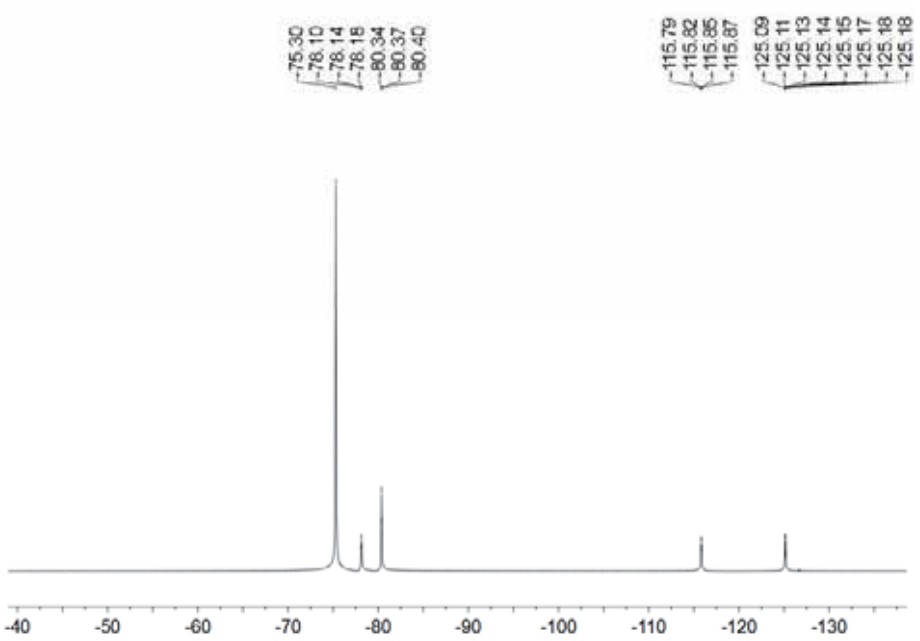

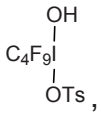

, **26**

^{1}H NMR (400 MHz, CD_3CN/DMSO-d_6, 20:1)

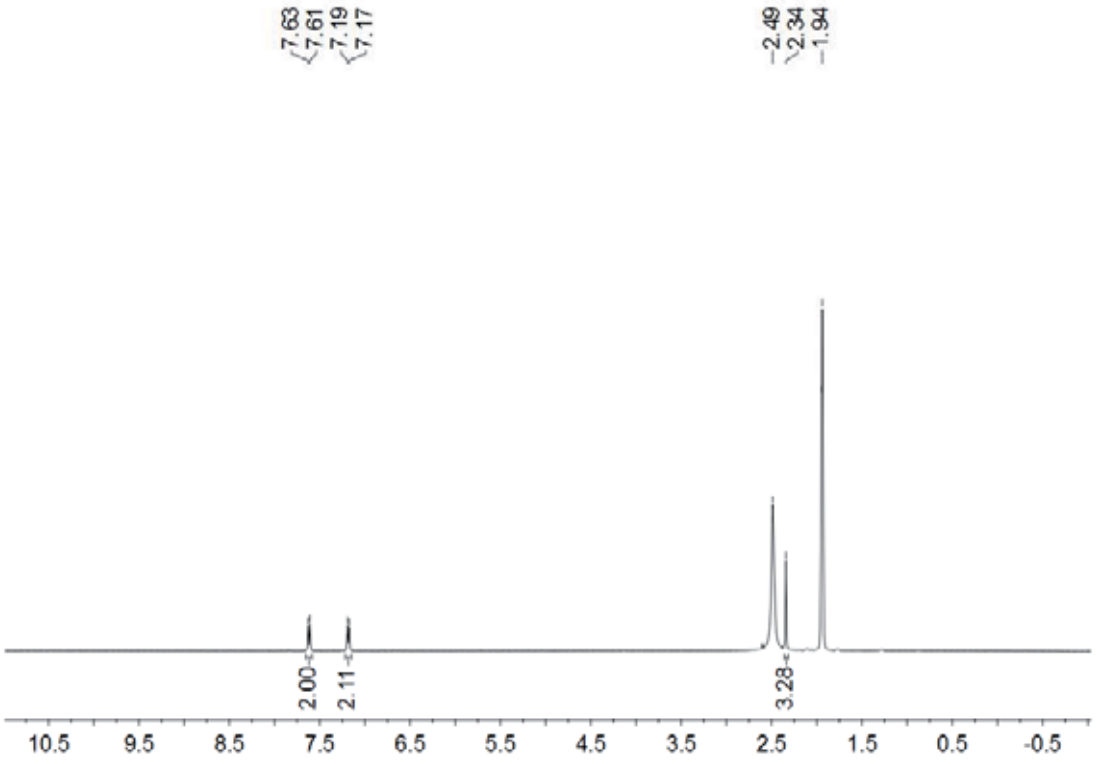

^{19}F NMR ((376 MHz, CD_3CN/DMSO-d_6, 20:1)

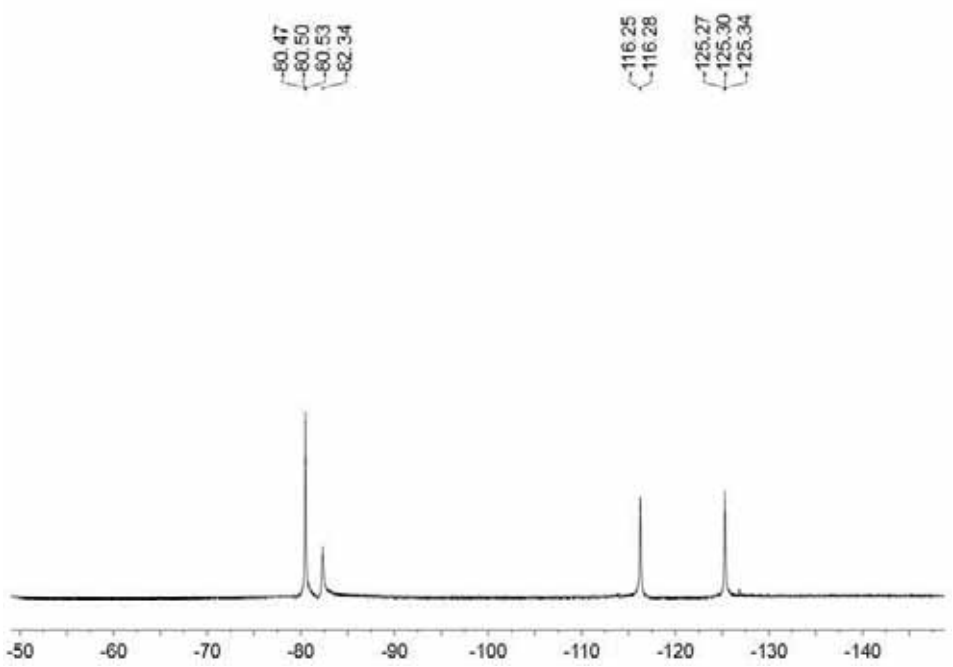

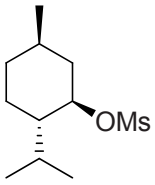

, **27**

^{1}H NMR (360 MHz, $CDCl_3$) δ (ppm)

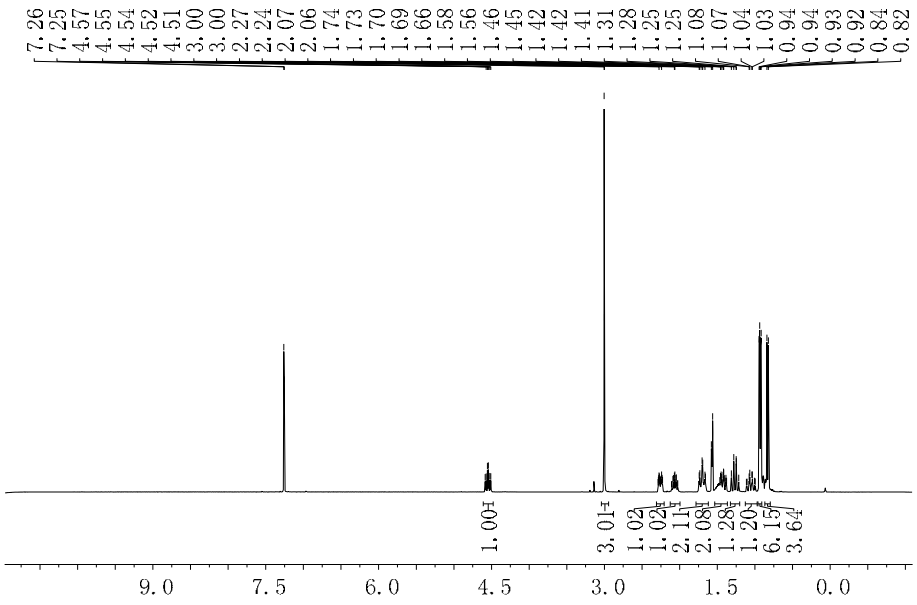

^{13}C NMR (90MHz, $CDCl_3$) δ (ppm):

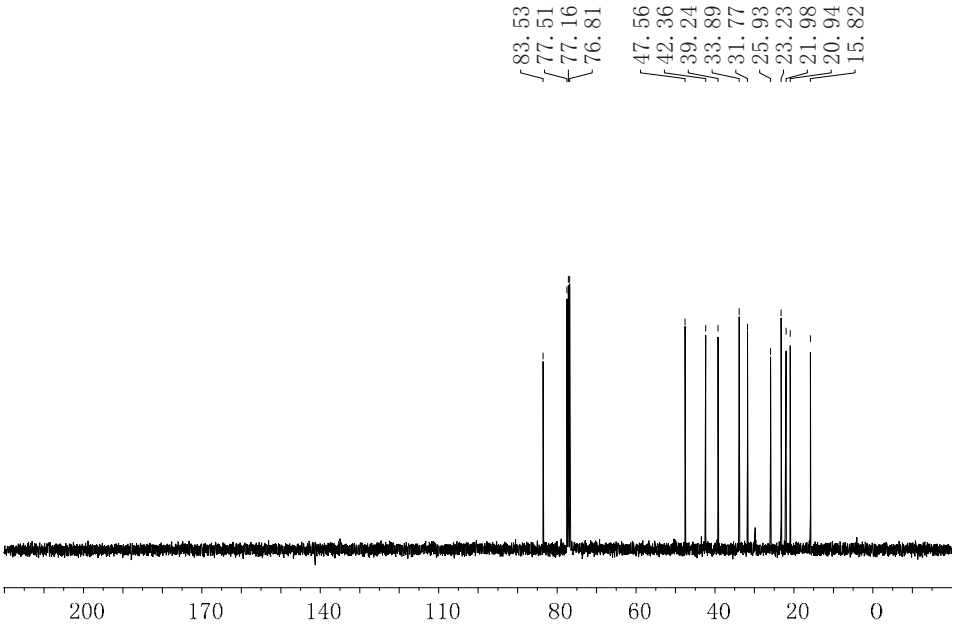

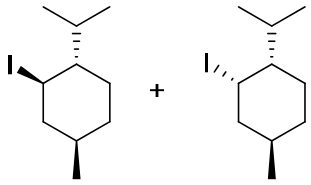

(Mixture of compounds **28** and **29** with a ratio of 10 : 1)

^{1}H NMR (360 MHz, $CDCl_3$)

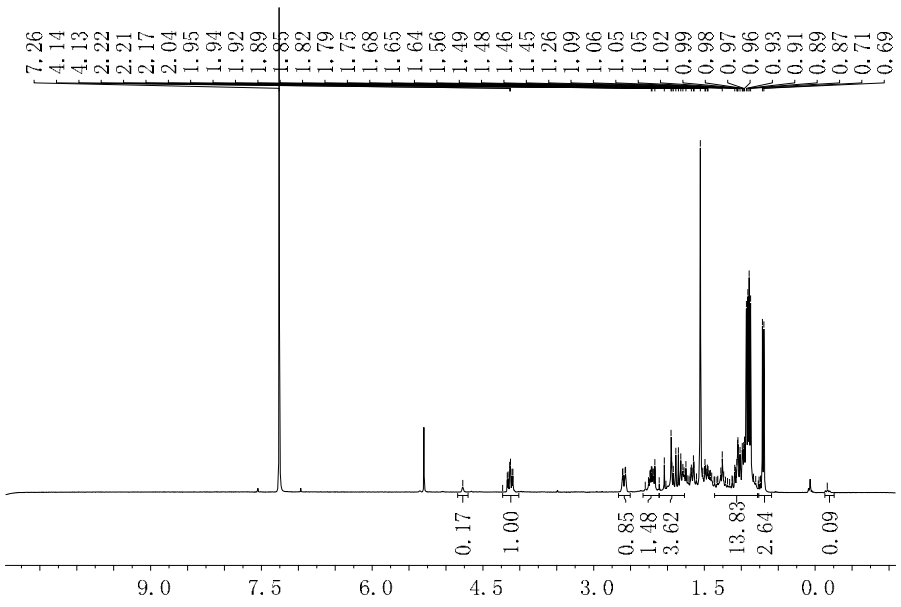

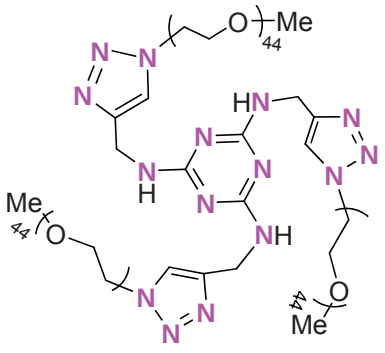

, **30**

^{1}H NMR (360 MHz, $CDCl_3$)

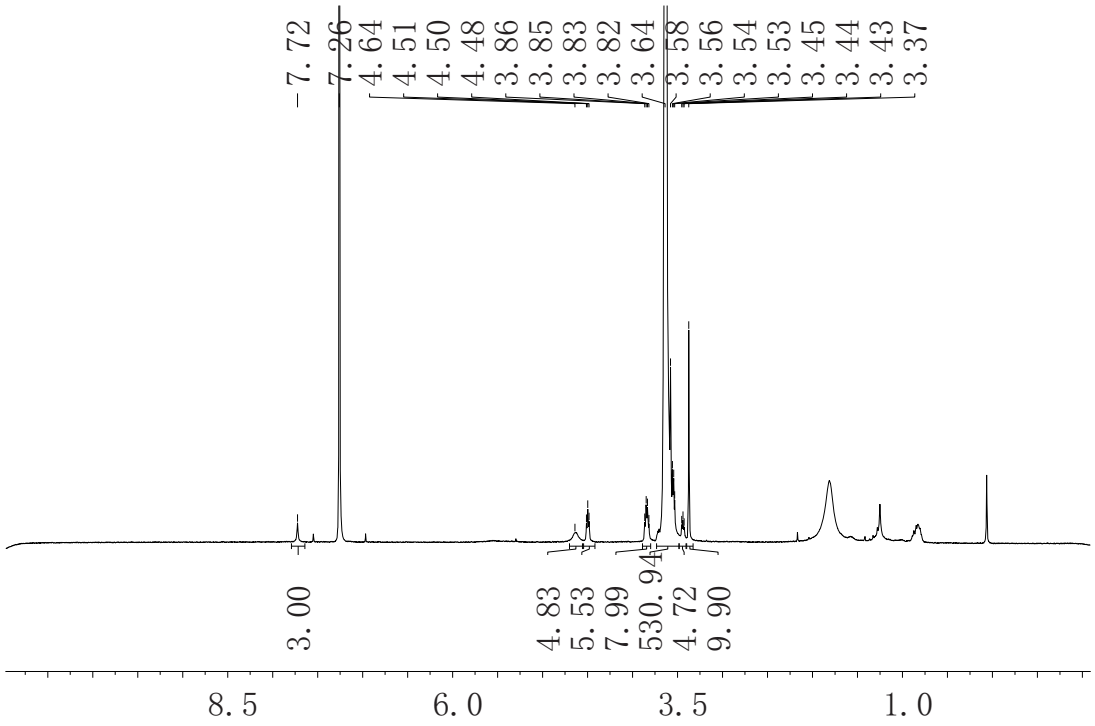

IR (ATR) *v* (cm^{-1})

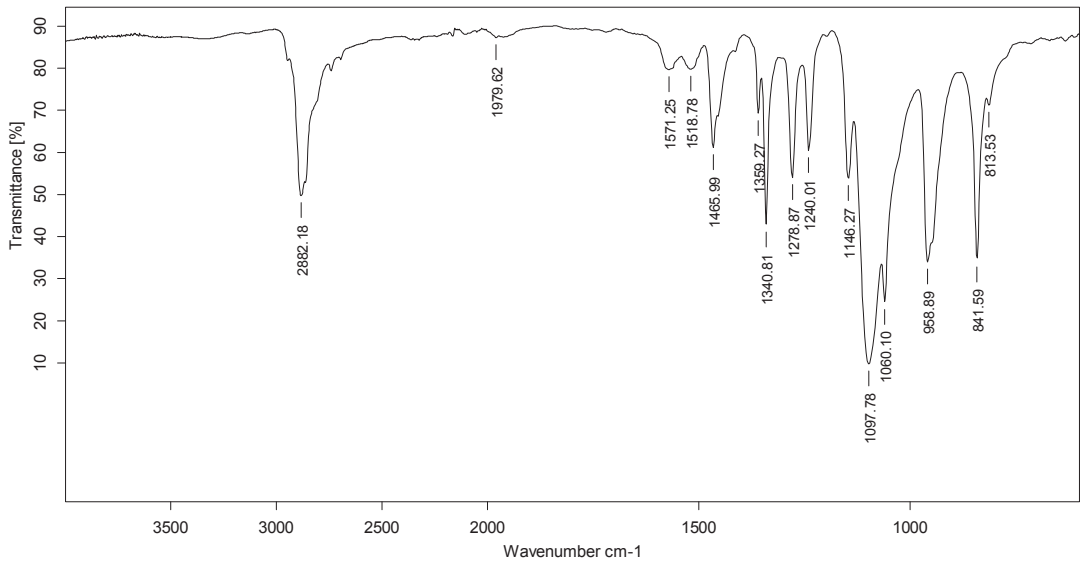

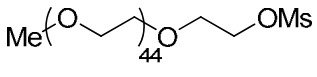

, **31**

^{1}H NMR (360 MHz, $CDCl_3$)

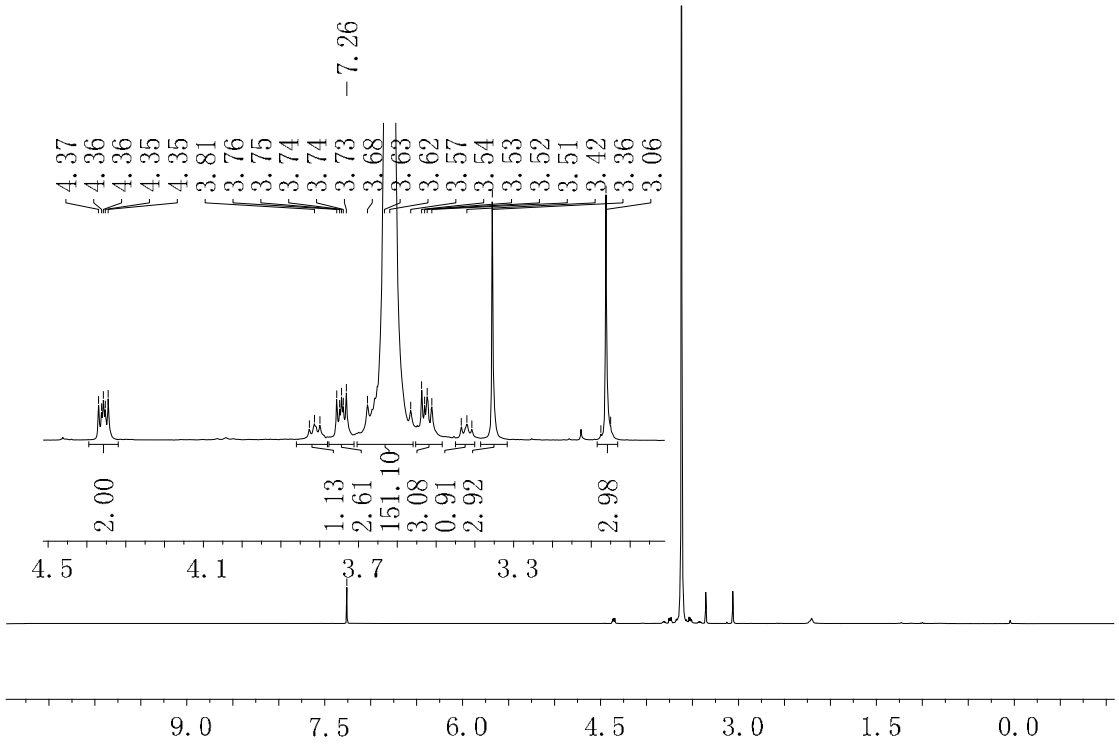

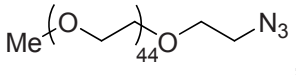

, **32**

^{1}H NMR (360 MHz, $CDCl_3$)

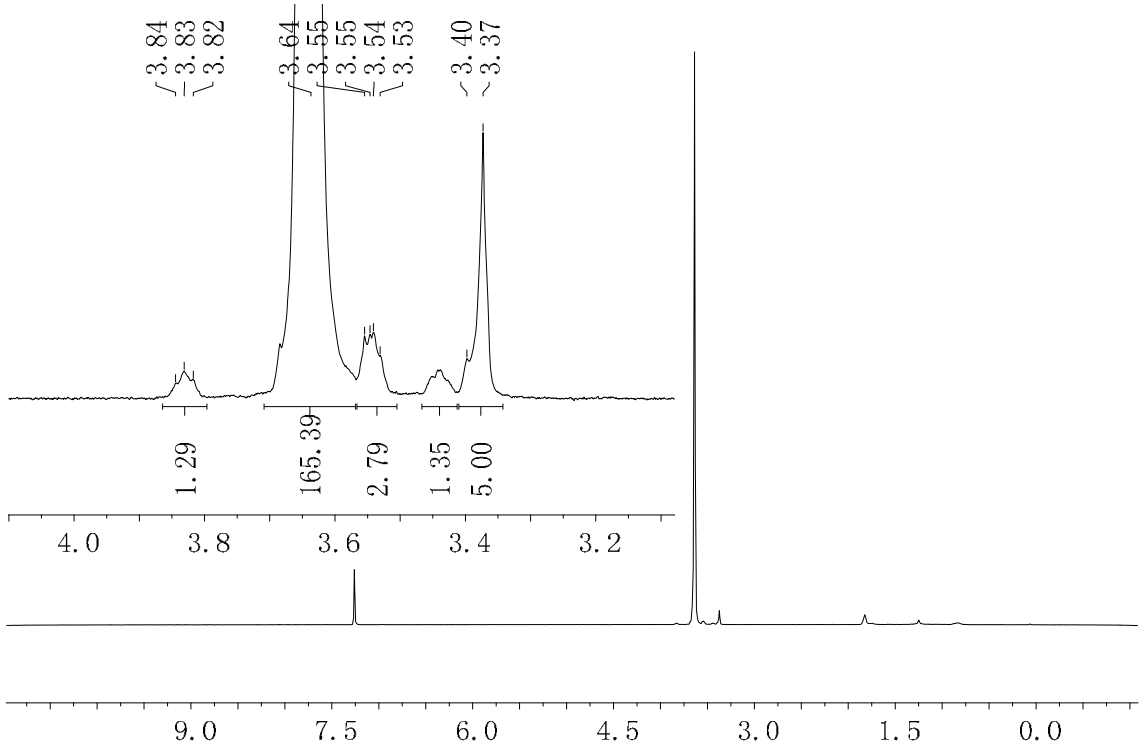

IR (ATR) ν (cm^{-1})

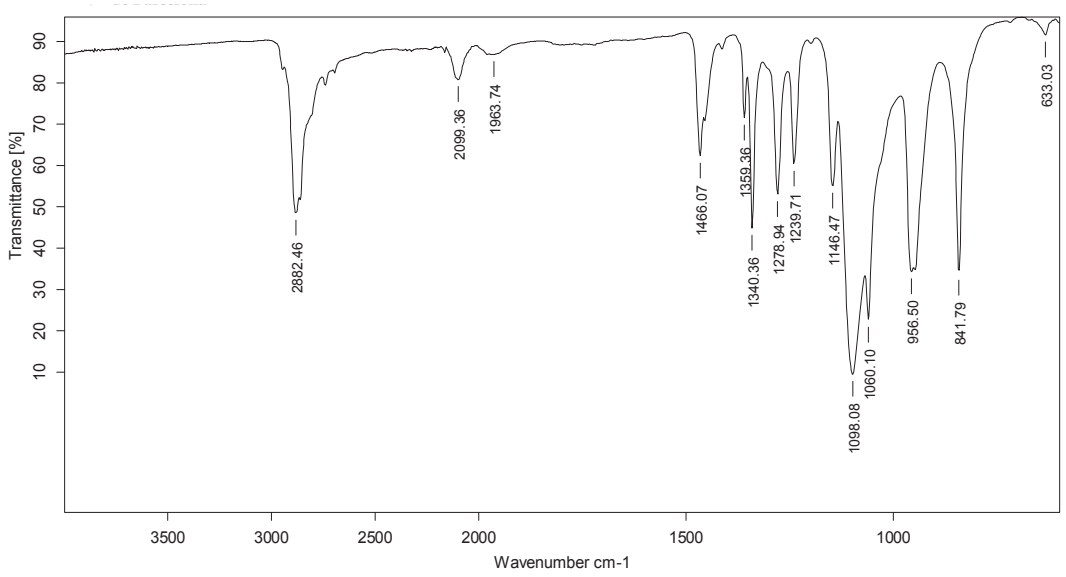

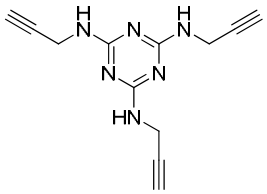

, **33**

^{1}H NMR (360 MHz, $CDCl_3$)

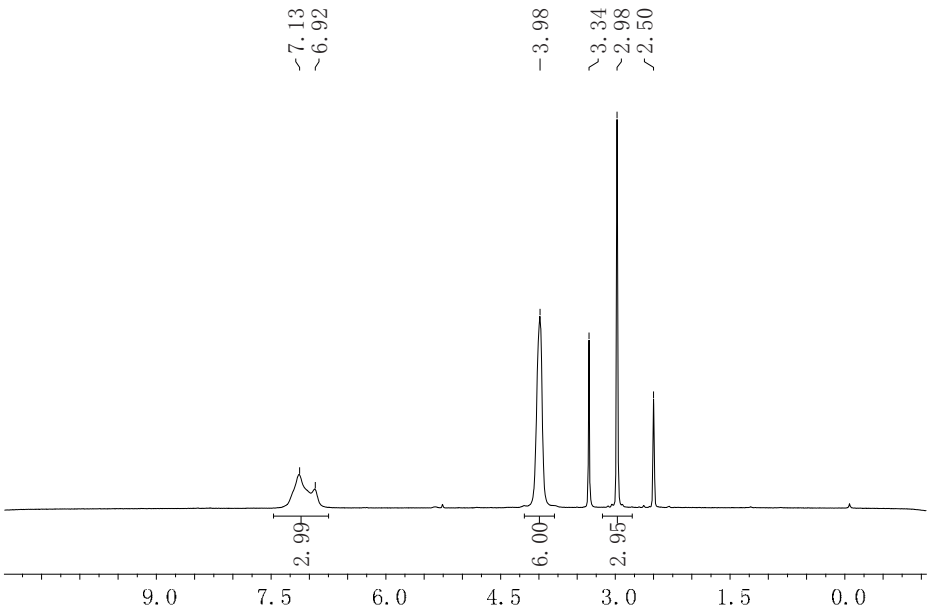

^{13}C NMR (90MHz, $CDCl_3$)

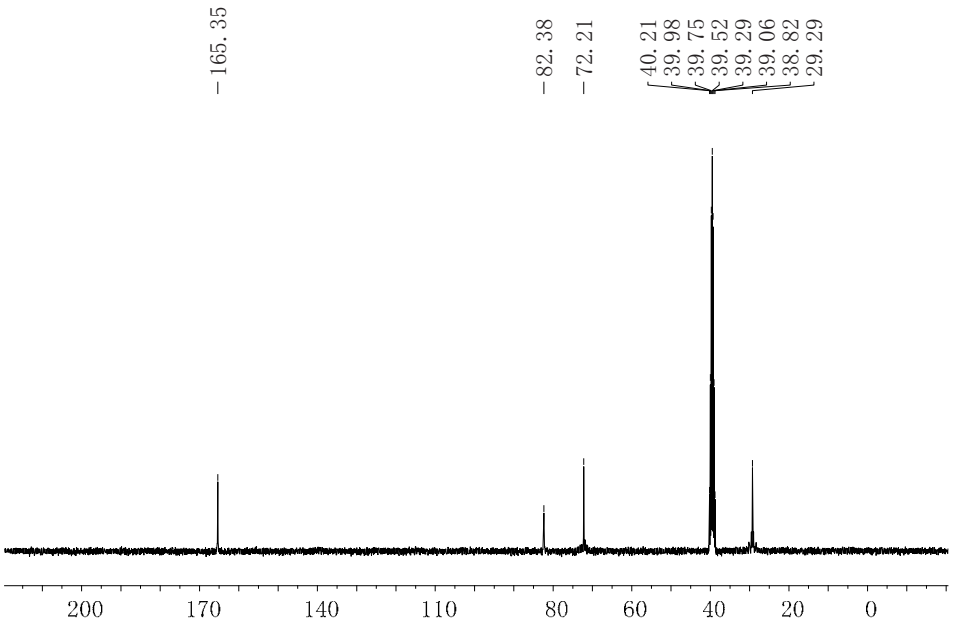

IR (ATR) *v* (cm^{-1})

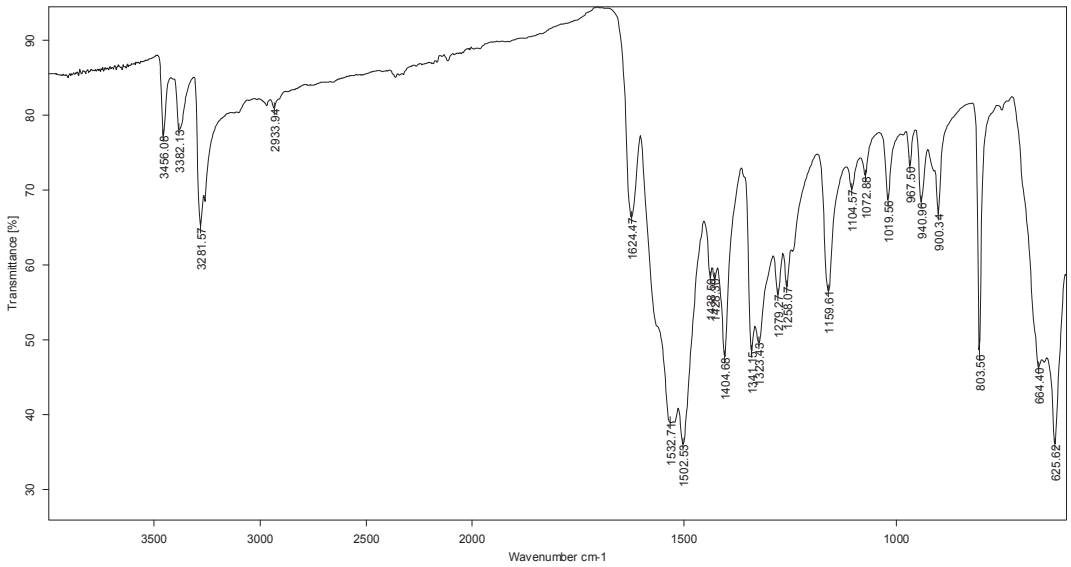

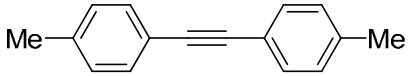

, **34a**

^{1}H NMR (400 MHz, $CDCl_3$)

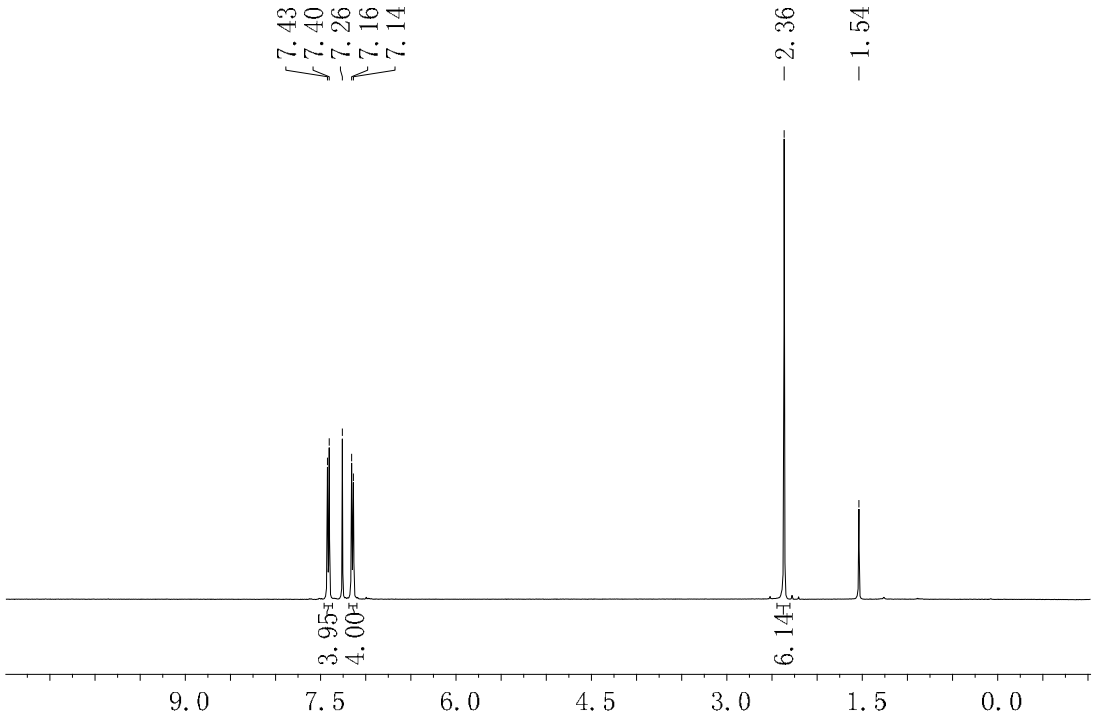

^{13}C NMR (101 MHz, $CDCl_3$)

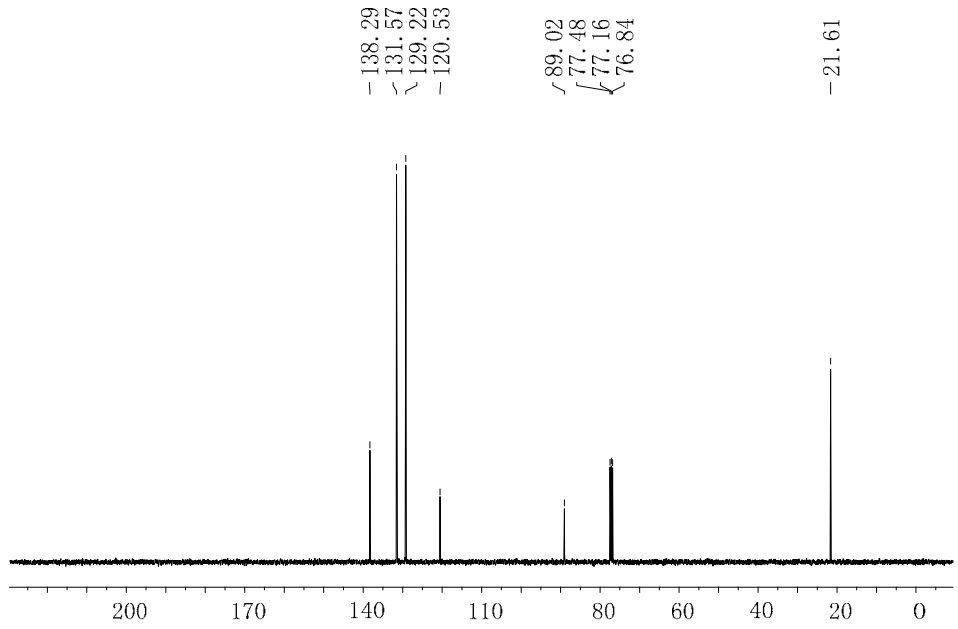

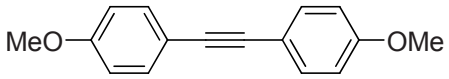

, **34b**

^{1}H NMR (400 MHz, $CDCl_3$)

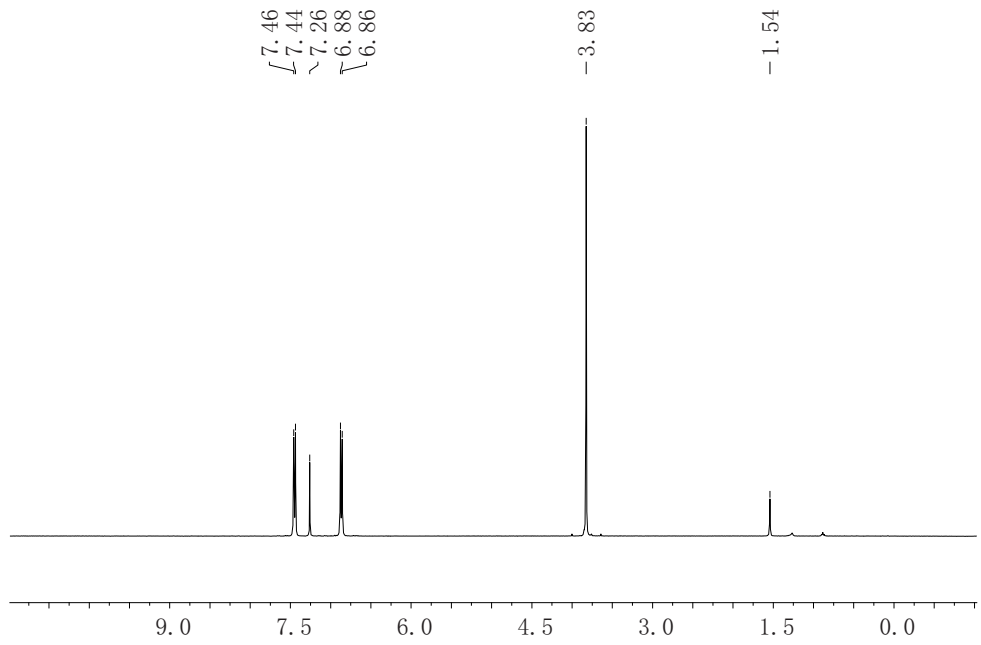

^{13}C NMR (101 MHz, $CDCl_3$)

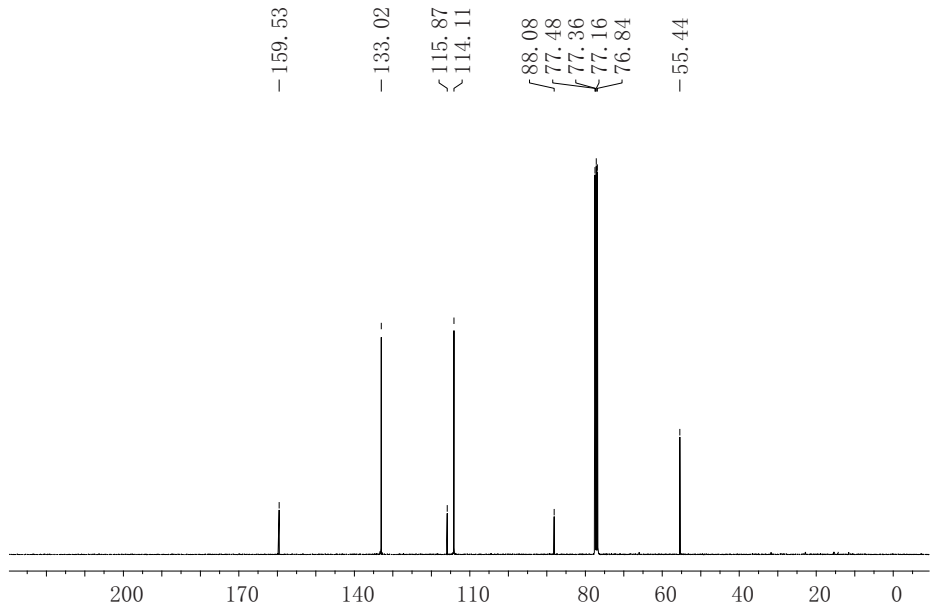

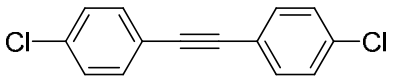

, **34c**

^{1}H NMR (360 MHz, $CDCl_3$)

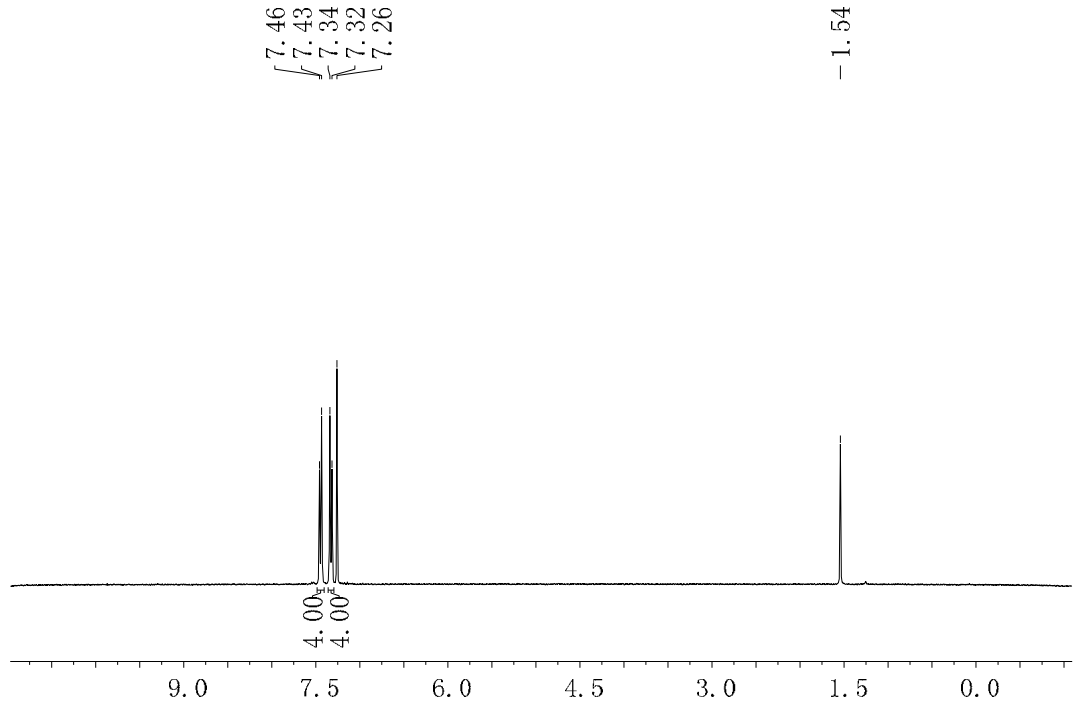

^{13}C NMR (101 MHz, $CDCl_3$)

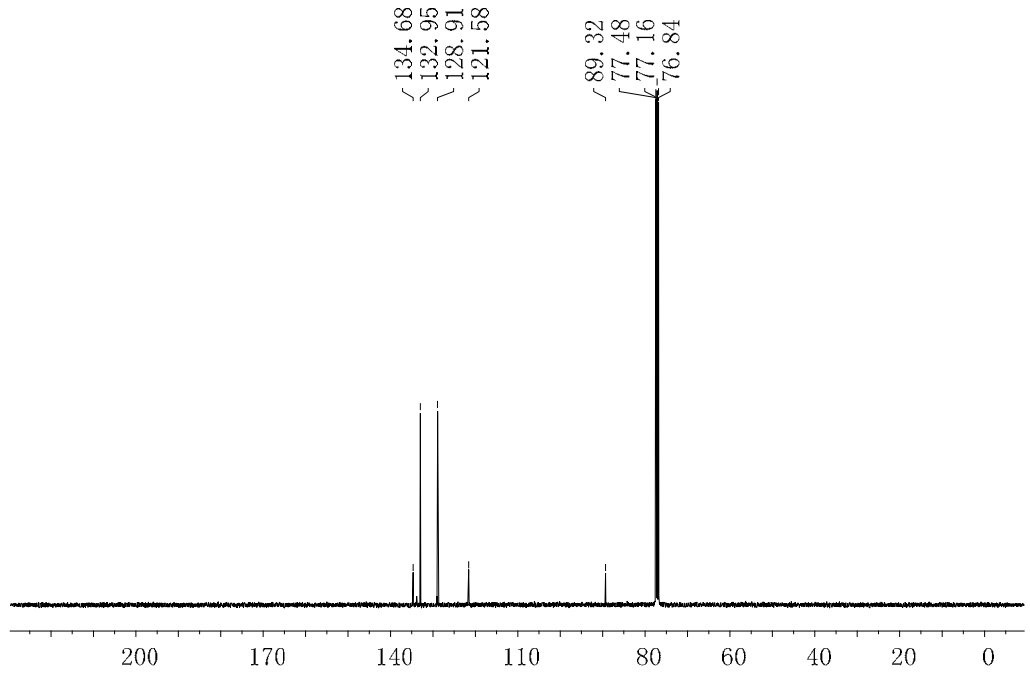

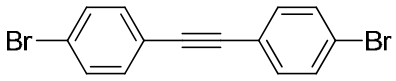

, **34d**

^{1}H NMR (360 MHz, $CDCl_3$)

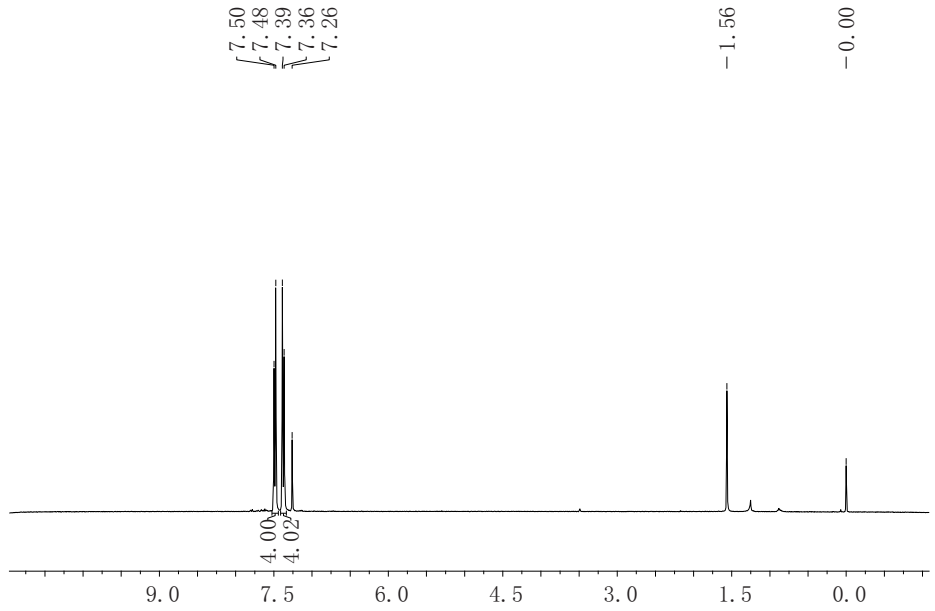

^{13}C NMR (90 MHz, $CDCl_3$)

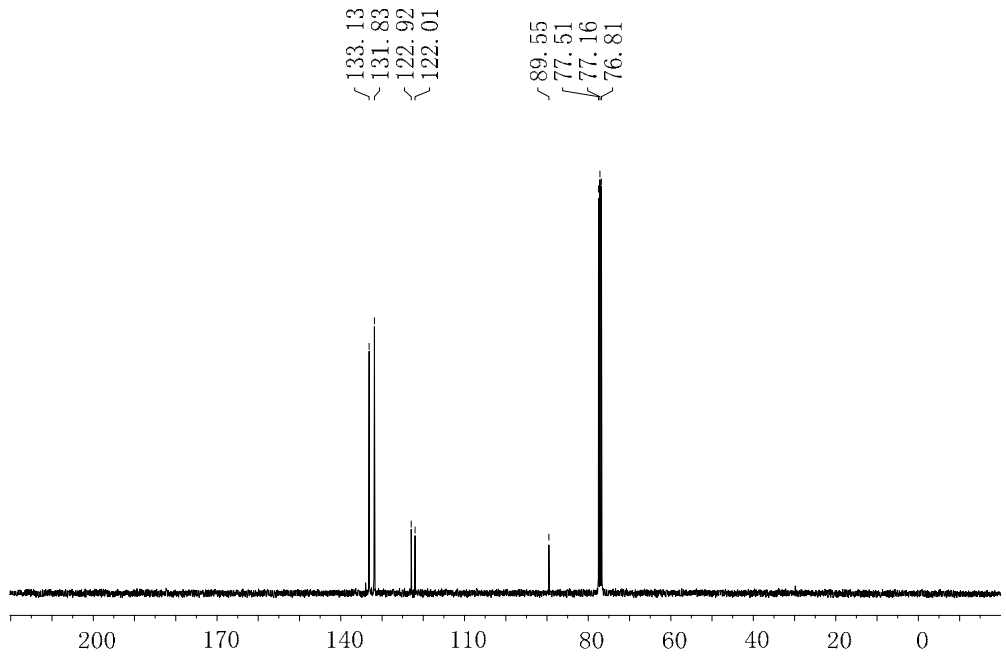

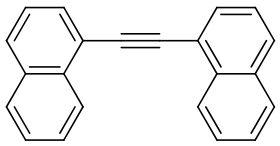

, 34e

^{1}H NMR (400 MHz, $CDCl_3$)

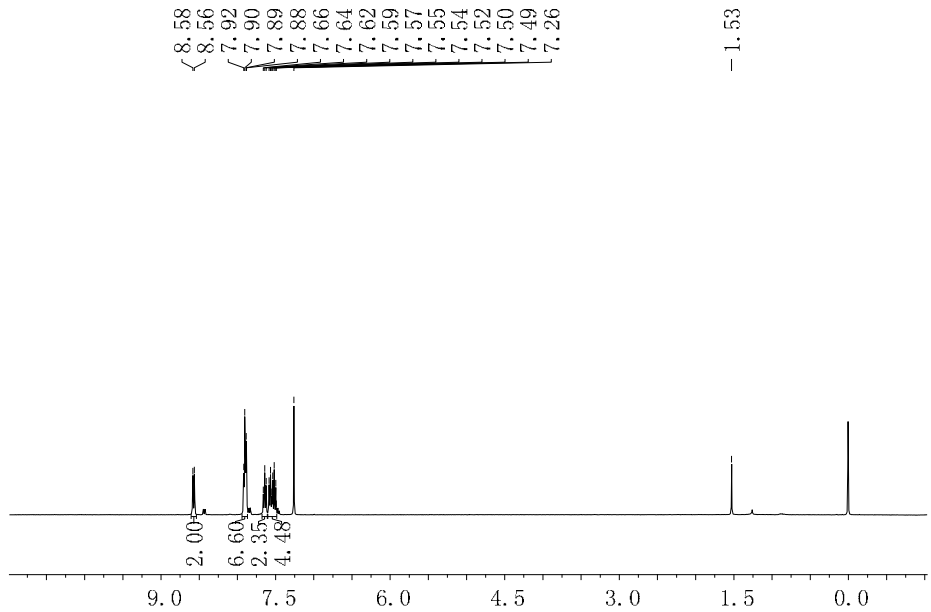

^{13}C NMR (101 MHz, $CDCl_3$)

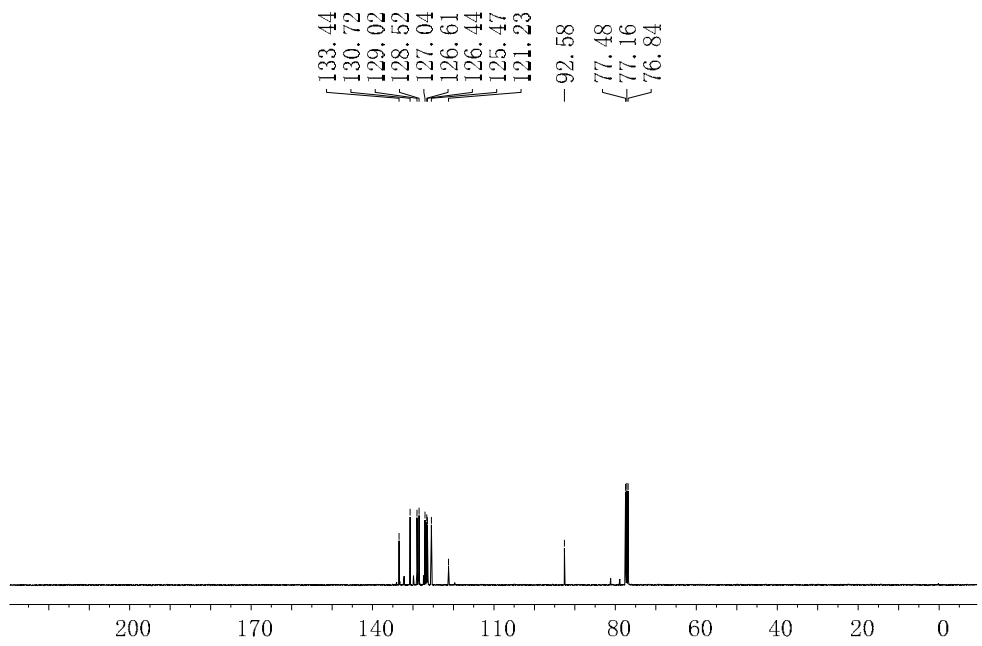

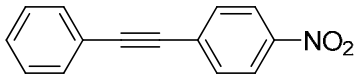

, **35f**

^{1}H NMR (400 MHz, $CDCl_3$)

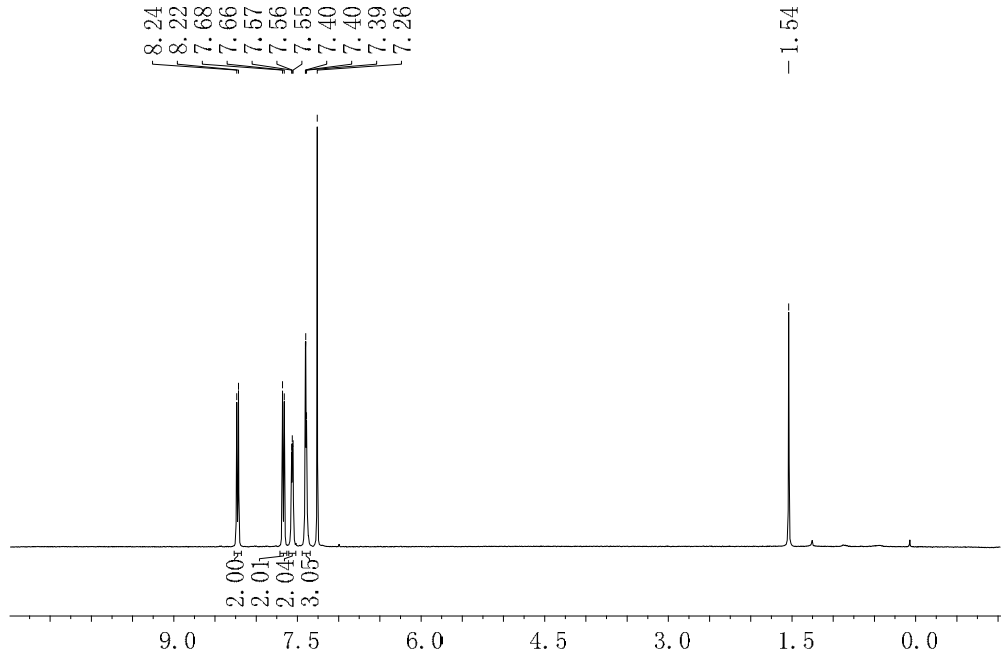

^{13}C NMR (101 MHz, $CDCl_3$)

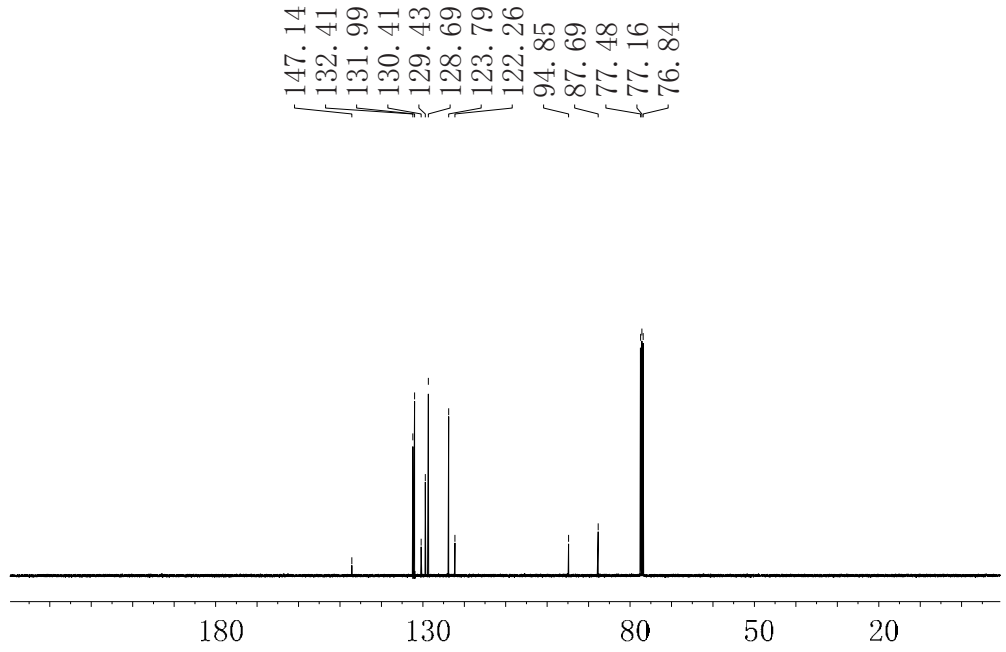

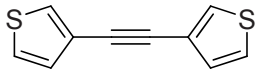

, **35g**

^{1}H NMR (400 MHz, $CDCl_3$)

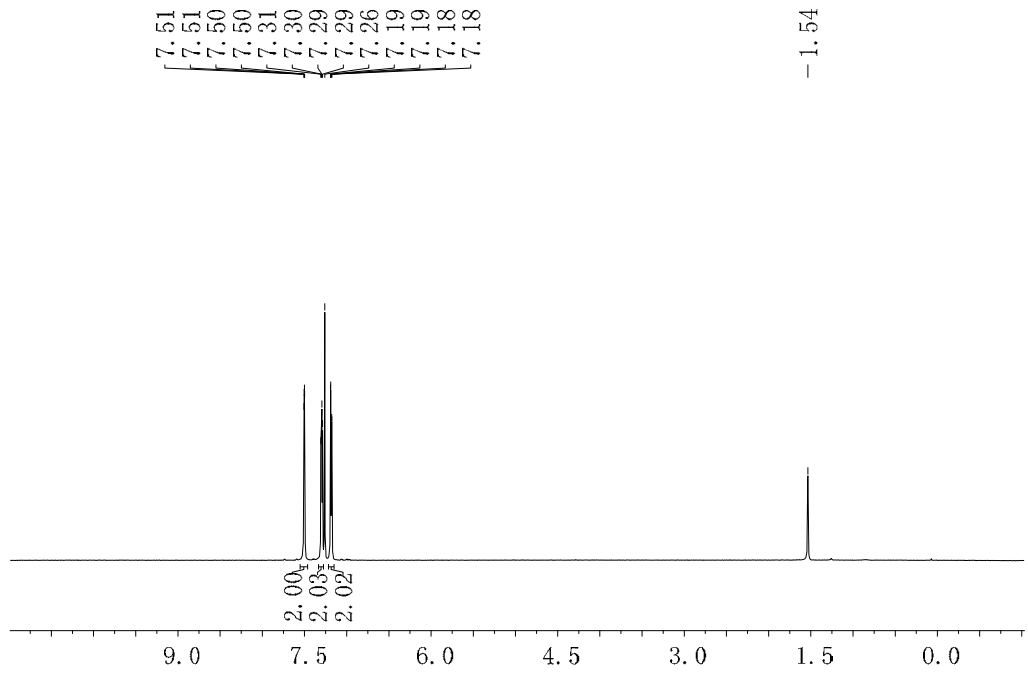

^{13}C NMR (101 MHz, $CDCl_3$)

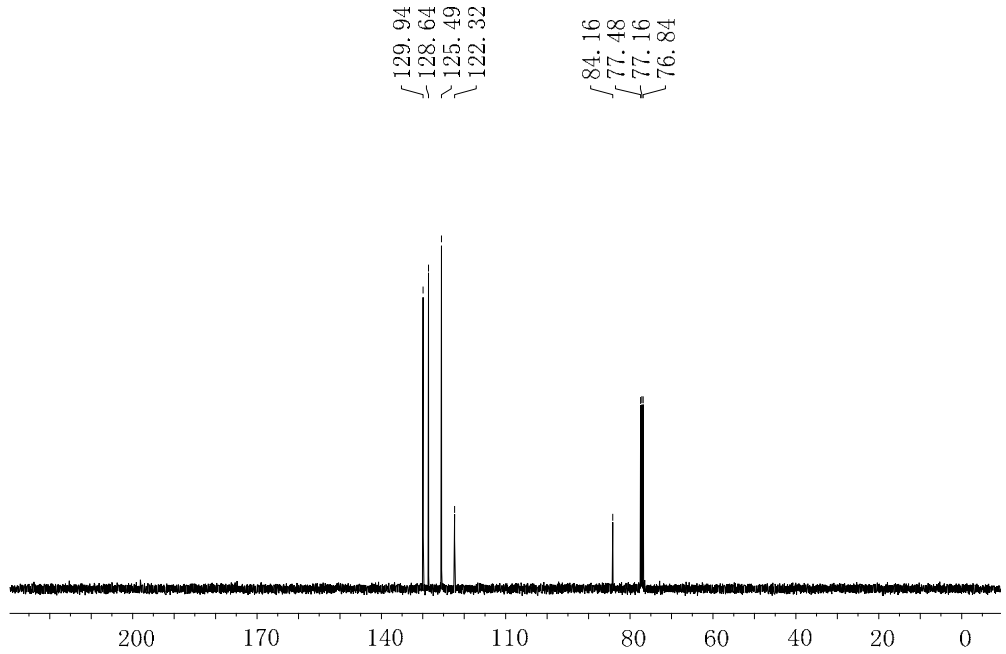

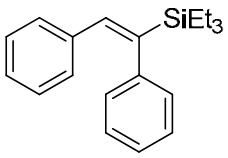

, **36a**

^{1}H NMR (360 MHz, $CDCl_3$) δ (ppm)

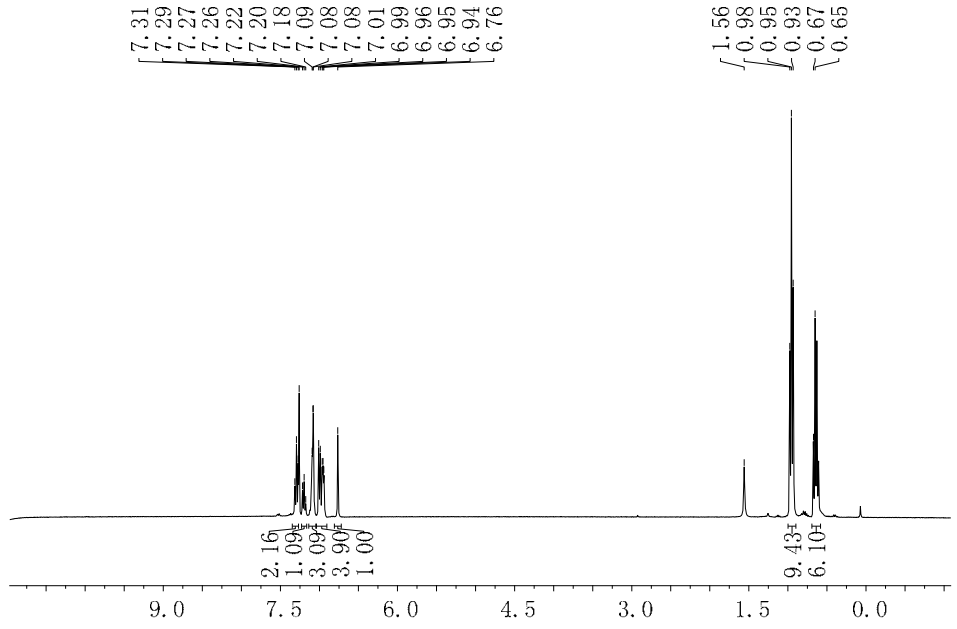

^{13}C NMR (90 MHz, $CDCl_3$)

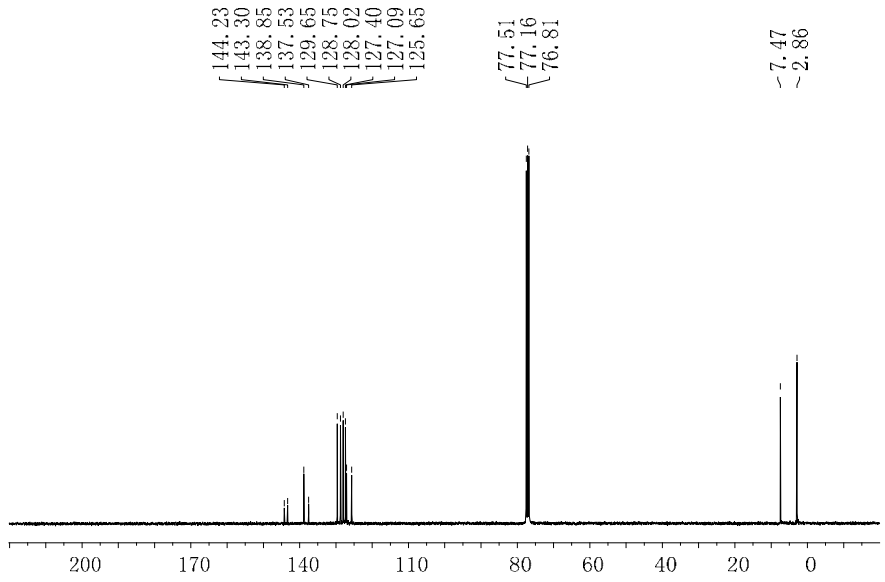

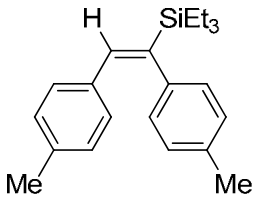

36b

^{1}H NMR (400 MHz, $CDCl_3$) δ (ppm)

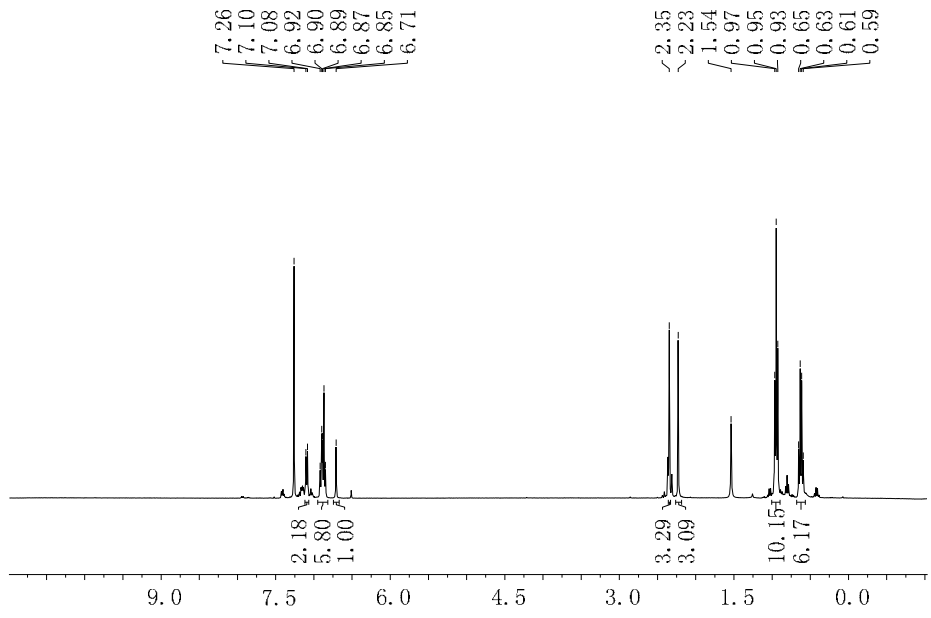

^{13}C NMR (100 MHz, $CDCl_3$)

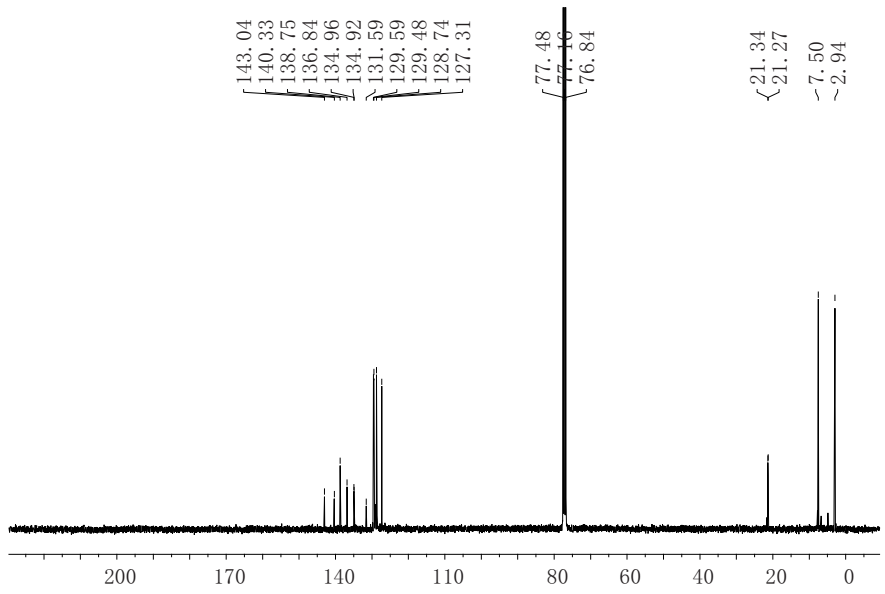

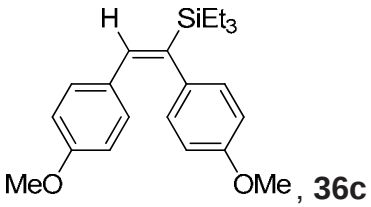

36c

^{1}H NMR (400 MHz, $CDCl_3$) δ (ppm)

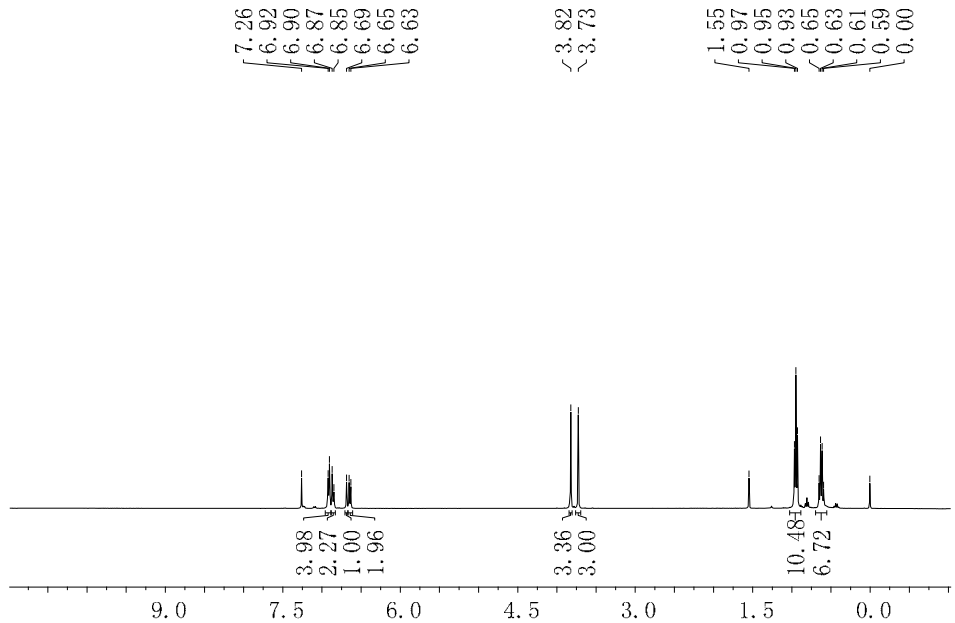

^{13}C NMR (100 MHz, $CDCl_3$)

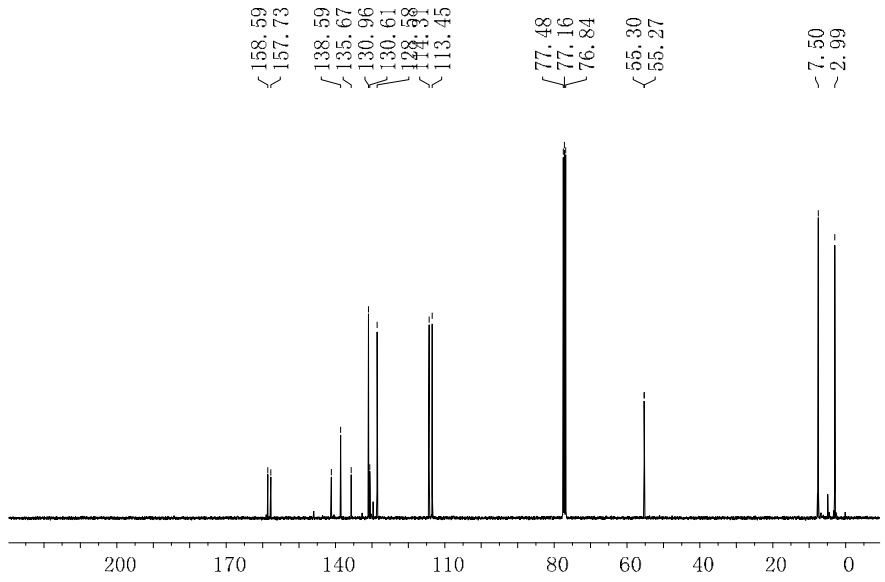

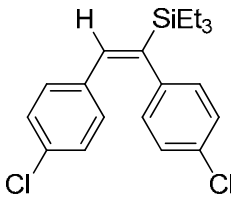

36d

^{1}H NMR (400 MHz, $CDCl_3$) δ (ppm)

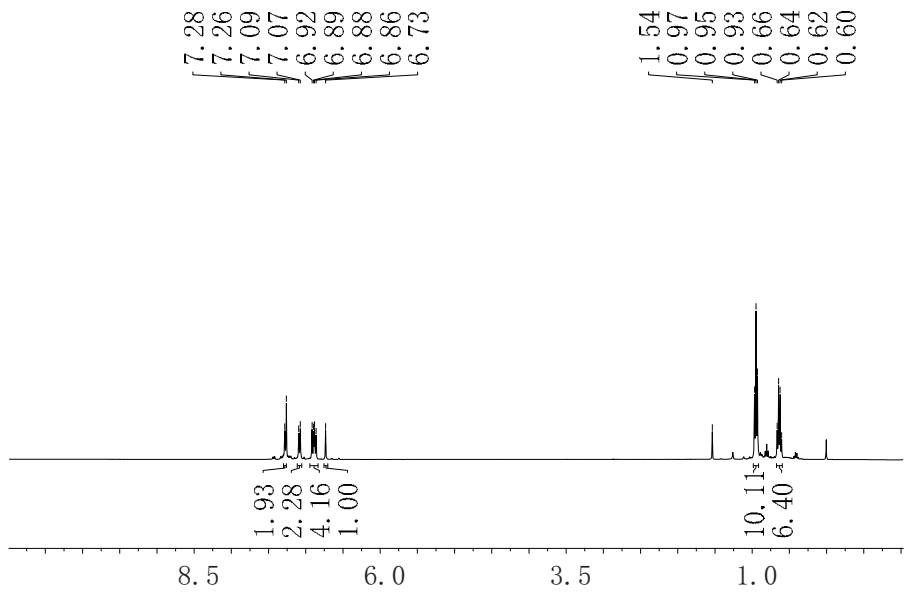

^{13}C NMR (100 MHz, $CDCl_3$)

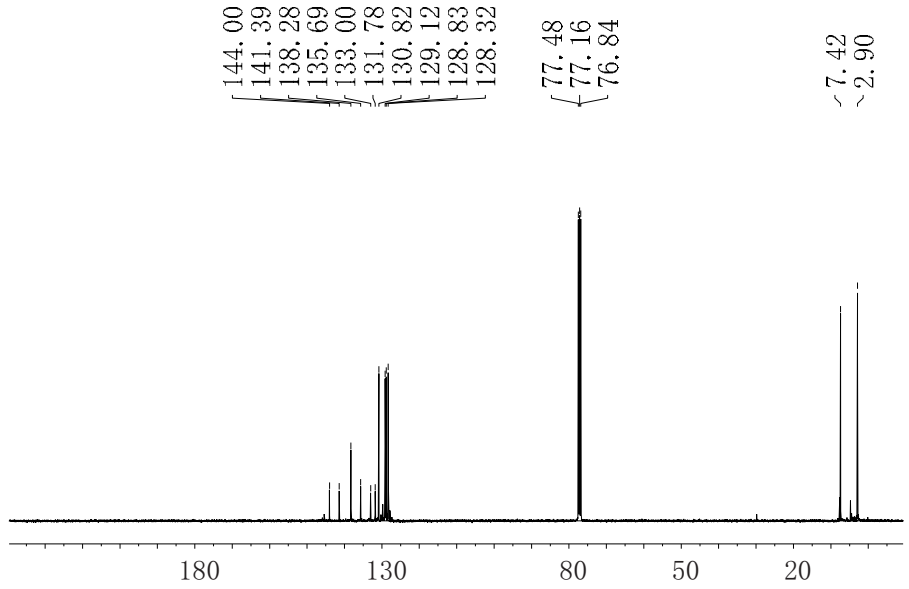

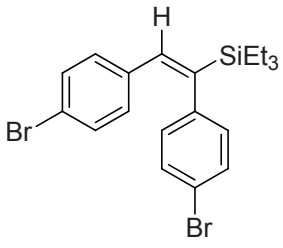

, **36e**

^{1}H NMR (400 MHz, $CDCl_3$) δ (ppm)

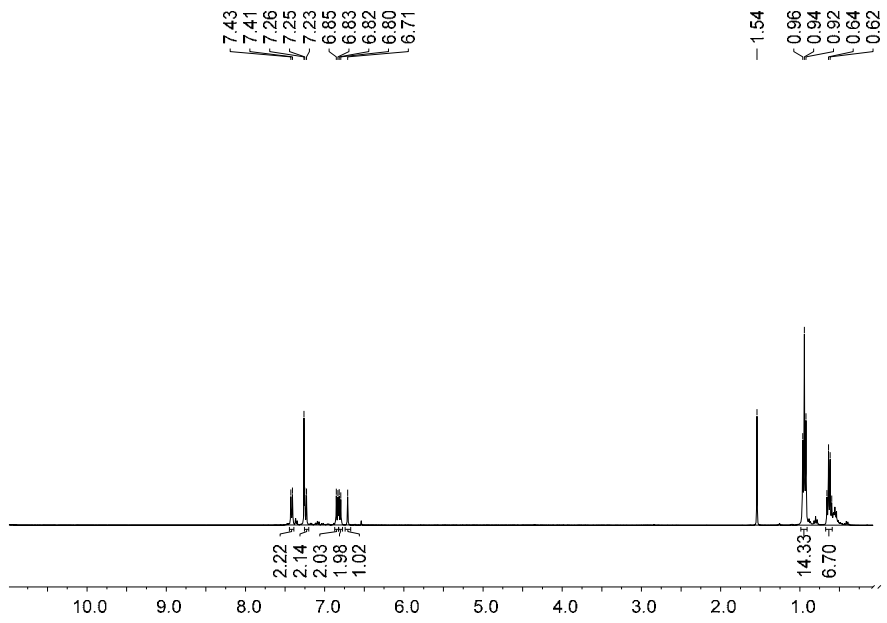

^{13}C NMR (100 MHz, $CDCl_3$)

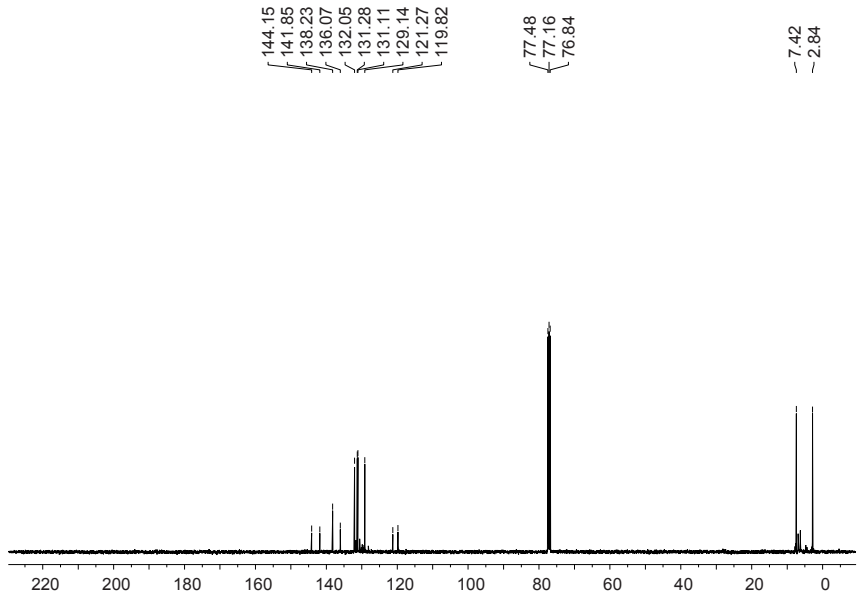

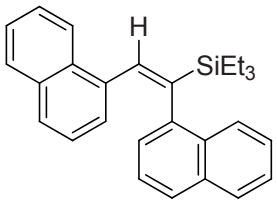

, **37**

^{1}H NMR (360 MHz, $CDCl_3$) δ (ppm)

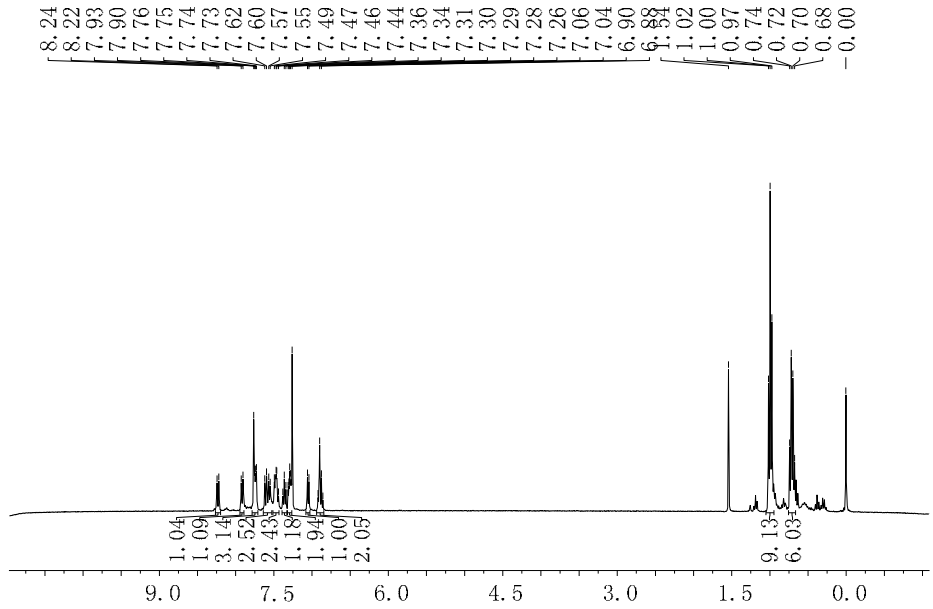

^{13}C NMR (90 MHz, $CDCl_3$)

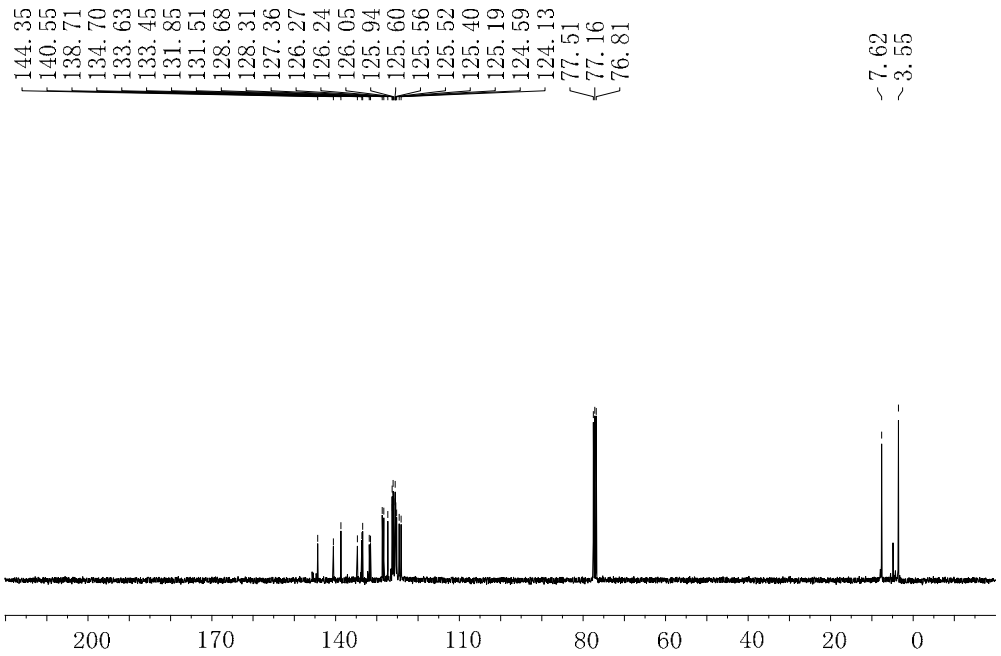

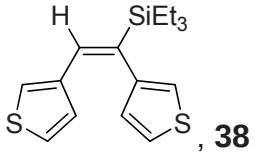

, **38**

^{1}H NMR (400 MHz, $CDCl_3$) δ (ppm)

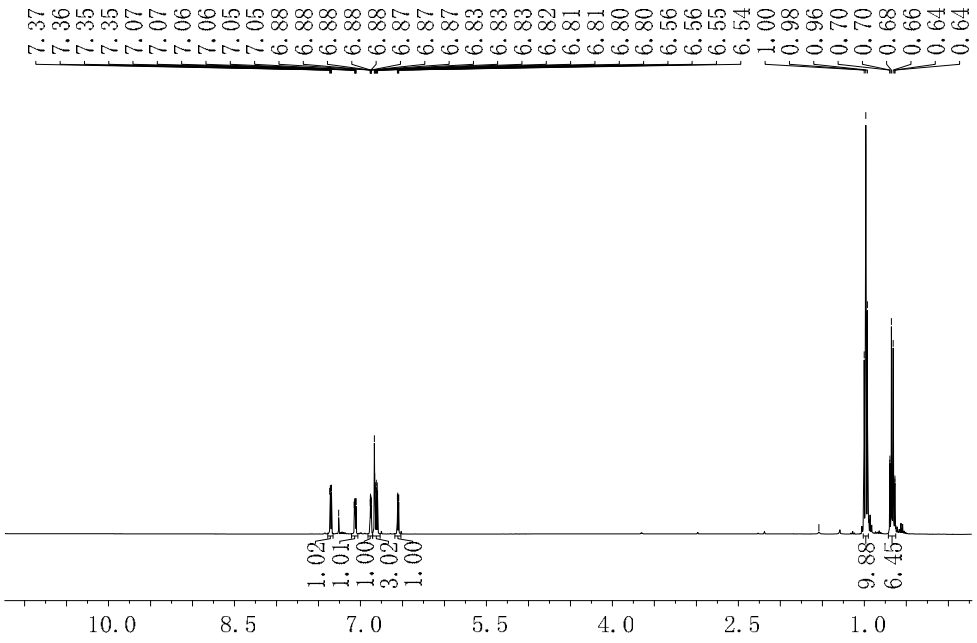

^{13}C NMR (100 MHz, $CDCl_3$)

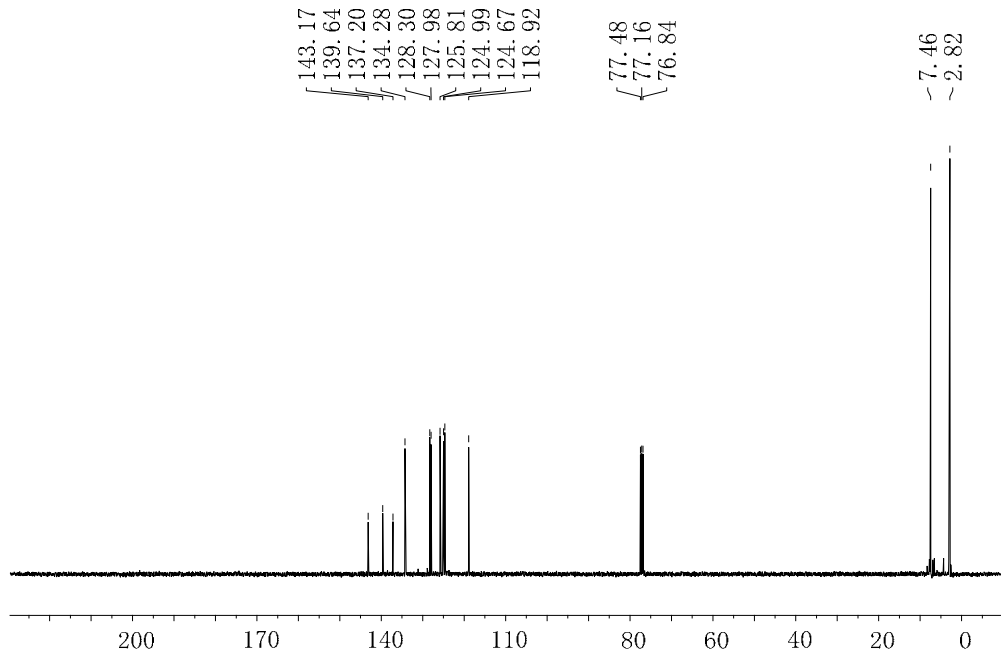

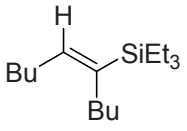

, **39**

^{1}H NMR (360 MHz, $CDCl_3$) δ (ppm)

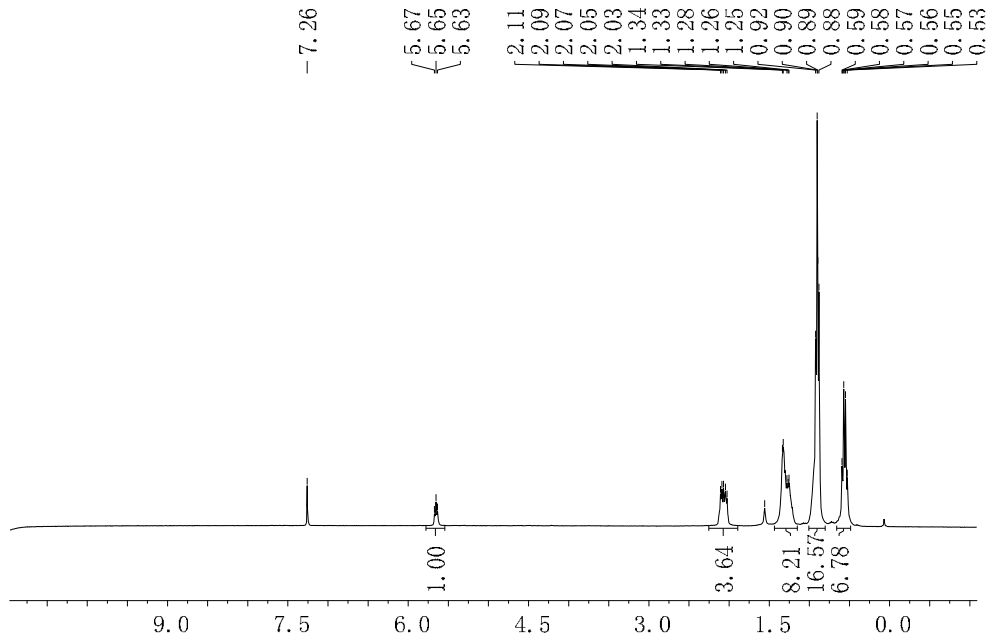

^{13}C NMR (90 MHz, $CDCl_3$)

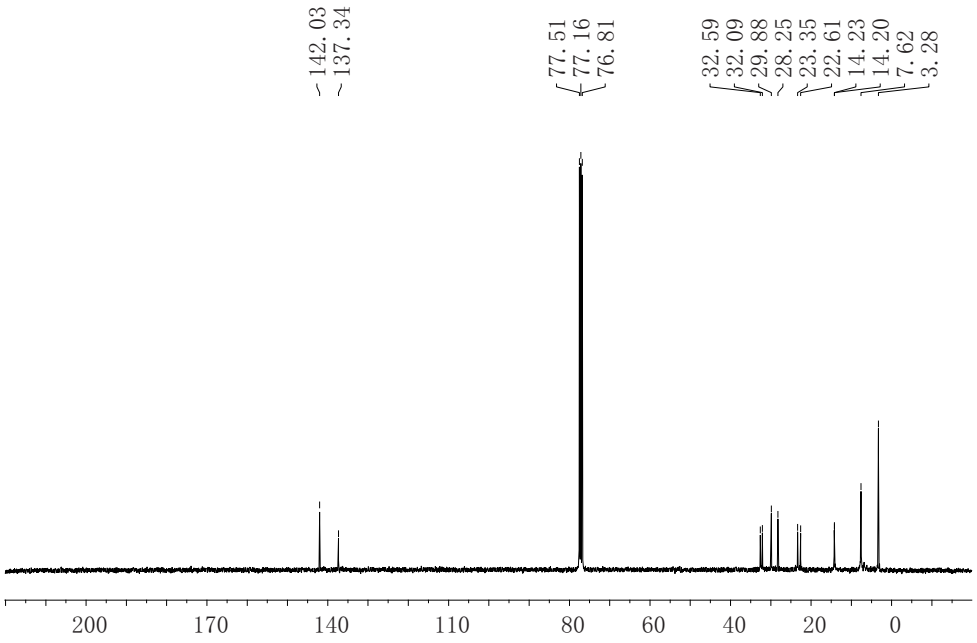

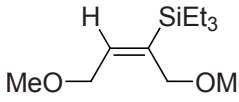

, **40**

^{1}H NMR (360 MHz, $CDCl_3$) δ (ppm)

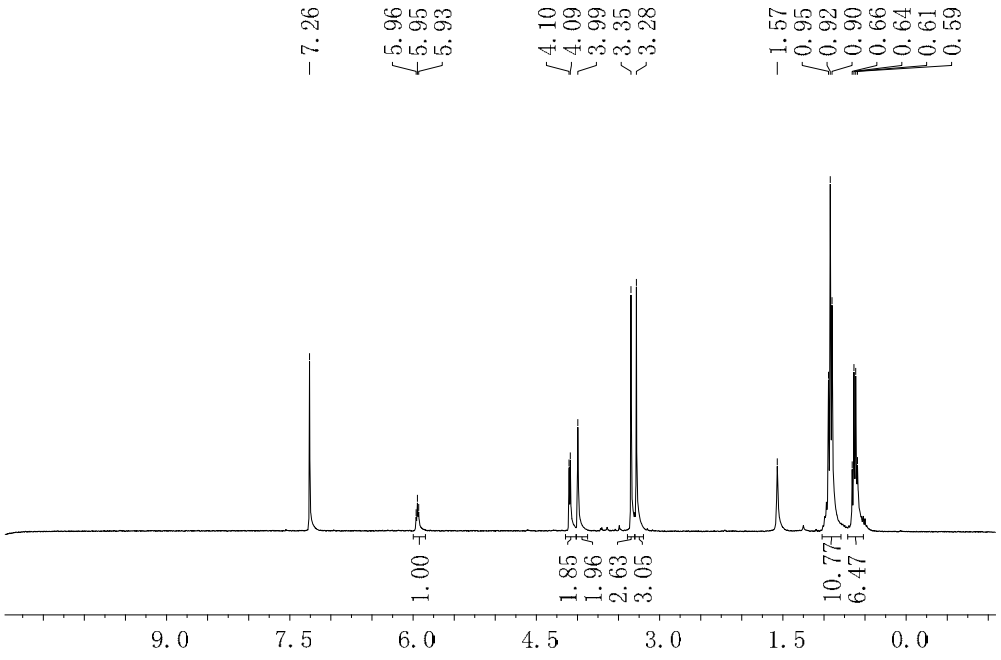

^{13}C NMR (90 MHz, $CDCl_3$)

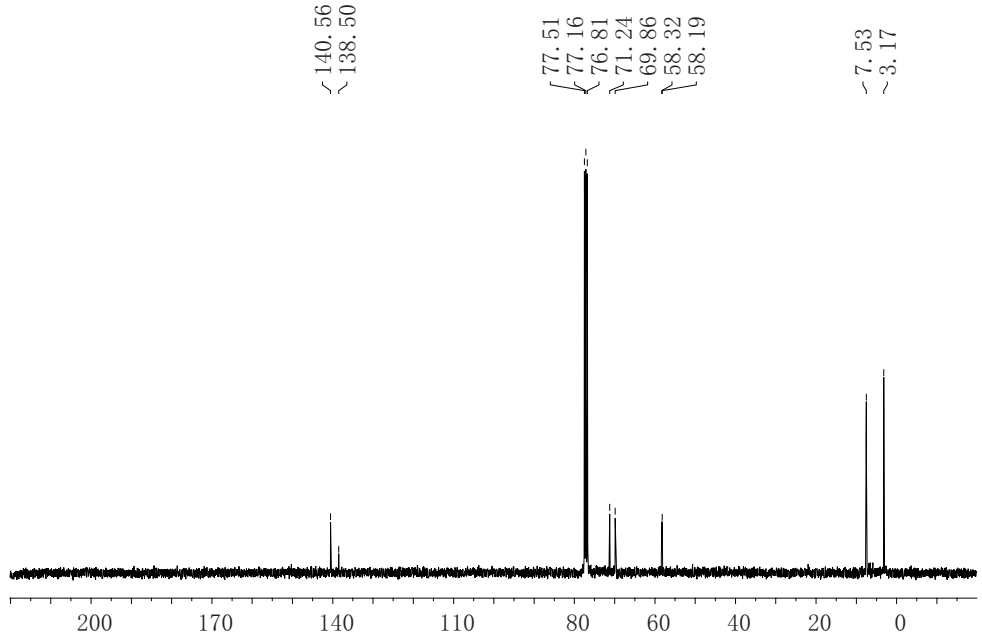

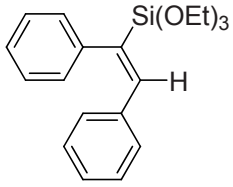

, **41a**

^{1}H NMR (360 MHz, $CDCl_3$) δ (ppm)

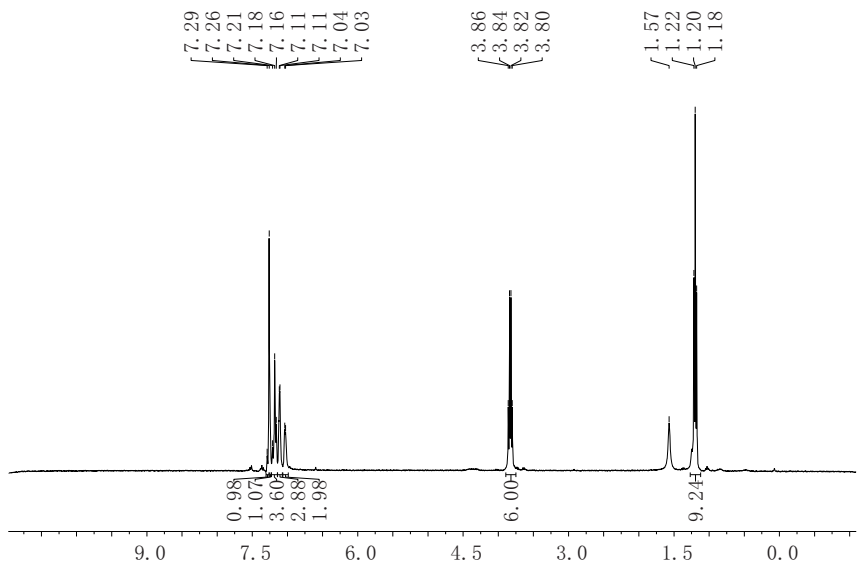

^{13}C NMR (90 MHz, $CDCl_3$)

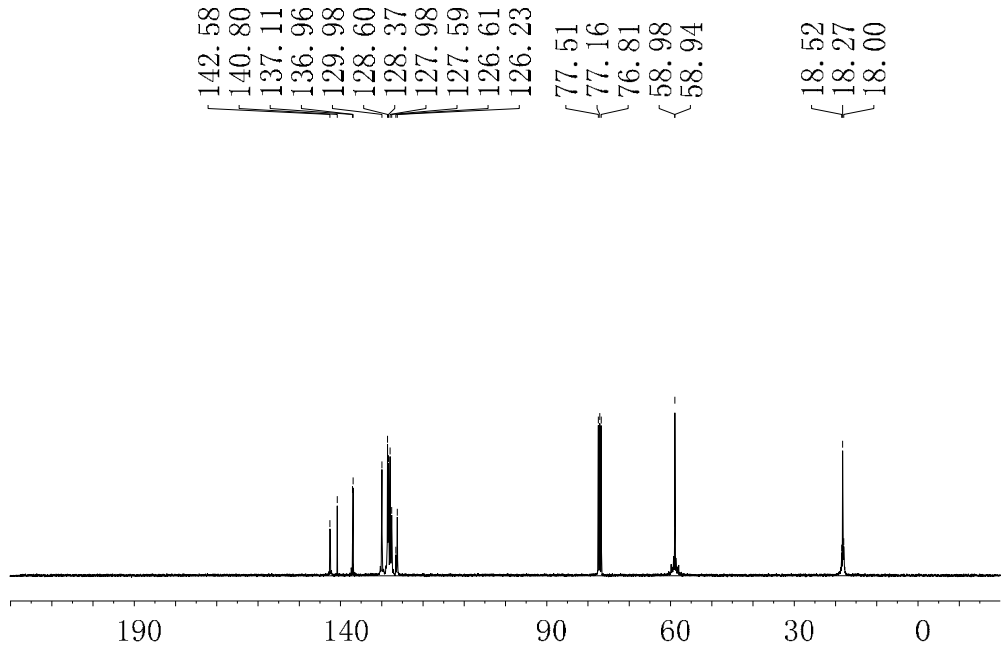

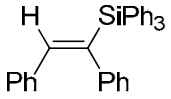

, **41b**

^{1}H NMR (250 MHz, $CDCl_3$) δ (ppm)

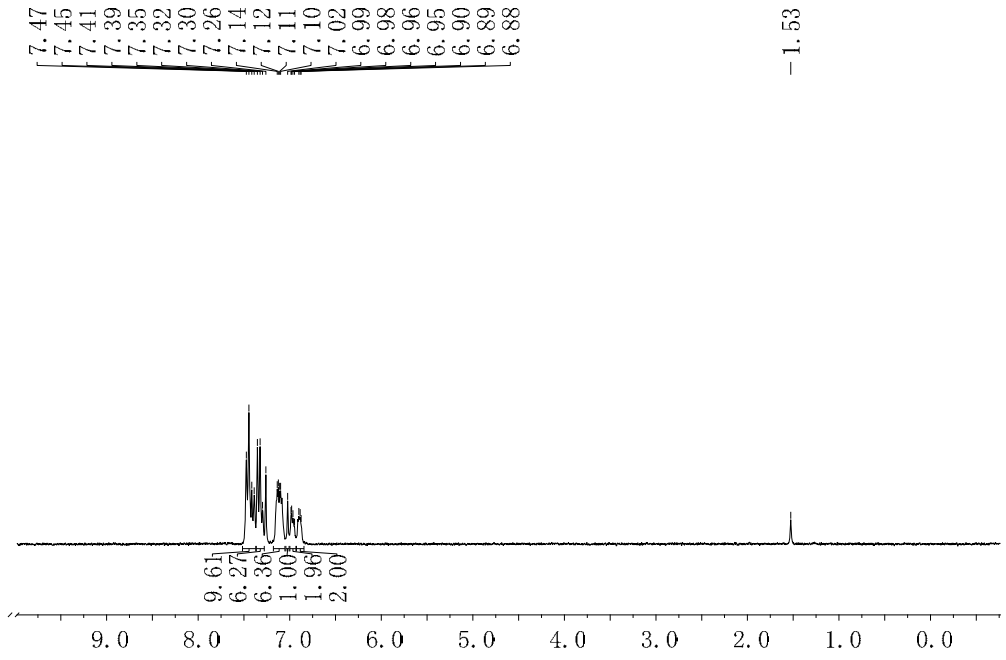

^{13}C NMR (100 MHz, $CDCl_3$)

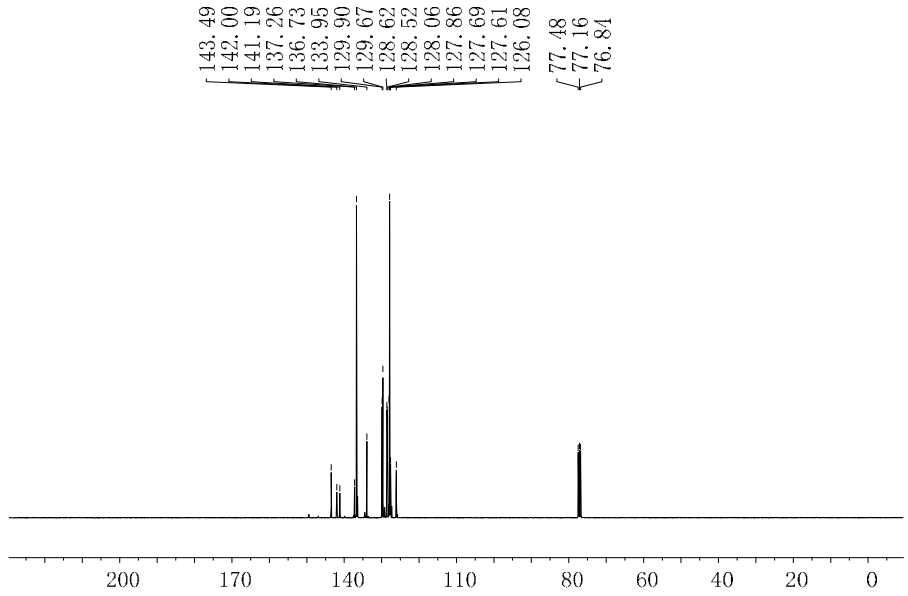

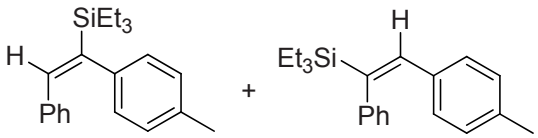

42a (42%) **43a** (58%)

^{1}H NMR (360 MHz, $CDCl_3$) δ (ppm)

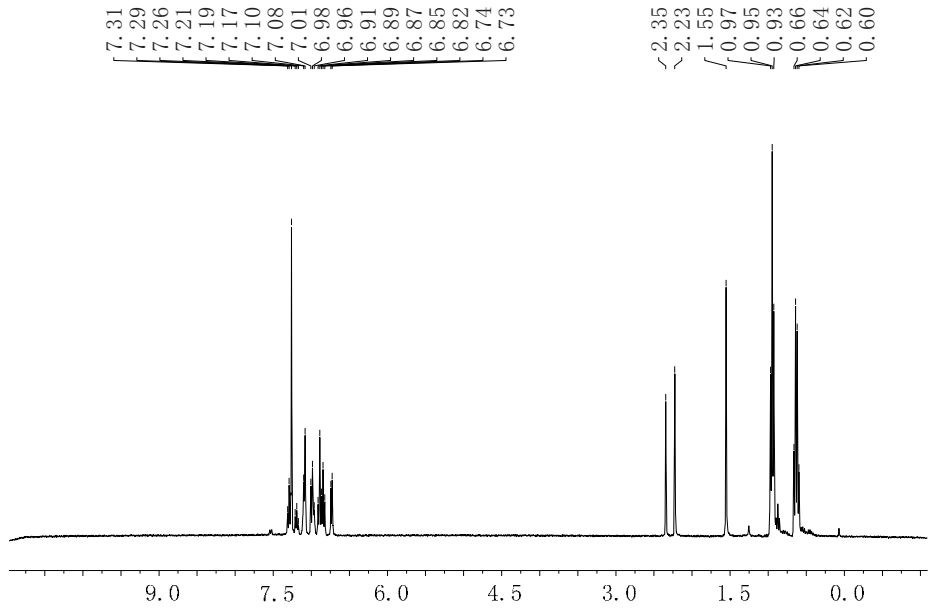

^{13}C NMR (90 MHz, $CDCl_3$)

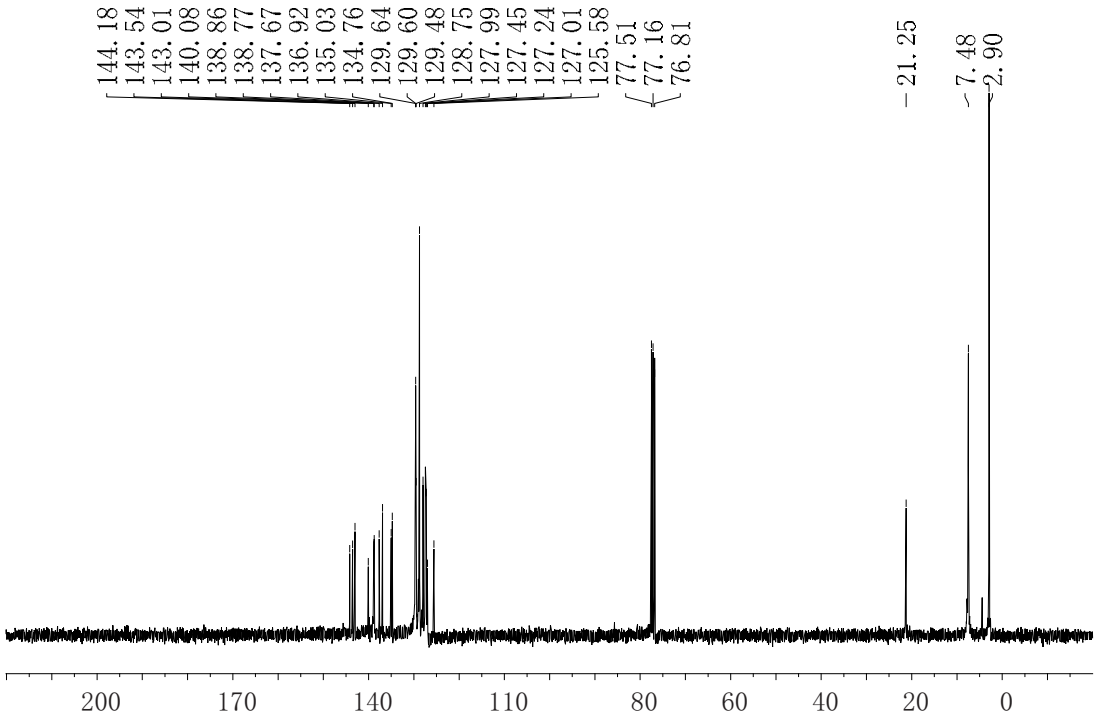

GC trace of the mixture with different isomers

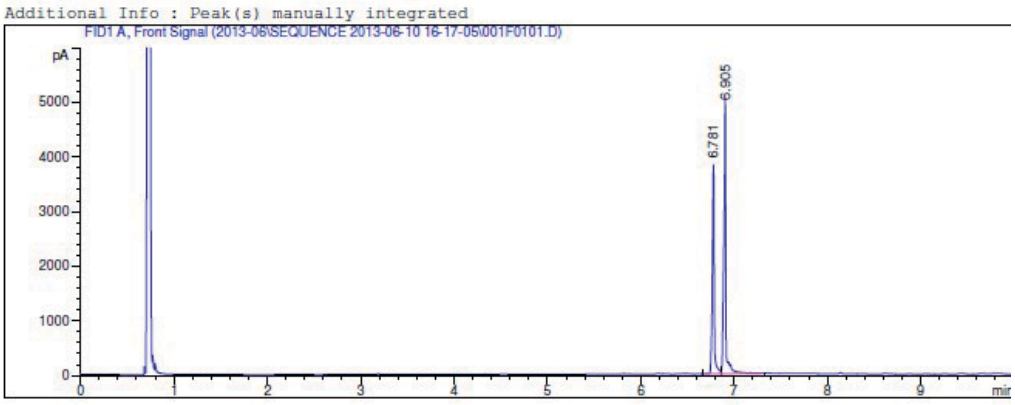


```
================================================================
                    Area Percent Report
================================================================

Sorted By             :      Retention Time
Multiplier:                   :      1.0000
Dilution:                     :      1.0000
Use Multiplier & Dilution Factor with ISTDs

Signal 1: FID1 A, Front Signal

Peak RetTime Sig Type    Area      Height     Area
  #   [min]           [pA*s]      [pA]        %
----|-------|---|----|----------|----------|--------|
   1   6.781  1  VV S 5582.74023 3858.37939 42.02570
   2   6.905  1  VB S 7701.36963 4953.28271 57.97430
```

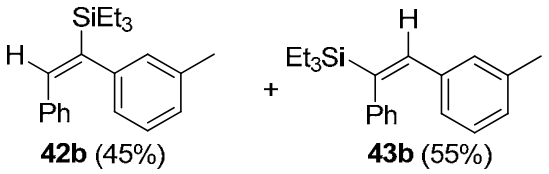

42b (45%) **43b** (55%)

^{1}H NMR (360 MHz, $CDCl_3$) δ (ppm)

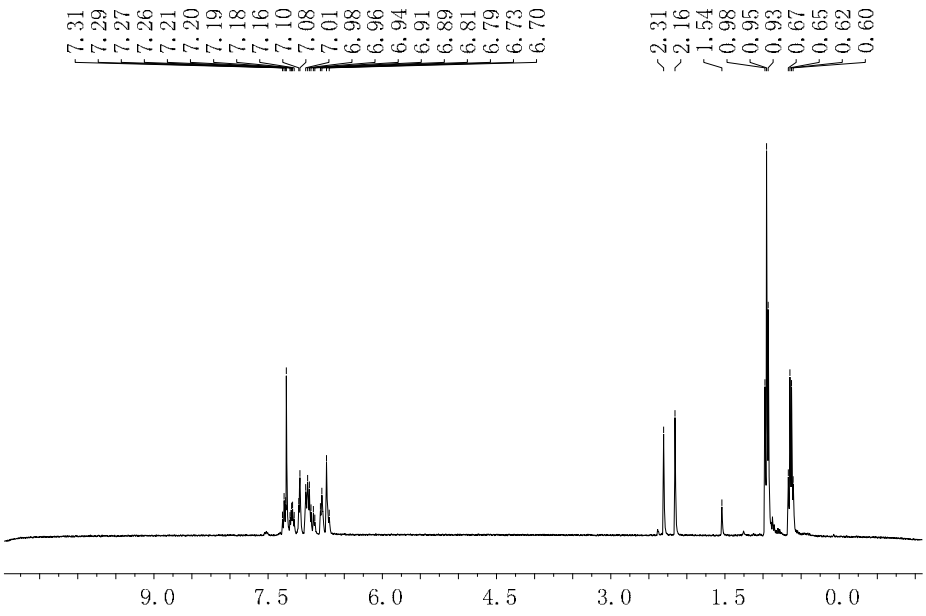

^{13}C NMR (90 MHz, $CDCl_3$)

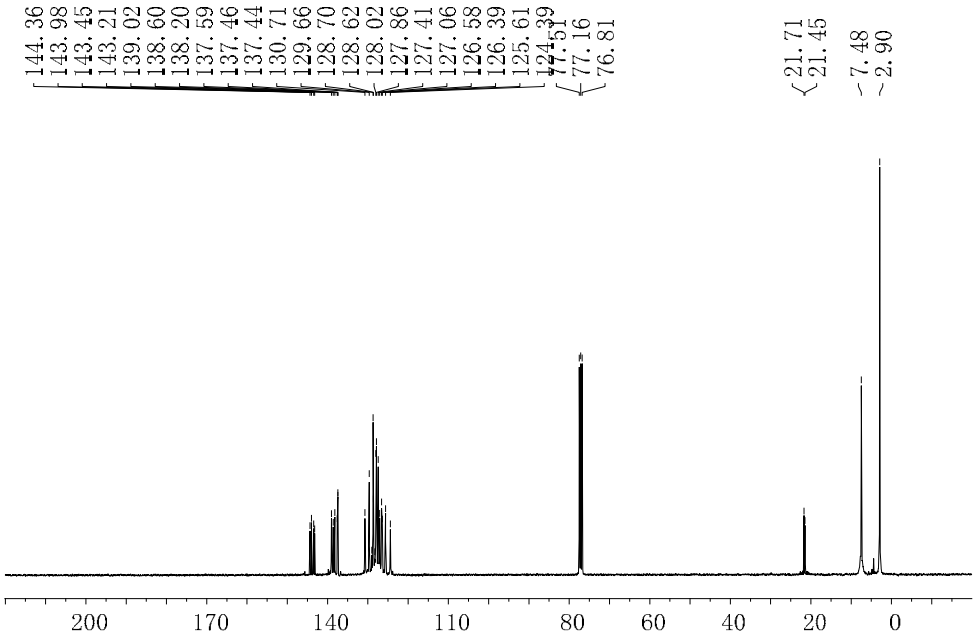

GC trace of the mixture with different isomers

Additional Info : Peak(s) manually integrated

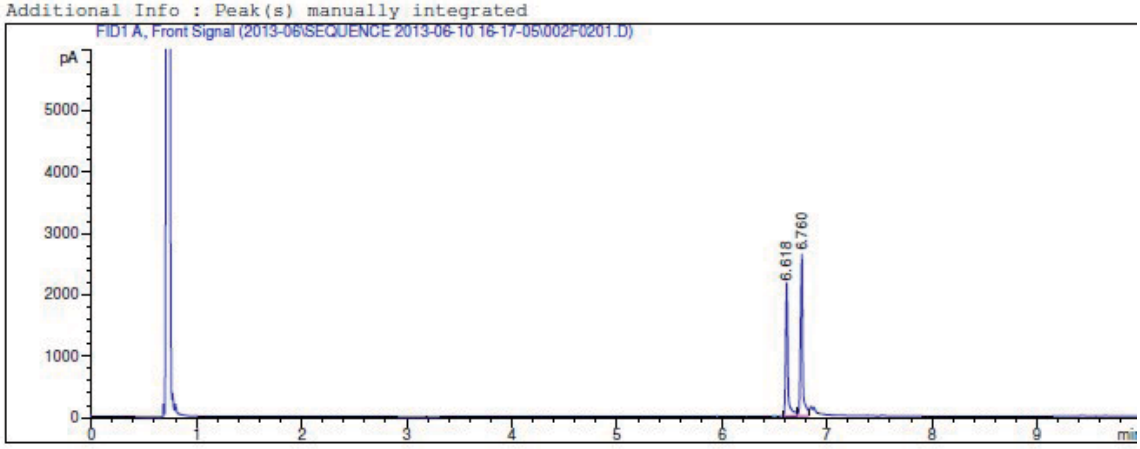


```
=====================================================================
                        Area Percent Report
=====================================================================

Sorted By             :      Retention Time
Multiplier:                   :      1.0000
Dilution:                     :      1.0000
Use Multiplier & Dilution Factor with ISTDs

Signal 1: FID1 A, Front Signal

Peak RetTime Sig Type    Area      Height     Area
  #   [min]            [pA*s]      [pA]       %
----|-------|---|----|----------|----------|--------|
   1   6.618  1  BV   3205.42993 2132.71289 44.79030
   2   6.760  1  VV   3951.09790 2616.25806 55.20970
```

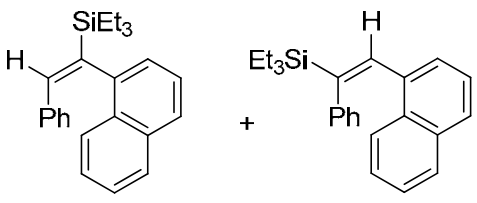

42c (88%)

+

43c (12%)

^{1}H NMR (360 MHz, $CDCl_3$) δ (ppm)

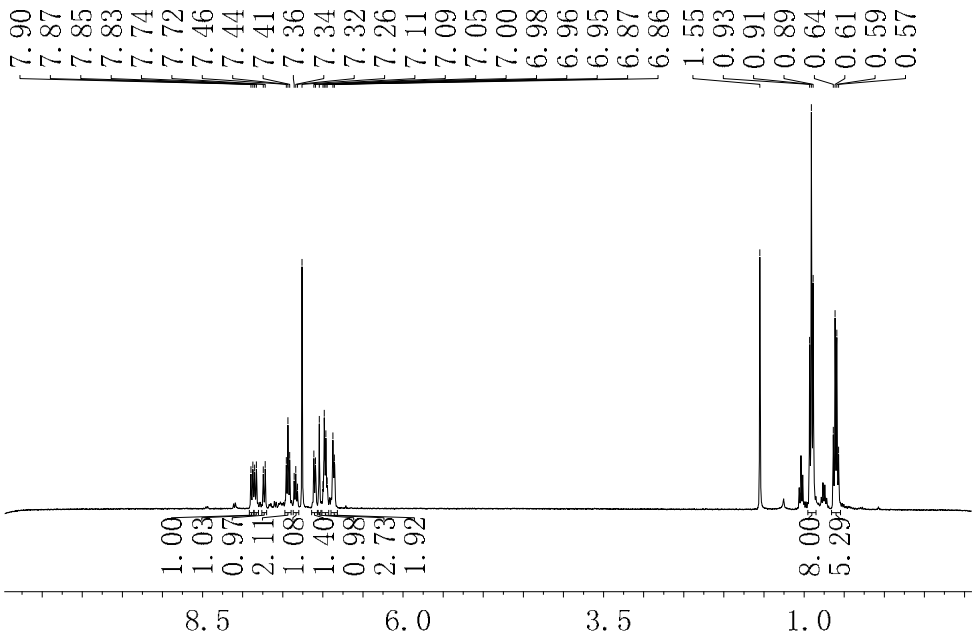

^{13}C NMR (90 MHz, $CDCl_3$)

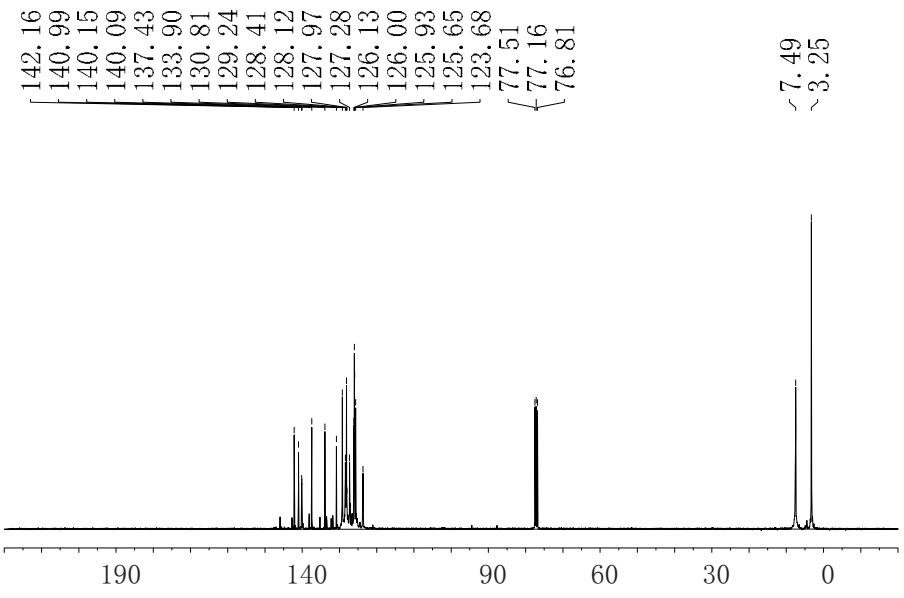

GC trace of the mixture with different isomers

Additional Info : Peak(s) manually integrated

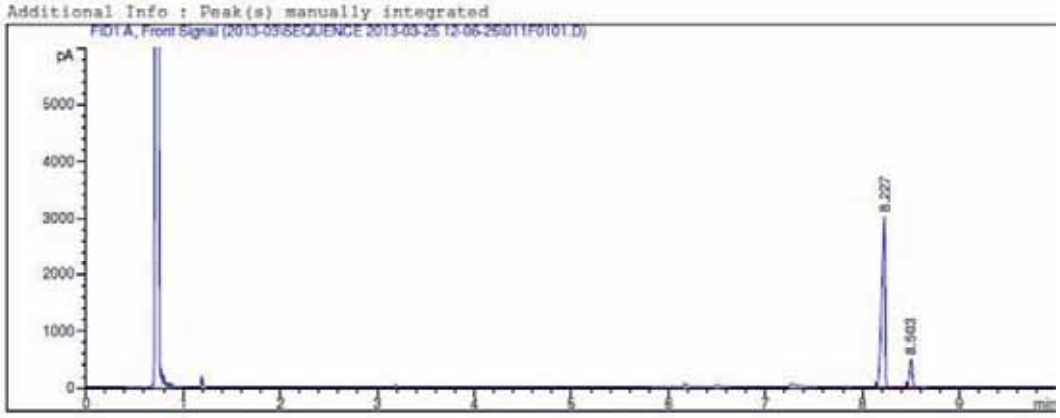

Area Percent Report

Sorted By : Retention Time
Multiplier: : 1.0000
Dilution: : 1.0000
Use Multiplier & Dilution Factor with ISTDs

Signal 1: FID1 A, Front Signal

Peak #	RetTime [min]	Sig	Type	Area [pA*s]	Height [pA]	Area %
1	8.227	1	BV	7154.22559	3022.07178	87.55518
2	8.503	1	BV	1016.87939	491.28317	12.44482

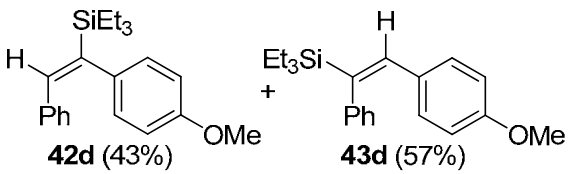

42d (43%)

+

43d (57%)

^{1}H NMR (360 MHz, $CDCl_3$) δ (ppm)

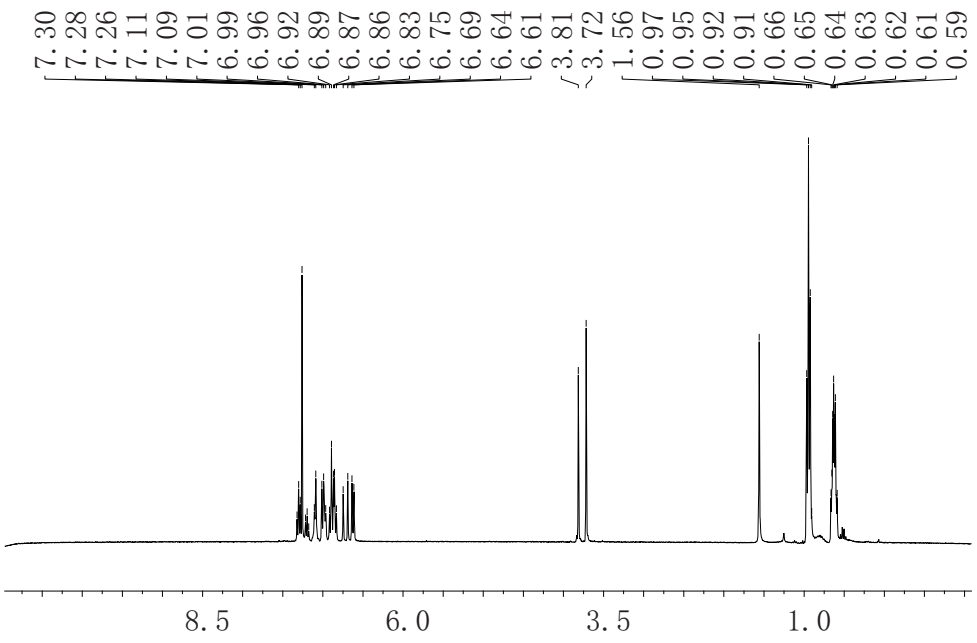

^{13}C NMR (90 MHz, $CDCl_3$)

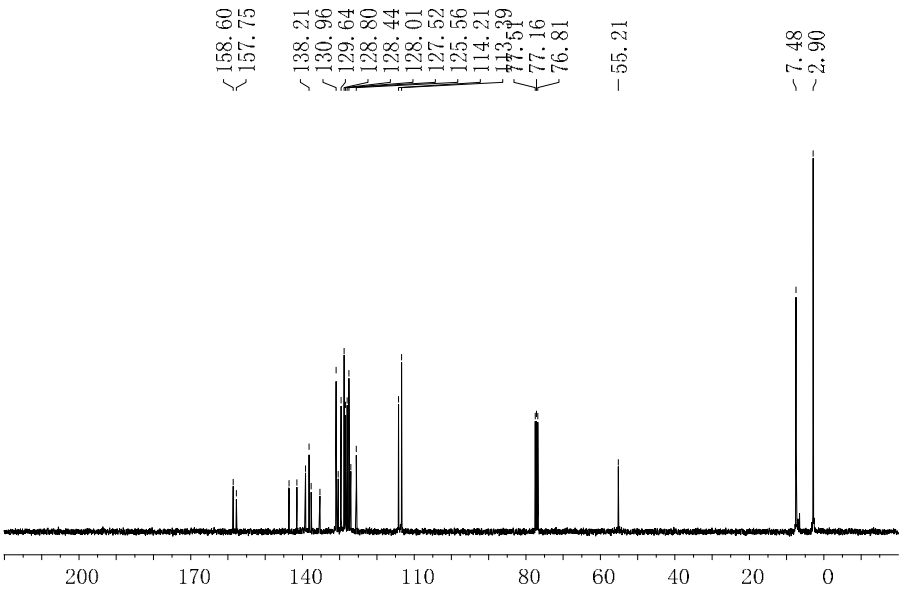

GC trace of the mixture with different isomers

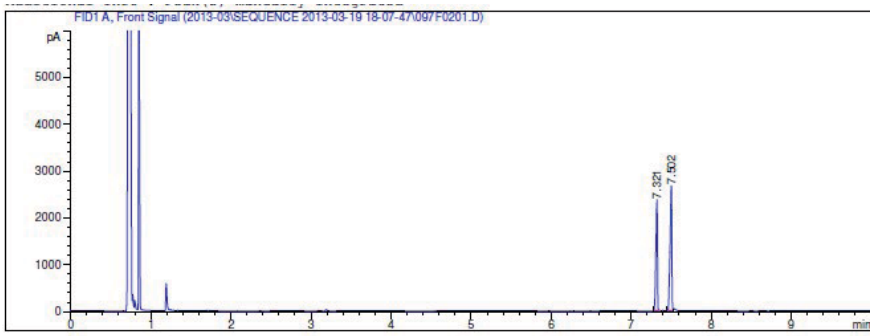


```
================================================================
                      Area Percent Report
================================================================

Sorted By             :      Retention Time
Multiplier:                   :      1.0000
Dilution:                     :      1.0000
Use Multiplier & Dilution Factor with ISTDs

Signal 1: FID1 A, Front Signal

Peak RetTime Sig Type    Area      Height     Area
  #   [min]            [pA*s]      [pA]       %
----|-------|---|----|----------|----------|--------|
   1   7.321  1  BV   3171.91187 2333.28149 42.92693
   2   7.502  1  VV   4217.18359 2644.90137 57.07307
```

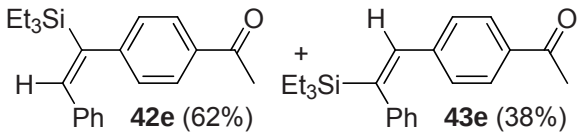

^{1}H NMR (360 MHz, $CDCl_3$) δ (ppm)

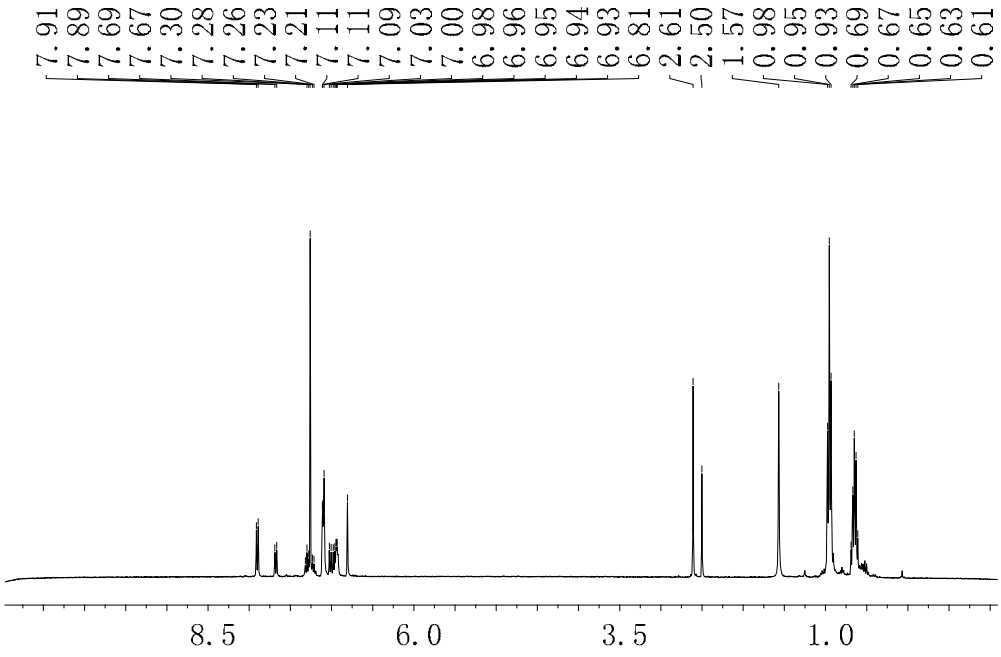

^{13}C NMR (90 MHz, $CDCl_3$)

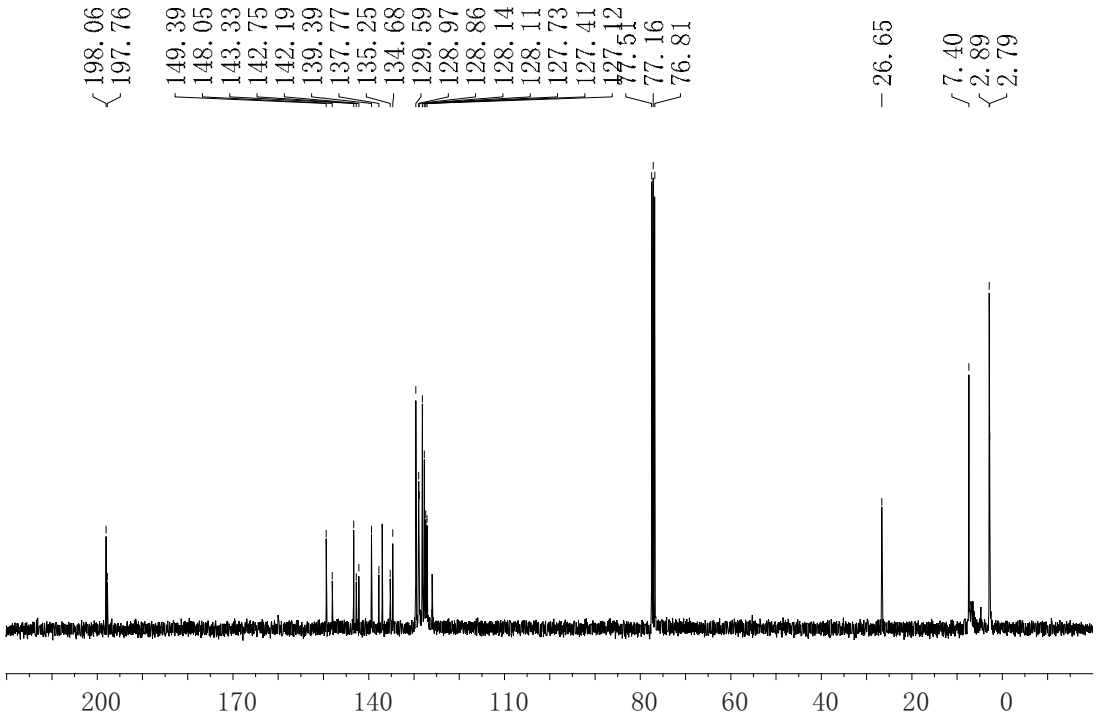

GC trace of the mixture with different isomers

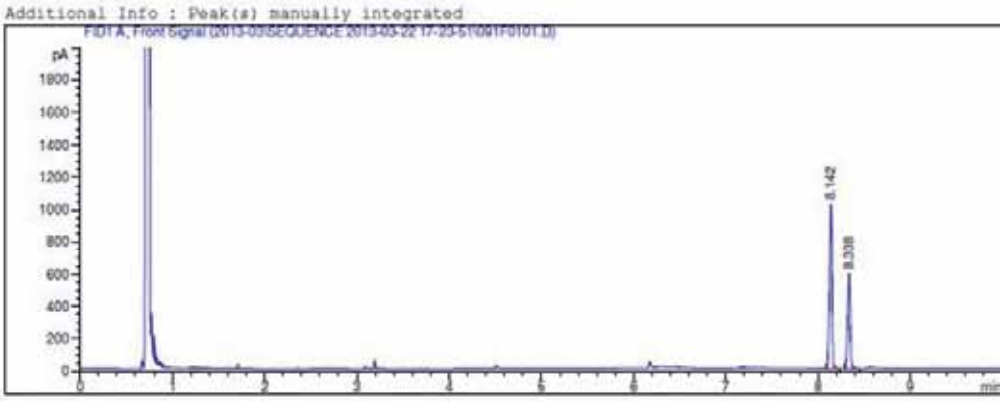

Area Percent Report

Sorted By : Retention Time
Multiplier: : 1.0000
Dilution: : 1.0000
Use Multiplier & Dilution Factor with ISTDs

Signal 1: FID1 A, Front Signal

Peak #	RetTime [min]	Sig	Type	Area [pA*s]	Height [pA]	Area %
1	8.142	1	BB	1955.00720	1016.42456	63.16070
2	8.338	1	BB	1140.28320	584.90894	36.83930

After stood in the air for some days, isomerisation happened and the NMR spectra were showed as follows:

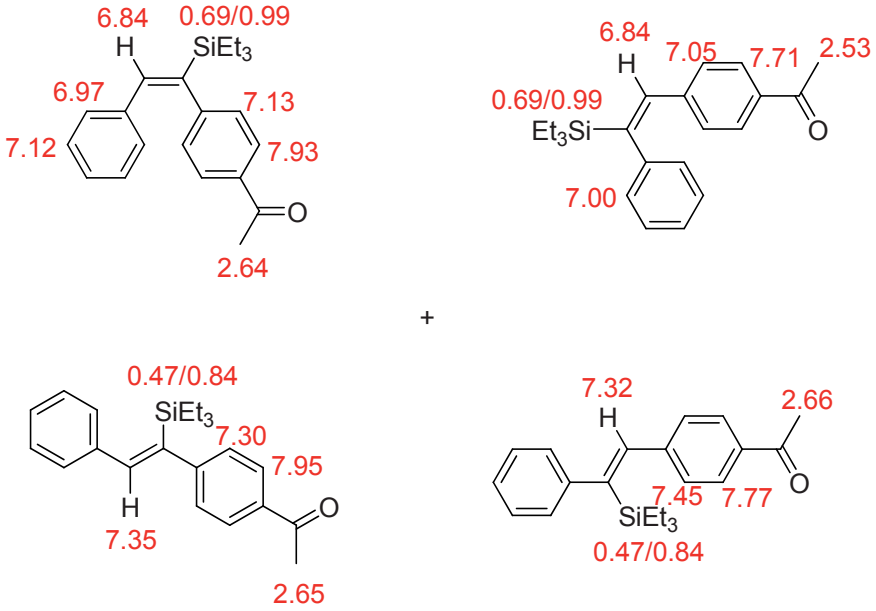

Ratio by NMR: from the first to last: 56:20:10:14

^{1}H-NMR (500 MHz, $CDCl_3$)

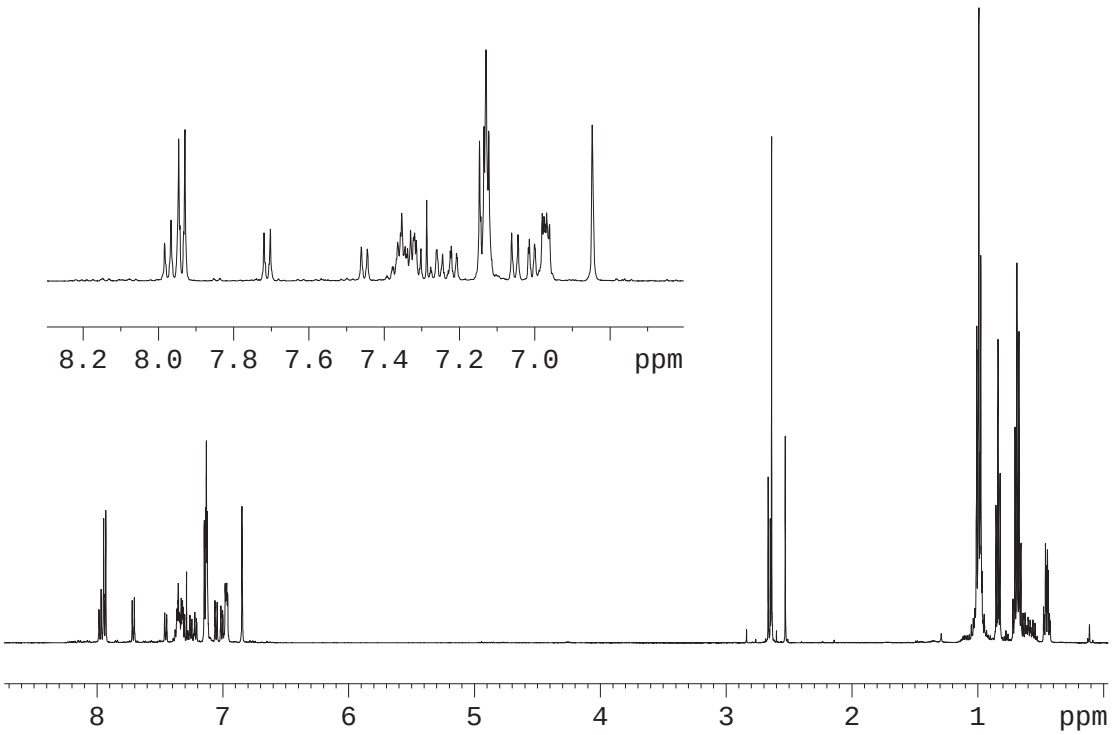

^{13}C-NMR (101 MHz, $CDCl_3$)

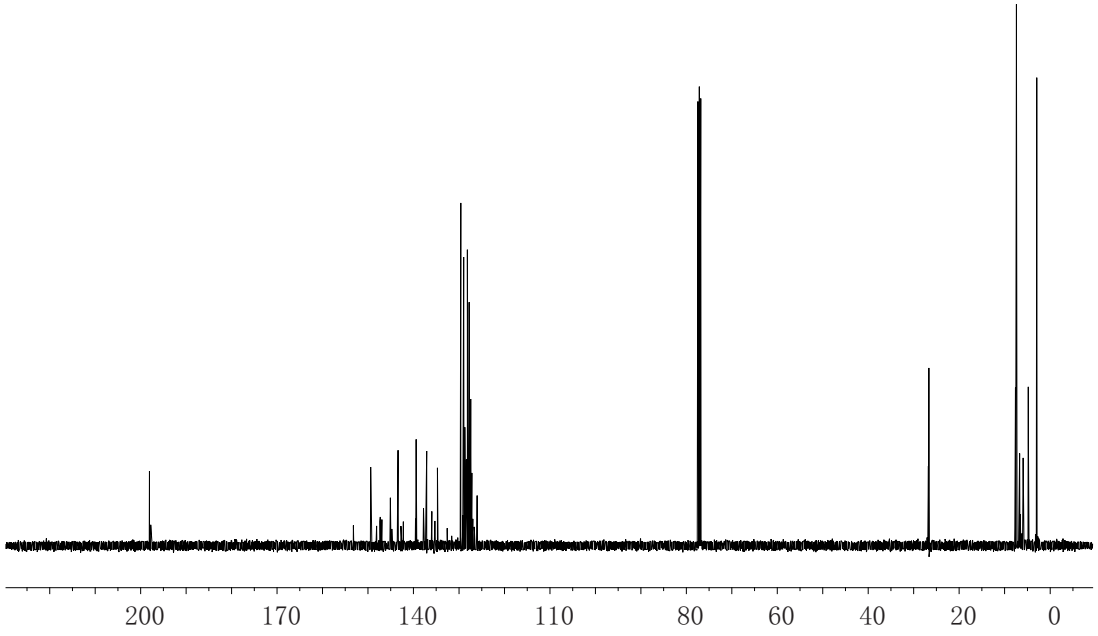

2D ^{1}H-^{1}H COSY (500 MHz, $CDCl_3$)

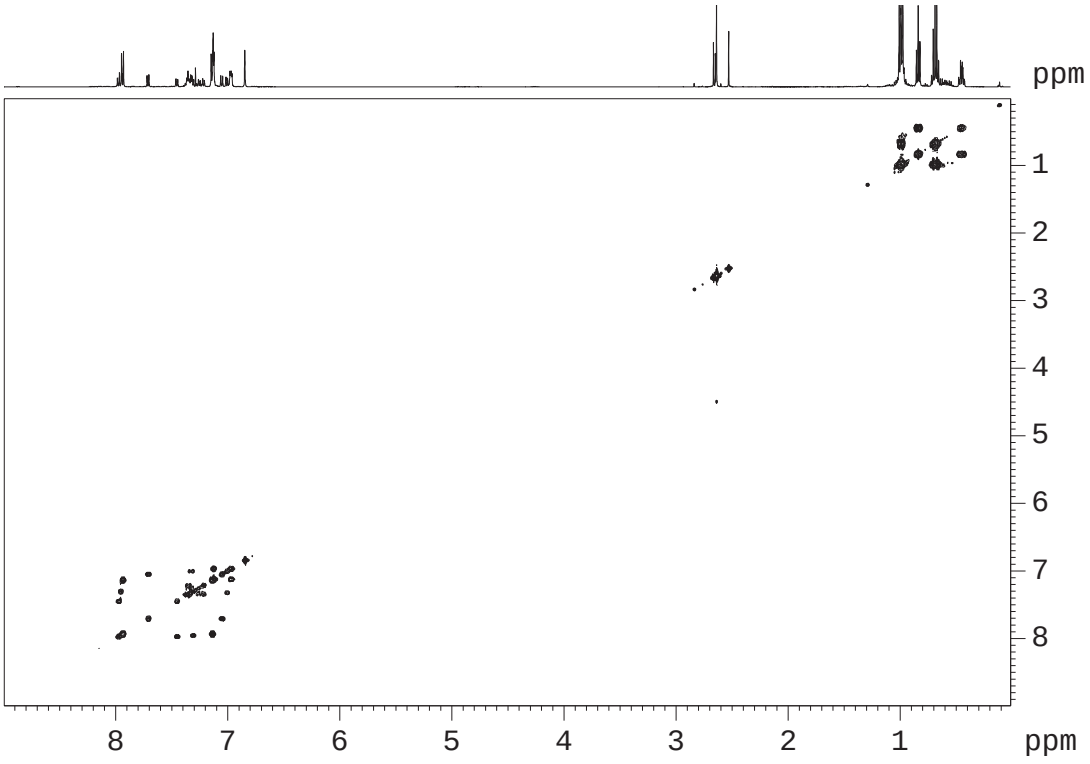

2D ^{1}H-^{13}C HSQC (500 MHz, $CDCl_3$)

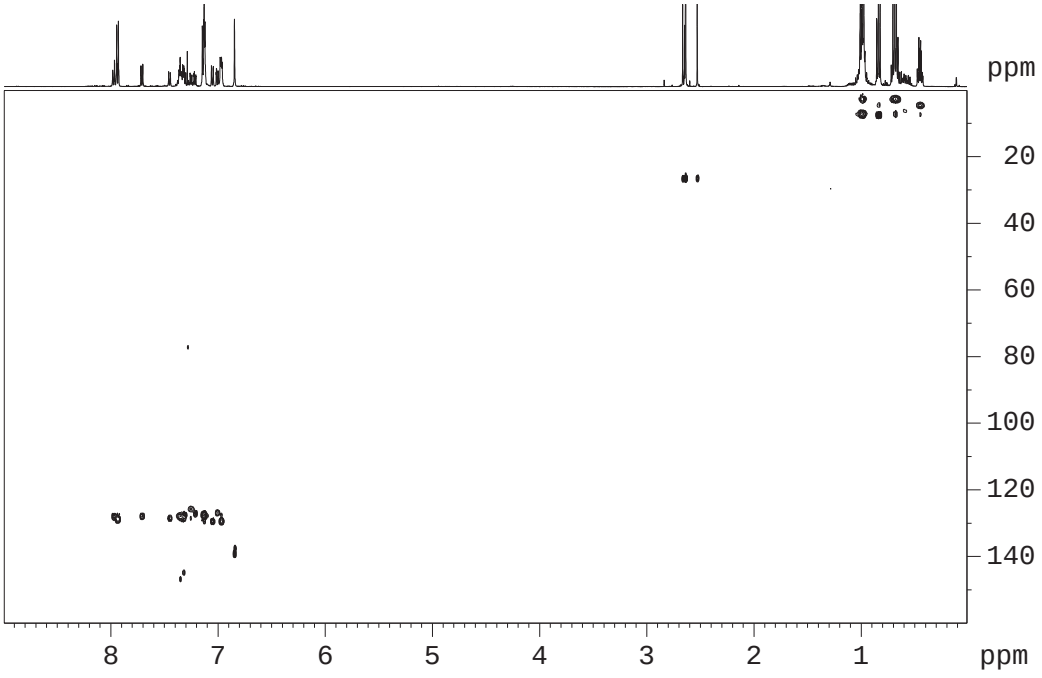

2D ^{1}H-^{13}C HMBC (500 MHz, $CDCl_3$)

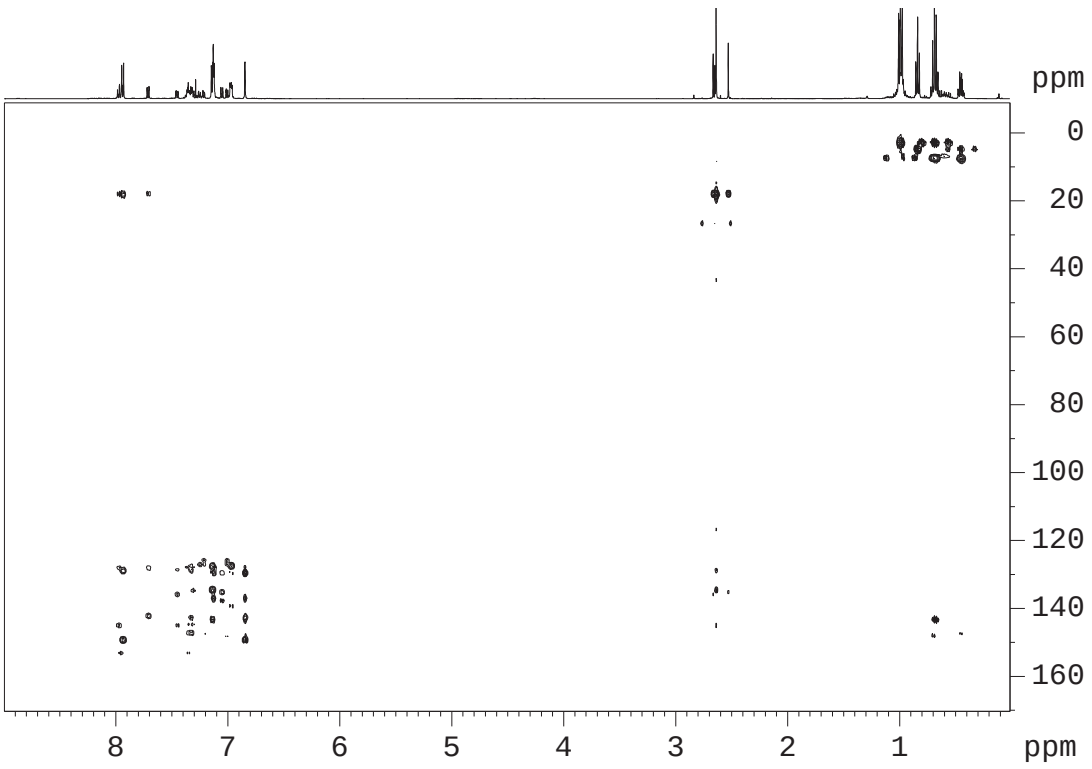

^{1}H-selective 1D NOESY (500 MHz, $CDCl_3$)

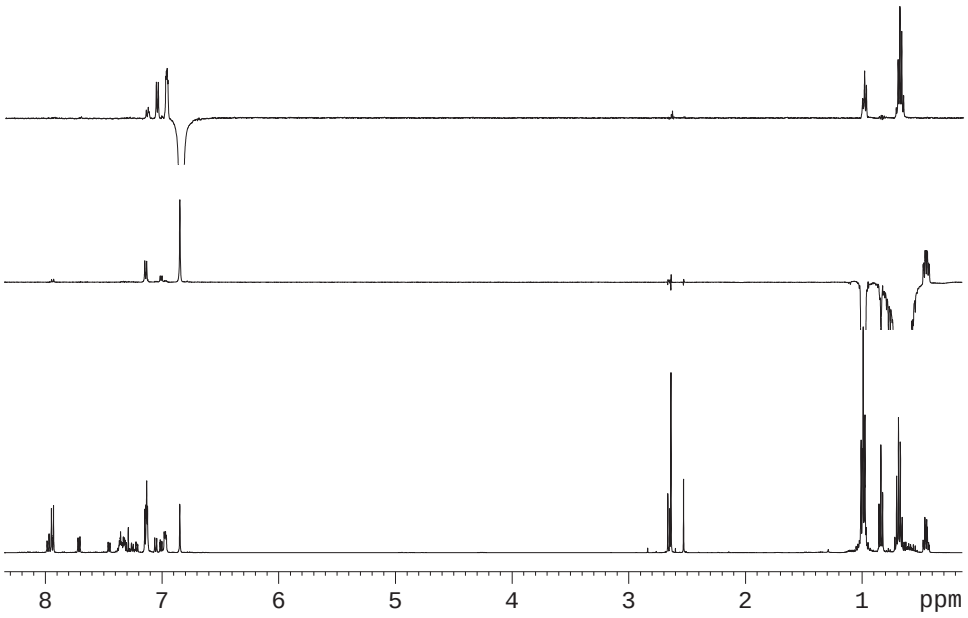

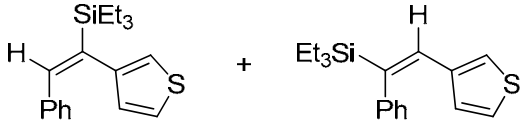

42f (50%)

+

43f (50%)

^{1}H NMR (500 MHz, $CDCl_3$) δ (ppm)

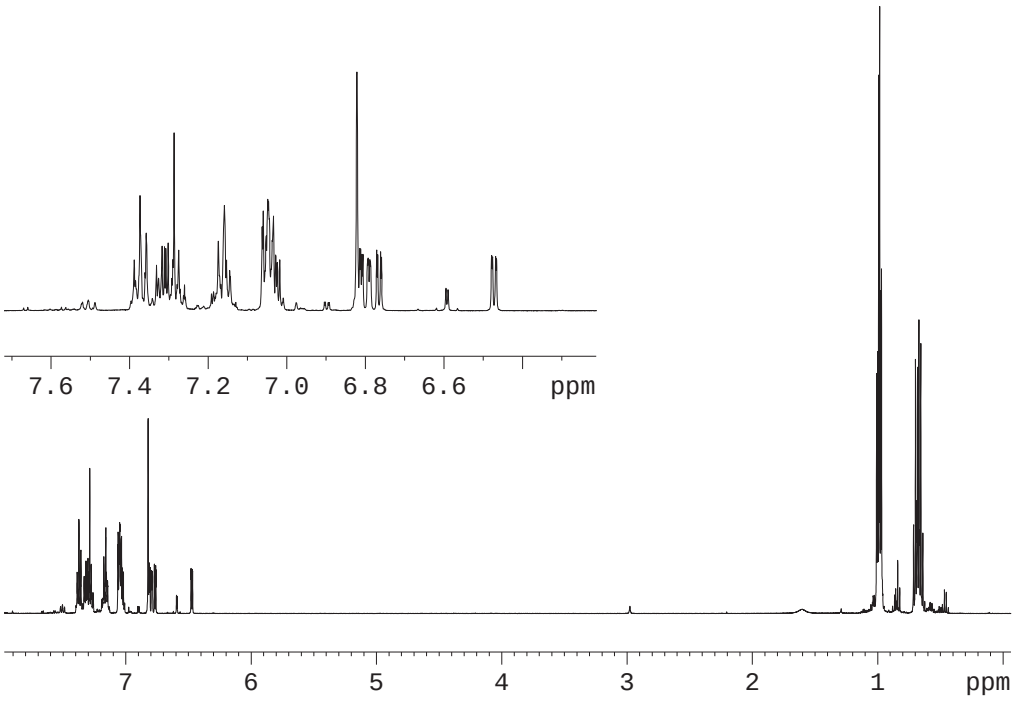

^{13}C NMR (125 MHz, $CDCl_3$)

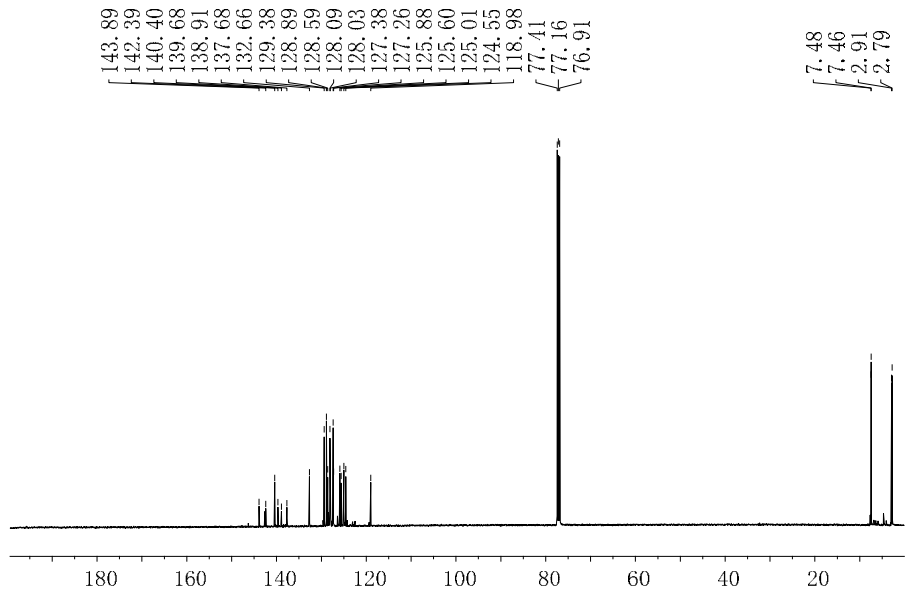

2D ^{1}H-^{1}H COSY (500 MHz, $CDCl_3$)

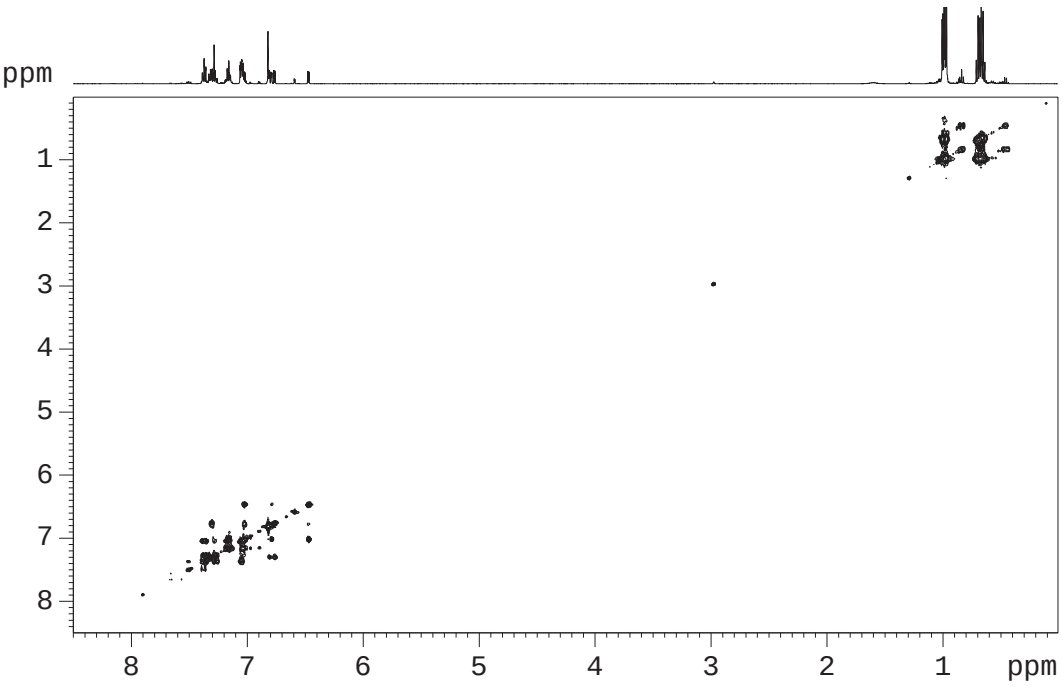

2D ^{1}H-^{13}C HSQC (500 MHz, $CDCl_3$)

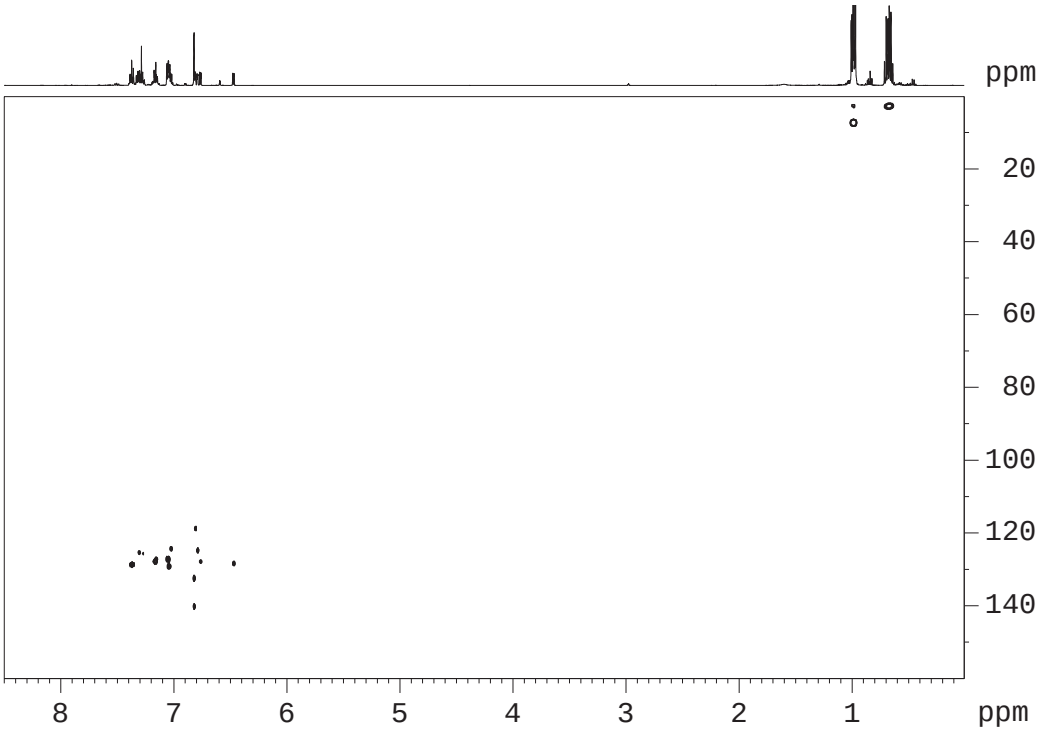

2D ^{1}H-^{13}C HMBC (500 MHz, $CDCl_3$)

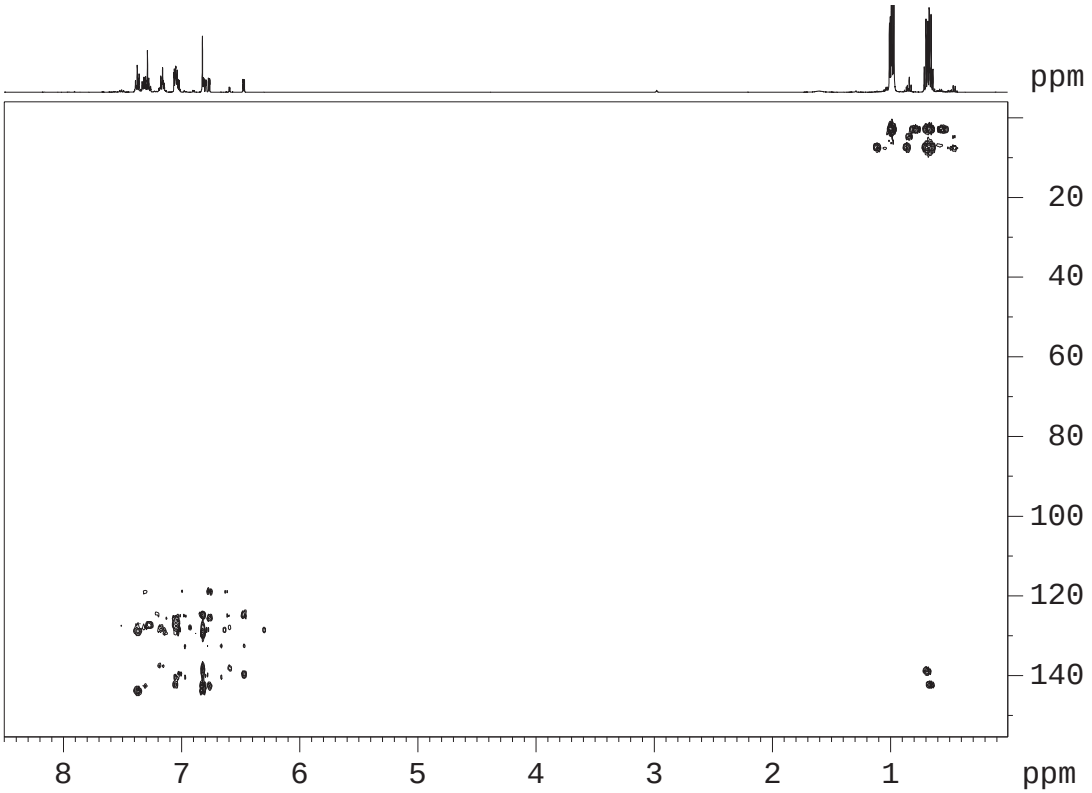

^{1}H-selective 1D NOESY spectra (500 MHz, $CDCl_3$)

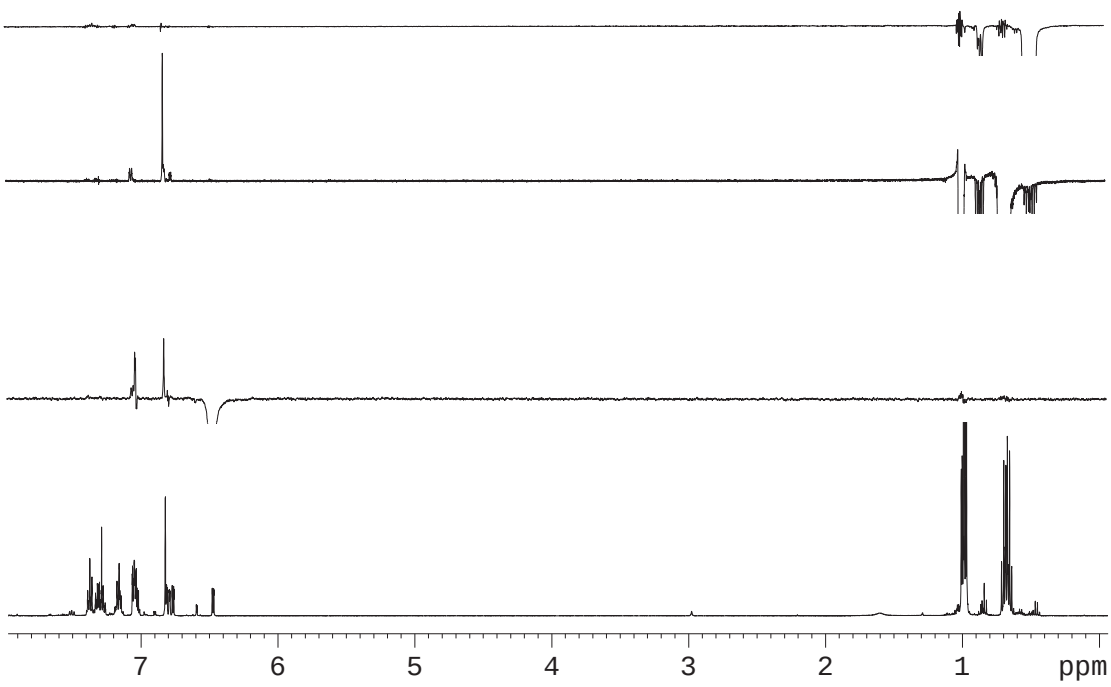

GC trace of the mixture with two different isomers

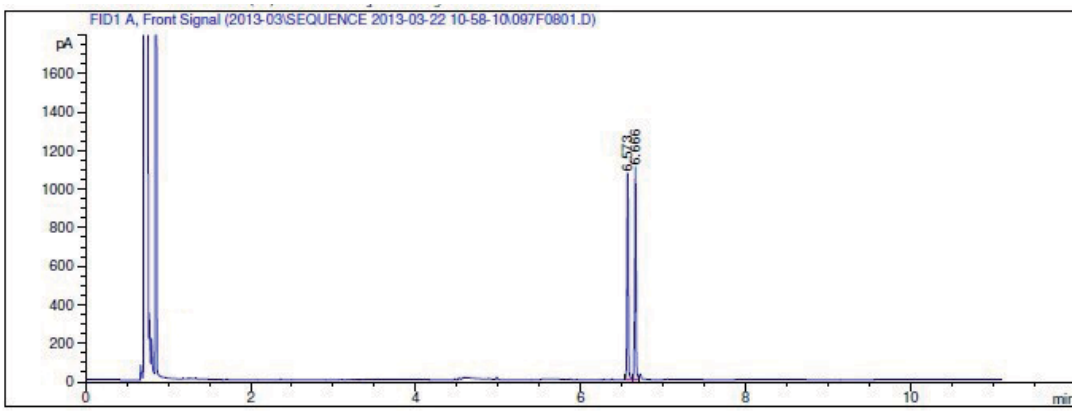

Area Percent Report

Sorted By : Retention Time
Multiplier: : 1.0000
Dilution: : 1.0000
Use Multiplier & Dilution Factor with ISTDs

Signal 1: FID1 A, Front Signal

Peak #	RetTime [min]	Sig	Type	Area [pA*s]	Height [pA]	Area %
1	6.573	1	BV	1189.80237	1055.22717	49.68588
2	6.666	1	VV	1204.84656	1087.97083	50.31412

After some days, GC trace of the mixture with different isomers

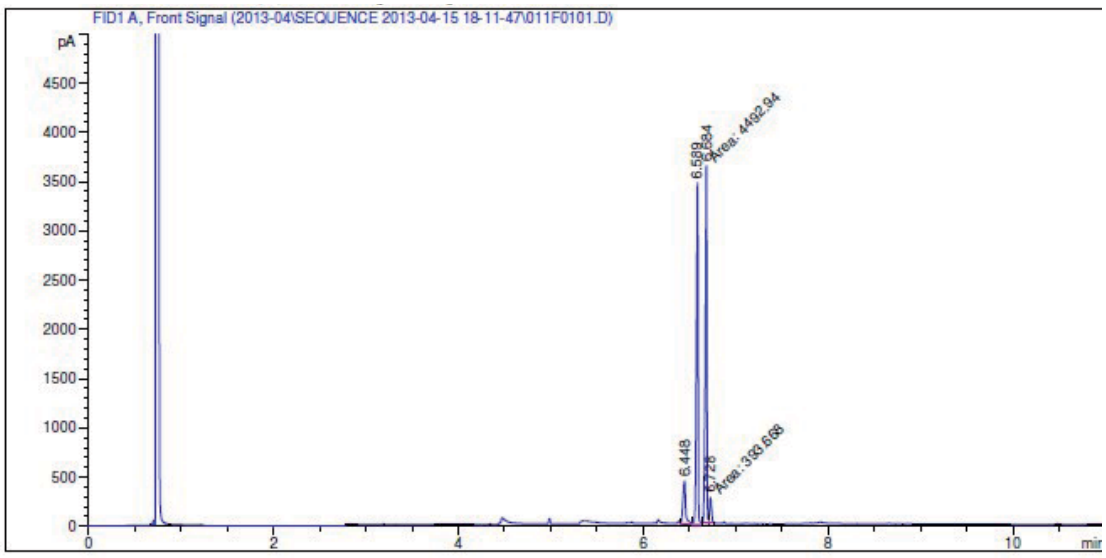


```
================================================================
                    Area Percent Report
================================================================

Sorted By             :      Signal
Multiplier:                   :      1.0000
Dilution:                     :      1.0000
Use Multiplier & Dilution Factor with ISTDs


Signal 1: FID1 A, Front Signal

Peak RetTime Type  Width     Area      Height     Area
  #   [min]        [min]   [pA*s]      [pA]        %
----|-------|----|-------|----------|----------|--------|
   1   6.448 VV    0.0311  955.49426  444.14081  9.30611
   2   6.589 VV S  0.0184 4425.28809 3458.08472 43.10042
   3   6.684 MM    0.0206 4492.93896 3629.22974 43.75931
   4   6.728 MM    0.0252  393.66830  260.87283  3.83416
```

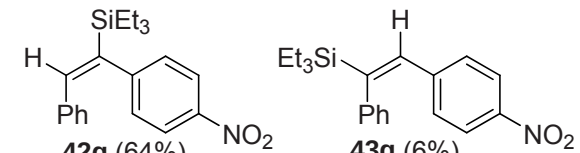

42g (64%)

43g (6%)

+

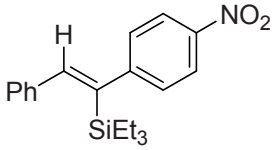

44g (20%)

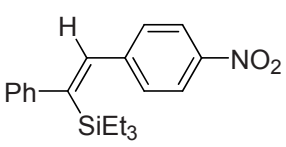

45g (10%)

^{1}H-NMR (500 MHz, $CDCl_3$)

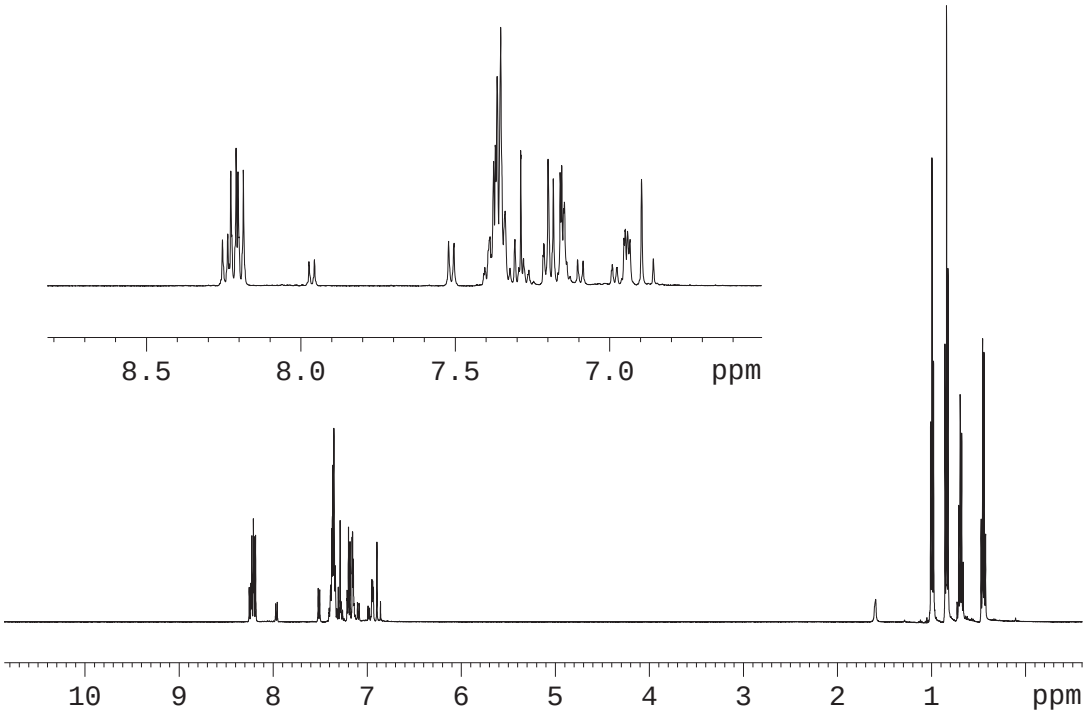

^{13}C-NMR (125 MHz, $CDCl_3$)

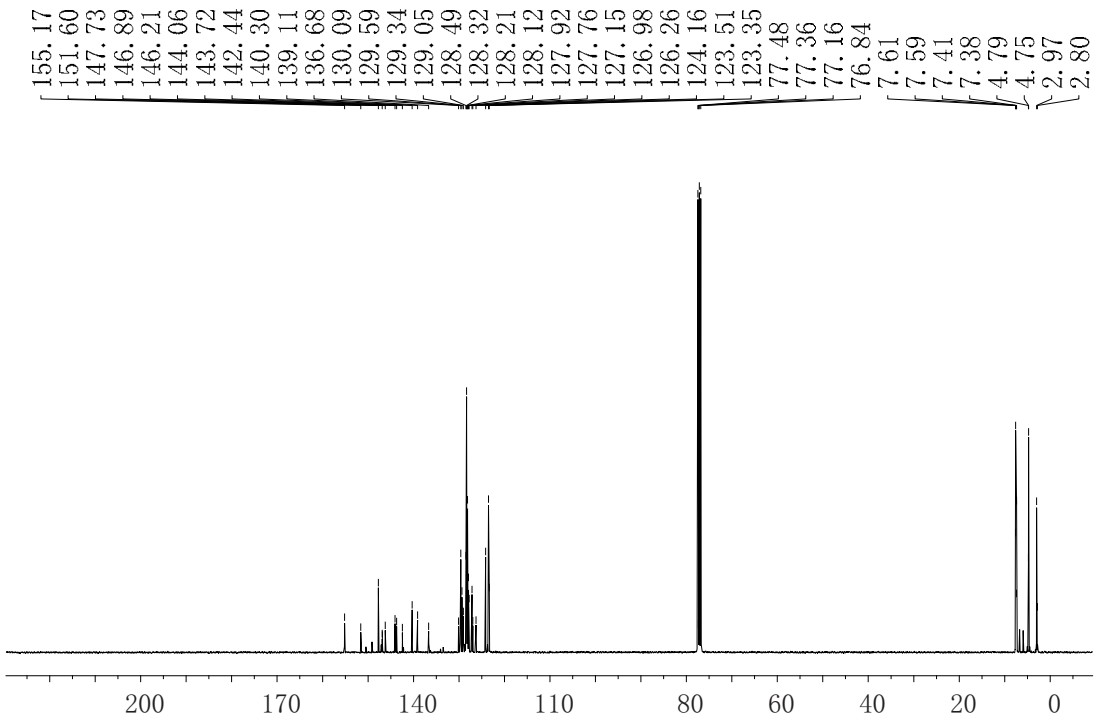

2D ^{1}H-^{1}H COSY (500 MHz, $CDCl_3$)

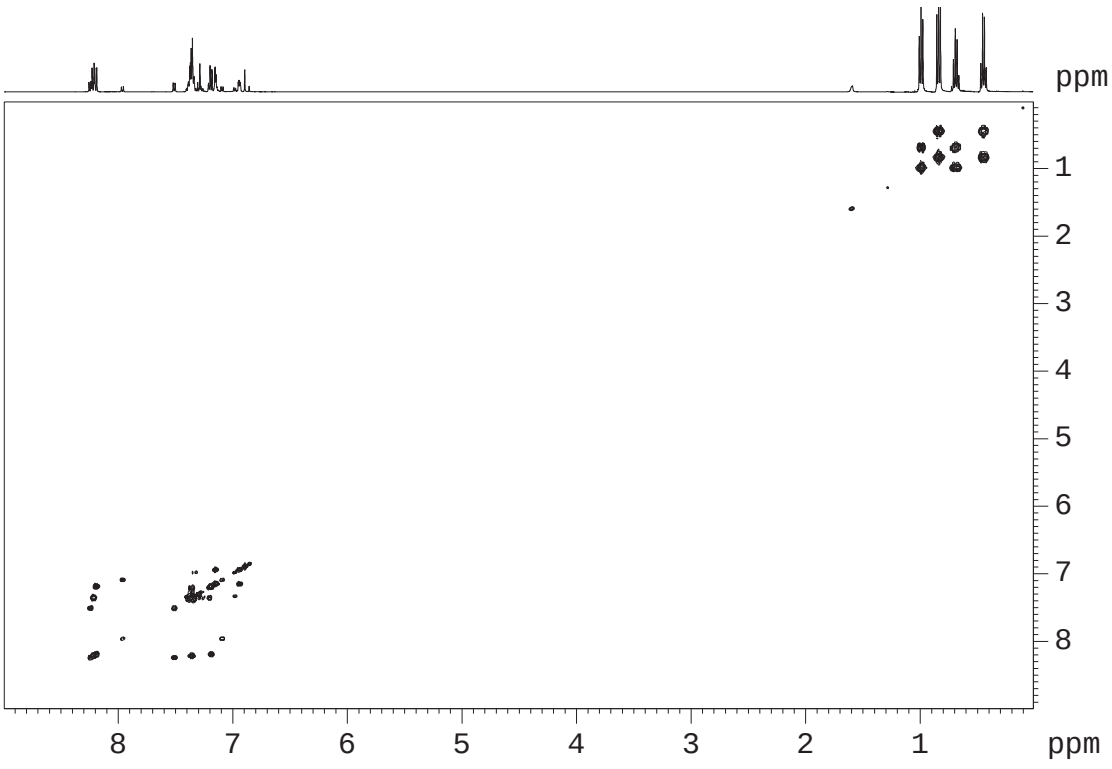

2D ^{1}H-^{13}C HSQC (500 MHz, $CDCl_3$)

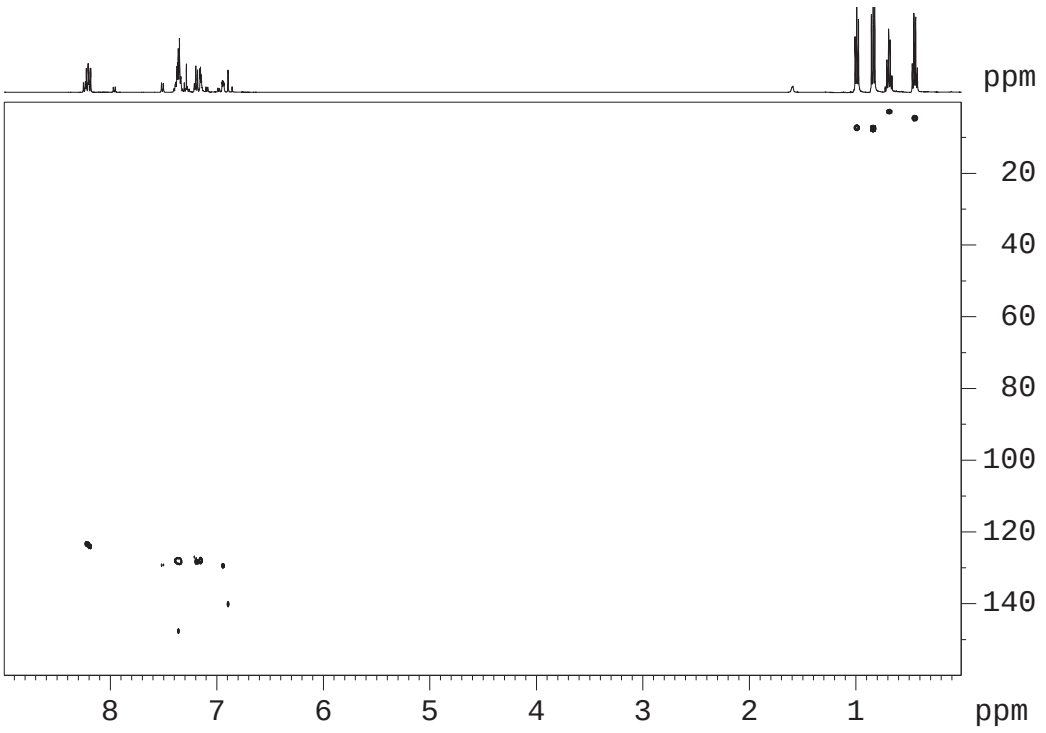

2D ^{1}H-^{13}C HMBC (500 MHz, $CDCl_3$)

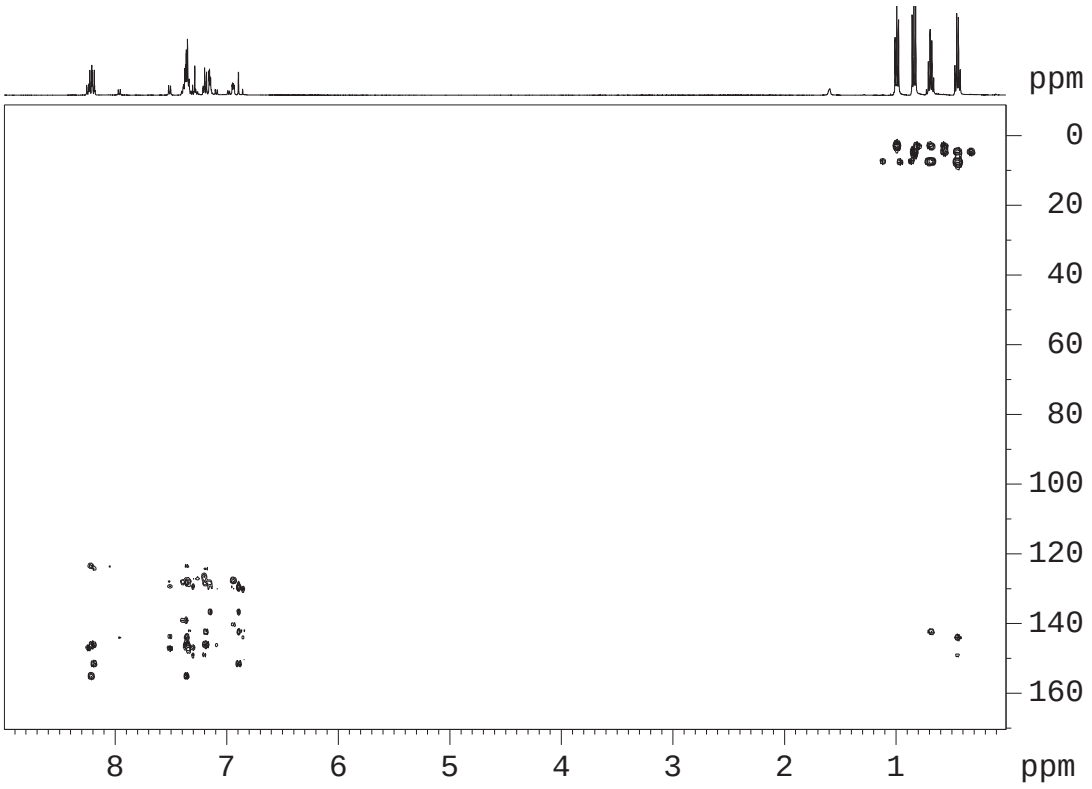

^{1}H-selective 1D NOESY (500 MHz, $CDCl_3$)

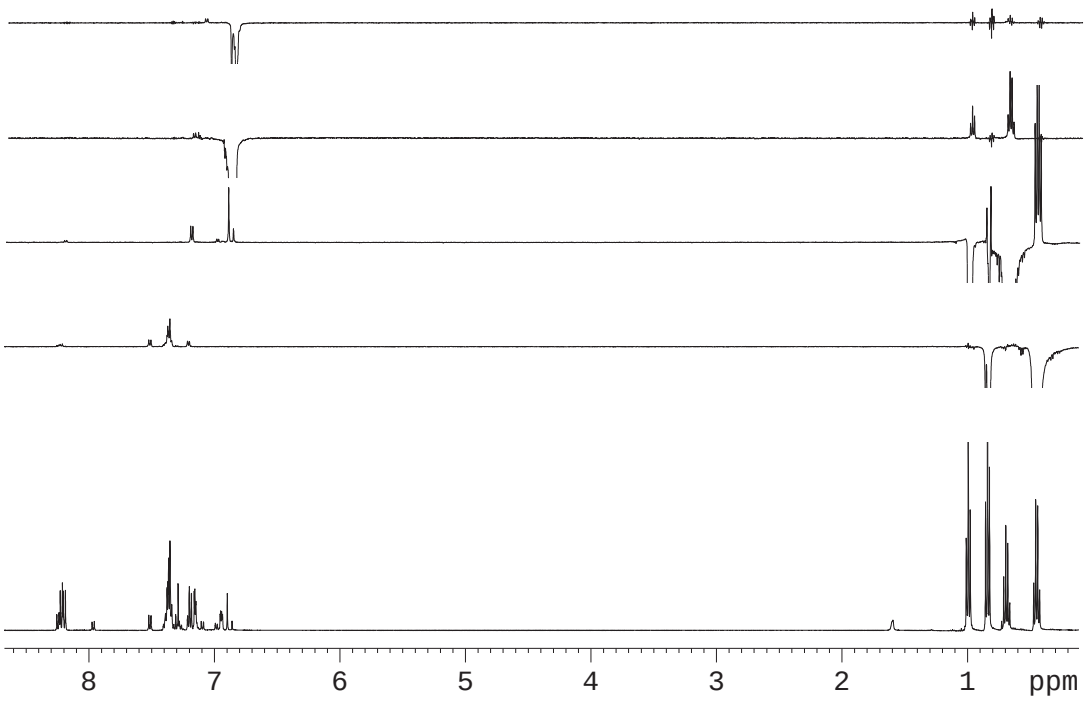

GC trace of the mixture with different isomers

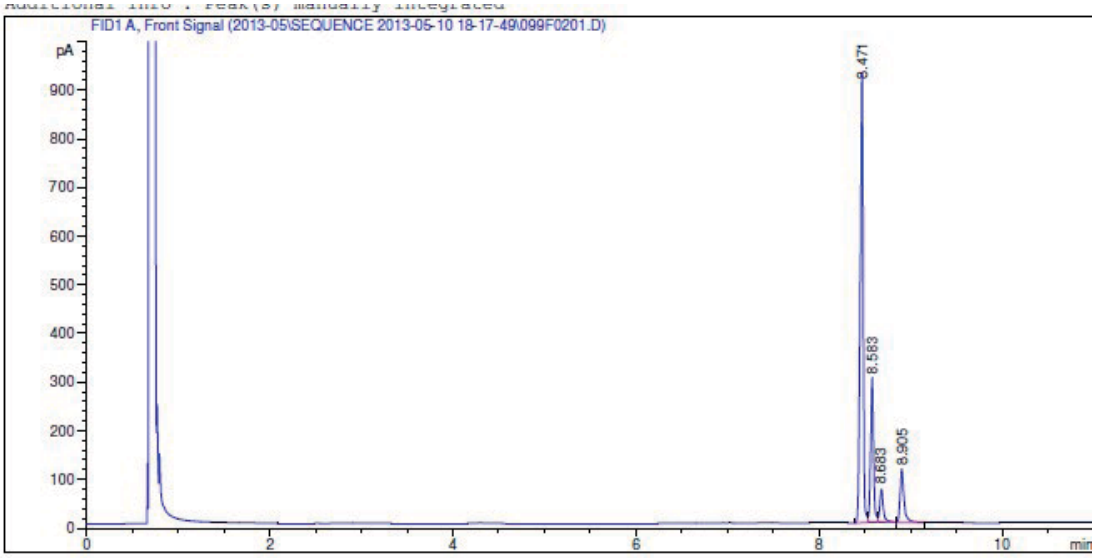


```
================================================================
                      Area Percent Report
================================================================

Sorted By             :      Signal
Multiplier:                   :      1.0000
Dilution:                     :      1.0000
Use Multiplier & Dilution Factor with ISTDs


Signal 1: FID1 A, Front Signal

Peak RetTime Type  Width     Area      Height     Area
  #   [min]       [min]   [pA*s]       [pA]        %
----|-------|----|-------|----------|----------|--------|
   1   8.471 BV    0.0338 2126.34961  924.64771 63.95895
   2   8.583 VV    0.0337  667.91095  297.12604 20.09024
   3   8.683 VV    0.0406  198.44659   68.46217  5.96912
   4   8.905 VB    0.0415  331.84641  110.52713  9.98168
```

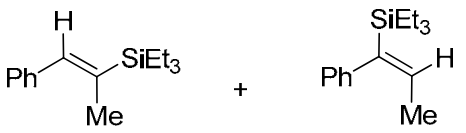

46a (45%)

\+

47a (55%)

^{1}H NMR (500 MHz, $CDCl_3$) δ (ppm)

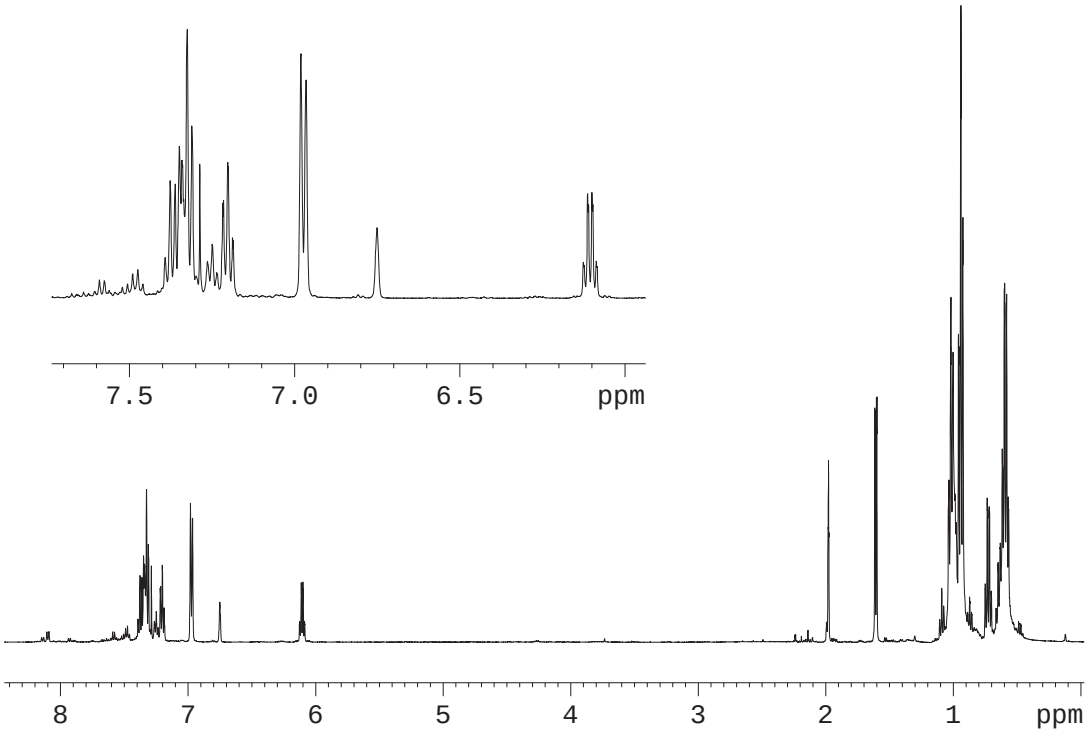

^{13}H NMR (101 MHz, $CDCl_3$) δ (ppm)

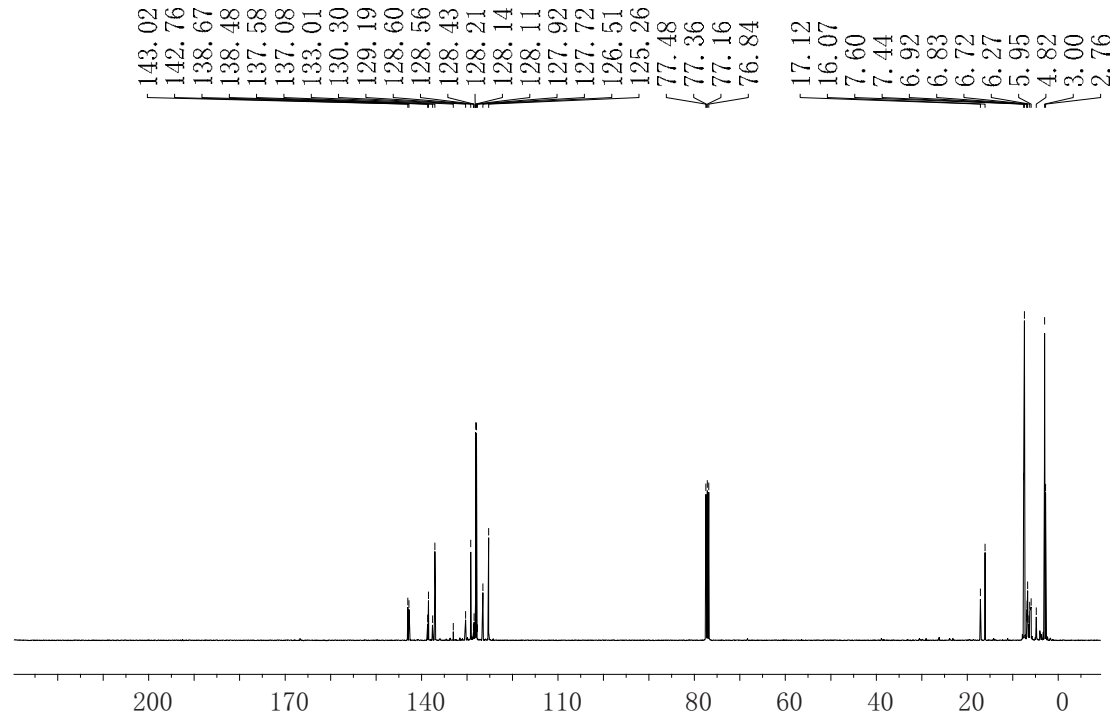

2D ^{1}H-^{1}H COSY (500 MHz, $CDCl_3$)

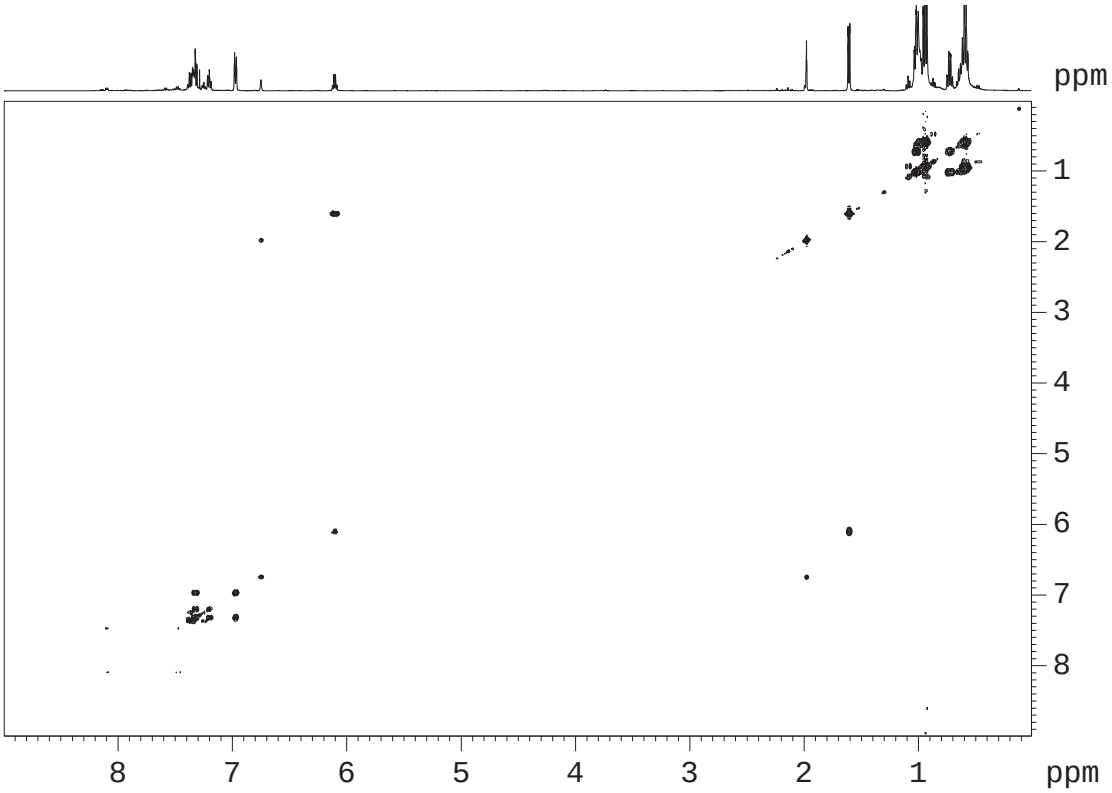

2D ^{1}H-^{13}C HSQC (500 MHz, $CDCl_3$)

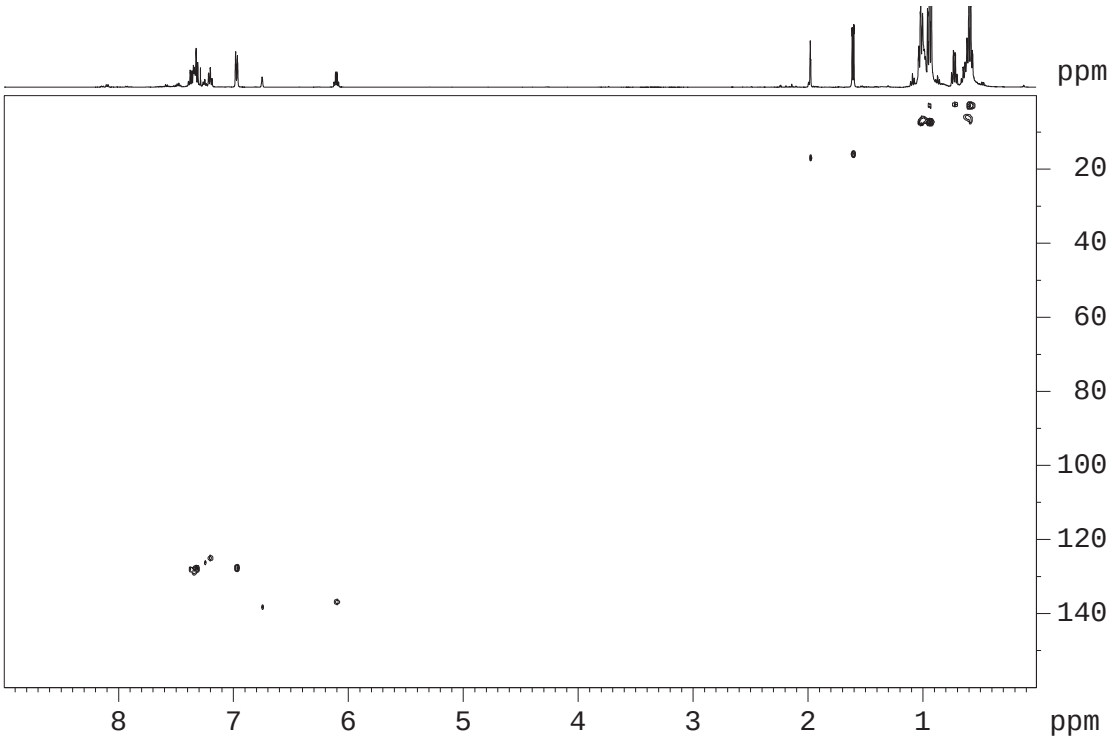

2D ^{1}H-^{13}C HMBC (500 MHz, $CDCl_3$)

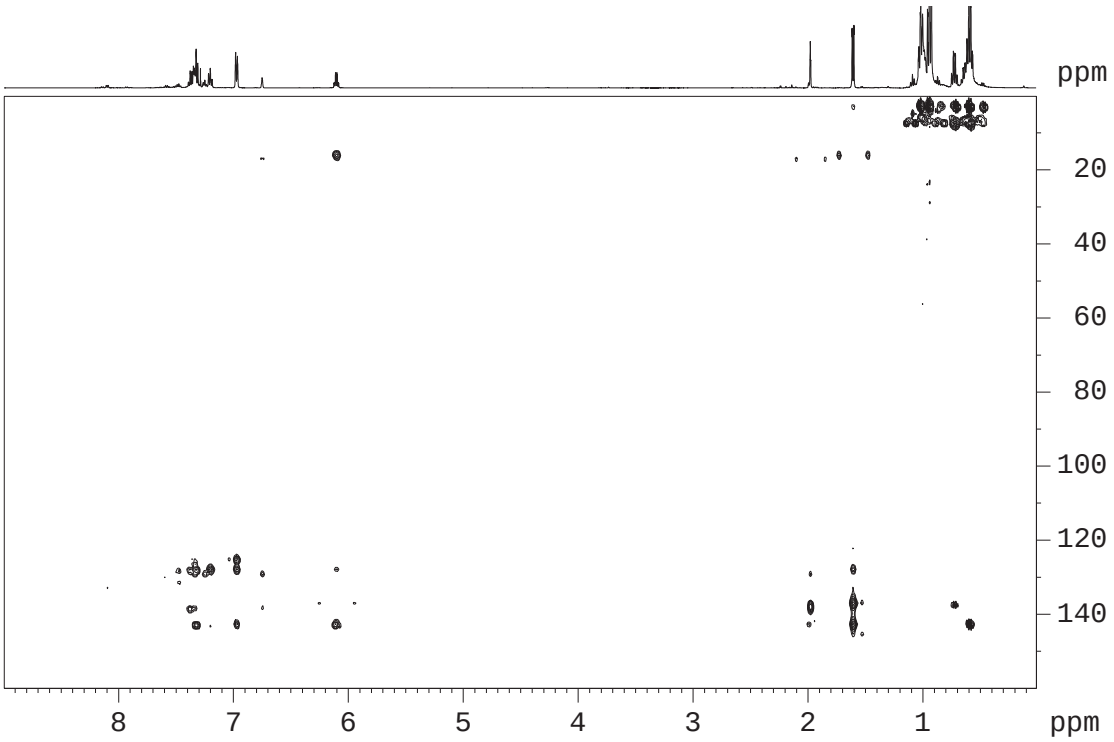

^{1}H-selective 1D NOESY (500 MHz, $CDCl_3$)

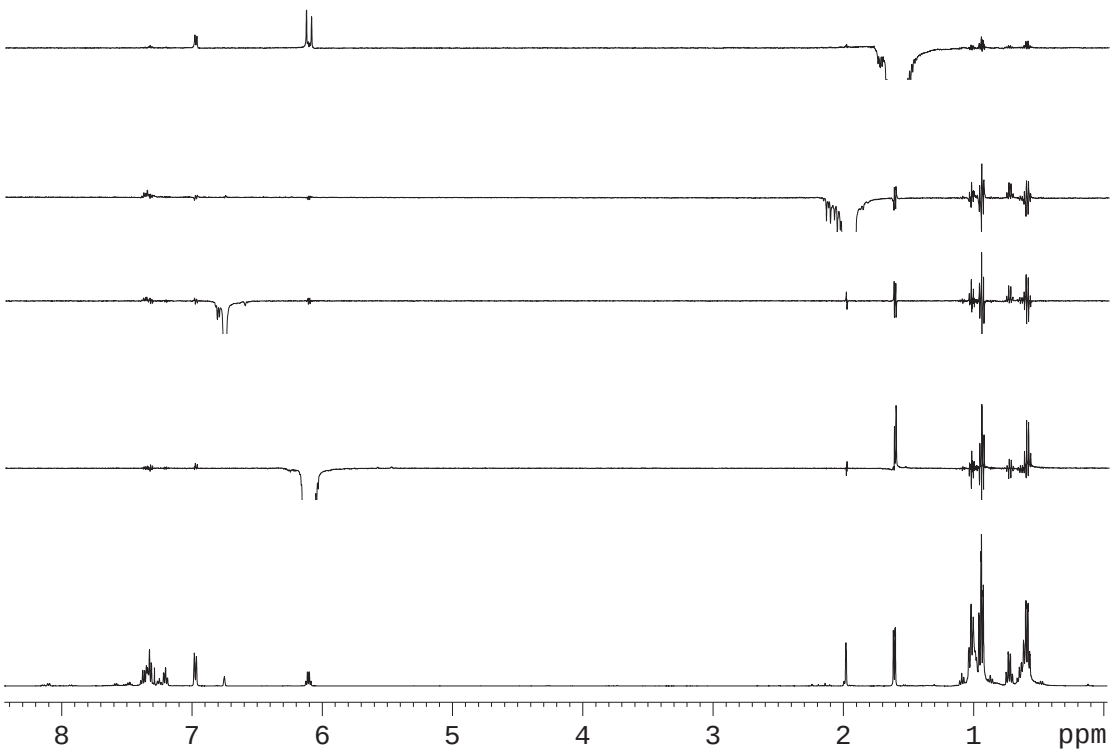

GC trace of the mixture with different isomers

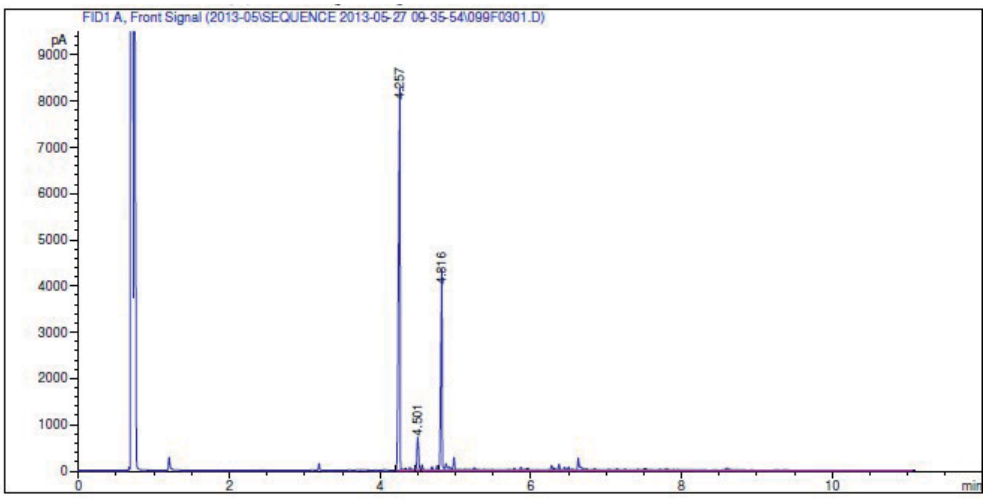


```
================================================================
                    Area Percent Report
================================================================

Sorted By             :      Signal
Multiplier:                   :      1.0000
Dilution:                     :      1.0000
Use Multiplier & Dilution Factor with ISTDs


Signal 1: FID1 A, Front Signal

Peak RetTime Type  Width     Area      Height     Area
  #   [min]        [min]   [pA*s]      [pA]        %
----|-------|----|-------|---------|----------|--------|
   1   4.257 VV S  0.0233 1.21016e4  7920.35742 53.08534
   2   4.501 VV T  0.0254 1025.58582  649.18958  4.49887
   3   4.816 VBAS  0.0262 9669.32422 3925.90723 42.41579
```

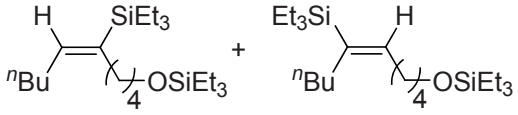

46b (50%)

+

47b (50%)

^{1}H NMR (500 MHz, $CDCl_3$) δ (ppm)

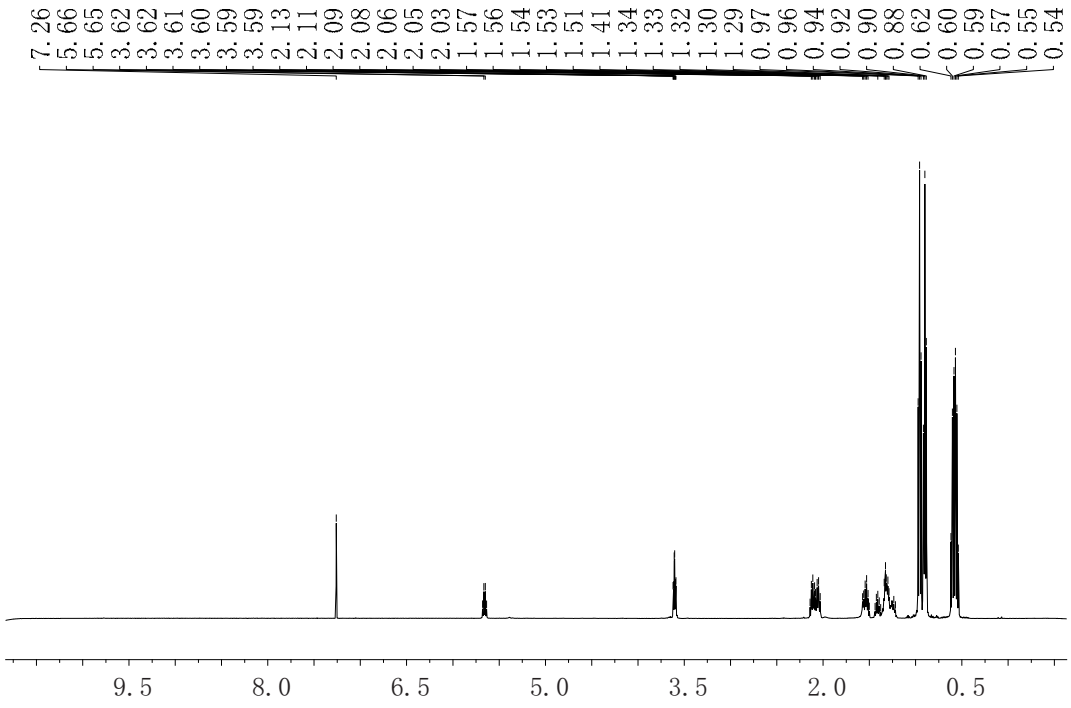

^{13}C NMR (125 MHz, $CDCl_3$)

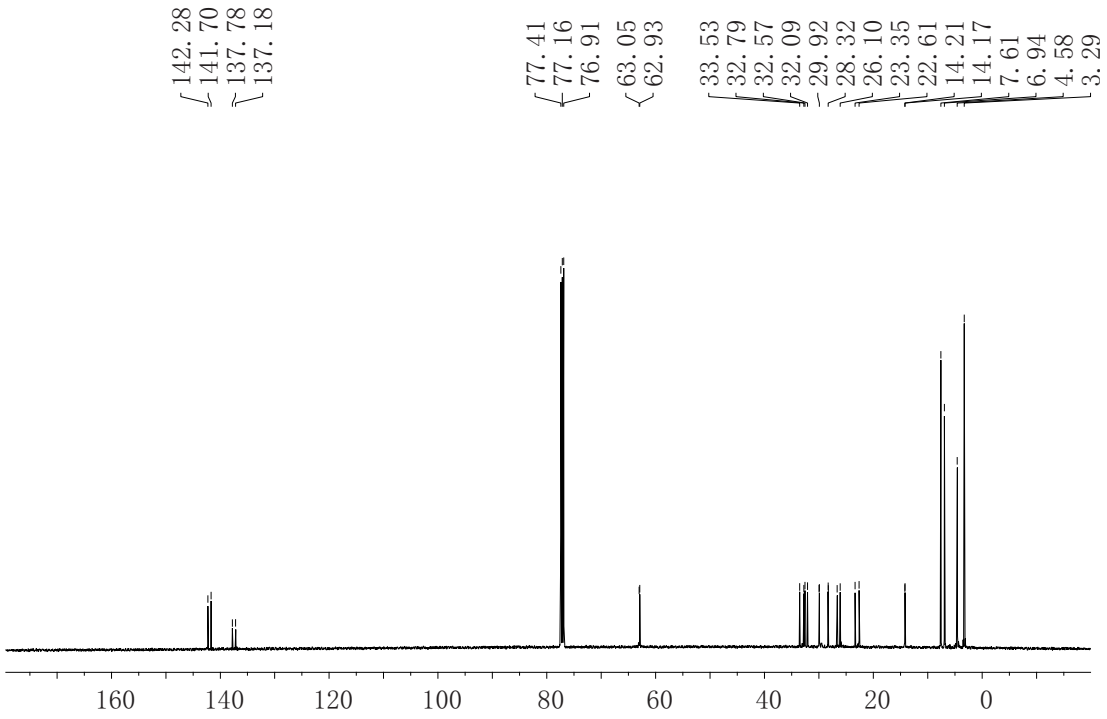

2D ^{1}H-^{1}H COSY (500 MHz, $CDCl_3$)

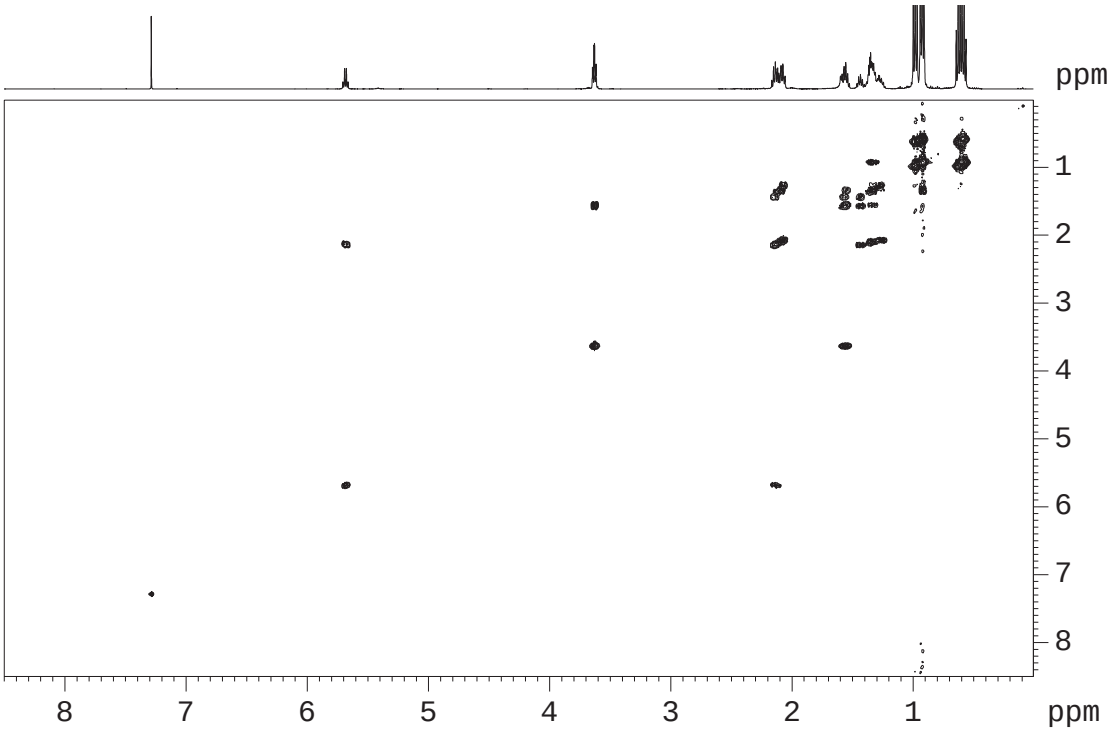

2D ^{1}H-^{13}C HSQC (500 MHz, $CDCl_3$)

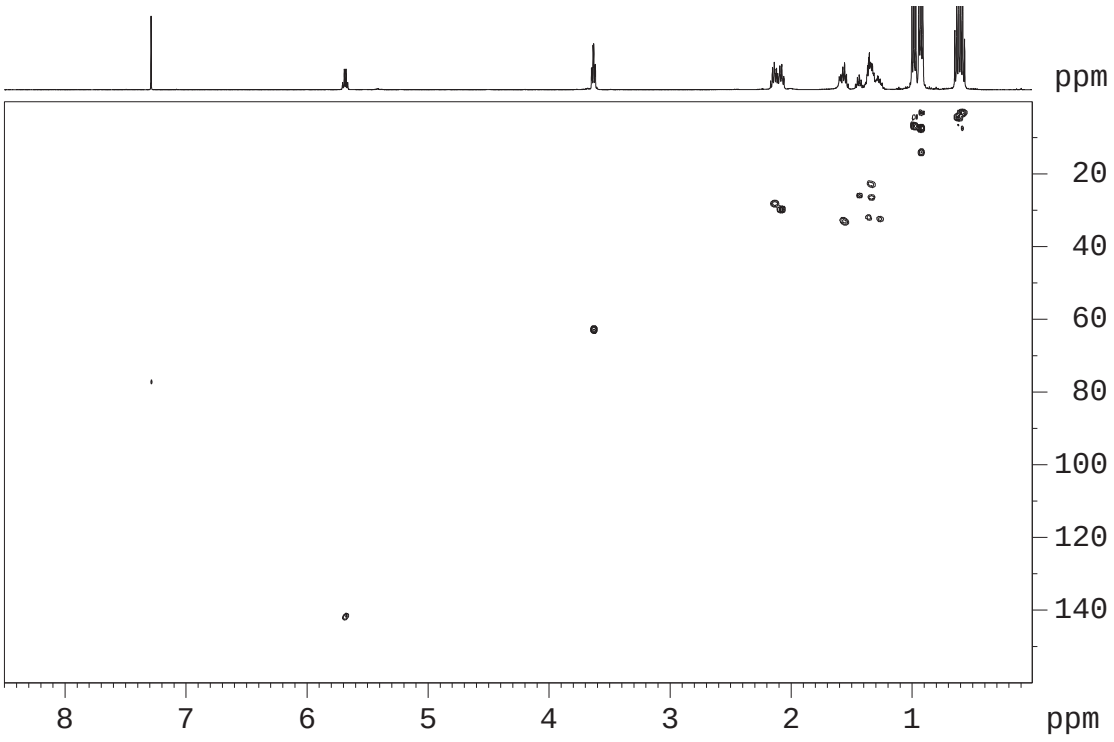

2D ^{1}H-^{13}C HMBC (500 MHz, $CDCl_3$)

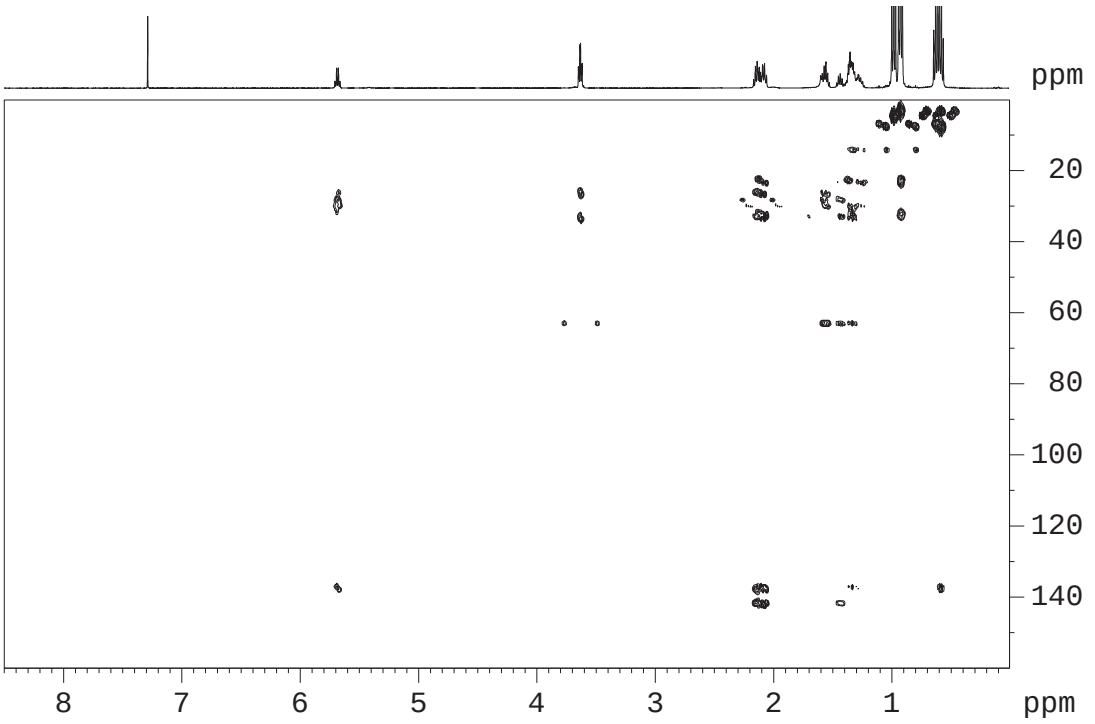

^{1}H-selective 1D NOESY (500 MHz, $CDCl_3$)

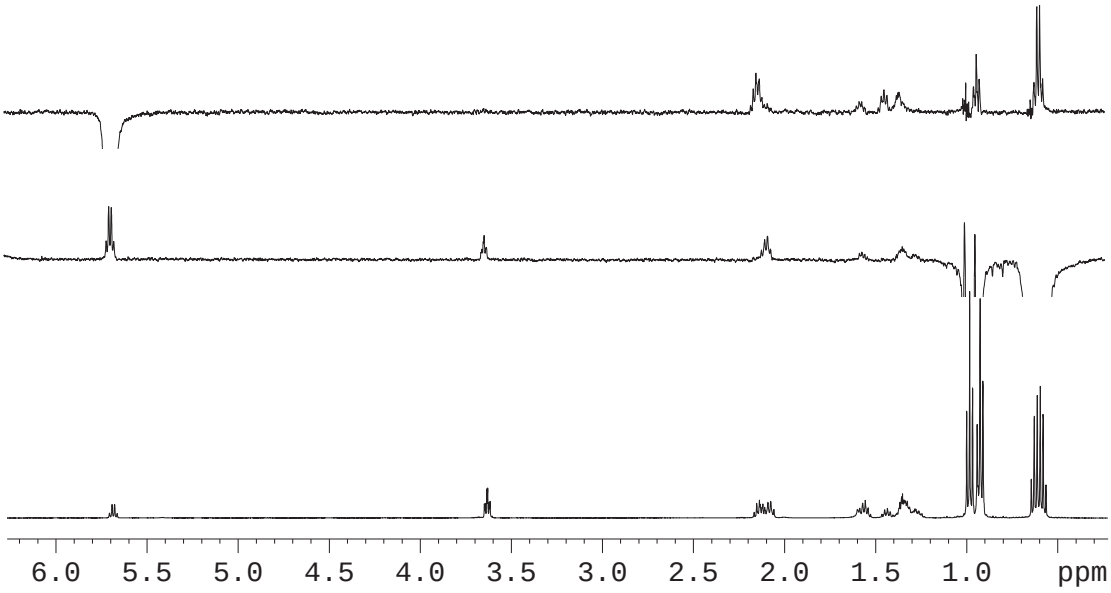

^{1}H-selective 1D TOCSY (500 MHz, $CDCl_3$)

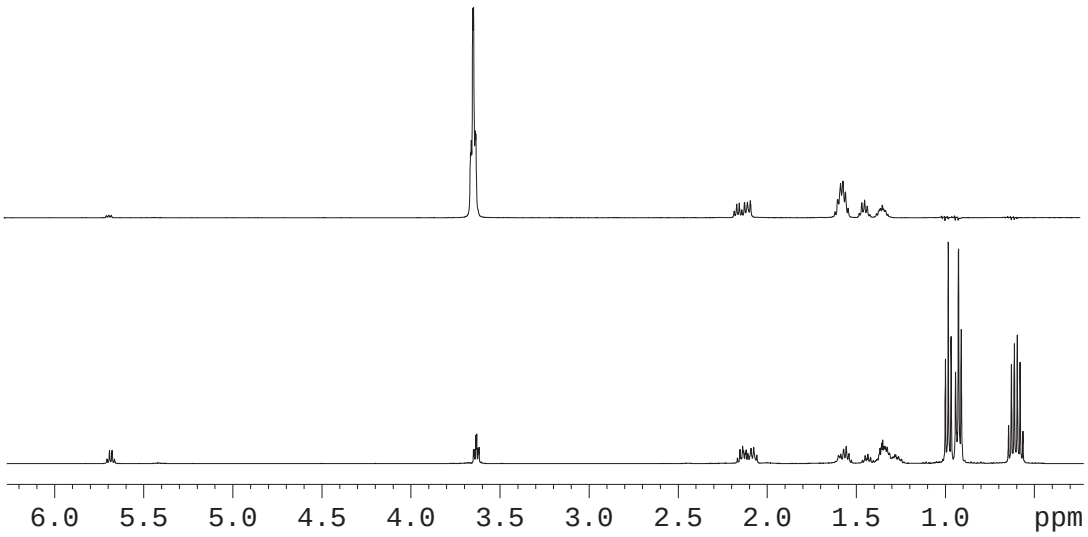

GC trace of the mixture with different isomers

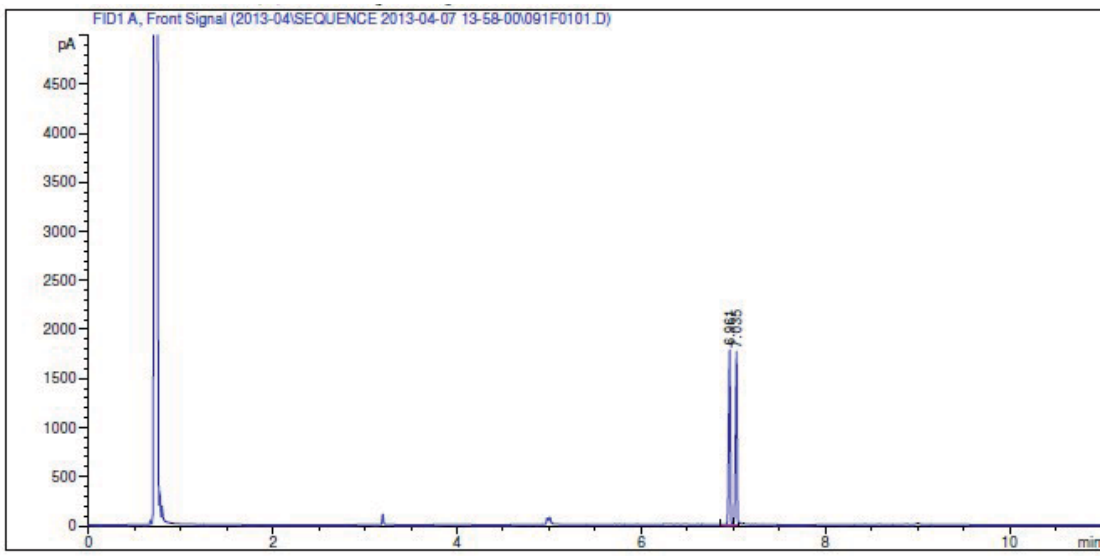


```
================================================================
                    Area Percent Report
================================================================

Sorted By             :      Signal
Multiplier:                   :      1.0000
Dilution:                     :      1.0000
Use Multiplier & Dilution Factor with ISTDs


Signal 1: FID1 A, Front Signal

Peak RetTime Type  Width     Area      Height     Area
  #   [min]       [min]   [pA*s]      [pA]        %
----|-------|----|-------|----------|----------|--------|
   1   6.961 VV    0.0188 2100.72949 1776.63489 50.51718
   2   7.035 VV    0.0186 2057.71655 1764.79529 49.48282
```

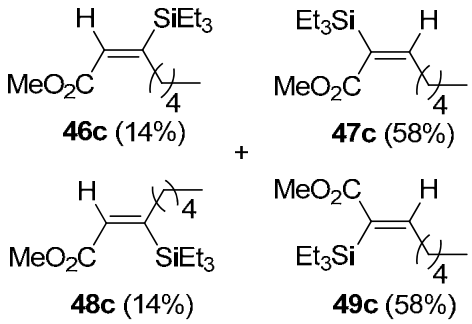

46c (14%) **47c** (58%)

48c (14%) **49c** (58%)

^{1}H-NMR (500 MHz, $CDCl_3$)

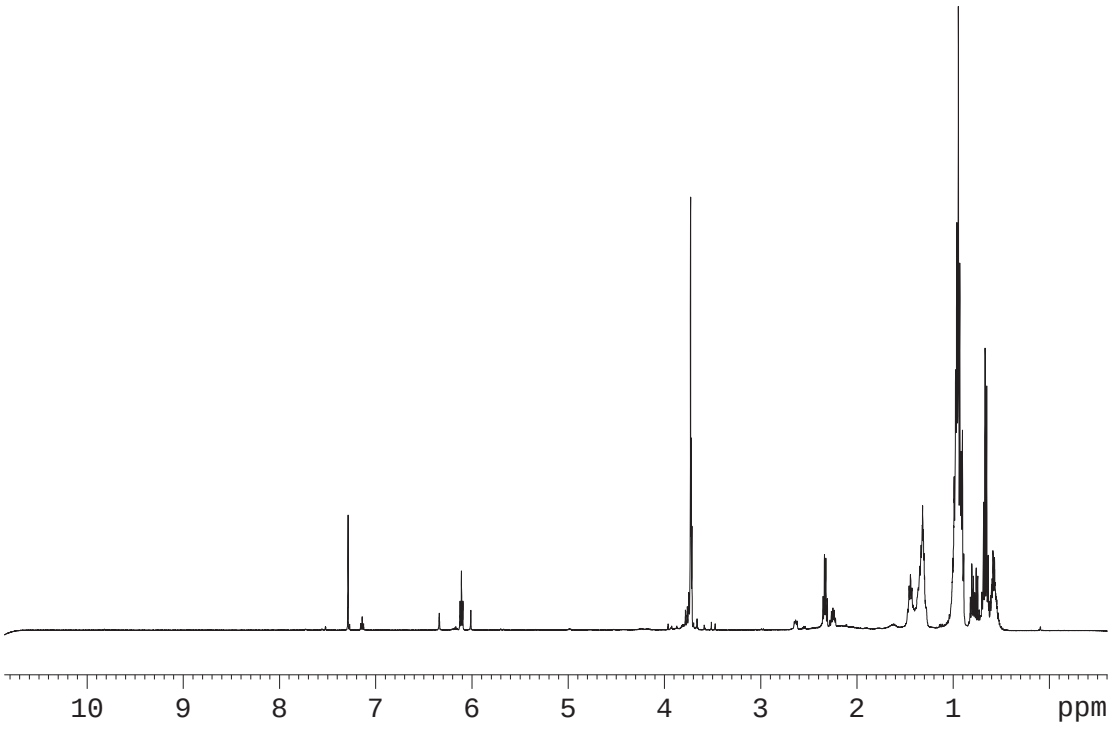

^{13}C NMR (100 MHz, $CDCl_3$)

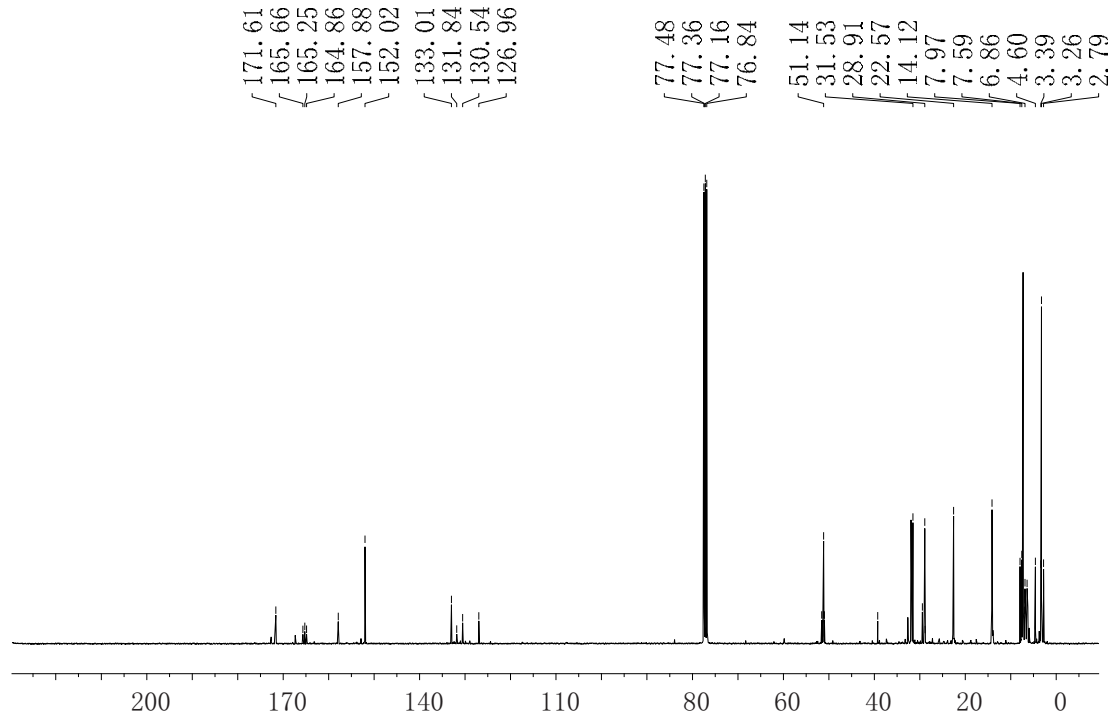

2D ^{1}H-^{1}H COSY (500 MHz, $CDCl_3$)

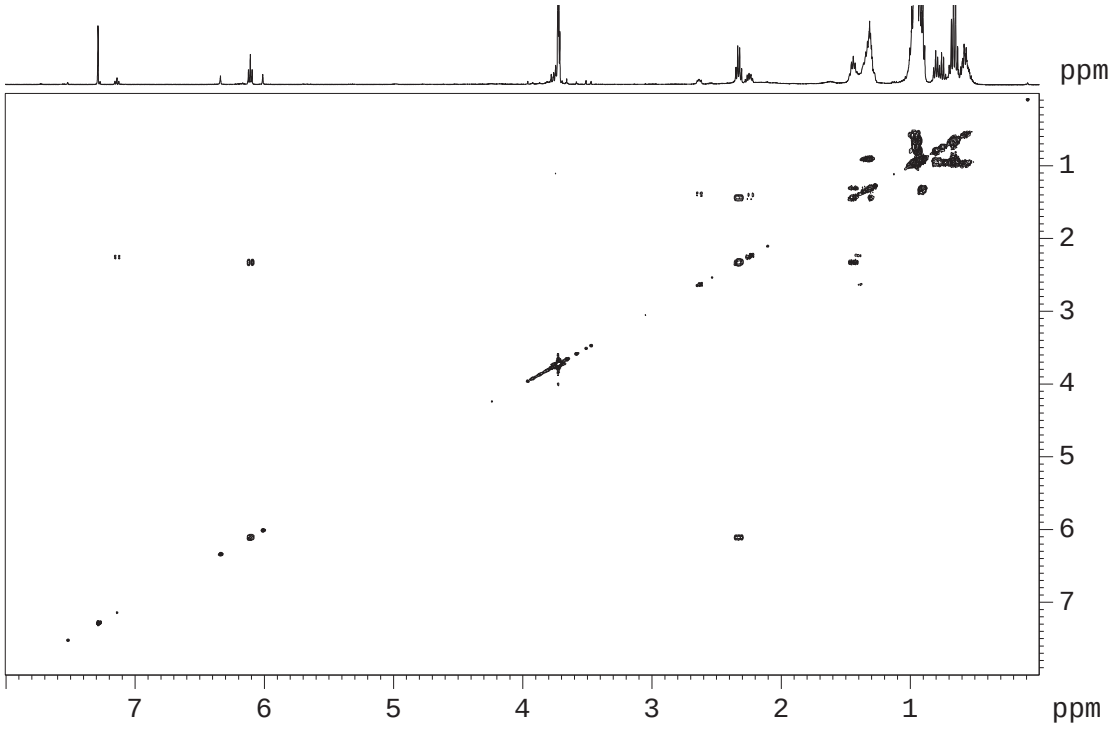

2D ^{1}H-^{13}C HSQC (500 MHz, $CDCl_3$)

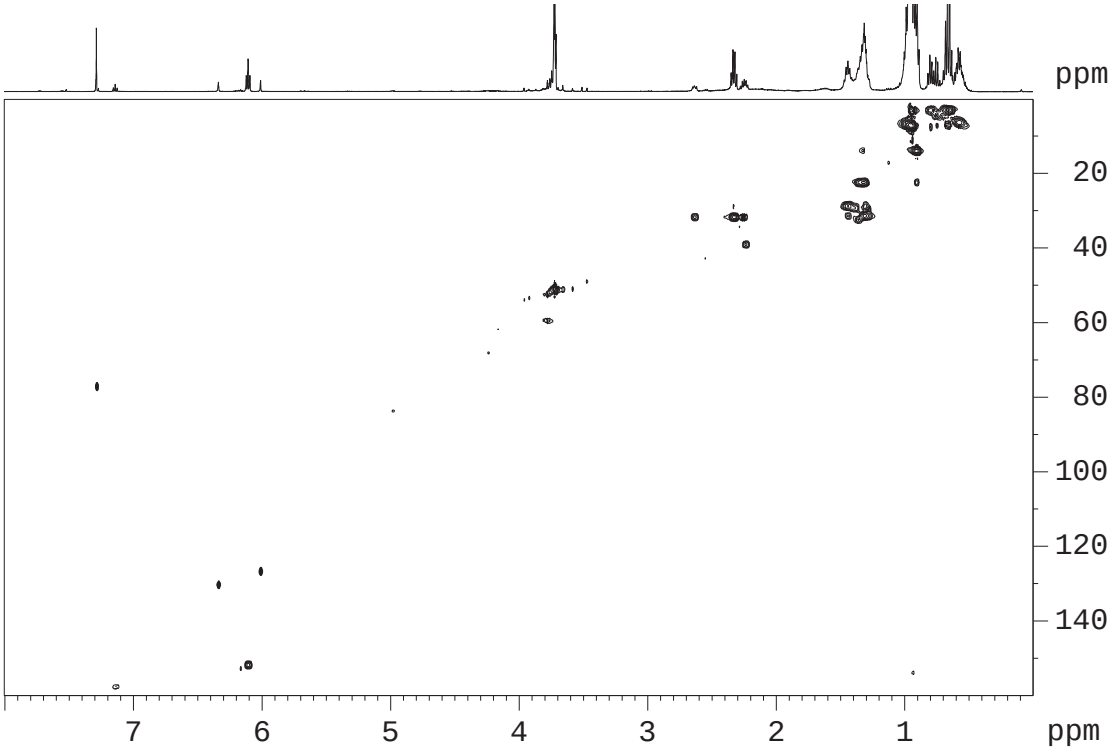

2D ^{1}H-^{13}C HMBC (500 MHz, $CDCl_3$)

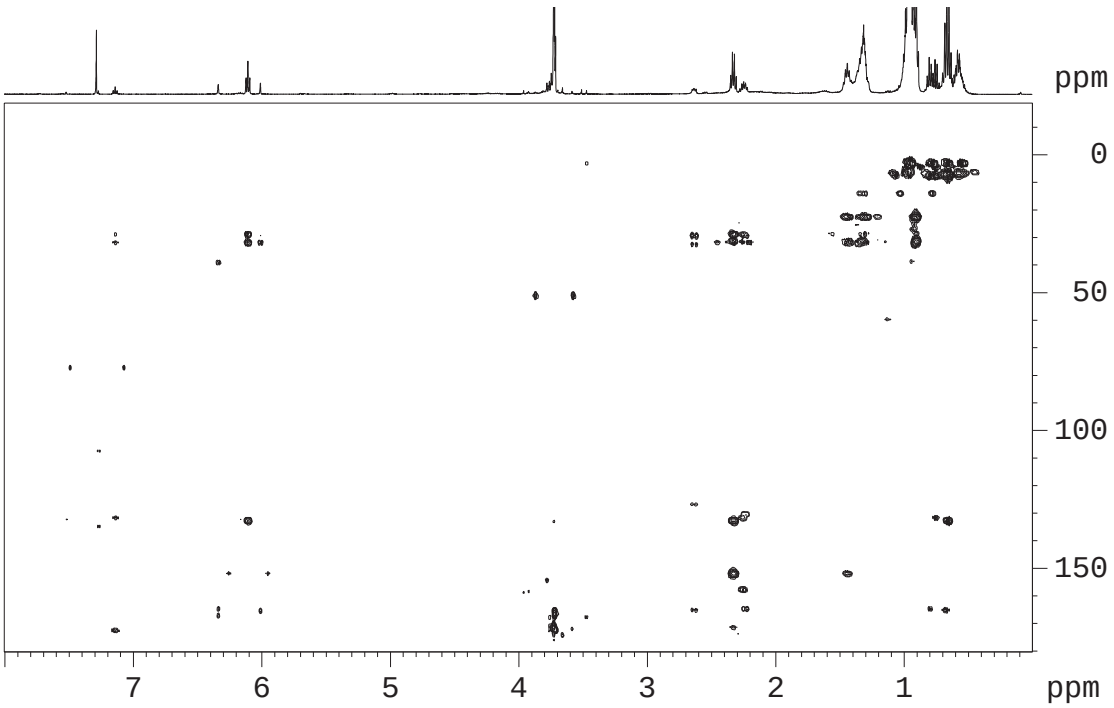

GC trace of the mixture with different isomers

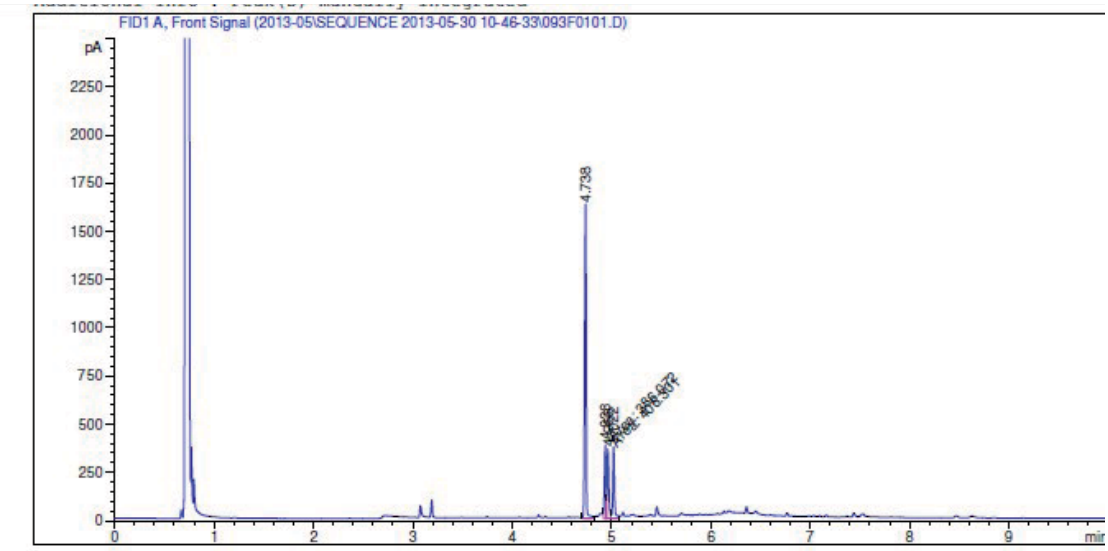


```
================================================================
                      Area Percent Report
================================================================

Sorted By             :      Signal
Multiplier:                   :      1.0000
Dilution:                     :      1.0000
Use Multiplier & Dilution Factor with ISTDs


Signal 1: FID1 A, Front Signal

Peak RetTime Type  Width     Area      Height     Area
  #   [min]        [min]   [pA*s]      [pA]        %
----|-------|----|-------|----------|----------|--------|
   1   4.738 VV    0.0174 1716.54785 1615.51929 58.25422
   2   4.938 MM    0.0167  386.07187  385.14551 13.10206
   3   4.966 MM    0.0189  406.30109  358.51141 13.78858
   4   5.022 VV    0.0188  437.72885  369.02307 14.85514
```

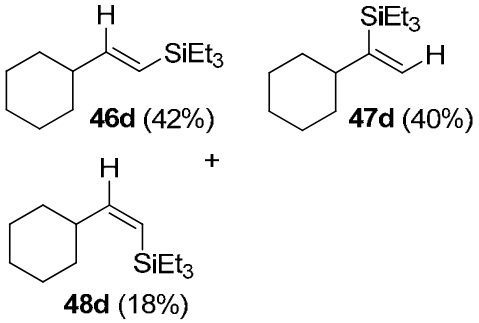

^{1}H NMR (500 MHz, $CDCl_3$) δ (ppm)

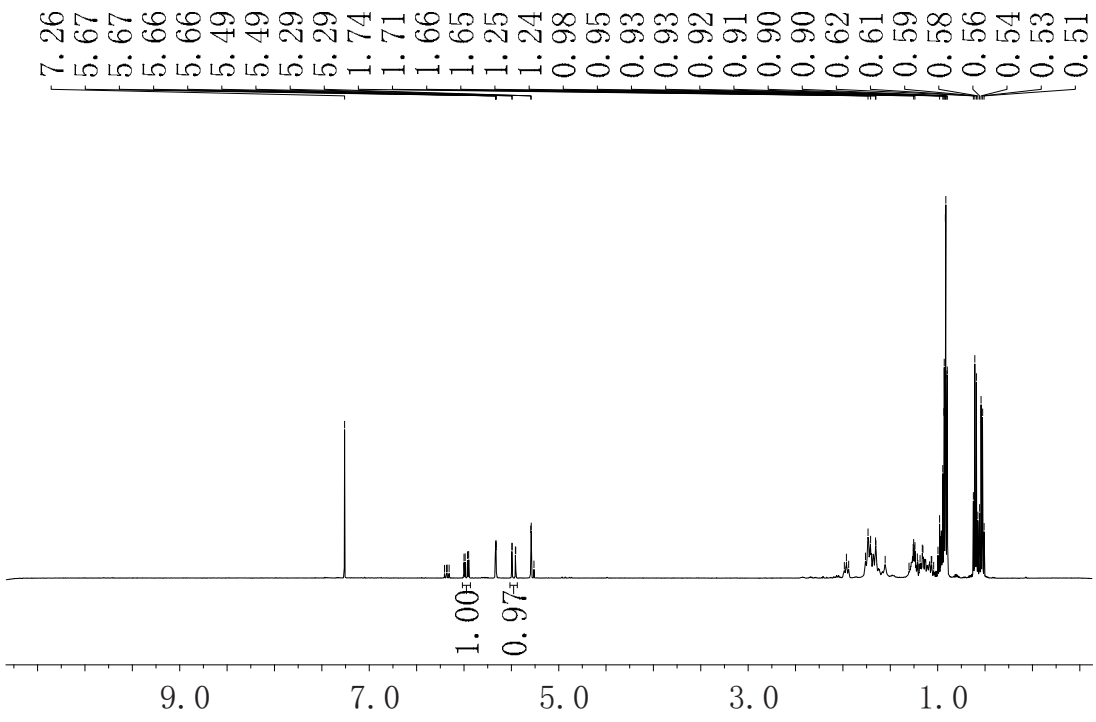

^{13}C NMR (125 MHz, $CDCl_3$)

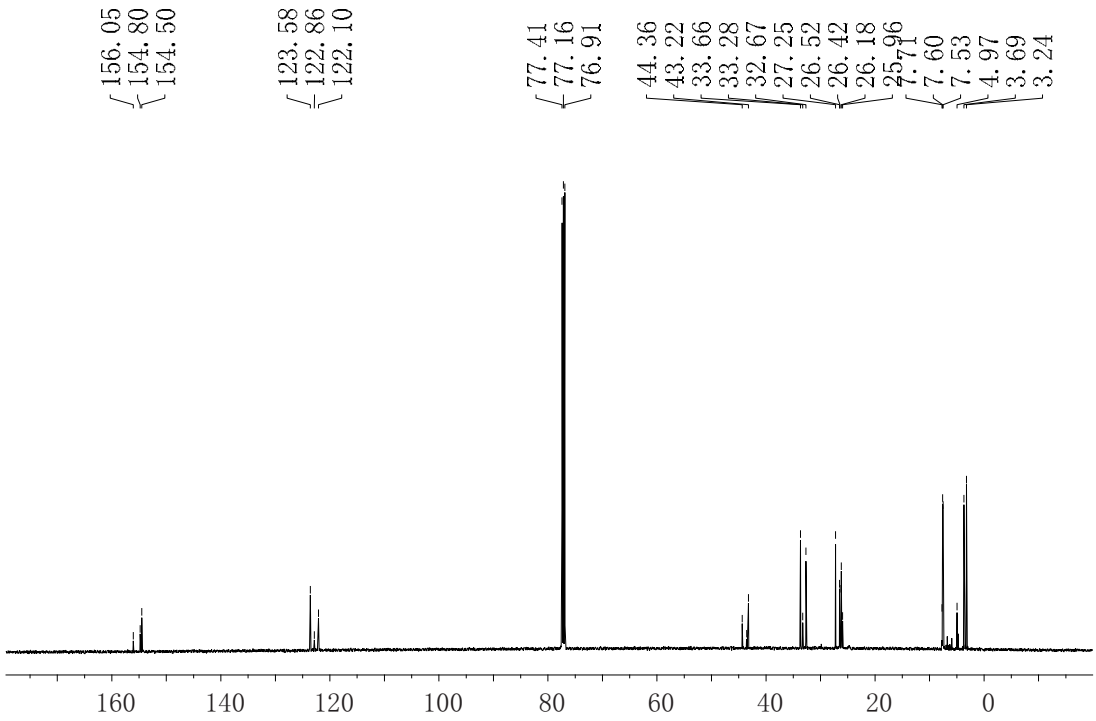

2D ^{1}H-^{1}H COSY (500 MHz, $CDCl_3$)

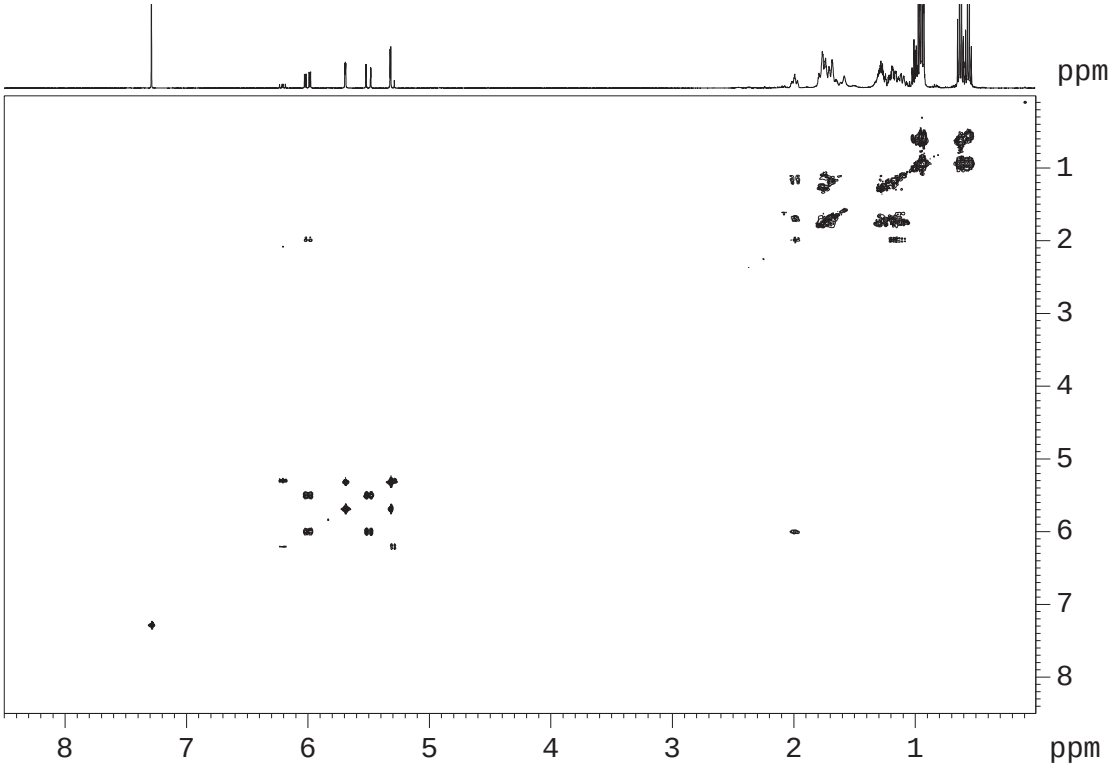

2D ^{1}H-^{13}C HSQC (500 MHz, $CDCl_3$)

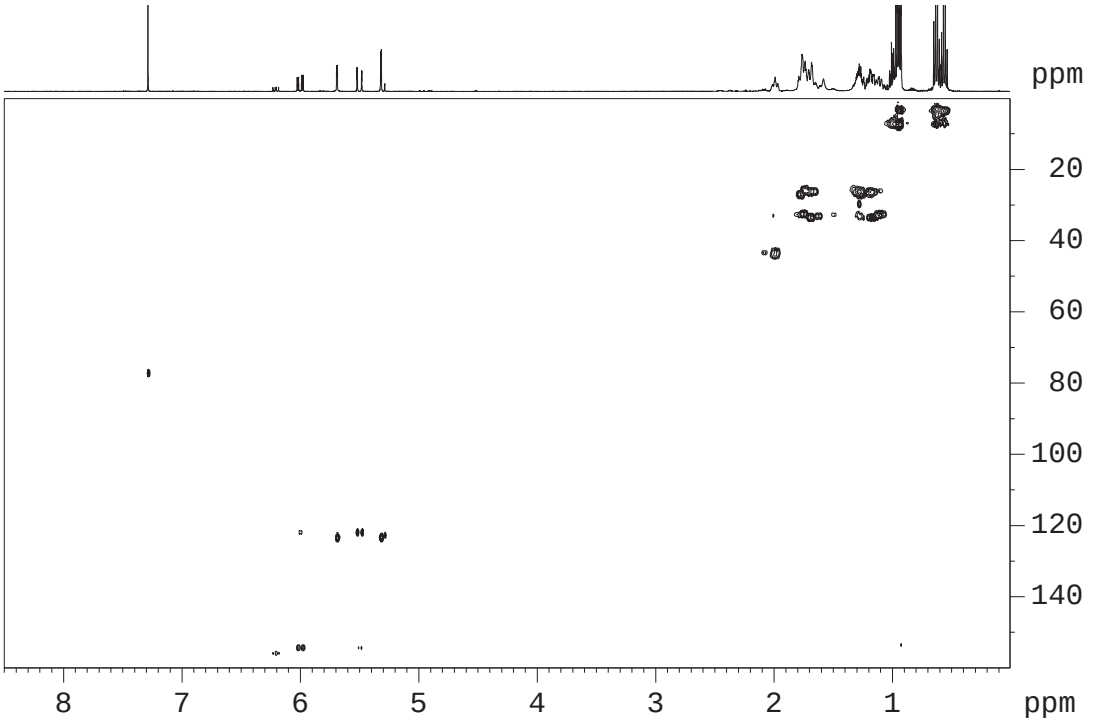

2D ^{1}H-^{13}C HMBC (500 MHz, $CDCl_3$)

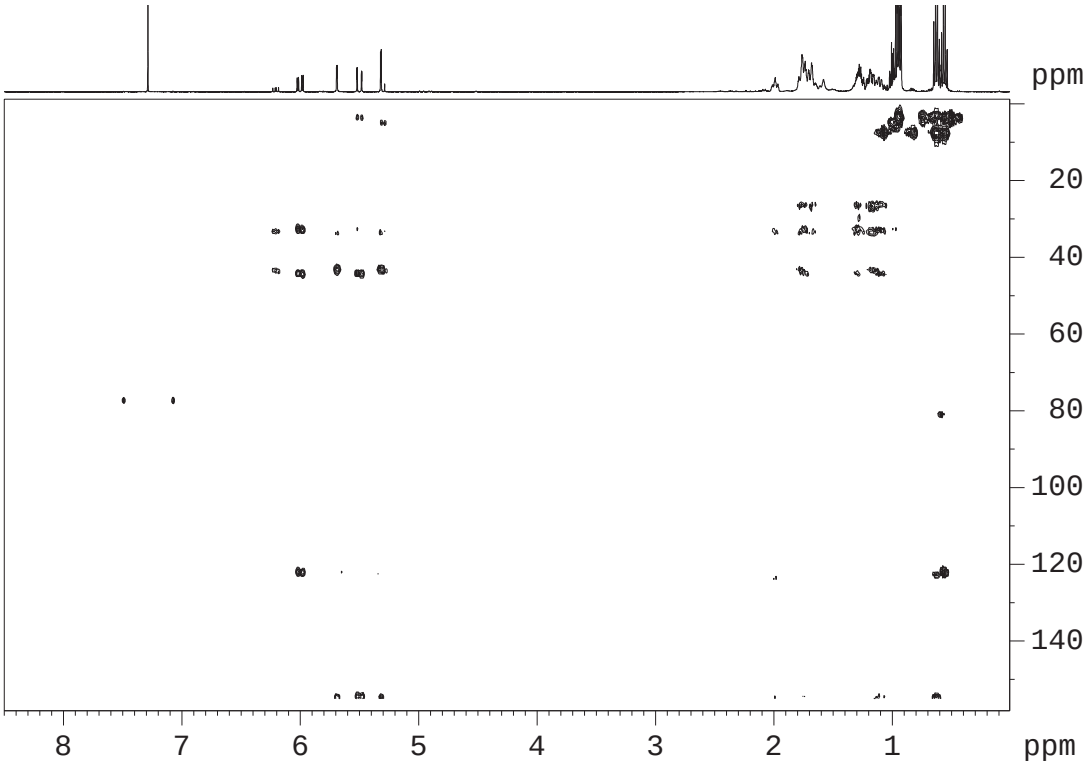

^{1}H-selective 1D NOESY (500 MHz, $CDCl_3$)

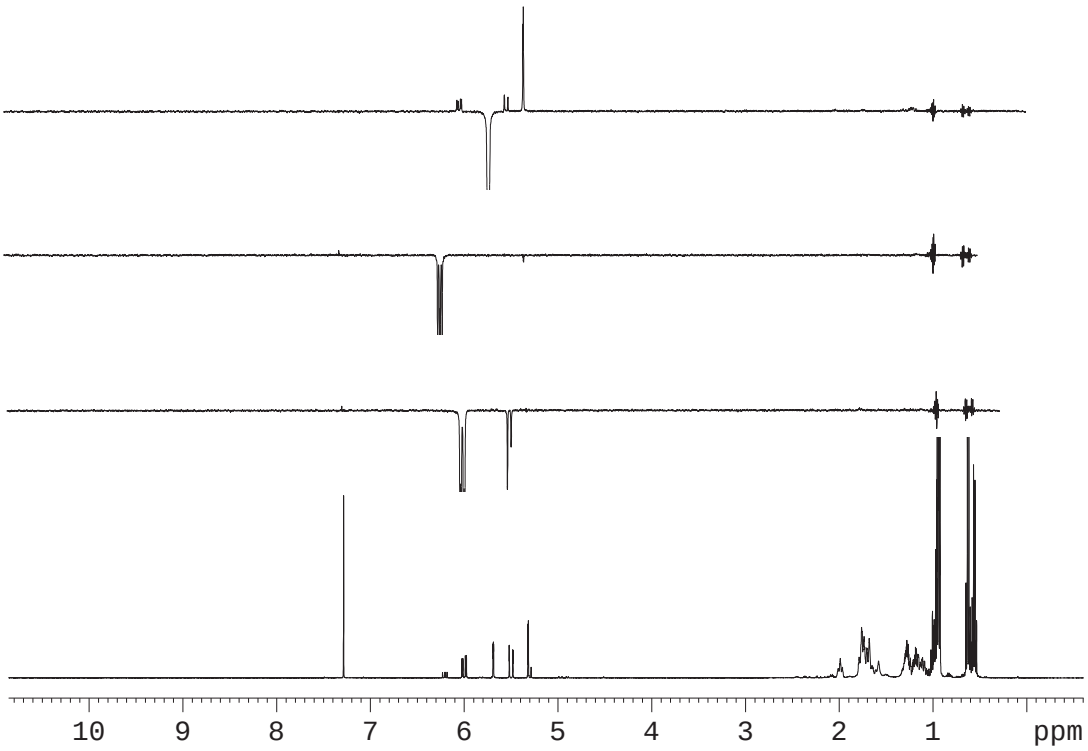

GC trace of the mixture with different isomers

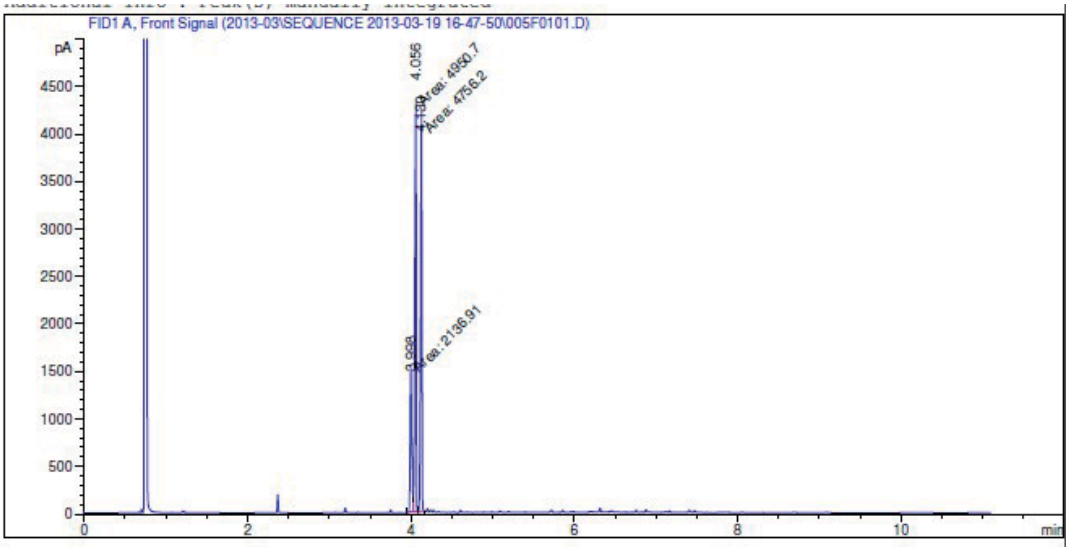


```
================================================================
                    Area Percent Report
================================================================

Sorted By             :      Signal
Multiplier:                   :      1.0000
Dilution:                     :      1.0000
Use Multiplier & Dilution Factor with ISTDs


Signal 1: FID1 A, Front Signal

Peak RetTime Type  Width     Area      Height     Area
  #   [min]        [min]   [pA*s]      [pA]        %
----|-------|----|-------|----------|----------|--------|
   1   3.998 MM    0.0247 2136.90649 1442.78308 18.04240
   2   4.056 MM    0.0183 4950.69629 4514.77637 41.79989
   3   4.130 MM    0.0201 4756.19971 3948.49023 40.15771
```

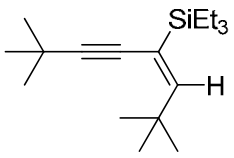

, **50**

^{1}H NMR (400 MHz, $CDCl_3$) δ (ppm)

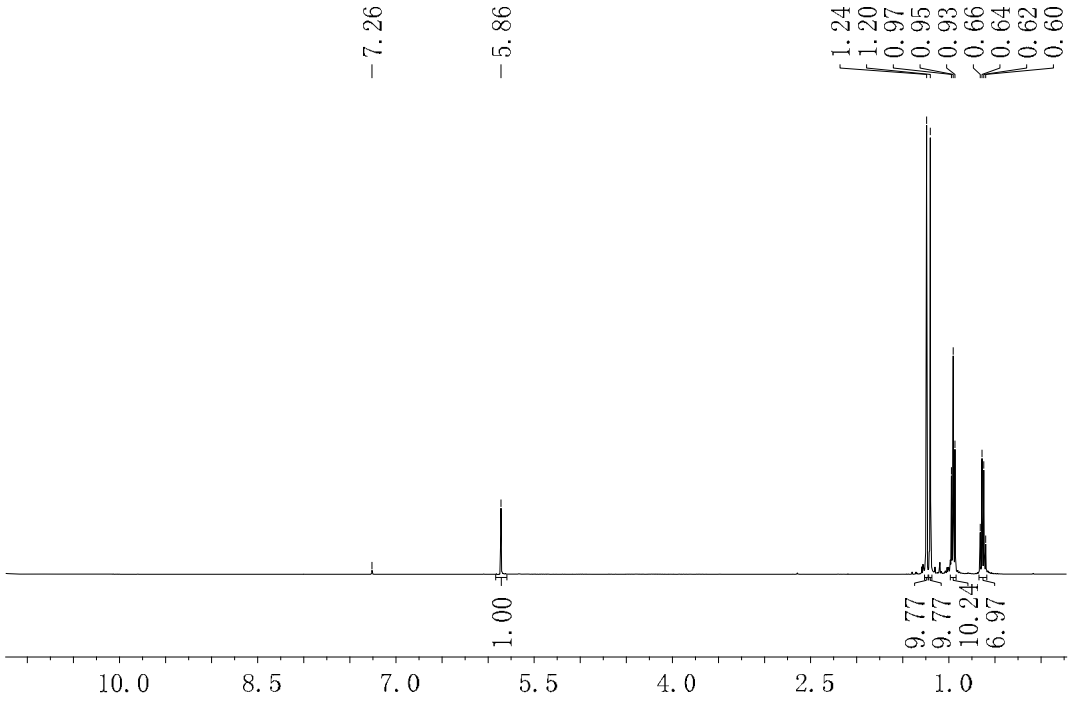

^{13}C NMR (100 MHz, $CDCl_3$)

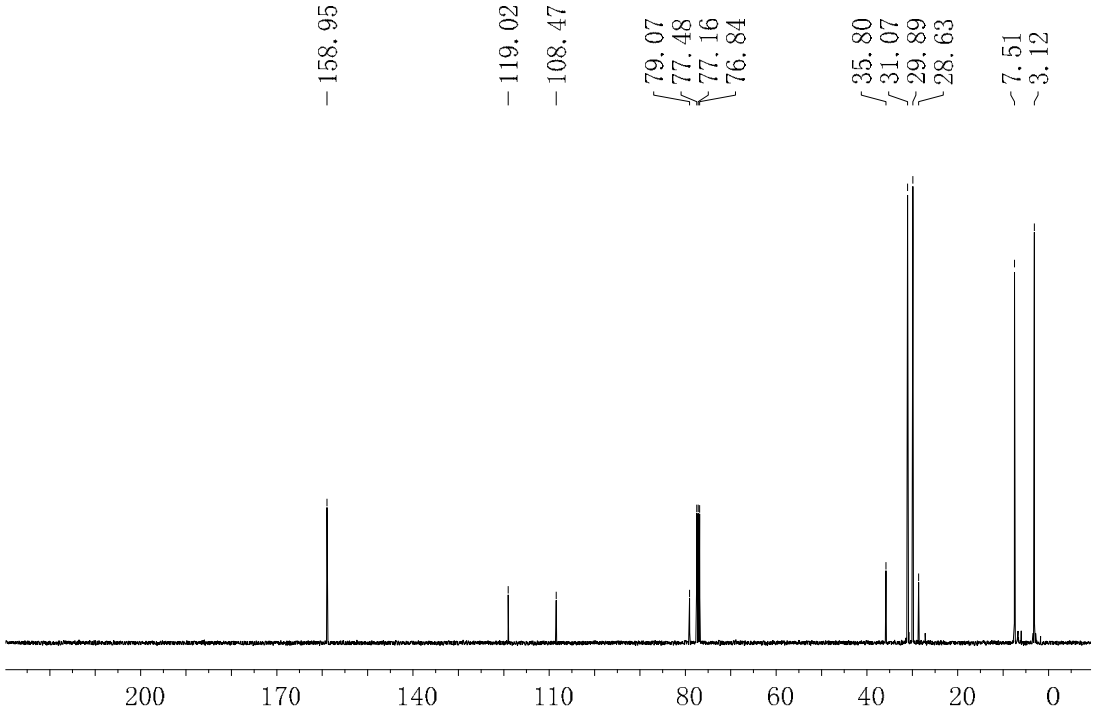

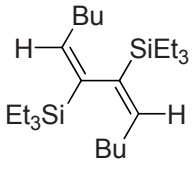

, **51**

^{1}H NMR (250 MHz, $CDCl_3$) δ (ppm)

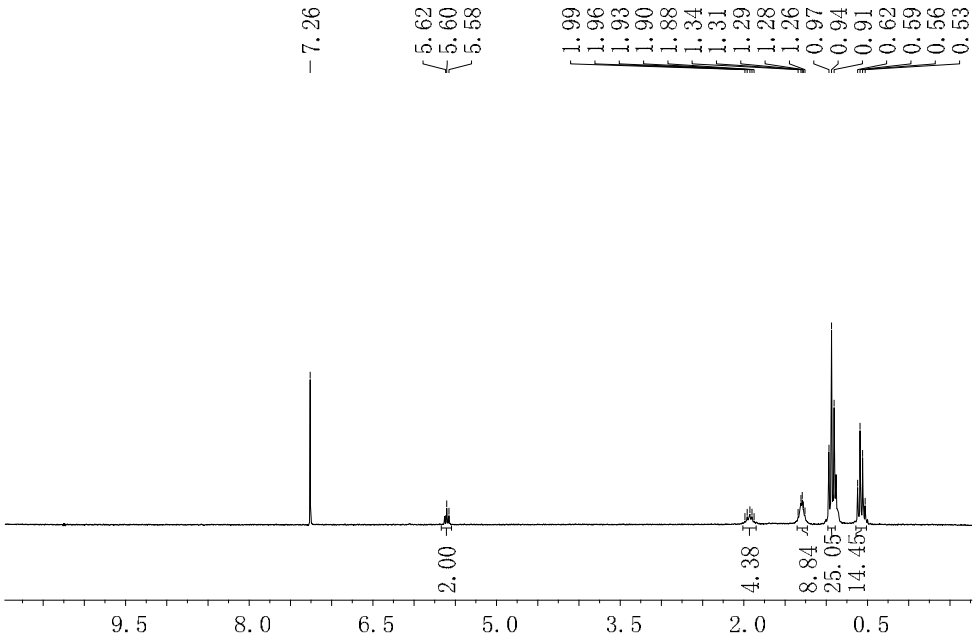

^{13}C NMR (90 MHz, $CDCl_3$)

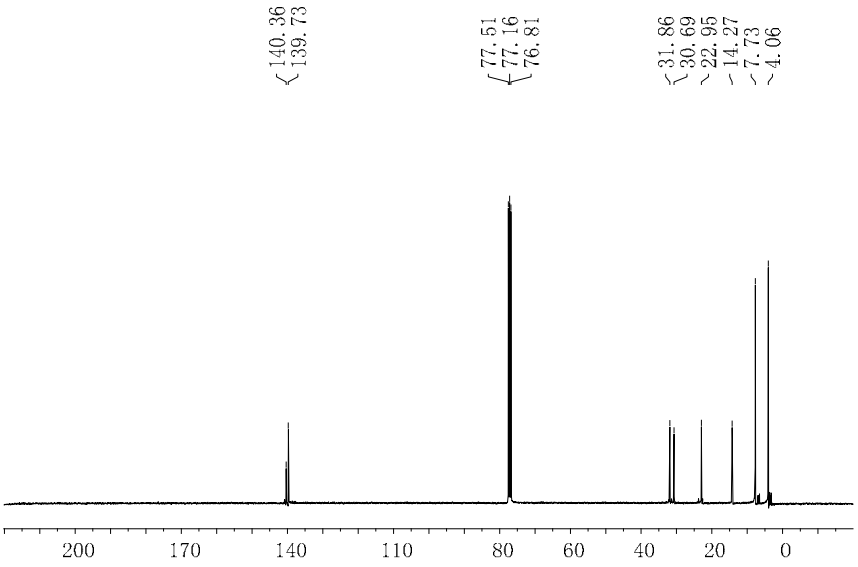

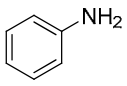

, **52**

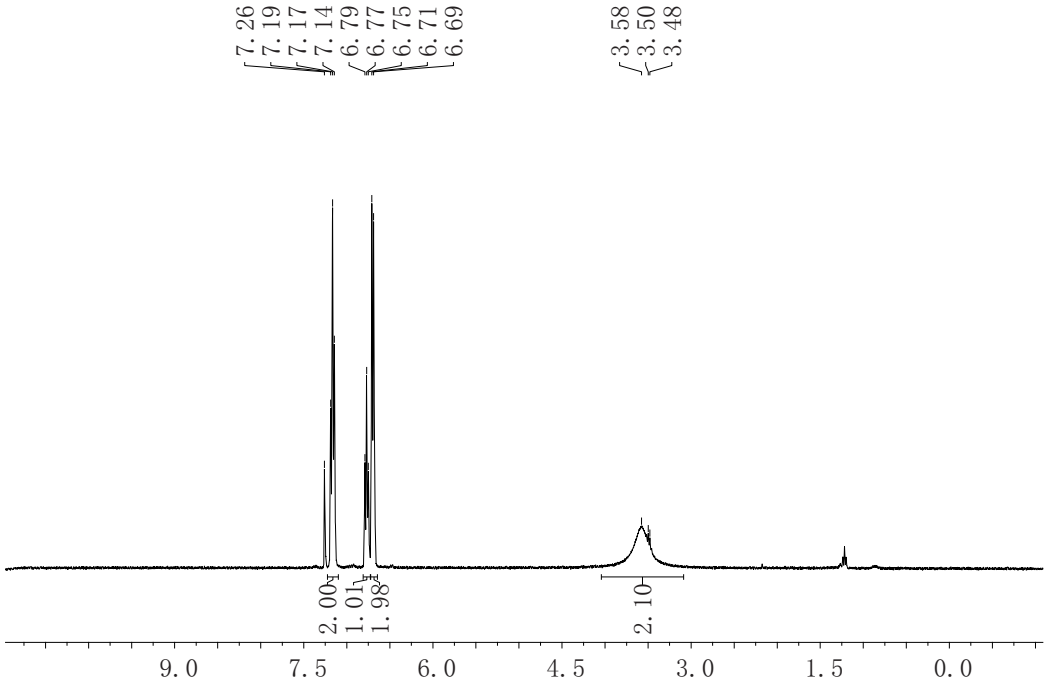

^{13}C NMR (90MHz, $CDCl_3$)

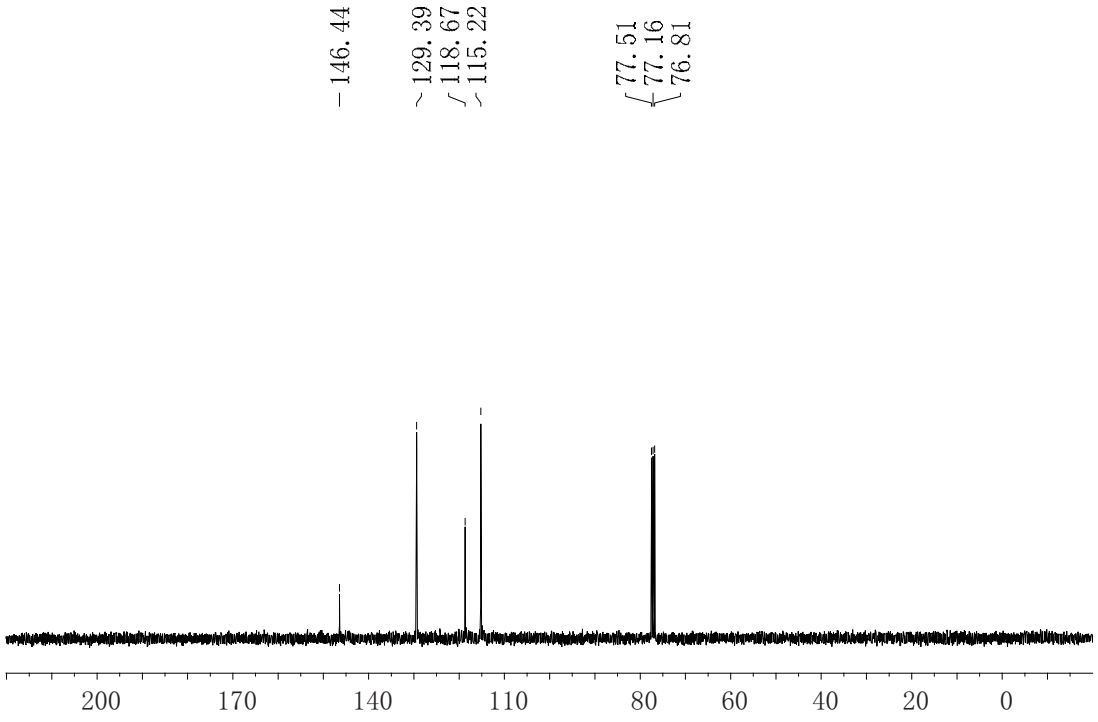

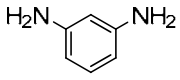

, **53**

^{1}H NMR (360 MHz, $CDCl_3$)

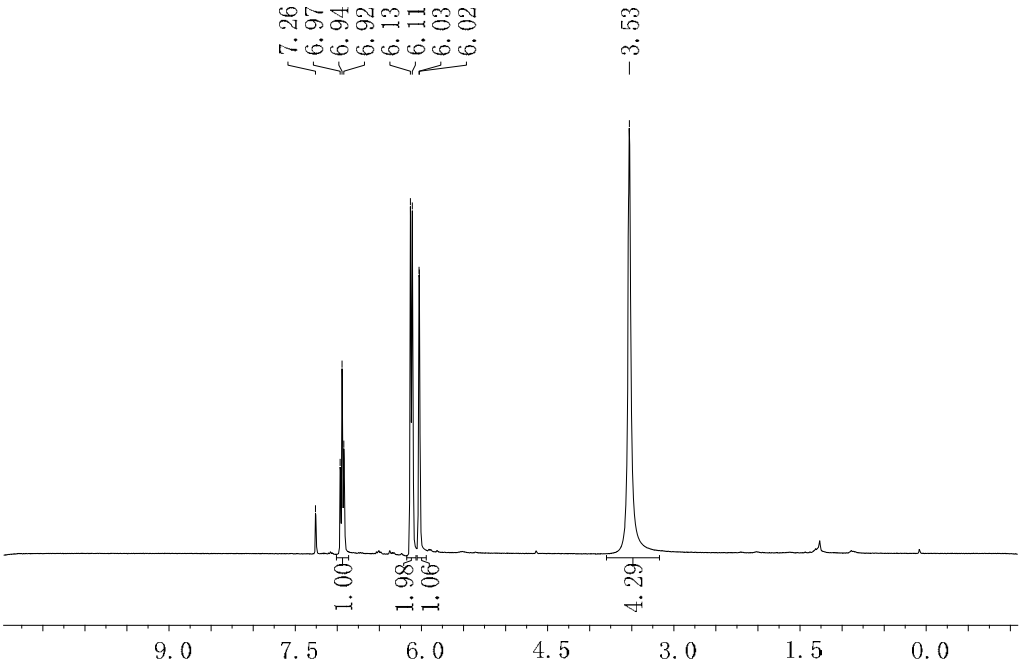

^{13}C NMR (90MHz, $CDCl_3$)

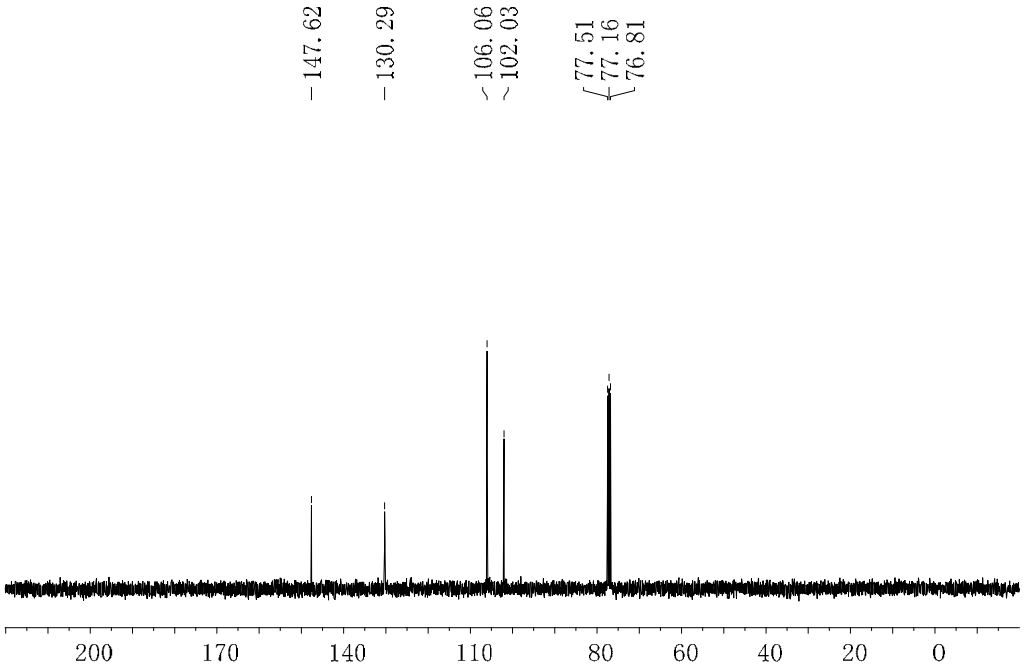

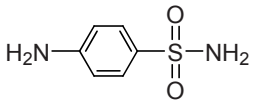

, **54**

^{1}H NMR (360 MHz, $(CD_3)_2SO$)

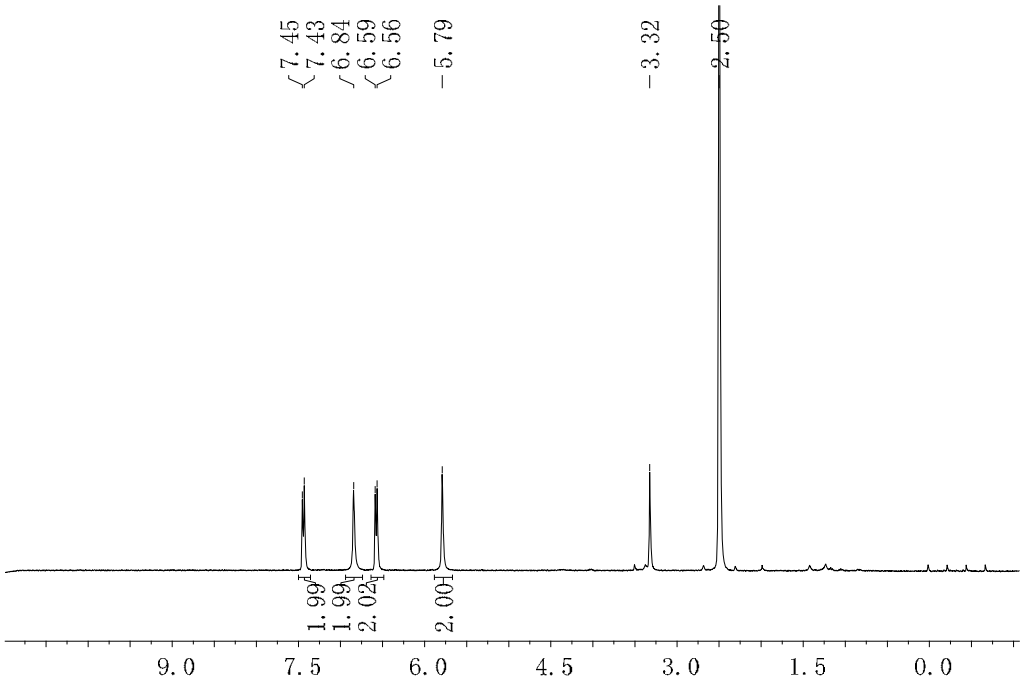

^{13}C NMR (90MHz, $(CD_3)_2SO$)

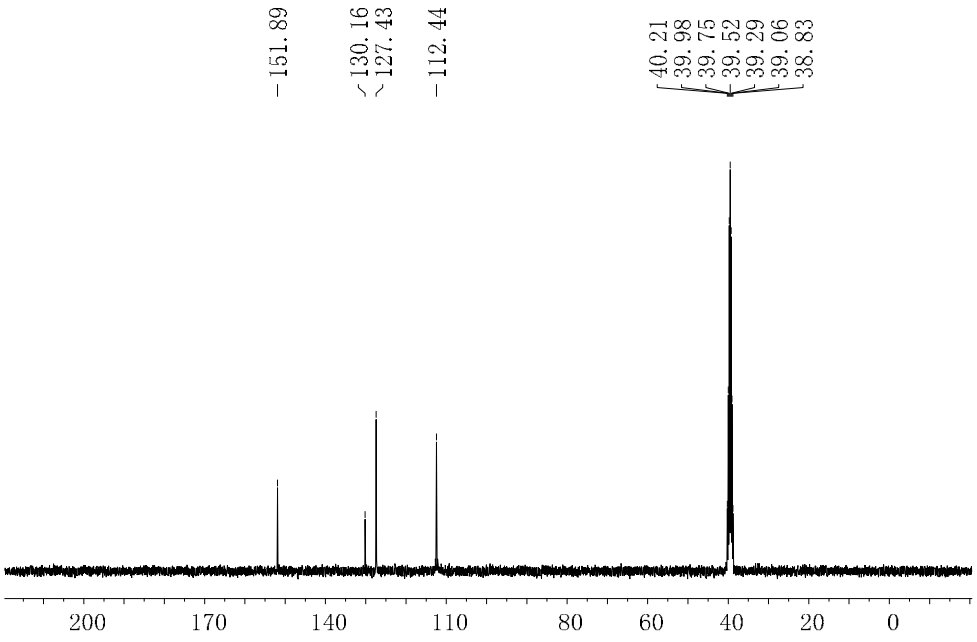

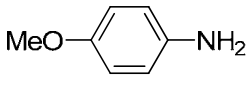

, **55**

^{1}H NMR (400MHz, $CDCl_3$)

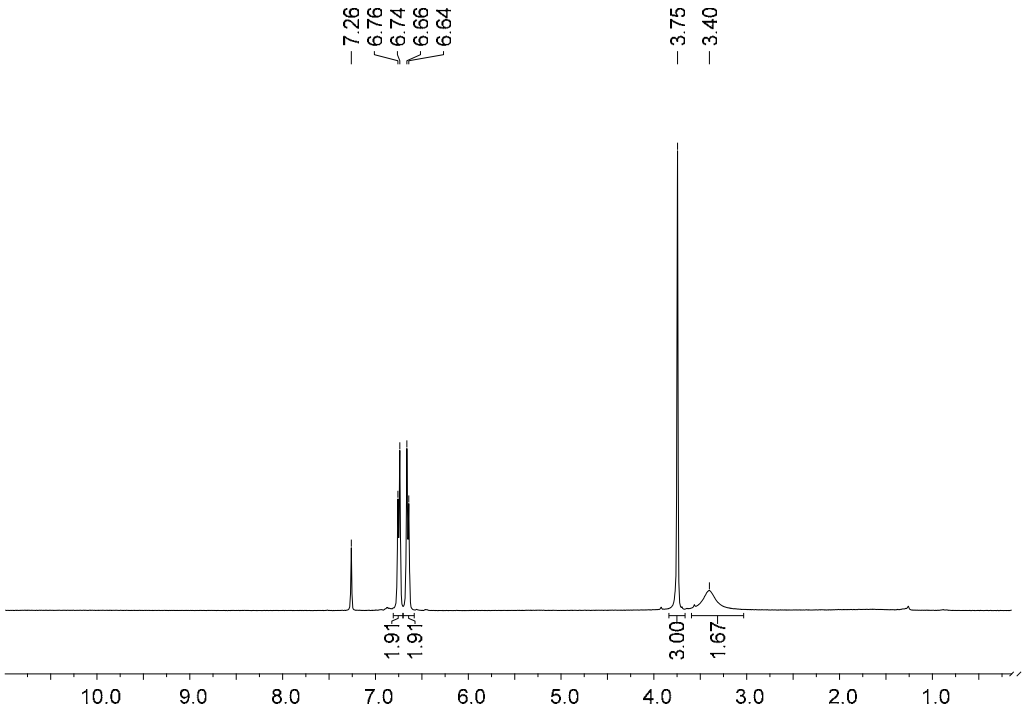

^{13}C NMR (100MHz, $CDCl_3$)

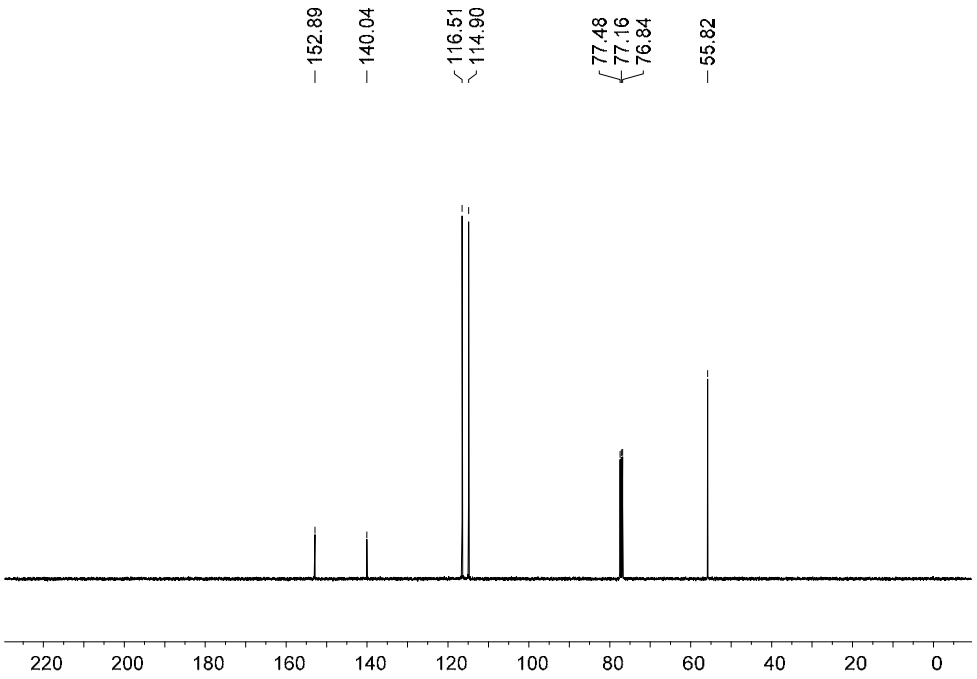

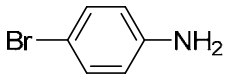

, **56**

^{1}H NMR (400MHz, $CDCl_3$)

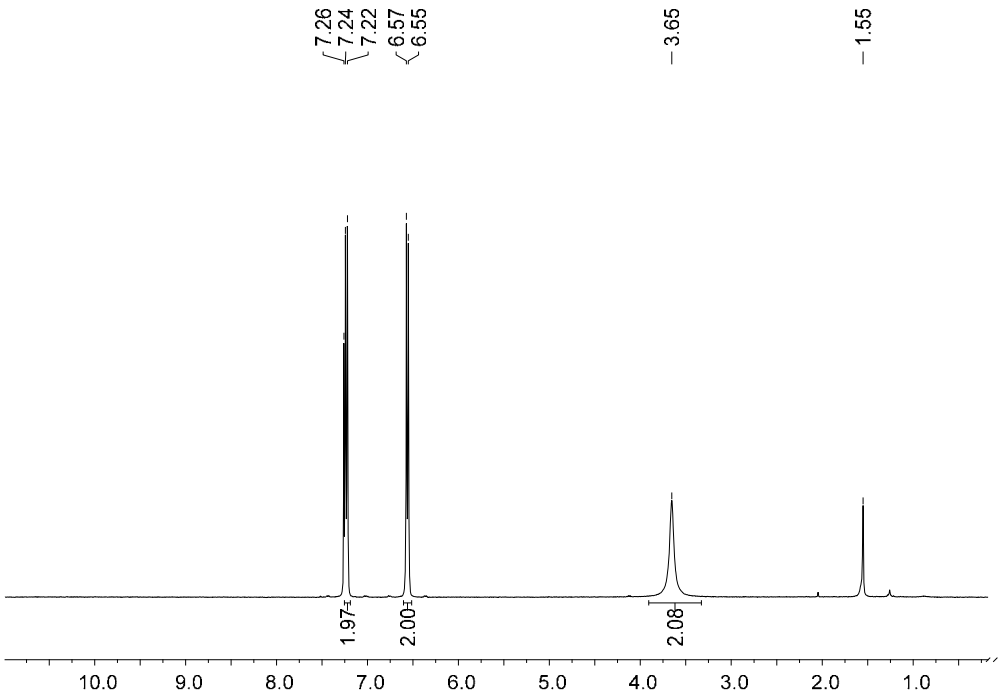

^{13}C NMR (100MHz, $CDCl_3$)

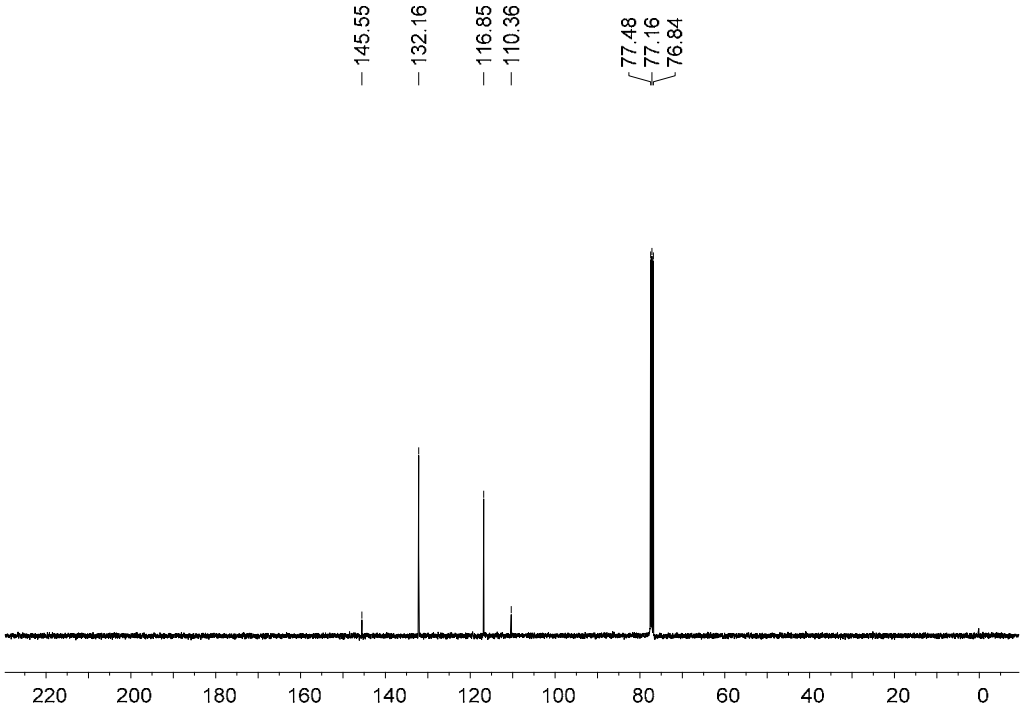

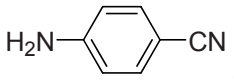

, **57**

^{1}H NMR (400MHz, $CDCl_3$)

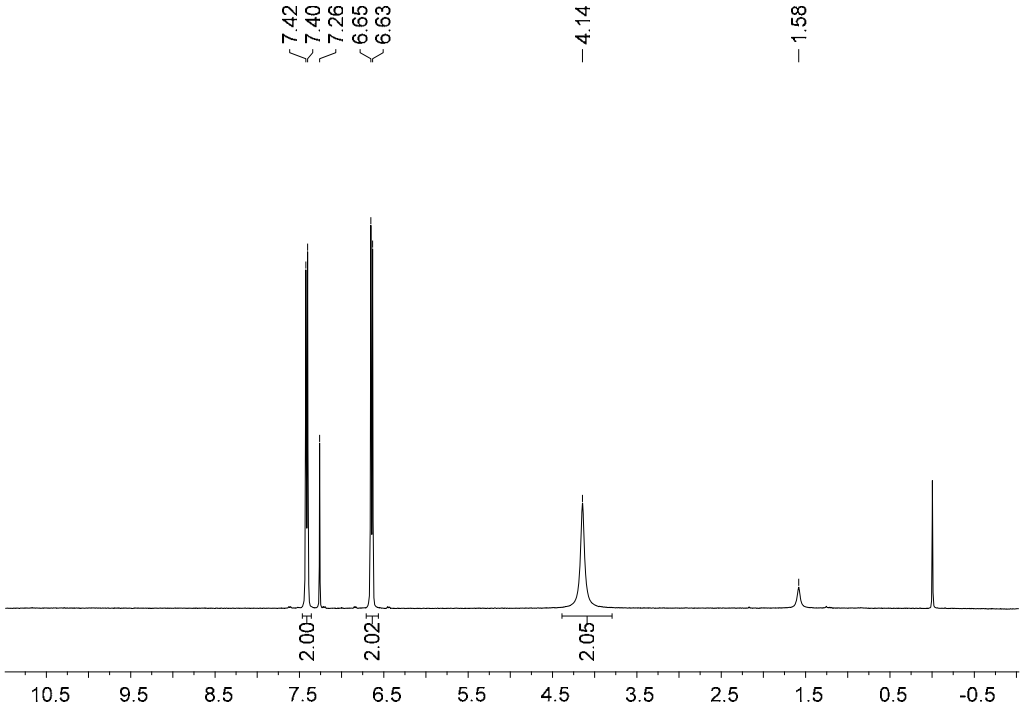

^{13}C NMR (100MHz, $CDCl_3$)

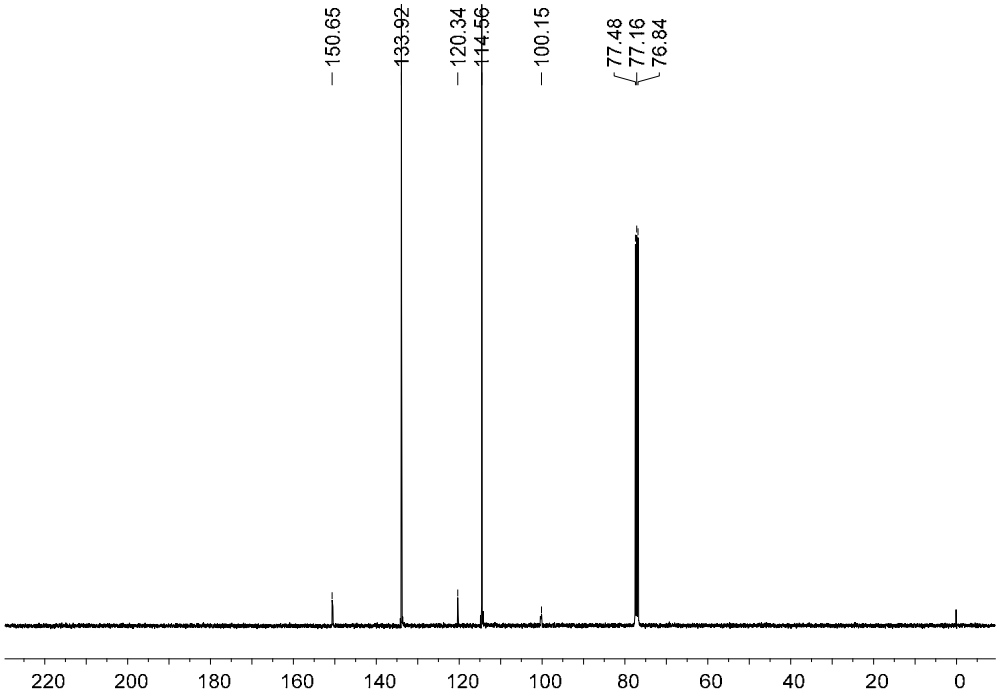

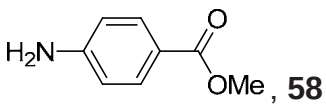

, **58**

^{1}H NMR (400MHz, $CDCl_3$)

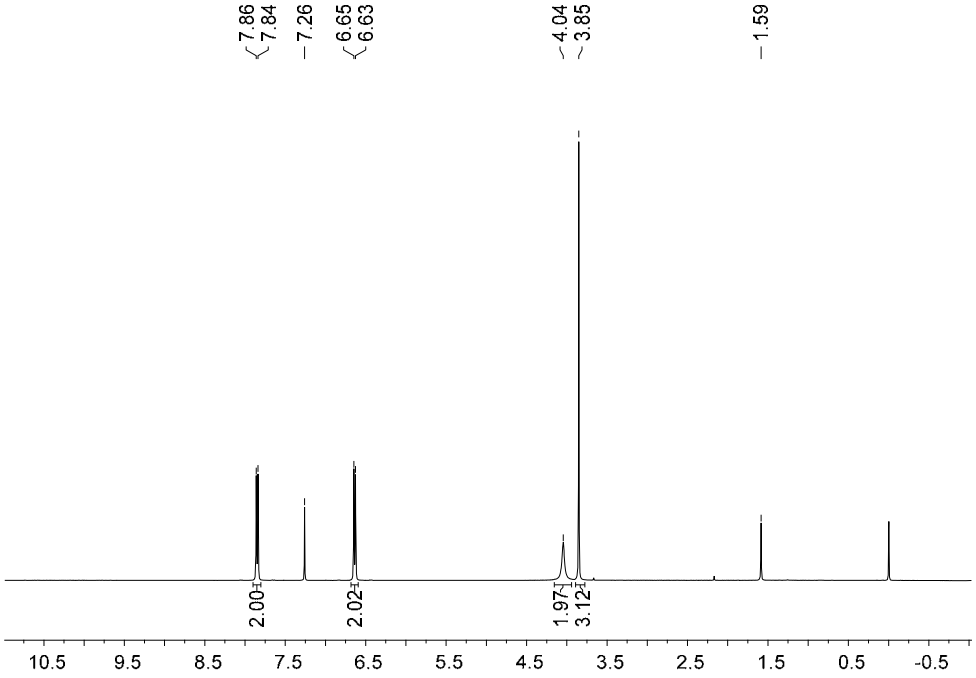

^{13}C NMR (100MHz, $CDCl_3$)

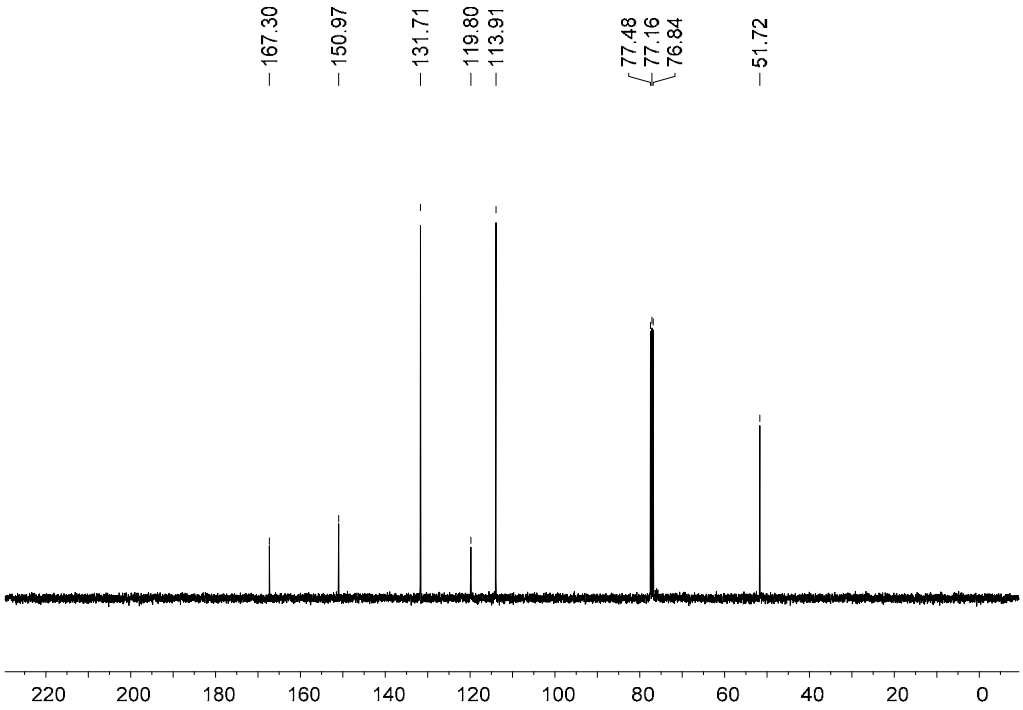

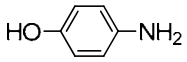

, **59**

^{1}H NMR (360 MHz, $(CD_3)_2SO$)

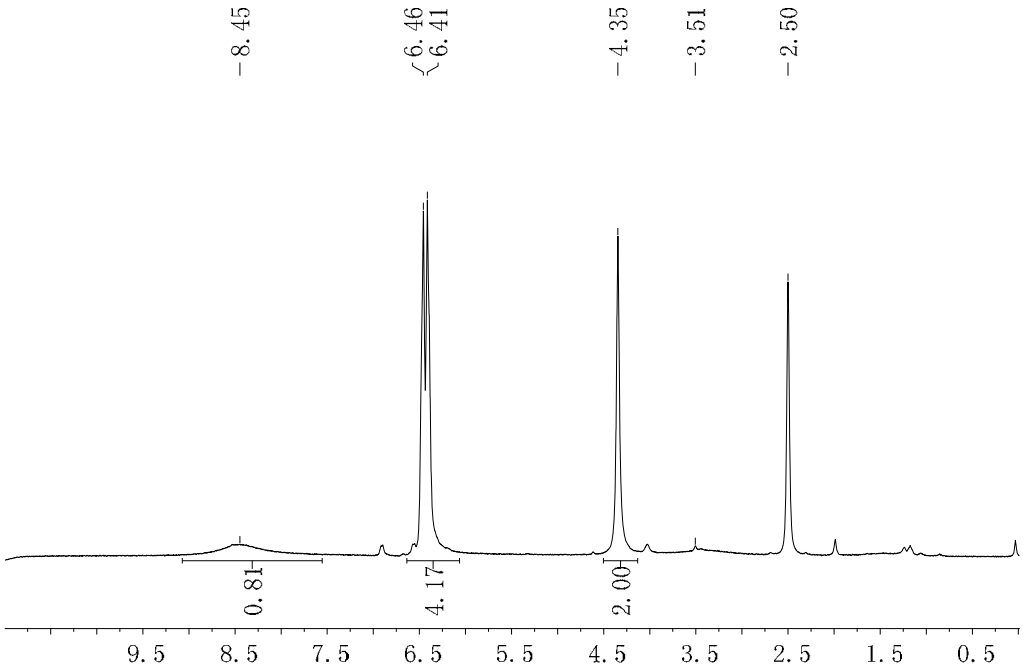

^{13}C NMR (90MHz, $(CD_3)_2SO$)